

## **General Disclaimer**

### **One or more of the Following Statements may affect this Document**

- This document has been reproduced from the best copy furnished by the organizational source. It is being released in the interest of making available as much information as possible.
- This document may contain data, which exceeds the sheet parameters. It was furnished in this condition by the organizational source and is the best copy available.
- This document may contain tone-on-tone or color graphs, charts and/or pictures, which have been reproduced in black and white.
- This document is paginated as submitted by the original source.
- Portions of this document are not fully legible due to the historical nature of some of the material. However, it is the best reproduction available from the original submission.

# LEGIBILITY NOTICE

A major purpose of the Technical Information Center is to provide the broadest dissemination possible of information contained in DOE's Research and Development Reports to business, industry, the academic community, and federal, state and local governments.

Although a small portion of this report is not reproducible, it is being made available to expedite the availability of information on the research discussed herein.



5101-242

Flat-Plate  
Solar Array Project

DOE/JPL--1012-94

DE85 000334

## Progress Report 22

for the Period January to September 1983

and Proceedings of the  
22nd Project Integration Meeting

Prepared for

U.S. Department of Energy

Through an Agreement with

National Aeronautics and Space Administration

by

Jet Propulsion Laboratory

California Institute of Technology

Pasadena, California

JPL Publication 84-2

### NOTICE

PORTIONS OF THIS REPORT ARE REPRODUCED FROM THE AVAILABLE COPY TO PERMIT THE WIDEST POSSIBLE AVAILABILITY.

Prepared by the Jet Propulsion Laboratory, California Institute of Technology,  
for the U.S. Department of Energy through an agreement with the National  
Aeronautics and Space Administration.

The JPL Flat-Plate Solar Array Project is sponsored by the U.S. Department of  
Energy and is part of the Photovoltaic Energy Systems Program to initiate a  
major effort toward the development of cost-competitive solar arrays.

This report was prepared as an account of work sponsored by an agency of the  
United States Government. Neither the United States Government nor any  
agency thereof, nor any of their employees, makes any warranty, express or  
implied, or assumes any legal liability or responsibility for the accuracy, com-  
pleteness, or usefulness of any information, apparatus, product, or process  
disclosed, or represents that its use would not infringe privately owned rights.

Reference herein to any specific commercial product, process, or service by trade  
name, trademark, manufacturer, or otherwise, does not necessarily constitute or  
imply its endorsement, recommendation, or favoring by the United States  
Government or any agency thereof. The views and opinions of authors  
expressed herein do not necessarily state or reflect those of the United States  
Government or any agency thereof.

This publication reports on work done under NASA Task RE-152 Amendment  
66, DOE/NASA IAA No. DE-A101-76ET20356.

## ABSTRACT

This report describes progress made by the Flat-Plate Solar Array Project during the period January to September 1983. It includes reports on silicon sheet growth and characterization, module technology, silicon material, cell processing and high-efficiency cells, environmental isolation, engineering sciences, module performance and failure analysis and project analysis and integration. It includes a report on, and copies of visual presentations made at, the 22nd Project Integration Meeting held at Pasadena, California, on September 28 and 29, 1983.

## NOMENCLATURE

A	Ampere(s)
Å	Angstrom(s)
ac	Alternating current
AM	Air mass (e.g., AM1 = unit air mass)
AR	Antireflective
AR&D	Advanced research and development
ASEC	Applied Solar Energy Corp.
a-Si	Amorphous silicon
AS/ISES	American Section, ISES (q.v.)
ASME	American Society of Mechanical Engineers
ASTM	American Society for Testing and Materials
BA	Butyl acrylate
BOS	Balance of System (non-array elements of a PV system)
BSF	Back-surface field
BSR	Back-surface reflection
C	Celsius (temperature scale)
CER	Controlled-environment reactor
CPVC	Chlorinated polyvinyl chloride
c-Si	single-crystal silicon
CVD	Chemical vapor deposition
CVT	Chemical vapor transport
Cz	Czochralski (classical silicon crystal growth method)
dc	Direct current
DGS	Dichlorosilane
DI	De-ionized
DOE	U.S. Department of Energy

EBIC	Electron-beam-induced current
EFG	Edge-defined film-fed growth (silicon ribbon growth method)
EMA	Ethylene methyl acrylate
EPDM	Ethylene-propylene-diene monomer
EPRI	Electric Power Research Institute
EPSDU	Experimental process system development unit
ESP	Edge-supported pulling (silicon-sheet production process)
EVA	Ethylene vinyl acetate
FBR	Fluidized-bed reactor
FF	Fill factor
FSA	Flat-Plate Solar Array Project
FSR	Free-space reactor
GE	General Electric Co.
GFCI	Ground-fault circuit interruptor
h	heat transfer coefficient; hour(s)
HEM	Heat-exchange method (silicon-crystal ingot-growth method)
$I_{sc}$	Short-circuit current
I-V	Current-voltage
ID	Inside diameter
IEEE	Institute of Electrical and Electronics Engineers
IIT	Illinois Institute of Technology
IITRI	IIT Research Institute
IPEG	Improved Price Estimation Guidelines
IPEG2	IPEG, non-computerized
IPEG4	IPEG, computerized
IR	Infrared
ISES	International Solar Energy Society
ITO	Indium-tin oxide

$J_{sc}$	Short-circuit current density
JPL	Jet Propulsion Laboratory
k	equilibrium constant
LAPSS	Large-area pulsed solar simulator
LASS	Low-angle silicon sheet growth method
LPE	Liquid-phase epitaxy
MBE	Molecular-beam epitaxy
MEPSDU	Module experimental process system development unit
mgSi	Metallurgical-grade silicon
MIS	Metal-insulator-semiconductor (cell configuration)
mod	Module
MPFA	Module Performance and Failure Analysis Area (of FSA)
MSEC	Mobil Solar Energy Corp.
m-Si	Microcrystalline silicon
MT	Metric ton(s)
MW	Megawatt(s)
NASA	National Aeronautics and Space Administration
NEC	National Electrical Code
NMA	Non-mass-analyzed
NOC	Nominal operating conditions
NOCT	Nominal operating cell temperature
OFHC	Oxygen-free hard copper
O&M	Operating and maintenance
P	Power
$P_{max}$	Maximum power
PA&I	Project Analysis and Integration Area (of FSA)
P/TR	Problem-failure report

PC	Power conditioner
PCS	Power-conditioning system
PC/TS	Performance Criteria/Test Standards (SERI)
PDU	Process development unit
PE	Polyethylene
PEBA	Pulsed electron beam annealing
PIM	Project Integration Meeting
PMMA	Polymethyl methacrylate
PnBA	Poly-n-butyl acrylate
ppba	Parts per billion, atomic
ppma	Parts per million, atomic
ppmw	Parts per million, weight
PU	Polyurethane
PV	Photovoltaic(s)
PVB	Polyvinyl butyral
PVC	Polyvinyl chloride
PVD	Physical vapor deposition
R&D	Research and development
RCA	RCA Corp.
RES	Residential Experiment Station
RH	Relative humidity
RTV	Room-temperature vulcanized
S	Incident solar energy density
SAMIS	Standard Assembly-Line Manufacturing Industry Simulation
SCE	Southern California Edison Co.
SEM	Scanning electron microscope
SERI	Solar Energy Research Institute
SIMRAND	<u>S</u> IMulation of <u>R</u> esearch <u>A</u> ND <u>D</u> evelopment Projects

SIMS	Secondary ion mass spectroscopy
SMUD	Sacramento Municipal Utility District
SOA	State of the art
SOC	Standard operating conditions (module performance)
SOLMET	Solar radiation surface meteorological observations
STC	Silicon tetrachloride
STC	Standard test conditions
T	Temperature
TCM	Transparent conducting material
TCS	Trichlorosilane
TEM	Transmission electron microscope
TMY	Typical meteorological year
TREI	Texas Research and Engineering Institute
TTU	Texas Tech University
U	Superficial velocity
$U_{mf}$	Minimum fluidization velocity
UCC	Union Carbide Corp.
UCP	Ubiquitous crystallization process
UL	Underwriters Laboratories
UV	Ultraviolet
$V_{oc}$	Open-circuit voltage
$W_p$	Peak watt(s)
y	mol % silane
$\eta$	Greek letter eta: efficiency
$\sigma_{xx}$	Greek letter sigma: lateral stress
$\Omega$	Greek letter omega: resistance in ohms



# METRIC CONVERSION FACTORS

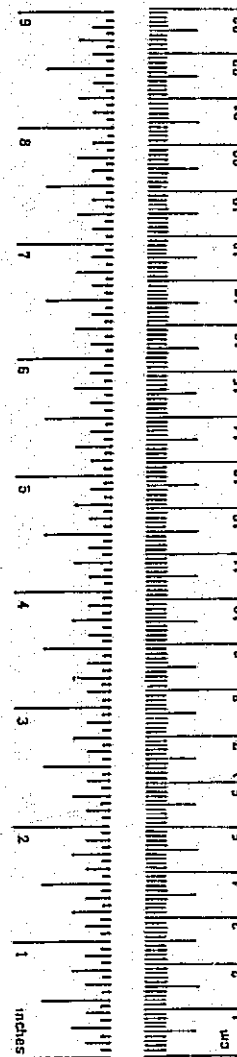
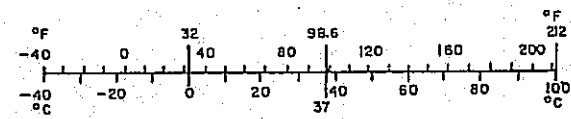
## Approximate Conversions to Metric Measures

Symbol	When You Know	Multiply by	To Find	Symbol
<b>LENGTH</b>				
in	inches	2.5	centimeters	cm
ft	feet	30	centimeters	cm
yd	yards	0.9	meters	m
mi	miles	1.6	kilometers	km
<b>AREA</b>				
in <sup>2</sup>	square inches	6.5	square centimeters	cm <sup>2</sup>
ft <sup>2</sup>	square feet	0.09	square meters	m <sup>2</sup>
yd <sup>2</sup>	square yards	0.8	square meters	m <sup>2</sup>
mi <sup>2</sup>	square miles	2.6	square kilometers	km <sup>2</sup>
	acres	0.4	hectares	ha
<b>MASS (weight)</b>				
oz	ounces	28	grams	g
lb	pounds	0.45	kilograms	kg
	short tons (2000 lb)	0.9	tonnes	t
<b>VOLUME</b>				
tsp	teaspoons	5	milliliters	ml
Tbsp	tablespoons	15	milliliters	ml
fl oz	fluid ounces	30	milliliters	ml
c	cups	0.24	liters	l
pt	pints	0.47	liters	l
qt	quarts	0.95	liters	l
gal	gallons	3.8	liters	l
ft <sup>3</sup>	cubic feet	0.03	cubic meters	m <sup>3</sup>
yd <sup>3</sup>	cubic yards	0.76	cubic meters	m <sup>3</sup>
<b>TEMPERATURE (exact)</b>				
°F	Fahrenheit temperature	5/9 (after subtracting 32)	Celsius temperature	°C

\* 1 in = 2.54 (exactly). For other exact conversions and more detailed tables, see NBS Misc. Publ. 286, Units of Weights and Measures, Price \$2.25, SD Catalog No. C13.1U 286.

## Approximate Conversions from Metric Measures

Symbol	When You Know	Multiply by	To Find	Symbol
<b>LENGTH</b>				
mm	millimeters	0.04	inches	in
cm	centimeters	0.4	inches	in
m	meters	3.3	feet	ft
m	meters	1.1	yards	yd
km	kilometers	0.6	miles	mi
<b>AREA</b>				
cm <sup>2</sup>	square centimeters	0.16	square inches	in <sup>2</sup>
m <sup>2</sup>	square meters	1.2	square yards	yd <sup>2</sup>
km <sup>2</sup>	square kilometers	0.4	square miles	mi <sup>2</sup>
ha	hectares (10,000 m <sup>2</sup> )	2.5	acres	
<b>MASS (weight)</b>				
g	grams	0.035	ounces	oz
kg	kilograms	2.2	pounds	lb
t	tonnes (1000 kg)	1.1	short tons	
<b>VOLUME</b>				
ml	milliliters	0.03	fluid ounces	fl oz
l	liters	2.1	pints	pt
l	liters	1.06	quarts	qt
l	liters	0.26	gallons	gal
m <sup>3</sup>	cubic meters	35	cubic feet	ft <sup>3</sup>
m <sup>3</sup>	cubic meters	1.3	cubic yards	yd <sup>3</sup>
<b>TEMPERATURE (exact)</b>				
°C	Celsius temperature	9/5 (then add 32)	Fahrenheit temperature	°F



## CONTENTS

### PROGRESS REPORT

PROJECT SUMMARY . . . . .	1
AREA REPORTS . . . . .	5
PHOTOVOLTAIC COMPONENTS RESEARCH AREA . . . . .	5
Advanced Materials Research Task . . . . .	5
Devices and Measurements Research Task . . . . .	19
Environmental Isolation Task . . . . .	23
Process Research Task . . . . .	29
PROJECT ANALYSIS AND INTEGRATION AREA . . . . .	33
ENGINEERING SCIENCES AREA . . . . .	35
MODULE PERFORMANCE AND FAILURE ANALYSIS AREA . . . . .	41

#### Table

1. Results of Environmental Tests . . . . .	44
---	----

# PROJECT INTEGRATION MEETING

## PROCEEDINGS

INTRODUCTION. . . . .	53
PLENARY SESSIONS. . . . .	55
Flat-Plate Module Requirements to Meet Program Goals (R.W. Aster, Jet Propulsion Laboratory) . . . . .	61
Silicon Sheet: Problems and Refocused Thrust (A.D. Morrison, Jet Propulsion Laboratory). . . . .	67
High-Speed Growth and Characterization of Crystals for Solar Cells Research Forum: Summary (Katherine A. Dumas, Jet Propulsion Laboratory). . . . .	81
Quantitative Process Control (M.H. Leipold, Jet Propulsion Laboratory) . . . . .	91
Metallization Research Forum: Summary (B.D. Gallagher, Jet Propulsion Laboratory). . . . .	95
Technical Challenges of Future Modules and Arrays (R.G. Ross, Jr., Jet Propulsion Laboratory) . . . . .	99
PV Module Standards (J.C. Arnett, ARCO Solar, Inc.) . . . . .	107
TECHNOLOGY SESSIONS . . . . .	111
SILICON SHEET GROWTH AND CHARACTERIZATION (A.H. Kachare, Chairman). . . . .	111
Advanced Dendritic Web Growth Development (Westinghouse Electric Corp.) . . . . .	113
Edge-Defined Film-Fed Growth (Mobil Solar Energy Corp.) . . . . .	121
Solid-Liquid Interface Studies (T.F. Ciszek, Solar Energy Research Institute) . . . . .	131
Ribbon Heat and Mass Transfer (H.M. Ettouney and R.A. Brown, Massachusetts Institute of Technology). . . . .	143
Ribbon Stress/Strain Analysis (University of Kentucky). . . . .	155
Ubiquitous Crystallization Process (William F. Regnault and Scott M. Johnson, Semix Inc.) . . . . .	169
Contactless Measurement of Free-Carrier Lifetime in Polycrystalline Si Ingots (S.M. Johnson, Solarex Corp.; L. Johnson, University of Pennsylvania) . . . . .	175

Refinement by Silane (Union Carbide Corp.) . . . . .	365
JPL In-House Fluidized-Bed Reactor Research (George Hsu, Jet Propulsion Laboratory) . . . . .	371
Electrochemical Production of Silicon (Energy Materials Corp.) . . .	381
Enhanced Silicon Purification in a Chemical Vapor Transport System (R. Powell and J.M. Olson, Solar Energy Research Institute). . . . .	385
Probabilistic Analysis of Silicon Cost (L. Reiter, Jet Propulsion Laboratory). . . . .	391
Device Structure and Analysis (G.T. Sah, G.T. Sah Associates) . . . . .	397
Solar Cell Efficiency Estimation Methodology and Analysis (Anant R. Mokashi, Jet Propulsion Laboratory) . . . . .	409
<b>CELL PROCESSING AND HIGH-EFFICIENCY CELLS</b>	
(D.B. Bickler, Chairman) . . . . .	415
Laser-Assisted Solar-Cell Metallization Processing (S. Dutta, Westinghouse Electric Corp.) . . . . .	417
Process Research on Polycrystalline Silicon Material (PROPSM) (Jerry Culik, Solarex Corp.) . . . . .	422
A Nonnoble Front Metallization Process (Alexander Garcia III, Spectrolab, Inc.; Brian Gallagher, Jet Propulsion Laboratory) . . .	437
Process Research of Non-Cz Silicon Material (G.M. Rose and R.B. Campbell, Westinghouse Electric Corp.) . . . . .	455
Thin-Film Diffusion Barriers (M.A. Nicolet, California Institute of Technology) . . . . .	461
Metallization Cost Comparison (R.W. Aster, Jet Propulsion Laboratory) . . . . .	467
Evaluation of the Ion Implantation Process for Production of Solar Cells From Silicon Sheet Materials (M.B. Spitzer, Spire Corp.) . . . . .	473
Cluster Ion Beam Deposition (D.J. Fitzgerald, Jet Propulsion Laboratory) . . . . .	487
Molecular-Beam Epitaxial Growth of Silicon Solar Cells (F.G. Allen, University of California, Los Angeles) . . . . .	491
Microcrystalline Solar Cells (Applied Solar Energy Corp.) . . . . .	495

Silicon Sheet Characterization (D. Ast, Cornell University) . . . .	179
Quantitative Analysis of Defects in Silicon Sheet (Materials Research, Inc.) . . . . .	191
Silicon-Sheet Cell Performance (Applied Solar Energy Corp.) . . . .	225
Silicon-Sheet Surface Studies (University of Illinois at Chicago). . . . .	233

#### MODULE TECHNOLOGY

(R.G. Ross, Jr., Chairman). . . . .	253
Long-Term Module Testing at Wyle Laboratories (D.H. Otth, Jet Propulsion Laboratory). . . . .	255
Solar-Cell Reliability Research (J.W. Lathrop, Clemson University) . . . . .	265
Solar-Cell Electrochemical Corrosion (G.R. Mon, Jet Propulsion Laboratory). . . . .	277
Transparent Conducting Materials Overview (D.R. Coulter, Jet Propulsion Laboratory). . . . .	297
TCM Technologies and Performance (Gary Wnek, Massachusetts Institute of Technology). . . . .	301
Organic Conducting Polymers: Interactive Modeling (G.F.J. Garlick, Consultant to Jet Propulsion Laboratory) . . . . .	307
Experimental Evaluation of TCMs (Alexander Garcia III, Spectrolab, Inc.) . . . . .	313
Encapsulation Design Analysis (Alexander Garcia III, Spectrolab, Inc.) . . . . .	317
Electrical Insulation Stability (Edward F. Cuddihy, Jet Propulsion Laboratory). . . . .	327
Theoretical and Experimental Encapsulant Stability (R. Liang, Jet Propulsion Laboratory) . . . . .	335
Polymer-Metal Interface Bond Stability (F.J. Boerio, University of Cincinnati) . . . . .	349

#### SILICON MATERIAL

(R. Lutwack, Chairman). . . . .	355
Dichlorosilane Research Process (Hemlock Semiconductor Corp.) . . .	357

High-Efficiency Cell Concept (M. Wolf, University of Pennsylvania) . . . . . 501

Crystalline Silicon Solar Cell Task: Status of High-Efficiency Programs (Joseph B. Milstein, Solar Energy Research Institute). . . 511

Status: Nonnoble Metal Systems (J. Parker, Electrink, Inc.). . . . 521

#### MODULE TECHNOLOGY

(L.D. Runkle, Chairman) . . . . . 523

Block V Test Results (John S. Griffith, Jet Propulsion Laboratory) . . . . . 525

Foreign Module Performance (L.D. Runkle, Jet Propulsion Laboratory) . . . . . 537

Module Durability: Five Years' Field Experience (R.W. Weaver, Jet Propulsion Laboratory). . . . . 545

Encapsulation Materials and Processing (Springborn Laboratories, Inc.) . . . . . 554

Hermetic Edge Sealing of Photovoltaic Modules (M.J. Nowlan, Spire Corp.). . . . . 589

SMUD Hot-Spot Test Results (C.C. Gonzalez, Jet Propulsion Laboratory) . . . . . 599

Bypass Diode Design Tradeoffs (N.F. Shepard, Jr., General Electric Co.) . . . . . 613

Bypass Diode Qualification Test Development (D.H. Otth, Jet Propulsion Laboratory). . . . . 623

Thermal Investigation of Residential Photovoltaic Arrays (L. Wen, Jet Propulsion Laboratory) . . . . . 631

Annual Energy Prediction Based on NOCT (C.C. Gonzalez, Jet Propulsion Laboratory). . . . . 643

# PROGRESS REPORT

## Project Summary

### INTRODUCTION

This report describes the activities of the Flat-Plate Solar Array Project (FSA) from February 1983 through September 1983, including the 22nd FSA Project Integration Meeting (PIM), held on September 28 and 29, 1983.

FSA, sponsored by the U.S. Department of Energy (DOE), has the responsibility for advancing solar array technology while encouraging industry to reduce the price of arrays to a level at which photovoltaic (PV) electric power systems will be competitive with more conventional power sources. This responsibility has included developing the technology for producing low-cost, long-life photovoltaic modules and arrays. More than 100 organizations have participated in FSA-sponsored research and development of low-cost solar module manufacturing and mass-production technology, the transfer of this technology to industry for commercialization, and the development and testing of advanced prototype modules and arrays. Economic analyses were used to select for sponsorship those research and development efforts most likely to result in significant cost reductions. An account of the progress that has been made during the reporting period is set forth here.

### SUMMARY OF PROGRESS

Large quantities of silane continue to be produced in the Union Carbide Corp. (UCC) experimental process system development unit (EPSDU) at Washougal, Washington, where operation continues under UCC funding. The silane EPSDU equipment title had previously been transferred to UCC in exchange for EPSDU operational data.

Quality of the silane is good, the resistivity being greater than 200  $\Omega$ -cm for silicon produced by epitaxial deposition. The carbon, oxygen, boron and phosphorus contents are low. The reasons for the higher-than-expected hydrogen content are being investigated. Pyrolysis of silane in a fluidized-bed reactor (FBR) that is now part of the EPSDU has been conducted for up to a 21 hours using 20 mol % silane in hydrogen.

In the 6-in.-dia research FBR at JPL, a test using 50% silane was successfully performed as part of the studies aimed at the characterization of the silicon-deposition process using high concentrations of silane.

An FBR study on a technique of heating the bed particles while maintaining cooler reactor walls was completed by Oregon State University.

## PROJECT SUMMARY

A technique for controlled nucleation of silicon particles for use as seed particles in direct pyrolysis of silane to silicon in a free-space reactor was demonstrated by a California Institute of Technology study. The research will be continued using a larger reactor.

The research by Hemlock Semiconductor Corp. on an advanced cold-metal-wall deposition reactor for converting dichlorosilane to silicon was completed. The attempt to eliminate excessive silicon deposition on the reactor walls was partially successful.

A study to define process parameters for hydrochlorination reaction was successfully completed by Solarelectronics, Inc.

Two advanced silicon purification studies, a electrochemical technique and a chemical vapor transport process, both initiated by J. Olson of SERI, have been initiated under FSA funding.

The silicon-sheet effort now has been focused on resolving the generic impediments to improved silicon-ribbon growth rates and quality. The relationships of crystallization rates, thermal stresses, and the mechanical and fracture properties of wide, thin silicon ribbons are being studied. An integrated multiple university, industry, and government-laboratory effort is applying advanced analytical and experimental techniques to this problem. The knowledge gained from those efforts will be applied to all ribbon investigations.

Work by Mobil Solar Energy Corp. on developing a model for obtaining temperature distribution--residual stress relationships in silicon ribbons grown at high speed is proceeding satisfactorily. Supplementary data from three universities together with the MSEC results will permit analytical models to be compared to experimental results.

Predicted ribbon results from computer models of dendritic-web ribbon grower thermal-element configurations were verified by a number of experimental runs at Westinghouse Electric Corp. The ability to adjust the grower thermal elements during growth enabled good ribbon to be grown at substantially faster rates.

Studies to determine the effect of defect structures in cast ingots and to investigate control of the crystallization front and its role in defect structure are being performed by Semix Inc. Two sources of subgrain structures, both showing deleterious effects on the performance of a solar cell, have been identified.

The strength of a good Czochralski-grown silicon wafer is greater when it is illuminated than when it is in the dark, but the strength of an indentation-damaged wafer is less in light than in the dark and the strength decreases with increasing size of the indentation, studies performed at JPL have shown.

Analytical methodology for designing encapsulation systems and determining their design sensitivities was devised by Spectrolab, Inc. Final reports were written in thermal, electrical, structural, and optical modeling.



## PROJECT SUMMARY

The most effective ultraviolet absorber for use in polymeric pottants, as determined in a study by the Polytechnical Institute of New York, are benzotriazoles.

Amorphous-metal diffusion-barrier studies at the California Institute of Technology have resulted in the characterization of an iron-tungsten film that is very stable. This has application in avoiding one of the problems with base-metal metallization systems.

A hermetic module edge-sealing process using an electrostatically bonded aluminum ribbon and an ultrasonically bonded foil back sheet was demonstrated by Spire Corp.

Two reports for use by residential PV system designers, "Fundamentals of Residential Photovoltaics" and "Residential PV Array Design," were submitted to Sandia National Laboratories as part of their residential PV documentation activities. The reports describe practical aspects of installation and safety issues.

An annual report, "Photovoltaic Module Bypass Diode Encapsulation," by General Electric Co., focused on design synthesis including electrical load sharing, cost comparisons, and reliability.

Module and solar-cell temperature and humidity endurance efforts continue with the completion of 365 days of testing modules in 85°C and 100°C chambers and the publishing of the fourth annual report on cell reliability.

Ten Block V, Group I modules have been received from each of four manufacturers and their Block V qualification testing is mostly completed. After satisfactory completion of the environmental testing of the Group I modules and resolution of their weaknesses, Group II module design reviews have been held with two manufacturers.

A procedure for secondary calibration of reference cells using the AM1.5 LAPSS and sun-calibrated reference cells was established.

The portable I-V data loggers were used in support of both FSA and non-FSA activities.

Workmanship in the assembly of modules still appears to be the major source of deficiencies that affect module durability and performance.

Now that a goal for the National Photovoltaics Program has been established, specific goals for each technical component that are of comparable technical feasibility are expected to be allotted. An analysis was performed comparing various balance-of-system efficiencies and costs versus module efficiencies and costs.

A study of polysilicon refinement costs versus processing sensitivities has been updated. A technically feasible price of \$20/kg (1982 dollars) or less is 90% probable in the long term.

An analysis of value-added cost and performance effectiveness of several state-of-the-art and advanced metallization techniques was performed.

# Area Reports

## PHOTOVOLTAIC COMPONENTS RESEARCH AREA

### Advanced Materials Research Task

#### INTRODUCTION

The objective of the Advanced Materials Research Task is to identify the critical technical barriers to low-cost silicon (Si) purification and sheet growth that must be overcome to produce a photovoltaic (PV) cell substrate material at a price consistent with Flat-Plate Solar Array Project (FSA) objectives and then to perform and support research and development to overcome those barriers.

Present solar-cell technology is based mainly on the use of Si wafers obtained by ID slicing of Czochralski (Cz)-grown ingots from Siemens-reactor-produced semiconductor-grade Si. This method of obtaining single-crystal Si wafers is tailored to the needs of semiconductor device production (e.g., integrated circuits and discrete power and control devices other than solar cells). The small market offered by present solar-cell users does not justify industry's development of the high-volume Si production techniques that would result in low-cost photovoltaic electrical energy.

It is important to develop alternative low-cost processes for producing refined Si and sheet material suitable for long-life, high-efficiency solar photovoltaic energy conversion. To meet FSA objectives, research must be performed to overcome the generic barriers to the success of the most promising processes for producing large quantities of pure Si and large areas of crystallized Si at a low, competitive cost. The form of the refined Si must be suitable for use in the sheet-growth processes, and these must in turn be suitable for direct incorporation into automated solar-array industry schemes.

Si purification processes involving deposition of the material from silane and dichlorosilane (DCS) are being pursued because these two substances can be purified relatively easily and, because of their high reactivity, they can be more readily decomposed or reduced to form Si than can trichlorosilane (TCS), which is used today in the conventional process. Research on two other processes that offer promise for making less-pure, solar-cell-grade Si by refinement of metallurgical-grade Si (mgSi) was recently undertaken because of the potential for further reduction of product cost.

FSA-funded improvements of the standard Cz ingot-growth process by reduction of expendable-material costs and improvement of ingot growth rate, together with improved slicing techniques, have developed the technology so that large areas of Si can be produced. Growth of large ingots by casting techniques, such as the semicrystalline casting process, may reduce sheet costs further.

Growth of crystalline Si material in a geometry that does not require cutting to achieve proper thickness is an obvious way to eliminate costly processing and material waste. Growth techniques such as edge-supported

## ADVANCED MATERIALS RESEARCH TASK

pulling (ESP), edge-defined film-fed growth (EFG), low-angle Si sheet (LASS) and dendritic-web growth are candidates for such solar-cell material.

In addition to research on processes for Si refinement and sheet formation, various supporting studies are under way to investigate key problems in both of these categories.

## SUMMARY OF PROGRESS

### Semiconductor-Grade Silicon Refinement Processes

#### Silicon Refinement Using Silane (Union Carbide Corp.)

Union Carbide Corp. (UCC) is conducting research on the pyrolysis of silane in a fluidized-bed reactor (FBR), a critical step in the process sequence of  $\text{mgSi}$  to silane to semiconductor-grade Si. Silane synthesis is under active investigation in UCC's own pilot plant at Washougal, Washington.

Installation of the FBR process development unit (PDU), which had been moved to the Washougal facility from its previous location in Tonawanda, New York, was completed. The unit was checked out, and bed heating and fluidization tests were conducted under hydrogen atmosphere. The 6-in.-dia FBR employed a dual-cone distributor, which had been adopted to obtain an expected improvement in fluidization over that provided by the single-cone distributor used in tests at Tonawanda. When the FBR was tested, however, bed agglomeration occurred, indicating improper fluidization. To avoid this problem, the dual-cone distributor was replaced by one with a single-cone design.

Using feeds of about 20 mol % silane in hydrogen, but ranging as high as 23%, tests of 20-h and 21-h duration were made. These are the longest tests made to date with this size FBR in the FSA-supported program. The reactor produced about 1 kg Si/h, and a very small amount of fines was obtained. Studies have shown that if silane feed concentrations of greater than 20 mol % silane can be used with total conversion to Si within the bed, the process is economically attractive.

The pressure drop across the distributor was unusually high during the entire 20-h test; it is believed that partial plugging had occurred during earlier short-duration tests. After this long test, the distributor cone was replaced with a new one. The following 21-h test was smooth throughout, and no distributor plugging occurred. However, the product withdrawal valve ruptured when it was operated, and the test was terminated at that point. Work is continuing to improve the system for long-duration operation.

Si samples were collected for preliminary purity investigation by neutron activation analysis.

#### Silicon Refinement Using Dichlorosilane (Hemlock Semiconductor Corp.)

Hemlock is investigating the critical portions of a process for making semiconductor-grade Si, in which DCS is made from TCS by a redistribution reaction using an organic amino functional catalyst, and the DCS is then reduced by hydrogen to produce Si in a chemical-vapor-deposition step using Siemens-type reactors.

## ADVANCED MATERIALS RESEARCH TASK

The program for research on an advanced cold-metal-wall Si deposition reactor was completed. The objective was to eliminate the excessive Si deposition on the inside surfaces of the reactor bell jar and thereby to allow operation at optimum efficiencies, so as to increase DCS-to-Si conversion efficiency, increase Si deposition rates, and decrease reactor energy consumption. This advanced reactor, of intermediate size, had an inside wall temperature of only about 300°C as compared with the wall temperatures of 500°C to 800°C in the quartz bell jars of conventional Siemens-type reactors.

The cooler wall temperatures permitted use of higher DCS feed rates. In one test a high Si deposition rate, 2.28 g/h-cm of deposition rod length (compared with the goal of 2 g/h-cm), was attained at an average power consumption of 59 kWh/kg, the lowest value obtained in the entire DCS program and slightly below the program goal of 60 kWh/kg. The conversion efficiency of DCS to Si was low, however, only 17% versus the goal of 40%, and a moderate amount of Si wall deposit was obtained, amounting to 2% of the amount deposited on the rods. In one series of tests, it was observed that more wall deposition occurred at low rod temperatures than at high rod temperatures, for reasons not yet understood. In general, however, the data on wall deposition scattered so badly that it was not possible to correlate this parameter with reactor operating parameters.

Screening of various materials of construction was conducted. Stainless steels (types 304 and 316), Hastalloy B, Monel 400, and carbon steel were placed individually in a small-scale reactor and Si was deposited using TCS feedstock. The Si was analyzed and found to contain no significant amounts of electrically active or metallic impurities; however, the carbon content was high, typically in the range of 1 to 10 ppma. It was concluded that low-carbon alloys should be considered as materials of construction for metal-walled reactors and that further testing would be required before a final choice could be made.

The results of the cold-wall reactor program indicate that with optimization of reactor operating conditions, the goals for Si deposition rate, conversion of DCS to Si, and power are attainable, particularly for large-size reactors.

The DCS PDU, the output of which had been tripled to about 200 lb DCS/h, continued to operate well during this period; no problems were encountered. The output was used to feed the cold-wall reactor as well as conventional Siemens-type reactors.

Final reports on the Phase I--Phase II effort and on the cold-wall reactor program are being prepared.

## Solar-Cell-Grade Silicon Refinement Processes

### Electrochemical Refining of Metallurgical Grade-Silicon (Energy Materials Corp.)

This program, which started in June 1983, is for study of an electrochemical process for purifying mgSi. It is based on the electrolysis of a

## ADVANCED MATERIALS RESEARCH TASK

system comprising a molten salt electrolyte, a carbon cathode, and an anode devised by J. Olson of SERI. The anode is formed from  $\text{Cu}_3\text{Si}$  and  $\text{mgSi}$ ; the purification has been postulated to depend on very large differences in the diffusion rates of Si and the metallic impurities in  $\text{Cu}_3\text{Si}$ . The primary objectives of this program are to establish the conditions for long-term, steady-state operation of an electrolysis cell sized to produce up to 5 g/h of Si and to evaluate the suitability of this process for large-scale production ( $\geq 1000 \text{ Mt/yr}$ ).

The program contains tasks for a theoretical analysis of the effect of Si depletion on anode morphology; a theoretical analysis and modeling of impurity behavior in the anode; an experimental determination of long-term, steady-state operation near the design limit; experimental determination of impurity distributions and anode changes as functions of current density and time, and an analysis of the production potential and economics for a large-scale plant.

Design of the electrolysis cell was completed, and design of the electrodes and fabrication of the cell are under way. The chamber containing the cell assembly was coated with Teflon to provide a corrosion-resistant surface.

### Chemical Vapor Transport Process for Purifying Metallurgical-Grade Silicon (Solar Energy Research Institute)

A study of a chemical vapor transport (CVT) process for purifying  $\text{mgSi}$ , started mid-September 1983, is under way at SERI under the direction of J. Olson. In this process, chlorosilanes (predominantly TCS) are produced by the reaction of  $\text{HCl}$  at the surface of a material prepared from  $\text{Cu}_3\text{Si}$  and  $\text{mgSi}$ ; the temperature is about  $700^\circ\text{C}$ . The TCS and other reaction products are transported to the surface, maintained at about  $900^\circ\text{C}$ , where Si deposition occurs. The purification depends upon not transporting and depositing impurities present in the  $\text{mgSi}$ .

The program contains tasks to determine the effects of the experimental variables of  $\text{H/Cl}$  ratio, temperatures, gas pressure, and reactor geometry on deposition rate and deposit characteristics; the energy use, and the reaction system behavior as a function of time.

## Silicon Refinement Process Supporting Studies

### Hydrochlorination Reaction Investigation (Solarelectronics, Inc.)

A research and development program was carried out to study the hydrochlorination of silicon tetrachloride (STC) and  $\text{mgSi}$  to TCS in a 2-in.-dia reactor. The objective of this program was to obtain experimental data to define process parameters for the hydrochlorination reaction. The contract was completed in April, 1983.

During the period from January to April, 1983, a quartz hydrochlorination reactor was built to study equilibrium formation of TCS at temperatures higher than  $500^\circ\text{C}$  and to study reaction mechanisms using the deuterium isotope.

## ADVANCED MATERIALS RESEARCH TASK

A series of experiments was conducted at atmospheric pressure and over a range of temperatures to investigate the influence of temperature on the equilibrium formation of TCS. The equilibrium constant values were determined to be  $1.17 \times 10^{-3}$ ,  $1.67 \times 10^{-3}$ ,  $2.24 \times 10^{-3}$ ,  $2.50 \times 10^{-3}$ , and  $2.65 \times 10^{-3}$  at temperatures of 500°, 550°, 600°, 650°, and 700°C, respectively. The Van't Hoff plot ( $\ln k$  vs  $1/T$ ) is linear up to 550°C. These results indicate that at 600°C and above, the thermal decomposition of TCS is taking place in parallel with the hydrochlorination reaction.

The hydrochlorination reaction mechanism was investigated based on the postulation that hydrogenation of the Si-Cl bond to form TCS and HCl is a rate-determining step. By replacing hydrogen with deuterium in the hydrochlorination reaction, a higher rate of reaction may be obtained, providing useful information on the mechanism of the reaction pathway. Two experiments at temperatures of 420° and 450°C and at atmospheric pressure were conducted using the deuterium isotope. Neither experiment showed any significant increase, caused by the use of the deuterium isotope, in the rate of reaction. These experimental results imply that hydrogenation of an Si-Cl bond is not a rate-determining step. A plausible mechanism may involve absorption of STC on the Si surface followed by the formation of reactive intermediates, such as the free radicals trichlorosilyl ( $\cdot\text{SiCl}_3$ ) and dichlorosilene ( $:\text{SiCl}_2$ ), as a rate-determining step. The rapid hydrogenation of these free radicals may form TCS and DCS.

The final report on this program was issued. The major technical results of the effort are summarized as follows: (1) the equilibrium constant for the reaction wherein mgSi and STC are converted to TCS increases with increase in temperature from 350° to 750°C; (2) the heat of reaction,  $\Delta H$ , was calculated to be 10.4 kcal/mol; (3) the reaction follows pseudo-first-order kinetics with an activation energy,  $\Delta E$ , of 13.2 kcal/mol; (4) the kinetic effect of the deuterium isotope on the reaction indicates that hydrogen is not directly involved in the rate-determining step; (5) a reaction mechanism was proposed involving adsorption of STC on the surface of Si particles to form an activated species, such as  $\text{SiCl}_2$ , as a rate-determining step; and (6) results of the corrosion study showed that type 304 stainless steel, Incoloy 800H, and Hastelloy B-2 are suitable materials of construction for the hydrochlorination reactor. The formation of silicide film on the surface of these alloys prevents corrosive attack of hydrochloric acid up to temperatures of 500°C.

### Fluidized-Bed Reactor Research (Oregon State University)

The study of radiantly heated fluidized-bed reactors for Si production from silane was completed by Oregon State University, and the final report was issued. This heating technique has the potential of heating the bed particles while maintaining cooler reactor walls. In this way silane reaction and Si condensation on the walls can be prevented. The study centered on the important characteristics of the effective absorptivity of heat by the bed from the electric heater source and of the heat-transfer coefficient between the hot bed and the cool distributor plate. The measurements were made in silane-free, non-reacting systems.

## ADVANCED MATERIALS RESEARCH TASK

The effects of the electric heater source power, the bed depth, the reactor geometry, and gas velocity on the prime characteristics were determined. The findings are summarized as follows: (1) the effective heat absorptivity and heat transfer coefficient are independent of the source power; (2) the bed depth affects the absorptivity but not the transfer coefficient; (3) the absorptivity increases strongly with gas velocity and inversely with distance between the source and the bed as well as being greater for tapered beds in comparison to non-tapered beds; and (4) the transfer coefficient,  $h$ , increases slowly and continuously in round beds, increases sharply and continuously in square beds, and first decreases and then increases slowly in tapered beds, so that for  $U/U_{mf}$  (ratio of superficial velocity to minimum fluidization velocity) greater than four,  $h_{round} > h_{round-tapered} > h_{square-tapered} > h_{square}$ . Using the assumptions that in a silane reactor the bed temperature is to be about 700°C and the distributor plate about 350°C, calculations based on the experimental values derived in this study showed that the desired distributor temperature cannot be maintained with a square or round bed. The alternatives are a tapered bed, a conical bed with no distributor, or a multiorifice or multicone bed.

Further calculations directed toward the consideration of a design of a scaled-up silane bed showed that: (1) the distance from the heat source to the bed should be minimized; (2) energy utilization efficiency increases with size; (3) the common vertical-sided bed resting on a distributor plate is not usable; (4) the multicone or multiorifice design is advantageous for large beds; and (5) the energy use is about 40/y kWh/kg Si (where y = mol % silane).

The need for further studies of the effects of particle size distribution, steady-state characteristics, seed addition and product removal, effects of reactor geometry and materials of construction, and the influence of the radiation source was cited.

### Silicon Particle Growth Research (California Institute of Technology)

Research focused on the problem of growing supermicrometer Si particles by direct pyrolysis of silane gas in an entrained flow system. A theoretical analysis of particle growth in the previous free-space reactor studies revealed that coagulation was too slow to grow very small particles to acceptable sizes within reasonable residence times. The larger particles can be produced by direct vapor deposition provided that the total number concentration of particles can be kept sufficiently small. This in turn requires that homogeneous nucleation of new particles be stopped once the required number of seed particles is generated. The theory of nucleation inhibition by growing aerosol particles was examined to identify aerosol reactor operating conditions.

A small, two-stage aerosol reactor was designed based on these theoretical predictions. The first stage was operated much like the previous free-space reactors to generate seed particles of Si by homogeneous nucleation. The seed aerosol was then diluted with a gas containing additional silane, thereby reducing the seed number concentration and providing the silane necessary for particle growth. After the seed aerosol and primary gases were

well mixed, they were heated to promote silane decomposition. The temperature in the second reaction stage was, however, maintained at a much lower level than in the seed generator. In this way the concentrations of condensable vapors can be kept low enough by diffusion to the seed particles that additional nucleation can be prevented.

The aerosol reactor was operated with primary reactant gases consisting of 1% to 2% silane in nitrogen. Seed particles smaller than  $0.5\ \mu\text{m}$  in diameter were grown to  $6.2\ \mu\text{m}$  mass median diameter with 1% silane and to  $9.0\ \mu\text{m}$  with 2% silane. The recovery of Si in these experiments was approximately 70% of the input silane. Particle deposition on the walls of the reactor and sampling system accounted for much of these losses. The small size of the prototype reactor aggravated these losses.

A larger reactor will be used for the continuation of this research. The more favorable volume-to-surface ratio should reduce the losses by wall deposition and should provide conditions for better growth. The objectives will be to characterize the system fully and to provide particles sufficiently large for use as seed particles for a silane fluidized-bed reactor or for use as Si for direct processing into ingots or ribbon materials.

### Research on Silane Pyrolysis in Fluidized-Bed Reactors (JPL)

JPL is conducting FBR research with the objective of characterizing the deposition of Si from silane and providing bases for significant improvements in this process. The 6-in. FBR was provided with a 1-in.-dia product-withdrawal tube. A high rate of product withdrawal, 3 kg/h, was demonstrated, enabling a steady inventory of Si in the bed. A long-duration experiment at 30% silane and  $700^\circ\text{C}$  for 8 h was successfully achieved with a continuous withdrawal rate of 1.5 kg/h.

A test of various FBR materials of construction was performed. Coupons of type 304 stainless steel, Incoloy 800H, Hastelloy G, and quartz were exposed to 20 mol % silane in hydrogen for five hours at  $650^\circ$  to  $700^\circ\text{C}$ . Analyses are in progress.

An FBR test at high silane concentration was successfully conducted at  $630^\circ\text{C}$  and 50% silane for a duration of 5 h. A total of 14 kg of Si was produced. A 4-in.-dia Cz ingot was pulled from the unetched FBR particles. The resulting ingot was partly polycrystalline, indicating that the material may have been contaminated. Solar cells,  $2 \times 2\ \text{cm}$ , were made from single-crystal regions of the top, middle, and bottom portions of the ingot. These cells are the first to be made from FBR material produced from silane. The cell efficiency averages for these three regions ranged from 12.1% to 12.5%, compared with control cells of 13.9% efficiency from a commercial source. These control cells were not fabricated from ingot material grown in the puller that was used to grow the ingot from FBR product. Therefore, the difference in performance of the cells does not necessarily indicate the purity of the FBR product. Although it appears that the Si was contaminated in the course of ingot pulling, the results of these experiments constitute a significant achievement in demonstrating the practicability of using FBR material in solar-cell fabrication.



Experiments to investigate the effect of multiple injection of silane for purposes of scavenging fine Si particles were carried out in the 2-in.-dia FBR. A feed of 65 mol % silane in hydrogen was introduced at the bottom of the bed, and a smaller volumetric flow rate of 20 mol % silane (amounting to only 1/30 of the amount of silane introduced from the distributor) was fed in at a point 6 in. above the distributor. The relatively small amount of silane being introduced under conditions that would favor chemical vapor deposition of Si, rather than homogeneous decomposition that would produce fines, was expected to cause scavenging of fines produced by the main flow. These preliminary experiments indicated that not only was the amount of fines reduced from 4% to 2%, but also the color of the bed particles was gray rather than dark brown, reflecting an increase in the size of the fines before they were scavenged by the bed particles.

Experiments were conducted to investigate the feasibility of fluid jet milling to prepare clean FBR seed. The results indicated that about 60% of 700- $\mu$ m-dia particles can be fractured to give material smaller than 500  $\mu$ m.

## Shaped-Sheet Technology

### Edge-Defined Film-Fed Growth (Mobil Solar Energy Corp.)

The primary goal of this program is to develop a model for obtaining temperature field--residual stress relationships applicable to Si ribbon grown at high speeds and subsequently to apply this model to a growth system that has been modified and improved to produce low-stress ribbons at high speeds.

During this report period, theoretical modeling work centered on the prediction of residual stress in Si sheet. The relevant ribbon temperature-field data, boundary conditions, and Si material characteristics at high temperatures are needed for input into the computer model. These will then be iterated to obtain an optimum growth configuration that can be translated to actual experimental parameters for confirmation.

The work performed can be summarized as follows: the computer model for residual stress calculation developed at Harvard University is operational and has been tested with two ribbon-temperature profiles. One was obtained experimentally from strategically placed thermocouples in the growth cartridge and the other obtained from theoretical approximations of an ideal stress-reducing thermal profile. The results agree qualitatively with the observed physical characteristics of actual ribbons produced under similar conditions. The material constants and boundary conditions, however, were not known, and the values used for this calculation were first-order approximations only. Actual boundary conditions, (i.e., the lateral stress,  $\sigma_{yy}$ , not equal to 0 at the growth interface) and material constants will be required to allow production of quantitatively meaningful results.

The fiber-optic temperature probe was constructed. This instrument will allow high-resolution, high-temperature measurements of the Si ribbon surface during growth. The fiber material consists of a combination of sapphire at the high-temperature region and quartz for transmission of signals to the detection circuitry. Calibration of the instrument is in progress. Problems have been encountered with excessive noise from emanation of stray radiation from the die top and surrounding hot region.

## ADVANCED MATERIALS RESEARCH TASK

A four-point high-temperature bending jig has been constructed for measurement of Si material constants at high temperatures. Experiments were conducted at 1000°, 1200°, and 1350°C with single-crystal Cz Si, polycrystalline Silso Si wafers, and EFG ribbon Si samples. Sample displacement versus time curves were obtained for various bending forces. These curves are being analyzed to obtain creep constants for the three forms of Si sheet. Examination of the cross sections of the Si material reveals dislocation generation that appears to be related to the amount of stress applied and temperature. The dislocation densities observed in single-crystal Si samples show substantial amounts at temperatures higher than 1000°C with the densities saturating at  $5 \times 10^5 \text{ cm}^{-2}$  in the highly stressed regions. Some dislocation movement and agglomeration were observed in the higher-temperature case (1350°C). Additional experiments will be performed to determine the influence of crystal orientation and grain boundaries upon dislocation formation and movement under high-temperature stress.

Initial modeling efforts on determination of the isotherm configurations in the melt region at the die top near the solid-liquid interface were begun at the Massachusetts Institute of Technology. This will provide insights into the behaviour of the solid-liquid interface shape and hence control of growth behavior with different thermal conditions and die configurations.

Residual stress measurements were made on stressed polycrystalline and single-crystal Si samples with the laser interferometric measurement system at the University of Illinois at Chicago. The experimentally obtained residual stress data agree with those calculated to within 10%. The apparatus is being modified to accept EFG ribbons for measurement and to obtain meaningful data from nonuniform surfaces.

Planned activities for the next reporting period will include a culmination of the above activities in the acquisition of relevant Si material parameters, accurate in-situ Si ribbon temperature measurements, dislocation formation and stress data, and nondestructively obtained residual stress of Si ribbon at room temperature. Work will begin on the modification of an existing EFG growth system to confirm experimentally the reduced-stress configurations predicted by the computer model with inputs from experimentally obtained data.

### Dendritic Web Ribbon Growth (Westinghouse Electric Co.)

Westinghouse is conducting research on the key problems associated with a process for making a thin, wide-ribbon form of single-crystal Si directly from melt. "Dendritic" refers to the wirelike supporting dendrites on each side of the ribbon, and "web" refers to the Si sheet that results from the freezing of the liquid film between the bounding dendrites as the latter are raised from molten Si.

Using parametric evaluation by computer models, two web-growth configurations with capability for dynamic positioning (i.e., movement during ribbon growth) of thermal elements were defined. The new designs were based on a well-characterized static configuration in order that a good comparison of performance results could be made. The two dynamic configurations were

## ADVANCED MATERIALS RESEARCH TASK

built and tested. Major improvements of linear growth speed at the standard ribbon thickness of 150  $\mu\text{m}$  were obtained, the first configuration giving a speed of 2.7 cm/min, compared with 1.9 cm/min for the otherwise-equivalent static configuration (an increase of 42%). The second configuration gave a speed of 3.0 cm/min, an increase of 58% over the equivalent static design. The increased growth speed and low stress that were achieved were consistent with model predictions. It should be noted that in these tests the ribbon widths were relatively small, in the range of 1.5 to 2 cm, because such widths give convenient starting conditions. Achievement of greater widths would be time-consuming. However, the model predictions indicate that the greater widths (up to 5.8 cm) achieved by the static configuration on which these dynamic designs were based should be attainable simultaneously with high growth speed by the dynamic hardware.

In tests of a static growth configuration that was designed and built late in the previous report period, a growth speed of 2.1 cm/min for a 150- $\mu\text{m}$  thickness was achieved, this being 10% higher than the highest non-transient growth speed previously attained with static configurations.

Computer models of web growth were used to define two new static configurations for growth of low-stress ribbon. The configurations were built, and tests verified the growth speed and stress predictions of the models. One of the configurations gave a growth speed of 2.2 cm/min at 150- $\mu\text{m}$  thickness, the highest non-transient speed ever attained for a static configuration.

Using an earlier, well-characterized static configuration, the widest (5.8 cm) low-stress dendritic web ribbon ever grown was produced. The previous greatest width was 5.5 cm.

Transient area growth rates (for ribbon lengths of a few centimeters) to as high as 42  $\text{cm}^2/\text{min}$  were demonstrated. This is the highest rate that has been attained in the program. It should be noted that this material was very thin, of the order of 12  $\mu\text{m}$ . The highest transient area growth rate achieved before these results was 27  $\text{cm}^2/\text{min}$ . The recent results constitute an increase of 56%.

As a consequence of major progress in the reduction of buckling (elastic) stress, emphasis on computer modeling for further reduction of thermal stress has shifted to the hotter region of the growing web nearer the solidification interface, where plastic (residual) stress is generated. Overall reduction of stress is the principal requirement for attaining an increased rate of area growth.

## Ingot Technology

### Semicrystalline Casting (Semix, Inc.)

The semicrystalline casting development effort with Semix is a continuation of the cooperative agreement established in 1980 between Semix and the U.S. Department of Energy. Technical assistance in the monitoring of

this agreement is being supplied by JPL. The initial agreement envisioned a large-scale development of the technology for casting and wafering of semicrystalline Si. Philosophical changes in the scope and direction of the DOE program have resulted in a reduction in scope of the Semix effort to fundamental studies of the semicrystalline material, to determine defect structure and to investigate control of the crystallization front and its role in defect structure.

Investigation of structural defects within the grain volume that affect the efficiency of the material was carried out, to determine the nucleating mechanisms of a dislocation subgrain structure that is occasionally found in Semix material. Defect etching showed dislocation densities of the order of  $10^5/\text{cm}^2$  in regions of subgrain rotations and a density of  $10^3/\text{cm}^2$  outside these regions. The etch pit pattern indicates the presence of dislocations due to slip along (111)-type planes.

Sources of harmful subgrain structure in cast ingots were investigated. Two sources have been identified, one a generalized stress on the grain resulting in deformation and polygonization, and the other a kink in a high-angle boundary. The kink acts as a source of new dislocation arrays.

The dislocation subgrain structure, which has a deleterious effect on the local PV properties of the material, grows as a way of relieving internal stresses. The driving force for this structure appears to be stress along discontinuities or imperfections in the grain boundaries.

Another source of structural imperfection arises when process parameters are exceeded and the large grains break down into regions of extremely fine-grain material. Accompanying this breakdown is the development of so-called sinuous grain boundaries. To investigate the factors causing the breakdown and to determine the conditions that may impose practical limits on the speed of crystal growth in ingot technologies such as Semix's, the effects of non-equilibrium solidification on the material properties of the brick Si were studied. The PV properties of the material containing the fine-grain structure or sinuous grain boundaries are, in general, quite poor.

It has been shown that as grain growth proceeds into the mush region, the larger grains break down into a cellular structure as predicted by constitutional supercooling theory. Optical and scanning electron microscopy have indicated the presence of a liquid second phase existing in the grain boundaries after the primary field has frozen. Electron microprobe analysis has shown silicon carbide to be one of the constituents of this solute. The poor photovoltaic performance of the sheet material containing mush is due to shunt paths created by the incorporation of silicon carbide trapped in the sinuous grain boundaries and by the high dislocation content of these grains caused by high strain levels associated with impurity buildup.

Work also was conducted on quality evaluation of cast bricks by a double-beam laser technique. The scheme is based on modulation of a transmitted laser beam by injection of free carriers in the beam path by pulsing a dye laser. The variation in modulated decay time, which is related to the minority carrier lifetime, can be observed as a function of position along the ingot. The feasibility of the scheme was demonstrated. The transient signal has been detected and resolved to a maximum depth of 2 cm in the brick.

## Silicon Sheet Technology Supporting Studies

### Modification of Silicon Surface Properties by Fluid Absorption (University of Illinois at Chicago)

The purpose of this study is to provide an understanding of the abrasion and wear of Si through modification of its surface properties by interaction with fluids.

The wear rate of {100}n-type Cz Si abraded in ethanol, acetone, methanol, and deionized water was obtained from the {110} surfaces for loading forces,  $F_N$ , of 0.098 N to 0.49 N. The abrasion rate varies with  $F_N$  and fluid, ethanol being highest and DI water being lowest. The wear mechanism is a combination of fluid interaction with the surface, causing the deformation modes to change, and lateral or median crack propagation. Several analytical models are being used to describe the experimental results.

The surface hardness of Si was found to vary when tested in toluene, acetone, ethanol, methanol, glycerol, and deionized water. The surface hardness varies with applied load, with the largest effect at 0.24 N, and a minimum in hardness is observed when the dielectric constant of the fluid is 24 (ethanol).

The microhardness of Si was also obtained in inorganic salts: NaCl,  $\text{CaCl}_2$  and  $\text{FeCl}_3$  in concentrations from 1 ppm to  $10^4$  ppm in deionized water. A minimum in hardness was observed at 200 ppm in each case. The soaking time in each fluid also influenced the hardness but stabilized at a constant value after 2 h.

The fracture strength of Si after abrasion of a linear scratch in the presence of fluids is being used to determine the damage zone beneath the abraded groove. The fracture strength and the depth of damage varies with the type of fluid used in the abrasion. The damage zone is also being studied by an etching technique of room-temperature microhardness indentations. The highly strained and fractured region in the vicinity of the indent is etched preferentially with respect to the surrounding Si surfaces. The extent and morphology of the etched indentations are measures of the damage zone.

### Analysis of Stress-Strain Relationships (University of Kentucky)

A 12-month contract was executed in June 1983 with the University of Kentucky for stress-strain analysis of Si ribbon. The approach in this effort is the development of stress-strain models that will include elastic and elastic-plastic Si-ribbon buckling analysis. Complementary analysis of Si structure will focus on establishing the role that defect structures play in creating or relieving ribbon-growth stress.

Accomplishments include development of a preliminary buckling model that describes torsional buckling of grown Si ribbon, and compilation of a significant amount of data on high-temperature mechanical properties for Si.

## ADVANCED MATERIALS RESEARCH TASK

### Solid-Liquid Interface Studies (Solar Energy Research Institute)

The objective of this new contract, which started July 15, is to determine the influence of the thermal environment and the effects of impurities upon the stability and shape of the solid-melt interface in high-speed Si-growth techniques.

During this reporting period the principal investigator, T. Ciszek, prepared a manuscript and made a presentation titled "Orientation and Morphology Effects in Rapid Silicon Sheet Solidification" at the FSA Research Forum on high-speed crystal growth. In this work, rapid Si sheet growth was studied by observing the free spreading of point-nucleated sheets on a super-cooled horizontal melt surface. These studies have yielded much information on steady-state forms, solid-liquid interface sheet tip morphologies, qualitative Wulff surface-free-energy polar plots, and growth rate anisotropies.

Before the commencement of any horizontal ribbon pulling experiments to test their data, SERI must complete several furnace modifications. Included among the changes are the fabrication and installation of a new seed holder and the design and construction of containment mechanisms for the Si melt. These efforts are under way. The pulling mechanism is being calibrated.

### Materials Properties Modification (JPL)

The effects of light and electric field on the mechanical properties of Si were investigated.

The effect of light on the mechanical strength of Si wafers was measured on 2-in.-dia chemical-polished (100) Si Cz wafers supplied by Spectrolab. Three surface conditions of wafer samples were tested by a biaxial strength test. Tests using both a 110-V tungsten lamp and a dark condition were done for comparison. The three surface conditions tested were as-received, chemical polished; microindentation, Vickers 100-g load; microindentation, Vickers 200-g load.

Results indicated that the strength of undamaged wafers is greater (up to 30%) in light than in dark. However, the strength of indentation-damaged wafers becomes less in light than in dark. The difference between the reduced strength in light and the strength in dark increases with increasing size of microindentation. The tungsten-lamp light source used in this study was measured using a Gamma Scientific spectroradiometer. The maximum power was measured to be  $8.39 \times 10^3 \mu\text{W}/\text{cm}^2$  at the 1060 nm wavelength.

The effect of an electric field on the fracture resistance of single-crystal Si was studied. The microindentation Vickers test was used to introduce controlled damage onto the (211) surface of Si samples. Electric field tests were done by impressing 6 V, 0.1 mA through the Si sample during some of the 100-g, 200-g, or 300-g indentation tests. Both lateral and radial fracture damage from a microhardness indentation was measured in these samples. For these indentation tests, the rectangular Si sample was hard-wired at each end of the sample to a battery creating 6 volts and 0.1 mA in the Si. Initial

## ADVANCED MATERIALS RESEARCH TASK

test results indicate that less lateral damage, measured as extent of lateral fracture (center of indentation to end of fracture surface), occurred when the Si was tested with the electric field. An apparent "toughening" of Si is observed when it is indented in an electric field. Toughening was observed through a quantitatively smaller extent of radial and lateral fracture damage ( $\approx 15\%$ ) for the electric field samples versus no-field samples. Fracture-mechanics-based toughness values can now be calculated.

The fundamental reasons for the above-noted effects of light and electric field on the mechanical properties of Si are not known. It is believed that these effects may be related to the enhanced mobility of electrons in the environments studied.

# Devices and Measurements Research Task

## INTRODUCTION

The objective of this task is to identify and implement research and development activities in the photovoltaic devices and measurements area to meet the near-term and long-term objectives of FSA. Task activities encompass research in device physics, device structure, material-device property interaction, and measurement techniques for physical, chemical and electrical evaluation of devices and materials.

## Technical Approach, Organization and Coordination

To meet FSA objectives, efforts are now directed toward characterization of various silicon-sheet materials, material-device property interaction investigation, and measurement techniques. The program of the Task is structured accordingly.

Ongoing research contracts awarded for material and device evaluation are listed in Table 1.

The program of the Task also includes JPL in-house activities to conduct basic research in materials and devices characterization to support contractor needs and other tasks of the Photovoltaic Components Research Area.

## SUMMARY OF PROGRESS

### Cornell University

The following materials have now been studied:

- (1) Processed HEM material.
- (2) Bicrystals grown at JPL,  $\langle 100 \rangle$  greater than tilt axis with nominally 5 deg and 20 deg misorientation.
- (3) EFG ribbons.

The HEM material was obtained in the form of a processed cell. Optical scanning and EBIC showed that the cell, fabricated from an upper corner section, collected only in the vicinity of grain boundaries. Subsequent TEM showed that the grain boundaries were heavily decorated and acted as gettering centers for adjacent regions.

The crystallographic orientation of both bicrystals was measured by electron diffraction and was found to be, in the case of the low-angle boundary,  $5.5 \pm 0.1$  deg  $[100]$  with an additional  $2.1 \pm 0.2$  deg  $[010]$  tilt and a  $0.7 \pm 0.1$  deg  $[001]$  twist component. The high-angle crystal had a  $17.2 \pm 0.1$  deg  $[100]$  misorientation, with an additional tilt component of  $1.3 \pm 0.2$  deg  $[010]$ . Both crystals contained  $5 \cdot 10^5$  cm<sup>-2</sup> dislocations. The recombination behavior of both boundaries was identical and was controlled by impurities.



## DEVICES AND MEASUREMENTS RESEARCH TASK

### Cell Fabrication and Silicon-Sheet Evaluation (Applied Solar Energy Corp.)

The purpose of this contract is to investigate silicon solar-cell processes, development, fabrication and analysis. The most recent studies included the fabrication and analysis of mesa diodes made from HEM and Silso material. The results of various measurements on these diodes indicated that the diodes not containing grain boundaries performed better than those dominated by grain boundaries, but the degree of difference varied from material to material.

To understand the roles of grain boundaries and material quality inside the grain better, a light-spot scan system was modified to include the capability of measuring localized diffusion lengths. This has been accomplished and calibrated.

### Quantitative Analysis of Defects and Impurity Evaluation Technique (Materials Research, Inc.)

A significant correlation has been observed between solar-cell efficiency and the location of the material in the ingot of Semix silicon. The solar-cell efficiency decreases dramatically for the material near the top center of the ingot. An attempt has been made to correlate this decrease with the densities of dislocations, precipitates, grain boundaries and twin boundaries. Only the twin-boundary density is found to increase, by approximately one order of magnitude, from the outside part of the ingot to the top center part. This correlates with a decrease in solar-cell efficiency from approximately 10.5% to 6.5%. In addition, comparing solar-cell efficiency for adjacent slices of silicon shows consistently lower efficiencies for the upper slices. These observations may be explained by a simple analysis of the solidification process. Impurities with distribution coefficients of less than unity are rejected at the growing interface and thus build up in the melt. The last part of the ingot to freeze would therefore have a much higher density of these impurities. They might have a deleterious effect on solar-cell efficiency or perhaps disturb the crystal growth process, producing twins which themselves act to reduce solar-cell efficiency.

### Effects of Impurities on Solar-Cell Performance (C.T. Sah Associates)

This project has two interrelated tasks and objectives: theoretical and experimental studies of impurity-related energy levels, densities of the levels and carrier capture rates, and generation of a mathematical model to describe the experimental results and to specify the material property and device requirements for high-efficiency cells.

A technical report that describes the effects of extended back-surface field on the performance of high-efficiency silicon solar cells has been completed. About 100 cells have been analyzed, each with a different emitter of base dopant impurity distribution whose selection was based on the expected physical performance improvements. The four principal performance parameters

## DEVICES AND MEASUREMENTS RESEARCH TASK

( $V_{oc}$ ,  $J_{sc}$ , FF and EFF) are computed using a FORTRAN program, called Circuit Technique for Solar-cell Analysis (CTSA), which numerically solves the seven Shockley equations under AM1 solar illumination ( $88.92 \text{ mW/cm}^2$ ), for a optimum cell thickness of  $50 \mu\text{m}$ . The results show that very significant performance improvements can be realized by extending the BSF layer thickness from  $2 \mu\text{m}$  (18% efficiency) to  $40 \mu\text{m}$  (20% efficiency). The immunity of cell performance to recombination defect or impurity center is also improved by a factor of 2 to 3 in the recombination center density. A  $20\text{-}\mu\text{m}$  BSF penetration is sufficient in 20% p+/n/n+ cells with about  $20\text{-}\mu\text{s}$  base lifetime. At this and deeper BSF penetrations, the interband Auger recombination in the emitter layer becomes the limiting factor and affects mainly the short-circuit current but not the open-circuit voltage, which has saturated to about 710 mV. Future work in this second task will include the use of Ti impurity as the recombination center and the exact (no physical nor analytical approximations) numerical analyses of other optimum cell structures currently being investigated by the various JPL and DOE basic-understanding projects.

### Microcrystalline Silicon Growth for Heterojunction Solar Cells (Applied Solar Energy Corp.)

The objective of this program is to investigate the feasibility of using microcrystal (m-Si) with a 1.72 eV band gap as a heterojunction on single-crystal Si or as a window layer in a heteroface structure on a single-crystal Si p-n junction. The goal is to obtain high  $V_{oc}$ .

Results of various structures show the best  $V_{oc}$  in a heterojunction is about 480 mV and only negative voltage gain has been observed in the heteroface structure. Dark currents in the heterojunction have shown interface problems. P m-Si and P c-Si testing structure in many cases gave a negative photovoltage, which suggests that physical properties of the interface of p m-Si on c-Si do not favor  $V_{oc}$  enhancement.

### Development and Analysis of Silicon Solar Cells of Near 20% Efficiency (University of Pennsylvania)

Questions concerning the electronic properties, especially minority carrier lifetime, of epitaxial layers; of the influence of potential defects at the substrate--epi layer interface; and of possible degradation of the lifetime in the substrate by the high-temperature CVD process, are being investigated. Obtaining answers to these questions, as well as finding CVD--epi process conditions that will yield the highest lifetime values, is the main objective of this work. An additional objective is to develop a measurement method that will permit the reliable determination of the minority carrier recombination lifetime in such layers.

The first tests were carried out on  $100\text{-}\mu\text{m}$  and  $2\text{-}\mu\text{m}$ -thick epi layers deposited by M-A/Com from  $\text{SiHCl}_3$  at approximately  $1100^\circ\text{C}$ . The layers are  $0.25 \Omega\text{-cm}$  (As). The substrates are  $0.4 \Omega\text{-cm}$  (B) WASO-S with  $120\text{-}\mu\text{s}$  original lifetime. The tests have achieved several of the objectives of the project.

- (1)  $12\text{-}\mu\text{s}$  lifetimes were measured by the spectral LBIC method ( $L = 80 \mu\text{m}$ ). These lifetimes are fully compatible with 20% efficiency.

## DEVICES AND MEASUREMENTS RESEARCH TASK

- (2) A saturation current density  $j_{01} \approx 3 \times 10^{-12} \text{ cm}^{-2}$  was measured. Using the measured lifetimes,  $j_{01}$  of  $2.5 \times 10^{-12} \text{ A cm}^{-2}$  and  $0.5 \times 10^{-12} \text{ A cm}^{-2}$  were calculated for the epi layer and the substrate, respectively. This indicates that the epi process cannot have substantially degraded the substrate lifetime.
- (3) The excess current density was adequately low for high-efficiency solar cells.

The intermediate conclusion is that CVD-epi processes can be compatible with achieving 20% efficient solar cells.

### High-Efficiency Solar-Cell Structures by Molecular-Beam Epitaxy (University of California at Los Angeles)

Although many diverse measurements have been proposed to determine parameters of material and structure of p/n junction devices such as diodes, transistors, and solar cells, apparently no attempt has been made previously to provide a systematic and detailed theoretical framework that can both unify the diverse methods and suggest new methods. To develop this framework and to demonstrate its utility by experiment is the main purpose of this contract.

The following work as already been completed:

- (1) A mathematical framework for a two-part description of the quasi-neutral base region.
- (2) Application of this mathematical framework in open-circuit-voltage decay measurements.
- (3) Application of this mathematical framework in short-circuit-current decay measurements (apparently a new method).

# Environmental Isolation Task

## INTRODUCTION

The objective of the Environmental Isolation Task is the development and qualification of the total encapsulation system required to protect the active optical and electrical elements of a photovoltaic array from the effects of the field environment. The most challenging technical problem has been the development of high-transparency materials for the photoactive side of the module that meet the Project's low-cost and 30-year-life objectives. The approach to the objective includes a combination of contractor and JPL in-house efforts, which can be divided into two technical areas:

- (1) Materials and Process Research. This effort includes all of the work necessary to develop, demonstrate, and qualify one or more encapsulation systems to meet FSA cost and performance goals. It includes the testing of off-the-shelf materials, formulation and testing of new and modified materials, identification of automated processes to handle these materials during formulation and fabrication of modules, and systems analysis and testing to develop optimal module designs.
- (2) Material Durability and Life Testing. This work is directed toward the attainment of the FSA 30-year-minimum-life goal for modules. It includes research aimed at the development of a life-assessment method applicable to terrestrial photovoltaic modules, and validation of that method by specific application to photovoltaic demonstration sites. Material degradation studies are being conducted to determine failure modes and mechanisms. This effort supports both the materials and process development work and the degradation model development.

## SUMMARY OF PROGRESS

### Isolation Materials and Process Research

Module encapsulation material systems and configurations that meet the original FSA performance and cost goals and have the potential of meeting the service-life goal of 20 to 30 years have been developed and are being evaluated extensively. Major PV module manufacturers, including ARCO Solar, Inc., Solar Power Corp. and Solarex Corp. are using and evaluating the FSA-developed pottant (EVA) and primer materials (silanes) in their current product lines.

More advanced encapsulation concepts as well as work on some identified problem areas with EVA have been worked on during this reporting period. A new area of research has been initiated to evaluate the potential of using transparent conducting materials (TCM), initially polymers, as a current-collecting layer on the front side of PV solar cells to replace grid lines or a conducting layer of indium titanium oxide.

## ENVIRONMENTAL ISOLATION TASK

### Encapsulation Materials and Process Research and Evaluation (Springborn Laboratories, Inc.)

The goal of this program at Springborn Laboratories, Inc. is to identify, develop and evaluate materials and processes for the low-cost encapsulation of silicon photovoltaic cells. Material selections are based on performance criteria and the FSA objective of achieving a solar flat-plate or concentrator array at a manufactured cost of \$0.70 per peak watt (\$70/m<sup>2</sup>, 1980 \$). This includes studies of substrates, pottants, outer covers, adhesives, sealants, and other components. Pottant materials are under continuing development with evaluations of UV absorbers, amine-type stabilizers, metal deactivators, etc. to optimize performance. These investigations have resulted in "advanced industrial grades" of EVA and EMA with faster cure chemistries and non-extractable UV stabilizers. Candidate materials are also assessed for relative life performance with the use of accelerated stress conditions, including RS/4 sun lamp, CER reactors, thermal aging and others. The test results to date indicate that degradation is predominantly induction-period type in appearance, and that color is the first property to change. RS/4 exposures at 50°C show that the commercial grade of EVA is stable to 40,000 hours before degradation is observed, indicating excellent stability. Other tests show that EVA survives 7200 hours of thermal aging at 90°C and 2000 hours at 130°C. In all of the pottants, the most severe condition observed is thermal aging in the presence of copper. This metal is found to accelerate the degradation reactions of polymers.

Adhesive bonding is essential to module integrity. Springborn is continuing to identify primers and adhesives for all possible interfaces. Additionally, experimental support is being provided to two universities for fundamental studies in adhesion science.

Anti-soiling treatments for the surface of PV modules is still under evaluation, with the use of outdoor exposures. The fluorosilane treatments still appear to be effective after two years of exposure and to enhance overall module output by about 1%.

The investigation of thin-film deposition techniques for polymers, a new study, has started at Springborn. This study is in support of the new JPL program concerned with TCM to replace indium tin oxide.

The three outdoor heating racks are now fully operational at Springborn. These racks operate at 80°C, 100°C, and 129°C, and are intended to accelerate the aging thermal of materials and modules being exposed to natural environmental conditions of oxygen, humidity, UV, pollution, etc. It is planned that aging data generated at elevated temperatures will be extrapolated to lower temperatures for lifetime estimates.

### Module Design Analysis and Verification (Spectrolab, Inc.)

The objective of this program was to develop analytical methodology for advanced encapsulation designs. From these methods, design sensitivities were established for the development of photovoltaic module criteria, and the definition of needed research tasks.

During this period, final reports have been written in thermal, electrical, structural and optical modeling areas. A structural master curve that enables the designer to predict stress in the solar cell for any module design was developed. The electrical isolation work has provided a theoretical background from which a life-prediction methodology for electrical breakdown has emerged.

Synthesis of UV Absorbers  
(Polytechnical Institute of New York)

Novel stabilizer systems for plastic materials are polymerizable, polymeric and polymerbound antioxidants, photostabilizers and flame retardants.

2(2-hydroxyphenyl)2H-benzotriazoles (2HB) are the most effective ultraviolet absorbers. Several vinyl and isopropenyl derivatives of 2HB have been synthesized and their polymerization and copolymerization have been demonstrated. The copolymers have significantly improved photoaging properties on long term exposure to the environment over similar compositions with low-molecular-weight ultraviolet stabilizers.

Two families of 2HB's with ultraviolet absorbing chromophors have recently been synthesized with high extinction coefficients with very broad absorptions (250 nm to 360 nm): compounds with more than one benzotriazole units substituted on resorcinol(1,3-dihydroxybenzene) and phloroglucinol (1,3,5-trihydroxybenzene), and compounds with 2-hydroxybenzo (or aceto) phenone and one or two benzotriazole groups in the molecule.

By controlling carefully the reaction conditions, monobenzotriazole-substituted resorcinol (BDH) or phloroglucinol (BTH) was prepared in high yield and purity; BDH gave 2(2-hydroxy-4-acryloxy(methacryloxyphenyl)2H-benzotriazole BDHA(M). Homopolymers and copolymers of BDHA(M) have been prepared and are being evaluated.

Reaction of 2(2,4,6-trihydroxyphenyl)2H-benzotriazole (BTH) with acryloyl chloride gave not the desired BTHA, but the cyclized dihydrocoumarine. On hydrolysis, a benzotriazole-substituted hydroxypropionic acid was obtained which is a candidate as ultraviolet stabilizer for polyesters or polycarbonates.

Synthesis of ultraviolet-absorbing compounds to be permanently incorporated into polyesters, polycarbonates and epoxides is under way: 2(2,4-dihydroxy-5-carboxyphenyl)2H-benzotriazole, 2,4-(1,3-dihydroxyphenyl)-di[2H-(4',4''-dihydroxybenzotriazole)], 2,4-(1,3,5-trihydroxyphenyl)-di[2H-(4',4''-dihydroxybenzotriazole)], and 2,4,6-(1,3,5-trihydroxyphenyl)-tri[2H-(4',4'',4'''-trihydroxybenzotriazole)]. Work has started to incorporate these 2(2-hydroxyphenyl)2H-benzotriazoles into condensation polymers and epoxy resins.

## Material Durability and Life Testing

### Photothermal Degradation of Polymers (JPL)

A report, Handbook of Photothermal Test Data on Encapsulants (JPL Publication 83-32, JPL Document No. 5101-230) has been published containing a summary of data on changes in physical and chemical properties of polymeric pottants and cover films caused by exposures to temperatures up to 135°C and accelerated UV intensities.

An FSA report on the current status of encapsulant interface bonding stability is in press. This report will serve as a baseline of bonding integrity data in support of the ongoing study of long-term (30 years) bonding stability with current bonding processes and materials.

### Advanced Encapsulation Materials Evaluation (JPL)

Test panels of wood hardboard (Dorlux) with barrier films (Scotchpar) are undergoing outdoor tests of dimensional stability as a function of humidity and temperature. The barrier film has reduced cyclic dimensional changes by a factor of up to 10 over bare hardboard.

Preheating and conditioning of Tedlar film has been found to effectively reduce film shrinkage, which was encountered as a problem in module back-cover films during qualification test temperature cycling.

The effect of aging, temperature, and moisture on the dielectric and leakage resistance of candidate pottant and film materials is in process as a follow-on to the experimental statistical evaluation of voltage breakdown of these electrical isolation materials.

### Interface Bonding Stability (Rockwell Science Center)

Three reactive silane coatings, Z-6020, Z-6030, and Z-6031 from Dow Corning Corp., are currently used in advanced encapsulation systems employing ethylene vinyl acetate (EVA) encapsulation. The chemical and physical processes of encapsulant bonding using these reactive silanes have been extensively evaluated. The early phases of this study involved computer modeling of the physical transitions and environmental responses of the polymerized silane primer coatings. Experimental studies of the bulk polymerized reactive silanes show that residual chemical reactivity may be an important reason for the outstanding durability and environmental resistance of these materials.

A second phase of study has determined the quantitative relations for the interface bond stability (IBS) of these silane primers as defined by experimentally determined Weibull statistical distributions for shear bond strength. The effects of chemical composition are shown to produce major

## ENVIRONMENTAL ISOLATION TASK

(tenfold) changes in shear bond strengths. Variations in silane coating and drying steps are shown to make substantial (+15% to 30%) changes in shear bond strength distributions. These strength distributions can be quantitatively evaluated by a precise (+1%) analytical measurement of both the mean strength  $\sigma_0$  and the Weibull modulus  $m(\sigma)$ .

These statistical evaluations of IBS using the Weibull statistical criteria are now being extended to characterize premanufactured solar modules with varied degrees of natural and accelerated environmental aging.

### Polymer/Metal Interface Studies (University of Cincinnati)

Specimens of ethylene vinyl acetate (EVA) bonded to copper, aluminum, and mild steel have been supplied to F.J. Boerio so that he may start an interface analysis. Separately, Boerio reaffirmed that keeping liquid water from forming on a metal surface is a necessary requirement for corrosion resistance, but he also pointed out that the localized pH on the metal surface is involved. Apparently, there is a pH range within which corrosion will not occur, even if liquid water is present on the metal surface; this phenomenon is neither clearly or conclusively understood. A natural question then arises as to the role of silane primers as corrosion-prevention agents at the polymer-metal interface. Do silane primers prevent formation of liquid water, or do they regulate local pH, or both? These questions will be included in Boerio's studies, and if pH is a factor, this information will be directed to E.P. Plueddemann for the development of pH-regulating primer systems.

### Degradation Computer Modeling (University of Toronto)

A computer model that simulates, in principle, the chemical changes in the photooxidation of hydrocarbon polymers, using elementary input data has been developed. Further computations on the refined model show:

- (1) Time to failure.  $\tau_f$ , (chosen as the level of 5% C-H bond oxidation, which is within the range that would be expected for marked change in mechanical properties), varies as the inverse square root of the light intensities. However,  $\tau_f$  is almost unaffected by both the photoinitiator type and concentration.
- (2) The time-to-failure decreases with the rate of abstraction of C-H by peroxy radicals but increases with the rate of bimolecular radical termination controlled by diffusion.
- (3) Of the various stabilization mechanisms considered, the trapping of peroxy radicals is distinctly the most effective.
- (4) For a partially crosslinked polymer where the physical properties are not steep function of crosslink density, it is unlikely that there will be dramatic failure modes due to net changes in molecular weight.



## ENVIRONMENTAL ISOLATION TASK

- (5) Energy loss (power loss) due to polymer light absorption (with yellowing discoloration) will not be a significant failure mode.
- (6) Since the all-important peroxy radicals terminate by bimolecular disproportionation, at low concentration they could have lifetimes of up to several hours, which would affect the extent of dark reactions in the diurnal cycle in outdoor applications.
- (7) The useful lifetime of the unstabilized polymer decreases with temperature from almost two years in cool weather (45°F) to just a few months in hot tropical weather (100°F).

# Process Research Task

## INTRODUCTION

The objective of this task is to conduct research in critical areas of photovoltaic device fabrication and module formation.

Process research is grouped in four categories for reporting convenience: surface preparation, junction formation, metallization and module completion.

## SUMMARY OF PROGRESS

Process research efforts have been very successful, and 12 technical papers have been prepared and published. Four new-technology reports were submitted, two of which qualified for patent application. Two unsolicited proposals were received and one contract has subsequently been awarded to Westinghouse Electric Corp. for laser-assisted metallization research and development. A request for proposals to adapt pulse excimer laser processing for fabrication of solar cells was issued.

The Photovoltaic Metallization Systems Research Forum was held in Pine Mountain, Georgia. A high level of interaction between industry, government and academic participants was achieved and some proposals for novel metallization-systems have been received as a direct result of the Forum.

A Task member chaired the Semiconductor Equipment and Materials, Inc. (SEMI) committee meetings on solar grade silicon. Task members were on the evaluation team for a Solar Energy Research Institute (SERI) proposal on novel processes.

Samples of solar cells made in the People's Republic of China were analyzed in the JPL process laboratory as part of the U.S. assessment of foreign capabilities. Results of the analyses were included in a 22nd PIM presentation by L.D. Runkle.

A task member served on a Thin-Film Task Force appointed by R. Annan of DOE. DOE has named SERI to coordinate amorphous silicon activities and JPL has undertaken to develop large-area amorphous-silicon deposition chamber parameters.

## Surface Preparation

The Spectrolab, Inc., study on a conductive transparent oxide antireflective coating has been dropped to permit increased concentration on the thick-film metallization system in the same contract.

## PROCESS RESEARCH TASK

### Junction Formation

Solarex Corp. developed a minicell process sequence that allows characterization of many different locations on a large-grain polycrystalline solar cell. Analysis of test data shows that bulk minority carrier lifetime, rather than grain-boundary effects, is the governing factor in performance of cells made with Semix material.

Development of a polymer liquid dopant belt-furnace diffusion process has been nearly completed by Westinghouse. In a continuation of Westinghouse's liquid-dopant effort, a phosphorus front junction equivalent to a gaseous diffusion junction was demonstrated. Again, the meniscus coating machine was an important part of the effort. As a result of the liquid-dopant success, a parallel ion-implantation study has been discontinued. High capital equipment cost and marginal cell performance were other deciding factors in the discontinuation.

Non-mass analyzed (NMA) ion-implantation research has been deferred at JPL to concentrate on ion-cluster beam technology. There are at least two NMA facilities in the industrial area, indicating a successful transfer of NMA technology.

Ion-cluster beam deposition techniques are applicable to both diffusion and metallization system processes. The major effort in the last six months has been on research equipment construction and installation.

### Metallization

Bernd Ross Associates pioneered use of a new measurement technique -- resonant nuclear reaction profiling with  $N^{15}++$  -- to determine hydrogen concentration near the silicon-metal interface. Additional work in this new area was cut short by Ross's death.

Use of carbon monoxide instead of hydrogen as ambient atmosphere improved the sintering of the molybdenum-tin-titanium hydride thick-film metallization system. Spectrolab is still working on the solderability problem with this base-metal system.

Electrink, Inc. has been working with JPL researchers in development of thick-film inks using thermogravimetric analysis and differential thermal analysis.

Additional work on amorphous metal diffusion barriers by California Institute of Technology has resulted in the characterization of an iron-tungsten film that is very stable. Nine technical papers were published as a result of this and other work in diffusion barriers.

Westinghouse has started a new program to develop direct writing of a front-surface metal grid using laser technology.

## PROCESS RESEARCH TASK

The JPL-developed contact-resistance measurement technique is now being tested for use in environmental degradation studies on conductor-semiconductor interfaces.

## Module Completion

Spire Corp. successfully demonstrated a hermetic edge-sealing process using an electrostatically bonded aluminum ribbon and an ultrasonically bonded foil back sheet.

Westinghouse demonstrated an automated cell-stringing machine design by Kulicke & Soffa, Inc., which is capable of bonding 180 cells in 10.5 minutes. This one machine would support a 2 MW/year factory production volume.

JPL assisted Boeing Aircraft Corp. in defining lamination parameters for its copper-indium diselenide photovoltaic module.

# PROJECT ANALYSIS AND INTEGRATION AREA

## INTRODUCTION

The objective of the Project Analysis and Integration Area (PA&I) is to support the planning, analysis, integration, and decision-making activities of FSA. Accordingly, PA&I supports the Project by developing and documenting Project plans, and by contributing to the generation and development of alternative plans through the assessment of technology options. The analysis function of PA&I generally involves the establishment of standards for the economic comparison of options under Project study, and development of capabilities to perform the trade-off analyses required. Supporting the integration of FSA entails integrating tasks within the Project, and interfacing between the Project and other elements of the National Photovoltaics Program. Assessments of progress toward achievement of goals are performed to guide decision-making within the Project, the Project goals having been established to reflect the requirements of the solar-array manufacturing industry and the National Photovoltaics Program.

## SUMMARY OF PROGRESS

The Photovoltaic Program's Five Year Research Plan contains a redefinition of Program goals to include a near-term (1985) goal of 12%, \$100/m<sup>2</sup> module technology and a long-term (1988) goal of PV technology capable of producing \$0.15/kWh electrical energy. (All monetary units are 1982 dollars.) An analysis has been performed to determine the effects of the Program goal changes on FSA goals. Results of the analysis were presented at the 22nd PIM. (See the Proceedings section of this document.)

The balance-of-system (BOS) efficiencies and costs, as well as module efficiency, influence the allowable cost for modules. The BOS efficiency assumed in the plan (81%) is essentially the present state of the art and leads to a range of allowable module costs in 1982 \$/m<sup>2</sup> of from \$25/m<sup>2</sup> for 10% module efficiency to \$80/m<sup>2</sup> for 16% module efficiency. If, on the other hand, BOS efficiencies are assumed to undergo some improvement in the future, say to 87%, this considerably relaxes the constraints on module cost to a range of \$43/m<sup>2</sup> for 10% module efficiency to \$109/m<sup>2</sup> for 16% efficient modules.

The silicon-cost-sensitivity study has been updated and a final report is being prepared. Distributions of possible costs for various silicon refinement process steps were developed to reflect uncertainty. These probability distributions were used as Improved Price Estimation Guidelines (IPEG) inputs for a probabilistic estimation of silicon manufacturing costs. Results of the study indicate that long-term silicon prices are 90% likely to be \$20 (1982 \$) or less. (This is a technologically feasible price and does not consider marketing costs or market conditions.) The silicon cost study methodology and results were presented at the 22nd PIM.

## PROJECT ANALYSIS AND INTEGRATION AREA

The value-added cost and performance effectiveness of several state-of-the-art and advanced metallization techniques were presented at the 22nd PIM. The study had recently been expanded to include a larger number of candidate processes. IPEG and a grid optimization model developed by PA&I were used to generate the cost and performance estimates, which were presented in "efficient frontier" format. Data for the cost estimates were gathered from FSA contractors and other sources. The metallization study will be expanded to include an analysis of the electrical and optical properties of transparent conducting materials. Equations solving for the transmission and reflection of absorbing films on an absorbing substrate will be used to determine what film characteristics will maximize the performance of a photoconductor as a solar cell when used alone or in combination with a metal grid.

PA&I, in cooperation with the Environmental Isolation Task, the Process Research Task and the Engineering Sciences Area, has completed an analysis of a wooden hardboard substrate module design. Solar cells and electrical circuitry were encapsulated and then bonded to the substrate in a separate nonvacuum process. The module manufacturing cost was about the same as that for superstrate modules because the lower material cost for the substrate module was offset by extra processing requirements. The cost equivalence assumed no penalty for soiling or for a possible increase in operating temperature for the substrate module. Neither did the analysis consider any possible effects on reliability and module lifetime.

Projections of PV module cost and performance by 1995 have been completed. Data were gathered from the technical staff of FSA and a revised version of SIMRAND (SIMulation of Research AND Development) was used to determine the probability of meeting or surpassing a goal that is a function of more than one variable, such as \$/kWh in the case of PV modules. Publication of the projections will follow.

# ENGINEERING SCIENCES AREA

## REQUIREMENTS RESEARCH

The Requirements Research activity addresses the identification and development of detailed design requirements and test methods at the array level. Continuing areas of activity that addressed improved definition of array requirements included the establishment of module and array electrical safety criteria, the development of residential array design documentation including associated array-to-power-conditioner electrical interface concerns, and hot-spot heating research documentation.

### Safety Requirements

Research aimed at developing module, panel and array subsystem safety requirements continued with the revision of Underwriters Laboratories' draft final report to incorporate JPL comments. The report includes work at the module level and emphasized array safety systems; a December, 1983 release is scheduled.

### Power-Conditioning Interface

Research activities during this reporting period focused on completing draft revisions of the array-to-power-conditioner input to the Residential PV Array Design document in preparation by JPL under contract to Sandia (see Residential Array Design, below). The revisions address specific array-to-power-conditioner system interface concerns for residential photovoltaics, such as the array power level required to prevent tripping of the PC power limiters under conditions of sporadic high insolation levels due to cloud reflections. Improper sizing of an array relative to a power conditioner can lead to unnecessary system down time on the one hand or to inefficient operation on the other. Conversations have been held with power-conditioner manufacturers and with Sandia Laboratories to clarify the issues.

### Residential Array Design

Development of a Residential Photovoltaics Design Documentation Effort sponsored by Sandia National Laboratories (SNLA) for use by residential-system designers included the preparation of two topical reports, Residential PV Array Design and Fundamentals of Residential Photovoltaics. The reports submitted to SNLA describe the practical aspects of system installation and alerts the system designer to problems and safety issues during installation, operation and maintenance of residential PV systems.

## ARRAY SUBSYSTEM STUDIES

These Engineering Sciences activities support the development of the technology base necessary for the effective integration of photovoltaic cells

## ENGINEERING SCIENCES AREA

and modules into cost-effective, reliable and safe arrays that meet the system needs of the end applications. Specific areas of activity included bypass diode integration techniques and a series-parallel circuit study.

### Bypass Diode Integration

Research continued on the development of techniques for the installation of p-n junction or Schottky diode chips as bypass diodes within glass-laminate-type PV modules with current ratings from 2 to 20 amperes. Efforts focused on design synthesis tasks including bypass diode cost comparisons, reliability considerations and parallel by-pass diode load-sharing considerations. Development activity in these areas was summarized in an annual report, Photovoltaic Module Bypass Diode Encapsulation, by N.F. Shepard, Jr., published by General Electric Co., June 20, 1983.

### Series-Parallel Circuit Study

Work on the SMUD 1-MW array has highlighted our inability to predict accurately the occurrence of hot-spot failures in complex series-parallel source circuits typical of those used in central-station PV arrays. An analytical study was initiated to generate the software for performing an array-cell failure analysis that determines the optimum series-parallel configuration for maximum reliability and minimum life-cycle cost due to cell failures. Efforts are focused on completing and debugging the computer program to be used in future circuit analysis.

## ARRAY SUBSYSTEM DEVELOPMENT

The Array Subsystem Development activity is directed toward the development of cost-effective residential-array support structures as a key approach to minimizing total array costs. Engineering Sciences Area in-house efforts have focused on the environmental durability of black polyvinyl chloride extrusions for direct-mounted residential array designs. Accelerated UV aging tests were continued on black polycarbonate (PC) and chlorinated polyvinyl chloride (CPVC) extrusions. These plastic extrusions have shown no changes in mechanical properties. However, a weight loss linear with time after an equivalent 12-year exposure was recorded. Both CPVC and PC extrusions are experiencing obvious cosmetic degradation on the sunlit surfaces. The tests are scheduled for 40 weeks, equivalent to a year's exposure of UV, with biweekly inspections, which are to gather a 20-year-life performance on these materials.

## RELIABILITY AND DURABILITY RESEARCH

Reliability and durability development efforts are addressed toward providing the technical base required to achieve reliable modules with 20-year lifetimes. Activities are conducted to clarify design tradeoffs, develop analysis tools and test methods, and provide generalized design solutions for the PV community. Specific activities during this reporting period included optimum rating conditions, electrochemical corrosion characterization, and module and cell temperature and humidity endurance.



## Optimum Rating Conditions

Efforts focused on a computer analysis for determining the optimum rating conditions (irradiance and temperature) for measuring array efficiency. The parameters included in the optimization task included site location, module thermal characteristics, and module I-V curve fill factor. The ultimate objective was to obtain a set of rating conditions for measuring module power output where the power value may be used as a predictor of array annual energy output. A technical paper titled "Energy Prediction Using NOCT-Based Photovoltaic Reference Conditions," by C.G. Gonzalez and R.G. Ross, Jr., was completed for the annual American Solar Energy Society meeting in Minneapolis, Minnesota, June 1-3, 1983. The paper updates the methodology for selecting the preferred irradiance level and ambient temperature for measuring module (or array) power output and shows that the NOCT-based power rating can predict annual PV energy production to within 1% accuracy for moderate climates. The paper also presents two approaches to fine-tuning the NOCT-based rating system for site-specific ambient temperature and I-V fill factor.

## Electrochemical Corrosion Characterization

Electrochemical corrosion research is directed toward the investigation of the degradation mechanisms of different metallization systems and their interaction with different encapsulant polymeric materials. In addition to the study of Ti-Pd-Ag and print-Ag contact deterioration reactions, the metallization coating types (i.e.,  $Ta_2O_5$ ,  $TiO_2O_3$  and SiO) also are being considered. Results have shown a migration of silver metallization materials into PVB encapsulants in both metallic and combined ( $Ag_2O$ ) states. However, no Ag migration has been detected in EVA encapsulants, showing an advantage EVA has over PVB in reducing electrochemical problems in modules. No electrical degradation in the overall cell performance was observed and  $Ta_2O_5$  has proven to be a better AR coating.

Several accelerated electrochemical tests are also being carried out to include encapsulated cells with Cr-Pd-Ag; Ti-Pd-Cu; Ni-Cu, and Pd-Ni-solder metallization systems. Various electron microscope analytical techniques are used in these studies, including EDAX, ESCA, ion microanalysis and X-ray diffraction, for the identification of the corrosion products.

Efforts have also focused on evaluating the electrical conductivity and water deabsorption kinetics of PVB, EVA and RTV silicone rubber encapsulants as a function of temperature and humidity. The results showed that water was highly absorbed in PVB, slightly absorbed in EVA and not absorbed in RTV. The kinetics of water deabsorption in PVB was found to obey the predictions of a simple model based upon volume diffusion in a quasi-infinite medium (flat plate).

A variety of single-crystalline and semicrystalline solar cells and metallizations from various manufacturers were used in a series of tests to determine the degradation kinetics of metallization corrosion. Initial results from solar cells exposed to an accelerated environment of  $10^{-4}$  molar solution of HCl and corrosion currents of  $10^{-2}$  and  $10^{-3}$  amps have shown the metallization corrosion rates to be highly dependent on both the metallurgical and

## ENGINEERING SCIENCES AREA

antireflection-coating materials. The effect of antireflective coatings on metallization systems ranges from a passivation to no effect in reducing the corrosion rates. Early results have also shown that corrosion rates in semi-crystalline cells appear to be dependent on the crystallographic orientation of the silicon substrate.

A series of in-house tests was completed after 2000 hours (83 days) of exposure with samples of EVA, PVB and RTV encapsulation using various solar cells with Ti-Pd-Ag, printed-Ag and Ni-solder contacts. All samples were aged under forward voltage bias and subjected to constant environment of 85°C/98% RH. Data obtained included cell capacitance, leakage current, series resistance and corona inception voltage. Results ranged from total destruction of the Ag/PVB systems to no apparent change in the Ni-solder/EVA systems.

### Module Temperature and Humidity Endurance (Wyle Laboratories)

Ninety minimodules, including Block III and IV designs, have been incorporated into the temperature-humidity test series at Wyle Laboratories. The reduction of visual and electrical performance data is being used in the development of humidity-degradation-rate curves based on comparisons of humidity testing cycles and temperature-humidity data from SOLMET weather tapes. Four environmental tests in progress include 85°C/70% RH, 70°C/85% RH, 85°C/85% RH and 40°C/93% RH temperature chambers with half of the test lot in a forward voltage-bias mode. Modules in the 85°C and 100°C chambers recently completed 365 days of exposure and are undergoing data reduction and examination. Additional test data are being obtained at 85°C/85% RH and 40°C/93% RH to define existing rate curves completely and to obtain more concise characterization of failure mechanisms.

A paper titled "Assessing Photovoltaic Module Degradation and Lifetime from Long-Term Environmental Tests," by D.H. Otth and R.G. Ross, Jr., was completed for the Institute of Environmental Sciences April 18, 1983, Annual Meeting in Los Angeles, California. The paper describes the accelerated test program at Wyle Laboratories for identifying key module temperature-humidity-bias degradation mechanisms, and the analytical structure used in assessing the significance of failure mechanisms to 20-year life. It illustrates the combined format by using current module temperature and humidity results.

A procurement of Block V minimodules that will add more recent designs to long-term endurance testing and provide performance comparisons to earlier technology is in progress.

### Cell Temperature and Humidity Endurance (Clemson University)

Research efforts have focused on preliminary results from cell reliability test data that have indicated that Schottky barrier formation may be a key degradation mechanism for p-on-n cells. Reliability results are contained in the Annual Report, Clemson Cell Reliability Research Activity, by J.W. Lathrop and E.L. Royal, dated September 1983. This was the fourth annual summary of research on reliability on temperature and humidity endurance conducted on encapsulated unencapsulated cells at Clemson.

## PERFORMANCE CRITERIA AND TEST STANDARDS

Active interfaces were maintained between FSA Engineering Sciences activities and the SERI Performance Criteria and Test Standards (PC/TS) Project to establish performance criteria and test standards covering both flat-plate and concentrator arrays. Arizona State University personnel who chaired the Electrical Performance Subgroup (EPS) during consensus standards development published a final report draft for JPL review that summarizes the test standards developed by the EPS on photovoltaic concentrators. The report also included important points of debate during the development of the standards and developments that have arisen since the publication of the Interim Performance Criteria Document--Issue 2 (IPC-2), which should be considered in future standards development.

## ENGINEERING SUPPORT

Engineering interface activities that provide for transfer of array requirements, design guidelines, analysis tools and test methods to the overall photovoltaic community continued in several areas.

The Engineering Sciences Area supported the development of the SMUD Project in several key areas, which included reviews of the Phase I module qualification tests results with SMUD Quality Assurance, the alignment and installation procedure at Acurex Corp. of the SMUD 10 kW verification array, and a draft of the technical specification for the second-phase procurement of SMUD modules. In addition, representatives of the Engineering Sciences and Module Performance and Failure Analysis Areas assisted in the performance of hot-spot tests on the SMUD verification array. A hot-spot test implementation plan was devised and the use of the JPL IR camera and portable data reduction system was demonstrated.

An Engineering Sciences Area representative moderated one of eight working-group sessions on Integrated Photovoltaic Central Station Conceptual Designs as part of an Electric Power Research Institute-sponsored design workshop, whose objective was to improve system design through feedback from the PV community, in Kansas City, Missouri, March 23-25.

R.G. Ross, Jr., Reliability and Engineering Sciences Manager, attended a meeting of the U.S. Technical Advisory Group (USTAG) supporting the U.S. delegation of the International Electrotechnical Committee Photovoltaic Standards Subcommittee (IEC/TC 82) in Los Angeles on July 17, as a member. The USTAG discussed proposed international standards covering PV measurements and system interfaces and made recommendations for U.S. positions at the upcoming general meeting to be held in Tokyo, Japan, in October.

An FSA research seminar titled "Results of Photovoltaic Research Investigations" was held at JPL on June 16, 1983. Guest speakers were Dr. E.K. Stefanokos and Dr. Y. Goswami of North Carolina A&T University. Technical presentation subjects included solar cell testing under high temperature and humidity conditions, and development of a solar-radiation design handbook.

Two Engineering Sciences Area representatives participated in the FSA Metallization Research Forum at Pine Mountain, Georgia, on March 16-18. A

## ENGINEERING SCIENCES AREA

brief summary of electrochemical degradation phenomena observed during accelerated module tests conducted in house at JPL and from the long-term Wyle test series was presented.

An Engineering Sciences Area representative visited the Lockheed Palo Alto Research Laboratory and participated in technical discussions on new methods available to evaluate failure mechanisms in solar cells. Lockheed demonstrated laboratory techniques that involve utilization of Auger surface analysis equipment to help understand changes that can occur in solar cells after environmental exposure.

As a result of the annual meeting of the National Electric Code (NEC) panels in Kansas City, Missouri, May 16-19, the proposed Article 690, Solar Photovoltaic Systems, was approved for incorporation into the 1984 edition of the NEC. FSA has supported work leading to the adoption of this article for four years. The achievement is particularly timely, as the NEC is revised every four years.

Engineering Sciences Area representatives discussed the use of buried wood in flat-plate solar arrays with members of the Western Wood Products Association during a meeting organized by the Photovoltaics Program Technology Development and Applications Lead Center at JPL. The WWPA, a trade association interested in furthering the use of wood, expressed great interest in providing data on long-life buried wood and making presentations at research forums and to individual manufacturers. The use of buried-wood foundations is rapidly expanding in the residential housing market, with 5% of new construction using plywood--stud builtup buried-wood foundations in 1982.

Engineering Sciences Area and Module Performance and Failure Analysis staff members met with Antony Desombre, Quality Manager of Photowatt S.A. in France, at JPL on March 21. Desombre is chairman of Working Group 2 of IEC subcommittee TC82, which is charged with developing international standards for photovoltaic module measurement and qualification testing. Discussions at JPL involved extensive review of FSA-developed measurement and qualification testing techniques.

R.G. Ross, Jr., and members of the Engineering Sciences Area met with Gunnar Bergman of Sweden on June 20, and described FSA activities in the area of module test standards and safety. Bergman is a consultant to the Swedish government; his assignment is to acquire an understanding of the technology and cost of PV, and project its future applicability as a power generating source in Sweden. He spent four weeks in the United States meeting key PV manufacturers and government laboratories.

R.G. Ross, Jr., participated in a Solaris Design Team Review on February 21-23, for a large Saudi Arabia PV installation. The review included an evaluation of system performance.

# MODULE PERFORMANCE AND FAILURE ANALYSIS AREA

## INTRODUCTION

The overall objective of the Module Performance and Failure Analysis Area (MPFA) is to evaluate the reliability and durability of modules that are constructed using the improved techniques researched in the other FSA Tasks and Areas. This is accomplished through a structured program of:

- (1) Procurement of modules to a specification.
- (2) Environmental stress testing.
- (3) Detailed failure analysis.
- (4) Operation in a field environment to obtain data that will:
  - (a) Confirm the reliability and durability of the tested article.
  - (b) Confirm the validity of the environmental test regimen imposed in item (2).

Accomplishment of this work also requires implementation of an accurate, repeatable, and reliable performance measuring system. Work activities and accomplishments in all of these activities of the Area during the reporting period are described below.

## MODULE DEVELOPMENT

### Block V, Group I

Five contractors are participating in the Block V, Group I module procurement activity. The full complement of 10 modules has been received from ARCO Solar, Inc., General Electric Co. (GE) and Mobil Solar Energy Corp. (MSEC). Solarex has delivered 10 modules of the design that uses a cell with a unique feed-through from the front to the back to make possible interconnects on the back side only. The Solarex module, using 10 x 15 cm semicrystalline cells, has not been delivered because of delays caused primarily by relocation of Solarex facilities. Spire has also experienced delays because of modification to its facilities and a spate of processing problems. The testing of these modules to the Block V requirements has proceeded and the results have been reported to the manufacturers, and are reviewed in a subsequent section of this report.

### Block V, Group II

The Block V, Group II activity involves four contractors; ARCO Solar, Inc., MSEC, Solarex and Spire. This activity is highly dependent upon the Group I contracts and involves delivery of design documentation, participation in design reviews, and delivery of hardware. Detailed design reviews have been held with ARCO Solar and MSEC. Upon satisfactory completion of the environmental testing of the Group I modules and resolution of weaknesses, the

## MODULE PERFORMANCE AND FAILURE ANALYSIS AREA

contractors will proceed with the fabrication of the Group II modules. The contract with Spire has been reduced in scope in favor of a new contract for the design of a high-efficiency module.

## MODULE TEST AND EVALUATION

### Performance Measurements

Activities involving reference cells have included (1) fabrication of new reference cells, (2) calibration of new reference cells, (3) recalibration of reference cells, (4) recalibration of the normal-incidence-pyrheliometer (NIP) against the JPL primary standard cavity radiometer, (5) work at DSET Laboratories, Inc. in fabricating and calibrating reference cells, and (6) comparison of reference cell cal-values at SERI and at JPL. New reference cells were fabricated and calibrated using EFG and web material produced by MSEC and Westinghouse respectively. A group of seven reference cells having various spectral response characteristics were recalibrated simultaneously and therefore under the same atmospheric or spectral irradiance conditions. The recalibration values correlated very well with the original values when turbidity and water-vapor conditions were considered. The NIP was found to correspond with the primary cavity radiometer within 0.2%. DSET is experiencing difficulty in achieving the desired atmospheric conditions to complete the calibration of 12 reference cells. The seven recalibrated reference cells, when measured using the SERI X-25 AM1.0 simulator and reference cell, produced calibration values that averaged 3.5% higher than those obtained during the sun calibration at JPL. The significance of this difference will be assessed in the next few months.

In addition to the continued support provided to the qualification testing program, other activities of the performance measurement team included:

- (1) Monitoring of the performance of the Schott GG-4 filters in the Large-Area Pulsed Solar Simulator (LAPSS) system, which provides an AM1.5 source and continues to show no significant degradation or change in output spectra with use.
- (2) Preparation and editing of a draft of a JPL LAPSS Operating Manual, Volume 1, and preparation of Volume 2.
- (3) Establishment of a procedure for the secondary calibration of reference cells using the AM1.5 LAPSS and sun-calibrated reference cells.
- (4) Measurement (sometimes called calibration) of transfer modules and cells for a varied group of users and manufacturers, including the Tennessee Valley Authority, Solec International, Inc., ARCO, British Petroleum and Hughes Aircraft Co..
- (5) Support to the Sacramento Municipal Utility District (SMUD) project by monitoring the calibration of the ARCO LAPSS at Camarillo, California.
- (6) Planning and implementing an upgrade in the PDP computer that is used for controlling and processing the LAPSS data.

## MODULE PERFORMANCE AND FAILURE ANALYSIS AREA

### Environmental Testing

Several categories of modules were subjected to the environmental test sequence at JPL during the reporting period. The tests were the Block V exposures, of which the most severe environments include a total of 200 thermal cycles from  $-40^{\circ}\text{C}$  to  $+90^{\circ}\text{C}$  and 10 humidity-freeze cycles from  $-40^{\circ}\text{C}$  to  $+85^{\circ}\text{C}$  at a relative humidity of 85%. Modules tested include some of the Block IV designs, Group I and Group II modules from Block V contractors and other involved module manufacturers, modules from foreign manufacturers and a set of modules for the Sandia Southwest Residential Experimental Station (SW RES) experiment.

The testing was not always a routine operation, as chamber failures at Convair and at JPL delayed completion of the thermal cycling tests. Chambers at Convair were used to accommodate large roof sections of modules.

Results of the environmental testing are shown in Table 1.

### Field Testing

Field-test activities for this reporting period included the daily acquisition of module data, periodic acquisition of array data, the acquisition of irradiance and weather data at five-minute and 15-minute intervals, and support to other FSA Areas and non-JPL installations in performing field tests. The daily data acquisition has suffered from problems associated with the instrumentation circuits. These problems generally involve computer-controlled switching circuits, which required modification from the original configuration for module measurements to the array configuration presently used in the field.

Nine months of array data have been acquired and analyzed. The results indicate only a slight, 2% to 4%, decrease in fill factor for the arrays. Further analysis of these data and the data taken daily for each module in the arrays is under way to determine if the problem is in the data system or if some of the modules have, in fact, degraded.

Data were taken for all of the Block I, II, and III modules that were either left at or relocated to the Goldstone, California, test site. The results indicate that degradation and failure are continuing at about the same rate as before the restructuring of the field test activity. (These results were presented in detail at the 22nd PIM).

The visual inspection of the Block IV modules under test at the Florida Solar Energy Center in Cape Canaveral indicate that there is a minor discoloration showing up on one of the module types. An electrical inspection is scheduled for October, 1983.

The portable I-V loggers were used on several occasions in support of both JPL and non-JPL efforts. The array logger was used to acquire data at the JPL field, for the SMUD project prototype array at Acurex Corp., and for the AMOCO Oil Co. in West Chicago, Illinois. The portable module logger was used to obtain data for the U.S. Coast Guard at their Fort Lauderdale, Florida, and Groton, Connecticut, sites. More than 275 modules were scanned and the data were reduced and presented to the Coast Guard for analysis.

Table 1. Results of Environmental Tests

Vendor Code	No. Of Modules Tested	Tests Completed	Results ( ) = No. of Modules Affected, if Less Than No. Tested
<u>Block V</u>			
G	6	T50~	Delamination and/or air bubbles at sides, all modules
	4	HF	Amber discoloration, more air bubbles
	2	T200~	More delamination and/or air bubbles
L5	(4 modules mounted in roof section)		
	4	Hi-pot, Continuity	Failed hi-pot, continuity; gasket electrically conductive; metal rain troughs not electrically connected; one cell string to J-box shorted
	6	T50~	Back surface delamination (5); electrical failure (10%), 1 module
	4	HF	Isolation to ground decreased during test, more delamination; hardware in J-box oxidized (1)
	2	T200~	Satisfactory
U	10	Hi-pot	4 of 10 failed initial hi-pot, were repaired by vendor, and returned to JPL
	6	T50~	Black edge sealant extruded (5), grid discoloration (2); two cells cracked (1)
	4	HF	Two cracked cells (1)



Table 1. Results of Environmental Tests (Cont'd)

Vendor Code	No Of Modules Tested	Tests Completed	Results ( ) = No. of Modules Affected, if Less Than No. Tested
<u>Block V</u>			
U	4	MI, Twist, Hail	Satisfactory
	2	HS	Satisfactory
	2	T200~	No IC fatigue; cement yellowed at terminals
	6	Final Hi-pot, Continuity	Failed hi-pot (6) and continuity (5)
Y	10	Hi-pot, Continuity	Hi-pot satisfactory; failed continuity with very high values of resistance, possible due to anodizing
	6	T50~	Electrical failure (5); Tedlar delamination and wrinkling, cell discoloration and air bubbles on some of the modules
	4	HF	Electrical degradation worse (-18%, -92%, -10%, resp.) (3); haze over grids and interconnects which decreased in time; air bubbles
	2	T200~	No IC fatigue noted; increased electrical degradation; discoloration, delamination, air bubbles (1)
	4	MI	Open circuit during test (1), more delamination (1); power unstable on all 4 modules

Table 1. Results of Environmental Tests (Cont'd)

Vendor Code	No Of Modules Tested	Tests Completed	Results ( ) = No. of Modules Affected, if Less Than No. Tested
<u>Commercial Modules Tested To Block V Specs</u>			
D	6	T50~	Back skin wrinkled, yellow discoloration at edge sealant and J-box
	4	HF	Electrical failure (-11%), 1 module
	2	T200~	Electrical failure, -96%, both modules; failed open circuit during test when hot; interconnect fatigue (2) with cracks on 4 ICs, 1 module
	1	Hot-spot	Satisfactory
F	6	T50~	Significant delamination, all modules
	4	HF	Electrical failure, -6% to -12%, 4 modules; discoloration of white insulating strips (2)
	2	T200~	Marginal degradation, -5%, 1 module; amber discoloration under interconnects and bus; no IC fatigue
	1	HS	Satisfactory
M2	6	T50~	Heavy concentration of bubbles to 3 cm and up to 50% coverage, mostly outside of cells; one cell cracked, and this module had 30% electrical loss
	4	HF	Zinc alloy feed through connectors at J-boxes oxidized
	2	T200~	More bubbles
Q3	6	T50~	Bubbles, some large (5); one cell crack (1)
	4	HF	Interconnect fatigue marks on two modules; seven ICs cracked on one module and -98% degradation; all have delamination at terminals, discoloration at edges, wrinkled top Tedlar surface, loose J-box, and busbar contamination; delamination at ICs (3), contamination at ICs (2)

Table I. Results of Environmental Tests (Cont'd)

Vendor Code	No. Of Modules Tested	Tests Completed	Results ( ) = No. of Modules Affected, if Less Than No. Tested
<u>Commercial Modules Tested To Block V Specs</u>			
V	6	T50~	Gaskets shrunk, laminates loose in frame; cell crack (1)
	4	HF	Backside material wrinkled, sealant softened and ran out of laminates, discoloration, all modules
	2	MI	One crack in one rail of each module at mounting hole; marginal design, needs metal doubler or large washer
W	6	T50~	Busbar elongation displaced interconnects sideways; some sealant extruding on backside (4)
	4	HF	Satisfactory
	2	T200~	More busbar elongation, ICs tearing away and in one case had torn loose; ICs between cells wrinkled; busbars are pure (99.7%) aluminum
	1	HS	Satisfactory
Z	6	T50~	Bubbles (2), sealant pulled away from J-box (1)
	4	HF	42-cm-long delamination strip (1)
	2	T200~	No IC fatigue; sealant migrated to diodes (1)

Table 1. Results of Environmental Tests (Cont'd)

Vendor Code	No. Of Modules Tested	Tests Completed	Results ( ) = No. of Modules Affected, if Less Than No. Tested
<u>Block IV Production Modules</u> <u>Tested to Block V Specs</u> <u>(JPL Document Nos. 5101-161, 5101-162)</u>			
G	2	T50~	Electrical degradation, -5% and -57%, resp.; collector discoloration
S	2	MI	Satisfactory
US	4	MI	Satisfactory
VS	6	T50~	Laminates loose in frame, gaskets shrunk, back skin wrinkled; cracked cells in 4 modules, delamination in one
	4	HF	Corner brackets rusted, delamination at one end; air bubbles (3), amber discoloration at terminals (2)
	2	T200~	No interconnect fatigue
	6	Hi-pot	One module failed
YR	6	T50~	Amber discoloration (2), small Tedlar split (1) cell crack (1)
	4	HF	Amber discoloration (2), cloudy film over cells (3), gasket loose (1)
	2	T200~	Amber discoloration at frame edge (2)
YS	2	T200~	Satisfactory
	4	MI	Bubbles up to 1-cm diameter along the side of one module

Table 1. Results of Environmental Tests (Cont'd)

Vendor Code	No. Of Modules Tested	Tests Completed	Results ( ) = No. of Modules Affected, if Less Than No. Tested
<u>Sandia, SW RES</u>			
LM	4	T50~	J-boxes and their covers warped (4) cells cracked, a J-box loose and delamination of back surface (2)
	4	HF	J-box hardware rusted (4), more Tedlar delamination (2), bubble-like inclusions with appearance of liquid (2)
	2	MI, Twist, HL	Satisfactory
	1	T200~	More back-surface delamination mesh interconnects have gray discoloration
Codes: T = Temperature cycles HF = 85°/85% humidity-freeze HS = Hot-spot test MI = Mechanical integrity (cycling) ~ = Cycles			

## MODULE PERFORMANCE AND FAILURE ANALYSIS AREA

Additional testing support was provided to the FSA Engineering Area in their studies and testing of the causes and effects of hot-spot heating of cells. Further testing at the JPL site is planned.

### Failure Analysis

Workmanship in the assembly of modules still appears to be the major source of deficiencies that affect module durability and performance. Problems still occur in new module designs and in changes to existing designs in an effort to improve module performance. The types of workmanship and design problems still being experienced are:

#### Design-Related

- High-voltage withstanding
- Ground continuity
- Cell interconnects
- Encapsulation discoloration
- Edge sealant
- Moisture penetration
- Delamination of module edges

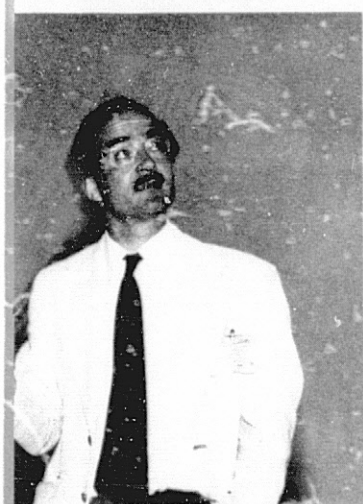
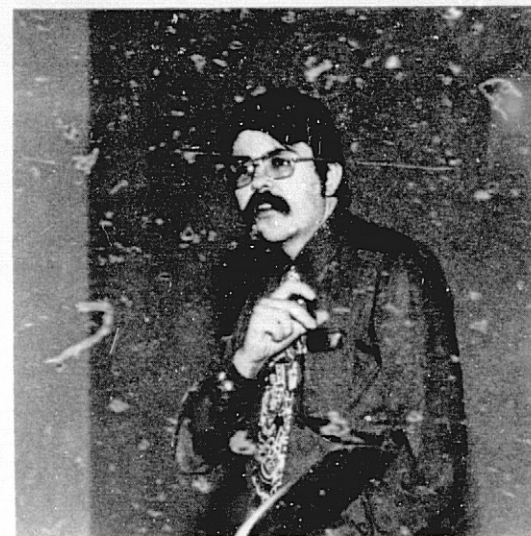
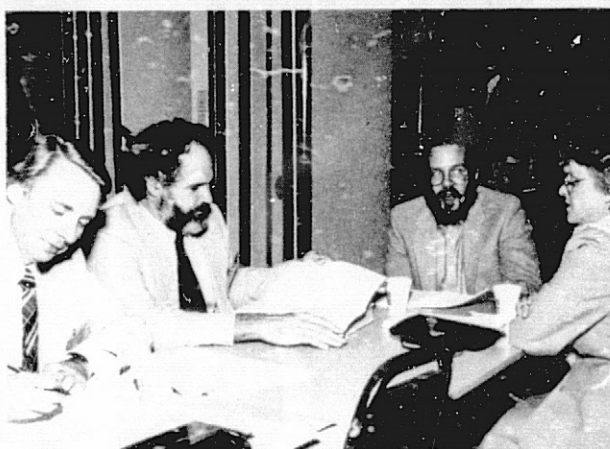
#### Workmanship-Related

- High-voltage withstanding
- Shorted cells
- Cracked cells
- Inadequate encapsulant cure
- Inadequate laminate deaeration
- Poor solder joints

The design-to-workmanship problem ratio appears to be 30% to 70%; early in the solar program this ratio was 50% to 50%.

The Problem/Failure Reporting system as of August 1983 has accumulated 1340 Problem/Failure Reports (PFRs), of which 1140 were closed.

The ongoing failure analysis effort still uses the laser-scan equipment to provide a graphic assessment of module performance. The high-voltage equipment provides verification and localization of leakage problems. The illumination equipment allows the study of I-V curves under stress conditions. The electron microscope identifies contaminants. The support of the Materials Laboratory pinpoints problems with the laminates, encapsulants and sealants.









# PROCEEDINGS

## INTRODUCTION

The 22nd Project Integration Meeting (PIM) of the Flat-Plate Solar Array Project (FSA) of the Jet Propulsion Laboratory (JPL) was held at the Pasadena Center, Pasadena, California, September 28 and 29, 1983. The PIM theme was "Crystalline Silicon Activities."

FSA has reoriented its activities to proceed toward goals that are compatible with the U.S. Department of Energy (DOE) Photovoltaics Five Year Research Plan, 1984-1988. The restructuring of FSA to accommodate this reorientation was described at the PIM.

In plenary session, presentations were made on the DOE PV Five Year Plan, and summaries were presented on the refocused thrust of FSA technical activities, on two recent FSA Research Forums (PV Metallization Systems, and High-Speed Crystal Growth), and on the status of standards for photovoltaics.

Presentations on, and discussions of, suggestions on the updating of the Five Year Plan produced valuable responses. Such responses had been solicited because the participation of industry and the user community along with the government in shaping the progress of photovoltaics is essential to the Plan's successful implementation as a basis for federal support of PV efforts over the next few years.

The DOE Plan says "Emphasis is placed on completing the development of flat-plate designs which yield improved conversion efficiencies and are amenable to automated production." This is important, because "Industry commitments and public observation suggest that crystalline silicon will continue to dominate the marketplace through this decade, if projected improvements are achieved." Continued improvements of crystalline silicon technology are vital to the PV community as it matures and strives to demonstrate its maturity to a wide-ranging user community and to be capable in the future of exploiting evolving technologies.

The success of the plan is highly dependent upon joint industry-government cooperation. As stated in the plan: "Implementation of the National Photovoltaics Program is based on the perpetuation of a mutually beneficial government/industry partnership .... To insure the success of this partnership, the federal research program includes provisions for: cost-shared research efforts which require long-term commitments by both industry and government, and prompt, accurate, and complete transfer of information gained from research and development."

A summary of plenary session presentations follows.

# Plenary Sessions

## SUMMARY

W. T. Callaghan, Manager of the Flat-Plate Solar Array Project, opened the meeting with a description of the restructuring of the Project to be compatible with the DOE Five-Year Plan. Project activities now focus on the most critical technical barriers that could inhibit the achievement of inexpensive, high-efficiency, highly reliable flat modules and arrays. He reported that FSA has dropped the support of production technology; as before, the Project relies primarily on universities and industry to perform much of the work in a cooperative, cost-sharing effort.

Robert Annan, Director, Photovoltaic Energy Technologies Division, U.S. Department of Energy, summarized the status of the DOE National PV Program Five-Year Plan and the status of PV within DOE. He reported a change at DOE in this past year; the new upper management at DOE has established a new policy that is positive and supportive of the development of renewable energy sources. Management, from Secretary of Energy Donald Hodel down, is committed to the support of photovoltaics. The Five-Year Plan is being accepted. The Plan can be looked at as a road map, or a way to move along a path toward bulk generation of electricity in the 1990's, with specific technology goals that will lead to a price of \$0.15/kWh for electricity. Annan noted that if the Plan is to succeed, it is necessary that it be supported by the PV community. Consequently, it is important to receive comments from the entire PV community on the Plan and how it might be improved. Complementary to the Plan, it is important that the government be supportive of industry. The industry doesn't want the government to help them make their sales, but it would be helpful if the financial environment for international PV sales were improved. Today's PV products are creditable and the government will be more supportive in acknowledging that fact. There is a need to educate, and to be sure that the colleges train technical people who can continue advancements during the coming decades.

A presentation on flat-plate module requirements to meet Program goals was presented by R. Aster of the FSA Project Analysis and Integration (PA&I) Area. The five-year goal of flat-plate collector research is to establish by 1988 technologies that industry can then apply to scaled-up production of modules. The modules should be compatible with a PV system capable of generating power at \$0.15/kWh. Module costs are parametric with module efficiencies and with balance-of-system (BOS) costs and efficiencies. Trade-offs between initial and operational efficiencies and costs of the power system, as components and as a total, have been estimated. Obviously there is a need to assess progress periodically as these parameters are better understood, and it is assessed where research and development can most effectively contribute to lower-cost electricity. In this context, some allowable module costs versus module and BOS efficiencies were presented. Suggested criteria for interpreting achievement of the goal also were presented. As a method of measuring progress, a near-term goal has been established; suggested criteria for meeting this goal were also described.

## PLENARY SESSION

Silicon-sheet growth progress, problems, and refocused thrust were reported by Andrew D. Morrison, Manager of the FSA Advanced Materials Research Task. Many growth techniques have been explored since 1975; silicon sheet growth has been one of the prime technology efforts in the PV program. Today, edge-defined film-fed growth (EFG) and dendritic-web ribbons are the two forerunners in silicon ribbon technology. Excellent progress has been made in demonstrating the technical feasibility of these techniques; now emphasis is on overcoming the generic barriers inhibiting the high-speed growth of quality ribbon that will be economically competitive. Extensive analytical and experimental efforts are being performed on the interrelationships in ribbons of heat flow, stress, and deformation when the ribbons are grown at high speeds. Also, an understanding of how the above parameters influence ribbon crystalline structure, and consequently the performance of solar cells, is being obtained.

M.H. Leipold, Manager, Process Sequences and Materials Research, presented an overview of process development. A key parameter in the continuing evolution to make higher-efficiency cells in more cost-competitive ways is to increase the yields of each production step. To achieve high yields, process sensitivity data must be determined for each significant processing step; for example, the time-temperature relationship for a specific process step is important and might degrade the effectiveness of previous steps. Consequently, each processing step must be improved to its practical extent and then possible interactions on previous steps must be evaluated for their final effect on cell and module yields and performance.

A Photovoltaic Metallization Systems Research Forum, sponsored by FSA, was held March 16 to 18, 1983. The objective of this Forum, which was chaired by Brian Gallagher of JPL, was to explore the status of commonly used metallization systems and of those that may be used on future materials or devices. During the Forum, presentations and discussions covered state-of-the-art assessments, system-characteristics analyses, and innovative ideas. The sessions covered the design, preparation of materials, and fabrication processes of metallization systems; operational degradation and corrosion considerations, and the influence of these factors on reliability and economics. People from universities, industry, and governmental laboratories made presentations on metallization systems based on thick film, nonnoble metal, polymer thick-film conductors, generic metallo-organics, laser-assisted deposition, and ionized-cluster beam deposition. Progress has been made toward inexpensive, durable metallization systems, and numerous novel techniques show promise for future use in both crystalline-silicon cells and thin-film cells. The Forum concluded that advanced metallization ideas require continued long-term research.

A High-Speed Growth and Characterization of Crystals for Solar Cells Research Forum, sponsored by FSA, was held July 25 to 27, 1983. The objective of this Forum, which was chaired by Katherine Dumas and James Liu (both of FSA), was to address the fundamental theoretical phenomena and operational constraints that limit the rate of growth of crystals suitable for processing into efficient, cost-effective solar cells. Sessions covered Theory of Crystal Growth; Melt Spinning; Ribbon Growth; Stress/Strain Effects in Ribbon; Laser Recrystallization; Material Characterization, and Ingot Growth and Characterization. The 35 invited papers were presented mainly by university and industry speakers, many of whom had not been associated previously with the FSA Project. The presentations and discussions provided a stimulating

## PLENARY SESSION

forum in which the state of the art, issues, most appropriate areas for research, and a perspective of the potential of the technology were discussed. It was concluded that there is practical limit to how fast silicon ribbon can be grown, but to define the limit a good understanding of stress and strain effects in ribbon must be developed.

Ron Ross, Manager, FSA Reliability and Engineering Sciences Area, presented an overview of the technical progress of flat modules since 1975 and of the key module and array technology items that should be worked upon for future modules and arrays. The evolution of solar cell, module encapsulation, and electrical circuit parameters and how these items have related to major reliability problems were discussed. During the past eight years many engineering developments have been made based upon the problems encountered during testing and needs for future applications. Development work that is or should be emphasized were listed, and the status of those efforts described. Strawman degradation allocations for baseline and advanced crystalline-silicon modules were presented. It is advocated that the power-degradation allocations for future flat modules and arrays be decreased. Thin-film modules will have unique engineering encapsulation and design requirements, and it is expected that a variety of problems will be encountered, some new, and others variations of problems with crystalline-silicon modules. The Project desires to obtain as many different types of thin-film modules as possible and as soon as possible so that unique thin-film module performance and durability problems can be detected.

A presentation on the status of photovoltaic module standards was made by J. C. Arnett of ARCO Solar, Inc. Many organizations have participated in the development of photovoltaic standards including the Department of Energy, national laboratories, photovoltaic users, photovoltaic manufacturers, national consensus standards organizations, and international organizations. Groups in the United States, Europe, and around the world are working on standards; however, national standards vary, and consequently an international group is very active in the matter. Progress is slow, for these reasons:

- (1) Nature of the consensus process.
- (2) Limited funding for support.
- (3) - Proprietary positions of manufacturers.
- (4) Tendency of users to over-specify.
- (5) Character questions for consensus bodies.

Support of these efforts was requested so that a useful body of standards will evolve.

Plenary-session presentations follow.

## DOE FIVE YEAR PHOTOVOLTAIC PLAN UPDATE

Suggestions for updating the DOE Five-Year Photovoltaic (PV) Plan were covered in a session chaired by M. Prince, Chief, Photovoltaics Collector R&D Branch, DOE. The session included formal presentations by two utility companies and two module manufacturers that have been investing significantly in PV R&D and manufacturing capabilities. These presentations are summarized below:

A letter from R.S. Allan, Program Manager, R&D, Florida Power and Light Co., was read by Prince. Highlights of the letter were:

- (1) The new federal emphasis on large-scale high-efficiency technology should be strongly supported.
- (2) Efficiency milestones are admirable but may be optimistic. It is to be hoped that the time for thin-film-cell, multijunction-cell, etc., technologies to mature will be less than the 30 years required for silicon cells.
- (3) Systems reliability of modules should be addressed more vigorously. Large-scale users will require substantial operational reliability data.
- (4) There is a need to understand the potential dynamic impact of a PV system on other generators in a utility network.

K.V. Ravi, General Manager, Mobil Solar Corp., commented on the Plan:

- (1) The plan is well thought through, well presented, and addresses many important research areas.
- (2) It is highly desirable that goals be expressed in non-monetary terms. Manufacturing costs are functions of technology and many nontechnical business issues.
- (3) The plan is incomplete because there is no budget; it should be modified when budget figures are available.
- (4) The de-emphasis of thick-film PV relative to thin-film PV is unfortunate. Generic research on thick-film silicon material and its influence on cell performance is still needed.
- (5) Some of the proposed balance-of-system technology effort does not appear to fit the Plan's purpose.
- (6) More focused, generic PV research at universities over sustained periods (three to five years) should be supported.

## PLENARY SESSION

Steve Hester, Pacific Gas & Electric Company (PG&E), commented:

- (1) PG&E expects to be a prime user of PV in the future.
- (2) Today PG&E has several customers with small PV arrays connected to the system, is planning for ARCO Solar, Inc., central-station interconnection in a few months, and is doing PV evaluation research.
- (3) DOE long-term goals will meet PG&E needs.

The PG&E research priority list, from its perspective, is:

- (1) Existing cell and module studies.
- (2) Analysis of impact of PV central stations.
- (3) Spinning reserve requirements.
- (4) Interconnection criteria.
- (5) Utility power quality and safety.

PG&E favors, for stimulating utilities' use of PV, tax incentives for utilities and third-party financing.

Charles Gay, Vice President R&D, ARCO Solar, Inc., presented comments highlighted as follows:

- (1) Five years is a short time for the Plan; 10 years would be more appropriate.
- (2) Emphasis on thin films and high efficiency is good.
- (3) Government-industry partnership has been beneficial, especially module block buys, PIM meetings, and SMUD efforts. Partnership should continue but must be adjusted as PV matures.
- (4) The correct federal role is to do R&D that is too risky and/or too costly for industry. However, there is a need to review the specific efforts that should be included. He recommended adding broad-based technology such as health and safety, insolation studies, performance measurement, and standards.

He made specific research suggestions:

- (1) Emphasize thin-film materials other than those being worked on widely, and ancillary materials for thin-film cells and modules.
- (2) Continue environment studies, module failure analysis, and module lifetime prediction and block procurement for thin-film modules.
- (3) Establish good world-wide solar resource information and methodology for measuring actual PV system efficiencies.

## PLENARY SESSION

- (4) R&D contracts should be for a minimum of three years.
- (5) Annual review articles on specific research activities should be written for major scientific and technical journals.

The presentations were followed by discussion from the floor. Many comments reinforced the above suggestions, and are summarized below:

- (1) People were supportive and positive about the Plan.
- (2) Concern about lack of a budget in the Plan and whether there would be adequate funding over time, to allow good planning and implementation to meet the goals, was expressed.
- (3) Contracts should be for longer periods of time, especially for universities.
- (4) The remote market must be recognized.
- (5) There is a large amount of good technology that has strong potential for making PV a viable, large-scale alternative energy source that could be worked on. It isn't obvious, nor is it easy to determine, which specific technologies are the most appropriate to support, especially with the uncertainty in the total energy situation, which could change quickly.
- (6) There is a need for periodic review of technology-support priorities and for the incorporation of their findings into DOE activities. The DOE Plan is good vehicle for conveying information on DOE PV activities to government officials and the PV community.

# FLAT-PLATE MODULE REQUIREMENTS TO MEET PROGRAM GOALS

Robert W. Aster

## JET PROPULSION LABORATORY

The Five Year Research Plan for Photovoltaics has two overall goals for flat-plate modules, one near-term and the other long-term. The near-term goal includes an efficiency target and a cost target. This cost target is expressed in terms of 1982 \$/m<sup>2</sup>, and is approximately equivalent to the old 70¢/W<sub>p</sub> target, in 1980 \$/W.

The long-term goal is an energy goal. Therefore, many module-related parameters must be optimized to be consistent with 15¢/kWh. This formulation of the goal allows a large number of important cost-and-performance tradeoffs.

## FSA Project Goals

- Near-term: 12% efficient module (at 28°C and AM 1.5) and \$100/m<sup>2</sup> by FY85
- Long-term: 15¢/kWh systems by FY88, requiring consistent FSA goals for:
  - Module cost
  - Module efficiency
  - Module lifetime
  - Module degradation rates
  - Module mismatch properties
  - Module soiling characteristics
  - Module-related O&M

---

From the National Photovoltaics Program Five Year Research Plan



## PLENARY SESSION

This viewgraph shows the criteria for accomplishing the near-term goal, a milestone that is scheduled for the end of fiscal year 1985 in the Five Year Research Plan.

### Criteria for Near-Term Goal Interpretation

- Physical demonstration of 12% modules (module elements should come from potentially low-cost processes)
- Key process step: (sheet formation, cell processing and module fabrication) are individually developed such that if scaled up to achieve economies of scale then \$100/m<sup>2</sup>, 12% modules could be obtained. SAMICS is utilized for economic assessment
- FSA's objective is to enable industry to adopt advanced PV technology within several years after development. Therefore:
  - 1985 commercial module price will not be the criterion for FSA success
  - Key process steps might not be adopted commercially by 1985
  - Economies of scale used in the analysis may not be consistent with 1985 commercial factory size

It is important to note that the FSA role is limited to R&D and does not include commercialization. That is the reason for the last three caveats on this viewgraph.

The long-term goal is an energy goal that allows a number of cost-and-performance tradeoffs and requires consideration of the entire system lifetime. The next two viewgraphs show the importance of several new performance parameters, such as degradation rates, mismatch, and soiling. These are included in a term called "Balance-of-System (BOS) efficiency," which is used in the Program plan.

BOS efficiency is defined in the Five Year Research Plan as a discounted average of all the efficiency terms in the system (with the exception of module efficiency). It is the product of each of the terms listed in the left-hand column. The Research Plan used a BOS efficiency of 0.81 for example calculations. The breakout in the "baseline" column came from the report referenced within the plan for these figures. This second column contains a different set of numbers. For example, there is a specific goal of 98%-efficient PCUs in the Program Plan, so this was included here. I have been informed that the "advanced" figures for module-related BOS efficiency are achievable, given a strong R&D effort in these areas. R. Ross will provide more information on this later this morning. What I want to do is to show the impact that this parameter has on the allowable flat-plate module cost and efficiency goals.

## BOS Efficiencies

Parameter	Baseline State of the Art	Advanced	Observations
<u>Module-Related</u>			
Degradation	0.95	0.96	Discounted average
Mismatch	0.97	0.99	Too small to measure
Soiling	0.95	0.97	0.94 to 0.98 reported
<u>Other</u>			
PCU	0.96	0.98	0.97 at SMUD
Shadowing, Wiring, Switchyard	0.96	0.96	
Total Product	0.81	0.87	

These are long-term flat-plate module goals that are consistent with 15¢/kWh. The algorithm and the financial factors given in the Five Year Research Plan were used. Only the BOS efficiency is varied. As expected, allowable module cost is parametric with module efficiency.

## Long-Term Goals

## CONSISTENT WITH 15¢/kWh SYSTEMS

(Module cost is parametric with module efficiency and also depends on BOS efficiency)

Module Efficiency (28°C, AM 1.5)	Allowable Module Cost, 1982 \$/m <sup>2</sup>	
	SOA BOS 81%	Advanced BOS 87%
10	25	43
11	34	53
12	44	63
13	53	73
14	62	83
15	72	94
16	81	104

## PLENARY SESSION

These 1982  $\$/m^2$  terms can be translated into 1980  $\$/W_p$  terms by dividing by 1.2 for inflation and then dividing by (module efficiency  $\times 1,000$   $W_p/m^2$ ). For example,  $\$25/m^2$ , 10% modules are equivalent to  $21¢/W_p$  (1980  $\$$ ). And  $\$81/m^2$ , 16% modules are equivalent to  $42¢/W_p$  (1980  $\$$ ).

In the other column,  $\$43/m^2$ , 10% modules are equivalent to  $36¢/W_p$  (1980  $\$$ ), and  $\$83/m^2$ , 15% modules are equivalent to  $52¢/W_p$  (1980  $\$$ ). The effect of flat-plate tracking is illustrated by the next viewgraph, which is the same as the last one but with an overlay.

### Long-Term Goals CONSISTENT WITH 15¢/kWh SYSTEMS

(Module cost is parametric with module efficiency and also depends on BOS efficiency)

Module Efficiency (28°C, AM 1.5)	Allowable Module Cost, 1982 $\$/m^2$	
	SOA BOS 81%	Advanced BOS 87%
10	25	43
11	34	53
12	44	63
13	53	73 72*
14	62	83 84*
15	72	94 97*
16	81	104 109*

\*Tracking flat-plate option

The overlay shows the value of flat-plate tracking. These figures come from increasing area-related BOS from  $\$50/m^2$  to  $\$70/m^2$  (Black & Veatch estimate) for single-axis tracking hardware, and by increasing the system capacity factor from 0.27 to 0.32 to account for increased energy output. Very similar results can be obtained with two-axis tracking, with suitable increases in area-related BOS and system capacity factor. With higher module efficiencies the additional investment in tracking hardware pays off. The  $\$84/m^2$ , 14% modules are equivalent to  $50¢/W_p$  (1980  $\$$ ). At the last PIM, Paul Henry described a candidate process sequence that might ultimately meet such a target. Clearly, there are more flat-plate module candidates for achieving the goals in the "advanced" column than in the "SOA BOS" column, and the probability of success for the Program would be greatly increased if these higher BOS efficiencies can be achieved. With this in mind, we are now ready to examine the criteria for accomplishing the long-term goal.

## PLENARY SESSION

The first order of business is to establish module-related BOS efficiencies. At that point, the criteria for module cost and efficiency are similar to what they were for near-term goals, except that there is more freedom to pick an appropriate module cost-and-efficiency pair of numbers. However, meeting the long-term goals will entail lower costs and higher module efficiencies than those stated as the near-term goals, under any foreseeable circumstances.

Again, it is worth noting that the FSA role is limited to R&D and does not include commercialization. For this reason, the last set of comments on this viewgraph apply to long-term goals as much as they do to near-term goals.

### Criteria for Long-Term Goal Interpretation

- Flat plate modules:
  - Module-related BOS efficiencies:
    - Degradation extrapolated from accelerated lifetime experiments
    - Mismatch and soiling should be physically demonstrated
  - Module efficiency should be physically demonstrated
  - Lifetime extrapolated from accelerated lifetime experiments
  - Key materials and process steps are individually developed such that efficiency and cost from a scaled-up factory are consistent with 15¢/kWh
- FSA's objective is to enable industry to adopt new commercial technology within several years after 1988. Therefore:
  - 1988 commercial module price will not be the criterion for FSA success
  - Key process steps might not all be adopted commercially by 1988
  - Economies of scale used in the cost analysis would not be restricted by the 1988 commercial factory size

## Summary

The \$100/m<sup>2</sup> (1982 \$) near-term flat-plate goal is approximately the same as the old 70¢/W (1980 \$) goal.

The 15¢/kWh long-term goal is significantly different, requiring higher efficiencies, lower costs, and excellent module performance characteristics. An aggressive effort to develop appropriate tradeoffs between these parameters is required to achieve this goal.

Criteria for measuring goal accomplishment are a combination of empirical measurement and extrapolation of experimental data with appropriate analytical tools. Commercialization within the timespan of the Five Year Research Plan is not a criterion and should not be expected.

# SILICON SHEET: PROBLEMS AND REFOCUSED THRUST

JET PROPULSION LABORATORY

A.D. Morrison

## Semiconductor Ribbon Innovation History

- 1956 WM. SHOCKLEY PATENT FILED "CRYSTAL GROWING APPARATUS" APPLIED HEAT FLUX CONTROL TO OBTAIN RIBBON. PATENT ALSO INCLUDED INVERTED STEPANOV PROCESS AND PERIODIC TEMPERATURE PULSES TO PROVIDE 'SCRIBE' LINES
- 1960 GAULE AND PASTORE PROPOSE DUMBELL SHAPED SEMICONDUCTOR RIBBON GROWTH USING ELECTROMAGNETIC FIELD PRESSURE TO OBTAIN RIBBON SHAPE, ALSO THE USE OF GUIDES TO SHAPE THE MENISCUS
- 1961 DERMATIS et. al. PATENT FILED "A PROCESS FOR PRODUCING AN ELONGATED UNITARY BODY OF SEMICONDUCTOR MATERIAL CRYSTALLIZING IN THE DIAMOND CUBIC LATTICE STRUCTURE AND THE PRODUCT SO PRODUCED". THE ORIGINAL DENDRITIC WEB PATENT
- 1965 La BELLE AND MLAVSKY, PATENT FILED ON EDGE-DEFINED FILM-FED GROWTH (EFG). APPLIED TO SILICON 1970
- 1969 C.E. BLEIL FILED FOR "HORIZONTAL GROWTH OF CRYSTAL RIBBONS" THE ORIGINAL HORIZONTAL RIBBON GROWTH WORK

Table 1. Laboratories Engaged in ERDA Program

LABORATORY	RESEARCH & DEVELOPMENT AREA
<u>RIBBON GROWTH PROCESS</u>	
MOBILTYCO	EDGE-DEFINED FILM-FED GROWTH (EFG)
IBM	CAPILLARY-ACTION SHAPING TECHNIQUE (CAST)
UNIV. OF S. CAROLINA	DENDRITIC WEB GROWTH
WESTINGHOUSE	DENDRITIC WEB GROWTH
RCA	INVERTED STEPANOV
MOTOROLA	LASER-ZONE RECRYSTALLIZATION (RTR)
<u>SHEET GROWTH PROCESSES</u>	
HONEYWELL	DIP-COATING (ON LOW-COST SUBSTRATES)
ROCKWELL	CHEMICAL VAPOR DEPOSITION (ON LOW-COST SUBSTRATES)
GENERAL ELECTRIC	FLOATING SUBSTRATE GROWTH (CHEMICAL VAPOR DEPOSITION ON LIQUID TIN)
UNIV. OF PENN,	HOT-FORMING OF SILICON
*FROM ZOUTENDYK (1)	

Table 2. Current Silicon Sheet Growth Research in U.S. Program

PROCESS	LABORATORY	FUNDING
EDGE-DEFINED FILM-FED GROWTH (EFG)	MOBIL SOLAR ENERGY CORP.	DOE-JPL (PARTIAL)
DENDRITIC WEB	WESTINGHOUSE ELECTRIC CORP.	DOE-JPL (PARTIAL)
LOW-ANGLE SILICON SHEET (LASS)	ENERGY MATERIALS CORP.	DOE-SERI (PARTIAL)
EDGE-SUPPORTED PULLING (ESP)	SERI	DOE-JPL-SERI
EDGE-STABILIZED RIBBON (ESR)	ARTHUR D. LITTLE	DOE-SERI (PARTIAL)

Table 3. Silicon Ribbon Growth Data

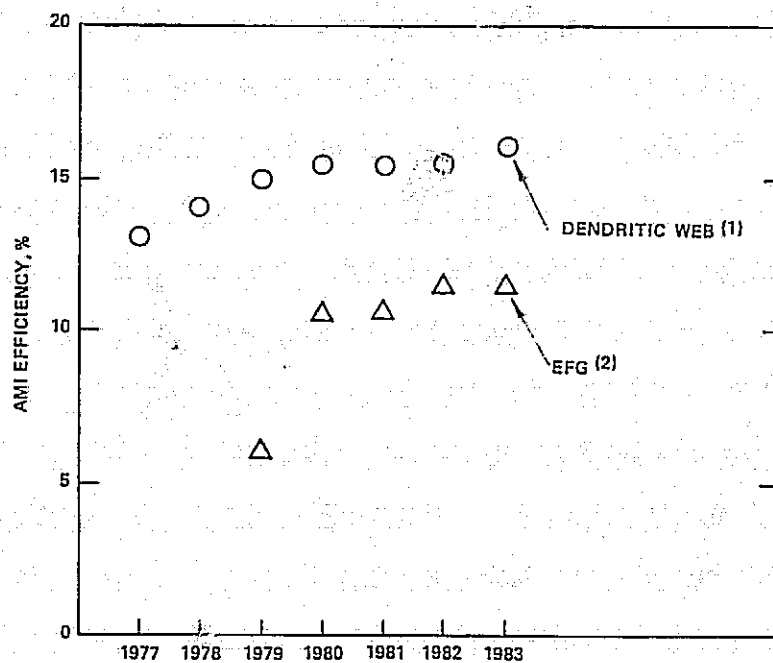
	THICKNESS, $\mu\text{m}$	WIDTH cm	LENGTH m	LINEAR GROWTH RATE cm/min	AREA GROWTH RATE $\text{cm}^2/\text{min}$	SURFACE	STRUCTURE
ESP ESR	4-400	10	5	18 max 6.8 SUSTAINED	$\approx 70$	RIPPLED, GRAIN BOUNDARIES, TWIN STRIA	FINE GRAINS AT EDGES, LARGE- GRAIN EQUILIBRIUM DEFECT STRUCTURE AT CENTER OF RIBBON
EFG	150-300	10	30	7 max 4.0 SUSTAINED	$\approx 50$ MULTIPLE RIBBON GROWTH	GRAIN BOUND- ARIES TWIN STRIA GROWTH STRIA	TWINS, GRAIN BOUNDARIES, SIC PARTICLES; EQUILIBRIUM DEFECT STRUCTURE
LASS	500-1000	10	34	85 max 30-40 TYPICAL	$\approx 500$ SINGLE RIBBON GROWTH $\approx 600$ MULTIPLE RIBBON GROWTH	COARSE DEN- DRITIC TOP SURFACE, SMOOTH ROUNDED BOTTOM SURFACE	DENDRITIC, RANDOM OR PARALLEL GRAINS, 1-5 mm WIDE, UP TO SEVERAL cm LONG
WEB	150	5.4	5	15 max 2 SUSTAINED	27 TRAN- SIENT 13 QUASI- STEADY STATE 9 SUSTAINED	FLAT, SPECULAR	SINGLE CRYSTAL, TWIN PLANE BUNDLE LIES IN THE PLANE OF THE RIBBON

### FSA Advanced Materials Research Task Advanced Dendritic Growth Development: Development Progress

DEVELOPMENT	1977	1978	1979	1980	1981	1982 EARLY	1982 LATE	1983 PLAN
AREA GROWTH RATE, $\text{cm}^2/\text{min}$								
1) TRANSIENT (LENGTHS OF SEVERAL CENTIMETERS)	2.3	8	23	27	27	27	27	30-35
2) QUASI-STEADY-STATE (LENGTHS OF 30 TO 100 cm)					7	8	13	18-20
3) STEADY-STATE (METERS OF LENGTH, HOURS OF GROWTH)					4	6	8	12-15
MAXIMUM UNDEFORMED WIDTH, CENTIMETERS	2.4	3.5	4.0	4.4	4.4	4.9	5.5	6-7
$W_{150}$ -UNDEFORMED WIDTH AT 150 $\mu\text{m}$ THICKNESS (AN INVERSE MEASURE OF BUCKLING STRESS)		2.0	2.7	3.2	3.2	3.8	4.9	6
MAXIMUM DEMONSTRATED SOLAR CELL EFFICIENCY, AM1	13	14	15	15.5	15.5	15.5	$\sim 16$	17-18

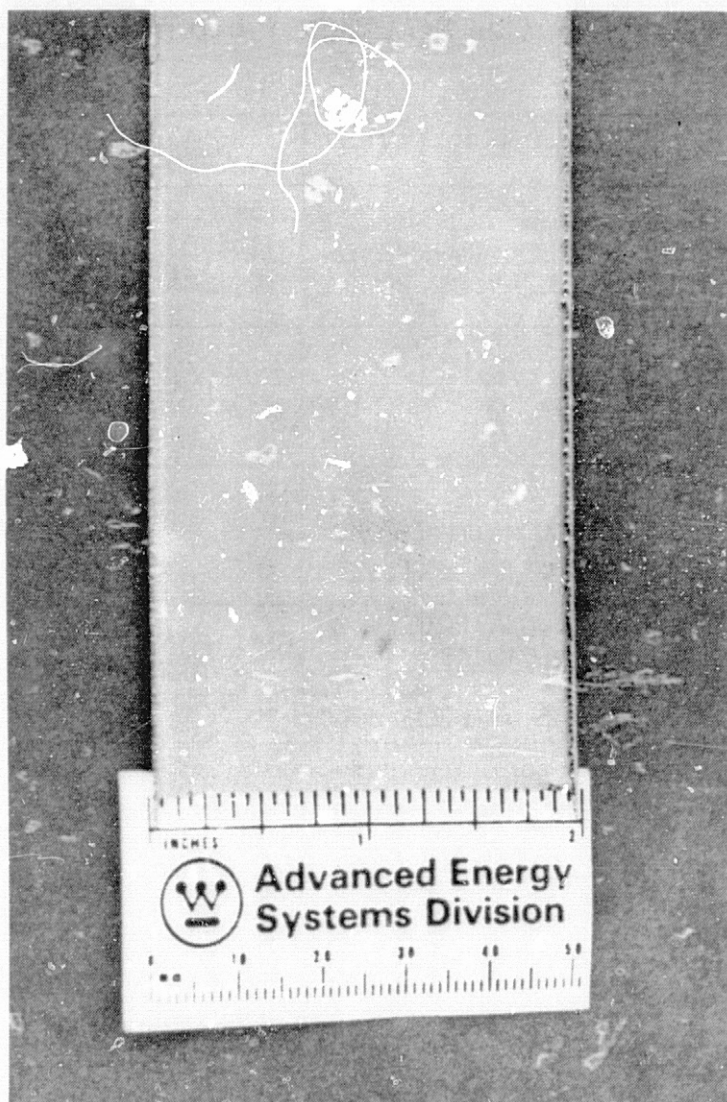


# Ribbon Solar Cell Efficiency Progress



(1) 2 x 2 cm CELLS, HIGHEST CELL EFFICIENCY DATA

(2) DATA FROM 5 cm WIDE SINGLE EFG RIBBON  
GROWN IN PILOT PLANT OPERATION

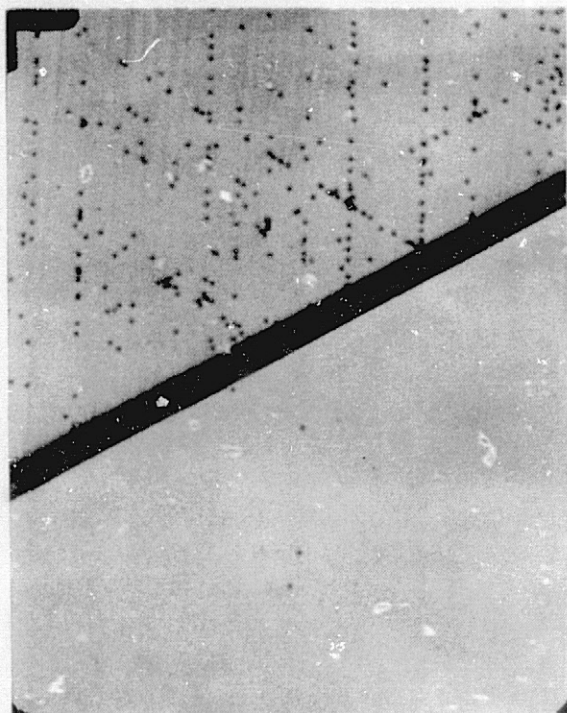


Dendritic Web Silicon Sheet (Westinghouse)

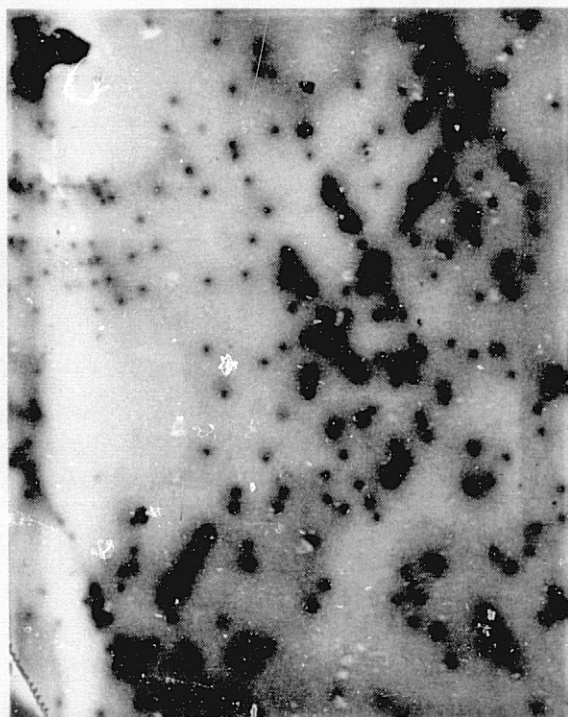
Table 4. Cell & Module Performance\*

	CELL EFFICIENCY ( $\eta$ ) AM1	MODULE EFFICIENCY
ESP/ ESR	1 cm <sup>2</sup> 8.2% MAXIMUM ACHIEVED (vs. 11.7% Cz CONTROL)	-----
(6) EFG	4 cm <sup>2</sup> 5 cm <sup>2</sup> > 50 cm <sup>2</sup> 14% 13% 11-12%	17 1/8" x 42 1/8" MODULE (34) 10% MAXIMUM
(32) LASS	4 cm <sup>2</sup> 12.0% MAXIMUM ACHIEVED 10.5% AVE.	-----
(33) WEB	≥ 16% REGULARLY ACHIEVED IN LABORATORY 8-10 cm <sup>2</sup> PRODUCTION LINE 13.3% AVE.	16" x 48" MODULE 12.4% MAXIMUM ACHIEVED 11.5% AVERAGE

\* RIBBON MODULES ARE IN PRODUCTION ONLY AT MOBIL SOLAR AND WESTINGHOUSE AND ARE COMMERCIALY AVAILABLE ONLY FROM MOBIL SOLAR.



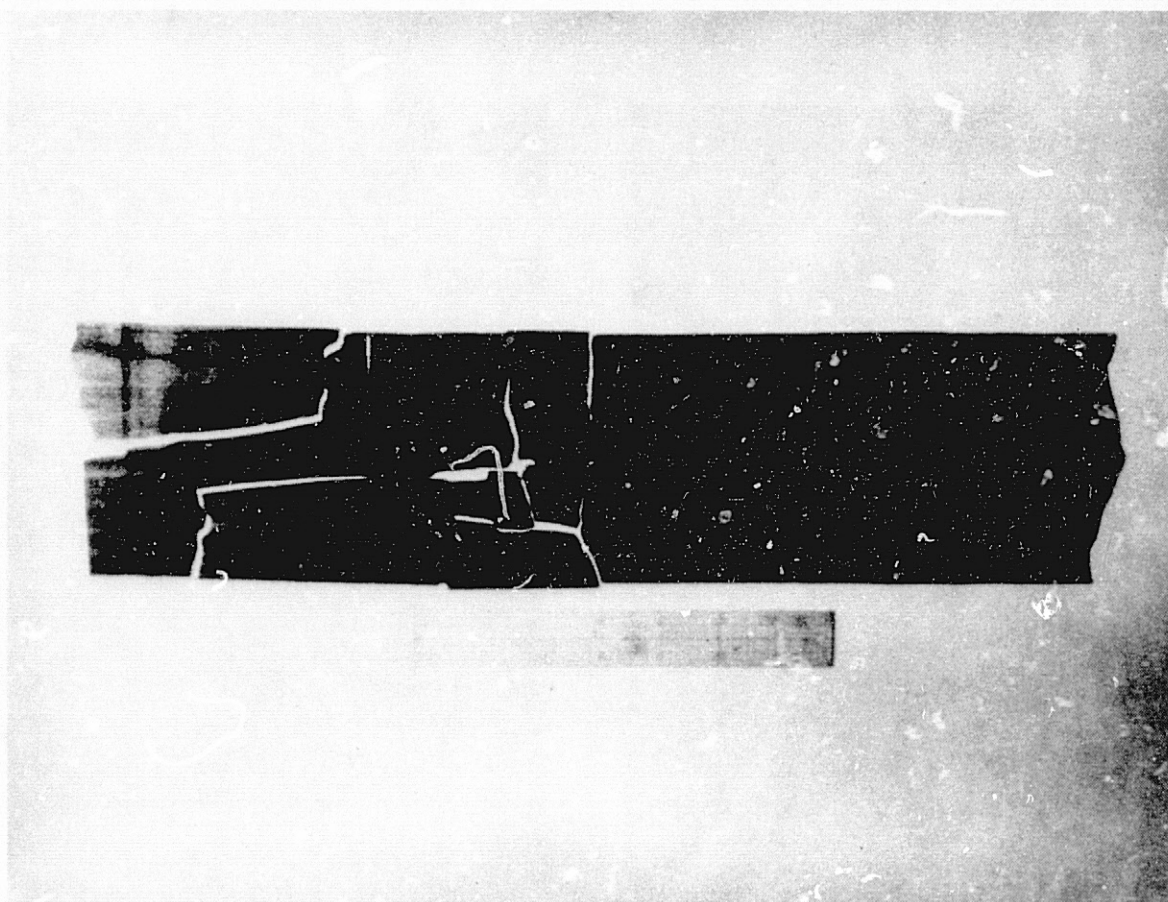
(a)



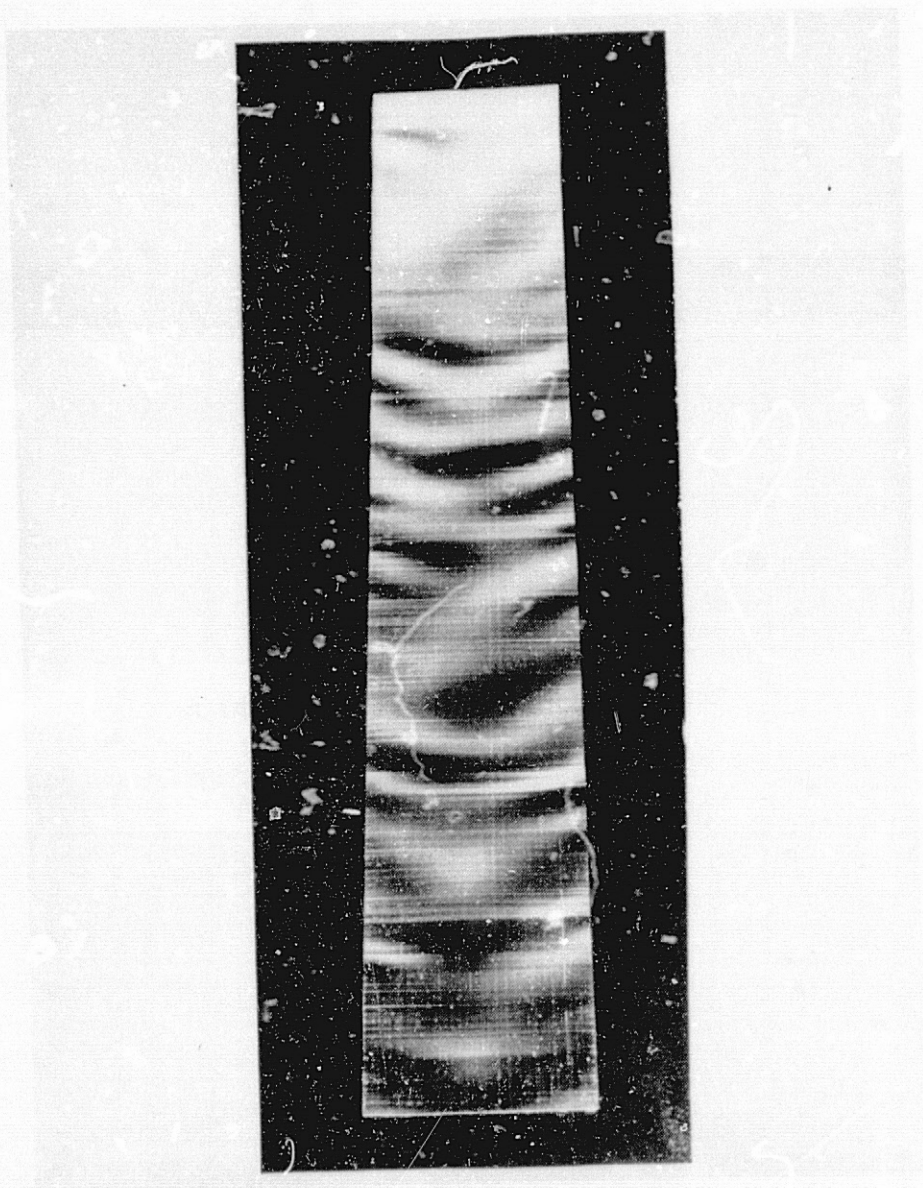
(b)

Dislocations Along (111) Slip Planes on Dendritic Web Delineated By Etch Pits (a) and Low-Temperature EBIC (b)



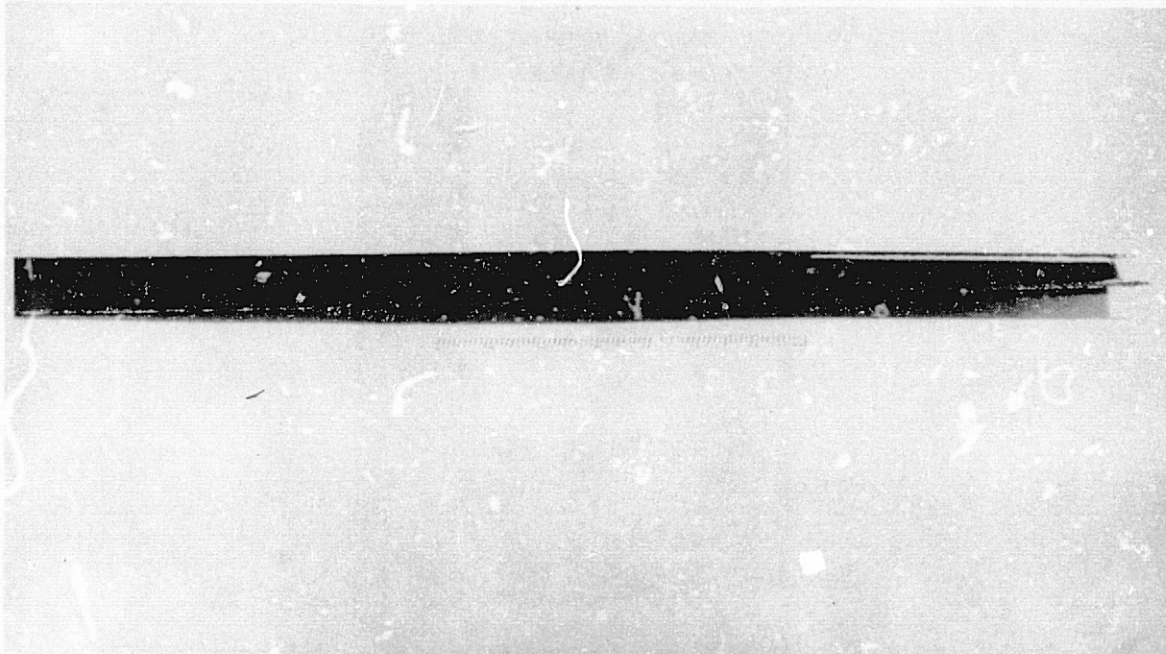


Catastrophic Failure Due to Residual Stresses  
in Silicon Ribbon

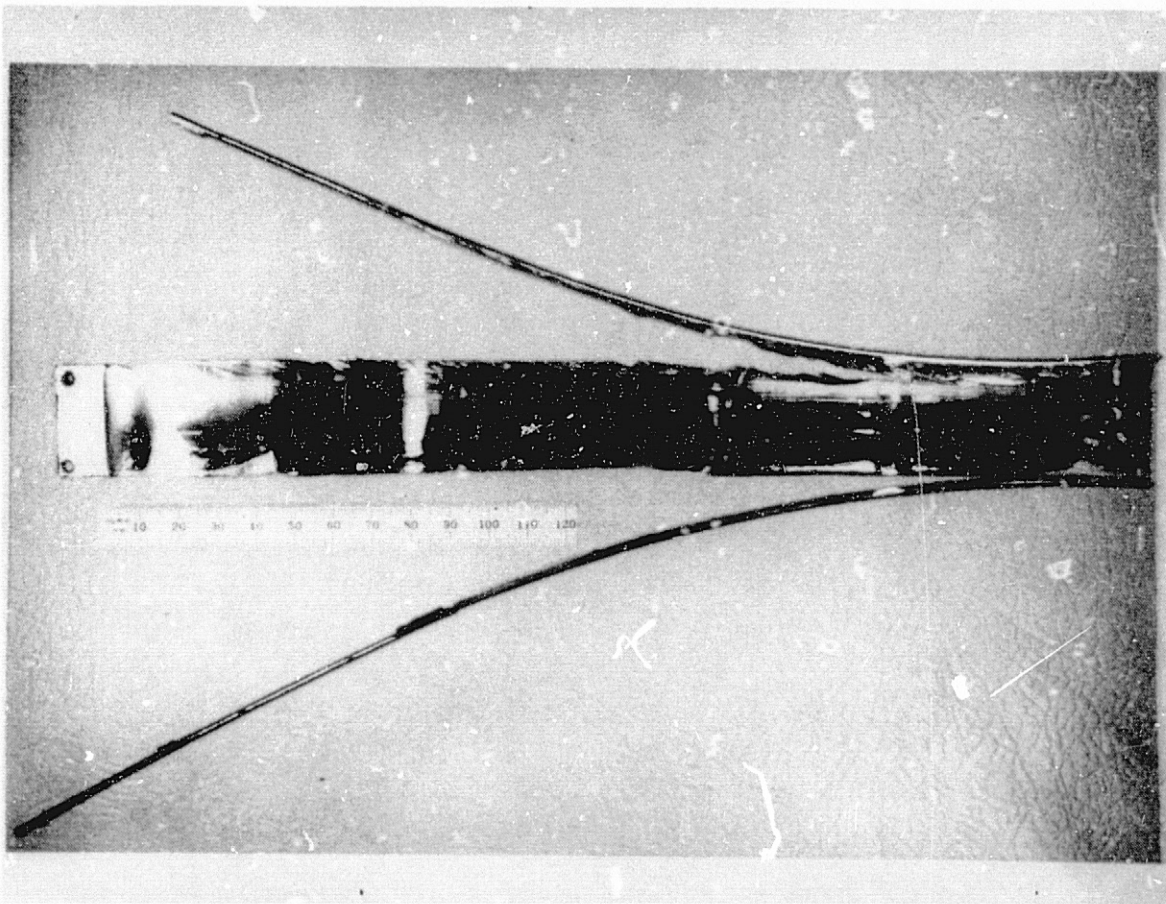


Silicon Ribbon Buckled Due to Stresses Occurring  
During the Growth Process





Torsionally Buckled Silicon Ribbon



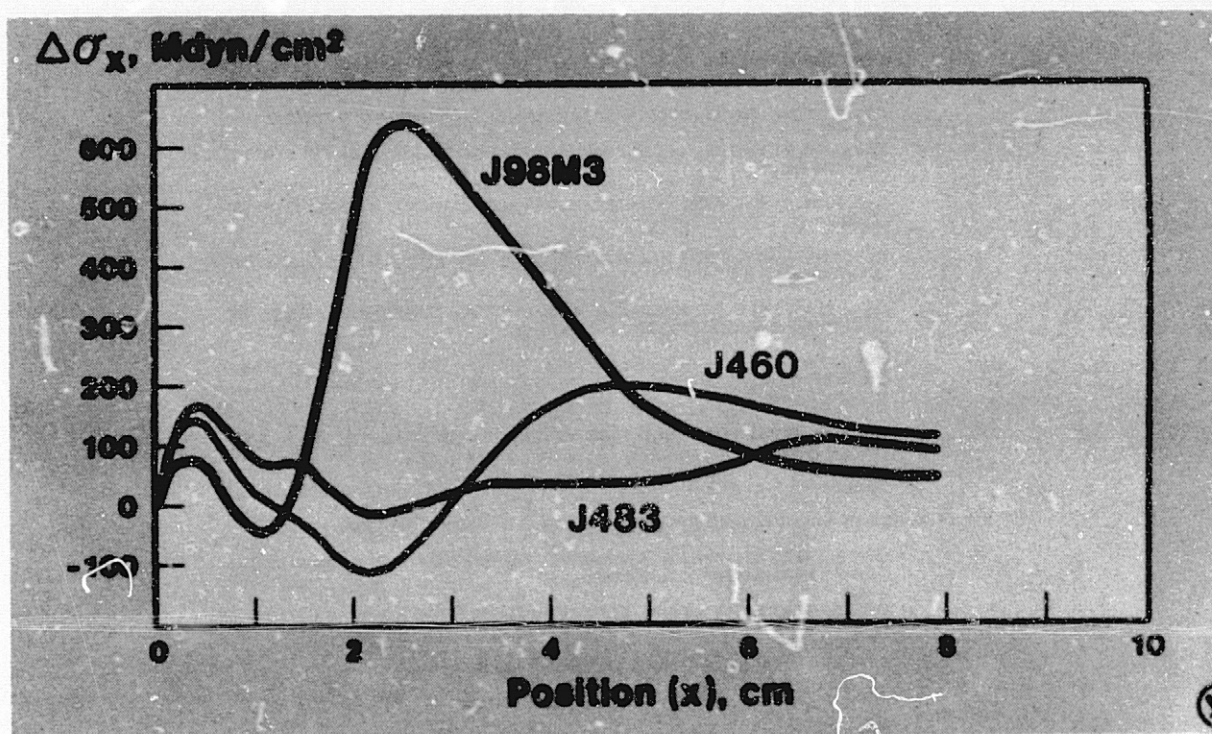
Ribbon Failure Due to the Difference in Coefficient of Thermal Expansion Between Ribbon and Filaments (ESP Process: Ciszek, SERI)

## Areas of Concern and Research

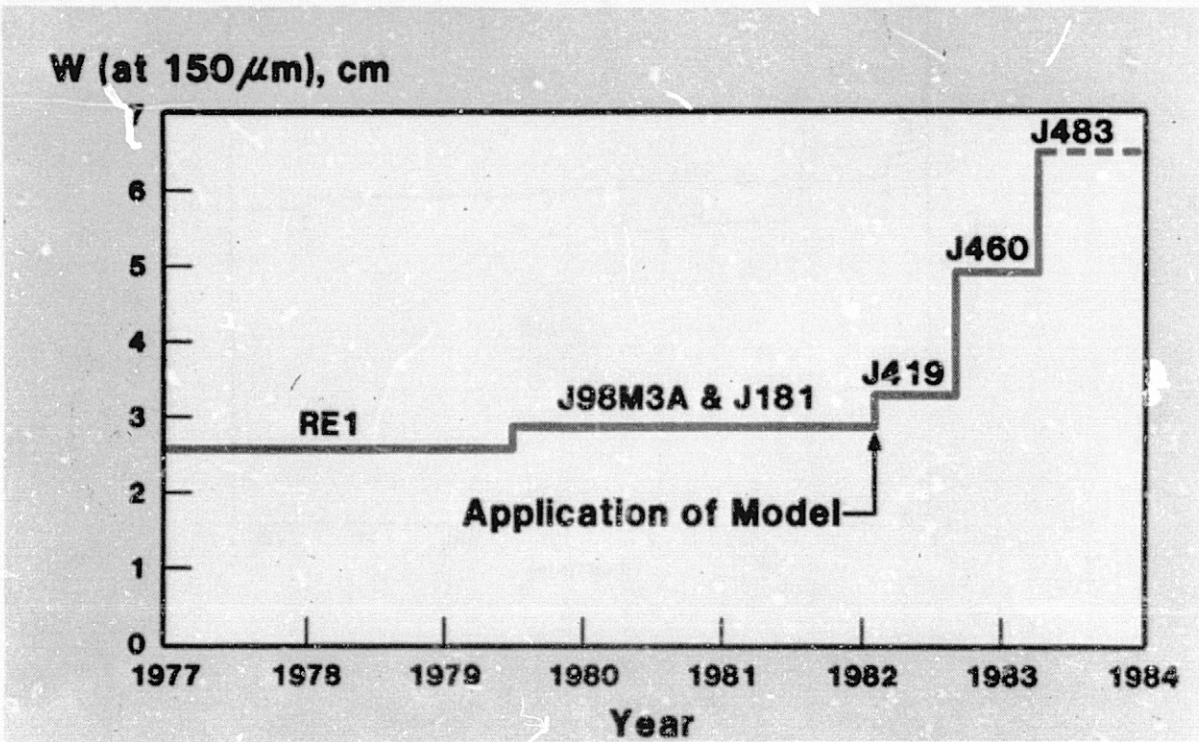
- STRESS AND STRAIN IN WIDE THIN RIBBONS GROWN AT HIGH SPEEDS
  - DEVELOP METHODS OF MEASURING THERMAL FIELDS IN GROWING RIBBONS
  - DEVELOP METHODS OF MEASURING RESIDUAL STRESS IN RIBBONS
  - DEVELOP METHODS OF OBSERVING RIBBON DEFORMATION ON A REAL-TIME BASIS
  - MEASURE THE HIGH TEMPERATURE MECHANICAL PROPERTIES OF SILICON
  - DEVELOP MODELS FOR PLASTIC DEFORMATION AND ELASTIC BUCKLING IN GROWING RIBBONS
  - VERIFY MODELS BY RELATING THE OBSERVED THERMAL FIELDS TO OBSERVED RIBBON STRESS AND STRAIN
  - USE VERIFIED MODELS TO DEFINE RIBBON THERMAL FIELDS AND GROWTH DYNAMICS THAT WILL YIELD LOW STRESS GROWTH ENVIRONMENTS
  - MODIFY PRESENT RIBBON GROWTH PROCESSES TO USE THE DATA OBTAINED ABOVE
  - DESIGN, FABRICATE AND TEST LOW-STRESS RIBBON GROWTH SYSTEMS
- IMPURITY EFFECTS AND INTERFACE STABILITY IN RIBBON GROWTH
  - MODEL HEAT FLOW AND INTERFACE STABILITY CRITERIA FOR RIBBONS GROWN IN THE VERTICAL MODE
  - MODEL HEAT FLOW AND INTERFACE STABILITY FOR RIBBONS GROWN IN THE HORIZONTAL MODE
  - EXPERIMENTALLY TEST AND VERIFY MODELS
- MATERIAL PERFECTION AND DEVICES PERFORMANCE
  - CHARACTERIZE RIBBON MATERIAL GROWN UNDER VARIOUS CONDITIONS
  - FABRICATE BASE-LINE CELLS ON RIBBONS GROWN UNDER VARIOUS GROWTH PROCESS CONDITIONS
  - RELATE CELL PERFORMANCE TO RIBBON GROWTH PROCESS VARIABLES AND SPECIFIC DEFECTS
  - OPTIMIZE GROWTH PROCESSES WHICH COMPENSATE FOR SPECIFIC RIBBON DEFECTS
  - FEED DEFECT DATA BACK TO THE GROWTH PROCESS TO REDUCE OR ELIMINATE DEFECTS WHICH ADVERSELY AFFECT CELL PERFORMANCE.



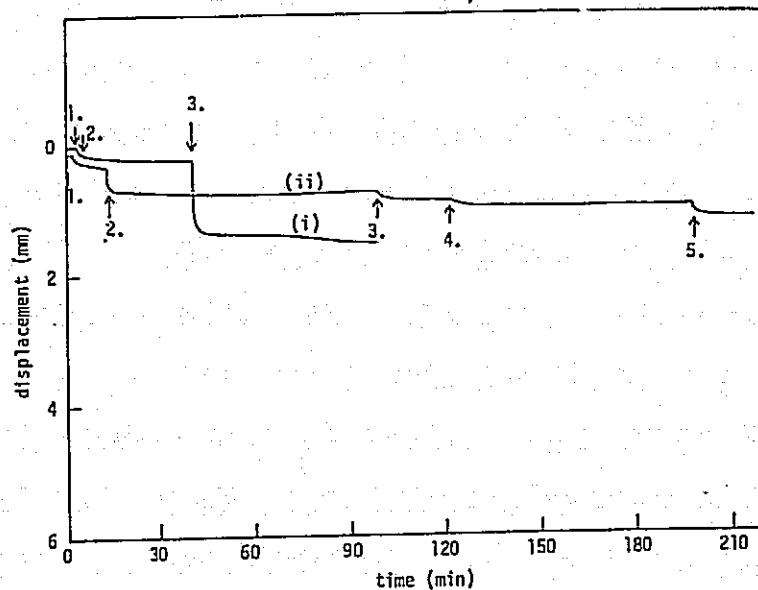
# Comparison of $\Delta \sigma_x$ for Three Web Growth Geometries



# Undeformed Web Width



## Stress Loading Conditions



### Load - Curve (i) (1215°C)

1.	27.0 g
2.	46.0 g
3.	90.0 g

### Load - Curve (ii) (1360°C)

1.	51.5 g
2.	81.0 g
3.	100.0 g
4.	118.0 g
5.	137.0 g

## Key Technical Issues

### • THROUGHPUT

LINEAR GROWTH RATE/AREAL THROUGHPUT

STRESS AND STRAIN PHENOMENA

INTERFACE STABILITY/IMPURITY REDISTRIBUTION

### • QUALITY

CRYSTAL PERFECTION/DEFECT CHARACTER

IMPURITY CONCENTRATION AND DISTRIBUTION

# HIGH-SPEED GROWTH AND CHARACTERIZATION OF CRYSTALS FOR SOLAR CELLS RESEARCH FORUM: SUMMARY

JET PROPULSION LABORATORY

Katherine A. Dumas

## Silicon Sheet Technology Objective\*

"THE OBJECTIVE OF SILICON SHEET RESEARCH IS TO RESOLVE GENERIC  
IMPEDIMENTS TO IMPROVE RIBBON GROWTH SPEED AND QUALITY."

---

\*FIVE YEAR RESEARCH PLAN, 1984-1988  
NATIONAL PHOTOVOLTAIC PROGRAM  
U. S. DEPARTMENT OF ENERGY

## Barriers Associated With Increased Growth Rates

- 1) HEAT FLOW LIMITS GROWTH VELOCITY
- 2) INCREASED CRYSTAL DEFECTS
- 3) DEGRADED DEVICE PERFORMANCE

## Forum Objectives

- ASSESS THE STATE - OF - THE - ART
- ADDRESS THE TECHNICAL BARRIERS
- DEFINE FUTURE AREAS OF RESEARCH

## Forum Statistics

- 68 ATTENDEES
- 35 TECHNICAL PAPERS
  - 16 INDUSTRY
  - 13 UNIVERSITY
  - 6 GOVERNMENT LABS
- 4 INTERNATIONAL PRESENTATIONS (ENGLAND, GERMANY, JAPAN)
- 8 SESSIONS

## Agenda

	MONDAY	TUESDAY	WEDNESDAY
8:00 AM - 12:00 PM	SESSION I OVERVIEW	SESSION IV RIBBON GROWTH	SESSION VII MATERIAL CHARACTERIZATION
1:00 PM - 5:30 PM	SESSION II THEORY OF CRYSTAL GROWTH	SESSION V STRESS/STRAIN EFFECTS IN RIBBON	SESSION VIII INGOT GROWTH AND CHARACTERIZATION
7:30 PM - 10:00 PM	SESSION III MELT SPINNING	SESSION VI LASER RECRYSTALLIZATION	



## Presentations

### SESSION I: OVERVIEW

K. KOLIWAD, JPL (CHAIRMAN)

HIGH SPEED GROWTH OF SILICON CRYSTALS:

FSA PROJECT PERSPECTIVE

K. KOLIWAD (JPL)

IS THERE A SPEED LIMIT?

B. CHALMERS (HARVARD UNIVERSITY)

OVERVIEW OF BULK SILICON SINGLE CRYSTAL GROWTH

J. MOODY (MONSANTO CO.)

CRYSTALLIZATION OF SILICON RIBBONS

M. LEIPOLD (JPL)

OVERVIEW OF CHARACTERIZATION APPROACHES FOR HIGH  
SPEED CRYSTAL GROWTH

K. RAVI (MOBIL SOLAR ENERGY CORPORATION)

### SESSION II: THEORY OF CRYSTAL GROWTH

W. WILCOX, CLARKSON COLLEGE OF TECHNOLOGY (CHAIRMAN)

NON-EQUILIBRIUM PROCESSES IN CRYSTAL GROWTH

R. SEKERKA (CARNEGIE MELLON UNIVERSITY)

TRANSPORT PROCESSES IN DENDRITIC CRYSTALLIZATION

M. GLICKSMAN (RENSSELAER POLYTECHNIC INSTITUTE)

USE OF THE BURTON-PRIM-SLICHTER EQUATION AT HIGH  
GROWTH RATES

W. WILCOX (CLARKSON COLLEGE OF TECHNOLOGY)

COMPUTER MODELS OF RAPID SOLIDIFICATION

G. GILMER (BELL LABORATORIES)

THE EFFECT OF GROWTH RATE ON INTERFACE MORPHOLOGY

R. TRIVEDI (IOWA STATE UNIVERSITY)

PLENARY SESSION

SESSION III: MELT SPINNING

D. AST, CORNELL UNIVERSITY (CHAIRMAN)

RAPIDLY SOLIDIFIED ALLOYS MADE BY CHILL BLOCK  
MELT-SPINNING PROCESSES

H. LIEBERMANN (METGLAS PRODUCTS)

POLYCRYSTALLINE SILICON SHEET BY THE IMPROVED  
SPINNING METHOD

Y. MAEDA (HOXAN CORPORATION)

RAPID SOLIDIFICATION PROCESSING (RSP) TECHNOLOGY  
(AS APPLIED TO METALS AND SOME CERAMICS)

W. GIESSEN (NORTHEASTERN UNIVERSITY)

SESSION IV: RIBBON GROWTH

M. LEIPOLD, JPL (CHAIRMAN)

ORIENTATION AND MORPHOLOGY EFFECTS IN RAPID SILICON  
SHEET SOLIDIFICATION

T. CISZEK (SOLAR ENERGY RESEARCH INSTITUTE)

SILICON FOILS GROWN BY INTERFACE - CONTROLLED  
CRYSTALLIZATION

D. HELMREICH (WACKER - HELIOTRONIC)

THE S-WEB-TECHNIQUE FOR HIGH-SPEED GROWTH OF  
SI-SHEETS

J. GRABMAIER (SIEMENS AG)

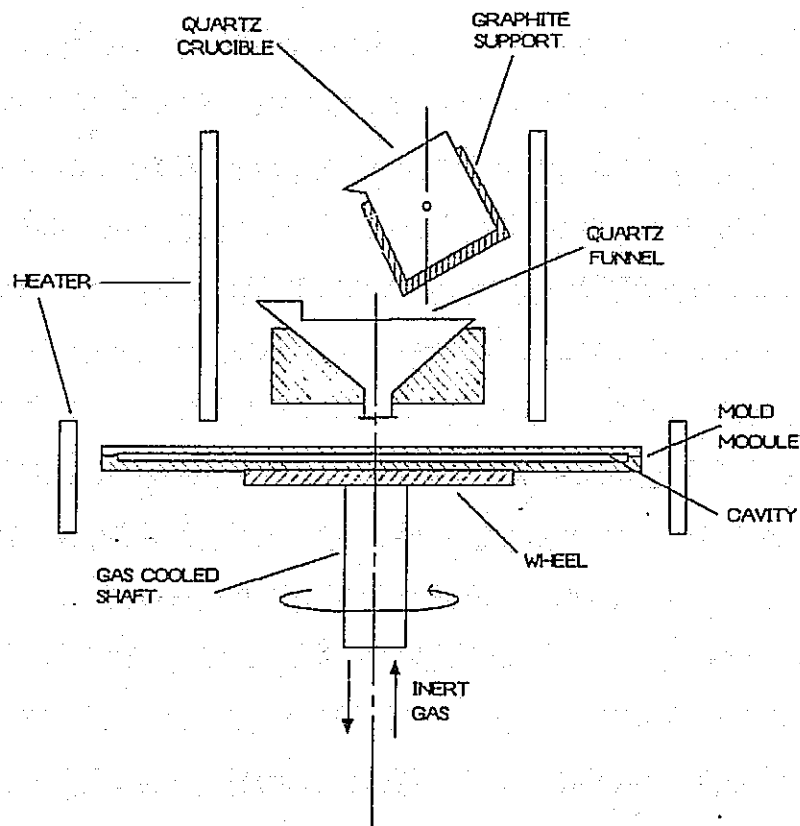
EDGE STABILIZED RIBBON: STRESS DISLOCATION DENSITY  
AND ELECTRONIC PERFORMANCE

E. SACHS (ARTHUR D. LITTLE, INC.)

LOW ANGLE SILICON SHEET GROWTH: A REVIEW OF  
PROGRESS, PROBLEMS AND PROMISE

H. BATES (ENERGY MATERIALS CORPORATION)

## Setup for Producing Sheet by the Improved Spinning Method\*



\*This technique is being developed by the Hoxan Corp. in Japan.



Table 1. Characteristics of Silicon Sheets \*

Growth rate	: 4 sheets per 15 seconds.
Size	: 50mm x 50mm.
Minimum thickness	: 0.1 mm.
Crystal structure	: Polycrystalline and dendritic.
Grain size	: 1 - 10 mm.
Resistivity	: 0.7 - 1.2 $\Omega$ cm.
Carrier lifetime	: 1.0 - 1.3 $\mu$ sec.

Table 2. PV Properties Under AM1.5 100 mW/cm<sup>2</sup> 28°C \*

Area	Open-circuit voltage (V)	Short-circuit current (mA/cm <sup>2</sup> )	FF	Efficiency (%)
2x2 cm	0.564	24.95	0.712	10.02
5x5	0.562	25.20	0.670	9.50
5x5	0.560	24.20	0.690	9.35
5x5	0.564	25.00	0.652	9.18

\*Tables 1 and 2 describe solar-cell results characteristic of the material produced by the spinning method developed by Hoxan Corp.

## Presentations (Cont'd)

### SESSION V: STRESS/STRAIN EFFECTS IN RIBBON

O. DILLON, UNIVERSITY OF KENTUCKY (CHAIRMAN)

MATHEMATICAL MODELLING OF HIGH-SPEED RIBBON SYSTEM:

A CASE STUDY OF EDGE-DEFINED FILM-FED GROWTH

R. BROWN (MASSACHUSETTS INSTITUTE OF TECHNOLOGY)

THERMAL BUCKLING OF SILICON SHEET

O. DILLON (UNIVERSITY OF KENTUCKY)

EXPERIMENTAL ASPECTS OF THE STUDY OF STRESS

GENERATING MECHANISMS IN SILICON SHEET GROWTH

J. KALEJS (MOBIL SOLAR ENERGY CORPORATION)

THE EFFECT OF CREEP ON THE RESIDUAL STRESSES

GENERATED DURING SILICON SHEET GROWTH

J. LAMBROPOULOS (HARVARD UNIVERSITY)

CONTROL OF THERMAL STRESS IN DENDRITIC WEB GROWTH

R. SEIDENSTICKER (WESTINGHOUSE R&D CENTER)

### SESSION VI: LASER RECRYSTALLIZATION

J. FAN, LINCOLN LABORATORY (CHAIRMAN)

HIGH SPEED CRYSTAL GROWTH BY Q-SWITCHED LASER  
MELTING

A. CULLIS (ROYAL SIGNALS AND RADAR ESTABLISHMENT)

HIGH-QUALITY SILICON FILMS PREPARED BY ZONE-MELTING  
RECRYSTALLIZATION

C. CHEN (LINCOLN LABORATORY)

NONEQUILIBRIUM CRYSTAL GROWTH DURING LASER  
ANNEALING OF SILICON

C. WHITE (OAK RIDGE NATIONAL LABS)

PLENARY SESSION

SESSION VII: MATERIAL CHARACTERIZATION

J. MILSTEIN, SOLAR ENERGY RESEARCH INSTITUTE (CHAIRMAN)

STRUCTURAL CHARACTERIZATION OF SOLAR SILICON  
D. AST (CORNELL UNIVERSITY)

A HIGH-SPEED CHARACTERIZATION TECHNIQUE FOR  
SOLAR SILICON  
J. GRABMAIER (SIEMENS AG)

DEFECTS IN HIGH SPEED GROWTH OF EFG SILICON RIBBON  
H. RAO (MOBIL SOLAR ENERGY CORPORATION)

ELECTRICAL AND STRUCTURAL CHARACTERIZATION OF  
WEB-DENDRITE  
G. SCHWUTKE (ARIZONA STATE UNIVERSITY)

REAL TIME X-RAY DIFFRACTION: APPLICATIONS TO  
MATERIALS CHARACTERIZATION  
R. ROSEMEIR (BRIMROSE CORPORATION OF AMERICA)

SESSION VIII: INGOT GROWTH AND CHARACTERIZATION

R. LANE, KAYEX CORP. (CHAIRMAN)

X-RAY TOPOGRAPHIC METHODS AND APPLICATION TO  
ANALYSIS OF MICROELECTRONIC MATERIALS  
W. MAYO (RUTGERS UNIVERSITY)

MAXIMIZATION OF GROWTH RATES DURING CZOCHRALSKI  
PULLING  
M. WARGO (MASSACHUSETTS INSTITUTE OF TECHNOLOGY)

SEGREGATION OF IMPURITIES IN DIRECTIONAL  
SOLIDIFICATION OF SILICON  
P. RAVISHANKAR (EXXON RESEARCH AND ENGINEERING CO.)

EFFECTS OF NON-EQUILIBRIUM SOLIDIFICATION ON THE  
MATERIAL PROPERTIES OF BRICK SILICON FOR  
PHOTOVOLTAICS  
W. REGNAULT (SEMIX CORP.)

## Conclusions

- THERE IS A PRACTICAL SPEED LIMIT
- VERY LITTLE UNDERSTOOD ABOUT STRESS/STRAIN EFFECTS
- THE UNDERSTANDING IS NECESSARY TO DEFINE THE LIMIT

## Future Areas of Research

1. STRESS/STRAIN IN WIDE THIN RIBBON
2. IMPURITY EFFECTS AND INTERFACE STABILITY
3. MATERIAL QUALITY AND DEVICE PERFORMANCE

# QUANTITATIVE PROCESS CONTROL

## JET PROPULSION LABORATORY

M.H. Leipold

### Process Development

- Assessment
- Process selection
- Process development
- Proof of performance
- Acceptance by industry

### Effect of Process Yields on Costs (per Cell Basis)

Sheet Processing Step	Yield Values					
	Unity	2.80 Watt	$\Delta 1$	$\Delta 2$	$\Delta 3$	$\Delta 4$
Clean	1.0	0.994	0.99	0.99	0.98	0.97
Dry	1.0	0.999	0.99	0.99	0.98	0.98
Diffuse junction	1.0	0.988	0.98	0.97	0.96	0.95
Aluminum BSF	1.0	0.99	0.98	0.96	0.95	0.93
Clean back	1.0	0.995	0.99	0.98	0.97	0.96
Print Ag back	1.0	0.99	0.98	0.97	0.97	0.96
Print Ag front	1.0	0.99	0.98	0.97	0.96	0.94
Laser cut	1.0	1.0	0.99	0.99	0.98	0.97
Test and sort	1.0	0.95	0.94	0.93	0.92	0.9
Cell layup	1.0	1.0	0.99	0.98	0.97	0.96
(Prepare mat'l)	1.0	1.0	1.0	1.0	1.0	1.0
Layup	1.0	0.999	0.99	0.98	0.97	0.96
Form module	1.0	0.998	0.99	0.98	0.97	0.96
Trim seal	1.0	0.999	0.99	0.99	0.99	0.98
Final test	1.0	0.99	0.98	0.98	0.97	0.94
Crate module	1.0	0.999	0.995	0.995	0.99	0.98
Cumulative yield	1.0	0.89	0.78	0.70	0.63	0.51

Step	Yield Values					
	Unity	2.80 Watt	$\Delta 1$	$\Delta 2$	$\Delta 3$	$\Delta 4$
Cumulative yield	1.0	0.89	0.78	0.70	0.63	0.51
Sheet cost	1.68	1.68	1.68	1.68	1.68	1.68
Process value added	0.96	0.96	0.96	0.96	0.96	0.96
Process value lost	0.0	0.25	0.56	0.81	0.14	1.82
Module cost	2.64	2.89	3.20	3.45	3.79	4.45

### Approaches to Proof of Performance

- Demonstration
  - Large scale
  - Resource limitations
  - Program limitations
- Interference
  - Limited scale
  - Resource-conservative
  - Minor program adjustment
- Synergistic process steps

### Process Design

Structure is a function of process

$$S_i = f[\sum(p_i)]$$

$$\left. \frac{\delta S_n}{\delta p_n} \right|_i = \text{Process sensitivity}$$

Detectability

## Cell Design

Efficiency is a function of structure

$$\eta = f(\sum(S_i))$$

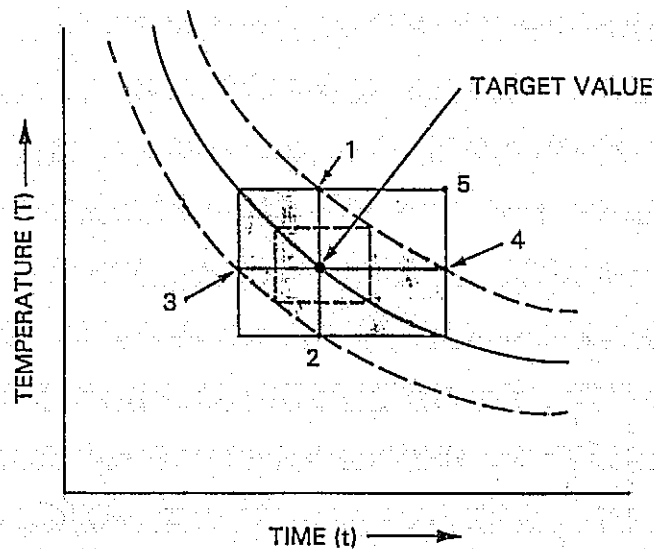
$$\left. \frac{\delta \eta}{\delta S_n} \right|_i = \text{Device sensitivity}$$

## Unified Model

Efficiency is a function of structure, which is a function of process

$$\eta = f\{ \sum |S_i(p_i)| \}$$

## Time-Temperature Relationship in a Process



## Typical Processes Requiring Sensitivity Data

- Back-surface field
- Hydrogen passivation
- Metallization-junction interaction
- Metallization integrity
- Junction isolation
- Sheet condition and breakage
- Junction formation



# METALLIZATION RESEARCH FORUM: SUMMARY

JET PROPULSION LABORATORY

B. D. Gallagher

## Research Forum Objectives

- To determine future metallization thrusts
  - Assess state of the art
  - Analyze system characteristics
  - Explore innovative ideas

## Audience and Speaker Mix

	Audience	Speakers
Industrial	36 (55%)	10 (44%)
Government	19 (29%)	8 (34%)
Universities	10 (16%)	5 (22%)
Totals	65	23

## Project Constraints

- Economic
  - Module \$0.70/watt
  - Metallization Variable
- Reliability
  - Module 30 years
  - Metallization Compatible
- Efficiency
  - Module 12% at NOC
  - Metallization Compatible

## Session I: Status of PV Metallization Systems

M. Wolf (University of Pennsylvania), Chairman

- Solar-Cell Metallization: Historical Perspective  
W. Taylor (Photowatt International)
- Economic Implication of Current Systems  
R. Daniel (JPL)
- Accelerated Degradation of Silicon Metallization Systems  
J. Lathrop (Clemson University)
- Field-Test Experience  
R. Weaver (JPL)
- Fundamentals of Semiconductor Metal Contacts  
D. Schroder (Arizona State University)

## Session II: Metallization System Design

D. Burger (JPL), Chairman

HANDOUT: "Getting the Current Out," D. Burger (JPL)

- A Microelectronic Test Structure for Interfacial Contact Resistance Measurement  
L. Linholm (National Bureau of Standards)
- Diffusion Barriers  
M. Nicolet (California Institute of Technology)
- Observation of Solar-Cell Metallization Corrosion  
G. Mon (JPL)
- Module Degradation Catalyzed by Metal Encapsulant Reactions  
B. Gallagher (JPL)
- Metallization Problems with Concentrator Cells  
P. Iles (Applied Solar Energy Corp.)
- Additional Discussion of Sessions I and II

### Session III: Thick-Film Metallization Systems

J. Parker (Electrlink, Inc.), Chairman

- Effects of Particle Size Distribution in Thick Film Conductor  
R. Vest (Purdue University)
- Particle Size Effects on Viscosity of Silver Pastes--A Manufacturer's View  
J. Provance (Thick Film Systems, Div. of Ferro Corp.)
- Non-Noble Metal-Based Metallization Systems  
A. Garcia (Spectrolab, Inc.)
- Polymer Thick Film Conductor and Dielectrics for Membrane Switches and Flexible Circuitry  
N. Nazarenko (du Pont)

### Session IV: Advanced Techniques

R. Landel (JPL), Chairman

- Ionized Cluster Beam Deposition  
A. Kirkpatrick (Eaton Ion Implantation Systems)
- Metallization with Generic Metallo-Organic Inks  
G. Vest (Purdue University)
- Dry Etching of Metallizations  
D. Bollinger (VEECO)
- Laser Assisted Deposition  
S. Dutta (Westinghouse R&D)

### Session V: Future Metallization Challenges

G. Schwuttke (Consultant), Chairman

- Transparent Conductive Coatings  
S. Ashok (Pennsylvania State University)
- A Metallization System for Thin Film Photovoltaic Modules  
A. Firester (RCA Laboratories)
- Ion-Copper Metallization for Flexible Arrays  
H. Lavendel (Lockheed Palo Alto Research Laboratory)

## Research Forum Summary

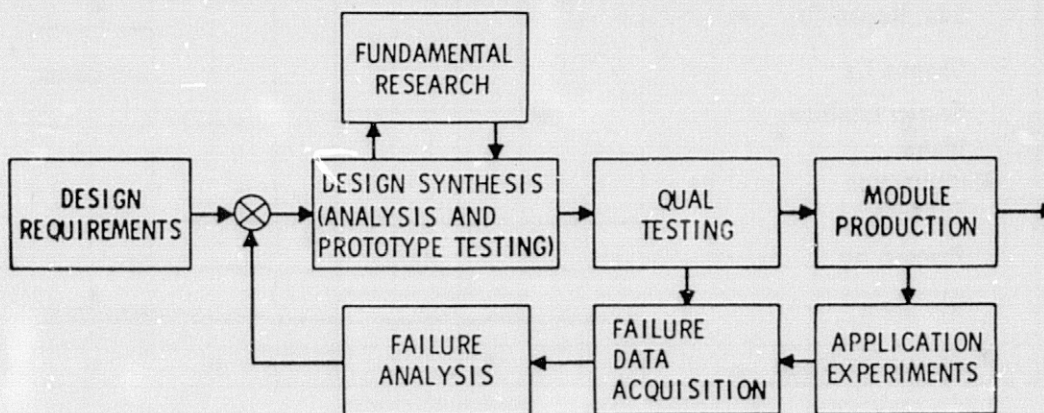
- **Information exchange excellent**
- **Project constraints are synergistic**
- **Process, as well as material, is a real variable**
- **Modes vs mechanisms**
- **Metallization system R&D required**
  - **RFP**
  - **Unsolicited proposals**

# TECHNICAL CHALLENGES OF FUTURE MODULES AND ARRAYS

JET PROPULSION LABORATORY

R.G. Ross, Jr.

## Module Research Approach (Closed-Loop Process)

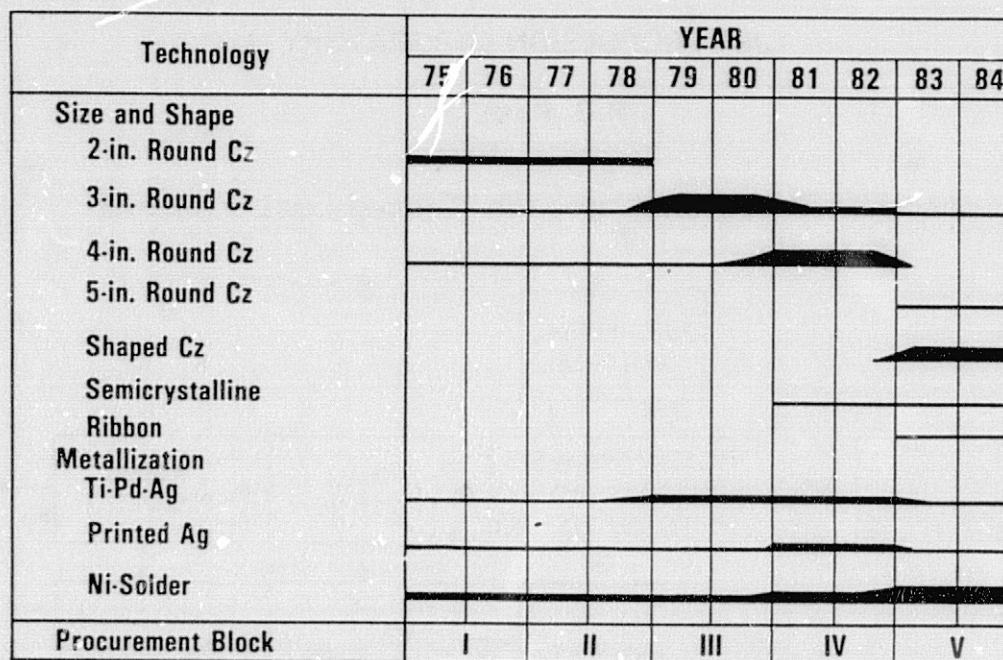


### APPROACH

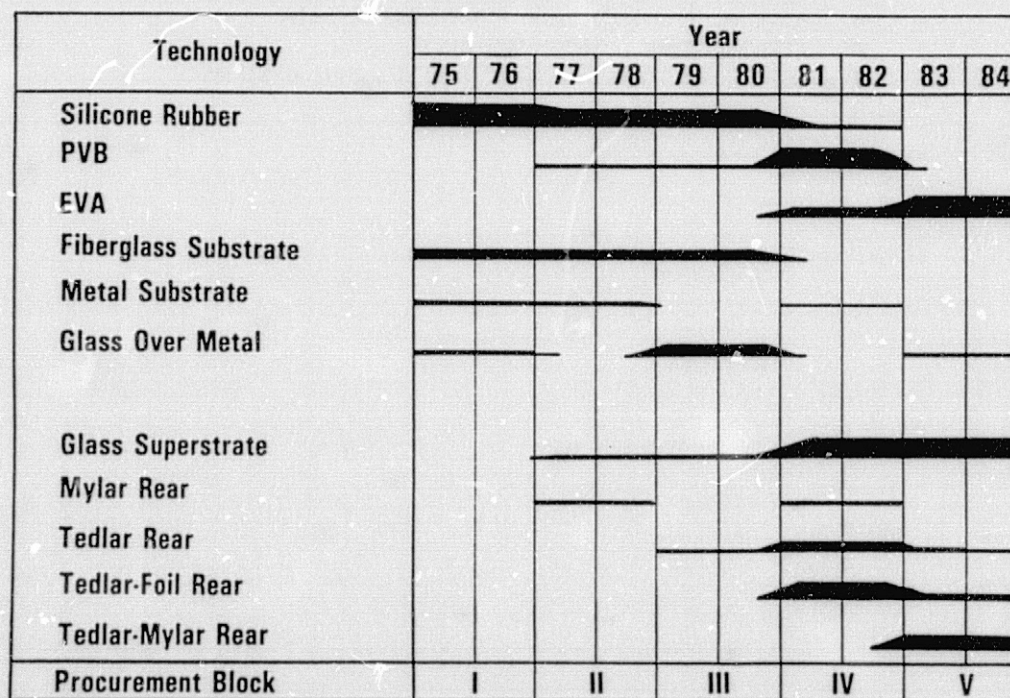
- SPECIFY REQUIREMENTS
- SYNTHESIZE DESIGNS
- SCREEN DESIGNS USING QUAL TESTS
- ACQUIRE AND FEED BACK PERFORMANCE DATA
- PERFORM FUNDAMENTAL RESEARCH
- USE FEEDBACK AND RESEARCH TO IMPROVE DESIGNS



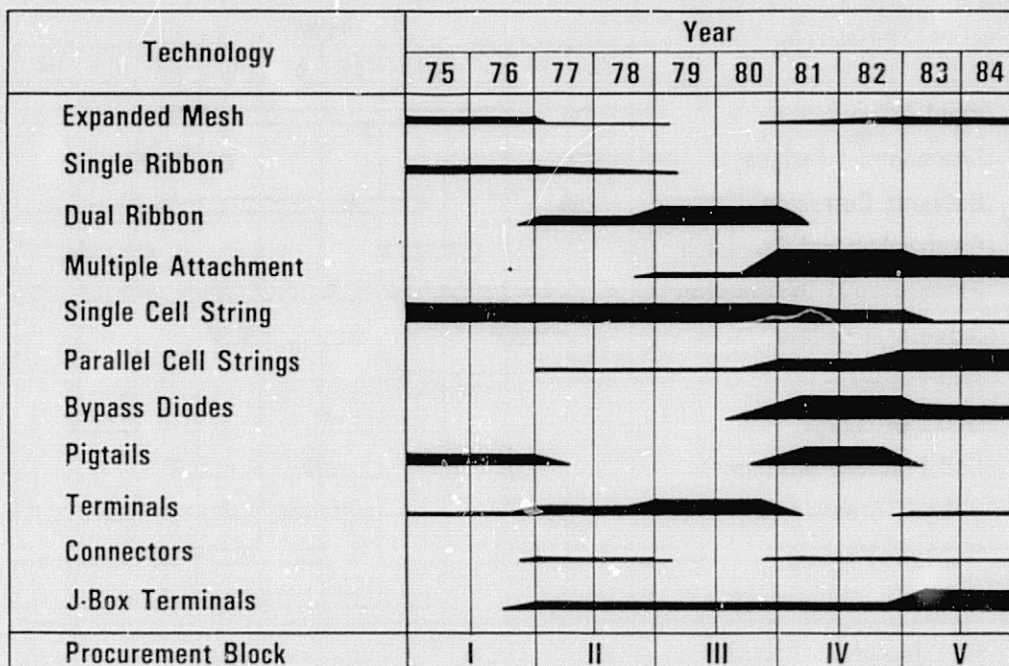
## Module Cell Evolution, 1975 to 1984



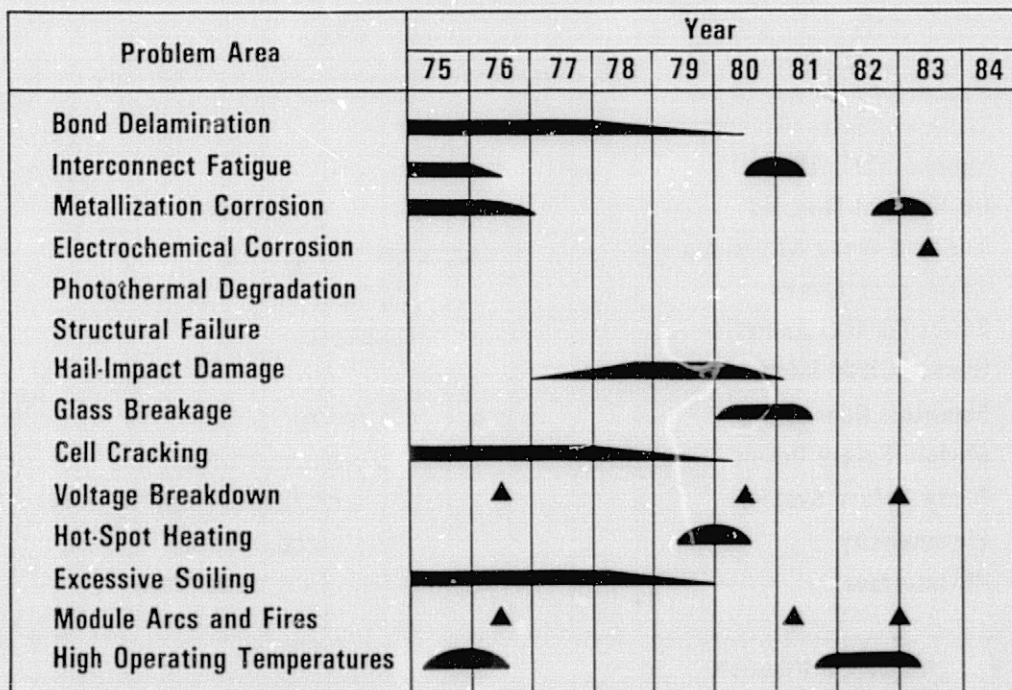
## Module Encapsulation Evolution, 1975 to 1984



## Module Electrical Circuit Evolution, 1975 to 1984

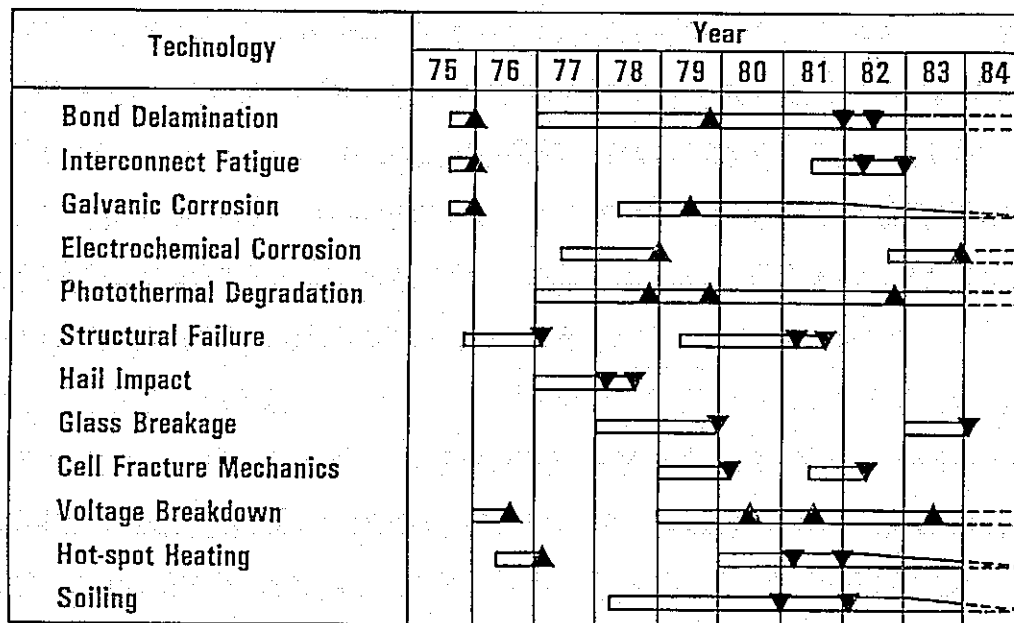


## Major Reliability Problems, 1975 to 1984





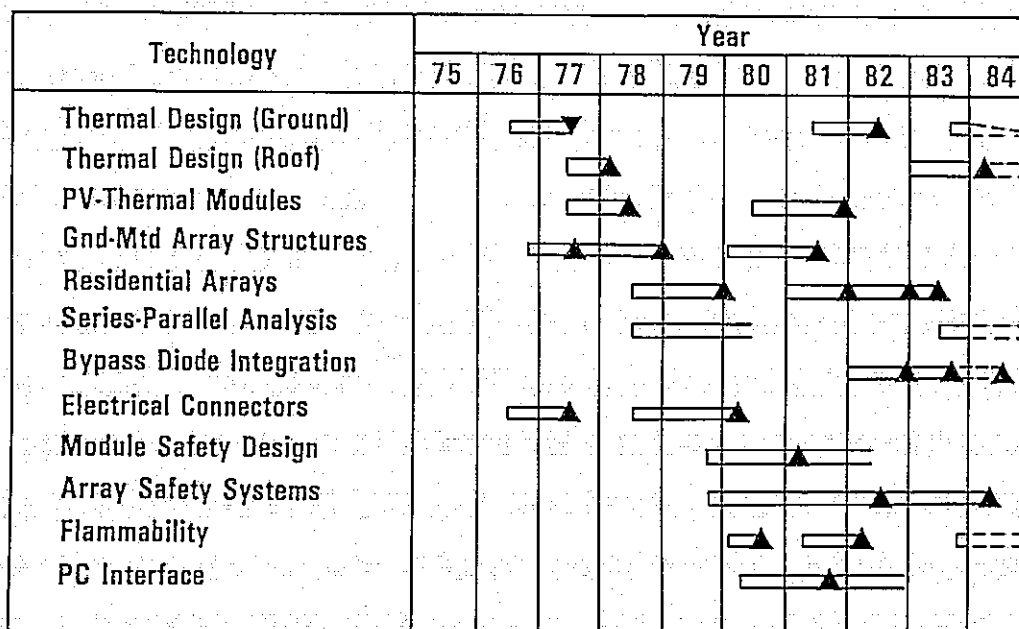
## Reliability &amp; Durability Developments, 1975 to 1984



▼ = Major Contribution

▲ = Significant Contribution

## Engineering Sciences Developments, 1975 to 1984



▼ = Major Contribution

▲ = Significant Contribution



## Key Near-Term Technical Thrusts

### Module and Cell Reliability

- Electrochemical corrosion
- Voltage breakdown
- Bond durability
- Photothermal degradation

### Engineering sciences

- Hot-spot heating in highly paralleled circuits
- Temperature prediction of residential arrays
- Module flammability
- Bypass diode optimization
- Series-parallel analysis for shorted cells
- IR reflectors for lower operating temperatures

### Module Performance and Failure Analysis

- Continued testing
- Continued failure analysis

### Module Development

- Block V and advanced designs

## Potential Fruitful Areas for Future Development

- AR Coatings for glass
- Gasket edge-seal technology
- Electrical termination technology
- Environmental durability of ribbon cells

## Thin-Film Differences Requiring New or Expanded Research

- New cell environmental durability (temperature/humidity/UV) failure modes
- Altered hot-spot heating failure mechanisms
- Short-circuit cell failure modes and effect on cell size and series/parallel redundancy
- New cell electrical interconnect failure modes
- Altered glass breaking strength
- Flexible substrate technology demands
- High cell stresses due to glass bending
- Non-linear electrical response and effect on module measurement
- Cell-to-cell electrical variability and effect on electrical mismatch and circuit design

## Strawman Degradation Allocations: 30-Year Baseline Technology, 1982 \$

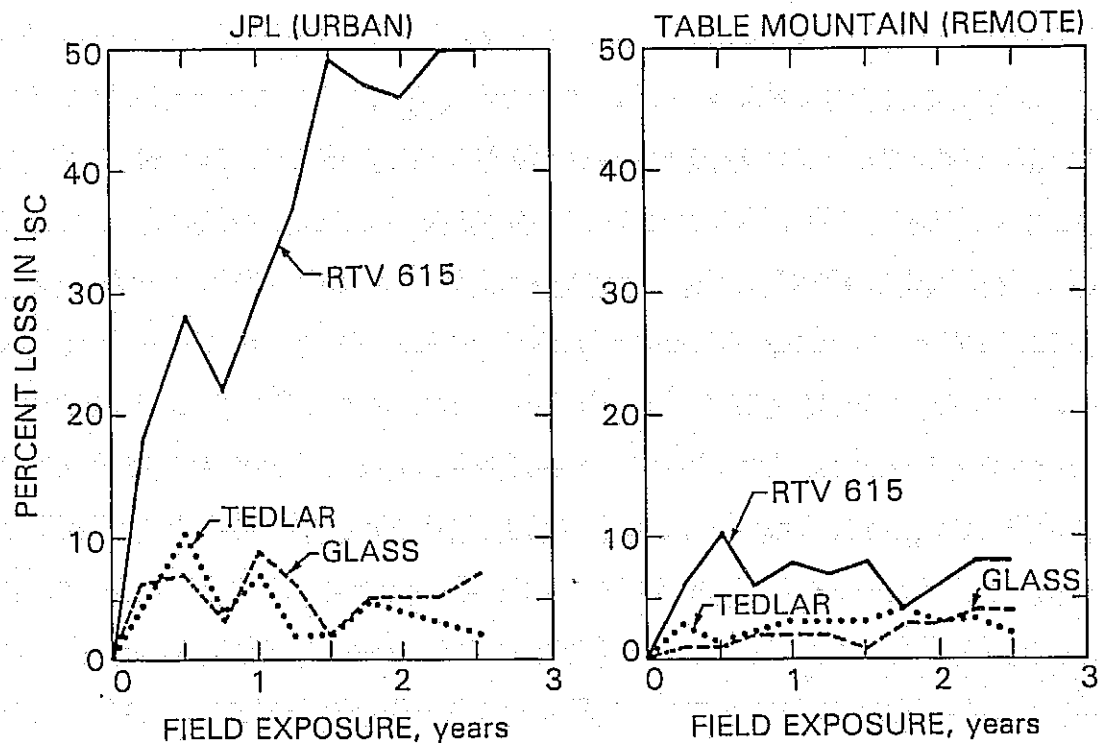
Type of Degradation	Program Allocation	Specific Mechanisms	Strawman Mechanism Allocation
Fixed Drop In Power	8%	Soiling Mismatch	5% 3%
Constant Power Degradation Rate	0.65%* per year	Cell Open Circuits Cell Corrosion Yellowing	0.0001 fraction per year 0.2% per year 0.2% per year
Constant O&M Rate	\$2.28/m <sup>2</sup> per year	Voltage Breakdown Glass Breakage Mod. Open Circuits Structures Upkeep Electrical Upkeep Grounds Upkeep	1.3/mile/year† 0.004 fraction per year† 0.004 fraction per year† \$560/acre/year \$500/acre/year \$500/acre/year

\*5% average loss of 30 years at 12½% discount rate

†At \$140 per replacement of 1.5m<sup>2</sup> module

□At 1350 m<sup>2</sup> of array per acre (1:3 packing)

# Array Loss Due to Soiling



## Cracked and Failed Cells Due to Field Exposure

SITE	TOTAL NUMBER OF CELLS IN FIELD	FRACTION* CRACKED PER YEAR	FRACTION FAILED PER YEAR
MEAD NEBRASKA	90,168	0.010	0.00021
MT. LAGUNA CALIF.	96,236	0.025	0.0010

\*30 TO 50% DUE TO HAIL IMPACT

## Strawman Degradation Allocations: 30-Year-Life Advanced Technology, 1982 \$

Type of Degradation	Program Plan Allocation	Revised Allocation	Specific Mechanism	Mechanism Allocation
Fixed Drop in Power	8%	4%	Soiling Mismatch	3% 1%
Constant Degradation Rate	0.65%* per year	0.45% per year	Cell open circuit Cell corrosion Yellowing	0.00001 per year 0.2% per year 0.2% per year
Constant O&M Rate	\$2.28/m <sup>2</sup> per year	\$1.07/m <sup>2</sup> per year	Voltage breakdown Glass breakage Mod. open circuits Structures upkeep Electrical upkeep Grounds upkeep	0.1/mile/year† 0.002 per year† 0.002 per year† \$200/acre/year \$500/acre/year \$200/acre/year

\*5% average loss over 30 years at 12½% discount rate

†At \$140 per replacement of 1.5 m<sup>2</sup> module

At 1350 m<sup>2</sup> of array per acre (1:3 packing)

### Challenges for the Future: Summary

- Achieving the technology for 30-year-life, low-cost modules with crystalline silicon cells
  - Voltage breakdown
  - Bond delamination
  - Corrosion
  - Flammability
- Meeting the demands of evolving new cell structures and materials
- Keeping abreast of the performance lessons arising from current products and applications

# PV MODULE STANDARDS

ARCO SOLAR, INC.

J.C. Arnett

## PV Standards Development Participants

NATIONAL LABORATORIES

PV USERS

PV MANUFACTURERS

NATIONAL CONSENSUS STANDARDS ORGANIZATIONS

DEPARTMENT OF ENERGY

## IEEE PVSCC Status

- FULL COMMITTEE MEETS SEMI-ANNUALLY (R D'AIELLO, CHAIRMAN;  
R. KLEIN, SECRETARY)
- SYSTEMS S/C: DRAFT INTERFACE DOCUMENT TO GO TO COMMITTEE  
BALLOT EOY (R. DeBLASIO, CHAIRMAN)
- POWER CONDITIONING S/C: DRAFT PC SUBSYSTEMS TEST METHOD IN  
S/C REVIEW. S/C MET IN APRIL WITH SANDIA SYSTEMS P I M  
(B. LYON, CHAIRMAN)
- CELL/ARRAY S/C: REORGANIZING AND CONDUCTING TASK ASSESSMENT  
(M. KEELING, CHAIRMAN)
- STORAGE S/C: MEETS 2-3/YEAR DRAFT DOCUMENTS IN WORKING  
GROUPS (B. BRENCH, CHAIRMAN)

# ASTM E44.09 Status

<u>STANDARD</u>	S/C	COMM	SOCIETY
NON-CONC. CELL TEST/REF.CELLS	X	X	PASSED
DIRECT NORMAL SPECTRUM/SIMULATORS	X	X	PASSED
CALIB. OF NON-CONC. REF. CELLS	X	FALL BALLOT	
TEST OF CONC. DEVICES	TABLED		
SPECTRAL RESPONSE OF CELLS	X	X	FALL BALLOT
SPECTRAL MISMATCH PARAMETER	X	X	FALL BALLOT
DEVICE LINEARITY	BALLOT 9/83		
NON-CONC. MODULE TEST/REF. CELLS	NEGATIVE	?	
HAIL TEST OF MODULES	X	FALL BALLOT	
GLOBAL CALIBRATION/REF. CELLS	X	FALL BALLOT	
E-891 AND E-892	IN REVIEW		

## IEC Technical Committee 82

- FORMALLY CONVENED AT STRESSA, MAY 1982
- THREE WORKING GROUPS FORMED
  - WG1: TERMINOLOGY/GLOSSARY (CANADA)
  - WG2: MODULES (FRANCE)
  - WG3: SYSTEMS (SWITZERLAND)

### ● PARTICIPANTS:

USA	BELGIUM
FRANCE	UK
GERMANY	SWITZERLAND
ITALY	CANADA
BRAZIL	CHINA

## IEC/TC 82

- NEXT MEETING: TOKYO - OCT. 24 - 28, 1983
- WORKING GROUPS MEET FIRST 2 DAYS
- WG1: DRAFT GLOSSARY WILL BE SUBMITTED
- WG2: GLOBAL AND DIRECT REFERENCE SPECTRUMS; REFERENCE CELL CONSTRUCTION; CELL AND MODULE PERFORMANCE MEASUREMENT
- WG3: TASK GROUPS WORKING STAND-ALONE, SYSTEM DESCRIPTION IN DEVELOPMENT STAGE BASED ON IEEE SYSTEMS S/C DRAFT
- IEC PROPOSAL TYPICALLY TAKES 2 1/2 TO 3 YEARS TO BECOME INTERNATIONAL STANDARD

## U.S. Participation in TC 82

- U.S. NATIONAL COMMITTEE (ANSI)
  - APPOINTS TECHNICAL EXPERTS TO WG'S
  - U.S. TECHNICAL ADVISORY GROUP (TAG) PROVIDES DELEGATES TO TC82
- DRAFT TC82 DOCUMENTS PREPARED AT WG LEVEL WITH U.S. REPRESENTATIVES PARTICIPATING
- U.S. COMMITTEE MEMBERS VIEWED AS AUTHORITIES IN MEASUREMENTS AND SYSTEMS DESIGN
- U.S. TAG MEETS REGULARLY AND PROVIDES COMMENTS ON TC82 DRAFTS
- U.S. TAG PREPARES AND PROVIDES TECHNICAL INPUT TO THE WG TECHNICAL EXPERTS

## Barriers to Standardization

- NATURE OF CONSENSUS PROCESS
- LIMITED FUNDING FOR SUPPORT
- PROPRIETARY POSITIONS OF MANUFACTURERS
- TENDENCY OF USERS TO OVER-SPECIFY
- CHARTER QUESTIONS FOR CONSENSUS BODIES

## U.S. Position on Standards

- SERI - IPC LARGE STEP FORWARD
- EUROPEAN STANDARDS IN PLACE
- OTHER COUNTRIES RAPIDLY CLOSING ON NATIONAL MODULE PERFORMANCE STANDARDS
- PARTICIPATION IN IEC/TC82 HAS TEMPORARILY DILUTED U.S. EFFORTS OF ATSM/IEEE
- AVAILABILITY OF U.S. TECHNICAL SUPPORT BY ACTIVE ASTM/IEEE PARTICIPANTS HAS STRENGTHENED U.S. POSITION IN THE WORLD STANDARDS ARENA



# Technology Sessions

## SILICON SHEET GROWTH AND CHARACTERIZATION

A.H. Kachare, Chairman

Progress reports on silicon (Si) sheet growth and characterization were presented by 10 contractors.

Westinghouse Research and Development Center, developing dendritic-web growth methods, reported experimental improvement of 42% in growth rate by using computer-modeled growth conditions. The increased growth speed from 1.9 cm/min to 2.7 cm/min and low stress were consistent with model predictions.

Mobil Solar Energy Corp. (MSEC), developing edge-defined film-fed Si ribbon growth (EFG), discussed the dependence of the stress distribution on details of the sheet temperature distribution and on the growth interface stress state. Work is being done to enable specification of variables needed to evaluate a model for obtaining temperature field-residual stress relationships applicable to EFG at high speeds.

Solar Energy Research Institute (SERI), conducting research on understanding of solid-liquid interface phenomena in high-speed growth, reported results on small cylindrical crystal growth (0.5-1.5 mm dia) by dipping a cylindrical seed of desired orientation into the melt and growing a thick neck from the seed, under rotation. Sheet was then propagated radially in all directions on the melt surface by setting the vertical pulling speed to zero.

The Massachusetts Institute of Technology reported on modeling of transport phenomena in edge-defined film-fed Si ribbon growth.

University of Kentucky reported on an elastic analysis of the prebuckled stress field and the critical buckling conditions for the case when the material can be considered to be elastic with constant material properties. It is shown that the mode of deformation during buckling is torsional when the only stresses are due to temperature.

Semix Inc., conducting research on the ubiquitous crystallization process, reported that certain grains in this material do develop a substructure that is characterized by numerous small subgrains, of millimeter size, that are delineated by pure dislocation boundaries.

Cornell University, studying silicon-sheet properties, presented results on EFG, bicrystals and HEM material.

Material Research Inc. (MRI) discussed dislocation results on Semix Si.

University of Illinois at Chicago reported the results of multiple-scratch diamond-abrasion tests and microhardness tests in organic and inorganic fluids.

Applied Solar Energy Corp. (ASEC) reported on use of light-spot scanning to measure spatial diffusion length in silicon solar cells.

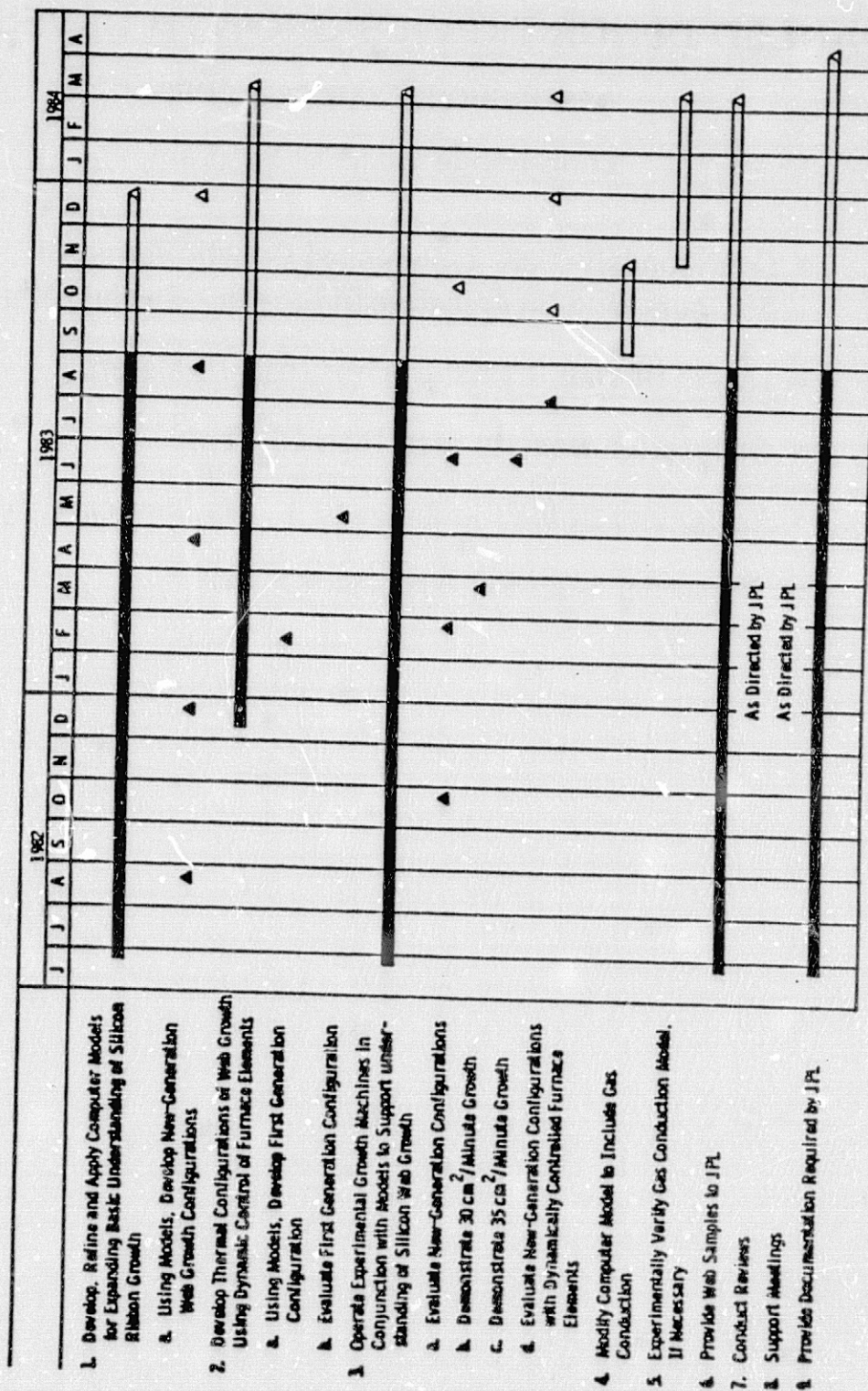
# ADVANCED DENDRITIC WEB GROWTH DEVELOPMENT

WESTINGHOUSE ELECTRIC CORP.

Long-Range Goals of Program

- Continuously-Melt-Replenished Growth Period Of 65 Hours With An Area Rate Of Growth  $> 25 \text{ cm}^2/\text{Minute}$
- Length Of Web Crystal Greater Than 10 Meters
- Dislocation Density Less Than  $10^4/\text{cm}^2$
- Resistivity Of Web In Range Of 1 To 3 Ohm-cm P-Type
- Terrestrial Solar Cell Efficiency  $> 15\%$

## Milestone Chart



Principal Tasks of the Current Phase  
of the Program

- **Develop Computer Specifications For Low-Stress Web Growth Configurations Having Thermal Elements In Fixed Position. Correlate With Experimental Web Growth.**
- **Develop Computer Specifications For Web Growth Configurations Incorporating Dynamic Positioning Of Thermal Elements. Correlate With Experimental Web Growth**

Web Growth Correlation With Model Prediction

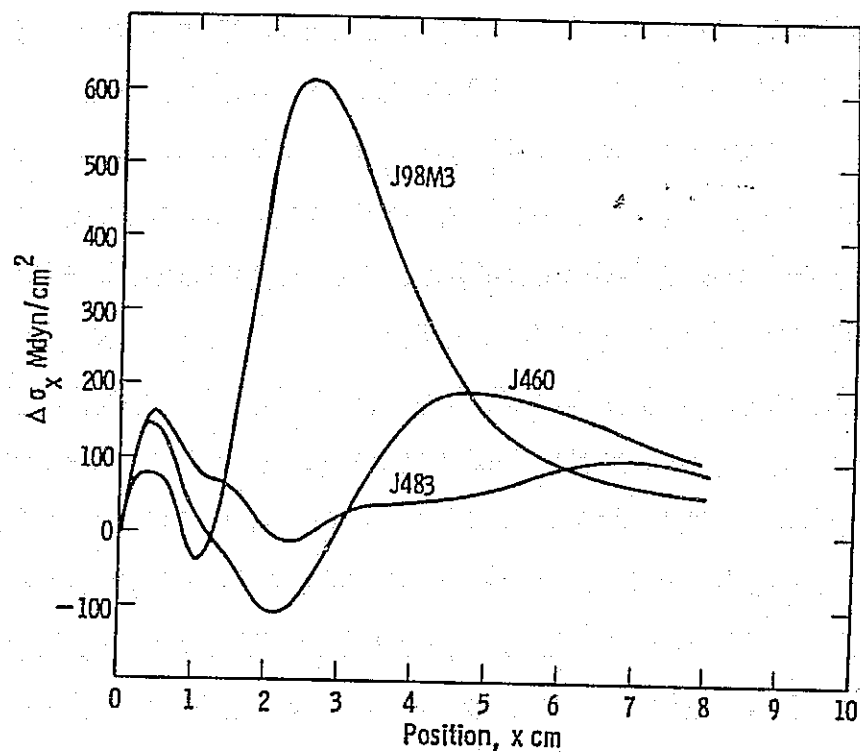
**(1) Experimental Growth System Must Duplicate Model Specification**

- **Fabricate Specified Hardware**
- **Monitor Temperature Of Thermal Elements While Performing System Adjustments**
- **Modify Growth System And Repeat Temperature Measurements As Needed To Obtain Specified Temperatures**

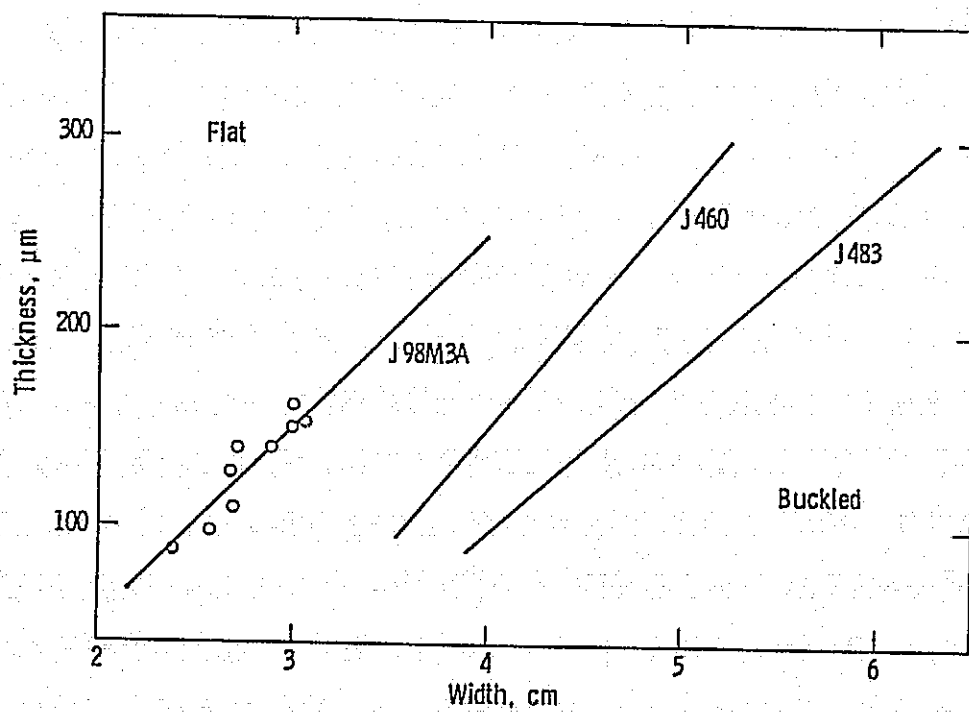
**(2) Grow And Evaluate Web Ribbon Consistent With Model Prediction**

- **Velocity And Thickness Relationship**
- **Buckling**

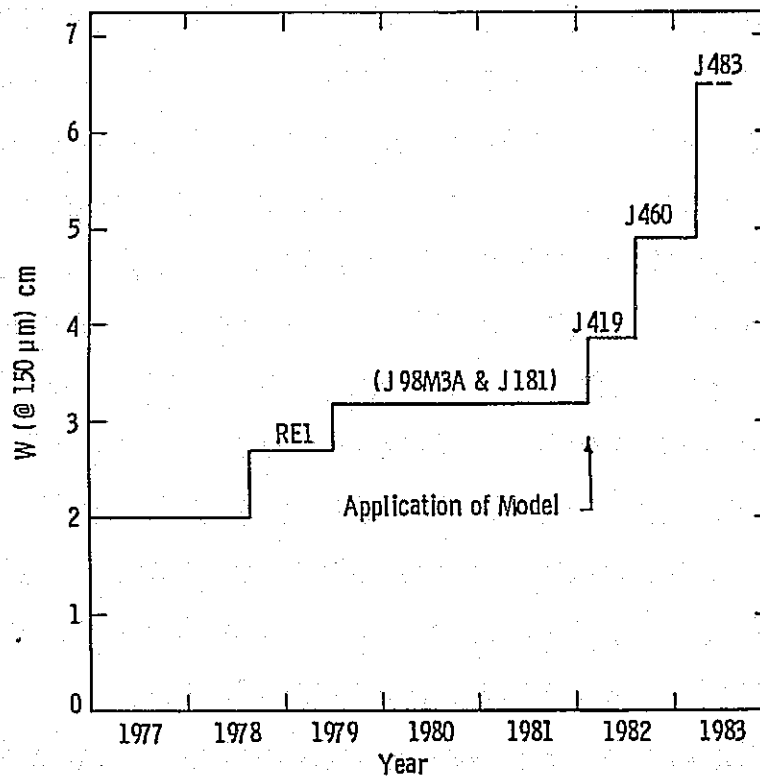
# SILICON SHEET GROWTH AND CHARACTERIZATION



## Buckling Model Results

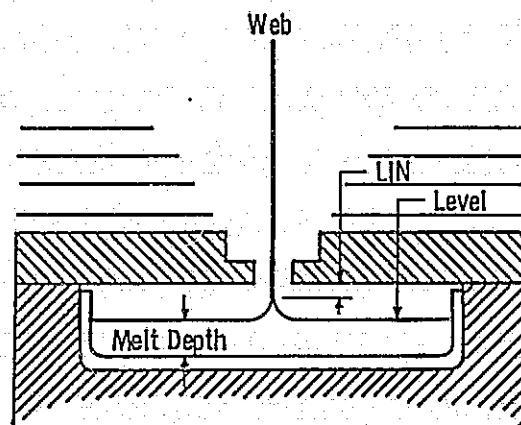


Undeformed Width at  $t = 150 \mu\text{m}$

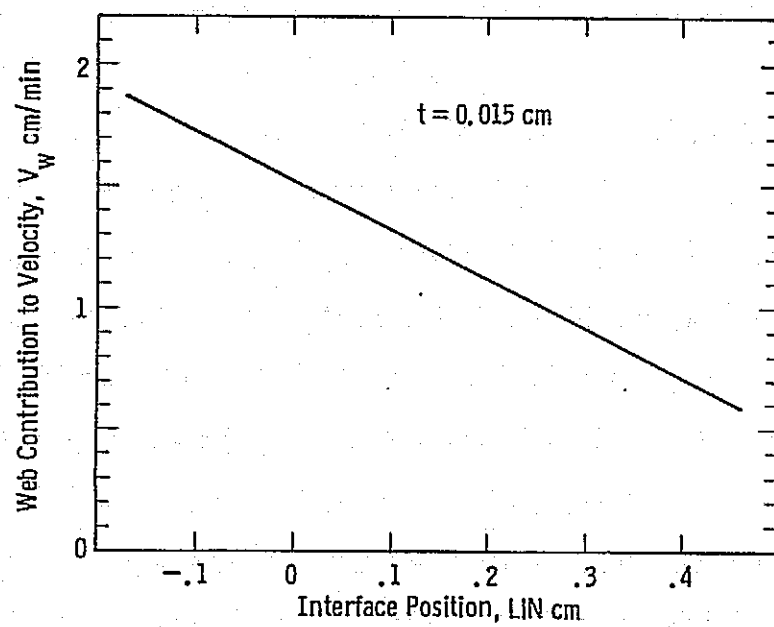


### Development of Dynamic Web Growth Configurations

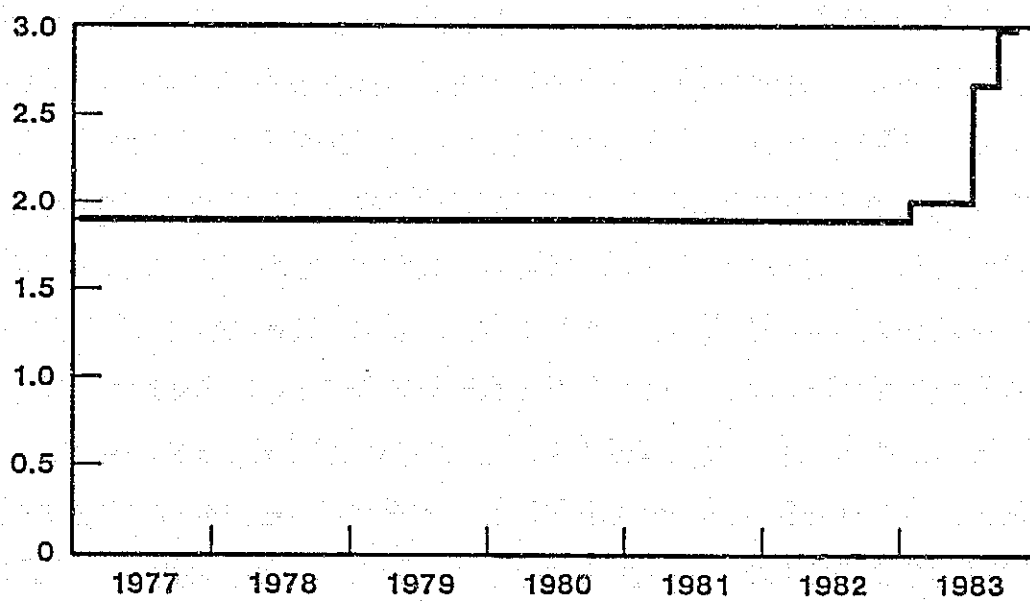
Parametric Study Using Computer Models Shows The Growth Interface-To-Lid Parameter (LIN) To Be A Prime Candidate For Attaining Increased Growth Speed



## SILICON SHEET GROWTH AND CHARACTERIZATION



Web Growth Speed at 150  $\mu\text{m}$  Thickness



## Summary

- **Program Is On Schedule**
- **Large Reduction In Buckling Stress/Increase In Allowable Ribbon Width**
- **Large Increase In Growth Speed**



# EDGE-DEFINED FILM-FED GROWTH

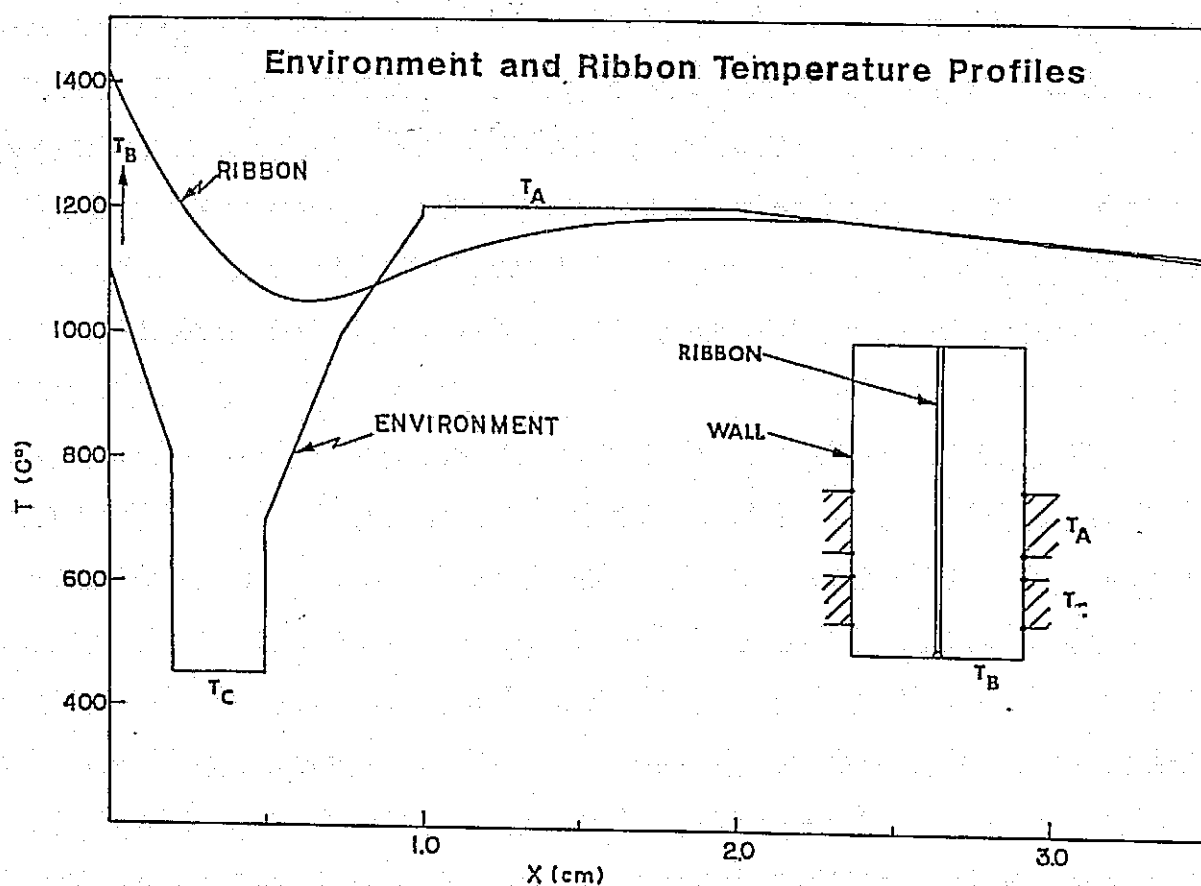
MOBIL SOLAR ENERGY CORP.

<p><u>TECHNOLOGY</u></p> <p>ADVANCED MATERIALS RESEARCH TASK</p>	<p><u>REPORT DATE</u></p> <p>SEPTEMBER 28, 1983</p>
<p><u>APPROACH</u></p> <p>STRESS STUDIES IN EFG</p>	<p><u>STATUS</u></p> <ul style="list-style-type: none"> <li>• COMPUTER CODE FOR CALCULATION OF STRESSES FOR A TWO-DIMENSIONAL MOVING SILICON SHEET IS FULLY OPERATIONAL.</li> <li>• MODELING AND EXPERIMENTAL TASKS ARE IN PROGRESS TO:                         <ul style="list-style-type: none"> <li>- OBTAIN TEMPERATURE DISTRIBUTIONS IN RIBBON.</li> <li>- DEVELOP UNDERSTANDING OF PLASTIC DEFORMATION (CREEP) PROCESS.</li> <li>- EVALUATE RESIDUAL STRESS.</li> </ul> </li> </ul>
<p><u>CONTRACTOR</u></p> <p>MOBIL SOLAR ENERGY CORPORATION, CONTRACT NUMBER 956312</p>	
<p><u>GOALS</u></p> <ul style="list-style-type: none"> <li>• DEVELOP UNDERSTANDING OF MECHANISM OF STRESS GENERATION IN SILICON SHEET GROWTH AND DEFINE MINIMUM STRESS GROWTH CONFIGURATIONS FOR 200 <math>\mu</math>M THICK 10 CM WIDE EFG RIBBON GROWING AT 4 CM/MIN.</li> </ul>	

## Status

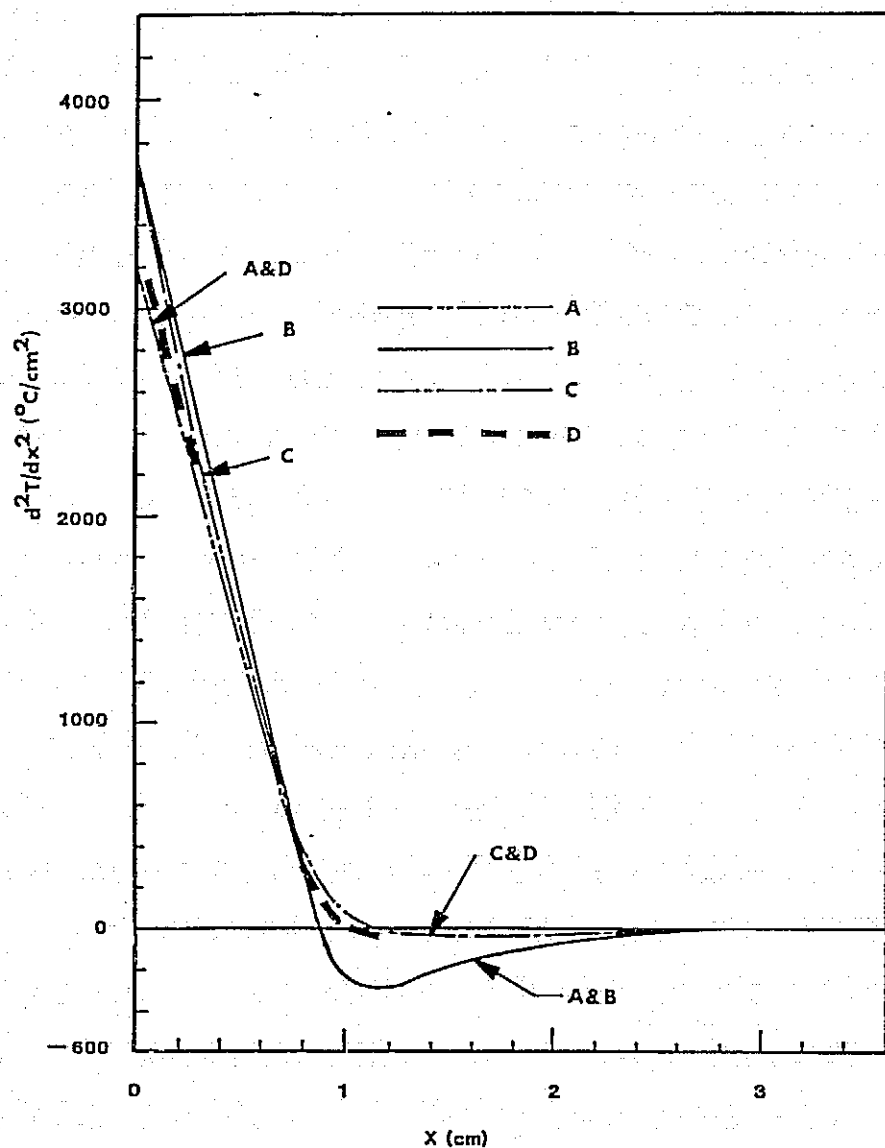
- STRESS ANALYSIS - COMPUTER CODE IS OPERATIONAL AND SENSITIVITY ANALYSIS IS UNDERWAY (HARVARD UNIVERSITY).
- TEMPERATURE FIELD MODELING - SCHEME FOR RIBBON FIELD IS DEVELOPED (MOBIL SOLAR); WORK ON INCLUDING HEAT TRANSFER IN MENISCUS IS UNDERWAY (MIT).
- EXPERIMENTAL WORK IN PROGRESS
  - STUDY OF DEFECT FORMATION PROCESSES, CREEP LAW FOR  $T \geq 1000^{\circ}\text{C}$  USING FOUR-POINT BENDING.
  - FIBER OPTICS PROBE IS OPERATIONAL AND CALIBRATED; USE IN GROWTH SYSTEM ENVIRONMENT IS A PROBLEM.
  - RESIDUAL STRESS MEASUREMENT USING LASER INTERFEROMETRY HAS BEEN DEMONSTRATED TO BE FEASIBLE ON CZ SILICON; WORK ON EFG RIBBON HAS STARTED (UNIVERSITY OF ILLINOIS).

## Environment and Ribbon Temperature Profiles



Thermal Conditions Used in Modeling:  
Ribbon Thickness is 300  $\mu\text{m}$ , Speed  $V = 0$

	CURVE A	B	C	D
$T_B$ , BASE PLATE TEMPERATURE	1500°C	1200°C	1200°C	1500°C
$T_C$ , COLD SHOE TEMPERATURE	450	450	400	400
$T_A$ , AFTERHEATER TEMPERATURE	1200	1200	960	960
$DT/DX _{X=0}$ , VERTICAL GRADIENT	1310	1370	1490	1427



## Temperature Field Modeling Conclusions

- HIGH INTERFACE VALUES OF  $a^2T/ax^2$  CANNOT BE AVOIDED WHILE MAINTAINING THE LARGE  $aT/\partial x$  NECESSARY FOR HIGH SPEED GROWTH ( $\geq 3$  CM/MIN).
- MATERIAL CONSTANTS OF SILICON SET MAIN CONSTRAINTS ON  $a^2T/ax^2$  NEAR INTERFACE AND REDUCE ITS SENSITIVITY TO ENVIRONMENT TEMPERATURE VARIATIONS.

## High-Temperature Creep Laws Used in Modeling

$$\dot{\epsilon}_{ij}^c = C[\exp(-\beta/T)/T] (\sigma_E/\mu)^{N-1} S_{ij}$$

REFERENCE	C (GPA-s) <sup>-1</sup>	$\beta$ (°K)	N	$\dot{\epsilon}$ (s <sup>-1</sup> )*
MYSHLYAEV ET AL. "LOW CREEP" CONDITION	$1.05 \times 10^{29}$	59,760	5	$1 \times 10^{-6}$
"HIGH CREEP" CONDITION	$1.05 \times 10^{31}$	59,760	5	$1 \times 10^{-4}$
SIETHOFF AND SHRÖTER	$5.85 \times 10^{22}$	41,800	3.6	$41 \times 10^{-4}$

\*CALCULATED STRAIN RATE FOR  $\tau/\mu = 10^{-3}$  AND  $T = 1300^\circ\text{K}$ .

## Stress Analysis Results

- LOW RESIDUAL STRESS STATE OF RIBBON FROM 10 cm CARTRIDGE SYSTEM IS CONSEQUENCE OF STRESS RELAXATION IN REHEAT REGION OF AFTERHEATER PROFILE
- BUCKLING STRESSES ORIGINATE CLOSE TO THE GROWTH INTERFACE AND ARE DEPENDENT ON DETAILS OF HEAT TRANSFER CONDITIONS WITHIN ~2 mm OF THE INTERFACE

## Experimental Support Work

### • RESIDUAL STRESS MEASUREMENTS

- MULTI-FINGER SCRIBE-AND-SPLIT APPROACH,
- LASER INTERFEROMETRY (U. OF ILLINOIS).

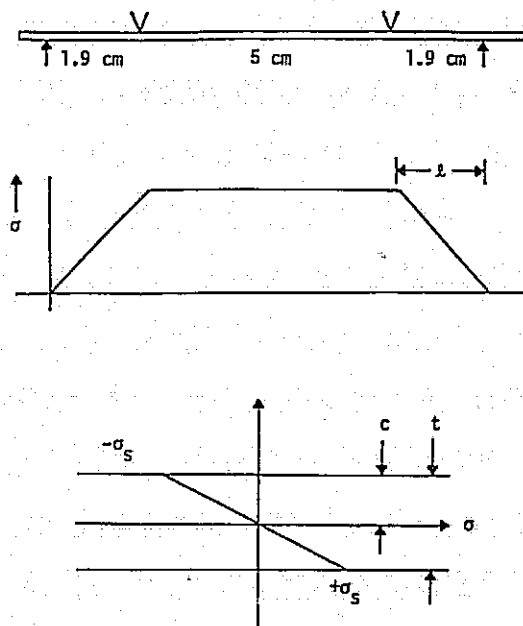
### • CREEP LAW STUDIES ( $\geq 1000^\circ\text{C}$ )

- THREE- AND FOUR-POINT BENDING,
- IMPACT OF IMPURITIES (CARBON) AND STARTING DEFECT DENSITY ON CREEP RESPONSE.

### • FIBER OPTICS TEMPERATURE SENSOR

- $\text{Al}_2\text{O}_3$  FIBER LIGHT-PIPING CHARACTERISTICS ARE UTILIZED,
- CAN PRODUCE HIGH RESOLUTION ( $\leq 0.25 \text{ mm}$ ),
- NON-CONTACT MEASUREMENT FOR MOVING RIBBON.

## Geometric and Stress Relationships



Geometric and stress relationships for sample of thickness  $t$  (and  $c = t/2$ ) in four-point bending.

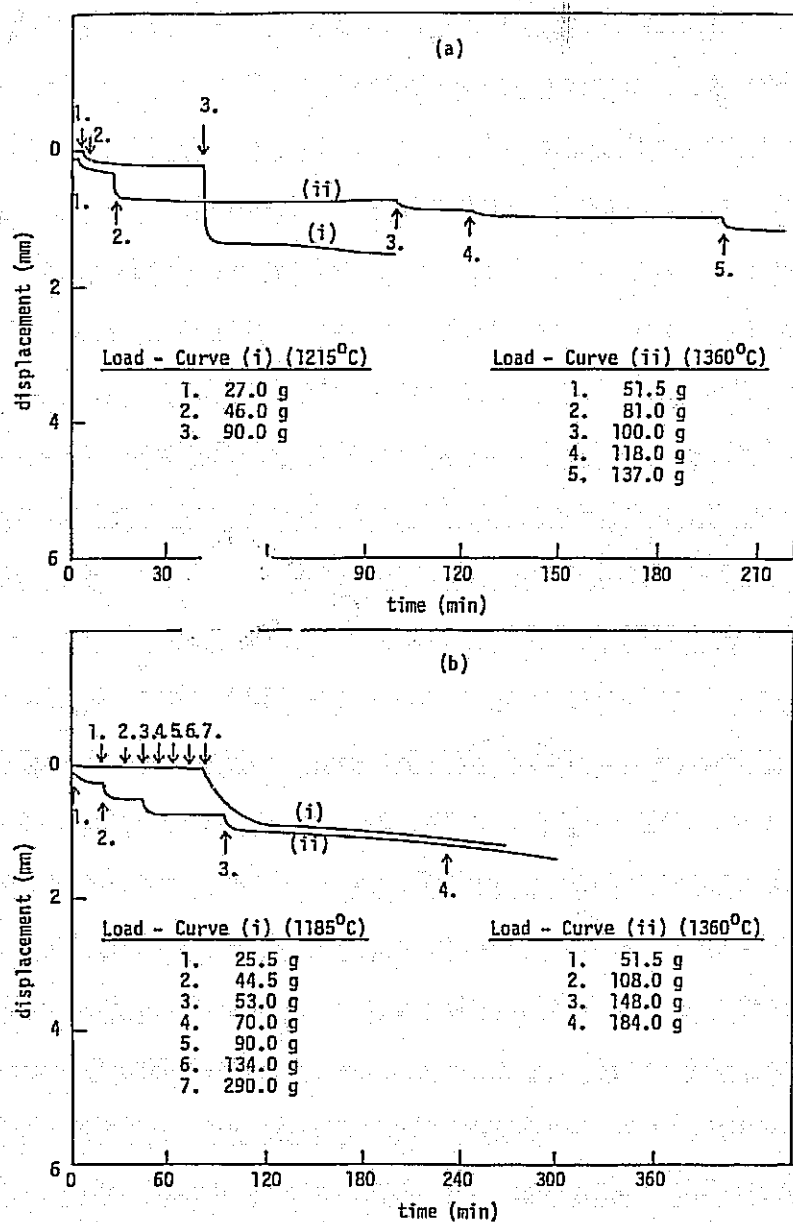
# SILICON SHEET GROWTH AND CHARACTERIZATION

## Four-Point Bending at 1050°C

1. 40 MINUTES HEAT-UP
2. 20 MINUTES UNDER LOAD  $L_1$
3. 20 MINUTES UNDER LOAD  $L_2$
4. COOL WITH NO LOAD

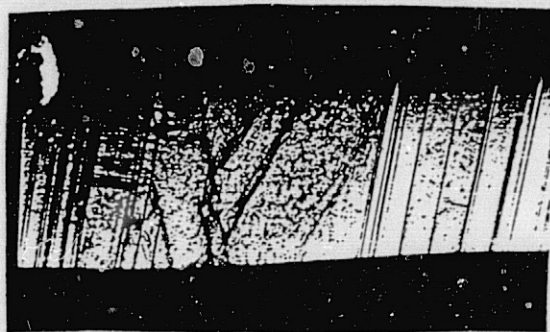
<u>SAMPLE NO.</u>	<u>t (MM)</u>	<u>L<sub>1</sub> (g)</u>	<u>a<sub>1</sub> (MM)</u>	<u>L<sub>2</sub> (g)</u>	<u>a<sub>2</sub> (MM)</u>	<u>FINAL a (MM)</u>
1	0,45	163	0,10	435	0,28	0,23
2	0,36	163	0,20	435	0,76	0,64
3	0,25	81	0,09	214	0,74	0,74
4	0,25	81	0,09	214	0,76	0,48

## Displacement vs Time

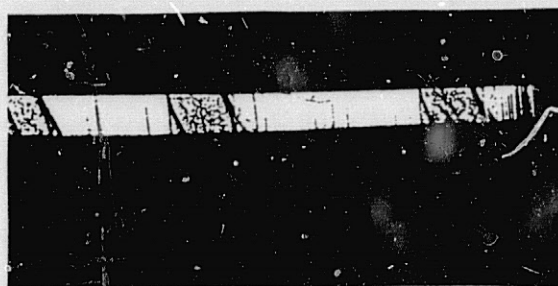


Displacement vs. time graphs for (a) CZ, and (b) Silso silicon wafers stressed by four-point bending.

## SILICON SHEET GROWTH AND CHARACTERIZATION



(a)



(b)

Cross-sectional micrographs of 10 cm wide ribbon grown at 2.6 cm/min and with afterheater setting of 1000°C. (a) Magnification X70.4, ribbon thickness is 0.55 mm; (b) magnification X45.2, thickness 0.15 mm.



## Fiber Optics Sensor Development

- PROBE FOR USE IN CARTRIDGE AND DETECTION SYSTEM  
CONSTRUCTED AND CALIBRATED AT ROOM TEMPERATURE.
- FIRST TESTS IN AFTERHEATER (900-1100°C) SHOW  
PROBE IS SENSITIVE TO STRAY RADIATION.
- PROBE IS BEING CONSTRUCTED TO TEST IN COLD SHOE  
REGION (COOLER ENVIRONMENT, HOTTER RIBBON).

## Summary

### RESULTS AT QUALITATIVE LEVEL INDICATE:

- (1) MATERIAL PROPERTIES OF SILICON RIBBON CONTRIBUTE TOWARD  
ESTABLISHING HIGH INTERFACE  $\partial^2 T / \partial x^2$  AND LIMIT  
FLEXIBILITY TO REDUCE IT BY ENVIRONMENT TEMPERATURE  
MANIPULATION WITHOUT DECREASING  $\partial T / \partial x$ .
- (2) HIGH CREEP LEVELS ARE OPERATIVE AND REDUCE STRESS FROM  
ELASTIC LEVELS IN 10 cm WIDE EFG SILICON RIBBON GROWN  
AT ~3 cm/min.

### CONCLUDE TENTATIVELY:

BUCKLE-FREE VERTICAL SILICON RIBBON GROWTH REGIME FOR  
ALL APPROACHES IS CREEP LIMITED TO BELOW SPEEDS OF THE  
ORDER OF 3 cm/min.

## Future Work

### • ADVANCED SYSTEM DESIGN

- MODEL TEMPERATURE FIELD-STRESS DISTRIBUTIONS TO DEFINE MINIMUM STRESS DISTRIBUTIONS (WITH HARVARD UNIVERSITY).
- DEFINE GROWTH SYSTEM TO TEST STRESS MODEL.
- DEVELOP HEAT TRANSFER MODEL TO INCLUDE MENISCUS EFFECTS (WITH MIT).

### • HIGH TEMPERATURE CREEP LAW/DEFECT STUDIES (WITH FOUR-POINT BENDING)

- VARY STRESS (LOADING) CONDITIONS.
- STUDY DEFECT STRUCTURE-ELECTRICAL ACTIVITY RELATIONSHIP.

### • DEVELOP MEANS TO USE FIBER OPTICS PROBE IN GROWTH SYSTEM.

### • DEVELOP LASER INTERFEROMETRY FOR MEASUREMENT OF RESIDUAL STRESS DISTRIBUTIONS IN EFG RIBBON.

# SOLID-LIQUID INTERFACE STUDIES

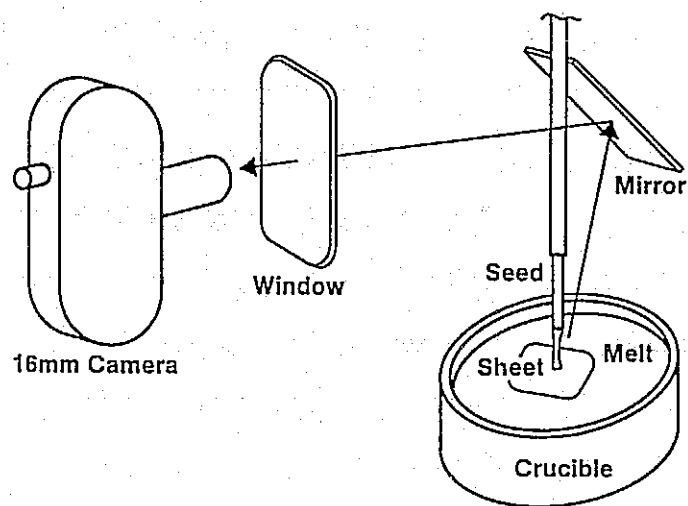
SOLAR ENERGY RESEARCH INSTITUTE

T.F. Ciszek

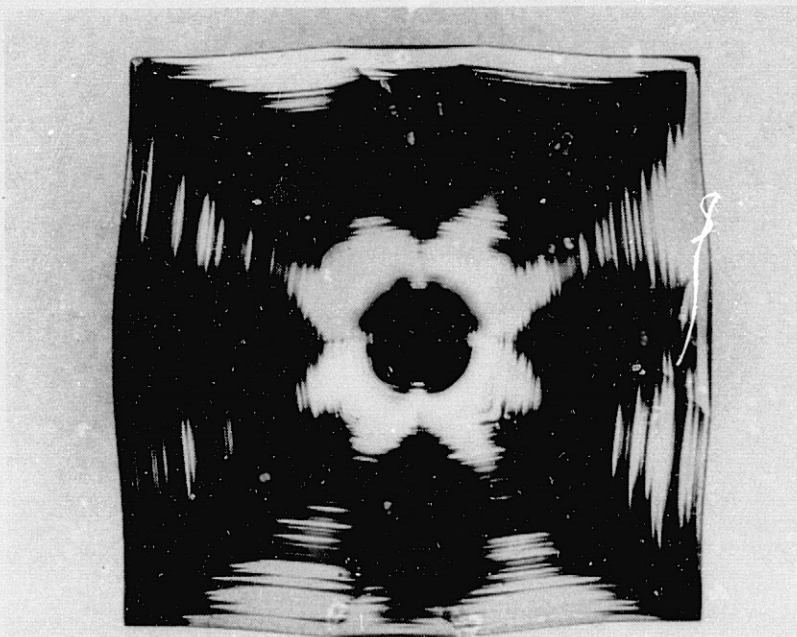
## Orientation and Morphology Effects in Rapid Silicon Sheet Solidification

<b>TECHNOLOGY</b> SOLID/MELT INTERFACE STUDIES OF HIGH SPEED SILICON SHEET GROWTH	<b>REPORT DATE</b> 8/22/83
<b>APPROACH</b> BASIC INVESTIGATIONS OF SOLID/LIQUID INTERFACE EFFECTS DURING HIGH SPEED SILICON CRYSTALLIZATION FROM AN EXTENDED MENISCUS.  <b>CONTRACTOR</b> SOLAR ENERGY RESEARCH INSTITUTE	<b>STATUS</b> * RADIAL GROWTH ANISOTROPIES AND LIMITING GROWTH FORMS OF POINT-NUCLEATED, DISLOCATION FREE SHEETS SPREADING HORIZONTALLY ON THE FREE SURFACE OF A SILICON MELT HAVE BEEN MEASURED FOR {110}, {100}, {111} AND {112} SHEET PLANES  * ANALYSIS OF THE SHEET EDGES HAS LEAD TO PREDICTED GEOMETRIES FOR THE TIP SHAPE OF UNIDIRECTIONAL HORIZONTALLY GROWN SHEETS PROPAGATING IN VARIOUS DIRECTIONS WITHIN THESE PLANES  * DENDRITE GROWTH RATES ON THE ORDER OF 2.5 METERS/MIN AND GROWTH RATE ANISOTROPIES OF 25 WERE MEASURED BY 16 MM PHOTOGRAPHY OF A SUPERCOOLED FREE MELT SURFACE
<b>GOALS</b> * INVESTIGATE THE INFLUENCE OF THERMAL ENVIRONMENT UPON THE STABILITY OF THE LEADING EDGE OF SILICON SHEET GROWTH FROM EXTENDED SOLID/MELT INTERFACES. * INVESTIGATE THE EFFECTS OF IMPURITIES ON INTERFACE STABILITY AND SHAPE. * ADAPT OR MODIFY AN EXISTING RIBBON GROWTH FURNACE FOR USE IN SUPPORT OF THESE INVESTIGATIONS.	

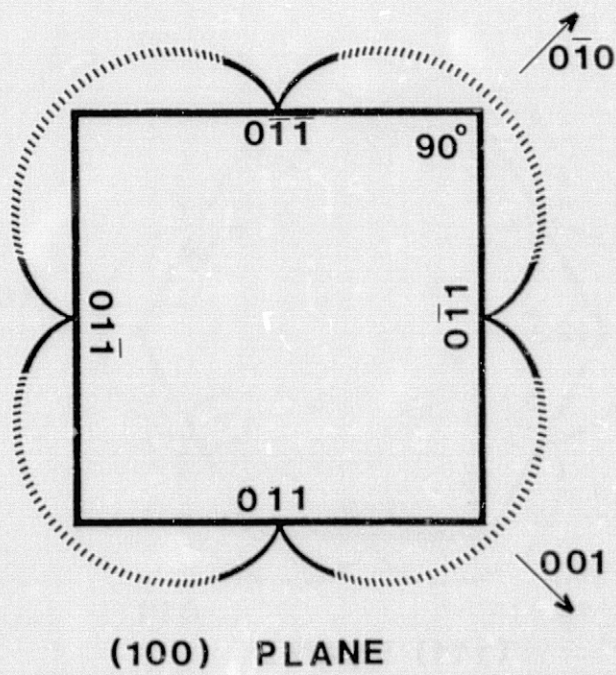
### Arrangement Used to Film Radially Growing Sheets



Final Shape of a (100) Sheet

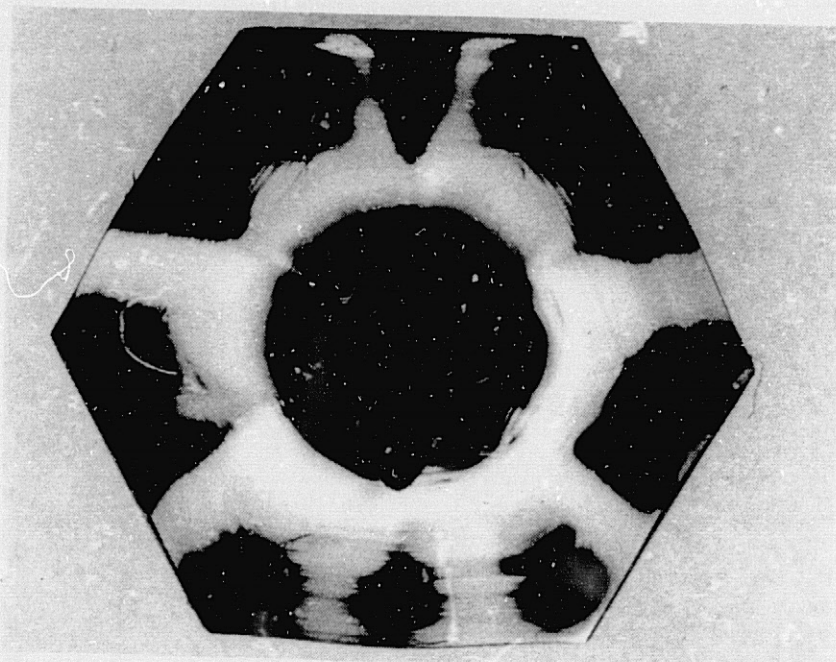


Idealized Form of a (100) Sheet

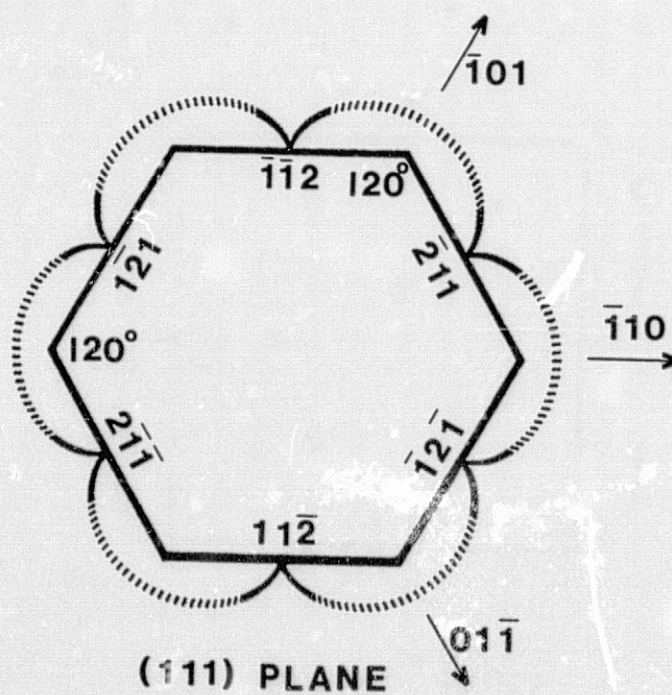




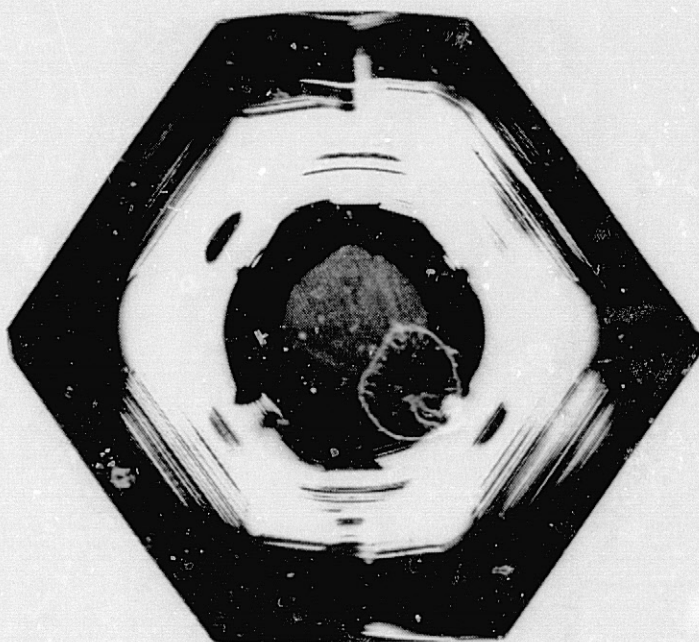
# Final Shape of a (111) Sheet



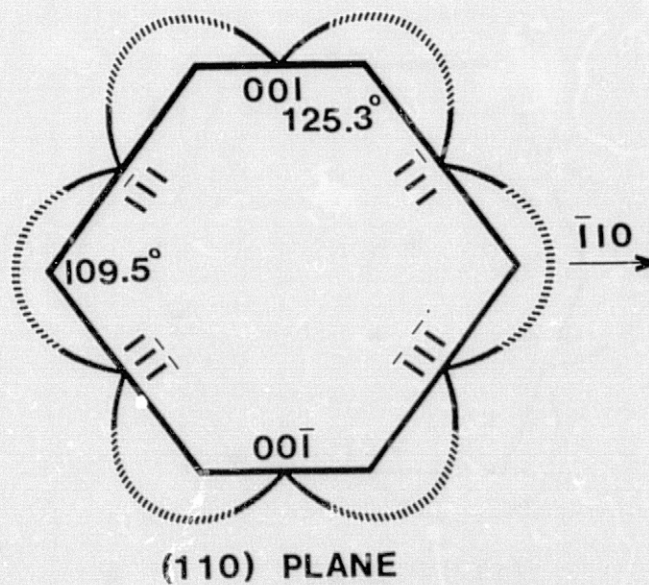
## Idealized Form of a (111) Sheet



Final Shape of a (110) Sheet

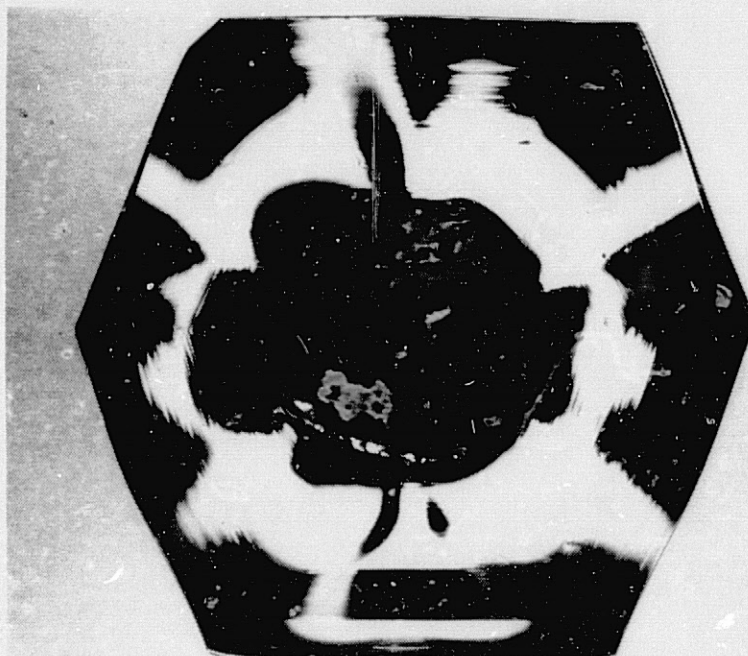


Idealized Form of a (110) Sheet

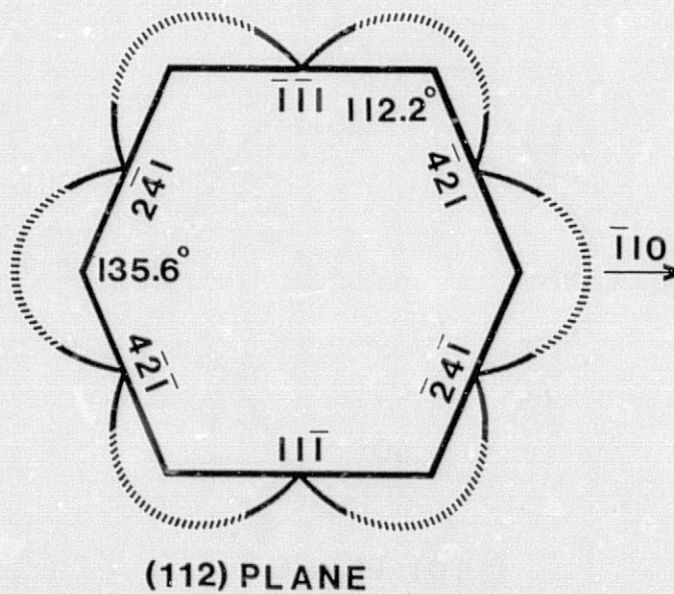




Final Shape of a (112) Sheet



Idealized Form of a (112) Sheet



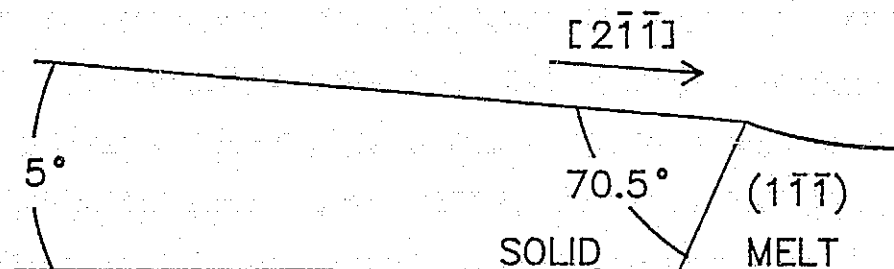


Edge Facets on a (111) Dislocation-Free Sheet

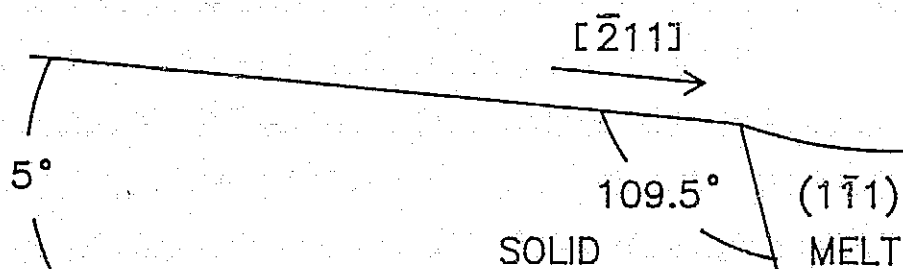


Predicted Tip Geometries

(111) SHEET

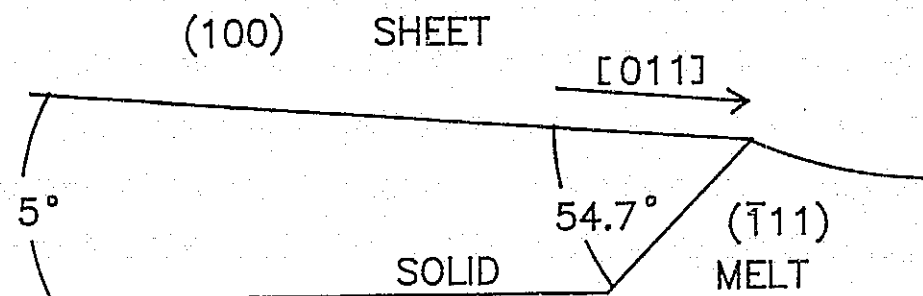


(111) SHEET

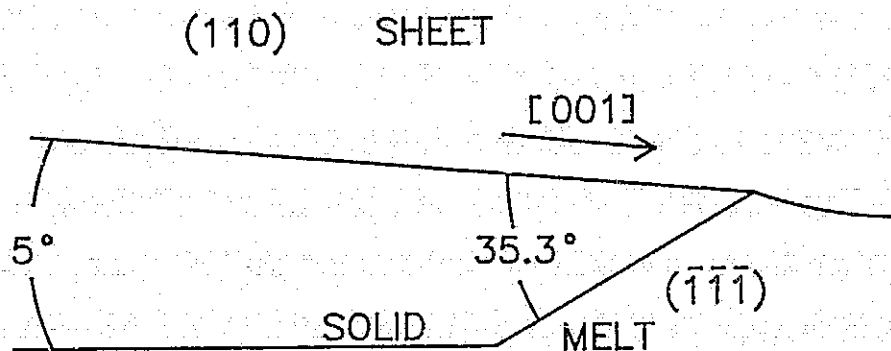
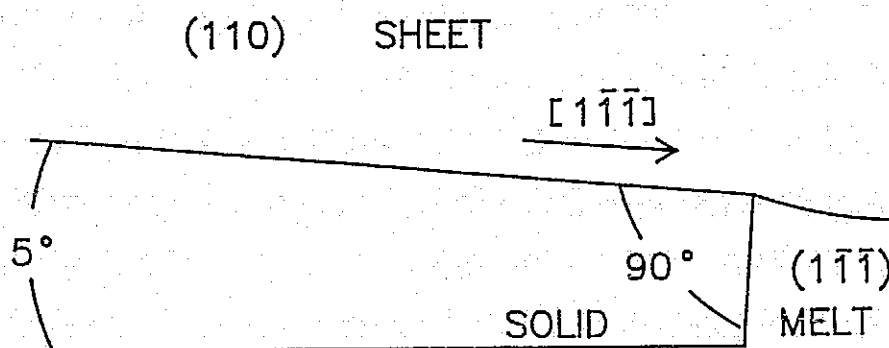


Predicted tip geometries for horizontally grown (111) sheets pulled in the  $\langle\bar{2}11\rangle$  and  $\langle 2\bar{1}\bar{1}\rangle$  directions

# SILICON SHEET GROWTH AND CHARACTERIZATION

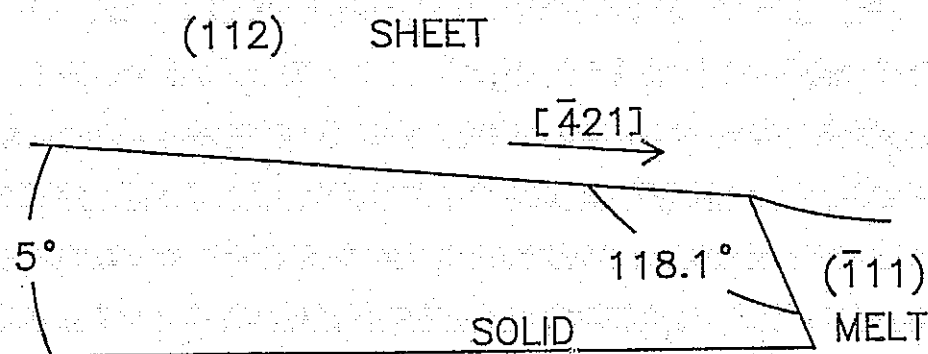
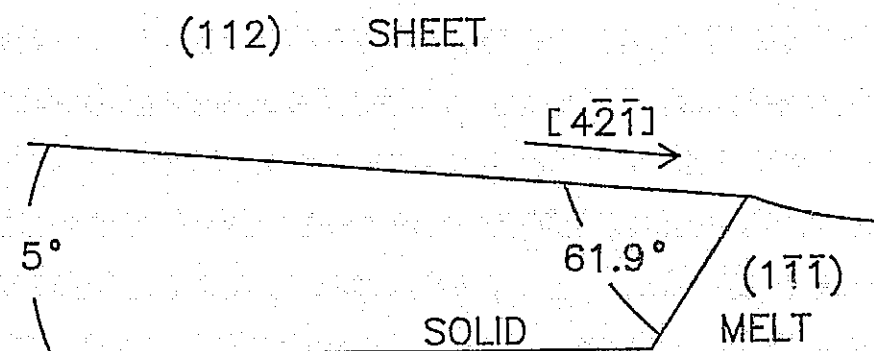
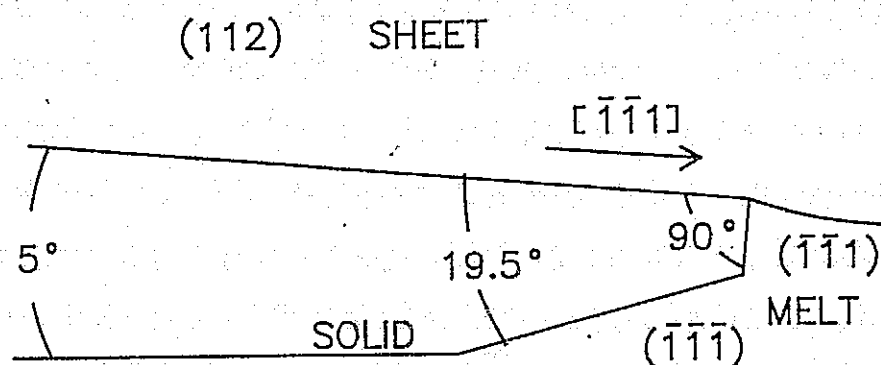
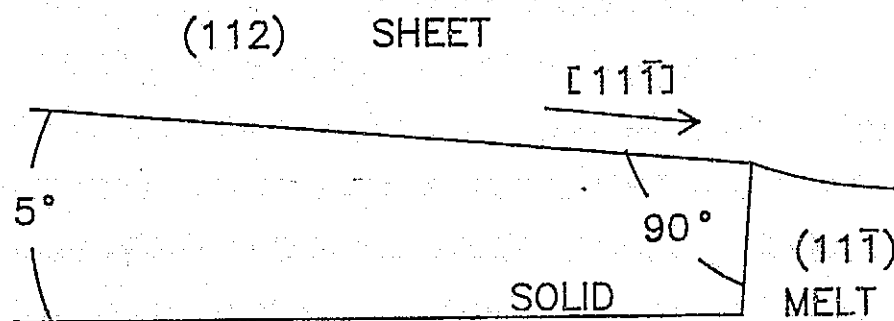


Predicted tip geometries for horizontal (100) sheets growing in the  $\langle 011 \rangle$  directions



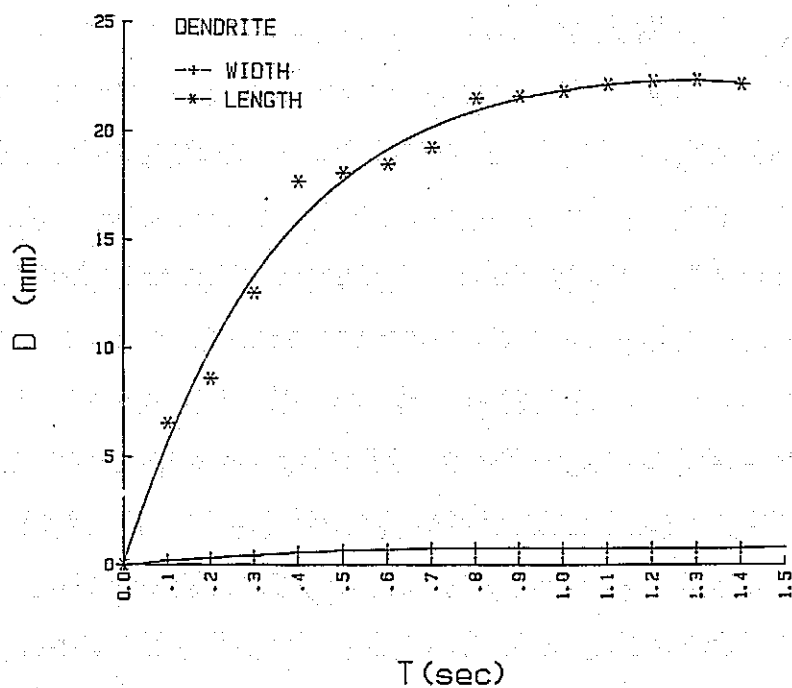
Predicted tip geometries for horizontal (110) sheets growing in the  $\langle 1\bar{1}\bar{1} \rangle$  and  $\langle 001 \rangle$  directions

# SILICON SHEET GROWTH AND CHARACTERIZATION

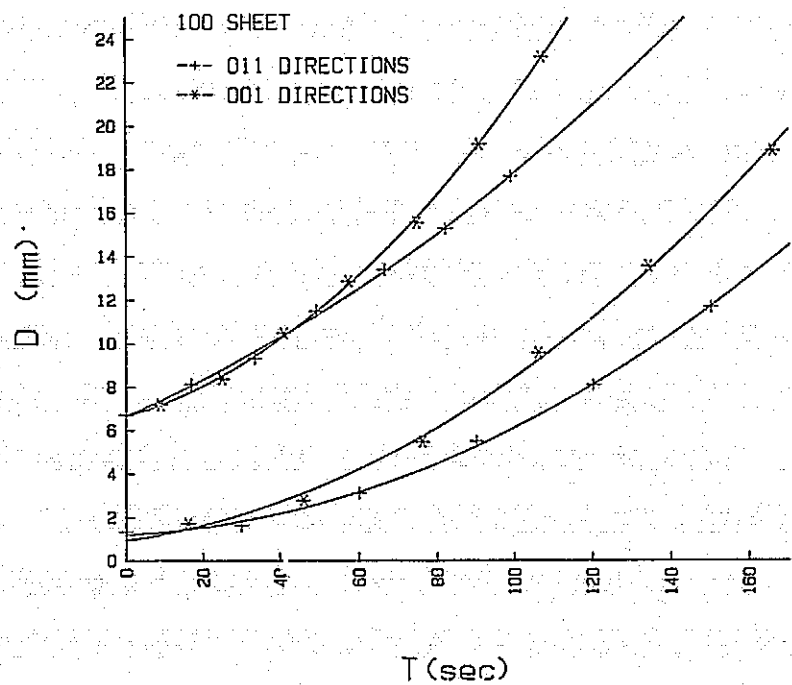


Predicted tip geometries for (112) sheets growing in the  $\langle 111 \rangle$ ,  $\langle \bar{1}\bar{1}1 \rangle$ ,  $\langle 4\bar{2}\bar{1} \rangle$ , and  $\langle \bar{4}21 \rangle$  directions

Size vs Time for a Dendrite



Size vs Time for (100) Sheets of Two Starting Diameters



# RIBBON HEAT AND MASS TRANSFER

MASSACHUSETTS INSTITUTE OF TECHNOLOGY

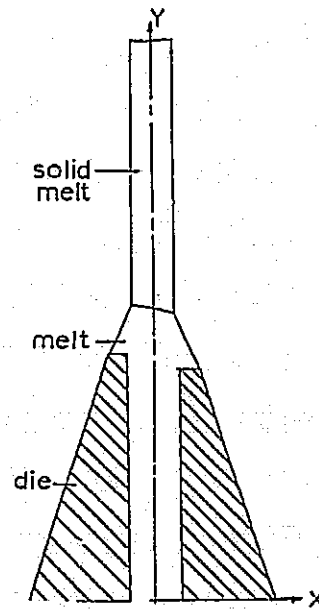
H.M. Ettouney

R.A. Brown

## Modeling of Transport Phenomena in Edge-Defined Film-Fed Crystal Growth

### GOALS

- USE MODELLING TO PREDICT QUANTITATIVELY OPERATING FEATURES OF MENISCUS-DEFINED GROWTH OF SILICON SHEETS
  - OPERATING LIMITS
  - PARAMETRIC SENSITIVITY
  - DOPANT DISTRIBUTION
  - STABILITY ANALYSIS



# Heat Transfer Model

## HEAT TRANSFER IN CRYSTAL

$$Pe_S \mathbf{e}_y \cdot \nabla T_S = \nabla^2 T_S$$

## MELT/SOLID INTERFACE

$$T_m = T_s = T_d$$

$$\hat{\mathbf{N}} \cdot \nabla T_s - (k_s/k_d) \hat{\mathbf{N}} \cdot \nabla T_d = Pe_L S (\hat{\mathbf{N}} \cdot \mathbf{e}_y)$$

$$\mathbf{v} \cdot \hat{\mathbf{N}} = Pe_L (\mathbf{e}_y \cdot \hat{\mathbf{N}})$$

$$\hat{\sigma}(\mathbf{v} \cdot \hat{\mathbf{N}}) = Pe_L (\mathbf{e}_y \cdot \hat{\mathbf{N}})$$

## MELT

$$Re \mathbf{v} \cdot \nabla \mathbf{v} = -\nabla p + \nabla^2 \mathbf{v}$$

$$\nabla \cdot \mathbf{v} = 0$$

$$Pe_L \mathbf{v} \cdot \nabla T_d = \nabla^2 T_d$$

## MENISCUS

$$2H = B(y + H_{eff})$$

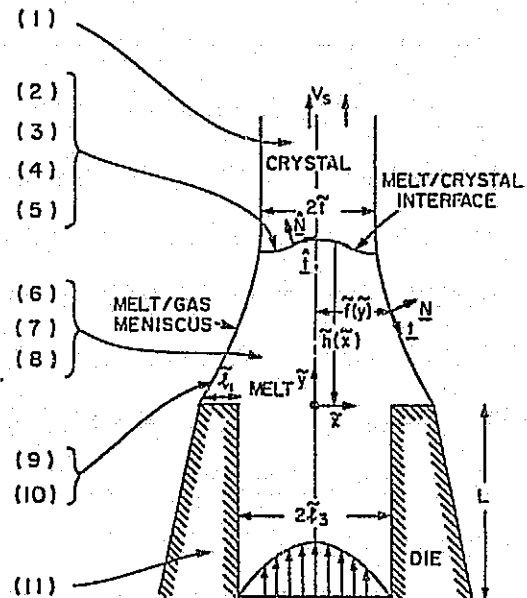
$$\mathbf{v} \cdot \hat{\mathbf{N}} = 0$$

## DIE

$$\nabla^2 T_d = 0$$

## ALL EXTERNAL SURFACES

$$-\hat{\mathbf{N}} \cdot \nabla T_l = Bi_l (T_l - T_\infty(y)) + Ri_l (T_l^4 - T_\infty^4(y)) \quad (12)$$



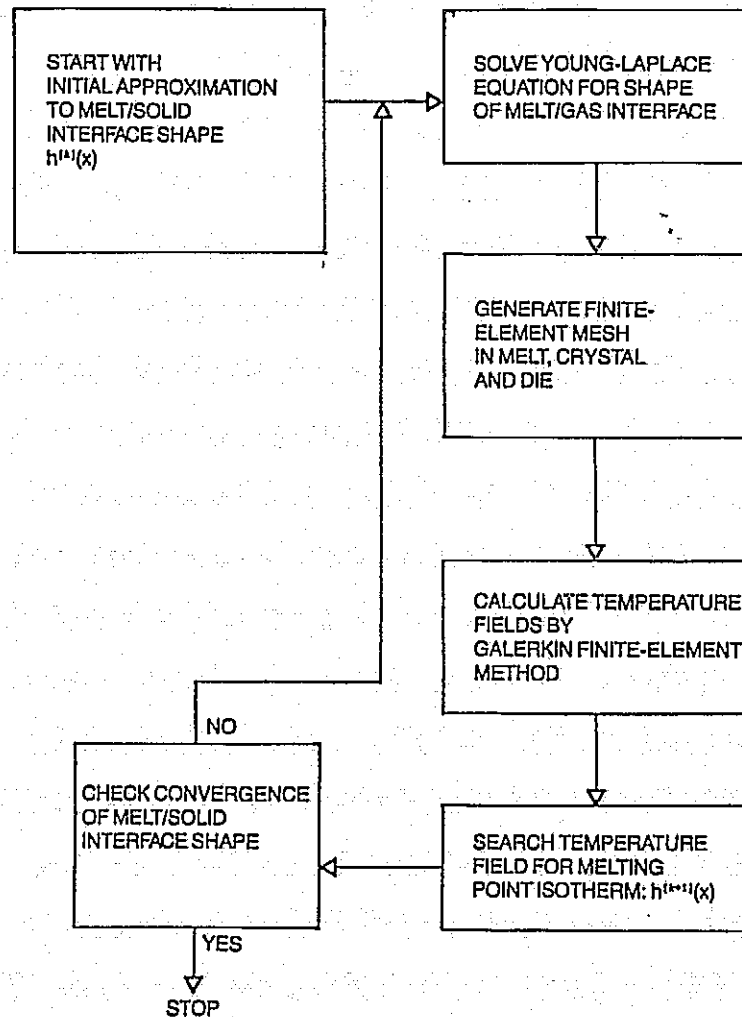
## Parameters Governing Heat Transfer Model

- DIMENSIONLESS GROWTH RATE
- DIE TEMPERATURE
- HEAT TRANSFER TO SURROUNDINGS
- STATIC HEAD

## Conduction-Dominated Heat Transfer Model

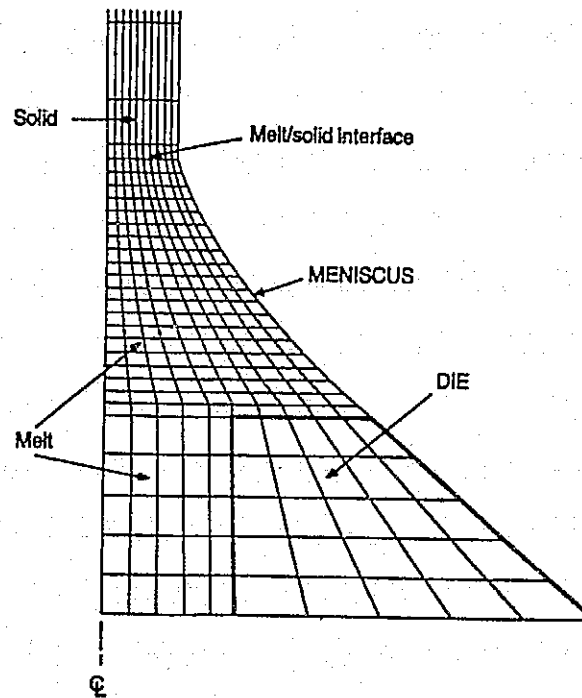
- HEAT TRANSFER DOMINATED BY CONDUCTION IN MELT  
SOLID AND DIE (DETAILS OF FLUID FLOW ARE UNIMPORTANT)
- MELT/GAS MENISCUS SHAPE IS STATIC
- CRYSTAL IS OPTICALLY OPAQUE
- VIEW FACTORS FOR AMBIENT ARE MODELLED BY SMOOTHED  
TEMPERATURE PROFILE

### Iteration Sequence for Successive Approximations





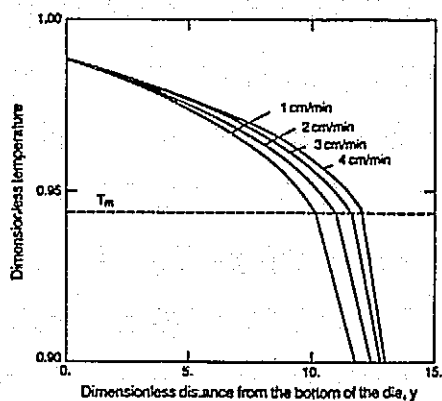
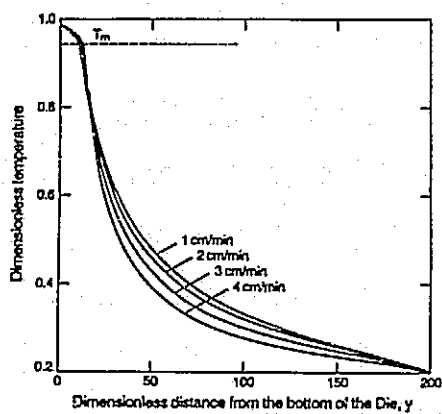
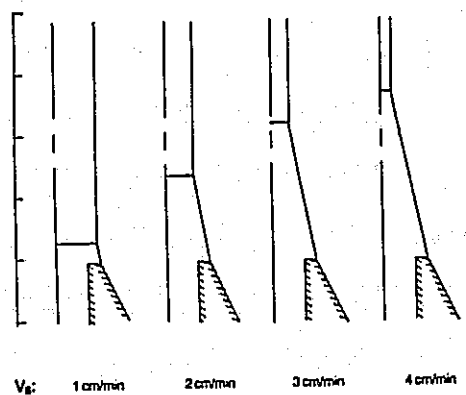
Sample Finite-Element Mesh



### Outline

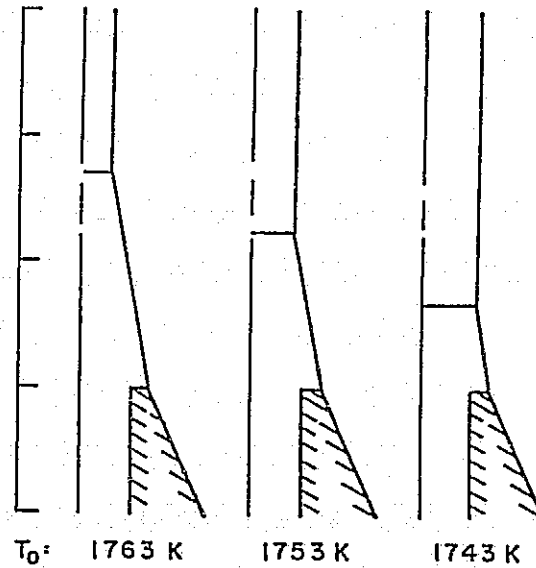
- GENERATE OPERATING DIAGRAMS OF
  - (1) crystal thickness-growth rate-die temperature
  - (2) crystal thickness-growth rate-static head
- PREDICT LIMITS ON OPERATING CONDITIONS AND STABILITY OF STEADY STATE SOLUTIONS
- COMPARISON WITH EXPERIMENTS FROM MOBIL SOLAR
  - (1) crystal thickness-growth rate
  - (2) dopant segregation

# Temperature Gradients in Melt and Solid Increase With Increasing Growth Rate

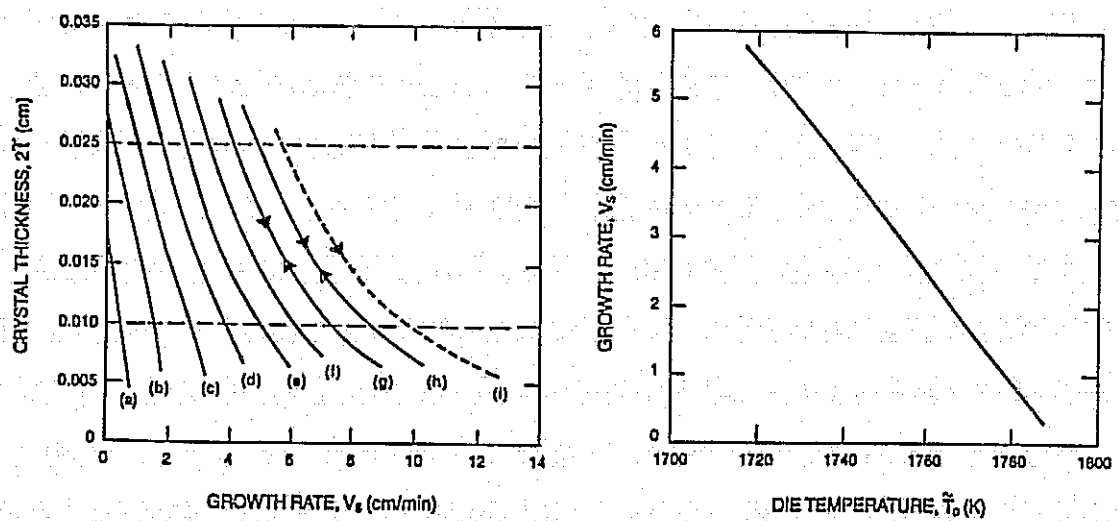


### Decreasing the Die Temperature

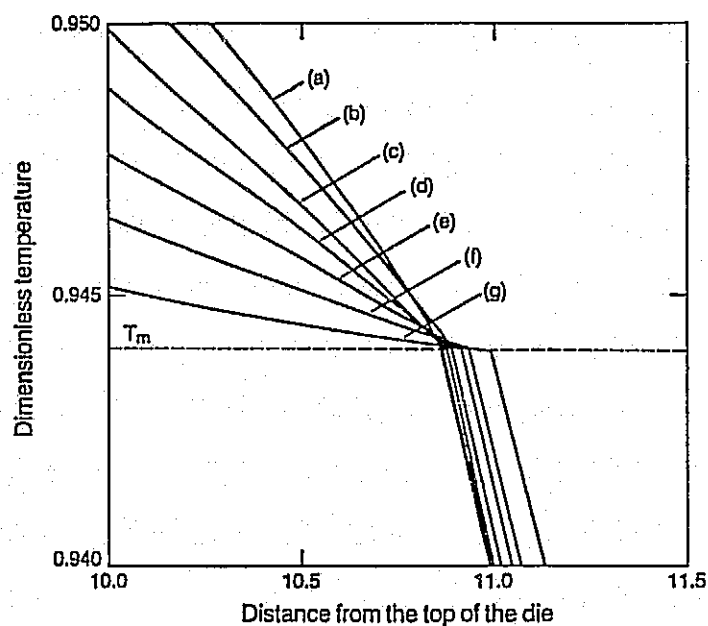
- DECREASES THE HEIGHT OF THE MELT
- INCREASES THE THICKNESS OF THE SHEET
- DECREASING THE TEMPERATURE GRADIENT



### Growth Rate — Die Temperature Operating Diagram for EFG

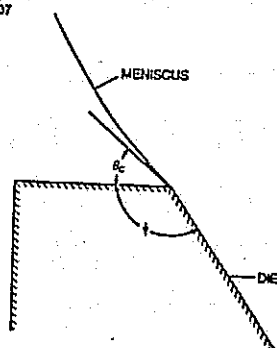
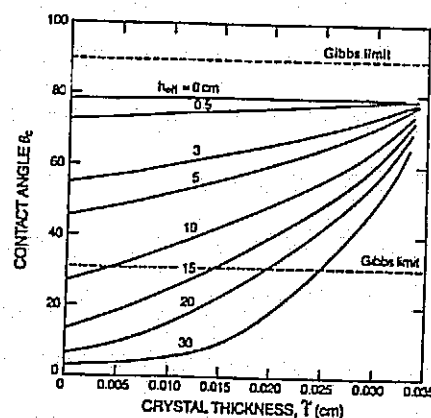
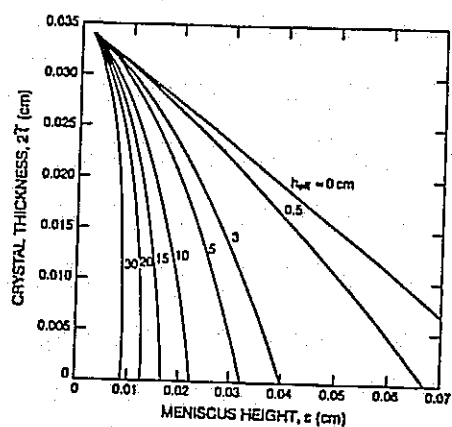


# Zero Temperature Gradient in Melt Occurs at Low Inlet Temperature and High Growth Rate

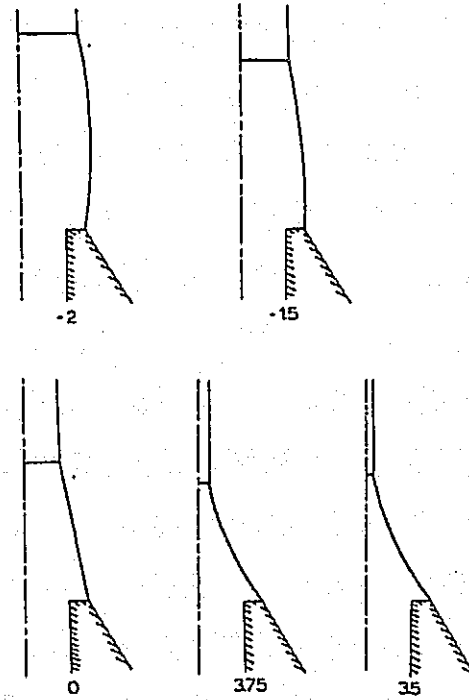
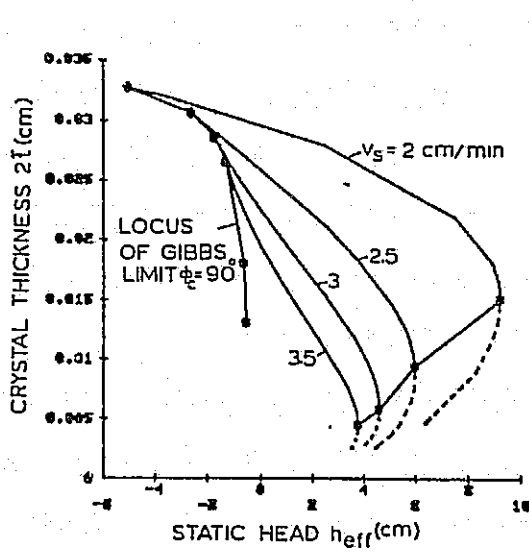


	$T$ °K	$V$ cm/min	$G_L$ °K/cm
(a)	1773	0.96	875
(b)	1763	1.81	743
(c)	1753	2.57	612
(d)	1743	3.41	475
(e)	1733	4.28	333
(f)	1723	5.15	186
(g)	1713	6.11	31

# Capillarity Gives Relationship Between Meniscus Shape and Crystal Thickness



# Interaction Between Capillarity and Heat Transfer Causes Loss of Steady State Beyond Limiting Value of Static Head



## Comparison of Calculations With Experimental EFG-Silicon Results

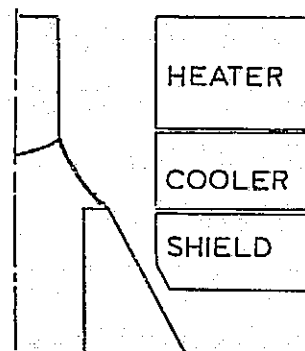
### BASIS OF COMPARISON

- $\dot{z}$  VERSUS  $V_g$  CURVE
- MELT/SOLID INTERFACE SHAPE

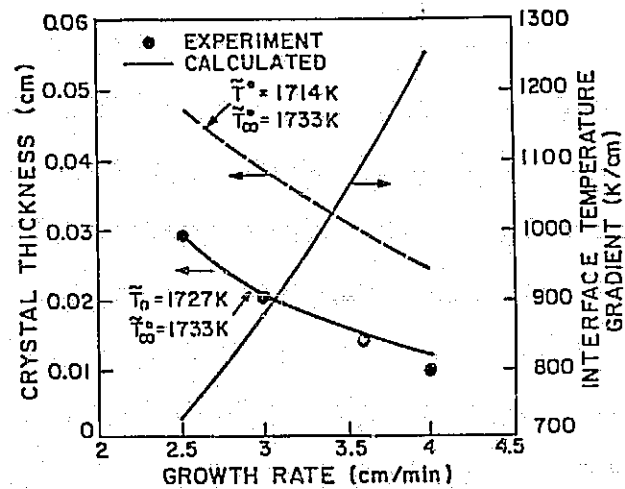
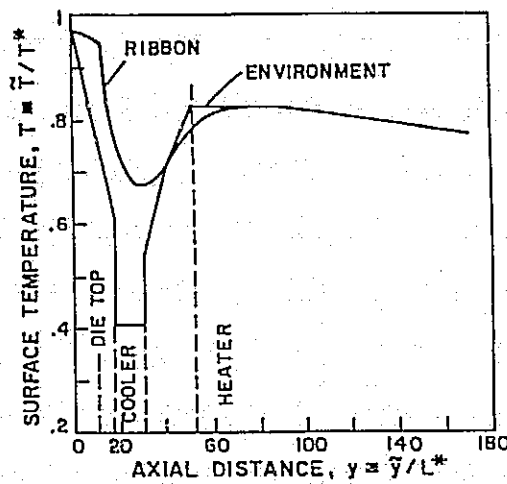
### INPUT

- AMBIENT TEMPERATURE DISTRIBUTION
- STATIC HEAD

TEMPERATURE PROFILE  
MEASURED BY KALEJS & BELL



## Calculations Agree Well With Experiments Using Reasonable Set-Point Temperatures



- PREDICTED TEMPERATURE GRADIENT INCREASES WITH INCREASING GROWTH RATE

## Summary and Future Directions

### NOW

THERMAL MODELLING OF MENISCUS-DEFINED GROWTH SYSTEMS IS POSSIBLE AT BOTH HIGH AND LOW GROWTH VELOCITIES. YIELDS

- OPERATING BOUNDS
- MODES OF FAILURE
- DETAILS OF THERMAL FIELDS AND MELT/SOLID INTERFACE SHAPE
- FLOW FIELD
- DOPANT DISTRIBUTION

### NEXT

- OPERATING STABILITY AND PROCESS DYNAMICS
- EXTENSION TO HIGH SPEED SYSTEM
- INTEGRATION INTO THERMAL STRESS PREDICTIONS



# RIBBON STRESS / STRAIN ANALYSIS

UNIVERSITY OF KENTUCKY

## Stress and Buckling Analysis



FSA PROJECT

<b>TECHNOLOGY</b> STRESS AND BUCKLING ANALYSIS	<b>REPORT DATE</b> 9/28/33
<b>APPROACH</b> MODEL MATERIAL BEHAVIOR MODEL BUCKLING DUE TO THERMAL STRESSES  <b>CONTRACTOR</b> UNIVERSITY OF KENTUCKY	<b>STATUS</b> <ul style="list-style-type: none"><li>• ELASTIC STRESS AND BUCKLING ANALYSIS COMPLETED FOR CONSTANT MATERIAL PROPERTIES.</li><li>• CRITICAL SHEET THICKNESS VS. SHEET WIDE COMPARED FOR FOUR THERMAL PROFILES.</li><li>• RESULTS ARE REASONABLY CONSISTENT WITH EXPERIMENT.</li></ul> SURVEY OF THE MECHANICAL PROPERTIES OF SILICON
<b>GOALS</b> <ul style="list-style-type: none"><li>• PROVIDE GUIDANCE BASED ON ANALYSIS FOR THERMAL PROFILES FOR REDUCING STRESSES AND IMPROVING FLATNESS IN WIDE RIBBON.</li><li>• HAVE RESULTS BE APPLICABLE TO ALL SHEET GROWTH SYSTEMS.</li></ul>	

# SILICON SHEET GROWTH AND CHARACTERIZATION

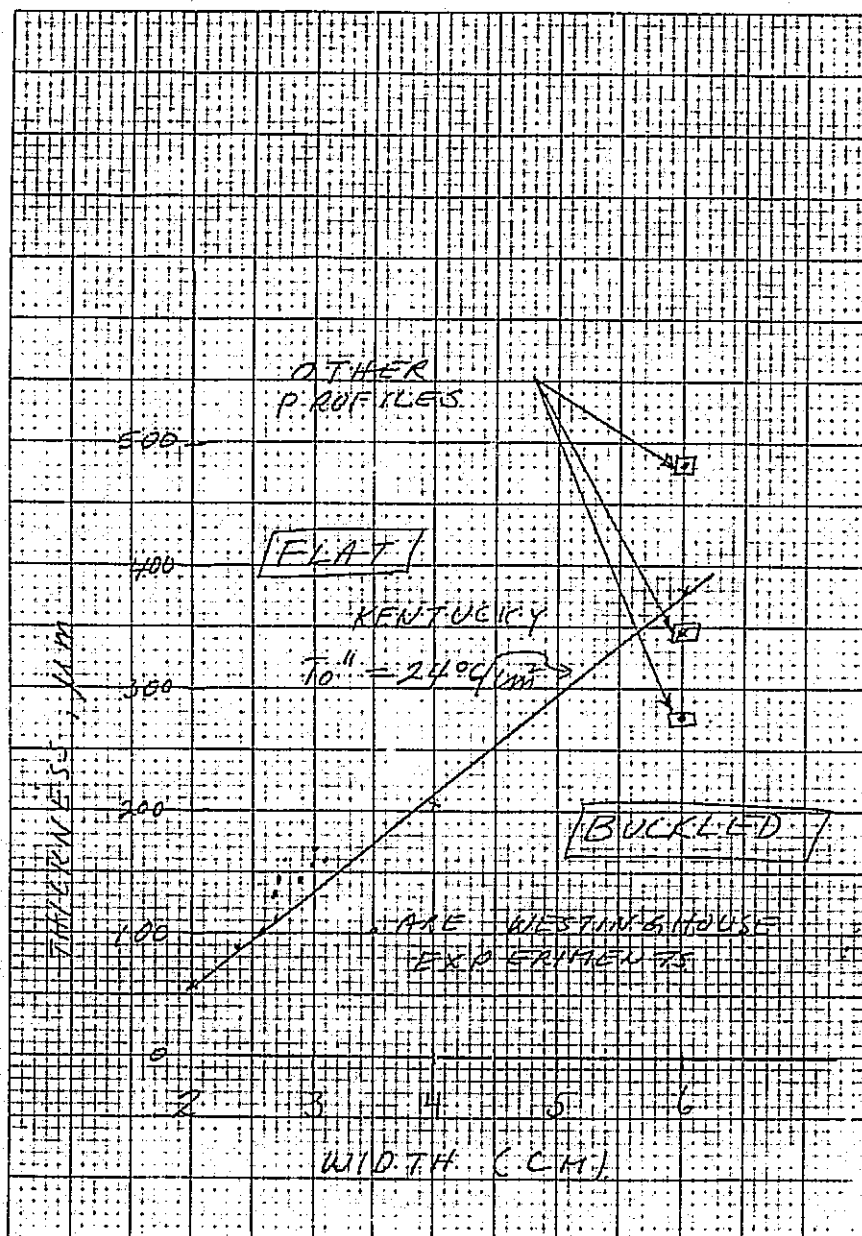


Table 1. Elastic Strain Rates for Various Growth Rates and Temperature Gradients

Growth Rate + $dT/dx$	1 cm/min	5 cm/min	10 cm/min
1°/cm	$8.1 \times 10^{-8}$	$4.1 \times 10^{-7}$	$8.1 \times 10^{-7}$
10°/cm	$8.1 \times 10^{-7}$	$4.1 \times 10^{-6}$	$8.1 \times 10^{-6}$
100°/cm	$8.1 \times 10^{-6}$	$4.1 \times 10^{-5}$	$8.1 \times 10^{-5}$
1000°/cm	$8.1 \times 10^{-5}$	$4.1 \times 10^{-4}$	$8.1 \times 10^{-4}$

\*  $\alpha = 4.88 \times 10^{-6}/^{\circ}\text{C}$  at  $1200^{\circ}\text{C}$

## Mobil Ribbon Process

$$\left(\frac{dT}{dx}\right) \sim 750^{\circ}\text{C/cm}$$

$$\left(\frac{dx}{dt}\right) = 4 \text{ cm/min}$$

$$(\dot{\epsilon})_{\text{avg.}} = 2.4 \times 10^{-4} \text{ sec}^{-1}$$

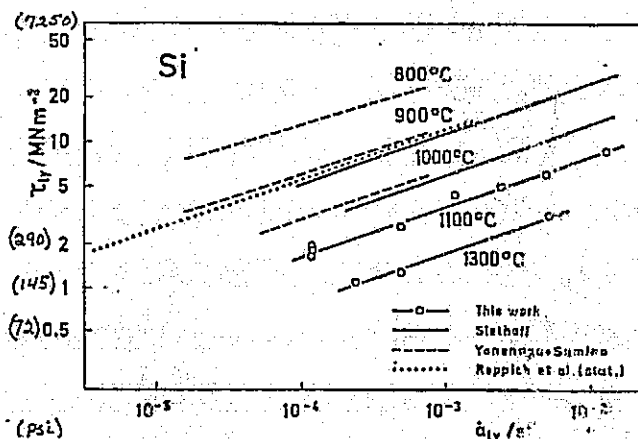


FIG. 1. Lower yield stress as a function of strain rate at different temperatures for silicon in a double-logarithmic plot. Results of Reppich et al.,<sup>2</sup> Yonemura and Sumino,<sup>3</sup> and Stethoff<sup>4</sup> are included.

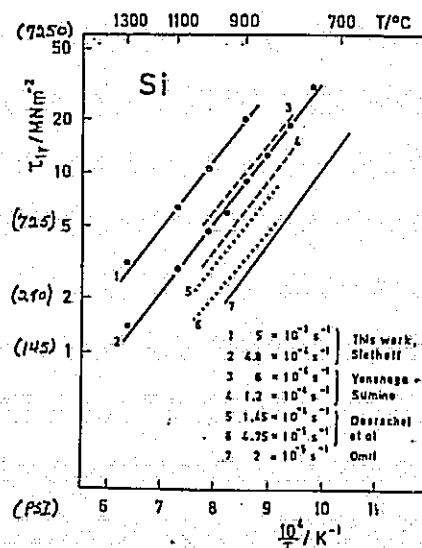


FIG. 2. Lower yield stress as a function of the reciprocal temperature at different strain rates for silicon in a semi-logarithmic plot. Results of Yonemura and Sumino,<sup>3</sup> Doerschel et al.,<sup>5</sup> Omri,<sup>7</sup> and Stethoff<sup>4</sup> are included.

# SILICON SHEET GROWTH AND CHARACTERIZATION

Table 2.

Extrapolated Values of Resolved Flow Stresses at the Lower and Upper Yield Points for Silicon as a Function of Temperature.

Temp °C	(a) $\tau_{LYP}$	(b) $\tau_{LYP}$	(b*) $\tau_{UYP}$
700	5767 psi	3434 psi	37,600 psi
800	2537	1422	11,140
900	1188	684	4,057
1000	536	369	1,731
1100	231	218	836
1200	107	138	446
1300	48	93	258
1400	22	65	159
1430	17	59	139

(a)  $\ln \tau_{LYP} = -0.008T + 25.3$  (J. R. Patel and A. R. Chaudhuri, J.A.P., 34 (1963) 2788).

(b)  $\tau_{LYP} = C \epsilon_n^{-1} \exp(U/nkT)$   
 $U = 2.3 \text{ eV}$ ,  $C = 4.5 \times 10^{-3} \text{ (kg/mm}^2\text{)}$ ,  $n = 2.3$ ,  $\dot{\epsilon} = 10^{-4} \text{ sec}^{-1}$   
H. Siethoff and P. Hassen

(b\*)  $U = 2.3 \text{ eV}$ ,  $C = 4.5 \times 10^{-3} \text{ (kg/mm}^2\text{)}$ ,  $n = 2.1$ ,  $\dot{\epsilon} = 10^{-4} \text{ sec}^{-1}$

Table 3.

Extrapolated Values of the Resolved Flow Stresses, Dislocation Densities and Dislocation Velocities at the Lower Yield Point as a Function of Temperature

Temp. °C	$\tau_{LYP}^*$		(a) $N_D \text{ cm}^{-2}$	(b) $\bar{v} \text{ cm/sec}$
	MPa	PSI		
700	40.	5770	$2.6 \times 10^8$	$9.3 \times 10^{-6}$
800	18.	2640	$4.4 \times 10^7$	$4.9 \times 10^{-5}$
900	8.2	1190	$1.0 \times 10^7$	$1.9 \times 10^{-4}$
1000	3.7	536	$3.0 \times 10^6$	$6.1 \times 10^{-4}$
1100	1.5	231	$1.0 \times 10^6$	$1.6 \times 10^{-3}$
1200	.74	107	$4.2 \times 10^5$	$3.8 \times 10^{-3}$
1300	.33	48	$1.9 \times 10^5$	$8.1 \times 10^{-3}$
1400	.15	22	$9.4 \times 10^4$	$1.6 \times 10^{-2}$
1430	.12	17	$7.8 \times 10^4$	$1.9 \times 10^{-2}$

\*  $\ln \tau_{LYP} = -0.008T - 25.3$  (MPa) (Ref. 1)

(a)  $N_D = 1.58 e^{1.8 \times 10^4/T}$  (Ref. 2)

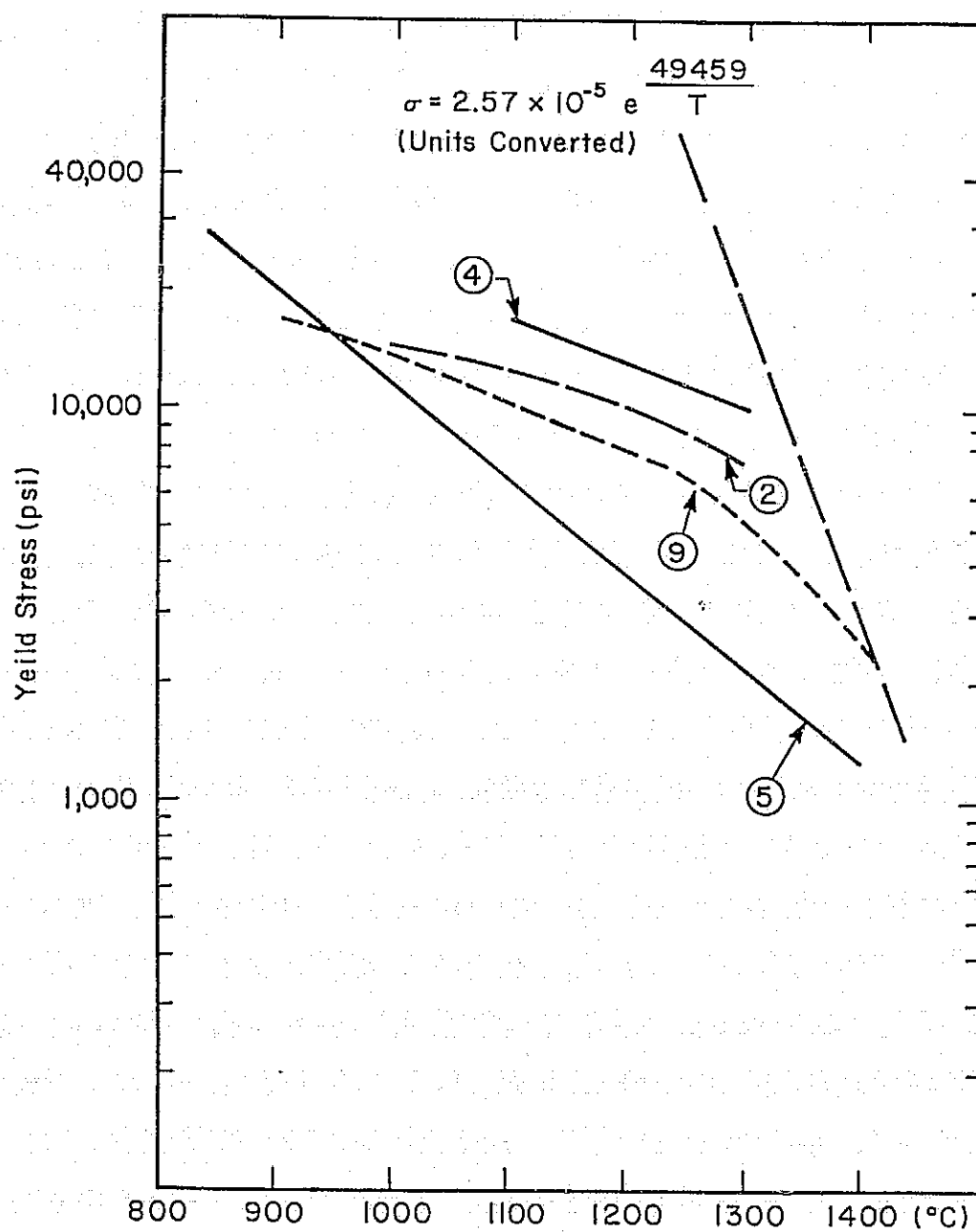
(b)  $\bar{v} = 4.74 \times 10^2 e^{-1.73 \times 10^4/T}$  (Ref. 2)

(a & b) were developed from the Average of three sets of data at  $\dot{\epsilon}$  of  $2.4 \times 10^{-4}$ ,  $1.2 \times 10^{-4}$  and  $0.6 \times 10^{-4}$ .

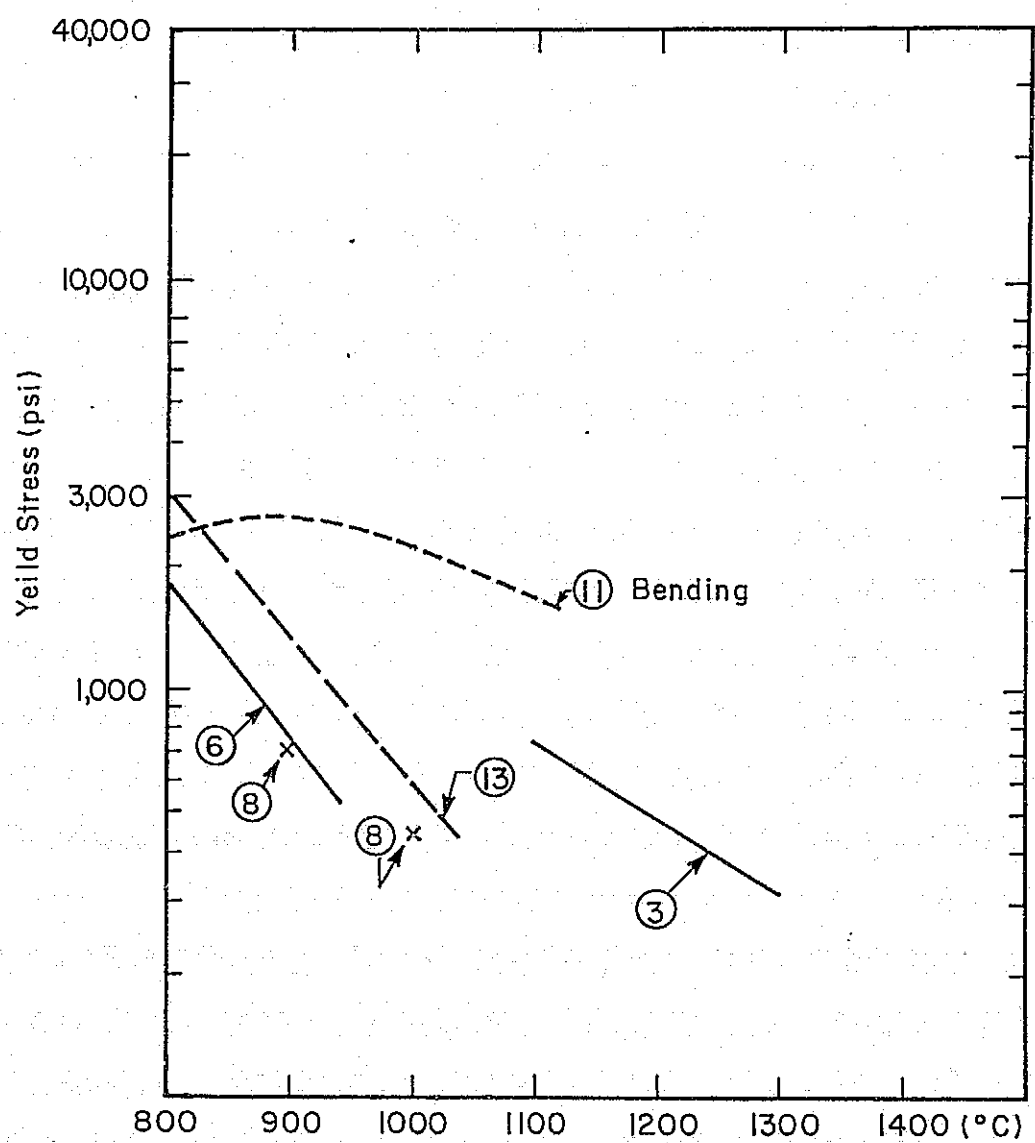
Ref. 1. J. R. Patel and A. R. Chaudhuri, J. Appl. Phys., **34** (1963) 2788.

Ref. 2. I. Yonenaga and K. Sumino, Phys. Stat. Sol., **50** (1978) 685.

# SILICON SHEET GROWTH AND CHARACTERIZATION

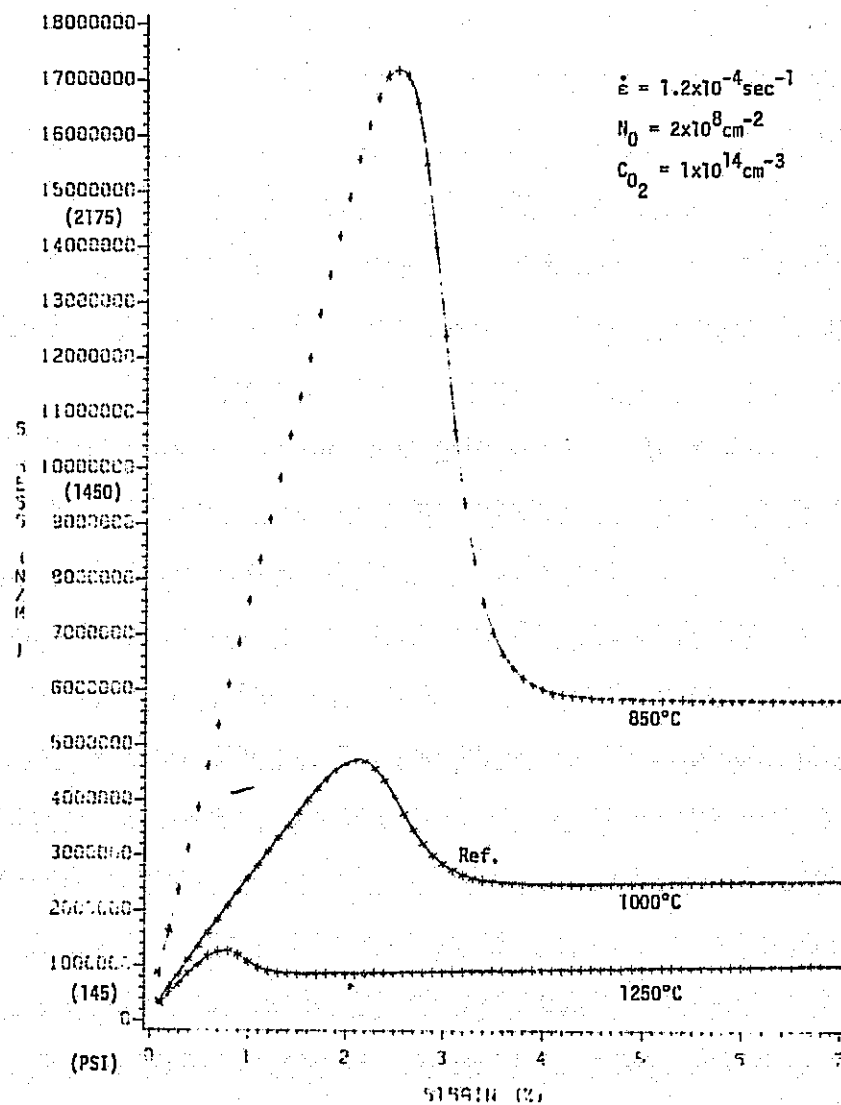


# SILICON SHEET GROWTH AND CHARACTERIZATION



# SILICON SHEET GROWTH AND CHARACTERIZATION

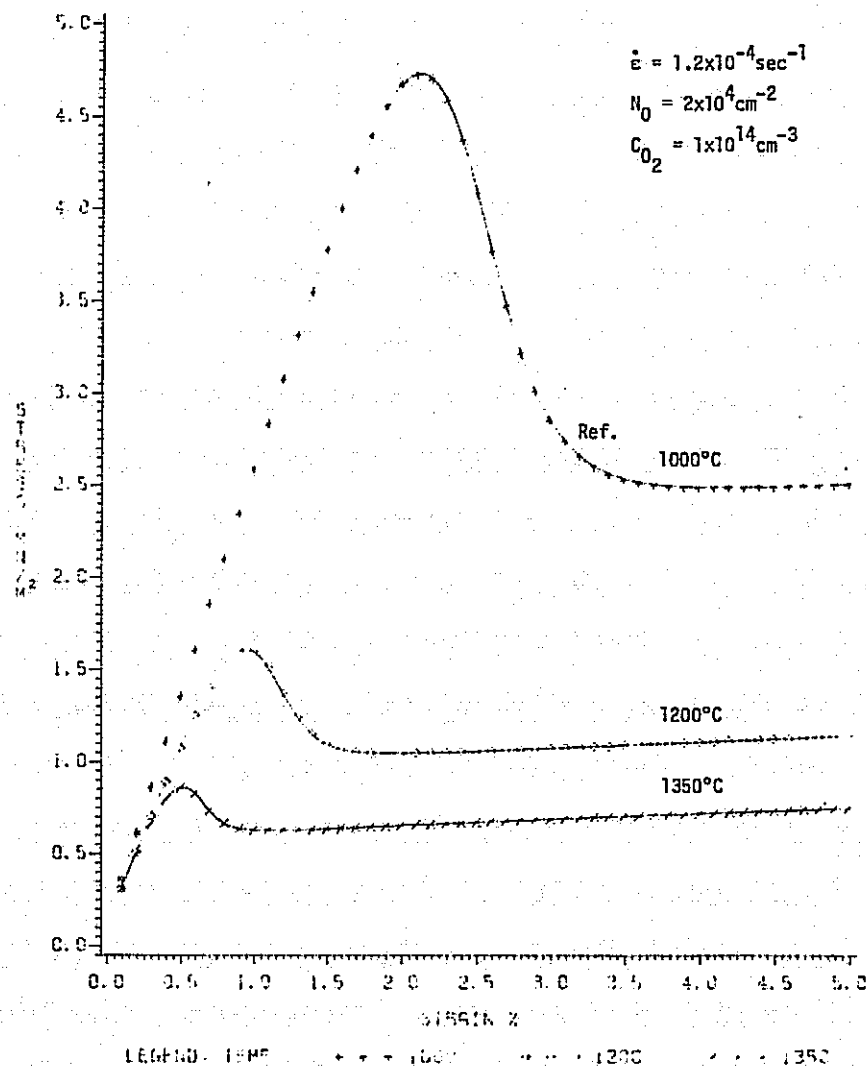
## Stress vs Strain



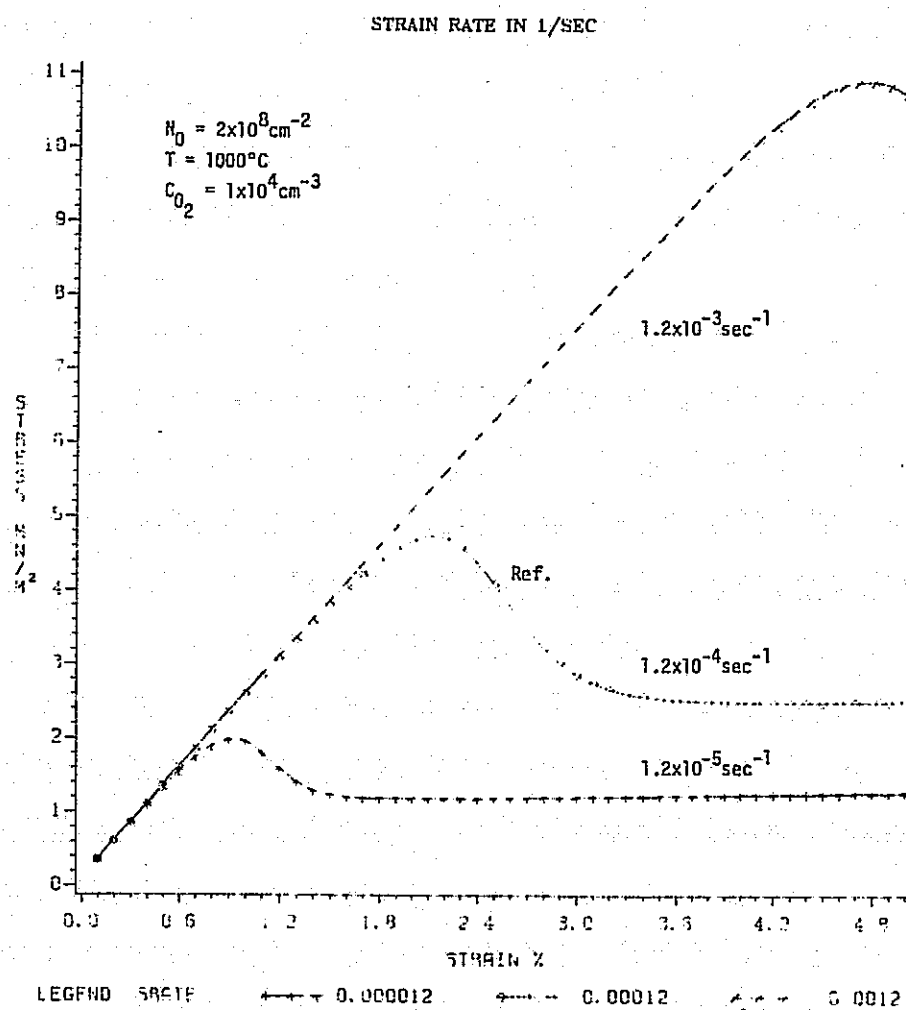


## Stress vs Strain for Si

TEMPERATURE IN DEGREES CENTIGRADE

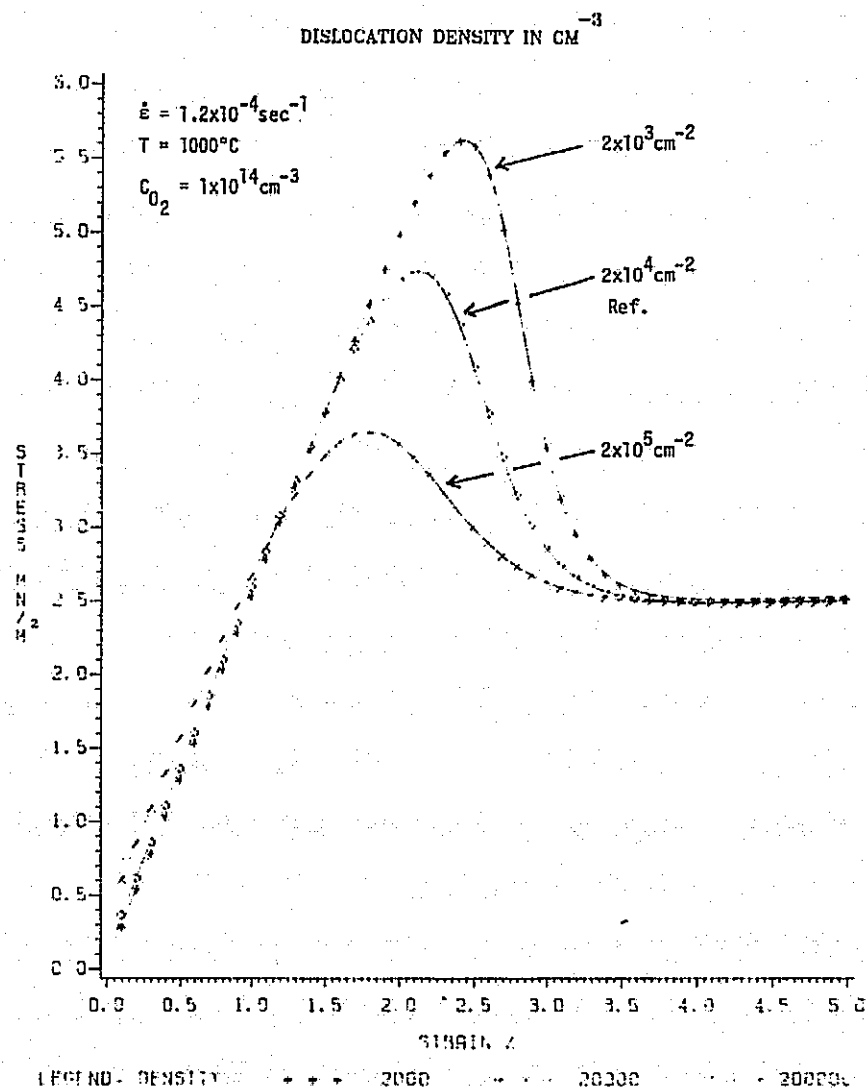


# SILICON SHEET GROWTH AND CHARACTERIZATION



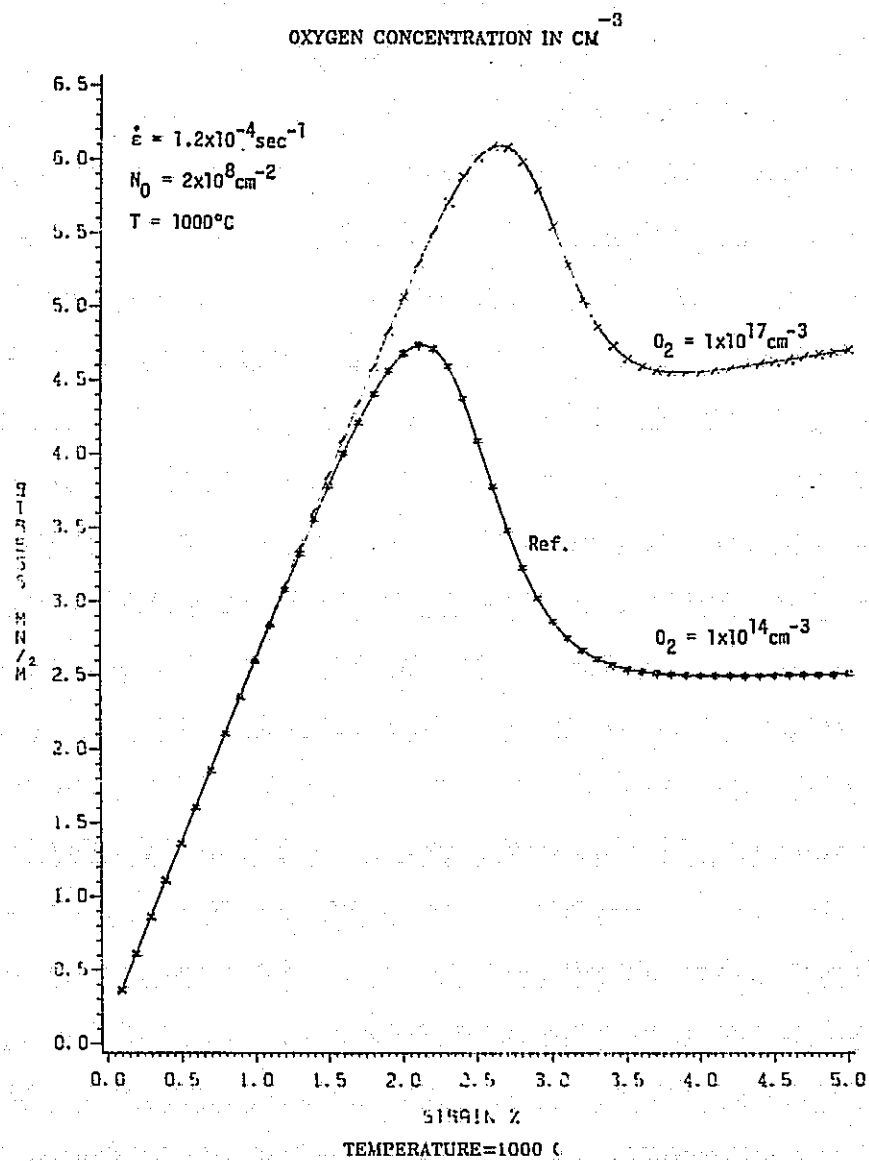
TEMPERATURE=1000 (

# SILICON SHEET GROWTH AND CHARACTERIZATION



TEMPERATURE=1000 (

# SILICON SHEET GROWTH AND CHARACTERIZATION



## SILICON SHEET GROWTH AND CHARACTERIZATION

### UNIVERSITY OF KENTUCKY

1. Savitskii, E. M. In Mechanical Properties of Intermettalic Compounds Wiley and Sons, N.Y. J. H. Wertbrook, Editor (1959).
2. Myshlysev, M. M., Nikitinko, V. I., and Nesterenko, V. I. Phys. Sol. Stat. 36, pp. 89-96. (1969).
3. Taylor, T. A. and Barrett, C. R., Mater. Sci. Eng. 10 pp 93-101 (1972).
4. Graham, C. D. Jr, Pope D. P., Kulkarni, S. and Wolf, M. Final Report on Hot Forming of Silicm Sheet, University of Pennsylvania; (April 14, 1978).
5. Sylwestrowicz, W. D. Phil Mag, Vol 7 pp 1825-1845 (1962).
6. Yonenaga, I. and Sumino, K., Phys Stat Sol (a), 50, p 685-693, (1978).
7. Pearson, G. L., Read W. T. Jr, Feldmoun W. L. Acta Metallurgica, 5, pp 181 ff. (April 1957).
8. Siethoff, H. and Haasen, P. "Lattice Defects in Semiconductors", edited by R. R. Hasiquti [University Press, Tokyo], p 491 ff. (1968).
- 8a. Correra, L. and Bentini, G. G., Jnl Appl Phys., 54, No. 8 pp 4330-4337.
9. Gurtler, R., J. Crystal Growth, 50, (1980).
10. Suzuki, T and Kojima, H. Acta Metallurgica Vol 14, p 913 f August (1966).
11. Sawada, R, Karaki, T. and Watanoke, J. Applied Physics A, Vol 31 pp 109-114 (1983).
12. Costaing, J.; Veyssiere, P.; Kubin, L. P.; and Rabies: Phil Mag A 44, No 6 pp 1407-1413 (1981).
13. Patel and Choudhuri, J. Appl Phys, 34, pp 2788 f (1963)

# UBIQUITOUS CRYSTALLIZATION PROCESS

SEMIX INC.

William F. Regnault  
Scott M. Johnson

## Semicrystalline Casting Process Development and Verification

INVESTIGATION OF STRUCTURAL DEFECTS WITHIN GRAIN  
VOLUMES THAT AFFECT THE EFFICIENCY OF SEMICRYSTALLINE  
SILICON SOLAR CELL MATERIALS

### PURPOSE:

DETERMINE THE NUCLEATING MECHANISMS OF A DISLOCATION  
SUBGRAIN STRUCTURE OCCASSIONALLY FOUND IN SEMICRYSTALLINE  
SILICON

### APPROACH:

PERFORM X-RAY TOPOGRAPHIC AND DEFECT ETCH STUDIES ON  
SEVERAL SAMPLES OF U C P MATERIAL.

DEFECT ETCHING SHOWS DISLOCATION DENSITY ON THE ORDER  
OF  $10^5/\text{cm}^2$  IN REGION OF SUBGRAIN ROTATIONS WITH A DEN-  
SITY OF  $10^3/\text{cm}^2$  OUTSIDE THESE REGIONS.

ETCH PIT PATTERN INDICATES DISLOCATIONS DUE TO SLIP  
ALONG (111) TYPE PLANES.

HIGH RESOLUTION LIGHT SPOT SCAN AT  $\lambda = 1.0\text{mm}$  SHOWS  
DEGRADATION OF SHORT CIRCUIT CURRENT DUE TO HIGH  
DISLOCATION CONTENT.

## Conclusions

DISLOCATION SUBGRAIN STRUCTURE HAS A DELETERIOUS EFFECT ON THE LOCAL PHOTOVOLTAIC PROPERTIES OF SEMICRYSTALLINE MATERIAL.

THE SUBSTRUCTURE ARISES AS A WAY OF RELIEVING INTERNAL STRESSES.

SLIP APPEARS TO BE IN  $\{111\}$  TYPE PLANES

THE DRIVING FORCE FOR THIS SUBGRAIN STRUCTURE APPEARS TO BE STRESS ARISING ALONG DISCONTINUITIES OR IMPERFECTIONS IN THE GRAIN BOUNDARIES.

## Effects of Nonequilibrium Solidification on the Material Properties of Brick Silicon for PV

### PURPOSE:

INVESTIGATE THE CAUSITIVE FACTORS IN THE BREAKDOWN OF LARGE GRAINS INTO REGIONS OF EXTREMELY FINE GRAIN MATERIAL.

DETERMINE CONDITIONS WHICH MAY IMPOSE PRACTICAL LIMITS ON THE SPEED OF CRYSTAL GROWTH IN INGOT TECHNOLOGIES LIKE U C P.

## SILICON SHEET GROWTH AND CHARACTERIZATION

### Approach

- GROW AN INGOT UNDER CONDITIONS KNOWN TO PRODUCE THE MATERIAL OF INTEREST AND TO COMPARE RESULTS WITH A CONTROL INGOT
- WAFER ONE QUADRANT OF THE INGOTS PERPENDICULAR TO THE GROWTH DIRECTION AND ANOTHER QUADRANT PARALLEL TO THE GROWTH DIRECTION
- ANALYZE THE WAFERS BY MEANS OF:

OPTICAL MICROSCOPY  
SCANNING ELECTRON MICROSCOPY  
X-RAY TOPOGRAPHY  
ELECTRON MICROPROBE ANALYSIS

THERMOCOUPLE RESPONSE MEASUREMENTS INDICATE AN AVERAGE GROWTH RATE OF 1.9CM/HR FOR MUSH INGOT AND 1.6CM/HR FOR CONTROL INGOT.

UCP MATERIAL HAS BEEN PRODUCED WITH AVERAGE GROWTH RATES AS HIGH AS 3.3CM/HR.

SOLAR CELLS FABRICATED ON SHEET MATERIAL CONTAINING EITHER MUSH OR SINUOUS GRAIN BOUNDARIES EXHIBIT:

VERY LOW SHUNT RESISTANCES  
POOR FILL FACTORS  
LOW MINORITY CARRIER LIFETIMES  
COMPLETE SHORTS  
LOW OPEN CIRCUIT VOLTAGE



## SILICON SHEET GROWTH AND CHARACTERIZATION

DUE TO THE HIGHLY STRAINED NATURE OF THIS MATERIAL, IT WAS POSTULATED THAT DIFFUSION DOWN THE GRAIN BOUNDARIES COULD BE RESPONSIBLE FOR THE SHUNTING OF THESE DEVICES.

BEVEL AND STAINING EXPERIMENTS WERE CARRIED OUT ON:

- A CONTROL SEMICRYSTALLINE SAMPLE
- A SAMPLE CONTAINING DISLOCATION SUB-  
GRAIN BOUNDARIES
- TWO SAMPLES CONTAINING MUSH; ONE  
DIFFUSED, ONE NOT

POLISHED TRANSVERSE SECTION OF REGION 3 SHOWS THAT THE GRAIN BOUNDARIES ARE DOTTED WITH INCLUSIONS APPROXIMATELY  $1\mu$  ACROSS.

THE ROUNDED CORNERS OF THIS INCLUDED MATERIAL INDICATE LIQUIFICATION AFTER THE PRIMARY FIELD OF SILICON HAS SOLIDIFIED.

OPTICAL AND SCANNING ELECTRON MICROSCOPY SHOWS THAT THESE GRAIN BOUNDARIES ETCH QUITE DEEPLY AND WITHIN THESE TRENCHES ARE FIBROUS INCLUSIONS.

ELECTRON MICROPROBE ANALYSIS, USING WAVELENGTH DISPERSIVE SPECTROSCOPY FOR CARBON AND OXYGEN, WAS CARRIED OUT ON THE FIBROUS INCLUSIONS AT THE GRAIN BOUNDARIES:

- THERE WAS NO CHANGE BETWEEN THE GRAIN  
VOLUME AND THE GRAIN BOUNDARIES FOR  
OXYGEN
- THERE WAS A MARKED INCREASE OF THE  
CARBON CONTENT OF THE INCLUSIONS OVER  
THE SILICON BACKGROUND

## SILICON SHEET GROWTH AND CHARACTERIZATION

FROM THE GRAIN MORPHOLOGY AND FROM THE HIGH INCLUSION CONTENT OF THE GRAIN BOUNDARIES, IT IS FELT THAT THIS MUSH STRUCTURE IS DRIVEN BY A BREAKDOWN IN GRAIN GROWTH, DUE TO CONSTITUTIONAL SUPERCOOLING.

USING THE SOLUTE REDISTRIBUTION MODEL OF TILLER/ JACKSON, RUTTER AND CHALMERS (ACTA MET, 1, 428, 1953), THE IMPURITY DISTRIBUTION IN THE SOLID CAN BE CALCULATED FROM:

$$C_s = C_0 (1-K) [1 - \exp(-K \frac{R}{D_L} x)]^{1+K}$$

THE FORM OF THE SOLUTE DISTRIBUTION IN THE LIQUID AT THE SOLIDIFICATION FRONT IS JUST:

$$C_T = C_s / K$$

AND THE TRANSIENT DECAY TO THE EQUILIBRIUM CONCENTRATION IS:

$$C_a = C_0 \left\{ \frac{1-K}{K} [1 - \exp(-K \frac{R^2}{D_L} T)] \exp(-\frac{R}{D_L} (X' - RT)) + 1 \right\}$$

WHERE  $C_0$  IS THE EQUILIBRIUM CONCENTRATION

$K$  IS THE SEGREGATION COEFFICIENT

$R$  IS THE SOLIDIFICATION RATE

$D_L$  IS THE DIFFUSION COEFFICIENT IN THE MELT

CONSTITUTIONAL SUPERCOOLING OCCURS WHEN THE ACTUAL THERMAL GRADIENT IN THE MELT IS LESS THAN THE LIQUIDUS TEMPERATURE. FROM HEAT AND MASS FLOW AT THE INTERFACE, THE GENERAL CONSTITUTIONAL SUPERCOOLING CRITERIA IS GIVEN AS:

$$\frac{G_L}{R} \geq \frac{M_L C_s (1-K)}{K D_L}$$

WHERE  $G_L$  IS THE THERMAL GRADIENT IN THE LIQUID

$M_L$  IS SLOPE OF THE LIQUIDUS CURVE

## SILICON SHEET GROWTH AND CHARACTERIZATION

COMBINING EQUATIONS AND SOLVING FOR X YIELDS

$$\frac{D_L}{KR} \ln \left\{ \frac{\frac{G_L KD_L}{RM_L C_L - K C_0} - K}{1 - K} - 1 \right\} = X$$

SOLVING, ONE OBTAINS A HEIGHT OF 1.5 cm FOR THE START OF THE BREAKDOWN IN GRAIN GROWTH WHICH IS IN FAIR AGREEMENT WITH THE 3 cm EXPERIMENTALLY OBSERVED HEIGHT.

## Conclusions

IT HAS BEEN SHOWN THAT AS GRAIN GROWTH PROCEEDS INTO THE MUSH REGION, THE LARGER GRAINS ARE SEEN TO BREAK DOWN INTO A CELLULAR STRUCTURE AS PREDICTED BY CONSTITUTIONAL SUPERCOOLING THEORY.

OPTICAL AND SCANNING ELECTRON MICROSCOPY HAVE INDICATED THE PRESENCE OF A LIQUID SECOND PHASE EXISTING IN THE GRAIN BOUNDARIES AFTER THE PRIMARY FIELD OF SILICON HAS FROZEN. ELECTRON MICRO-PROBE ANALYSIS HAS SHOWN SILICON CARBIDE TO BE ONE OF THE CONSTITUENTS OF THIS SOLUTE.

THE POOR PHOTOVOLTAIC PERFORMANCE OF SHEET MATERIAL CONTAINING MUSH IS DUE TO SHUNT PATHS CREATED BY THE SOLUTE TRAPPED IN THE SINUOUS GRAIN BOUNDARIES AND BY THE HIGH DISLOCATION CONTENT OF THESE GRAINS CAUSED BY STRAIN ENERGY ASSOCIATED WITH THE IMPURITY BUILD UP.

ULTIMATELY, THE RATE OF SOLIDIFICATION IN INGOT TECHNOLOGIES SUCH AS UCP IS DICTATED BY THE GENERAL CONSTITUTIONAL SUPERCOOLING CRITERIA.

$$\frac{G_L}{R} \geq \frac{M_L C_S (1-K)}{KD_L}$$

IF THE GOAL IS TO LOWER THE THERMAL GRADIENT WITHIN THE MATERIAL AND TO USE A STARTING MATERIAL WITH A CERTAIN IMPURITY LEVEL, THEN THERE IS A SOLIDIFICATION RATE WHICH BECOMES A PRACTICAL UPPER LIMIT.

# CONTACTLESS MEASUREMENT OF FREE-CARRIER LIFETIME IN POLYCRYSTALLINE Si INGOTS

SOLAREX CORP.

S.M. Johnson

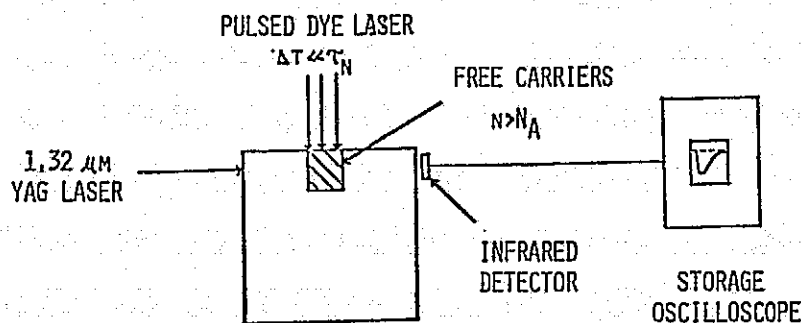
UNIVERSITY OF PENNSYLVANIA

L. Johnson

**OBJECTIVE:** DEVELOP A TECHNIQUE TO DETERMINE THE MINORITY CARRIER LIFETIME IN POLYSILICON INGOTS BEFORE WAFERING.

**APPROACH:** MEASURE THE TIME DEPENDENT TRANSMISSION OF A CW INFRARED LASER DUE TO THE ABSORPTION OF FREE CARRIERS INJECTED WITH A PULSED LASER ( $E_p \geq E_{gap}$ )

10 x 10 cm Polysilicon Brick



# SILICON SHEET GROWTH AND CHARACTERIZATION

## Probe and Excitation Source

PROBE: CW Nd:YAG LASER OPERATING AT  $\lambda = 1.32 \mu\text{H}$

EXCITATION SOURCE: PULSED DYE LASER TUNABLE BETWEEN 1.09 - 1.12  $\mu\text{H}$  WITH A PEAK PULSE ENERGY OF APPROXIMATELY 100 HJ

## Theory

FOR AN EXCITATION SOURCE PULSE WIDTH  $\Delta t \ll \tau$

$$(1) I(t) = I_0 [\exp(-D_H \alpha_{FC})] \exp(-t/\tau)$$

$I(t)$  = TIME DEPENDENT TRANSMITTED PROBE LASER INTENSITY

$I_0$  = UNMODULATED (D.C.) TRANSMITTED PROBE LASER INTENSITY

$D_H$  = WIDTH OF MODULATED REGION

$\alpha_{FC}$  =  $\alpha_{FC}^E + \alpha_{FC}^H$  FREE CARRIER ABSORPTION COEFFICIENT AT PROBE WAVELENGTH

$M$  = INJECTION LEVEL =  $N/N_A = P/N_A$

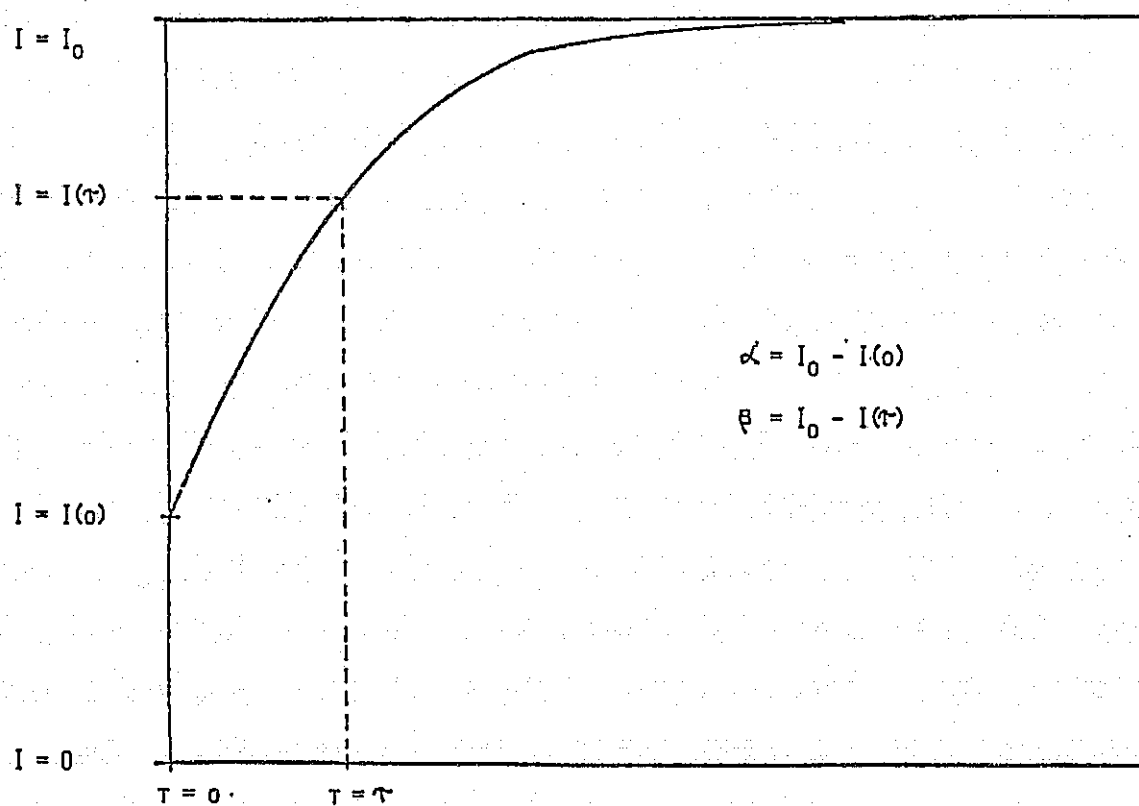
$\tau$  = FREE CARRIER LIFETIME (ASSUMING  $\tau_E = \tau_N = \tau$ )

$N_A$  = DOPANT CONCENTRATION,  $\text{CM}^{-3}$

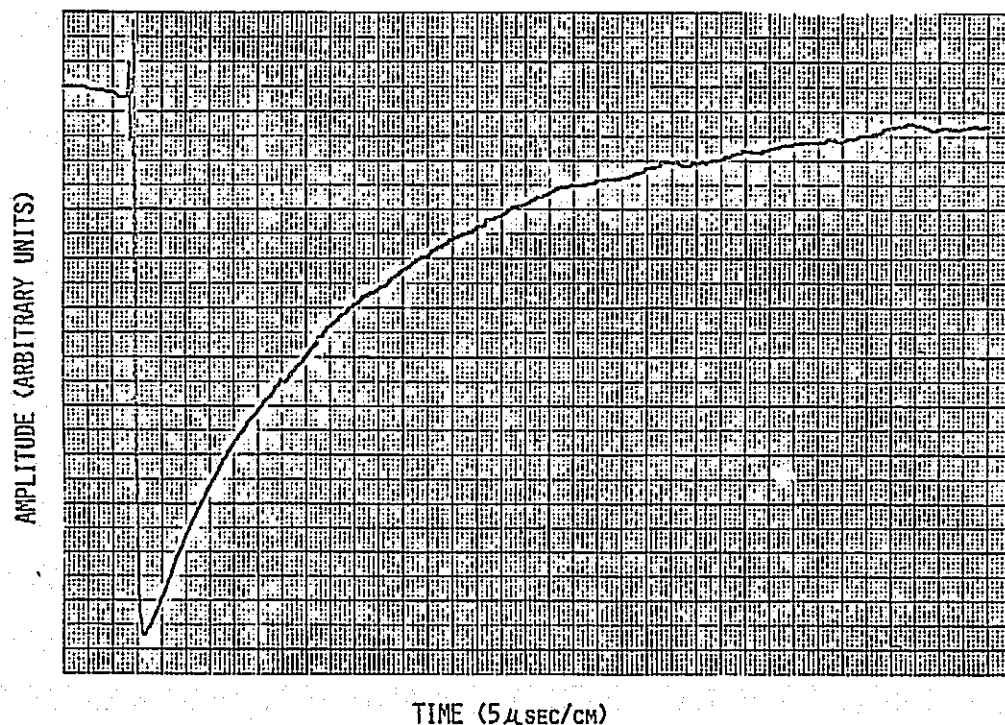
AT  $t = \tau$

$$(2) \frac{I(\tau)}{I_0} = \left[ \frac{I(0)}{I_0} \right]^{.368}$$

## Transient Signal Analysis



### Example of a Transient Signal



### Summary

1. FEASIBILITY OF THE CONTACTLESS INFRARED FREE-CARRIER ABSORPTION TECHNIQUE HAS BEEN DEMONSTRATED.
2. THE TRANSIENT SIGNAL HAS BEEN DETECTED AND RESOLVED TO A MAXIMUM DEPTH OF 2.0 CM IN THE BRICK.

### Future Work

1. CORRELATE FREE-CARRIER LIFETIME MEASUREMENTS MADE ON POLY-SILICON BRICKS WITH MEASUREMENTS MADE ON WAFERS BY OTHER TECHNIQUES.
2. RELATE THE EXPERIMENTAL RESULTS TO A THEORETICAL MODEL.
3. USE THE ABOVE RESULTS TO PREDICT THE FEASIBILITY OF PROBING DEEPER INTO THE BRICK USING ALTERNATE EXCITATION SOURCES.

# SILICON SHEET CHARACTERIZATION

CORNELL UNIVERSITY

D. Ast

- 1) Carbon - Oxygen - Selfinterstitial Interactions (Goesele model).
- 2.) Ebic studies of the influence of a high temperature pre-anneal on the structure & electrical activity of defects.
- 3.) Ebic studies of low angle g.b. in bicrystals (YPL grown)
- 4.) TEM studies of HEM material.



Models

(A) Structural → High T changes  
dislocation cores  
(constricted)  
→ Reduces dislocations  
in twin g.b.

(B) T.H. gettering → High T anneal  
generates  
homogeneously  
con level of EBIC)  
distributed  
gettering centers  
[Goesele model]

(C) Dissolving → High T anneal  
disperses carbon  
[Cusp model]

## Goesele Model

### Assumptions:

- 1.) Swirl like defects exist in EFM  
( $V/E$  argument)  
→ explains inability to find  $c$   
related precipitates
- 2.) In the as grown state, defects  
are strain free ( $c/I$  ratio)  
and electrically inactive  
→ strain free → TEM invisibility
- 3.) High temperature preanneal  
( $1200^\circ\text{C}$ ) reduces  $I$  content  
(carbon rich) → centers of  
contraction  
→ "Bleichmann" effect
- 4.)  $P$  diffusion restores "correct"  
 $I$  content. In addition,  $I$   
act as nucleation sites for  $\text{SiO}_2$   
precipitates → light enhancement.)

Pre-Anneal

Standard  
(900° -  $\text{Pt}_2$ )

High residual  
stress

"Normal" defect  
structure

Strongly EBIC  
active defects

Electrical  
activity

→ second phase  
( $\text{SiO}_2$ ?)

→ Broken bonds

→ dislocations  
(pile up at  
turns, inlv.)

Pre-anneal  
(~1200°C)

Low residual  
stress

→ Higher amount of  
g.b. (~20° → poly-  
gonization.)

→ Less dislocations  
in twin boundaries

→ Less bulk dislocations  
(~10 to 40% of STD)

→ Essentially no  
electrical activity  
at defects

Mechanical  
properties

Eb weak

strain fields

Incipient crack

(Stroh mechanism)

# Bicrystals

①  $5.5 \pm 0.1 [100]$

+  $\rightarrow 2.1 \pm 0.2 [010]$  tilt

+  $0.7 \pm 0.1 [001]$  twist

②  $17.2 \pm 0.1 [100]$

+  $1.3 \pm 0.2 [010]$  tilt

$\rho \approx 5 \cdot 10^5 \text{ cm}^{-2}$

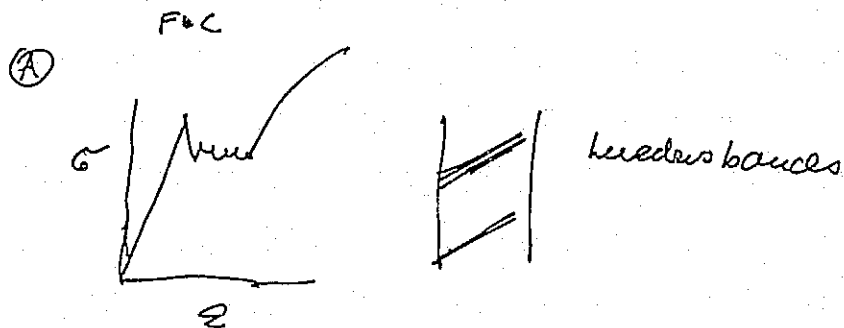
(denuded zones at f.b.)

Identical EBIC contrast [high]

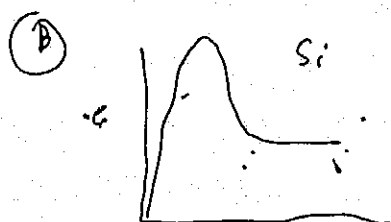
TEM  $\rightarrow$  precipitates

Electrical behavior controlled by  
impurity segregation

# SILICON SHEET GROWTH AND CHARACTERIZATION

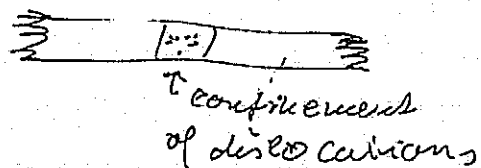


Mechanism - Carbon pinning

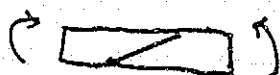


Mechanism - dislocation multiplication

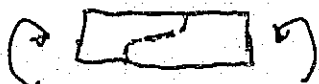
→ two boundaries



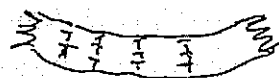
Initial:



Stress redistribution:



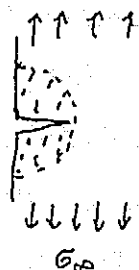
→ polygonization



## Fracture

$$K > K_c$$

$$K_c = \underset{\substack{\uparrow \\ \text{geometry}}}{C} \cdot \sigma_{\infty} \cdot \sqrt{c}$$

Surface energy  $\propto c$ Elastic unloading  $\propto c^2$ 

$$E_{tot} = C_1 \cdot c - \frac{\pi \cdot C^2}{2} \cdot \frac{\sigma_{\infty}^2}{2E}$$

$$\frac{\partial E}{\partial c} = 0$$

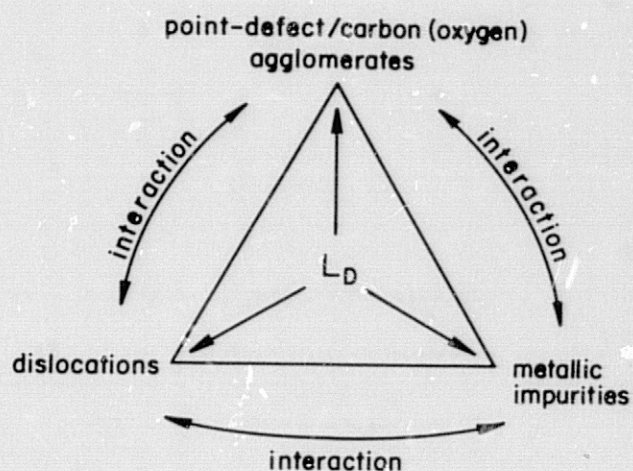
$$C_1 = \frac{\pi}{2} \cdot \frac{1}{E} \cdot C \cdot \sigma_{\infty}^2$$

$$\sigma_{\infty} \cdot C_{crit} = \sqrt{\frac{C_1 \cdot E \cdot 2}{\pi}}$$

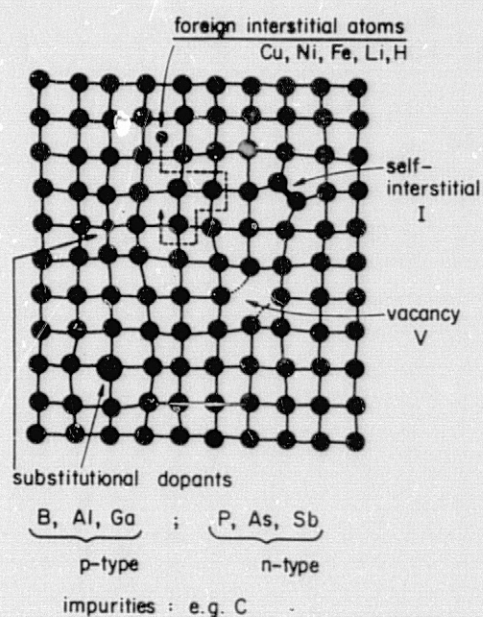
Asymmetric g.b.  $[110] \rightarrow$  broken bonds  
( $0 \dots 108^\circ$ )

Symmetric g.b.  $[110] \rightarrow$  no broken b.

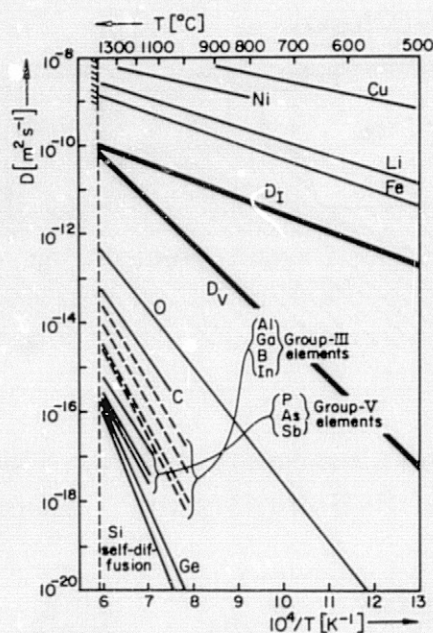
## Limiting Factors of Minority Carrier Diffusion Length



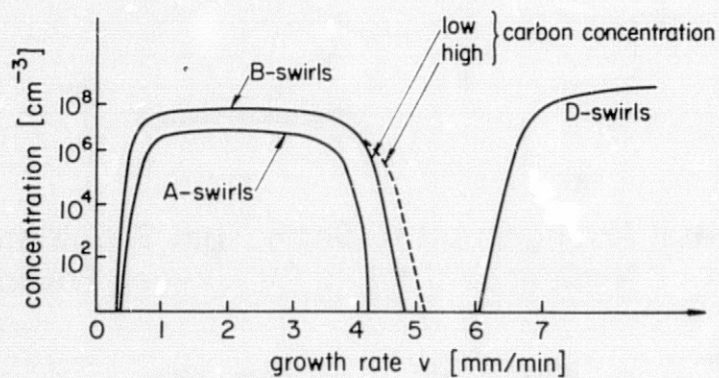
## Point Defects in Silicon





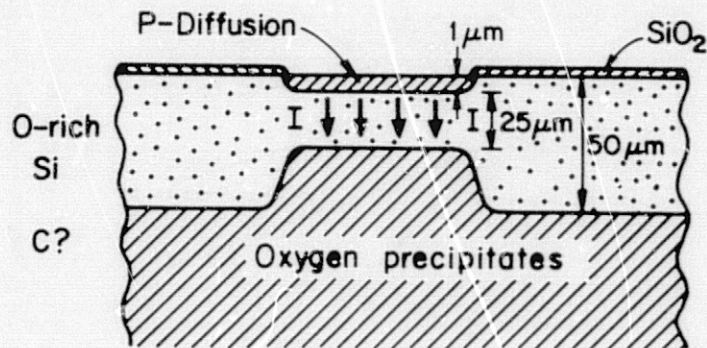
Diffusivity of Si-Selfinterstitials ( $D_I$ ) and Si Vacancies ( $D_V$ )

Appearance of Swirl Defects in Silicon  
(Horizontal Axis Should Be  $v/G$  ( $G$  = Temperature Gradient))

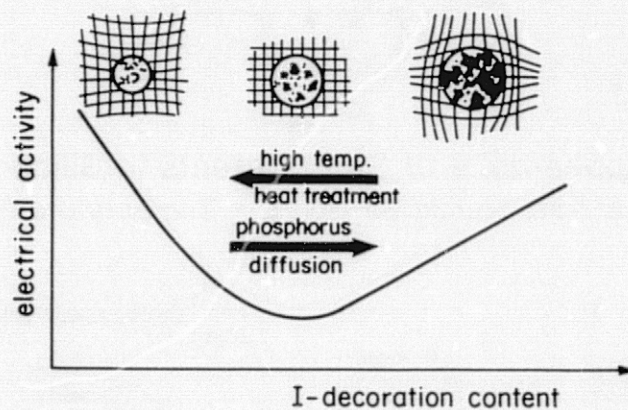




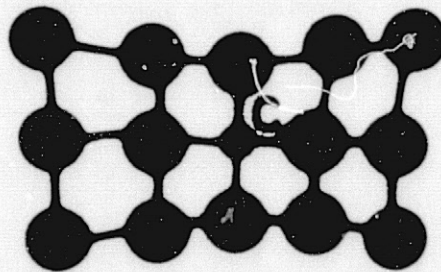
### Substitutional Carbon Incorporated in Silicon



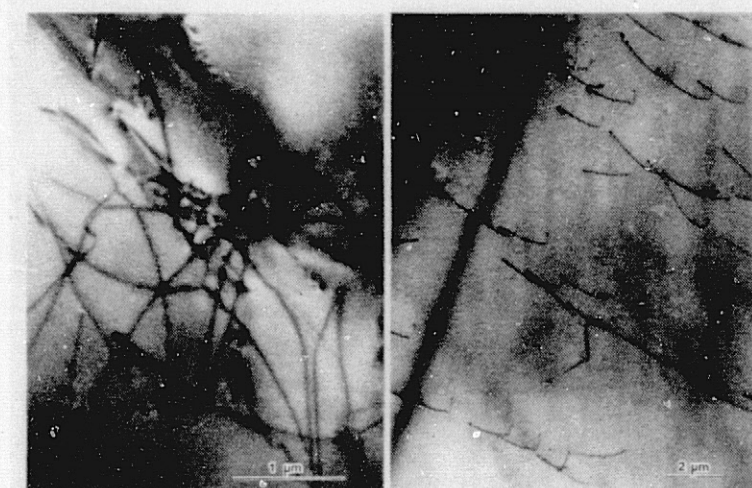
### Relation Between Composition Strain Field and Electrical Activity of Si-Selfinterstitial/Carbon Defects



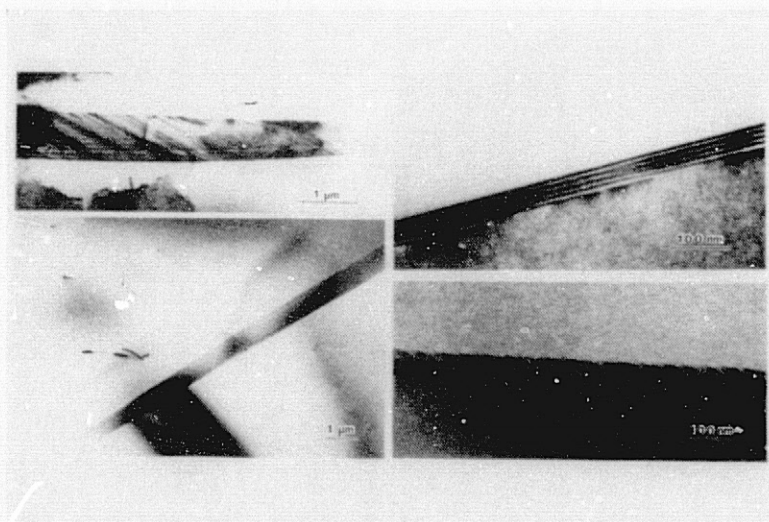
### Experimental Arrangement to Show That Si-Selfinterstitials Can Act as Nucleation Centers for Oxygen Precipitation



Top: Dislocations in Standard EFG Cell  
Bottom: Dislocations in Pre-Annealed EFG Cell

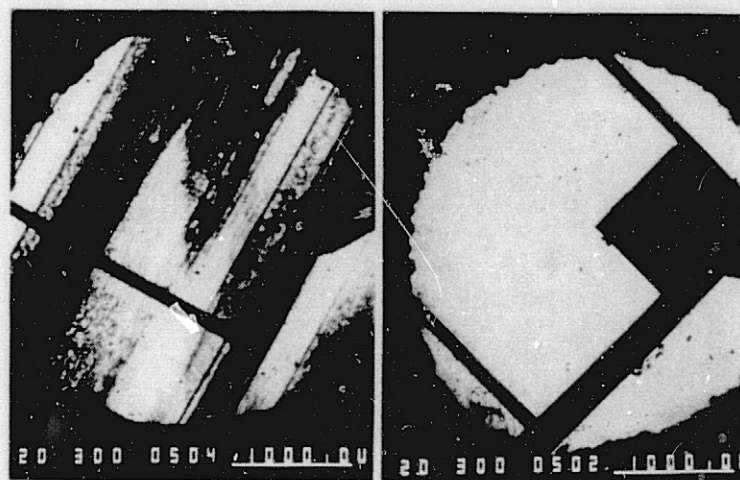


Examples of High-Angle ( $\theta \approx 20$  Deg)  
Grain Boundaries Formed During Anneal





Comparative EBIC Activity (Identical Imaging Conditions)  
Left: Standard Cell      Right: Pre-Annealed Cell



# QUANTITATIVE ANALYSIS OF DEFECTS IN SILICON SHEET

MATERIALS RESEARCH, INC.

## Circumference and Field of View of Olympus Inverted PME Microscope

Eye- piece Lens	Object- ive Lens	Magnifi- cation	Diameter of field of view (cm)	Circum- ference of field of view ( cm )	Area of field of view ( cm <sup>2</sup> )
10X	5X	50X	0.36	1.13	0.102
10X	10X	100X	0.175	0.55	0.0241
10X	20X	200X	0.089	0.28	0.00622
10X	40X	400X	0.0435	0.137	0.00149
10X	100X	1000X	0.0174	0.055	0.000238

Sample Calculation:

$$\text{Circumference at 50X} = \pi D = (\pi) (0.36 \text{ cm}) = 1.13 \text{ cm}$$

$$\text{Area of field of view at 50X} = \frac{\pi D^2}{4} = \frac{\pi (0.36)^2}{4} = 0.102 \text{ cm}^2$$

### Grain Boundary and Twin Boundary Length per Unit Area for Semix Samples

SEMIX Sample Number	Grain Boundary Length per unit area (cm/cm <sup>2</sup> )	Twin Boundary Length per unit area (cm/cm <sup>2</sup> )
A - 13	8.2 $\bar{x} = 2.9$ $\sigma = 2.0$	99.0 $\bar{x} = 34.6$ $\sigma = 56.5$
B - 2	4.5 $\bar{x} = 1.6$ $\sigma = 2.2$	15.8 $\bar{x} = 5.6$ $\sigma = 9.3$
C - 12	13.4 $\bar{x} = 4.7$ $\sigma = 2.7$	31.9 $\bar{x} = 11.2$ $\sigma = 11.1$
D - 8	13.8 $\bar{x} = 4.8$ $\sigma = 3.2$	44.5 $\bar{x} = 15.6$ $\sigma = 17.1$
E - 13	7.1 $\bar{x} = 2.5$ $\sigma = 2.1$	68.5 $\bar{x} = 24$ $\sigma = 38$
F - 2	5.4 $\bar{x} = 1.9$ $\sigma = 2.6$	12.2 $\bar{x} = 4.3$ $\sigma = 6.8$
G - 12	12.1 $\bar{x} = 4.2$ $\sigma = 2.6$	40.7 $\bar{x} = 14.3$ $\sigma = 15.5$
H - 8	9.4 $\bar{x} = 3.3$ $\sigma = 1.9$	35.9 $\bar{x} = 12.6$ $\sigma = 13.3$
Average	9.2	43.6

$$\bar{x} = \text{arithmetic mean} = \frac{\sum \text{features in all fields}}{\text{Total number of fields}}$$

$$\sigma = \text{standard deviation} = \left[ \frac{1}{n-1} \sum_{i=1}^n (x_i - \bar{x})^2 \right]^{1/2}$$

# Precipitate Particle and Dislocation Pit Density in Semix Samples

SEMIX Sample Number	Precipitate Particle Density (particles/cm <sup>2</sup> )			Dislocation Pit Density (pits/cm <sup>2</sup> )
	small	large	total	
A - 13	$22 \times 10^3$ $\bar{x} = 33$ $\sigma = 36.5$	745 $\bar{x} = 1.1$ $\sigma = 1.5$	$23 \times 10^3$	$4.9 \times 10^4$ $\bar{x} = 12$ $\sigma = 23$
B - 2	$19.5 \times 10^3$ $\bar{x} = 29.1$ $\sigma = 18.1$	444 $\bar{x} = 0.66$ $\sigma = 0.95$	$20 \times 10^3$	$9.5 \times 10^4$ $\bar{x} = 23$ $\sigma = 45$
C - 12	$6.2 \times 10^3$ $\bar{x} = 9.2$ $\sigma = 7.7$	65 $\bar{x} = 0.1$ $\sigma = 0.4$	$6.3 \times 10^3$	$37 \times 10^4$ $\bar{x} = 89$ $\sigma = 62$
D - 8	$2.5 \times 10^3$ $\bar{x} = 3.8$ $\sigma = 4.0$	152 $\bar{x} = 0.23$ $\sigma = 0.46$	$2.7 \times 10^3$	$10 \times 10^4$ $\bar{x} = 24$ $\sigma = 51$
E - 13	$9.1 \times 10^3$ $\bar{x} = 13.5$ $\sigma = 10.6$	400 $\bar{x} = 0.6$ $\sigma = 0.7$	$9.5 \times 10^3$	$37 \times 10^4$ $\bar{x} = 89$ $\sigma = 96$
F - 2	$4.8 \times 10^3$ $\bar{x} = 7.2$ $\sigma = 10.5$	740 $\bar{x} = 1.1$ $\sigma = 2.1$	$5.6 \times 10^3$	$17 \times 10^4$ $\bar{x} = 40$ $\sigma = 111$
G - 12	$6.4 \times 10^3$ $\bar{x} = 9.6$ $\sigma = 8.0$	140 $\bar{x} = 0.21$ $\sigma = 0.41$	$6.6 \times 10^3$	$45 \times 10^4$ $\bar{x} = 108$ $\sigma = 161$
H - 8	$9.5 \times 10^3$ $\bar{x} = 14.1$ $\sigma = 10.9$	250 $\bar{x} = 0.4$ $\sigma = 0.8$	$9.7 \times 10^3$	$46 \times 10^4$ $\bar{x} = 204$ $\sigma = 235$
Avg.	$10.0 \times 10^3$	367	$10 \times 10^3$	$31 \times 10^4$

For precipitate particle density, 2.3% of the total area was measured.

For dislocation density, 0.37% of the total area was measured.

### Defect Density, Conversion Efficiency and Diffusion Length of Semix Samples

Semix sample number	Small precipitate density ( $\text{cm}^{-2}$ )	Large precipitate density ( $\text{cm}^{-2}$ )	Total precipitate density ( $\text{cm}^{-2}$ )	Dislocation density ( $\text{cm}^{-2}$ )	Grain boundary length per unit area ( $\text{cm}^{-1}$ )	Twin boundary length per unit area ( $\text{cm}^{-1}$ )	Cell efficiency (%)	Diffusion length ( $\mu\text{m}$ )
A - 13	$22 \times 10^3$	745	$23 \times 10^3$	$4.9 \times 10^4$	8.2	99.0	7.2	53
B - 2	$19.5 \times 10^3$	444	$20 \times 10^3$	$9.5 \times 10^4$	4.5	15.8	10.0	51
C - 12	$6.2 \times 10^3$	65	$6.3 \times 10^3$	$37 \times 10^4$	13.4	31.9	9.7	41
D - 8	$2.5 \times 10^3$	152	$2.7 \times 10^3$	$10 \times 10^4$	13.8	44.5	10.8	47
E - 13	$9.1 \times 10^3$	400	$9.5 \times 10^3$	$37 \times 10^4$	7.1	68.5	6.2	35
F - 2	$4.8 \times 10^3$	740	$5.6 \times 10^3$	$17 \times 10^4$	5.4	12.2	9.6	22
G - 12	$6.4 \times 10^3$	140	$6.6 \times 10^3$	$45 \times 10^4$	12.1	40.7	9.5	19
H - 8	$9.5 \times 10^3$	250	$9.7 \times 10^3$	$86 \times 10^4$	9.4	35.9	10.7	31

### Area of Influence of Structural Defects per Unit Volume of Semix Samples

Semix sample number	Surface area of small and large precipitates $4\pi r_1^2 d_1 + 4\pi r_2^2 d_2$ $r_1 = 3/2 \mu\text{m}$ $r_2 = 15/2 \mu\text{m}$ $d_1, d_2$ are precipitate densities $\text{cm}^2/\text{cm}^3$	Surface area of dislocation $2\pi R \Gamma$ where $\Gamma$ is dislocation density and $R = 20 \text{ \AA}$ $\text{cm}^2/\text{cm}^3$	Grain boundary surface area $\text{cm}^2/\text{cm}^3$	Twin boundary surface area $\text{cm}^2/\text{cm}^3$	Total areas of all types of structural defects $\text{cm}^2/\text{cm}^3$	Cell efficiency (%)
A - 13	0.011	0.06	8.2	99.0	107.27	7.2
B - 2	0.008	0.12	4.5	15.8	20.428	10.0
C - 12	0.002	0.46	13.4	31.9	45.762	9.7
D - 8	0.002	0.126	13.8	44.5	58.428	10.8
E - 13	0.005	0.46	7.1	68.5	76.065	6.2
F - 2	0.006	0.214	5.4	12.2	17.82	9.6
G - 12	0.003	0.565	12.1	40.7	53.368	9.5
H - 8	0.004	1.081	9.4	35.9	46.385	10.7

## Defect Densities in Unprocessed Wafers

Semix sample number	Small precipitate density ( $\text{cm}^{-2}$ )	Large precipitate density ( $\text{cm}^{-2}$ )	Dislocation density ( $\text{cm}^{-2}$ )	Grain boundary length per unit area ( $\text{cm}^{-1}$ )	Twin boundary length per unit area ( $\text{cm}^{-1}$ )
1-10-13 (T)	44200	2035	6.0	7.88	79.2
1-12-14 (U)	29970	1705	1.1	3.14	29.2
2-5-1 (V)	26250	812	20.6	32	36.3
3-4-12 (W)	40370	2092	10.9	16.9	40
3-4-16 (X)	39050	2405	15.2	28.8	27.0
4-2-4 (Y)	23879	1916	37.2	16.9	34.8
4-2-8 (Z)	11430	693	16.9	13.9	51.2

## Results and Sample Calculations

3.3.1 THICKNESS

The calibration of the filar eyepiece on the Olympus microscope when using the 10X objective is  $0.9909 \mu\text{m}/\text{div}$ . Data taken for the three pieces from sample G-12 is shown in Table 1. Final results for all eight samples is shown in Table 2.

TABLE VII  
THICKNESS MEASUREMENTS ON SAMPLE G-12

	INITIAL READING	FINAL READING	d(div)	d( $\mu\text{m}$ )
1	276	564	288	285
2	361	653	292	289
3	208	526	318	315

$d = 296 \mu\text{m}$  max. % deviation = 6.4%

TABLE VIII  
THICKNESS DATA FOR ALL SAMPLES

sample	d( $\mu\text{m}$ )	max. % deviation
A - 13	266	2.4
B - 2	315	3.1
C - 12	304	1.2
D - 8	277	5.5
E - 13	305	3.5
F - 2	290	0.8
G - 12	296	6.4
H - 8	285	1.7



## Hall Const., Mobility, Carrier Conc., Carrier Type

The Hall const., mobility, carrier conc., and carrier type were determined using the configurations shown in Fig. 3. Data taken for sample G-12-2 is shown in Table 3. This is followed by sample calculations.

Sample: G-12-2

$I = 1\text{mA}$ ,  $B = 8\text{KG}$ ,  $d = 296\mu\text{m}$ ,  $\rho = 2.1\Omega\text{-cm}$

TABLE IX  
MEASURED VOLTAGES ON SAMPLE G-12-2

Configuration 1				Configuration 2		
	$V_1(B/O)$	$V_2(B/O)$	$V_H$	$V_1(B/O)$	$V_2(B/O)$	$V_H$
+I +B	.05	.0515	.0015	.056	.055	.001
-I +B	.056	.057	.001	.052	.051	.001
+I -B	.056	.055	.001	.052	.051	.001
-I -B	.051	.05	.001	.056	.057	.001

$$\overline{V_1 - V_2} = \overline{V_H} = .0011\text{V}$$

$$\text{Hall const. } R_H = \frac{\overline{V_H} d}{B I} = \frac{(.0011\text{V})(296 \times 10^{-4}\text{cm})}{10^{-3}\text{amps } 8.5 \times 10^{-5}\text{W/cm}^2} = 393\text{cm}^2/\text{coul}$$

$$\text{Hall mobility } = \mu_H = \frac{R_H}{\rho} = \frac{393}{2.1} = 187\text{cm}^2/\text{v-sec}$$

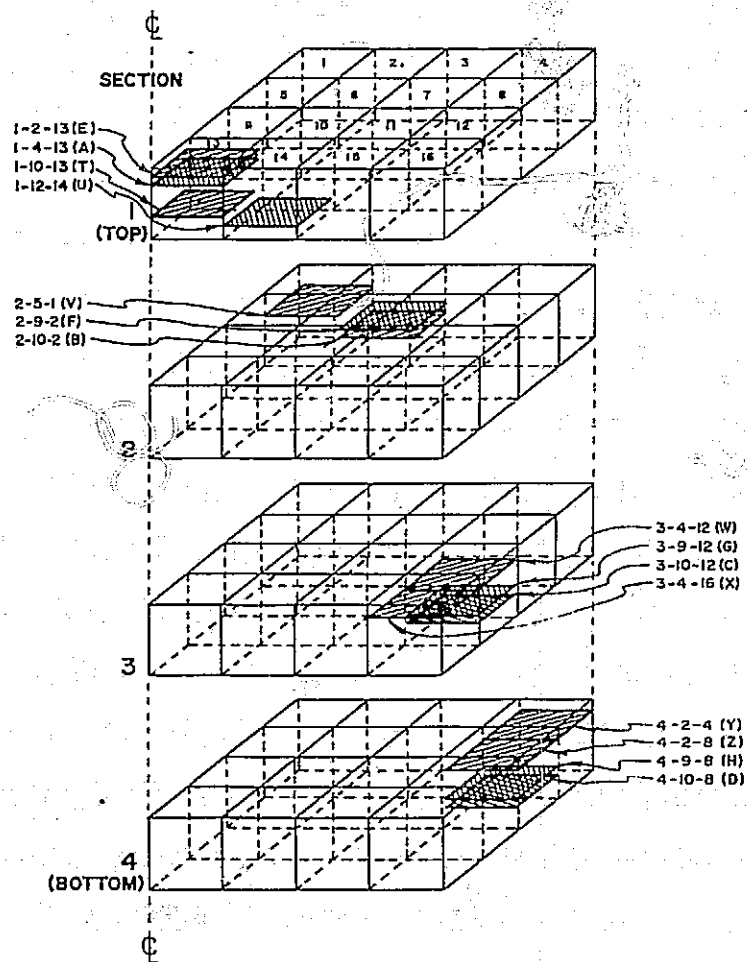
$$\text{Carrier conc. } p = \frac{1}{R_H q} = \frac{1}{393(1.6 \times 10^{-19}\text{coul})} = 1.58 \times 10^{16}\text{cm}^{-3}$$

where  $q$  = charge of an electron.

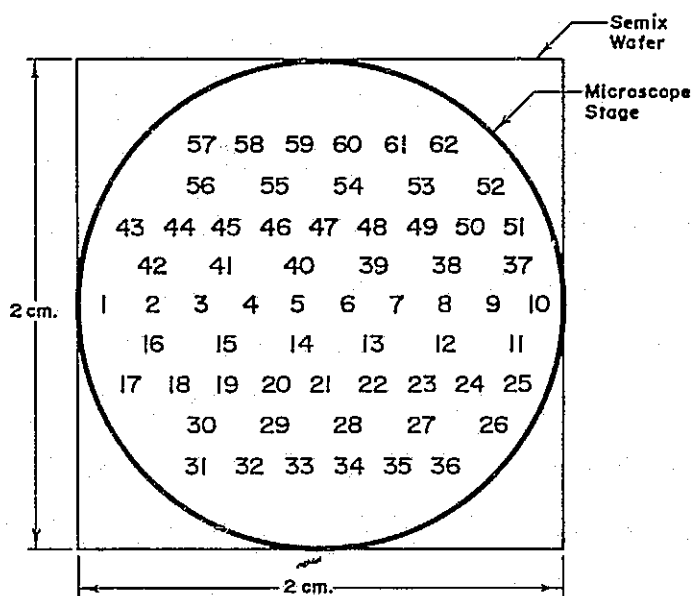
# Resistivity, Hall Mobility, Carrier Concentration, Hole Mobility, Normalized Hole Mobility, and Grain Boundary Density for All 20 Specimens

SAMPLE	$t(\mu\text{-m})$	$\mu_H(\text{cm}^2/\text{v-sec})$	$P \times 10^{16}(\text{cm}^{-3})$	$\mu_P(\text{cm}^2/\text{v-sec})$	$\frac{\mu_H}{P}$	$\mu_P(\text{cm}^2/\text{v-sec})$	G.B. (cm/cm <sup>2</sup> )
A-1	1.65	201	1.80	370	1.10	221	4.42
B-1	2.45	176	1.44	385	1.05	185	9.06
B-2	3.00	213	.97	408	1.00	213	16.97
B-3	1.85	212	1.58	379	1.07	227	12.41
C-1	1.80	337	1.02	405	1.00	337	2.17
C-2	1.69	198	1.86	368	1.10	218	15.17
C-3	2.20	187	1.51	382	1.06	198	11.86
D-1	2.20	178	1.59	378	1.07	190	9.85
D-2	2.15	177	1.64	376	1.08	191	6.63
D-3	3.10	85	2.36	351	1.16	99	16.16
E-1	1.86	274	1.26	393	1.09	262	0
E-2	1.75	226	1.58	379	1.07	242	.32
F-1	2.30	199	1.36	388	1.05	209	15.23
F-2	2.60	104	2.30	353	1.15	120	20.66
F-3	2.15	242	1.15	399	1.02	247	15.61
G-1	2.05	240	1.26	393	1.03	247	10.00
G-2	2.10	187	1.58	379	1.07	200	12.79
H-1	1.50	380	1.07	402	1.01	385	2.52
H-2	1.55	124	2.00	363	1.12	139	13.25
H-3	1.58	202	1.90	366	1.10	226	18.55

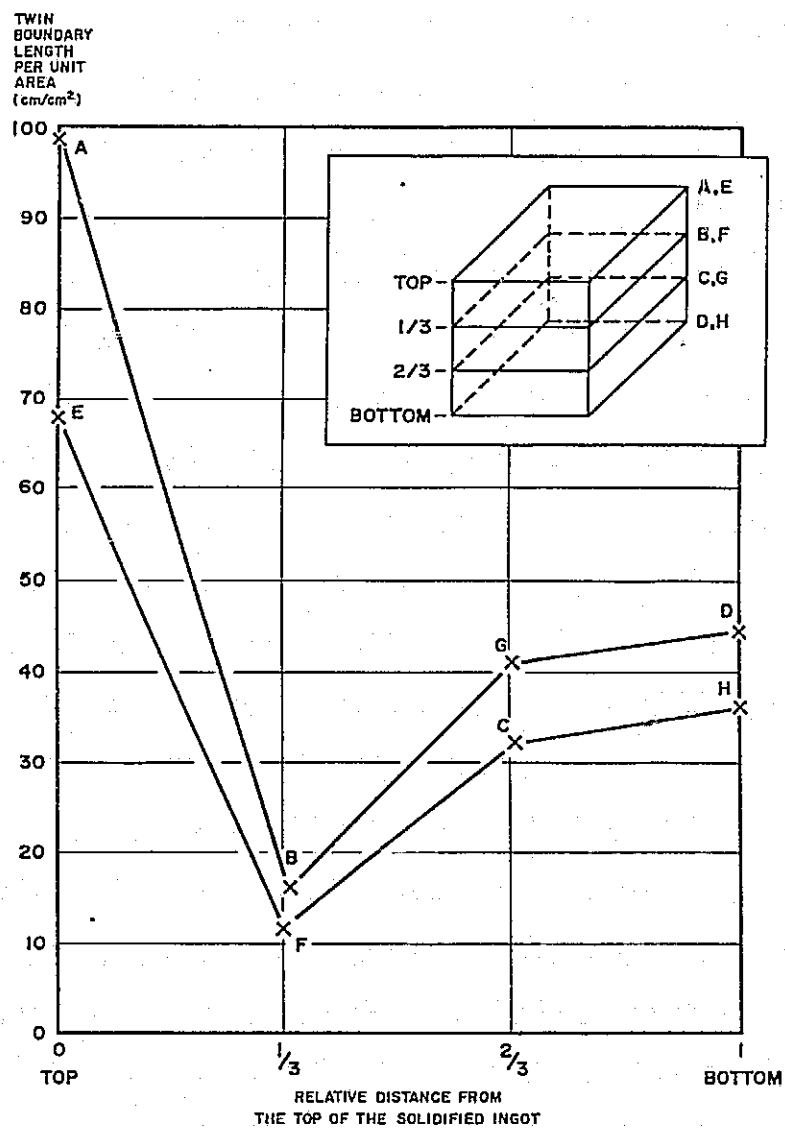
# Position of Wafers From UCP Ingots 5848-13C

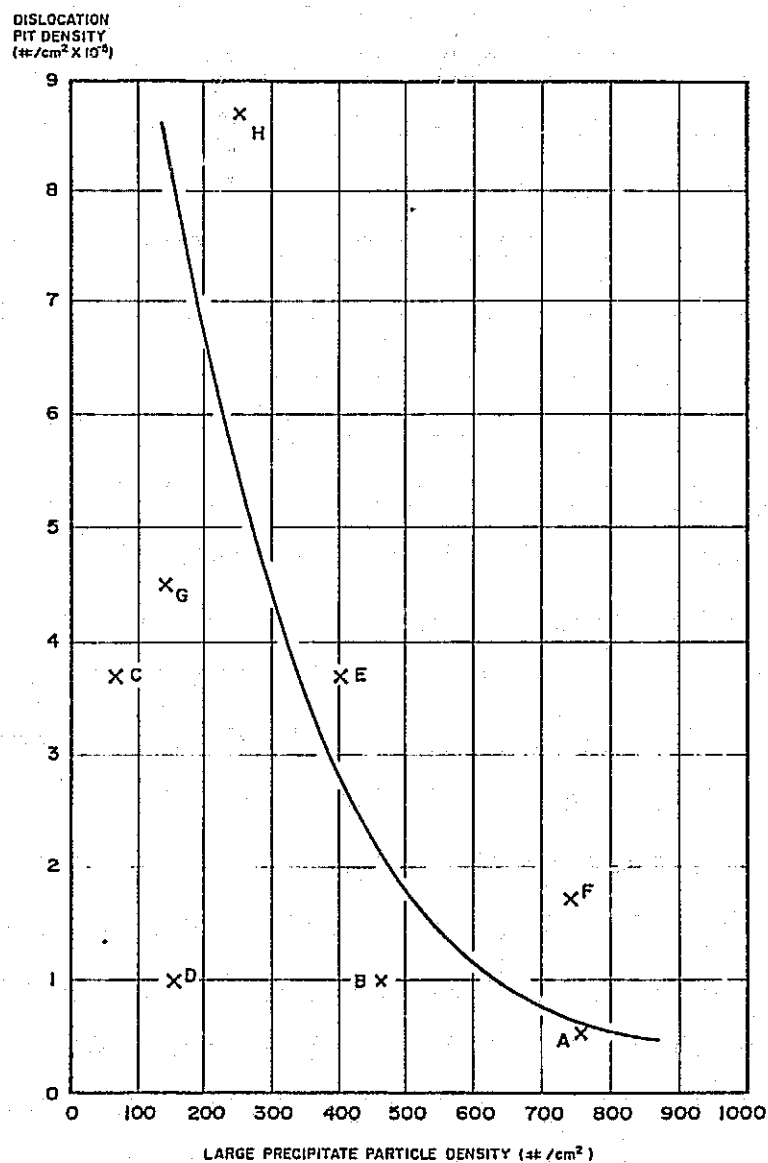


# Relative Positions of Measured Fields on Semix Wafers

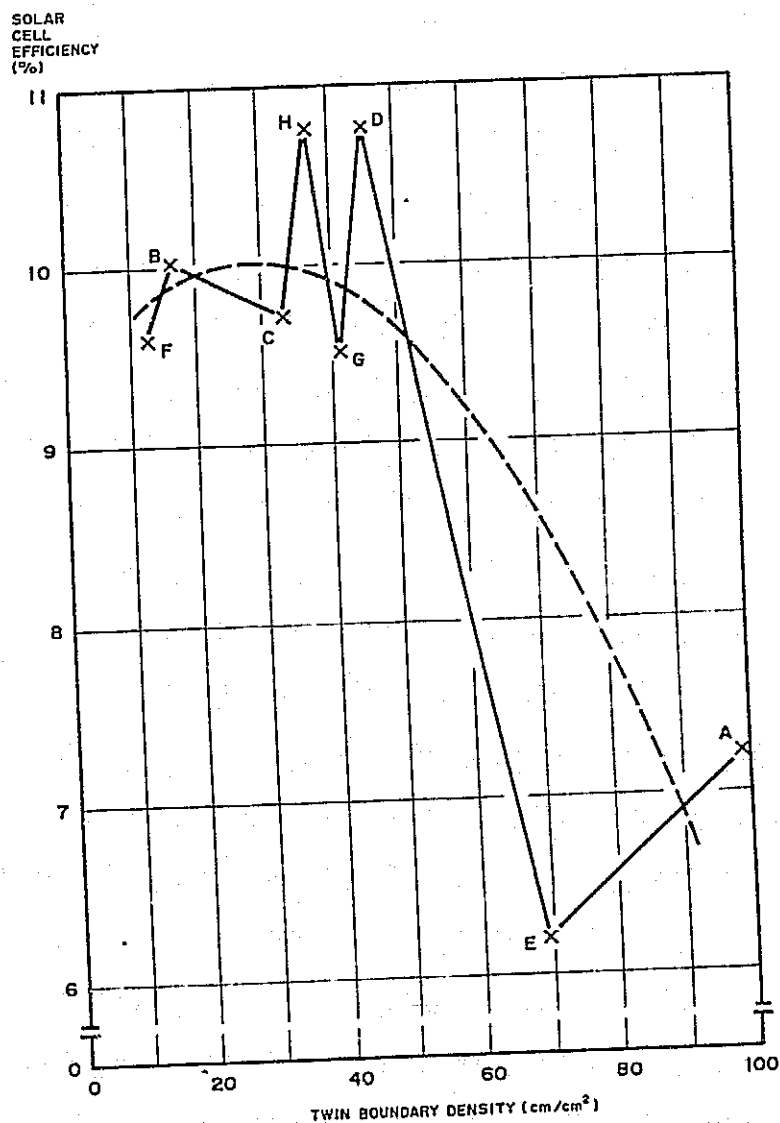


# Twin Boundary Length per Unit Area vs Relative Position of the Wafer in the Ingot From the Top of the Solidified Ingot

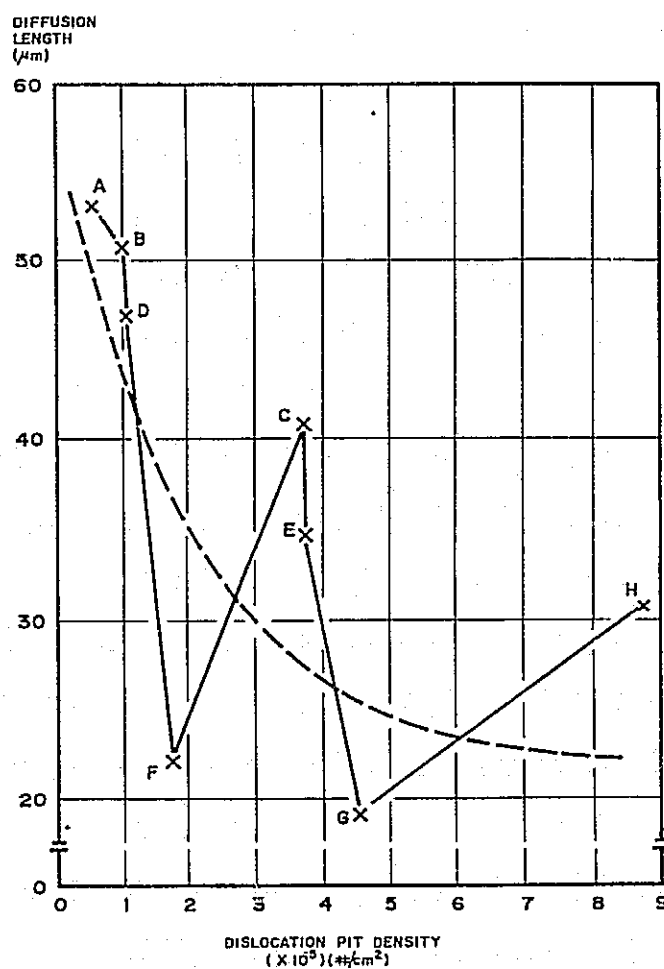


Dislocation Pit Density vs Large  
Precipitate Particle Density

# Solar-Cell Efficiency vs Twin-Boundary Density

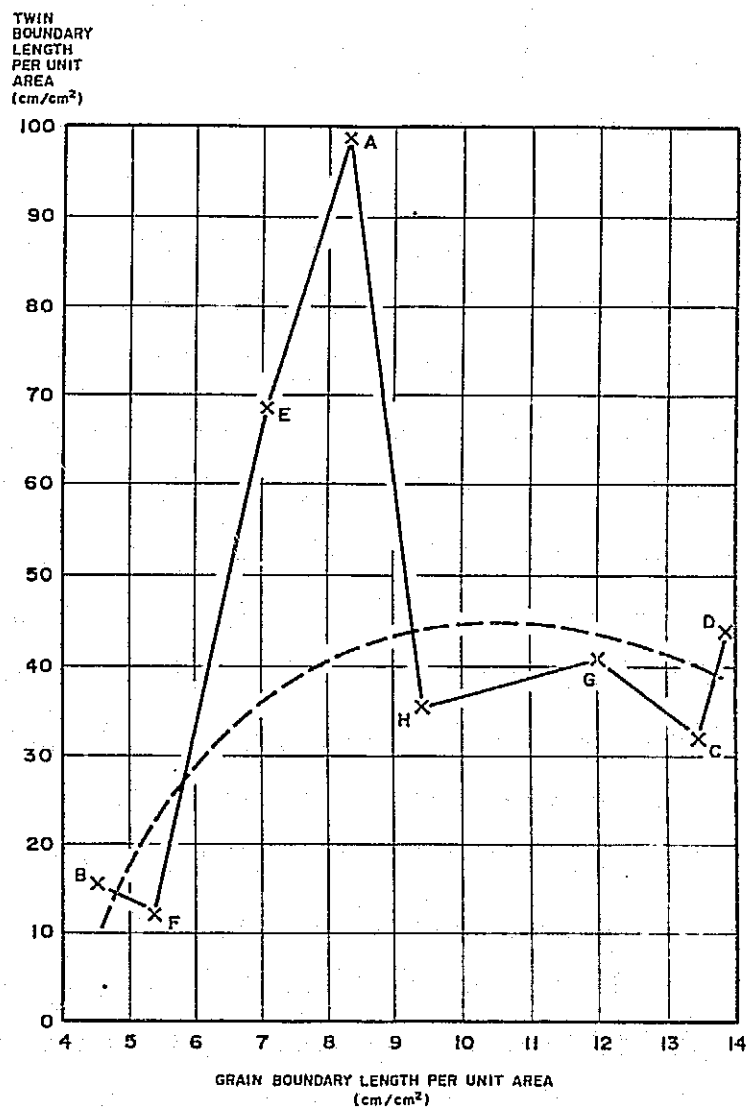


## Diffusion Length vs Dislocation Pit Density

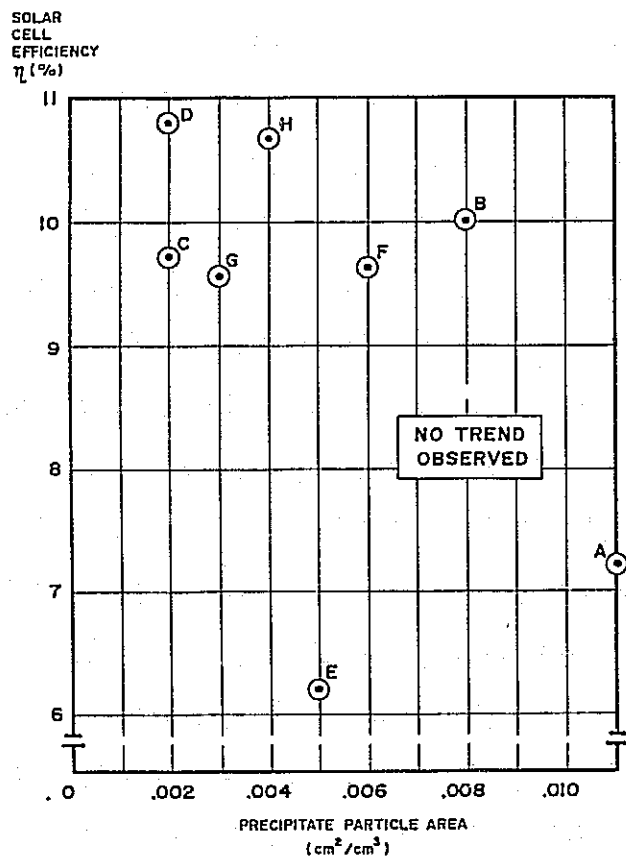




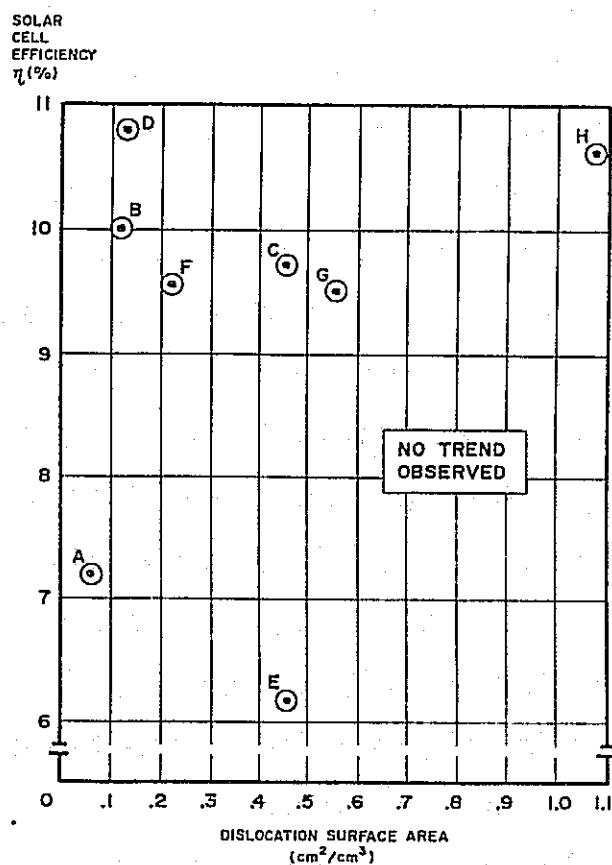
# Twin Boundary Length per Unit Area vs Grain Boundary Length per Unit Area



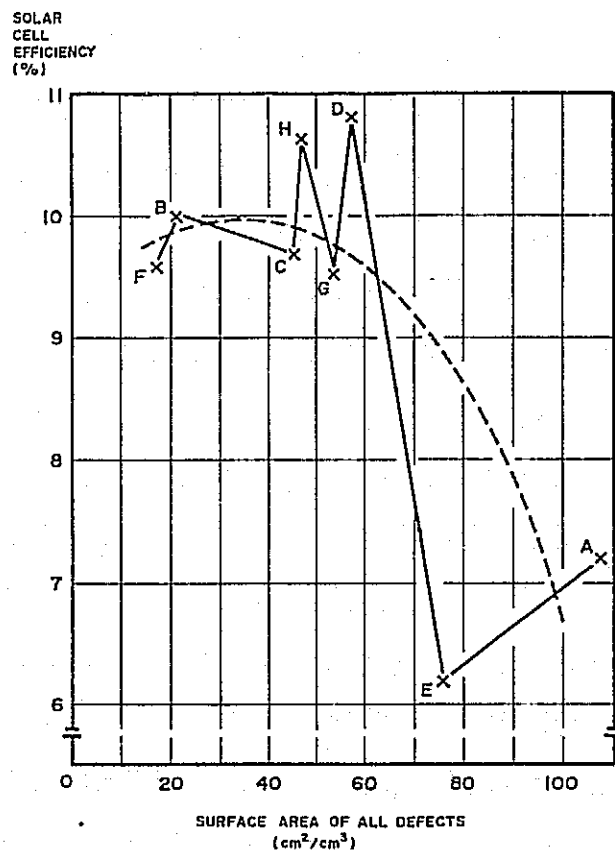
## Solar-Cell Efficiency vs Precipitate Surface Area



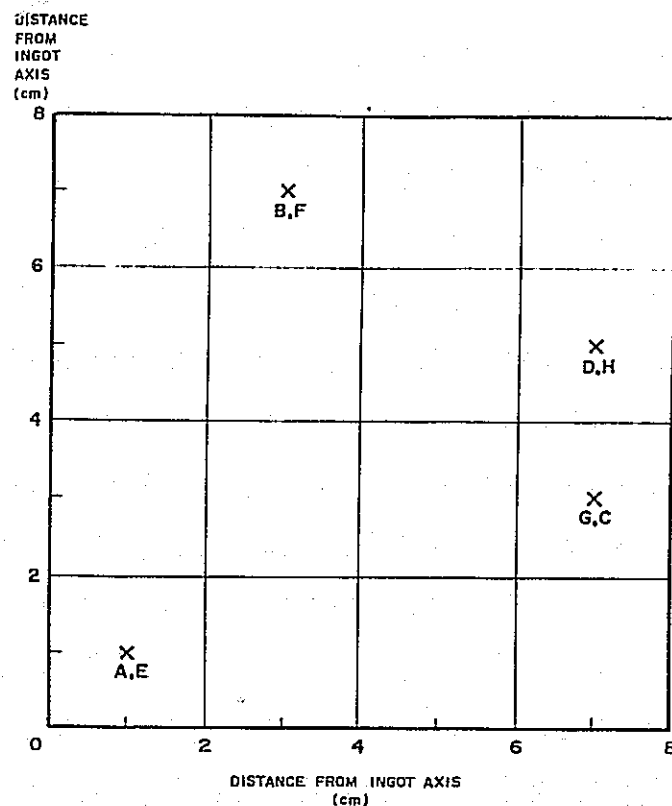
## Solar-Cell Efficiency vs Area of Influence of Dislocations



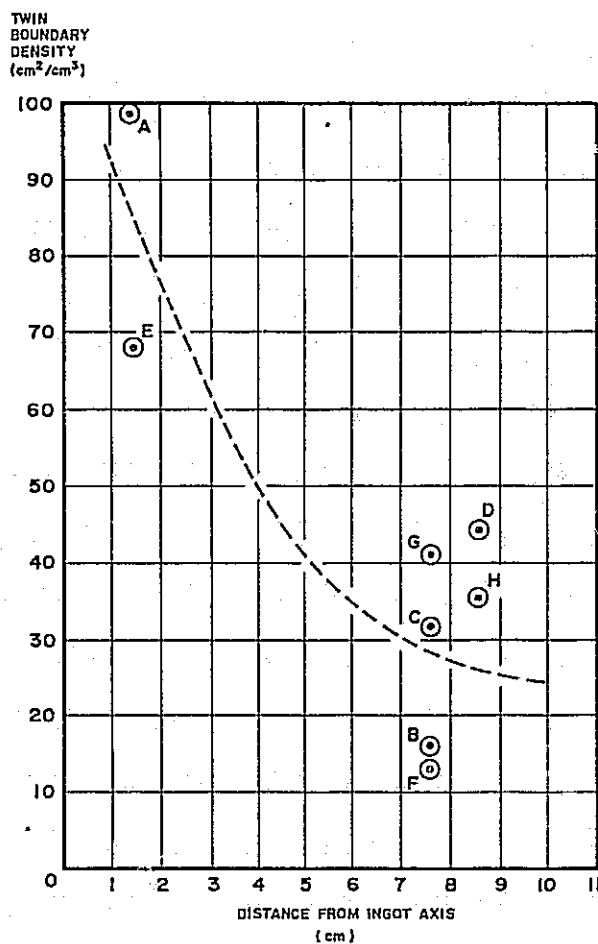
## Solar-Cell Efficiency vs Area of All Structural Defects



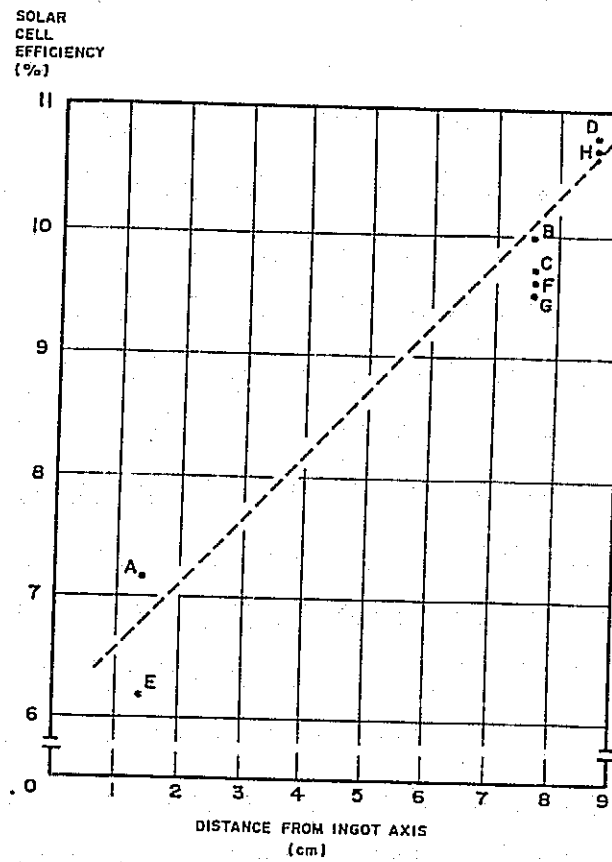
## Cell Map Showing Locations of Wafers



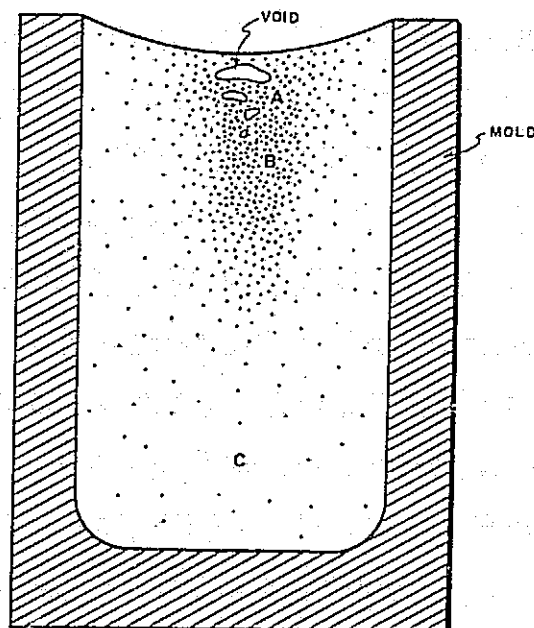
## Twin Boundary Density vs Distance From Ingot Axis



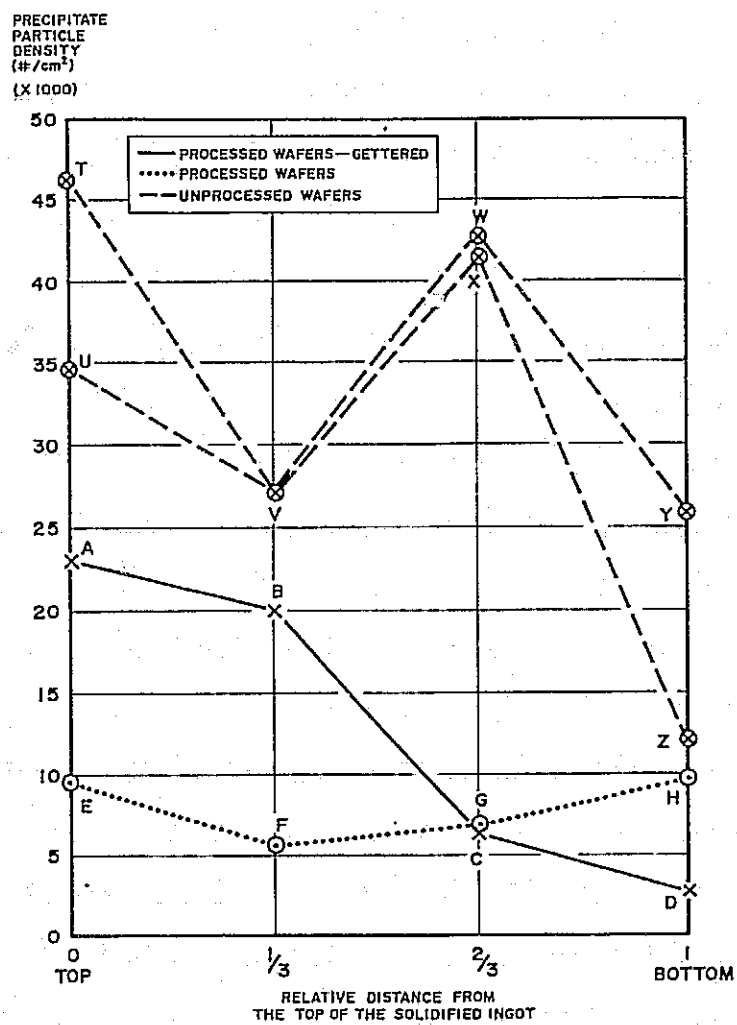
# Solar-Cell Efficiency vs Distance From Ingot Axis



## Segregation of Impurities in Cast Silicon

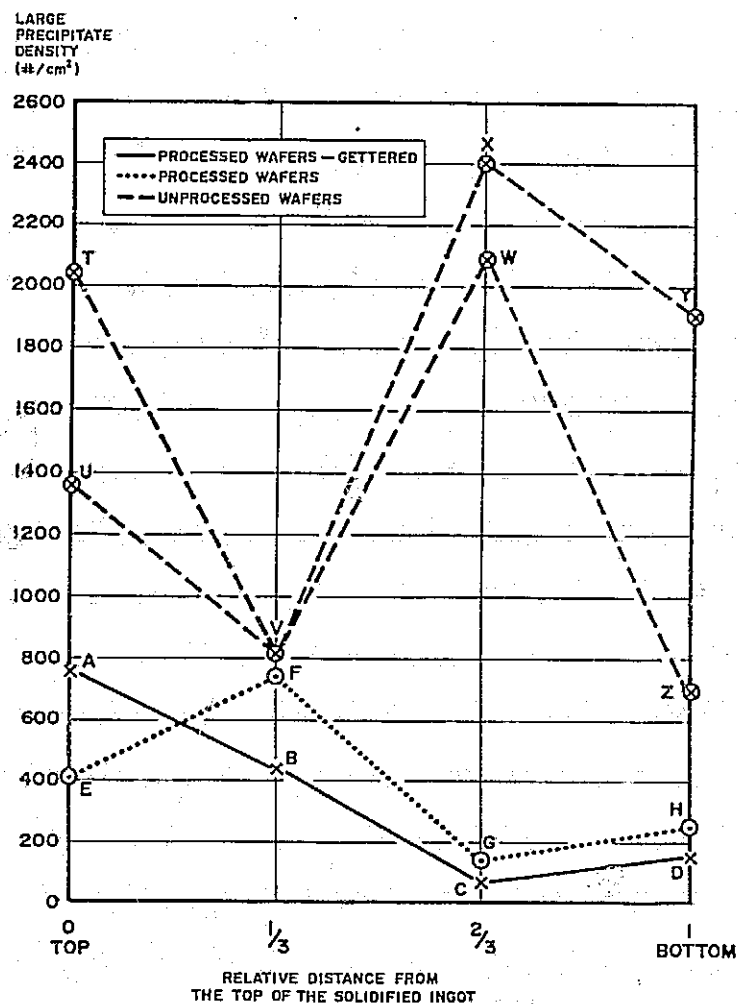


## Precipitate Density vs Relative Position in Ingot

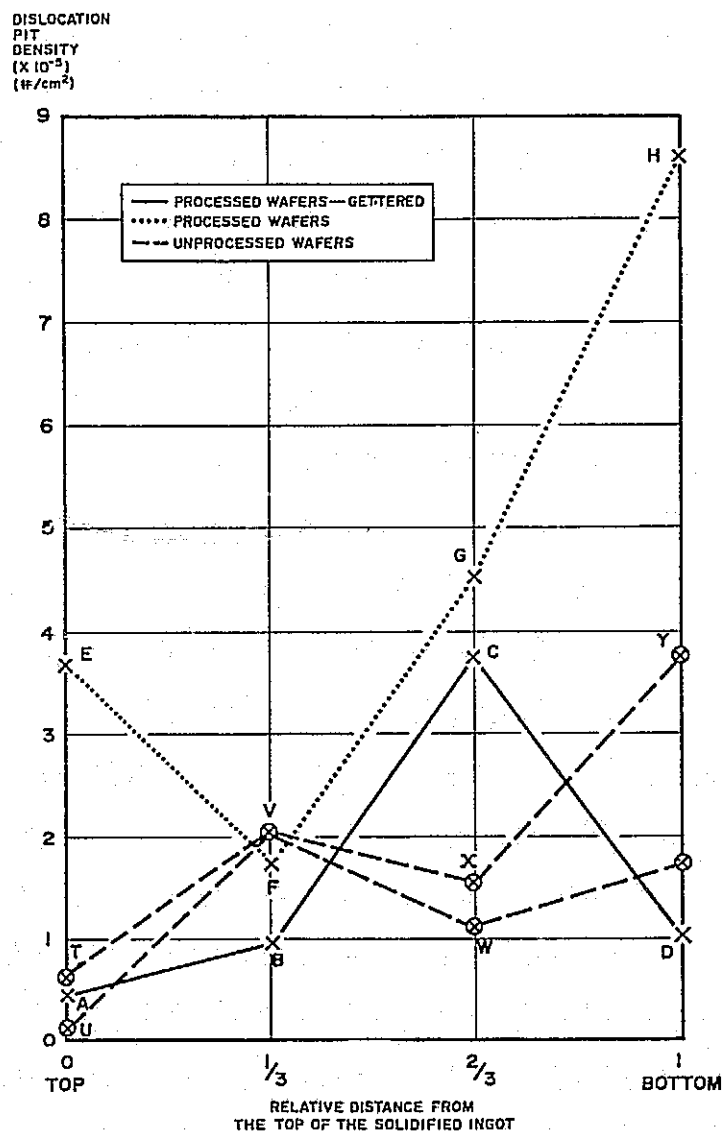




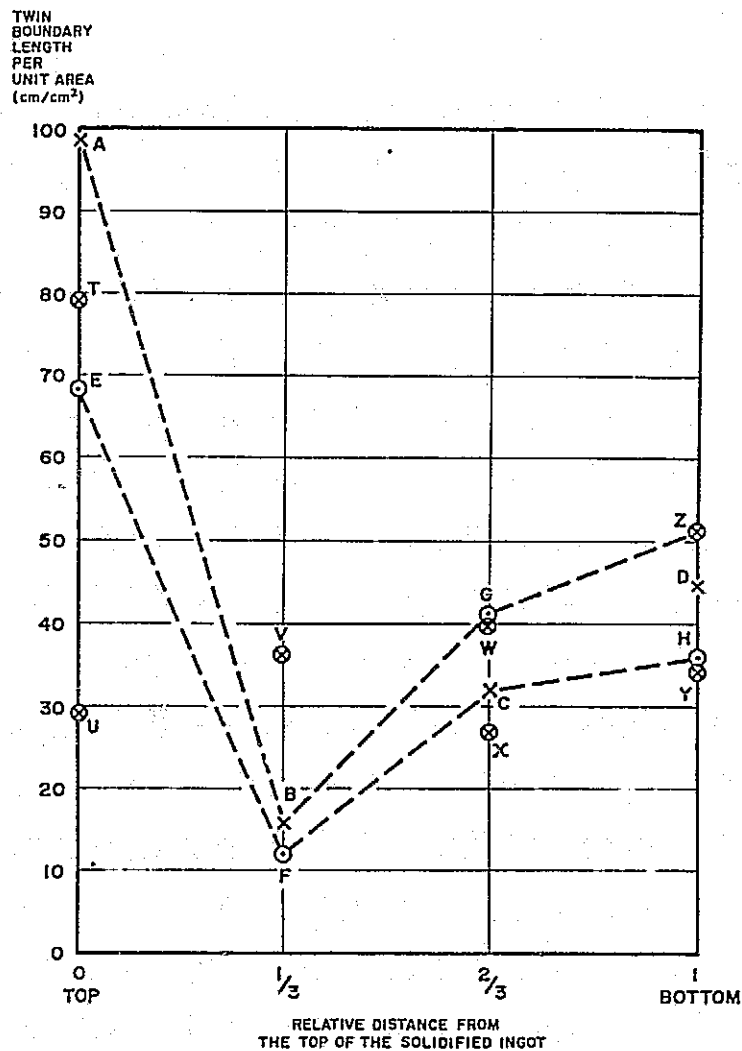
## Large Precipitate Density vs Relative Position in Ingot



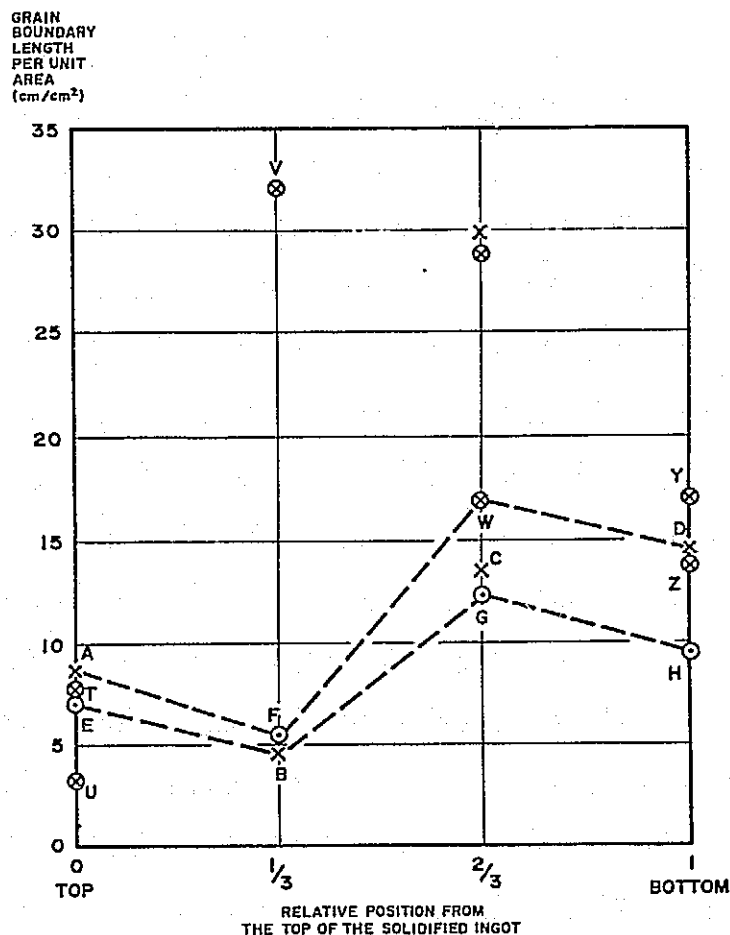
## Dislocation Pit Density vs Relative Position in Ingot



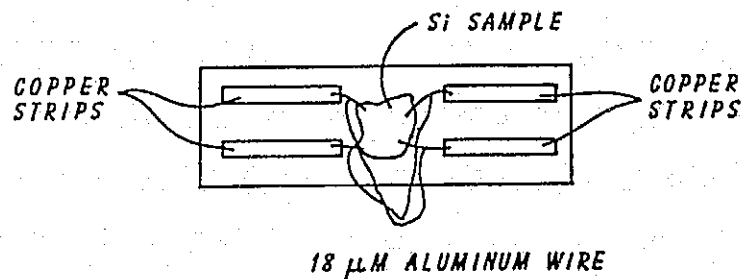
# Twin Boundary Length per Unit Area vs Relative Distance From Top of Ingot



# Grain Boundary Length per Unit Area vs Relative Distance From Top of Ingot

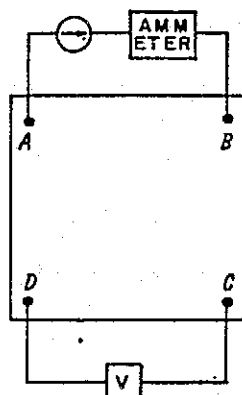


## Electrical Connections to Obtain Small Contact Area and Reduce Contact Influence on Measurements

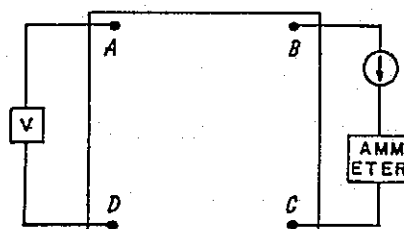


## Two Configurations Used for Resistivity Measurements

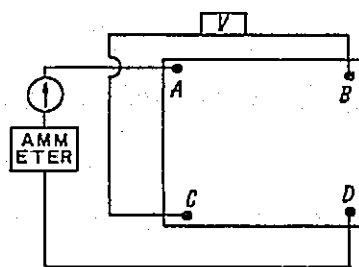
CONFIGURATION (1)



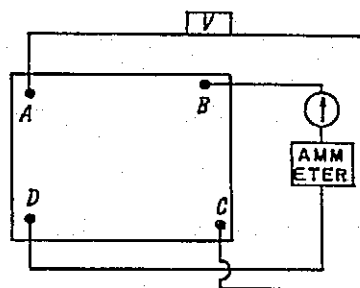
CONFIGURATION (2)



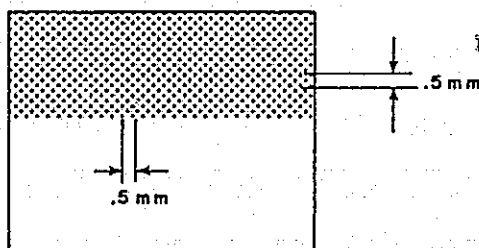
## Two Configurations Used for Hall Voltage Measurements



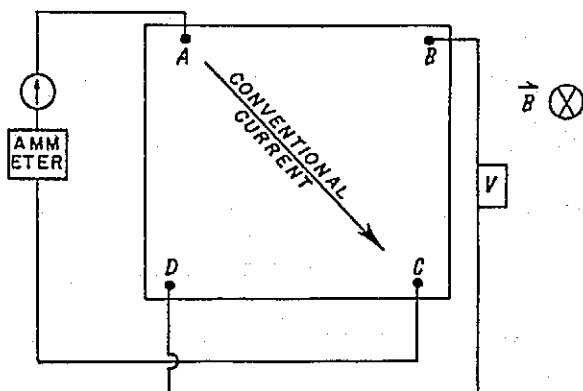
CONFIGURATION (1)



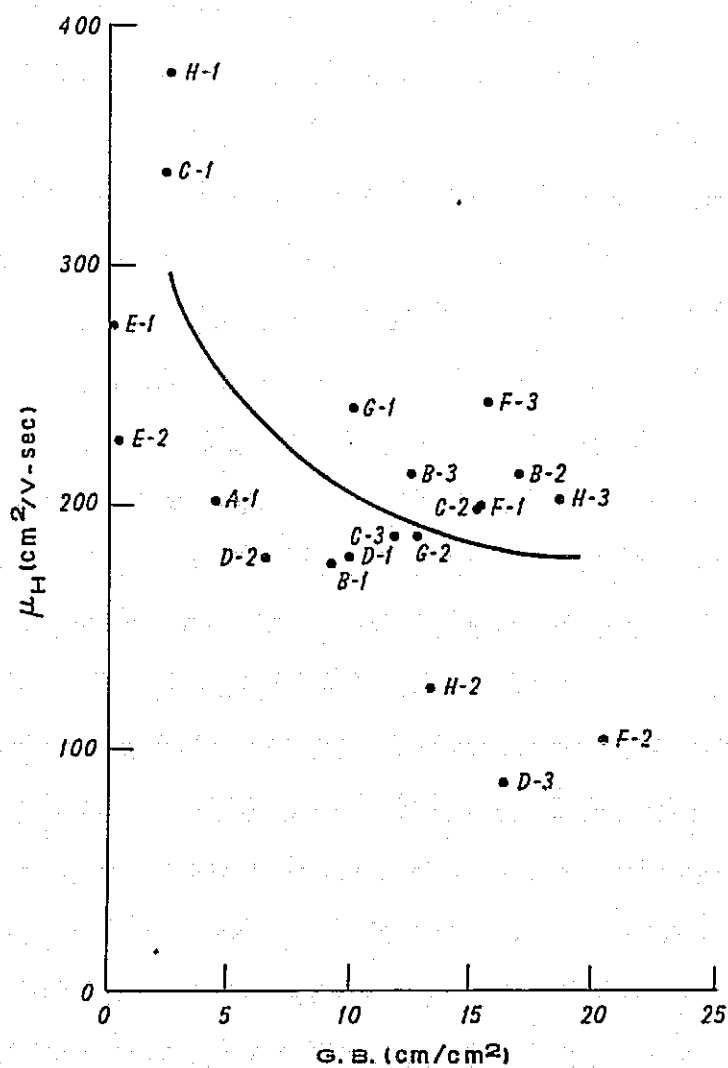
CONFIGURATION (2)



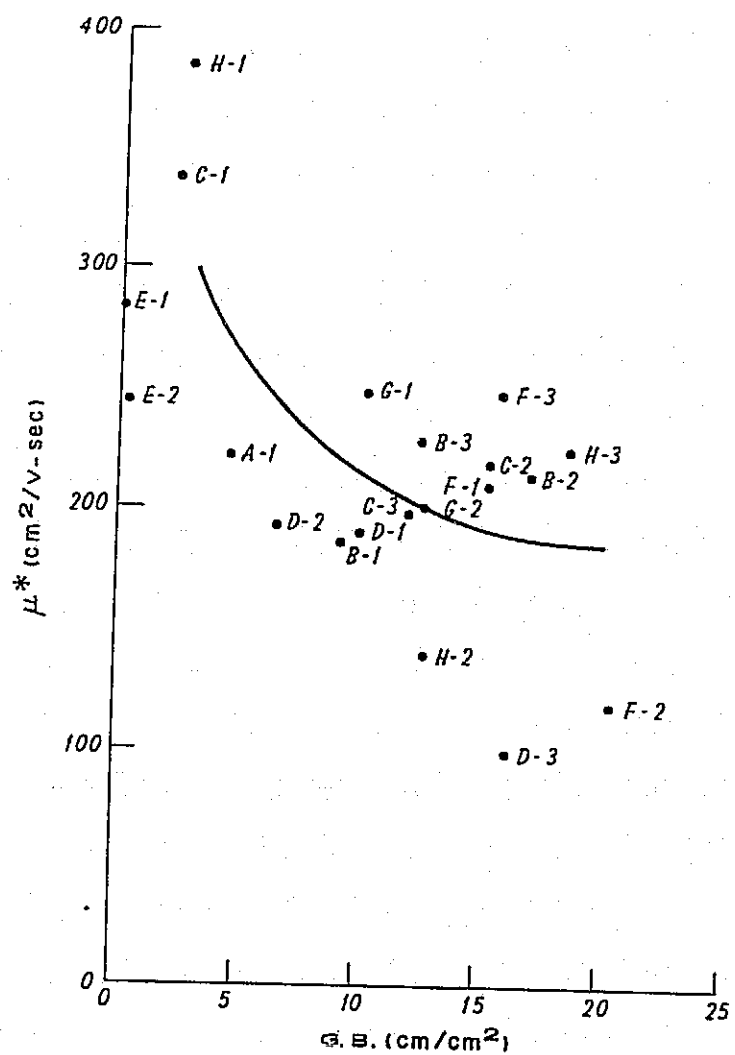
### Configuration Used to Determine Carrier Type



### Mobility vs Grain Boundary Density



# Normalized Mobility vs Grain Boundary Density



## Czochralski Blanks: Solar Cell Junction Removed

<u>TANNEAL</u>	<u>SAMPLE #</u>	<u>PROCESS</u>
AS GROWN	T5-3	SOLAR CELL
	T5-11	NO PROCESS
450°C/150 hr.	T3-8	SOLAR CELL
	T3-14	NO PROCESS
650°C/4 hr.	T5-8	SOLAR CELL
	T5-15	NO PROCESS
1000°C/1 hr.	T11-8	SOLAR CELL
	T11-13	NO PROCESS

## EXAMINE AFTER:

- a) Mechanical Polishing
- b) Chemical Polishing
- c) Chemical Etching

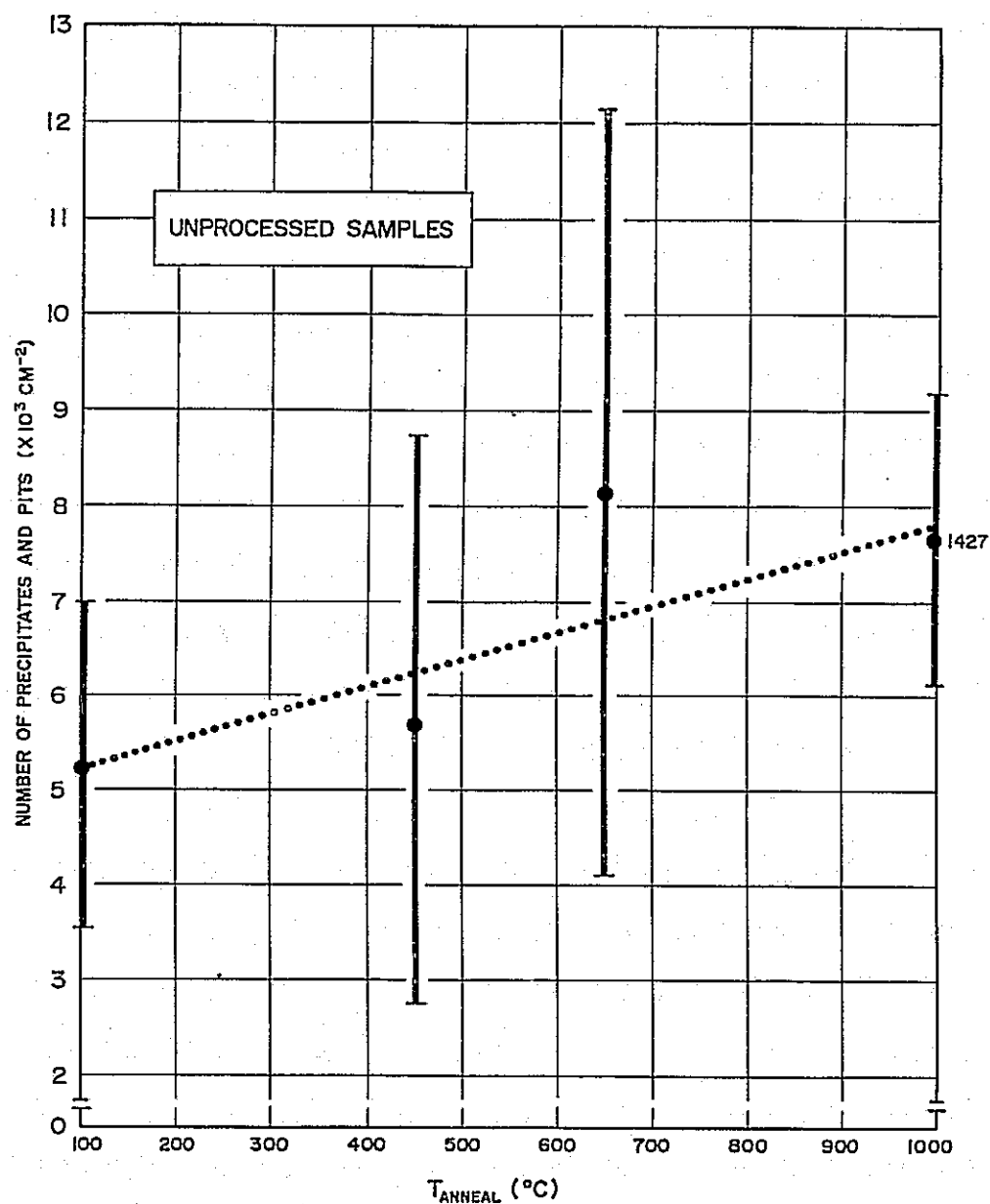
## EXAMINE:

- a) Optically at 1000 x  
≥ 100 fields of view
- b) FTIR from 400 cm<sup>-1</sup> to 4000 cm<sup>-1</sup>

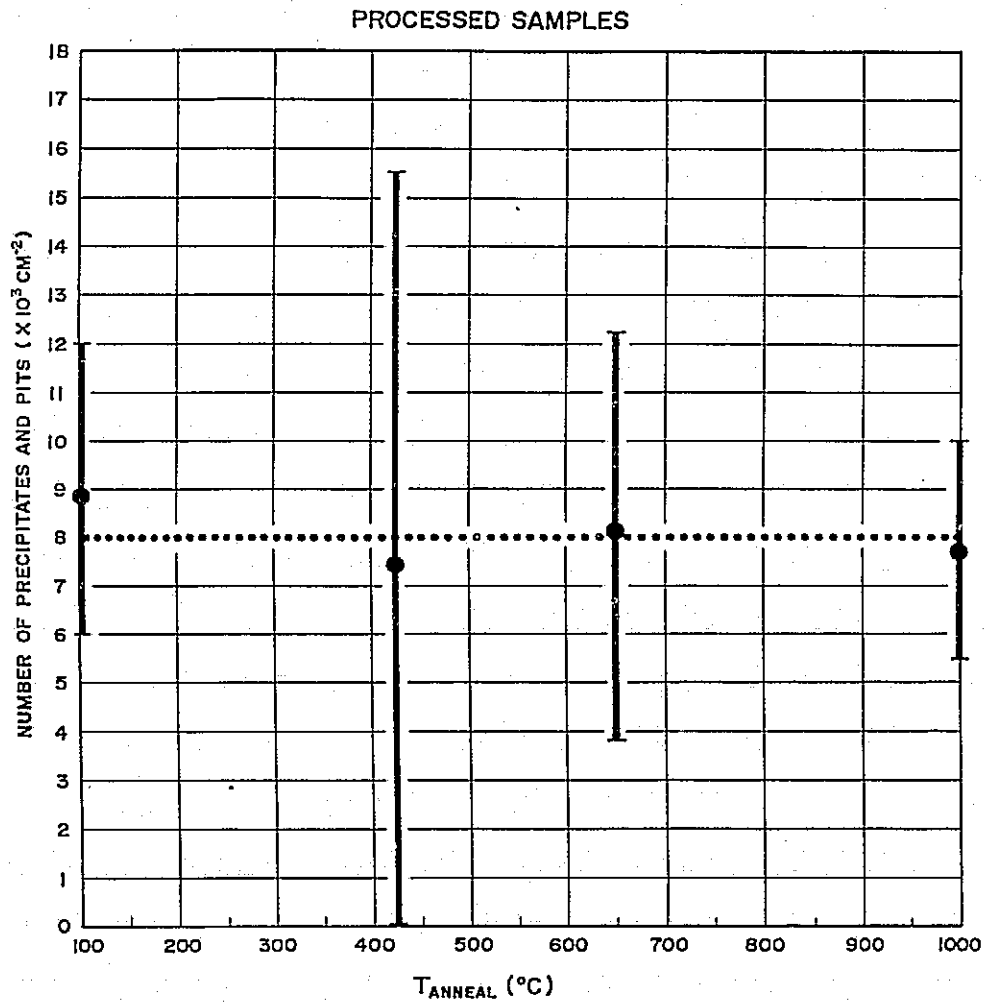
SAMPLE NO.	TANNEAL	NUMBER OF PITS AND PRECIPITATES (CM <sup>-2</sup> )			
		MECHANICAL POLISH	CHEMICAL POLISH	CHEMICAL ETCH	$\eta$
T5-3	As grown	10591	3301	8252	5.03 %
T3-8	450°C	1395	3576	23461	6.36 %
T5-8	650°C	6720	4951	12811	6.36 %
T11-8	1000°C	8920	5187	9038	5.68 %
T5-11	As grown	6982	4047	3733	—
T3-14	450°C	10414	4716	4150	—
T5-15	650°C	3694	11318	5462	—
T11-13	1000°C	9745	10846	8016	—



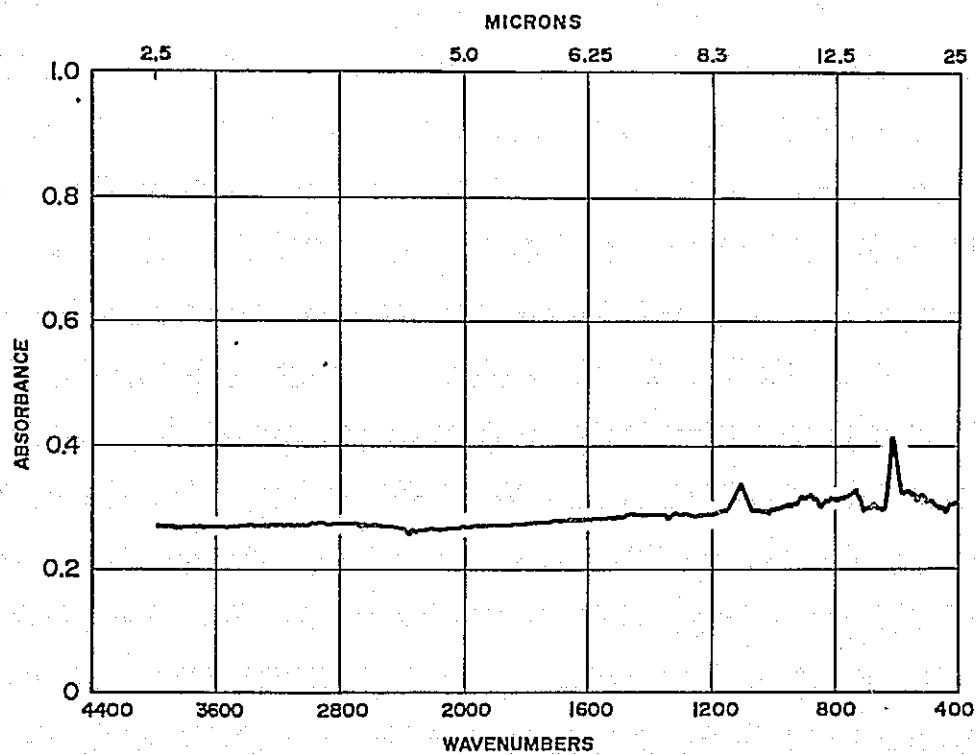
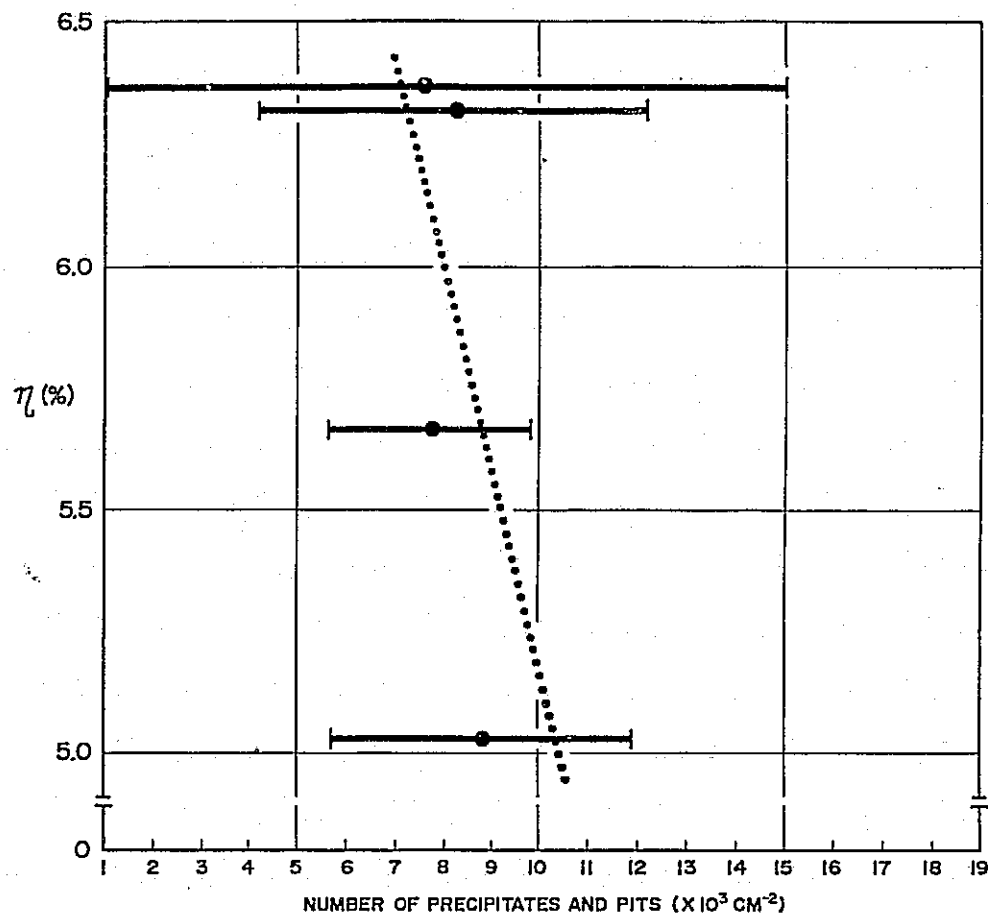
# SILICON SHEET GROWTH AND CHARACTERIZATION



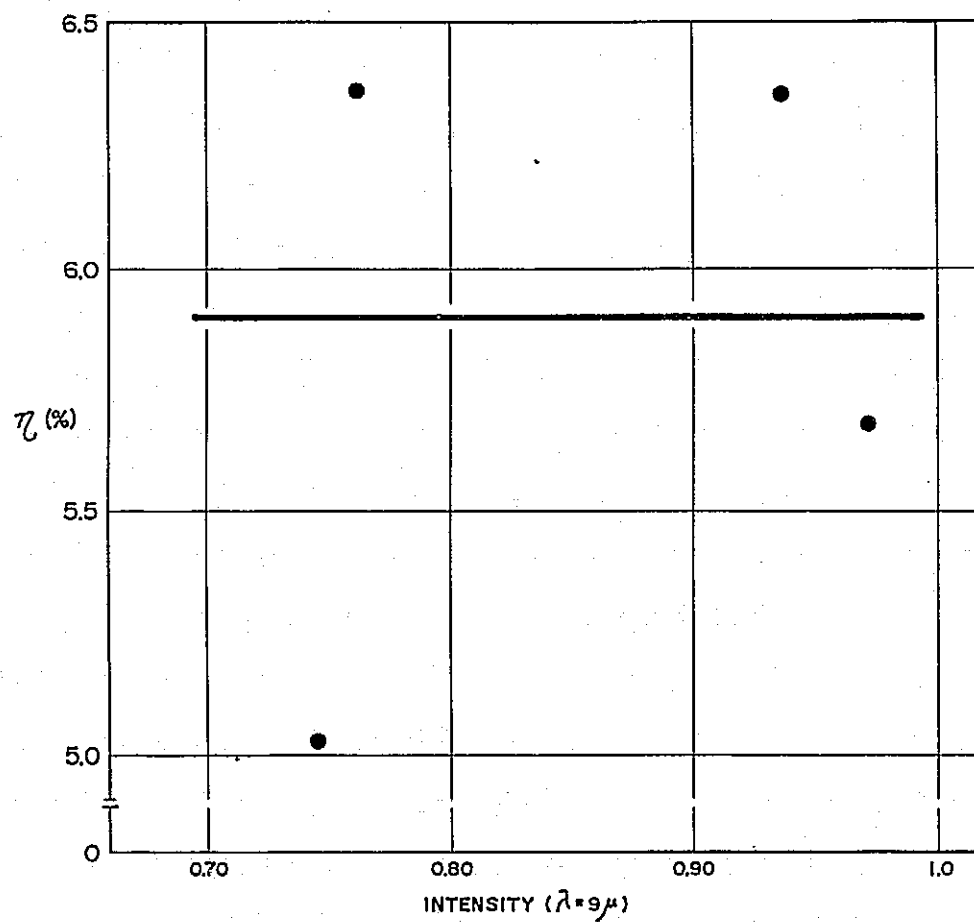
# SILICON SHEET GROWTH AND CHARACTERIZATION

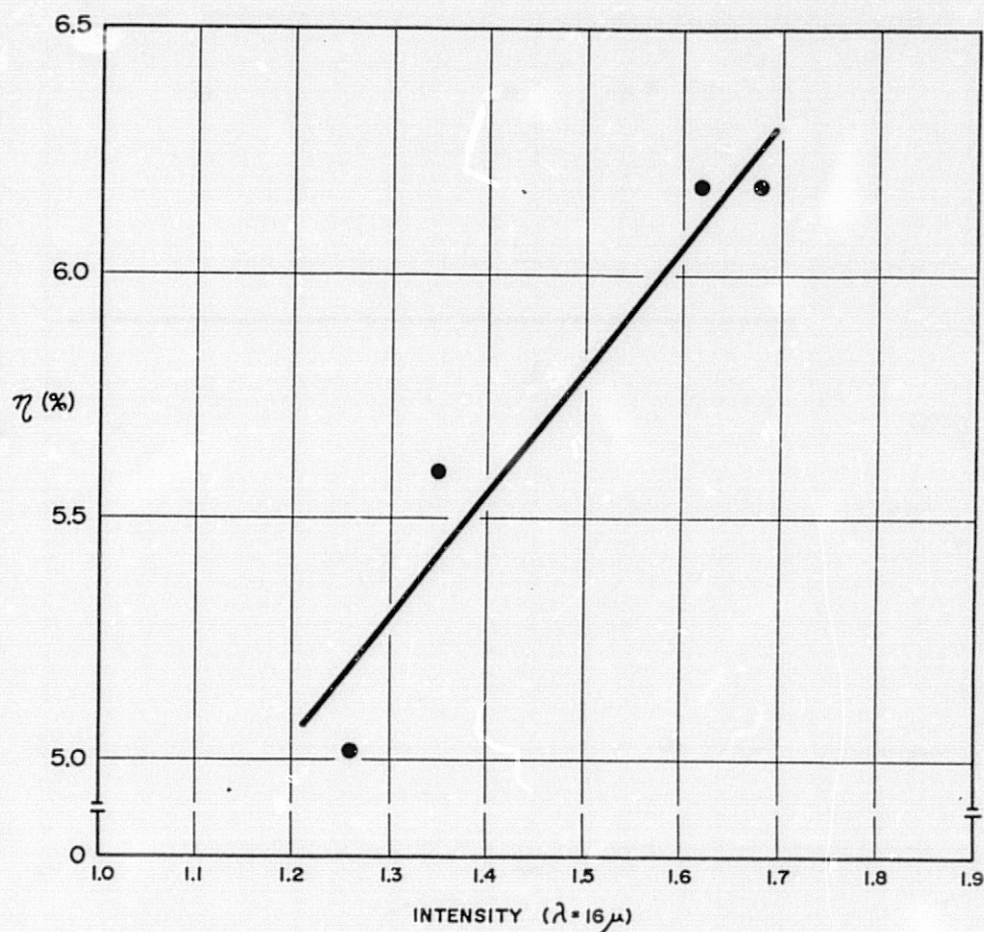


# SILICON SHEET GROWTH AND CHARACTERIZATION



# SILICON SHEET GROWTH AND CHARACTERIZATION





### Conclusion

- 1. Large number of precipitates may act as recombination centers**
- 2. Correlation of efficiency with one IR peak**

# SILICON-SHEET CELL PERFORMANCE

APPLIED SOLAR ENERGY CORP.

TECHNOLOGY SOLAR CELL FABRICATION & ANALYSIS	REPORT DATE 9-28-83
APPROACH 1) FABRICATION OF SOLAR CELLS BY BASELINE & ADVANCED PROCESSES POSSIBLY INCLUDING GETTERING AND ANNEALING. 2) ANALYSIS USING DARK AND LIGHT I-V, DIFFUSION LENGTH MEASUREMENTS, SPECTRAL RESPONSE. CONTRACTOR APPLIED SOLAR ENERGY CORPORATION	STATUS
GOALS 1) AN UNDERSTANDING OF THE MECHANISMS THAT LIMIT THE DEFICIENCIES OF SOLAR CELLS MADE FROM VARIOUS SILICON SHEETS. 2) AN UNDERSTANDING OF THE EFFECT ON SOLAR CELL EFFICIENCY OF VARIATIONS IN GROWTH PARAMETERS.	

1. SMALL DIODE STUDY:

SIZE OF DIODE -  $0.25 \times 0.125 \text{ cm}^2$  WITH A METAL PATCH THE SIZE OF  $0.072 \times 0.007 \text{ cm}^2$ .

2. LIGHT SPOT SCAN:

SIZE OF LIGHT SPOT -  $\sim 120 \mu\text{m}$

# Summary of Results of Baseline Cells for Comparing 3 Cast Si Materials

		Voc(mV)	Jsc(mA/cm <sup>2</sup> )	CFF(%)	$\eta$ (%)
<u>UCP</u>					
A	AVE.	514	25.6	74	10.1
	RANGE	20-550	24.4-26.1	25-78	0.1-11.2
B	AVE.	555	25.8	76	10.9
	RANGE	534-568	24.1-27.0	68-79	8.8-12.1
C	AVE.	550	25.3	72	10.1
	RANGE	512-564	24.4-26.5	38-79	4.8-11.8
UCP OVERALL	AVE.	539	25.6	74	10.4
	RANGE	20-568	24.1-27.0	25-79	0.1-12.1
<u>SILSO</u>					
D(Long Grain)	AVE.	552	24.4	72	9.8
	RANGE	526-564	21.6-26.6	46-79	6.1-11.3
E (Medium Grain)	AVE.	556	26.2	76	11.1
	RANGE	552-564	25.4-27.0	72-78	10.1-11.6
F(Fine Grain)	AVE.	547	23.7	75	9.7
	RANGE	536-552	22.6-24.4	61-78	7.9-10.5
SILSO OVERALL	AVE.	552	24.7	74	10.2
	RANGE	526-564	21.6-27.0	46-79	6.1-11.6
<u>HEM</u>					
G(Single Crystal)	AVE.	579	27.7	73	11.7
	RANGE	574-588	26.9-28.5	66-79	10.1-13.2
H(Poly)	AVE.	566	26.7	76	11.5
	RANGE	552-576	25.4-27.5	70-78	10.3-12.2
I(Poly)	AVE.	564	26.6	74	11.1
	RANGE	550-574	25.0-27.6	67-78	9.7-12.1
J(Poly)	AVE.	551	24.8	74	10.1
	RANGE	538-560	23.6-25.5	65-78	8.5-11.0
HEM OVERALL	AVE.	565	26.5	74	11.1
	RANGE	538-588	23.6-28.5	65-79	8.5-13.2
<u>CZ CONTROL</u>					
	AVE.	586	29.0	77	13.1
	RANGE	586-586	28.8-29.3	76-77	12.9-13.3

### Summary of $V_{oc}$ and $I_{sc}$ Measurement of Silso and HEM Diodes

	Single Crystal Diodes (Ave. Of 5 or More Diodes)		Grain Boundary Dominated Diodes (Ave. of 5 or More Diodes)	
	$V_{oc}$ (mV)	Normalized ( $I_{sc}$ )	$V_{oc}$ (mV)	Normalized ( $I_{sc}$ )
SILSO (Long Grain)	520	.851	518	.800
SILSO (Med. Grain)	531	.900	519	.844
SILSO (Fine Grain)			511	.765
HEM (Upper Central of Ingot 4141C)	516	.922	520	.834
HEM (Lower Central Of Ingot 4141C)	538	.922	532	.892
CZ Control	535	1		

### Summary of $V_{oc}$ and $I_{sc}$ Measurements of UCP Diodes

	Single Crystal Diodes (Ave. Of 5 or More Diodes)		Grain Boundary Dominated Diodes (Ave. of 5 or More Diodes)	
	$V_{oc}$ (mV)	Normalized ( $I_{sc}$ )	$V_{oc}$ (mV)	Normalized ( $I_{sc}$ )
1-C (Top of Ingot C4-21A)	545	.966	535	.897
4-B (Bottom Of Ingot C4-21A Outside)	529	.824	525	.839
4-C (Bottom Of Ingot C4-21A Center)	512	.785	517	.764
5-A From Random Source	541	.931	525	.868
Control	555	1	-	-



### Minority Carrier Diffusion Lengths of Diodes Made From UCP Silicon

WAFER	DIODE #	$L_D$ (um)	CHARACTER
A (Top Of C4-21A)	1	141	Single Crystal
	2	162	Single Crystal
	3	44	Grain Boundary
	4	48	Grain Boundary
B (Bottom Of C4-21A)	1	69	Single Crystal
	2	26	Single Crystal
	3	22	Grain Boundary
	4	28	Grain Boundary
C (Random Source)	1	71	Single Crystal
	2	126	Single Crystal
	3	42	Grain Boundary
	4	118	Grain Boundary
Cz Control	1	204	Single Crystal

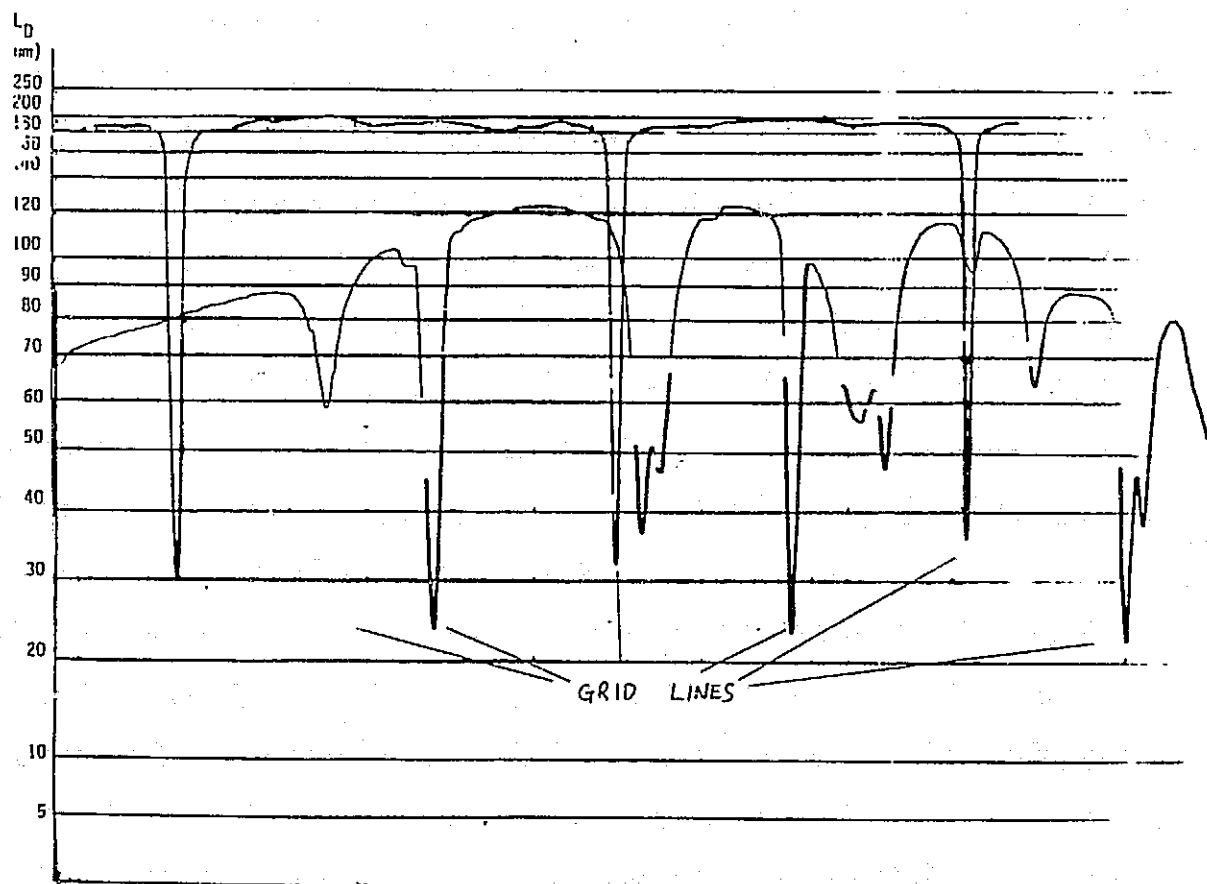
# SILICON SHEET GROWTH AND CHARACTERIZATION

	DIODES NUMBER	$L_D(\mu\text{m})$ FOR GRAIN BOUNDARY DIODES	DIODES NUMBER	$L_D(\mu\text{m})$ FOR NON-GRAIN BOUNDARY DIODES
SILSO (LONG GRAIN)	1 3 5	24 25 17	2 4 5	25 12 37
SILSO (MED. GRAIN)	7 9 11	22 19 16	8 10 12	58 45 48
SILSO (FINE GRAIN)	13	17		
HEM	1 3 5 7	45 82 78 90	2 4 6 8	47 108 52 34
CZ			1	183

## Modified Light-Spot Scan

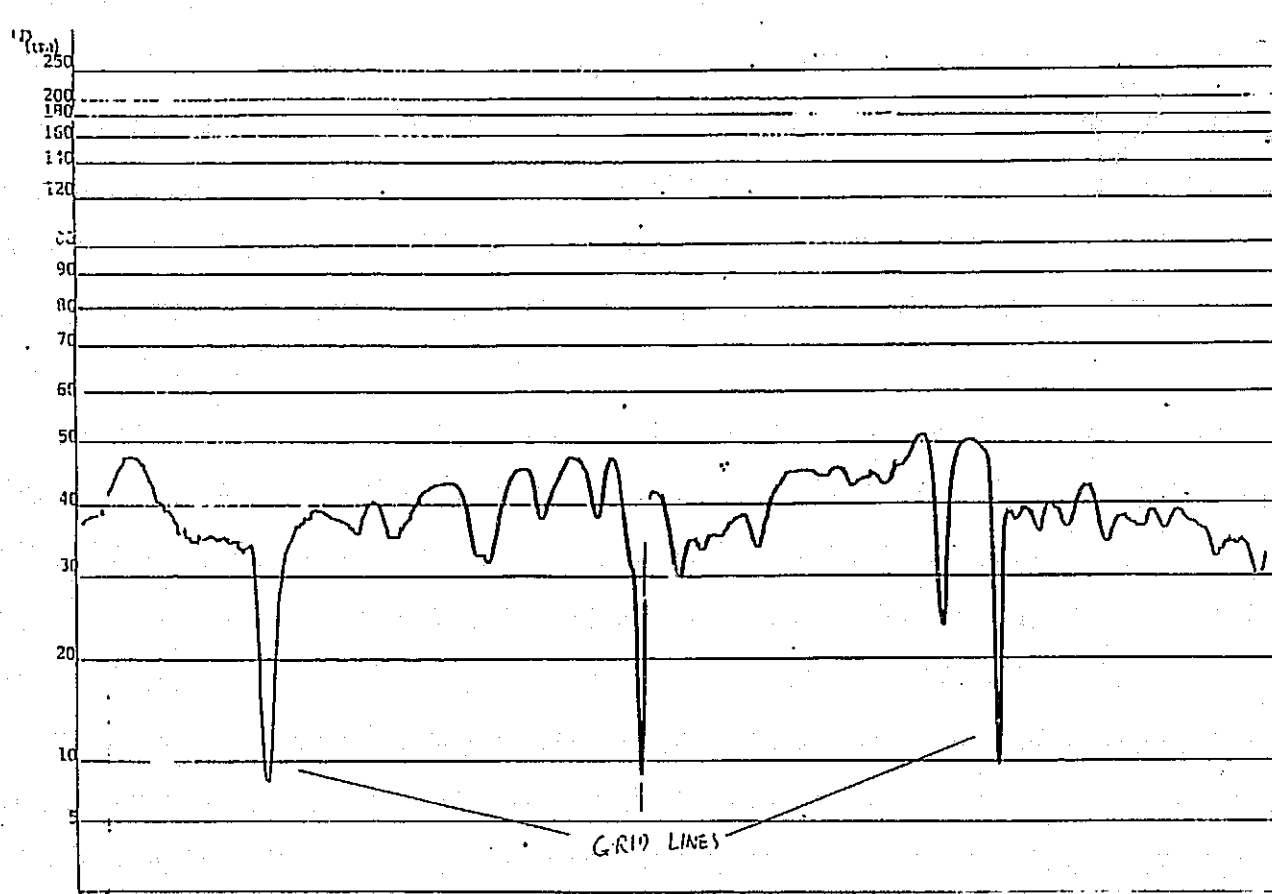
1. LIGHT SPOT SCAN:  $\sim 120\mu\text{m}$
2. MONOCHROMATIC INPUT: ( $\lambda = 0.97\mu\text{m}$ )  
RESPONSE AS A FUNCTION OF DIFFUSION LENGTH CAN BE  
CALCULATED AND SCALED.
3. MEASUREMENT IS CALIBRATED BY SOLAR CELL WITH KNOWN DIFFUSION  
LENGTH.

### Scaled Light-Spot Scan of HEM Poly Cell and Cz Control



# SILICON SHEET GROWTH AND CHARACTERIZATION

## Scaled Light-Spot Scan of HEM Poly Cell From Lower Part of Ingot 4141C



# SILICON-SHEET SURFACE STUDIES

UNIVERSITY OF ILLINOIS AT CHICAGO

<b>TECHNOLOGY</b> INFLUENCE OF FLUIDS ON WEAR AND FRACTURE OF SILICON; RESIDUAL STRESSES IN SILICON SHEET	<b>REPORT DATE</b> September 28, 1983
<b>APPROACH</b> Multiple-scratch; microhardness; three- and four-point bend; laser interferometry  <b>CONTRACTOR</b> University of Illinois at Chicago	<b>STATUS</b> <ul style="list-style-type: none"><li>- Wear rate and mechanism for Si deformation in a number of fluids has been determined.</li><li>- Bend tests of silicon abraded in fluids and etched microhardness indentations reveal the size of the damaged zone.</li><li>- Laser interferometry being used to determine residual stresses in sheet silicon.</li></ul>
<b>GOALS</b> <ul style="list-style-type: none"><li>- Determine influence of fluids on wear and damage zone; microhardness; fracture strength</li><li>- Utilize laser interferometry technique for measurement of residual stresses</li></ul>	

## Influence of Fluids on the Surface Mechanical Properties of Silicon

### RESIDUAL STRESSES IN SHEET SILICON

#### OBJECTIVES

#### I. CONTRIBUTE TO AN UNDERSTANDING OF WAFERING

- FRACTURE AND DEFORMATION OF SILICON IN FLUIDS

WEAR RATE IN FLUIDS

MECHANISM OF DEFORMATION

PLASTICITY/FRACTURE

DEPTH/DAMAGE

MICROCRACKS


PLASTIC ZONE

#### II. CONTRIBUTE TO AN UNDERSTANDING OF RESIDUAL STRESSES IN SHEET SILICON

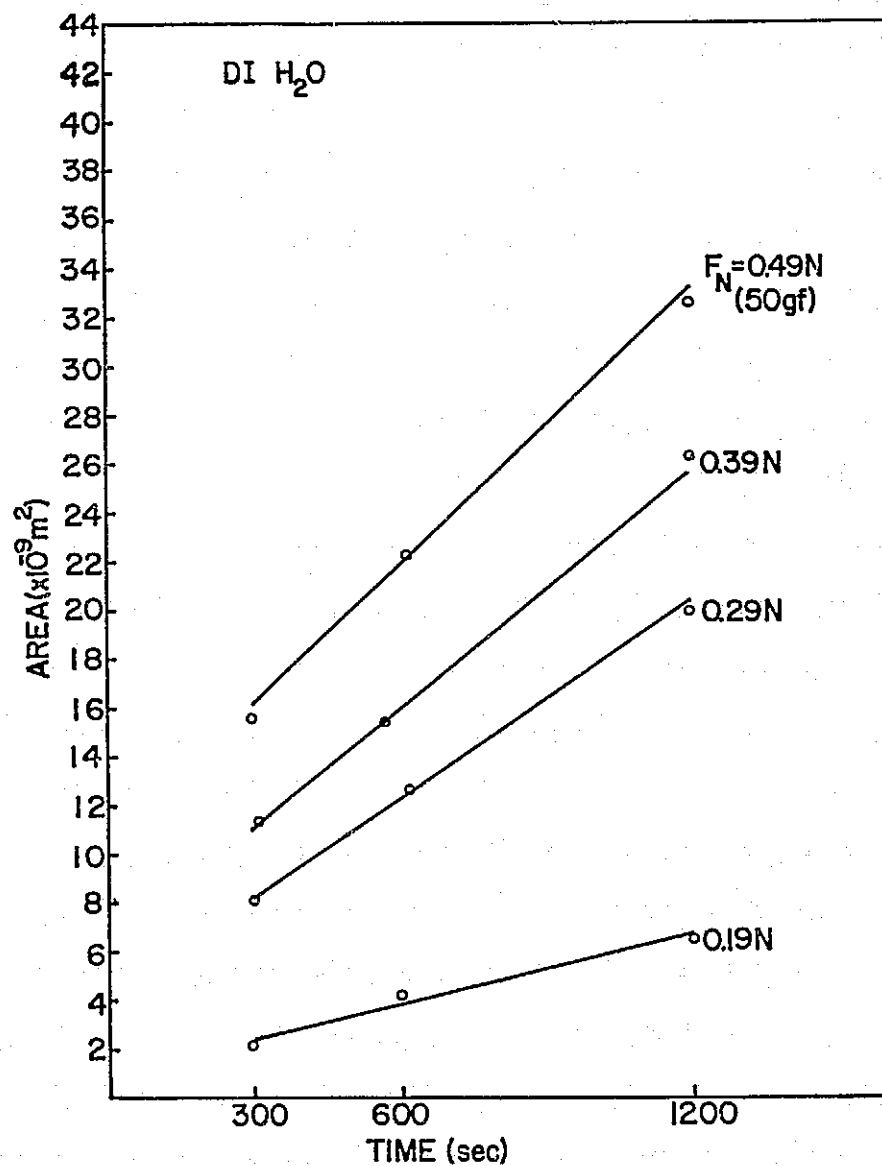
- DEVELOP LASER INTERFEROMETRY TECHNIQUE
- DETERMINE RESIDUAL STRESSES IN EFG RIBBON

## Surface Mechanical Properties of Silicon

### PROBLEM AREAS

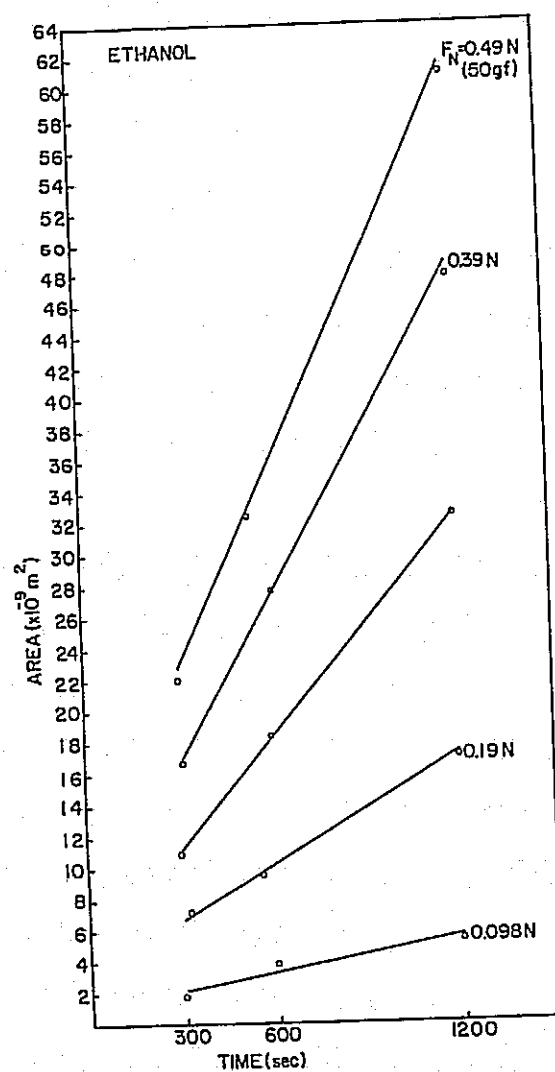
1. SILICON SLICING 
  - MAXIMIZE CUTTING SPEED
  - MINIMIZE DAMAGE ZONE
- MULTIPLE-SCRATCH TEST IN FLUIDS
  - MEASURE WEAR RATE AND COMPARE TO ANALYSIS
2. INFLUENCE OF FLUIDS ON DEFORMATION
  - INDENTATION
    - MEASURE MICROHARDNESS IN FLUIDS
    - DEVELOP THEORY
  - FRACTURE STRENGTH
    - MEASURE STRENGTH AFTER ABRASION IN FLUIDS
3. RESIDUAL STRESSES IN SHEET SILICON
  - DEVELOP LASER INTERFEROMETRY SYSTEM
  - ADAPT TO MEASUREMENT OF RIBBON

# SILICON SHEET GROWTH AND CHARACTERIZATION



Cross-sectional area (x10<sup>-9</sup> m<sup>2</sup>) versus abrasion time (s) of a circular multi-scratch groove formed by a 90° pyramidal diamond with de-ionized water in contact with the silicon surface. The force on the diamond varied from 0.19 to 0.49N.

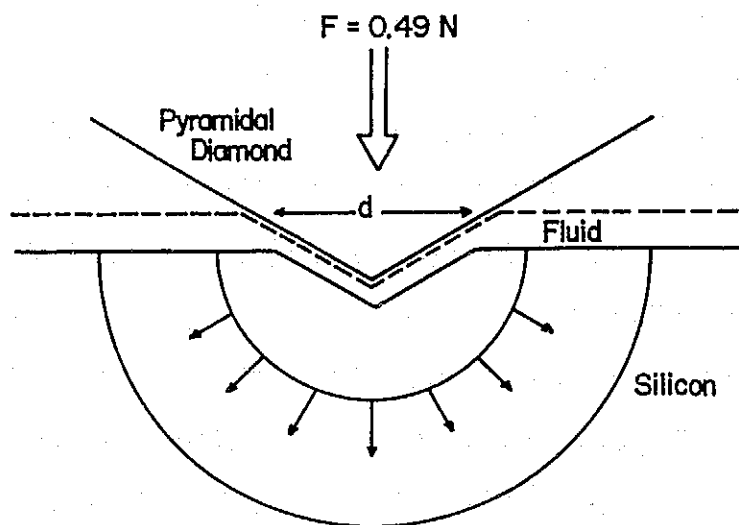
# SILICON SHEET GROWTH AND CHARACTERIZATION



Cross-sectional area ( $\times 10^{-9} \text{ m}^2$ ) versus abrasion time (s) of a circular multi-scratch groove formed by a  $90^\circ$  pyramidal diamond with ethanol in contact with the silicon surface. The force on the diamond varied from 0.19 to 0.49N.



# SILICON SHEET GROWTH AND CHARACTERIZATION

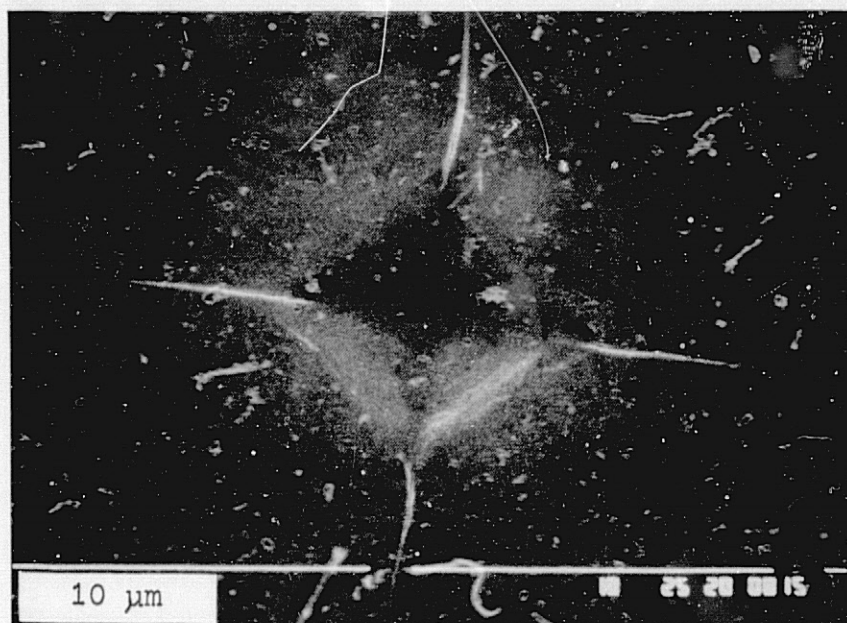


Hardness

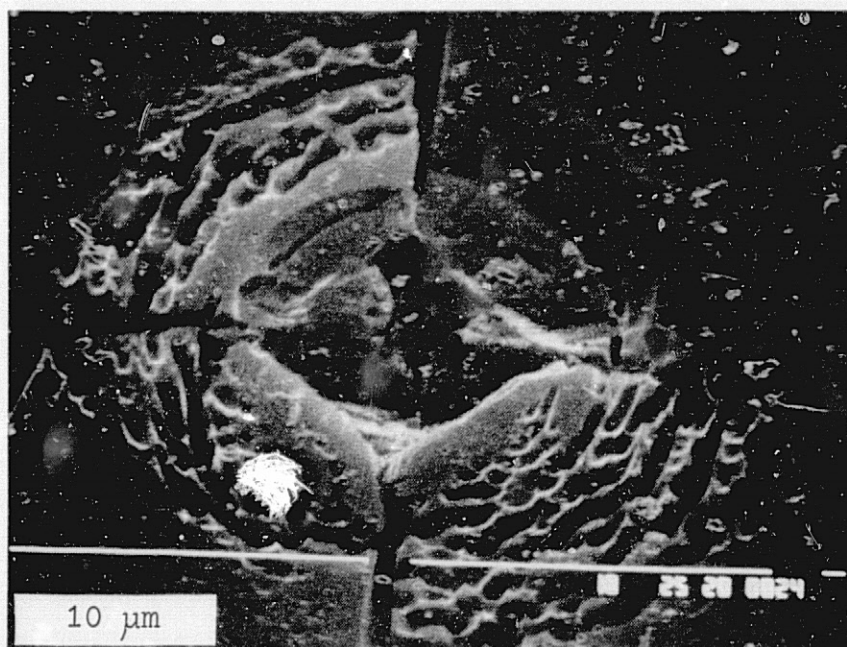
$$H = \frac{1854.4 F}{d^2}$$

where  $d$  is length of diagonal in  $\mu$  meters.

Schematic diagram of a microhardness indentation formed in silicon by a pyramidal diamond in the presence of a fluid. The indentation width is ' $d$ ' and the force on the diamond is ' $F$ '.



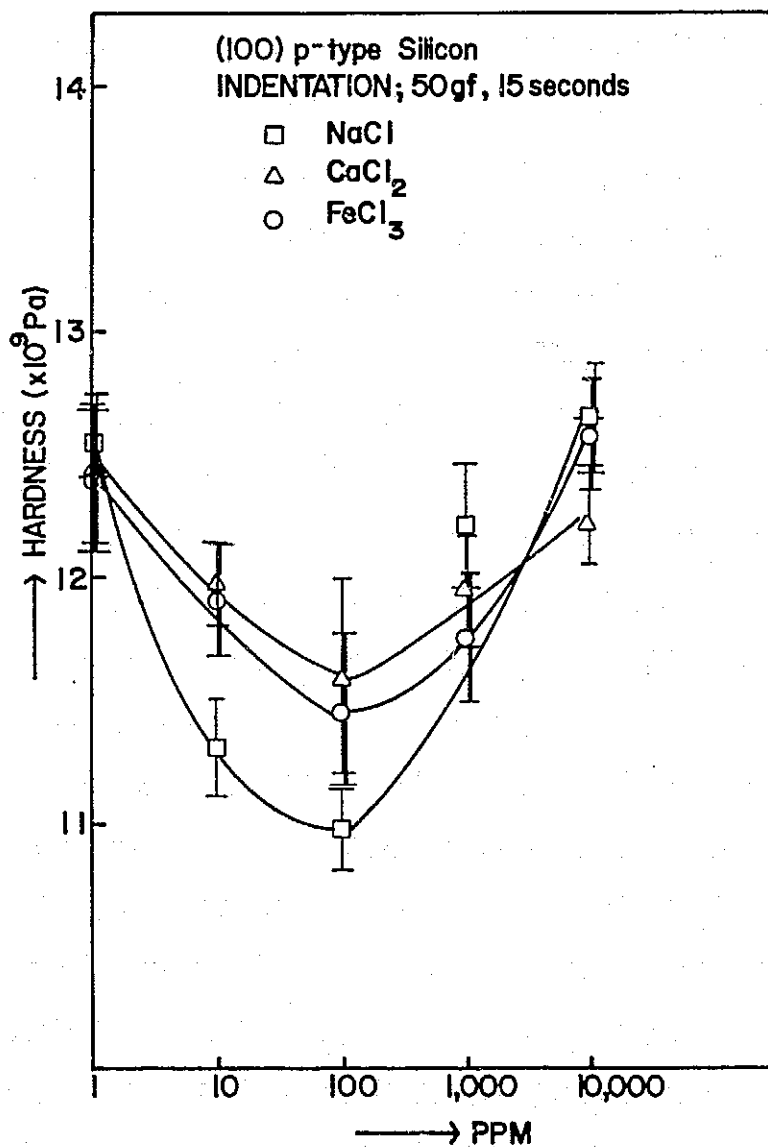
(a)



(b)

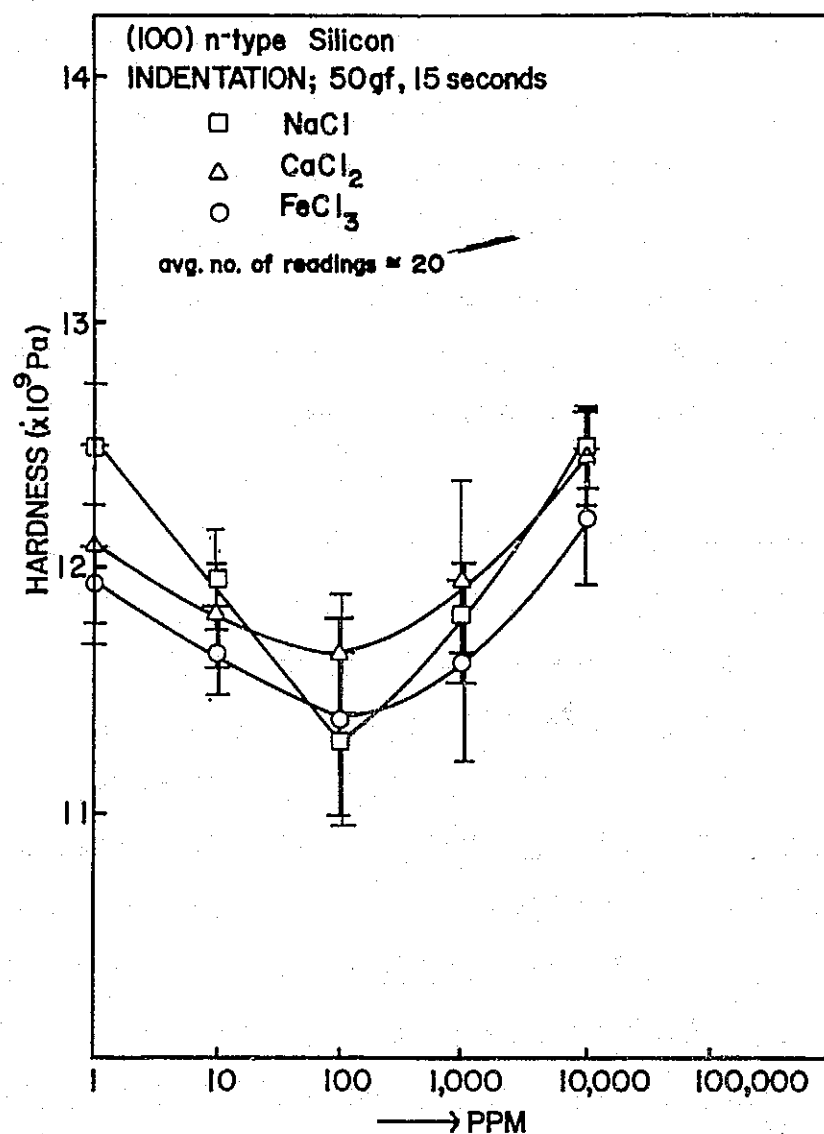
Scanning electron micrographs of (a) pyramidal diamond indentation in (100) n-type Cz silicon, (b) the indentation after exposure to a Sirtl etch for 25 s. The indentation was formed with a force of 0.49N in de-ionized water containing  $10^5$  ppm NaCl. The diameter of the etched region is related to the damage zone created by the indenter.

# SILICON SHEET GROWTH AND CHARACTERIZATION



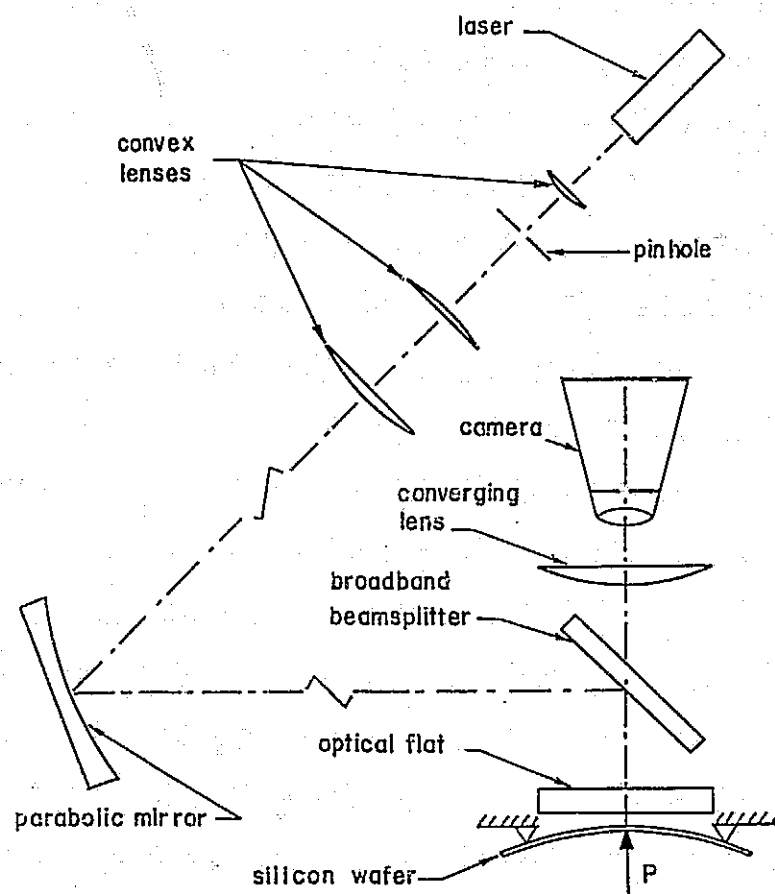
Hardness ( $10^9$  Pa) versus inorganic ion concentration (ppm) in de-ionized water of (100) p-type Cz silicon indented by a pyramidal diamond for 15 s with a force of 0.49N. The inorganic salts were NaCl, CaCl<sub>2</sub> and FeCl<sub>3</sub>. A minimum in hardness is seen at 100 ppm.

# SILICON SHEET GROWTH AND CHARACTERIZATION



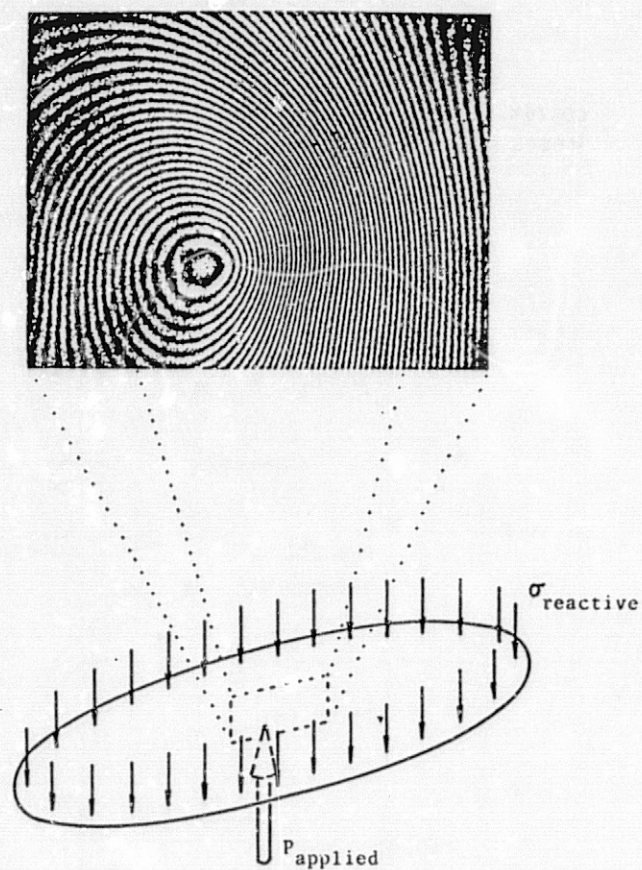
Hardness ( $10^9$  Pa) versus inorganic ion concentration (ppm) in de-ionized water for (100) n-type Cz silicon indented for 15 s with a force of 0.49N. The inorganic salts, NaCl, CaCl<sub>2</sub> and FeCl<sub>3</sub>, cause a minimum in hardness at 100 ppm.

# SILICON SHEET GROWTH AND CHARACTERIZATION

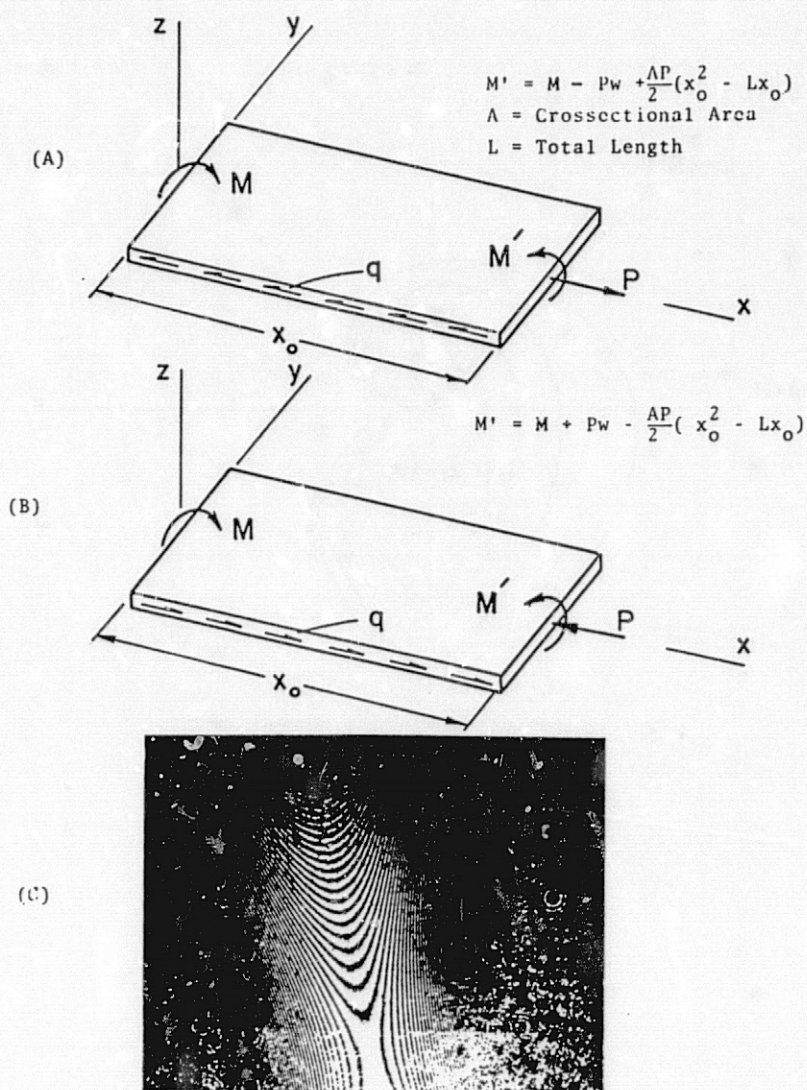


Schematic of the experimental setup to determine residual stresses in simply supported Silicon wafers under centric loading.





Partial interference pattern of a simply supported circular wafer under centric loading as viewed from the top.



(A)-State of loading for a rectangular plate under bending, in-plane tension and side shear. (B)-State of loading for a rectangular plate under bending, in-plane compression and side shear. (C)-Partial interferogram of the deflected surface as viewed from the top.

# SILICON SHEET GROWTH AND CHARACTERIZATION

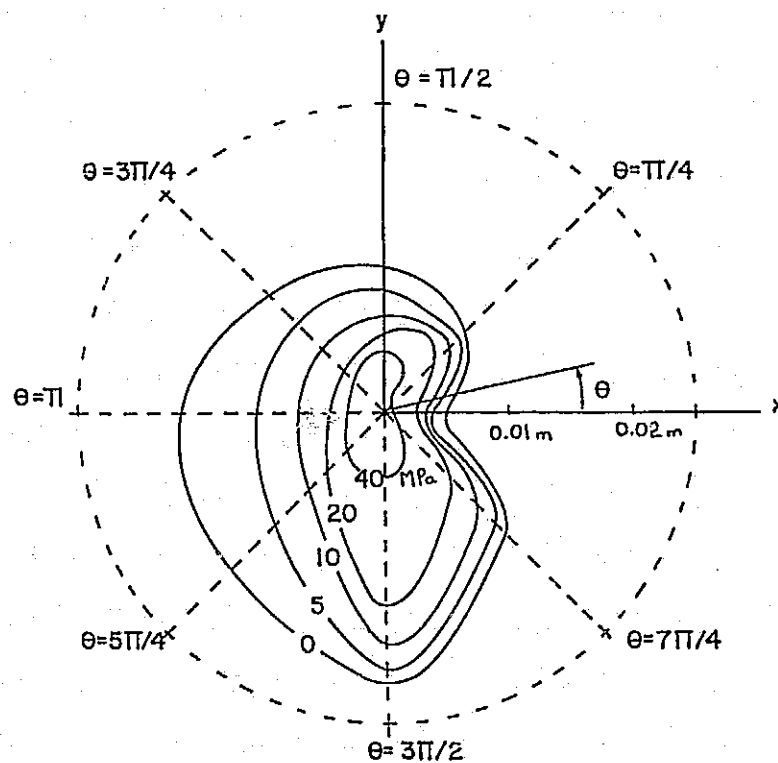


Figure 6. Distribution of the average residual stress  $\bar{\sigma}_r$  in a 0.575mm thick silicon wafer.



# SILICON-SHEET CELL PERFORMANCE

APPLIED SOLAR ENERGY CORP.

<b>TECHNOLOGY</b> SOLAR CELL FABRICATION & ANALYSIS	<b>REPORT DATE</b> 9 - 28 - 83
<b>APPROACH</b> 1) FABRICATION OF SOLAR CELLS BY BASELINE & ADVANCED PROCESSES POSSIBLY INCLUDING GETTERING AND ANNEALING. 2) ANALYSIS USING DARK AND LIGHT I-V, DIFFUSION LENGTH MEASUREMENTS, SPECTRAL RESPONSE. <b>CONTRACTOR</b> APPLIED SOLAR ENERGY CORPORATION	<b>STATUS</b>
<b>GOALS</b> 1) AN UNDERSTANDING OF THE MECHANISMS THAT LIMIT THE DEFICIENCIES OF SOLAR CELLS MADE FROM VARIOUS SILICON SHEETS. 2) AN UNDERSTANDING OF THE EFFECT ON SOLAR CELL EFFICIENCY OF VARIATIONS IN GROWTH PARAMETERS.	

1. SMALL DIODE STUDY:

SIZE OF DIODE -  $0.25 \times 0.125 \text{ cm}^2$  WITH A METAL PATCH THE SIZE OF  $0.072 \times 0.007 \text{ cm}^2$ .

2. LIGHT SPOT SCAN:

SIZE OF LIGHT SPOT -  $\sim 120 \mu\text{m}$

### Summary of Results of Baseline Cells for Comparing 3 Cast Si Materials

		Voc(mV)	Jsc(mA/cm <sup>2</sup> )	CFF(%)	$\eta$ (%)
<u>UCP</u>					
A	AVE.	514	25.6	74	10.1
	RANGE	20-550	24.4-26.1	25-78	0.1-11.2
B	AVE.	555	25.8	76	10.9
	RANGE	534-568	24.1-27.0	68-79	8.8-12.1
C	AVE.	550	25.3	72	10.1
	RANGE	512-564	24.4-26.5	38-79	4.8-11.8
UCP OVERALL	AVE.	539	25.6	74	10.4
	RANGE	20-568	24.1-27.0	25-79	0.1-12.1
<u>SILSO</u>					
D(Long Grain)	AVE.	552	24.4	72	9.8
	RANGE	526-564	21.6-26.6	46-79	6.1-11.3
E (Medium Grain)	AVE.	556	26.2	76	11.1
	RANGE	552-564	25.4-27.0	72-78	10.1-11.6
F(Fine Grain)	AVE.	547	23.7	75	9.7
	RANGE	536-552	22.6-24.4	61-78	7.9-10.5
SILSO OVERALL	AVE.	552	24.7	74	10.2
	RANGE	526-564	21.6-27.0	46-79	6.1-11.6
<u>HEM</u>					
G(Single Crystal)	AVE.	579	27.7	73	11.7
	RANGE	574-588	26.9-28.5	66-79	10.1-13.2
H(Poly)	AVE.	566	26.7	76	11.5
	RANGE	552-576	25.4-27.5	70-78	10.3-12.2
I(Poly)	AVE.	564	26.6	74	11.1
	RANGE	550-574	25.0-27.6	67-78	9.7-12.1
J(Poly)	AVE.	551	24.8	74	10.1
	RANGE	538-560	23.6-25.5	65-78	8.5-11.0
HEM OVERALL	AVE.	565	26.5	74	11.1
	RANGE	538-588	23.6-28.5	65-79	8.5-13.2
<u>CZ CONTROL</u>					
	AVE.	586	29.0	77	13.1
	RANGE	586-586	28.8-29.3	76-77	12.9-13.3

# Summary of $V_{oc}$ and $I_{sc}$ Measurement of Silso and HEM Diodes

	Single Crystal Diodes (Ave. Of 5 or More Diodes)		Grain Boundary Dominated Diodes (Ave. of 5 or More Diodes)	
	$V_{oc}$ (mV)	Normalized ( $I_{sc}$ )	$V_{oc}$ (mV)	Normalized ( $I_{sc}$ )
SILSO (Long Grain)	520	.851	518	.800
SILSO (Med. Grain)	531	.900	519	.844
SILSO (Fine Grain)			511	.765
HEM (Upper Central of Ingot 4141C)	516	.922	520	.834
HEM (Lower Central Of Ingot 4141C)	538	.922	532	.892
CZ Control	535	1		

Summary of  $V_{OC}$  and  $I_{SC}$  Measurements of UCP Diodes

	Single Crystal Diodes (Ave. Of 5 or More Diodes)		Grain Boundary Dominated Diodes (Ave. of 5 or More Diodes)	
	$V_{OC}$ (mV)	Normalized ( $I_{SC}$ )	$V_{OC}$ (mV)	Normalized ( $I_{SC}$ )
1-C (Top of Ingot C4-21A)	545	.966	535	.897
4-B (Bottom Of Ingot C4-21A Outside)	529	.824	525	.839
4-C (Bottom Of Ingot C4-21A Center)	512	.785	.517	.764
5-A From Random Source	541	.931	525	.868
Control	555	1	-	-

Minority Carrier Diffusion Lengths of  
Diodes Made From UCP Silicon

WAFER	DIODE #	$L_D$ ( $\mu m$ )	CHARACTER
A (Top Of C4-21A)	1	141	Single Crystal
	2	162	Single Crystal
	3	44	Grain Boundary
	4	48	Grain Boundary
B (Bottom Of C4-21A)	1	69	Single Crystal
	2	26	Single Crystal
	3	22	Grain Boundary
	4	28	Grain Boundary
C (Random Source)	1	71	Single Crystal
	2	126	Single Crystal
	3	42	Grain Boundary
	4	118	Grain Boundary
Cz Control	1	204	Single Crystal

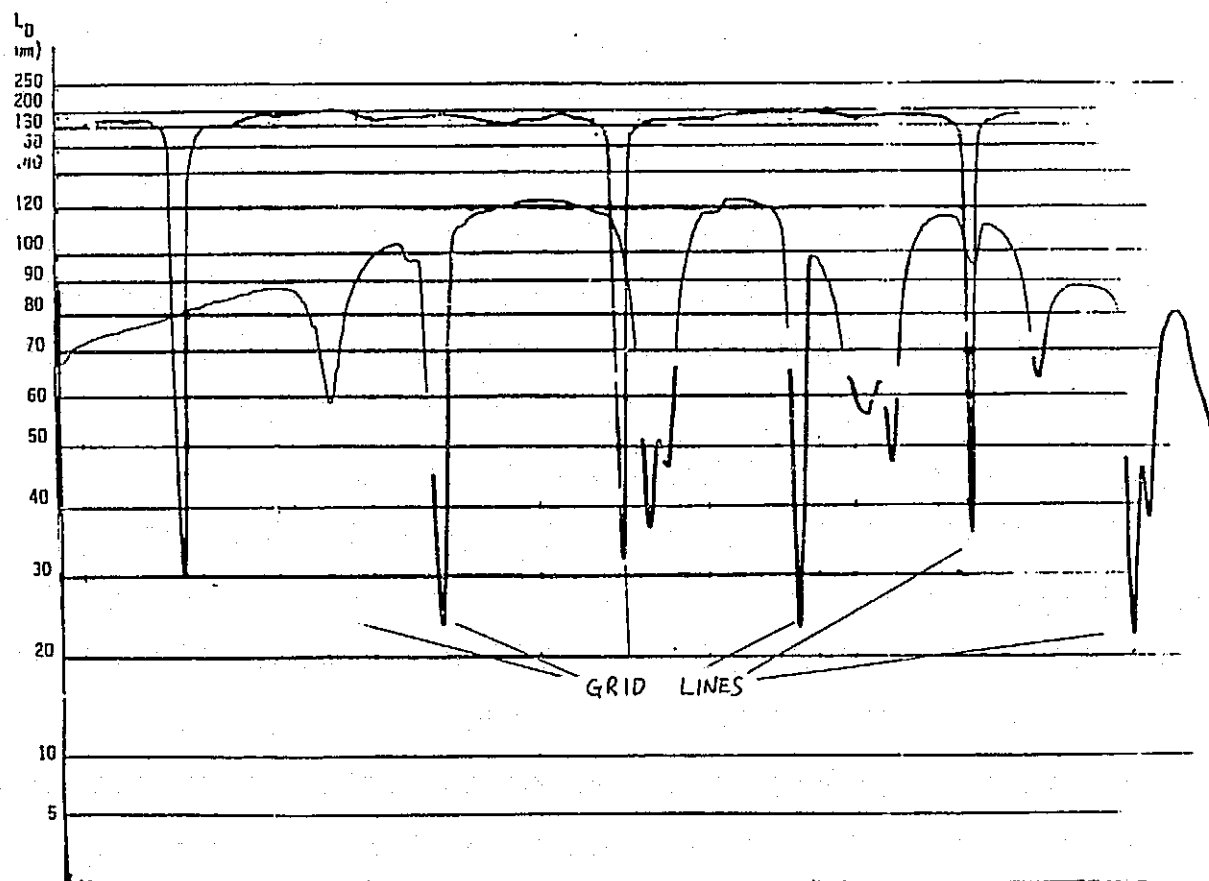
# SILICON SHEET GROWTH AND CHARACTERIZATION

	DIODES NUMBER	$L_D(\mu\text{M})$ FOR GRAIN BOUNDARY DIODES	DIODES NUMBER	$L_D(\mu\text{M})$ FOR NON-GRAIN BOUNDARY DIODES
SILSO (LONG GRAIN)	1 3 5	24 25 17	2 4 6	25 12 37
SILSO (MED. GRAIN)	7 9 11	22 19 16	8 10 12	58 45 48
SILSO (FINE GRAIN)	13	17		
HEM	1 3 5 7	45 82 78 90	2 4 6 8	47 108 62 34
CZ			1	183

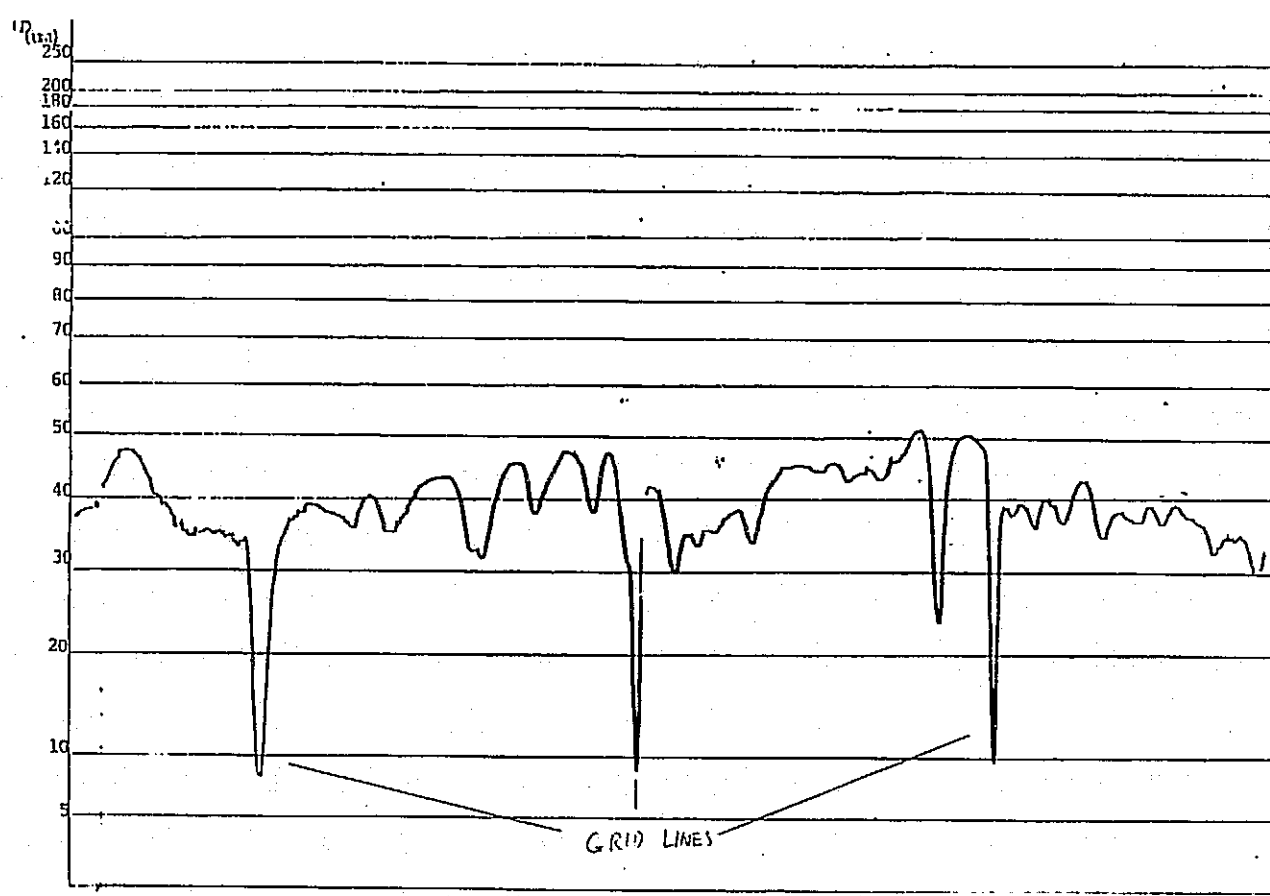
## Modified Light-Spot Scan

1. LIGHT SPOT SCAN:  $\sim 120\mu\text{m}$
2. MONOCHROMATIC INPUT: ( $\lambda = 0.97\mu\text{m}$ )  
RESPONSE AS A FUNCTION OF DIFFUSION LENGTH CAN BE  
CALCULATED AND SCALED.
3. MEASUREMENT IS CALIBRATED BY SOLAR CELL WITH KNOWN DIFFUSION  
LENGTH.

# Scaled Light-Spot Scan of HEM Poly Cell and Cz Control



Scaled Light-Spot Scan of HEM Poly Cell  
From Lower Part of Ingot 4141C



# MODULE TECHNOLOGY

R.G. Ross, Jr., Chairman

D.H. Otth of JPL presented the latest results of environmental endurance testing at Wyle Laboratories. The summary focused on long-term temperature-only degradation and the recent use of densitometric measurements to obtain degradation rates for PVB and EVA discoloration. Results from the 85°C/85% RH and intermediate temperature-humidity studies (70°C/85% RH and 85°C/70% RH levels) showed that combined environments have consistently led to additional degradation modes and to greater degradation than temperature environments alone.

J.W. Lathrop, Clemson University, reported on current FSA cell-reliability research activities. Included were results of the encapsulated-cell testing study and a discussion of the Schottky barrier formation failure mechanism in silicon solar cells.

G.R. Mon gave a presentation on bare cell and module electrochemical degradation studies at JPL. Data were presented that exhibited the time variation of many parameters resulting from exposures at different combinations of humidity and voltage-bias application while maintaining temperature constant. The results are preliminary to determining electrochemical degradation rates for photovoltaic modules in field applications.

An overview of the Transparent Conducting Materials Task was presented by D.R. Coulter of JPL. The major focus was on the development of organic and/or inorganic conductors for replacement of metals or semimetals as charged collectors and conductors in PV devices.

Gary Wnek, Professor of Material Science at MIT, described in general the science of conducting polymers and some preliminary considerations of the antireflection application. Wnek, a new FSA consultant, is providing guidance related to applications of conducting polymers as antireflection coatings on solar cells.

The optical transmission of commercially available, state-of-the-art conducting polymers is inadequate for antireflection application on solar cells. It is generally observed for these conducting polymers that increases in electrical conduction are accompanied by decreases in optical transmission. Is this behavior a consequence of state-of-the-art chemistry, or a fundamental law of nature? John Garlick, a joint consultant to JPL and Spectrolab, presented the background for developing a quantum mechanical model that addresses these questions.

Alex Garcia presented the details of a new program at Spectrolab that includes experimental studies of solar cells having conducting polymer antireflection coatings and a laboratory facility to permit routine deposition of conducting polymers on solar cells. Garcia also presented some early experimental measurements of solar cells coated with conducting polymers.



## MODULE TECHNOLOGY

E.F. Cuddihy of JPL described the theoretical background leading to the possible identification of the fundamental electrical-strength property of polymeric insulation materials. In a photovoltaic module, encapsulation pottants such as EVA must function as electrical insulation for the dc voltages established by the solar cell and associated electrical circuitry. For a desired 30-year module life, the electrical insulation qualities of the encapsulating pottant must not weather, degrade or deteriorate to a state that would permit electrical breakdown or allow hazardous levels of leakage current to human-contact areas. A recent theoretical analysis suggests that the fundamental dielectric strength of insulation materials can be defined, easily measured experimentally and monitored for its aging behavior.

R. Liang of JPL gave a presentation on theoretical modeling and experimental investigation of encapsulant degradation. The theoretical model predicts the serviceable lifetime of EVA systems in various conditions, including elevated temperature. Experimental studies have been concentrated on development of valid accelerated testing technology and of different means of stabilizing polymeric systems.

Jack Koenig of Case Western Reserve University updated his efforts at developing a technique to monitor chemically bonded interfaces directly, between any and all nonmetallic module interfaces, as for example between EVA and glass. The experimental modules will be used to track directly the chemistry of a bonded interface undergoing weather aging, for both fundamental understanding as well as kinetic information for life modeling.

James Boerio of the University of Cincinnati has initiated a new FSA program related to the studies of a chemically bonded interface between modules and encapsulation pottants. In conjunction with Case Western, all bonded interfaces of a photovoltaic module are being investigated. An additional feature of Boerio's program includes investigation of the role of silane primers as interfacial agents, which appear to be effective at stopping galvanic corrosion. Boerio described his program and some preliminary experiments related to the behavior of silanes in stopping the corrosion of aluminum.

# LONG-TERM MODULE TESTING AT WYLE LABORATORIES

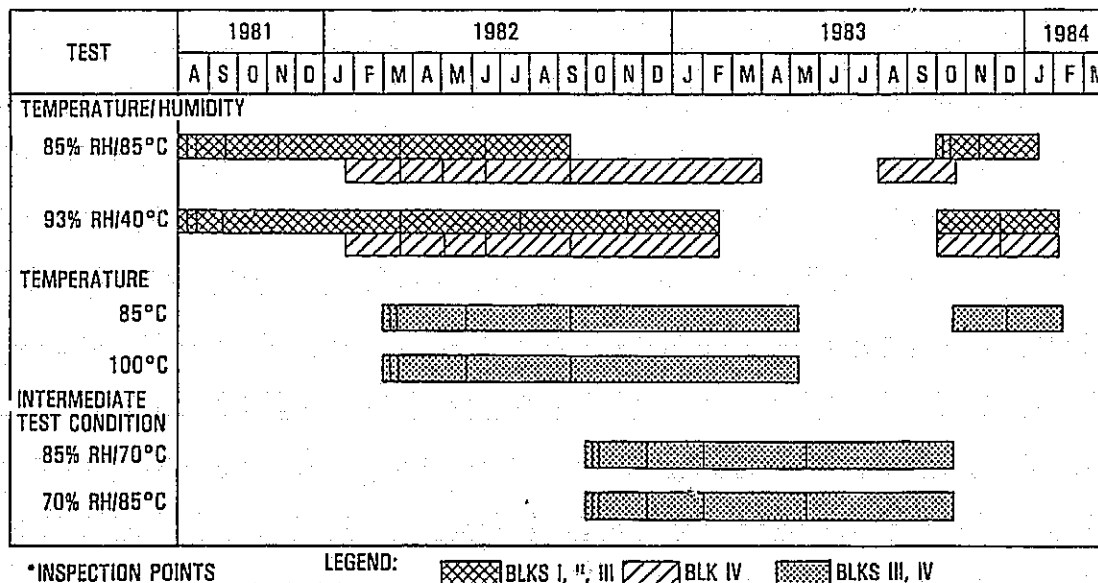
## JET PROPULSION LABORATORY

D.H. Otth

### Objectives

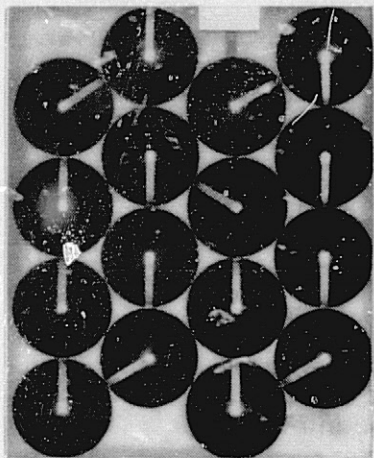
- Understand temperature/humidity-bias failure mechanisms of typical photovoltaic modules and materials
  - Cells, encapsulants, interconnects
  - Back covers, edge seals
- Establish generic functional relationships among temperature, humidity, bias and time for observed failure mechanisms
- Determine relative lifetimes of roof-mounted vs ground-mounted arrays
- Understand relative severity (acceleration factor) of candidate T/H-B qualification tests and define recommended levels

### Long-Term Module Testing Schedule

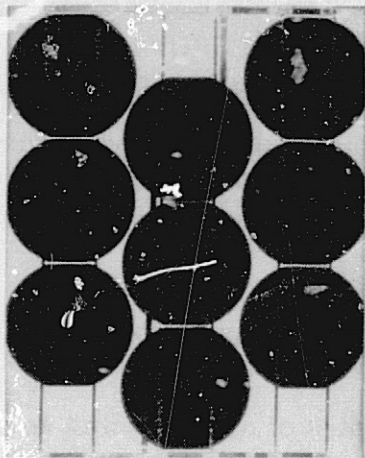


Module Design Comparisons at Day 365: 85°C / 0% RH

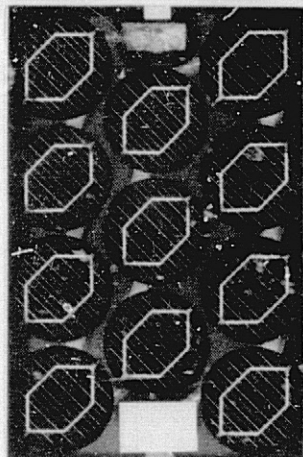
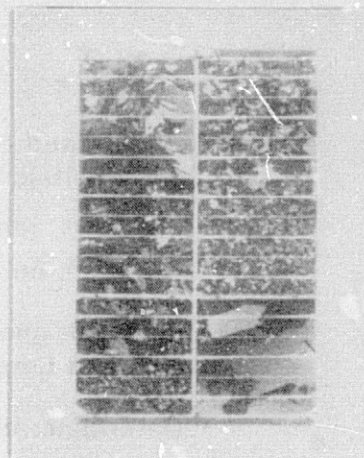
PVB, TEDLAR  
WITHOUT FOIL



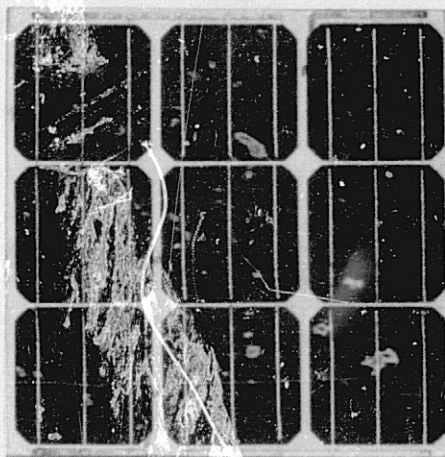
PVB, TEDLAR  
WITH FOIL



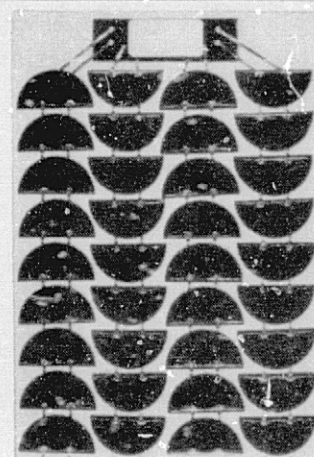
EVA, TEDLAR  
WITHOUT FOIL



PVB, TEDLAR  
WITHOUT FOIL



PVB, TEDLAR  
WITH FOIL

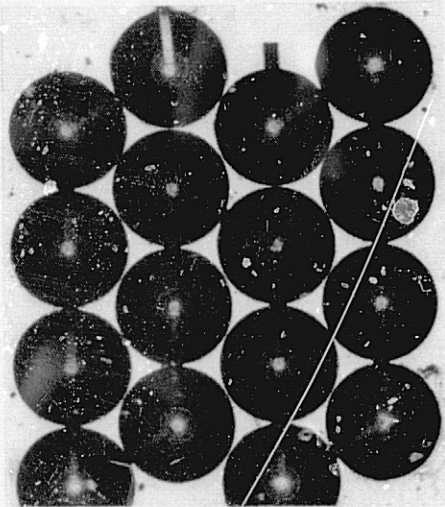


SILICONE, MYLAR  
WITHOUT FOIL

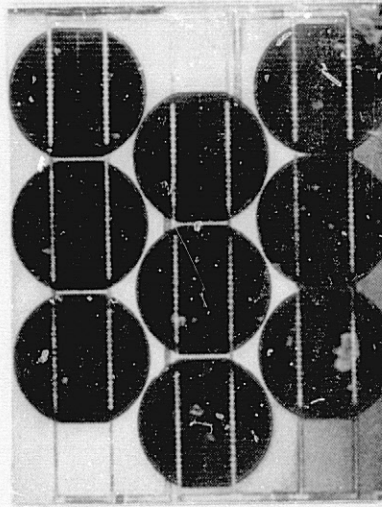


Module Design Comparisons: 85°C / 85% RH

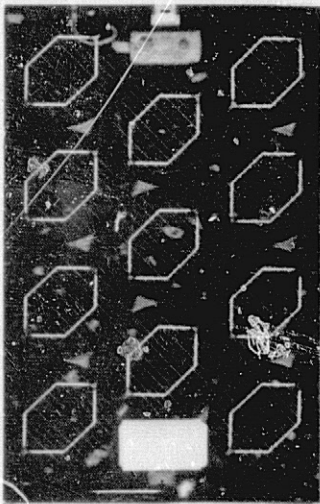
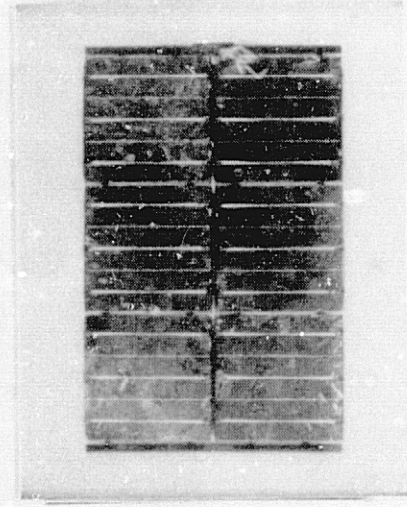
PVB, TEDLAR  
WITHOUT FOIL  
DAY 145



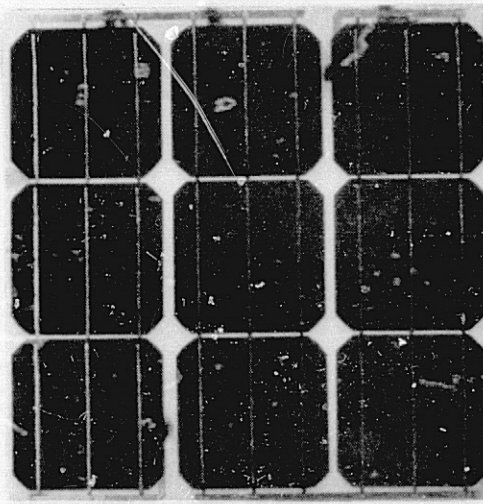
PVB, TEDLAR  
WITH FOIL  
DAY 294



EVA, TEDLAR  
WITHOUT FOIL  
DAY 294



PVB, TEDLAR  
WITHOUT FOIL  
DAY 280

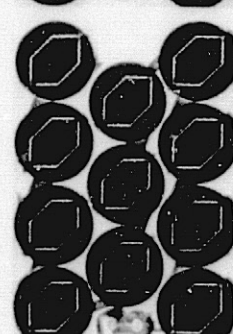
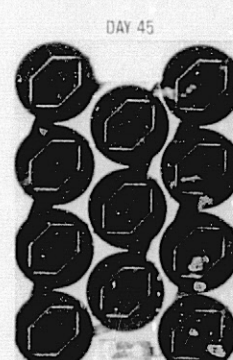
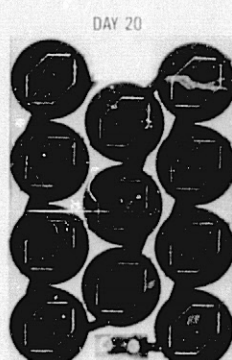
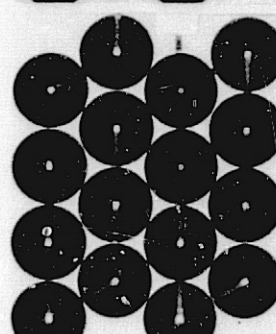
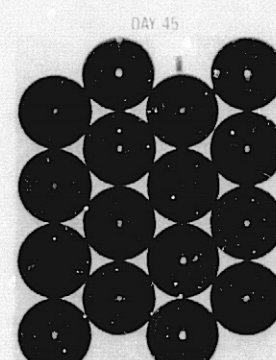
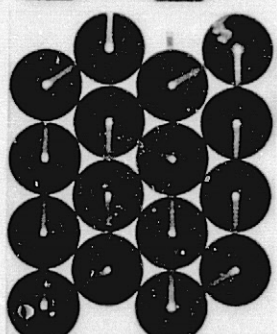
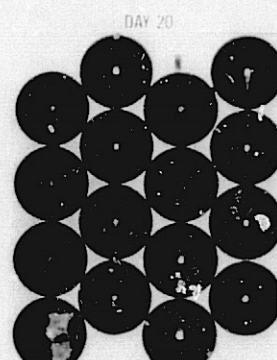
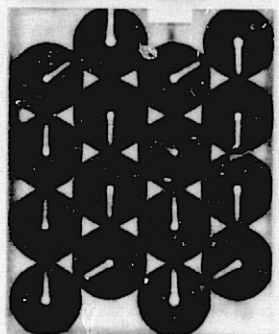
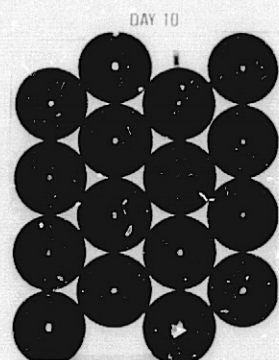


PVB, TEDLAR  
WITH FOIL  
DAY 204

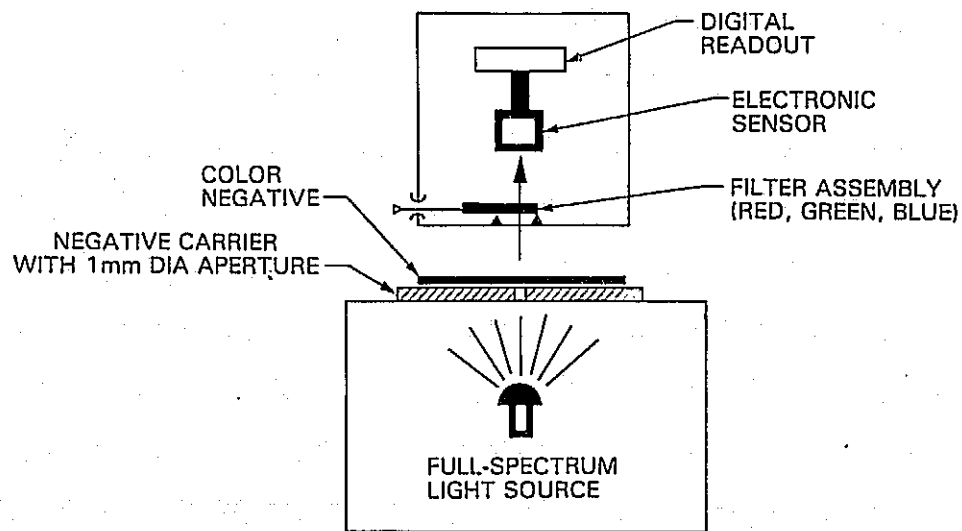


SILICONE, MYLAR  
WITHOUT FOIL  
DAY 280

Temperature Acceleration at 85°C / 0% RH:  
PVB, Tedlar (Without Foil) Modules

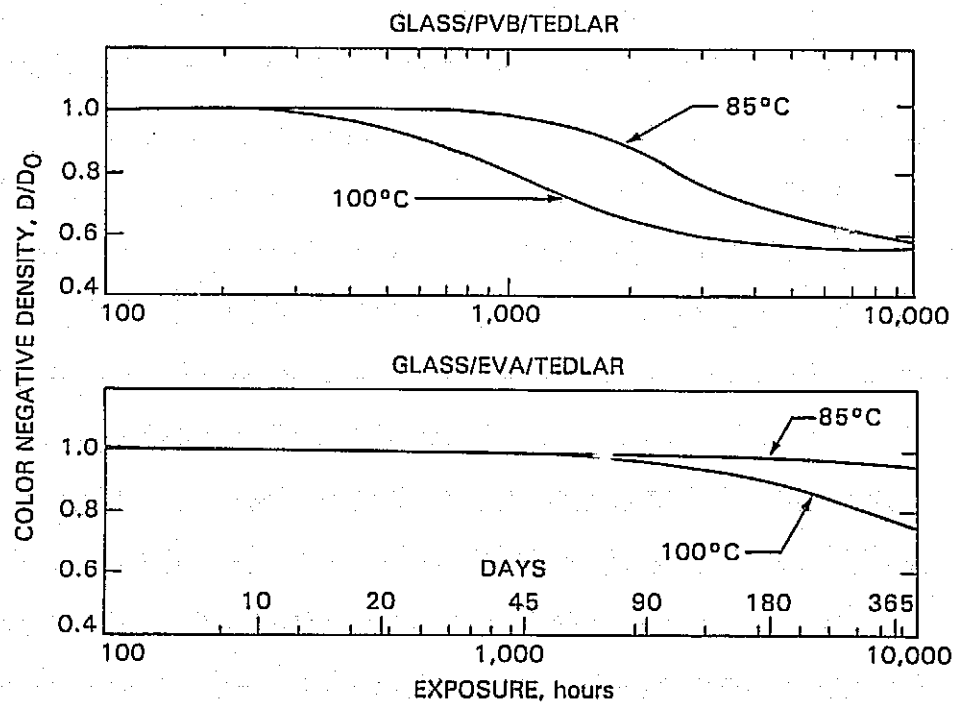


## Densitometer

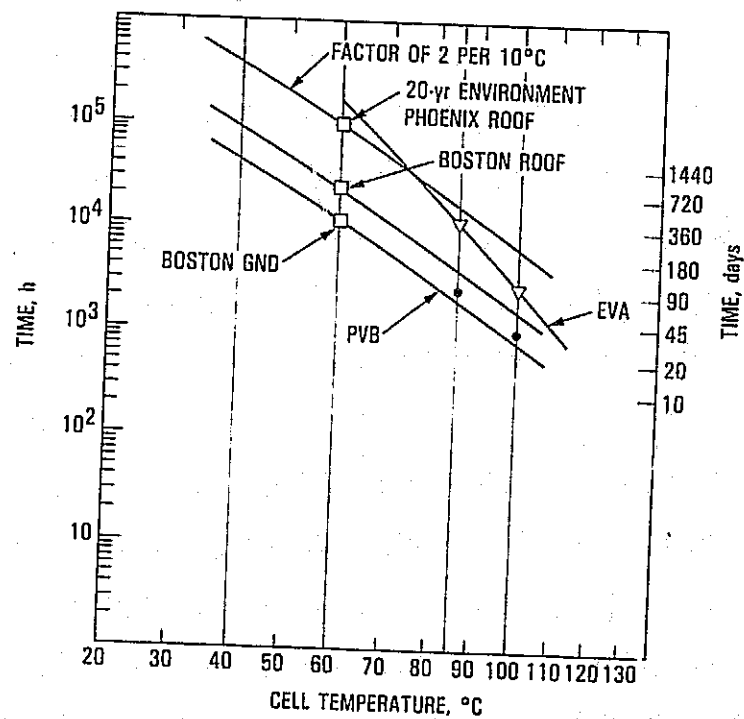


$$\text{COLOR DENSITY} = f\left(\frac{1}{\text{TRANSMITTANCE}}\right)$$

## Encapsulant Yellowing (PVB vs EVA)

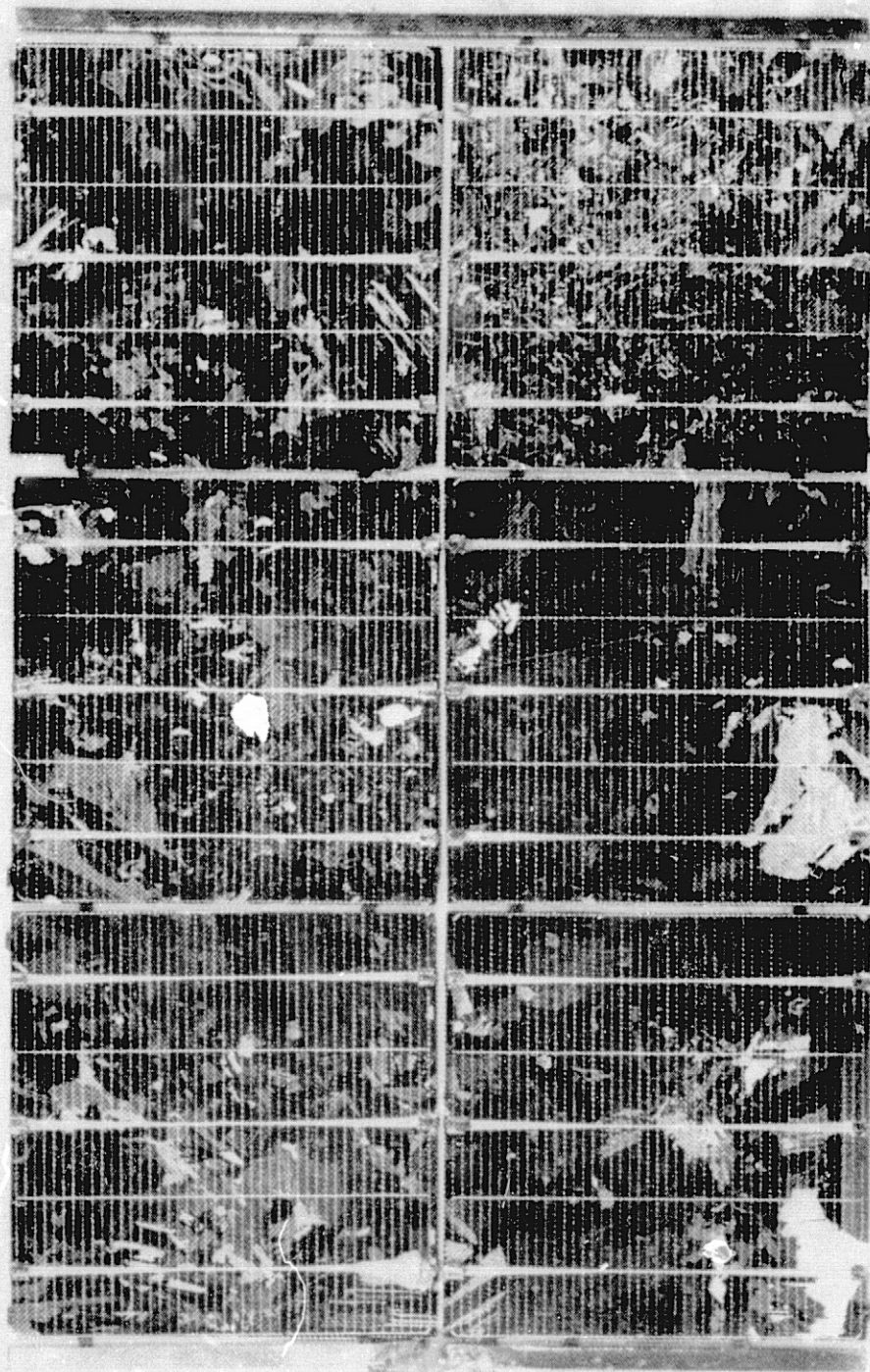


## Arrhenius Plot: Time to Degradation vs Cell Temperature



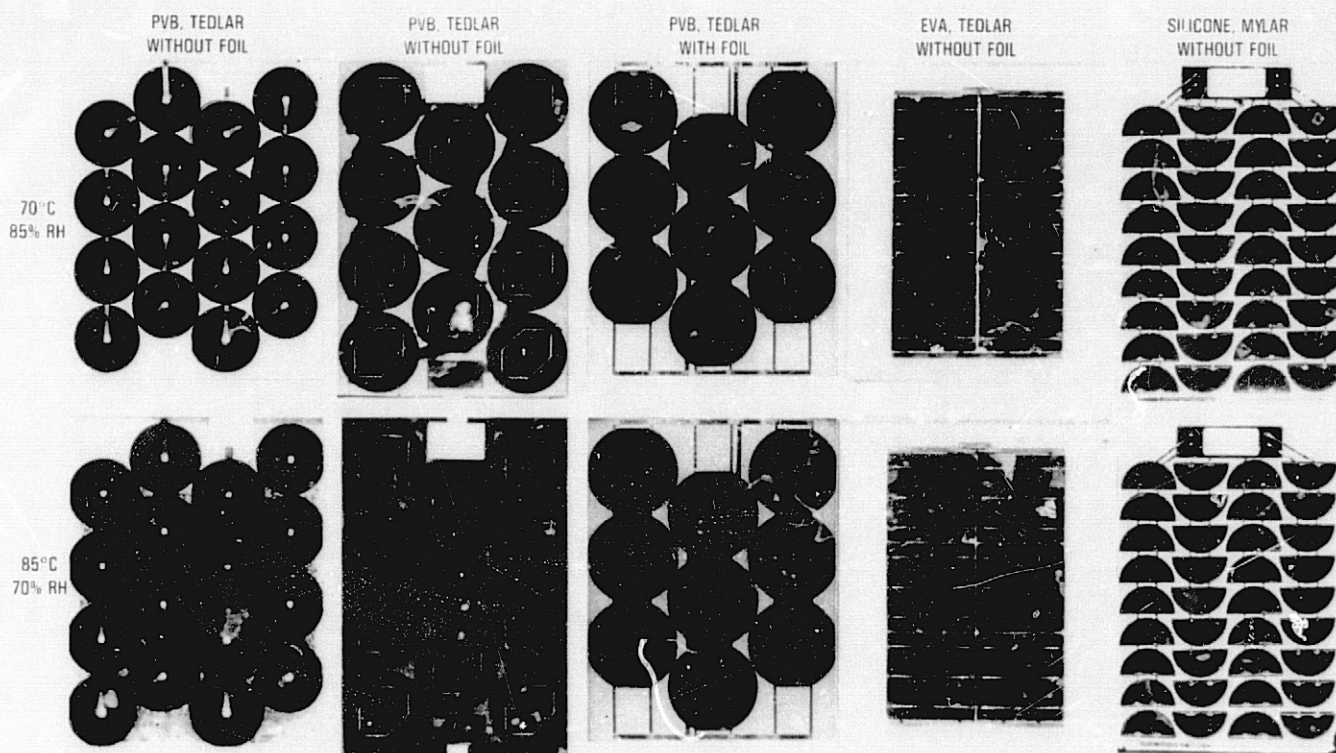


Day 365: 85°C

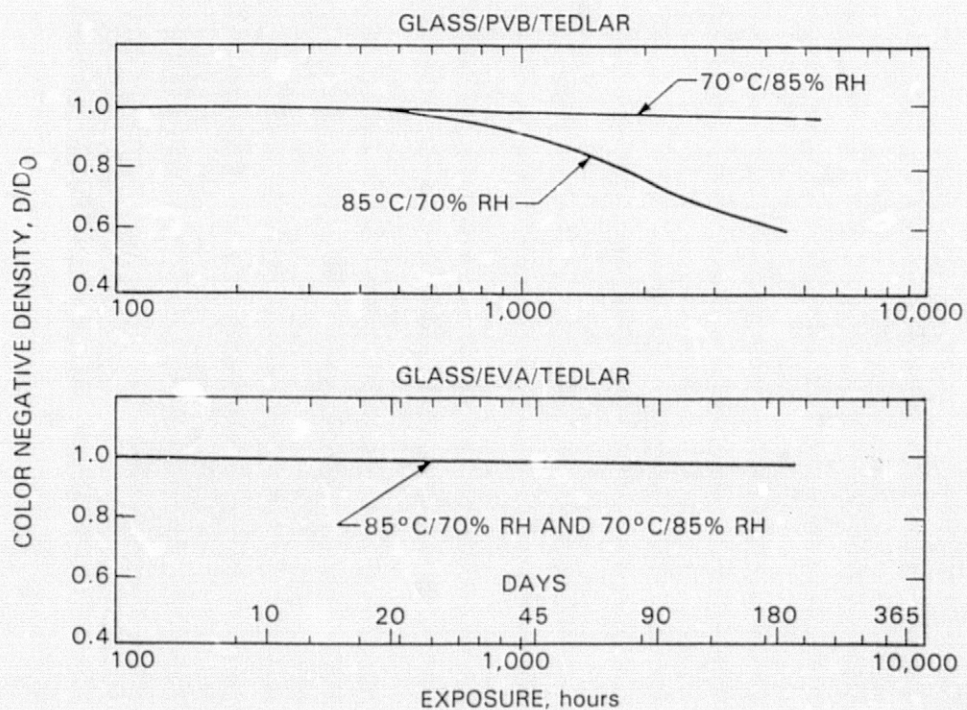




## Module Design Comparisons at Day 135



## Encapsulant Yellowing (PVB vs EVA)



## Performance Degradation at Day 365: 85°C/0% RH

(APPROX. 20 YEAR EQUIVALENT FIELD)

Encapsulant	Metallization	P/P <sub>0</sub> Power Loss	
		Transmissivity	Series Resistance
Glass/PVB/Tedlar	Ti-Pd-Ag	0.97	0.97
	Print-Ag	0.95	0.99
Glass/PVB/Foil	Print-Ag	0.99	1.00
	Ni-Solder	0.98	0.98
Glass/EVA/Tedlar	Ti-Pd-Ag	0.96	0.93
Glass/Silicone/Mylar	Ni-Solder	0.99	0.89
Strawman 20-year goal for total degradation in all environments		0.96	0.96

## Conclusions

- Long-term temperature-only degradation of a variety of encapsulants and metallizations appears to be consistent with 30-year life program goal
- Temperature-humidity environments have led to additional degradation modes and greater degradation than have temperature environments
- Quantification of long-term temperature-humidity degradation requires additional data and analysis

# SOLAR-CELL RELIABILITY RESEARCH

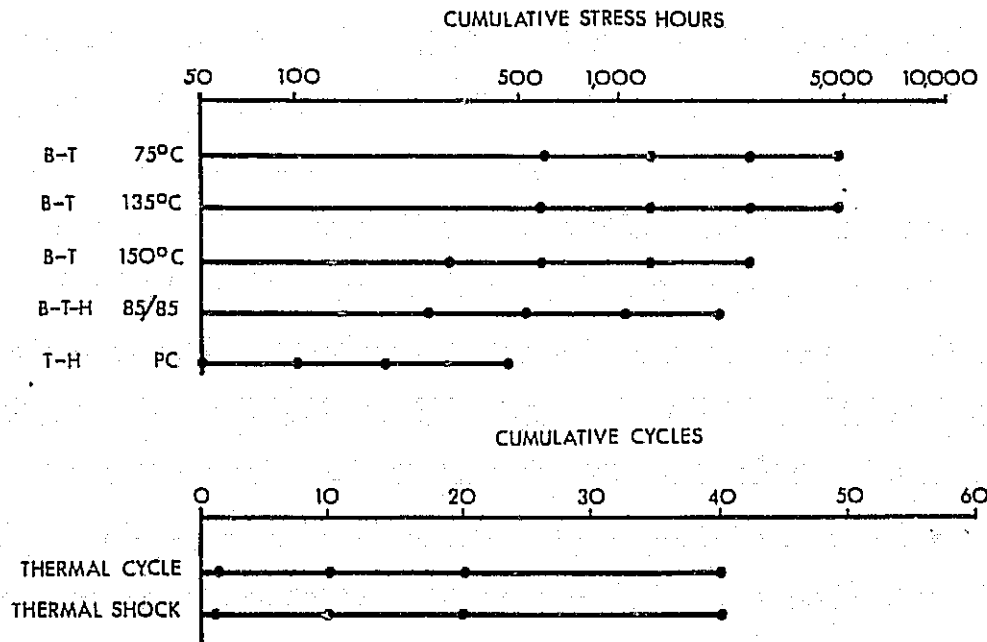
CLEMSON UNIVERSITY

J.W. Lathrop

## Unencapsulated Cell Types Classified by Primary Metallization

CELL TYPE	CONDUCTING LAYER	SOLDER
N	nickel plate	yes
O	nickel plate	yes
P	nickel plate	yes
Q	nickel plate	yes
R	copper plate	no
V	copper plate	yes
W	nickel plate	yes
X	nickel plate	yes
Y	silver paste	no
Z	silver paste	no

## Clemson Accelerated Test Schedule for Unencapsulated Cells



# MODULE TECHNOLOGY

## Hours of 85/85 Testing Completed on Encapsulated Cell Coupons

COUPON	CELL TYPE										
	N	O	P	Q	Q	R	V	V	W	X	Y
	SPR	SPR	SPR	SPR	MFG	SPR	SPR	MFG	SPR	SPR	SPR
G/EVA	---	---	---	---	---	---	---	2000	---	---	---
G/EVA/T	2000	2000	2000	2000	---	---	2000	2000	---	2000	2000
G/EVA/F1	2000	---	2000	2000	---	2000	---	2000	2000	2000	2000
G/EVA/F2	---	---	---	---	---	---	---	2000	---	---	---
G/EVA/G	2000	---	2000	2000	---	---	---	---	---	2000	2000
G/EMA/T	2000	2000	2000	2000	---	---	2000	---	---	2000	2000
T/EVA/S	2000	2000	2000	2000	---	---	---	---	2000	---	2000
G/SR/G	---	---	---	---	TBS	---	---	---	---	---	---

--- = Tests not planned

SPR = Coupons fabricated by Springborn Laboratories

MFG = Coupons fabricated by cell manufacturers

TBS = To be started

G = glass, T = Tedlar, F = foil, S = steel, SR = Silicone Rubber

All tests are scheduled to end at 2000 hours

## Power Decrease

Average % Decrease in Maximum Power for Encapsulated Cell

Coupons Subjected to 2000 Hours of 85/85 Testing.

	N	O	P	Q	Q	R	V	V	W	X	Y
COUPON	SPR	SPR	SPR	SPR	HFG	SPR	SPR	HFG	SPR	SPR	SPR
G/EVA	---	---	---	---	---	---	---	2	---	---	---
G/EVA/T	31	19	4	42	---	---	-1	1	---	20	-21
G/EVA/F1	15	---	1	53	---	10	---	-1	5	8	-28
G/EVA/F2	---	---	---	---	---	---	---	-2	---	---	---
G/EVA/G	0	---	1	23	---	---	---	---	---	13	-14
G/EVA/T	24	14	1	53	---	---	0	---	---	10	-8
T/EVA/S	-8	5	1*	6	---	---	---	---	2	---	-9
G/SR/G	---	---	---	---	TBS	---	---	---	---	---	---
UNENCAP	6	3	2	12			1		4	2	

--- = Tests not planned

SPR = Coupons fabricated by Springborn Labs

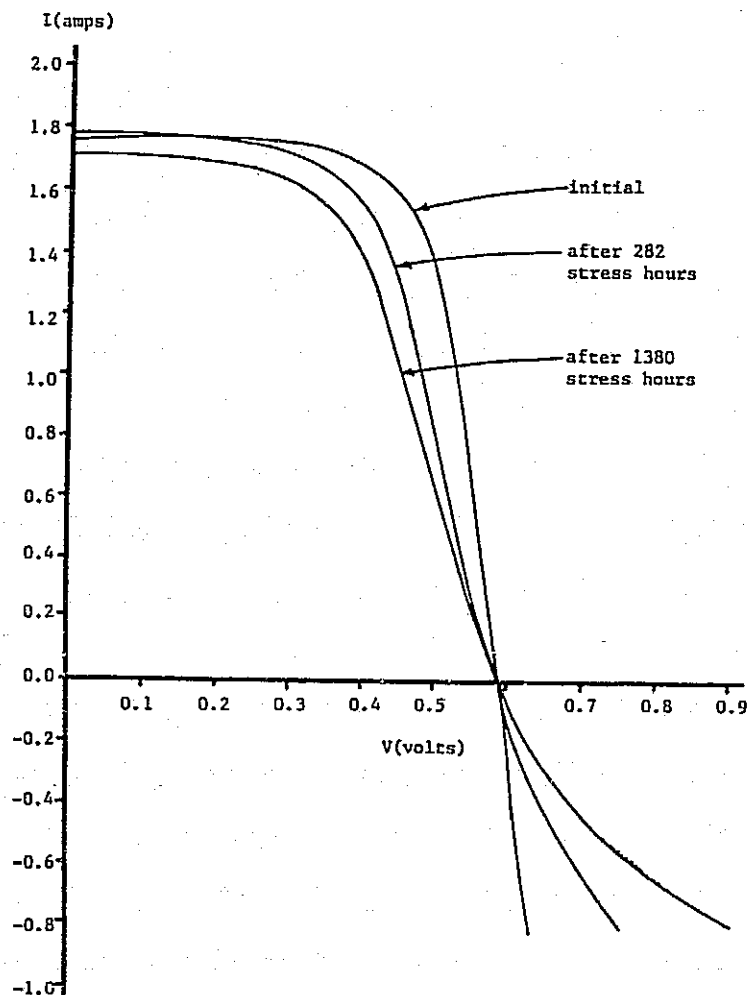
HFG = Coupons fabricated by cell manufacturer

TBS = To be started

G = glass, T = Tedlar, F = foil, S = steel, SR = Silicone Rubber

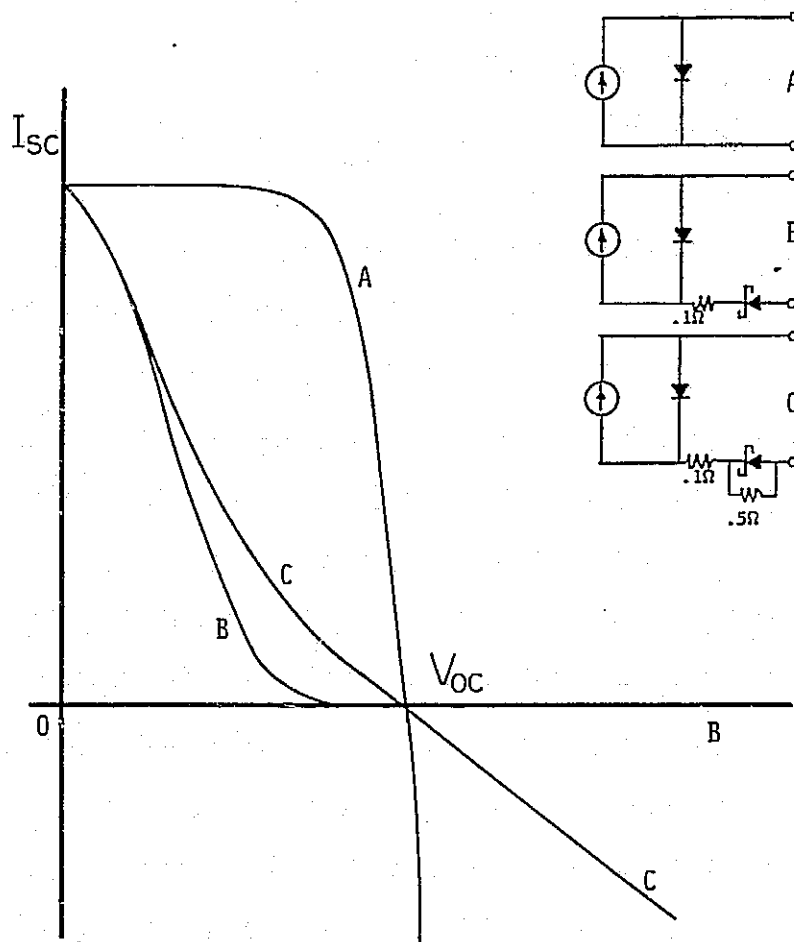
\* = all leads off after 1000 hours

# I-V Characteristics for a Typical $p^+n$ Solar Cell

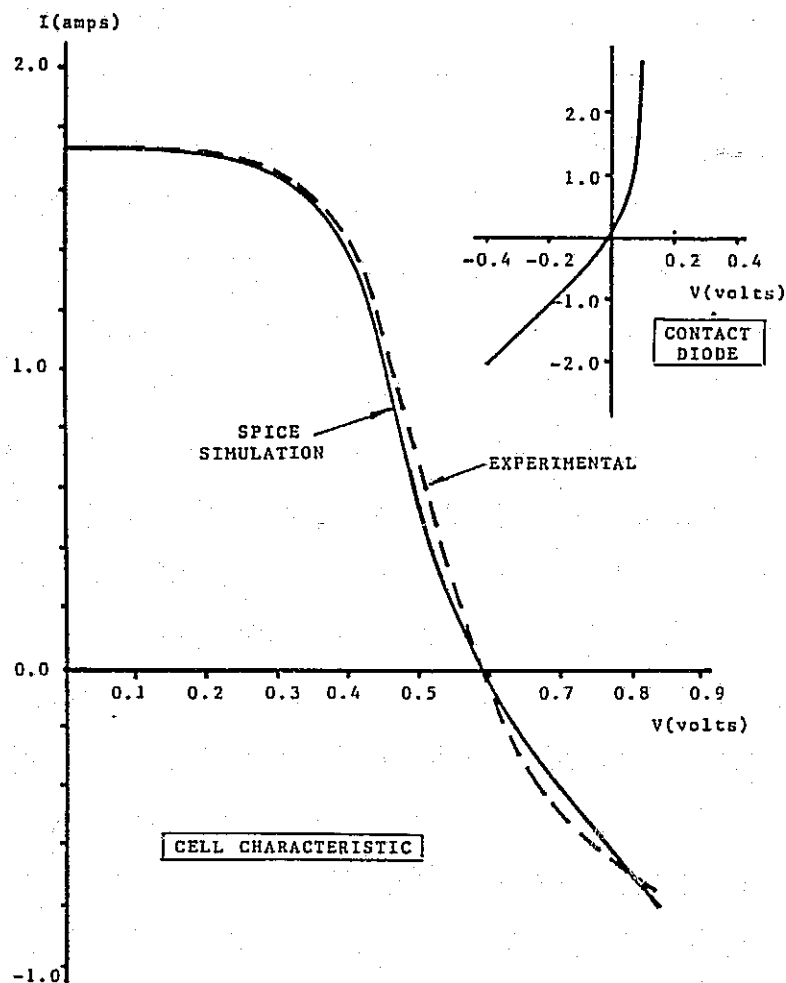


IV CHARACTERISTICS FOR A TYPICAL  $p^+n$  SOLAR CELL  
HAVING Au-N-SOLDER CONTACTS SUBJECTED TO  $150^{\circ}\text{C}$   
BIAS TEMPERATURE STRESS

# Simulation of Nonlinear Contact Degradation



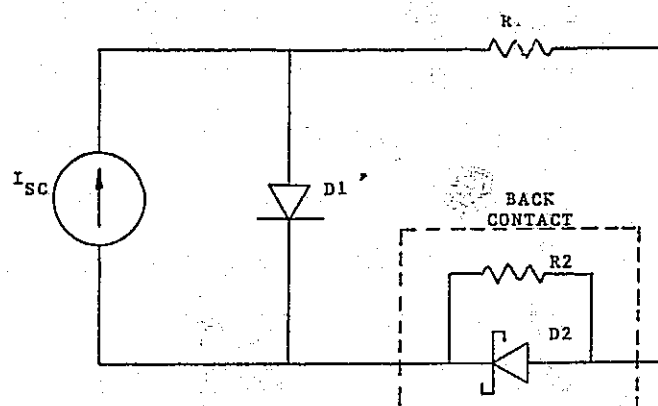
# I-V Characteristics of a Q-Cell



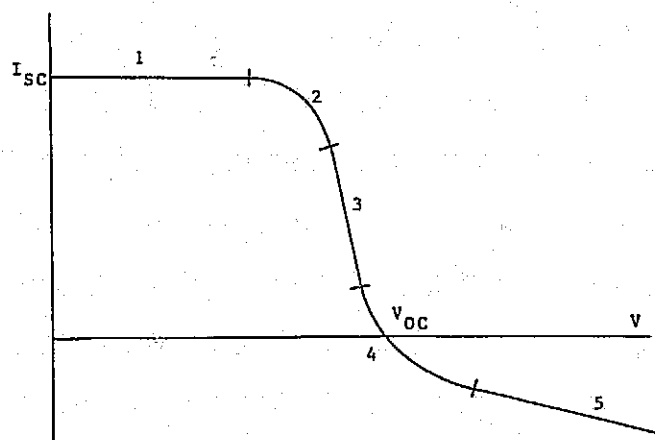
IV Characteristic of a Q-Cell After  
600 Hours at 150° as Fitted by SPICE  
Model Incorporating a Rectifying Circuit



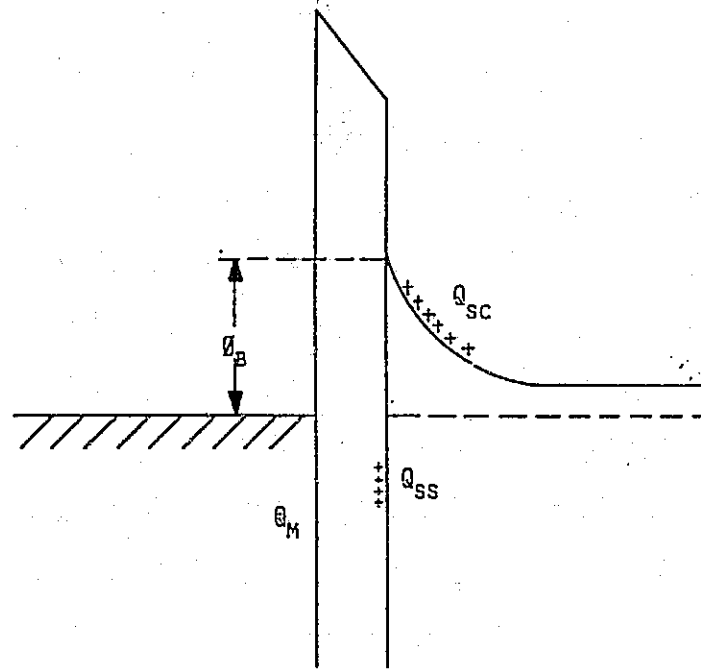
### Degraded-Cell Equivalent Circuit



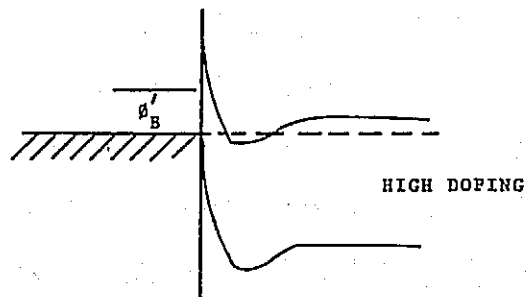
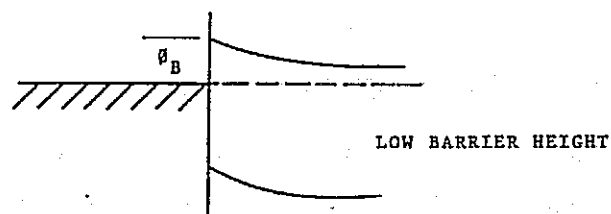
### Degraded-Cell I-V Characteristics



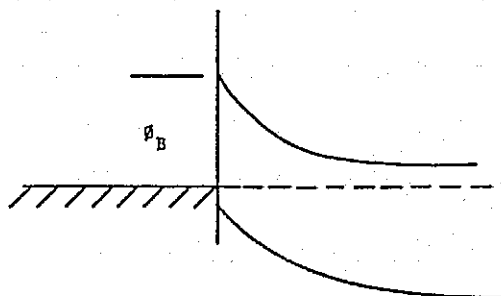
## Energy-Band With Thin Interfacial Layer Containing Positive Charge



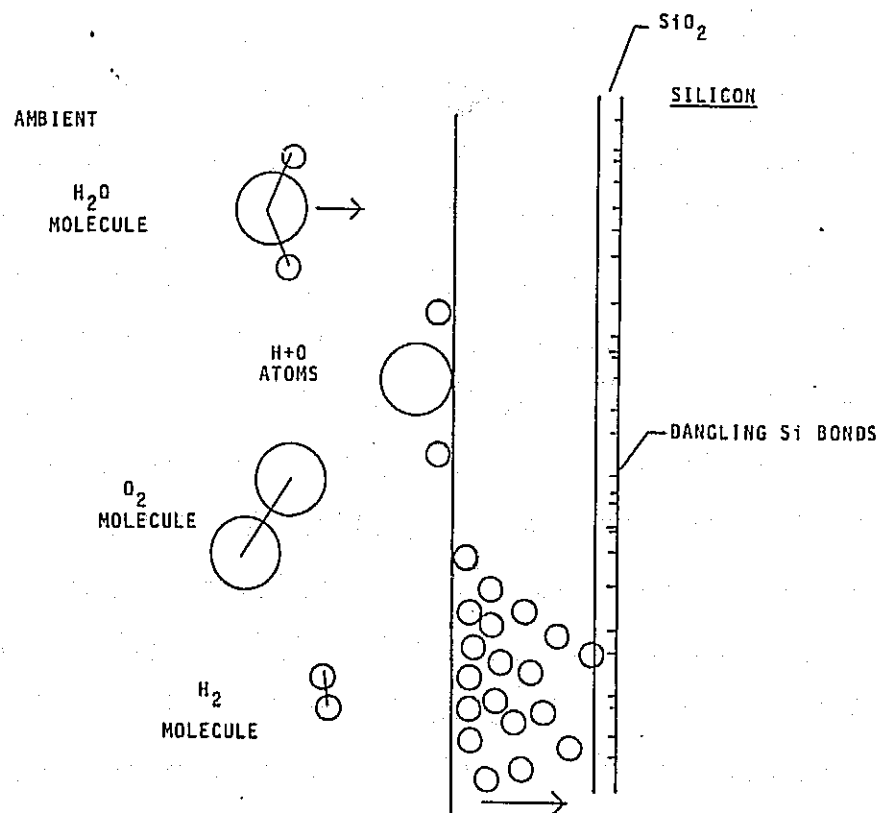
# Rectifying (Schottky) Contact Ohmic and Rectifying Barrier Configurations



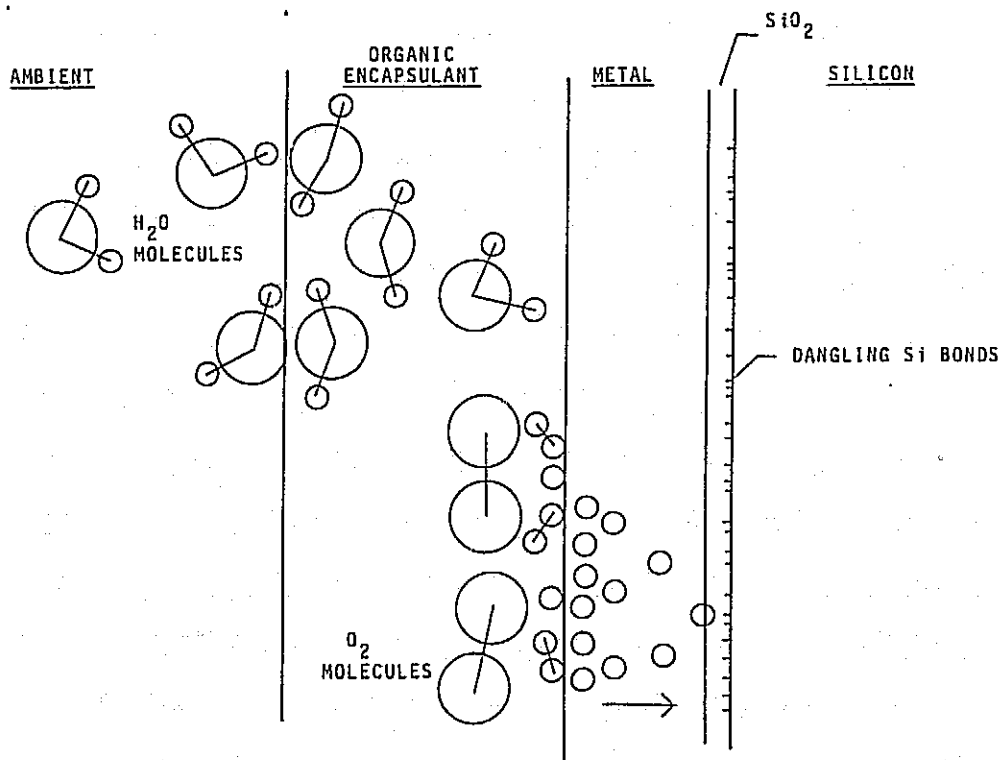
OHMIC CONTACT



# Atomic and Molecular Species at Unencapsulated Cell Surface



## Atomic and Molecular Species at Encapsulated Cell Surface



USE OF A LIGHTLY DOPED N-TYPE SILICON  
SUBSTRATE IS PRONE TO SCHOTTKY BARRIER  
CONTACT FORMATION AND SHOULD BE AVOIDED.

(Besides, a back surface field improves efficiency)

## MODULE TECHNOLOGY

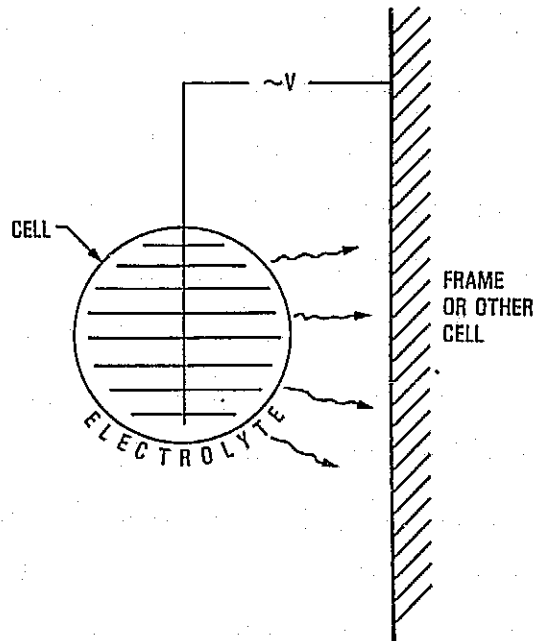
- A stable cell is a stable cell is a stable cell is a.....
- An unstable cell can be stabilized by use of a "proper" encapsulation system
- An unstable cell can be made more unstable by use of a "wrong" encapsulation system
- Metal foil does not provide an effective barrier against moisture related degradation

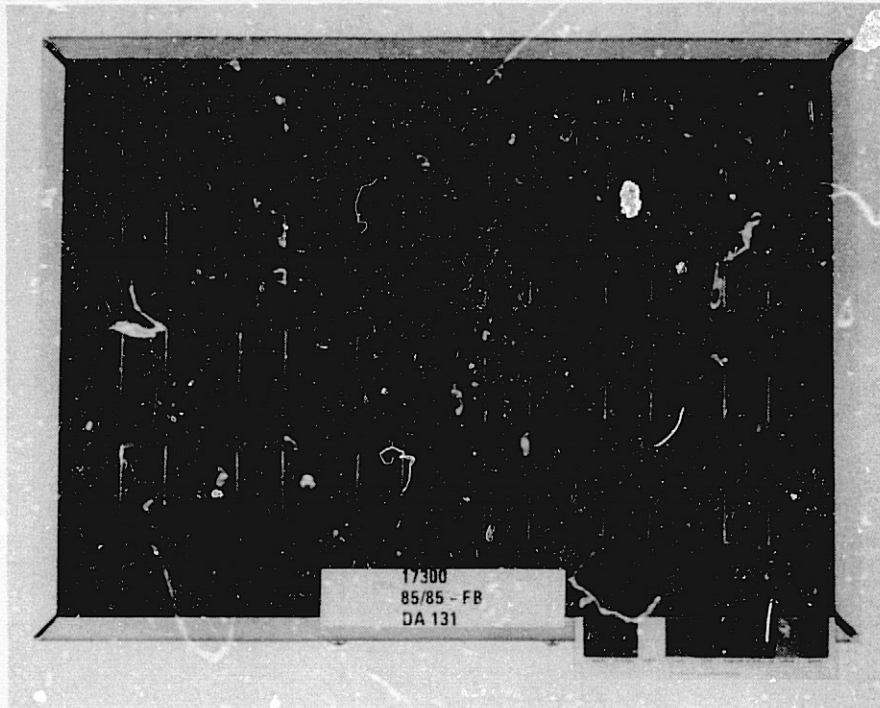
# SOLAR-CELL ELECTROCHEMICAL CORROSION

JET PROPULSION LABORATORY

G. R. Mon

## Corrosion Mechanism Overview





## Objectives

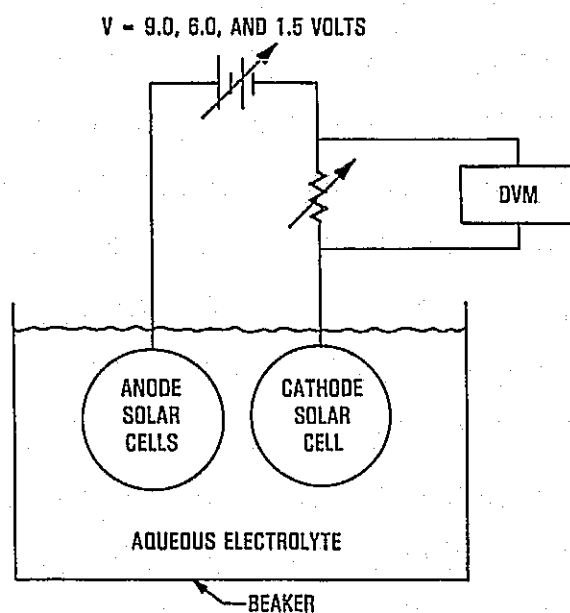
- Understand corrosion mechanisms contributing to module degradation
- Identify key rate dependencies
  - Environmental parameters
    - Temperature
    - Humidity
    - Applied voltage bias
  - Materials parameters
    - Encapsulants (electrolytic behavior)
    - Metallizations
    - AR coatings
    - Primers
- Develop techniques to eliminate or control potentially life-limiting mechanisms



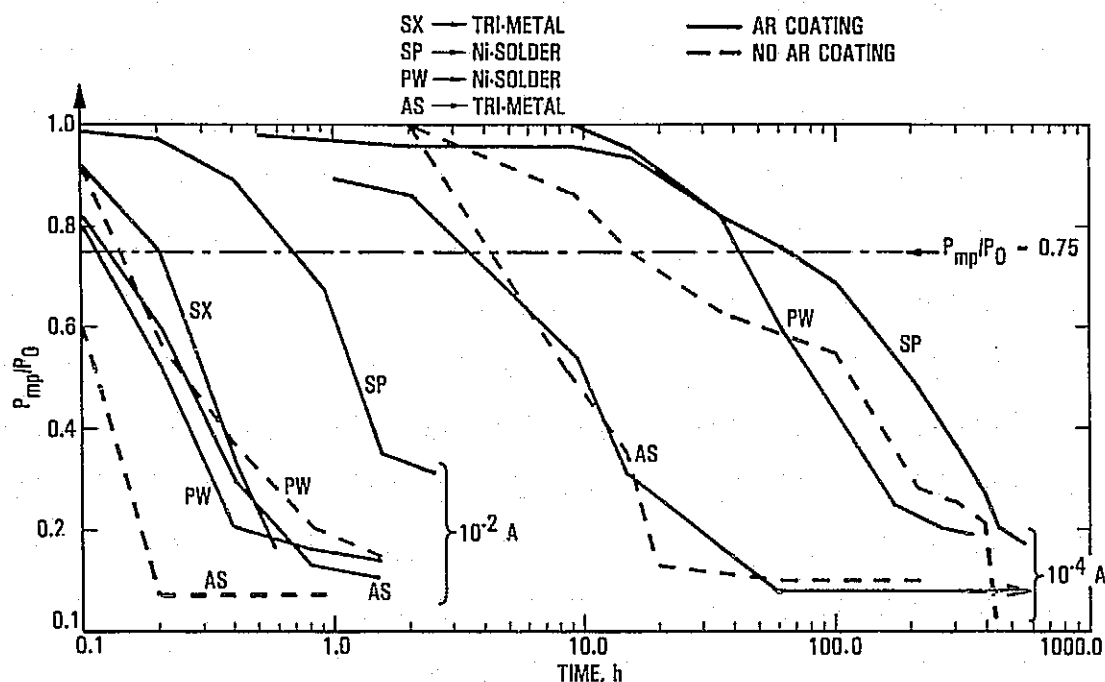
## Building the Corrosion Data Base

- Module temperature and humidity endurance testing (Wyle Laboratories)
- Cell temperature and humidity endurance testing (Clemson U.)
- In-house electrochemical corrosion characterization
  - Unencapsulated solar-cell electrode-electrolyte reactions
  - Encapsulated solar-cell electrode-electrolyte reactions
  - Module intercell and cell-frame reactions

### Experimental Arrangement for Accelerated Corrosion Testing of Unencapsulated Solar Cells



### Fraction of Maximum Power vs Exposure Time at Current Levels Indicated ( $[H^+] = 10^{-4}$ Molar)



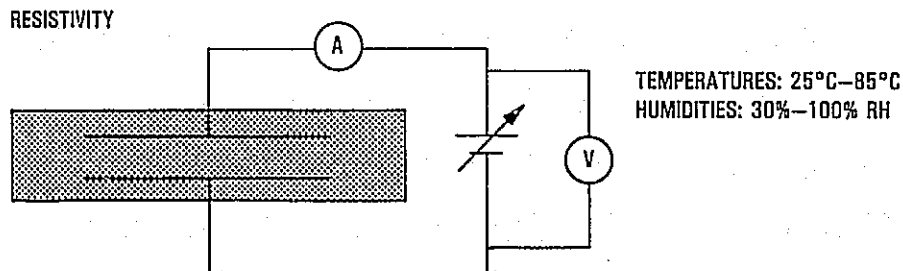
### Conclusions

- Electrode-electrolyte reactions are an important cell metallization corrosion mechanism
- For a fixed corrosion current density, the time to 25% power reduction is an order of magnitude greater for SP cells (Ni-solder metallization) than for SX cells (tri-metal)
- For unencapsulated solar cell electrodes, AR coatings apparently afford little protection against electrolytic corrosion
- The time to achieve a particular power reduction level is inversely proportional to the corrosion current density, as expected.

## Investigation of Physical Properties of EVA, PVB, and RTV Encapsulants

**Resistivity as a function of temperature, humidity, composition, and time of exposure**

### Experimental Setup



### Remarks

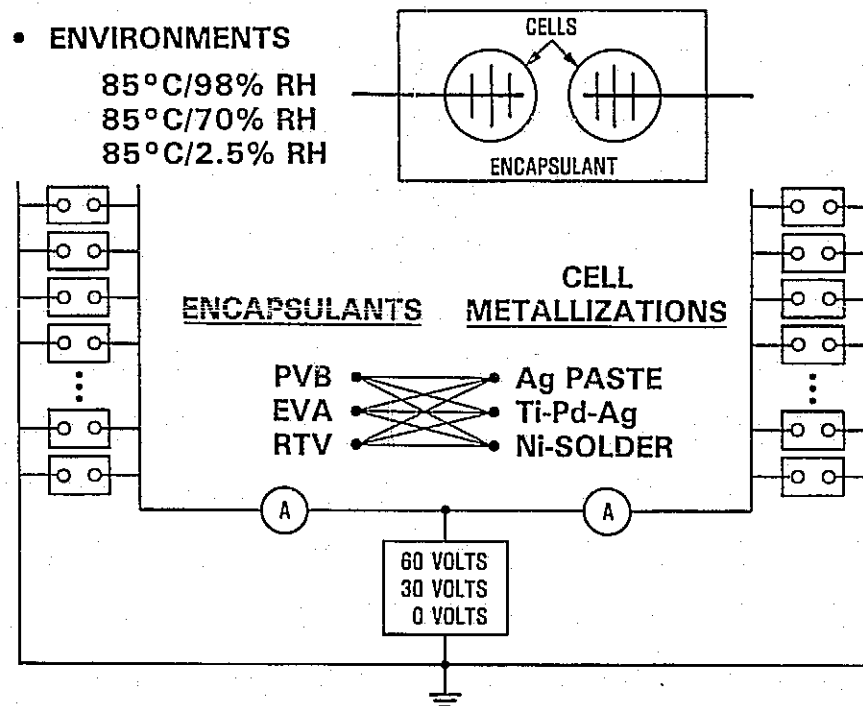
- The resistivities of both PVB and EVA exhibit similar response to temperature, decreasing two orders of magnitude over the range 25°C–85°C
- The resistivity of EVA is approximately constant, while that of PVB changes by two orders of magnitude over the relative humidity range 30%–100%
- At elevated temperature and humidity there is a difference in the resistivities of EVA and PVB of as much as five orders of magnitude

## Intercell and Cell-Frame Corrosion Experiment

- Develop correlations between measured changes in cell and/or pottant property values and observed corrosion
- Develop circuitry and instrumentation to monitor corrosion in situ
- Develop automated measurements capability for accelerated medium-term module reliability research

• ENVIRONMENTS

85°C/98% RH  
85°C/70% RH  
85°C/2.5% RH



## Variables Monitored in Corrosion Experiment

### ■ Light I-V curves (pre-test and post-test)

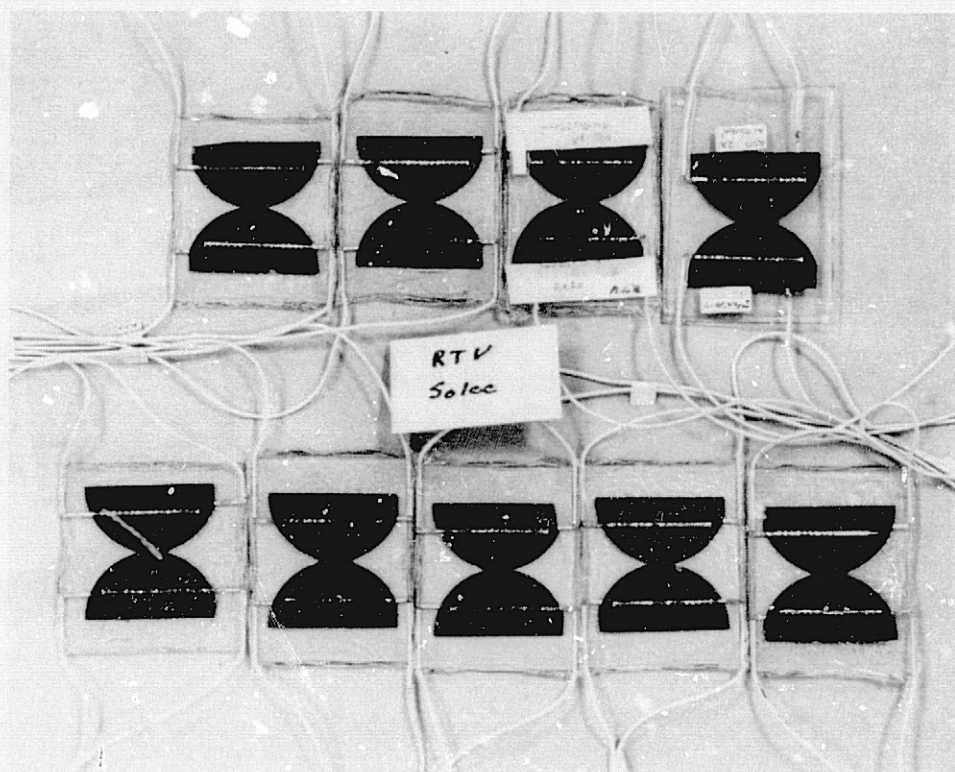
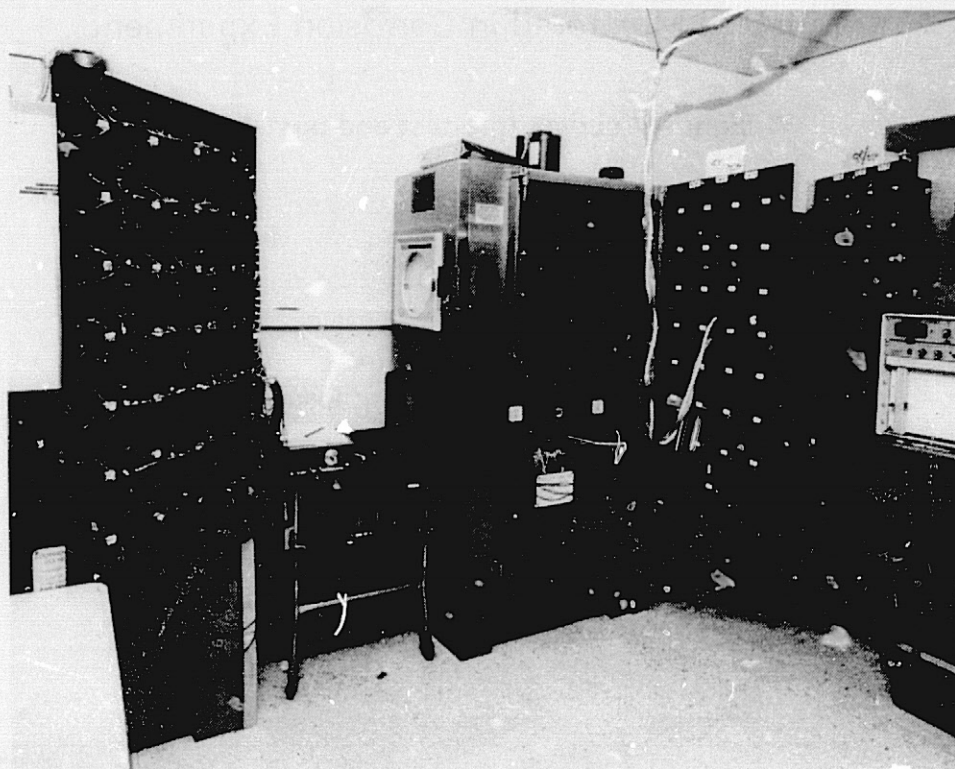
### ■ In situ

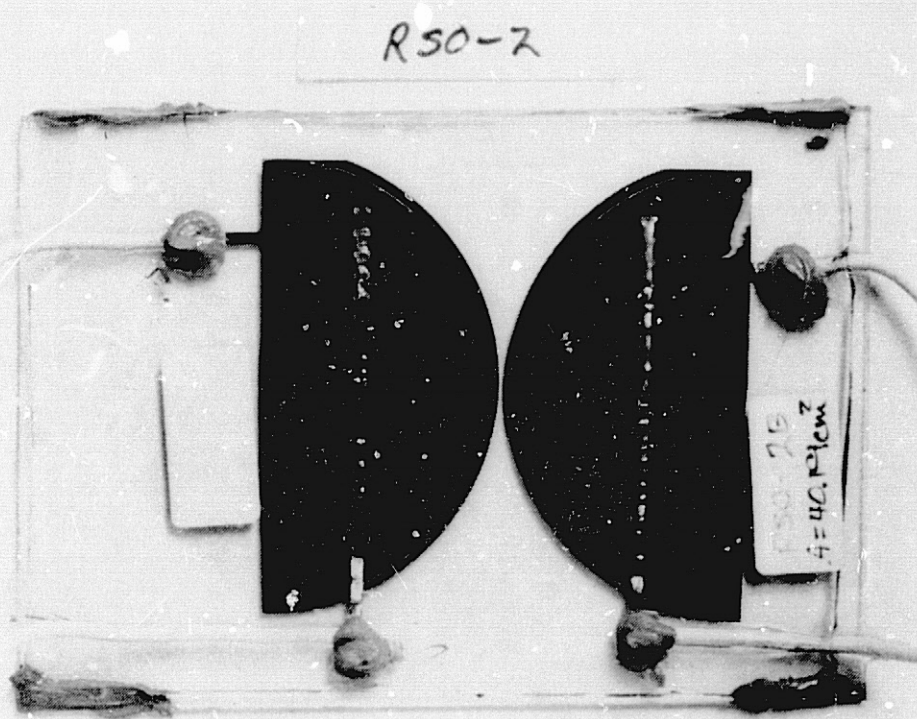
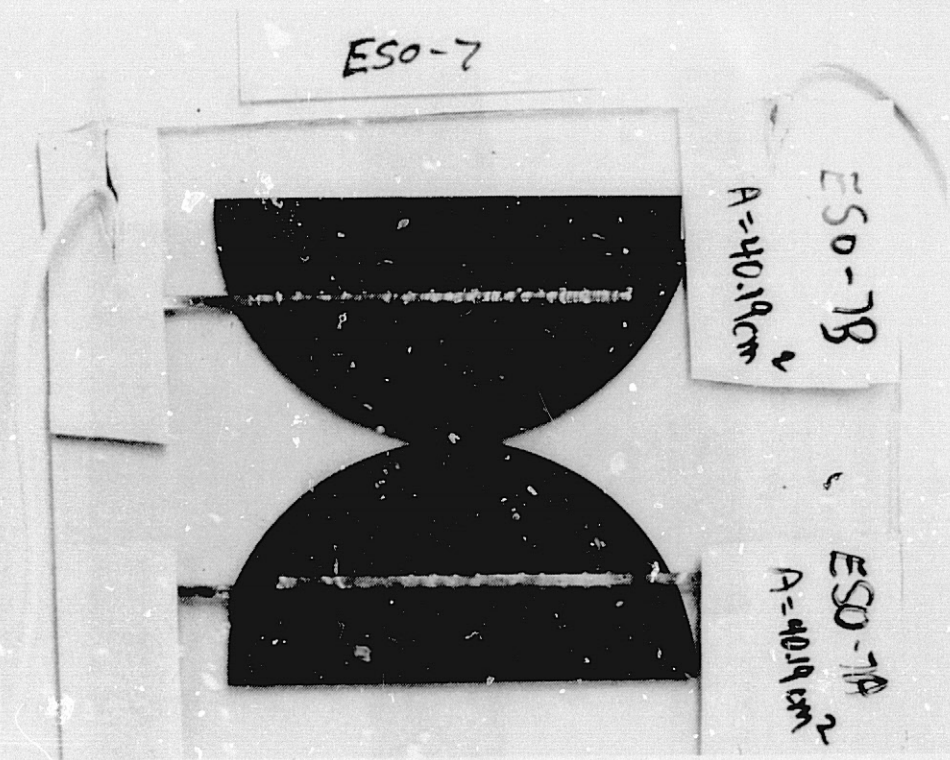
- Series resistance  $R_S$
- Shunt resistance  $R_{SH}$
- Junction capacitance  $C_J$ ; loss factor  $D_J$
- Insulation resistance  $R_I$
- Insulation capacitance  $C_I$ ; loss factor  $D_I$
- Dc discharge inception voltage DIV



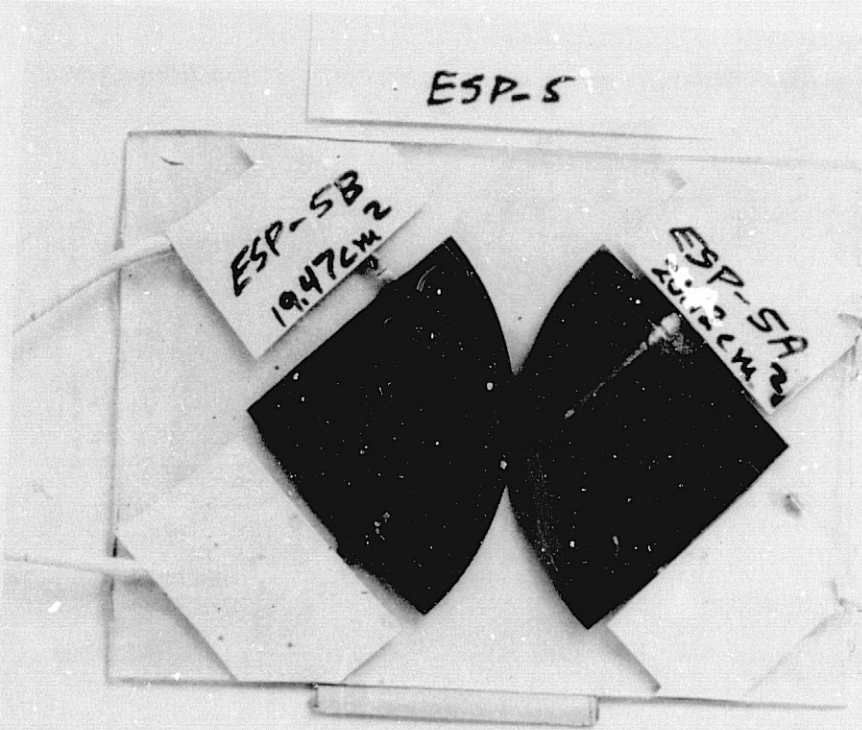


# MODULE TECHNOLOGY



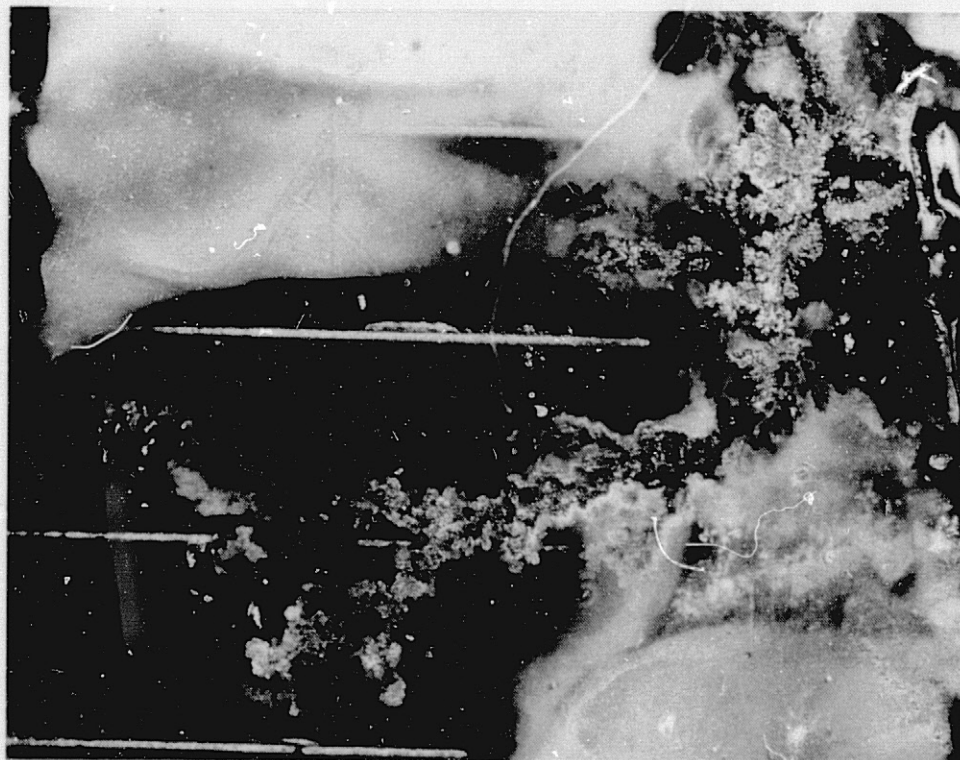
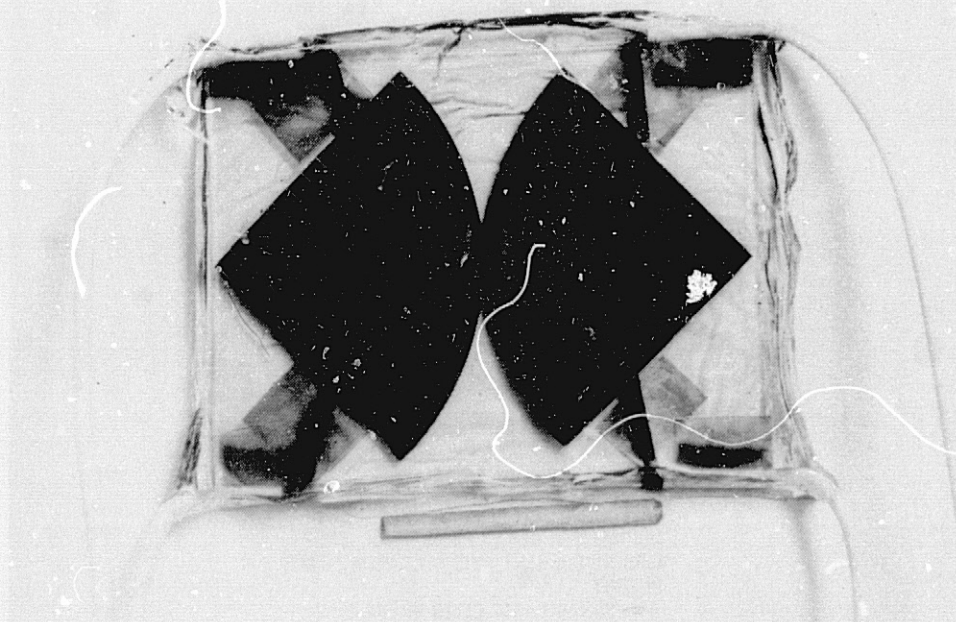




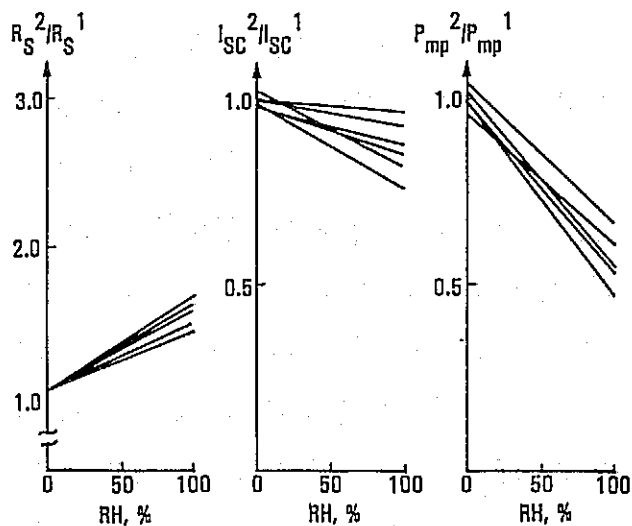




RSP-3

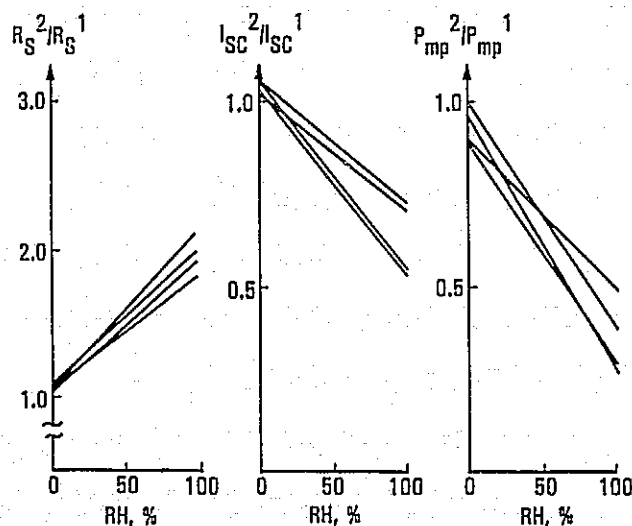


# Light I-V Curve Data



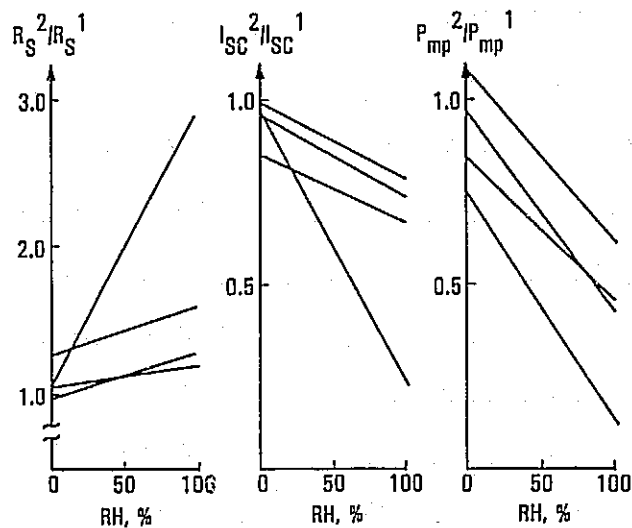
DEPENDENCE ON RELATIVE HUMIDITY OF  
NORMALIZED SERIES RESISTANCE, SHORT  
CIRCUIT CURRENT, AND MAXIMUM POWER  
OUTPUT

→ SILVER PASTE CELLS IN EVA  
AFTER 1944 h EXPOSURE

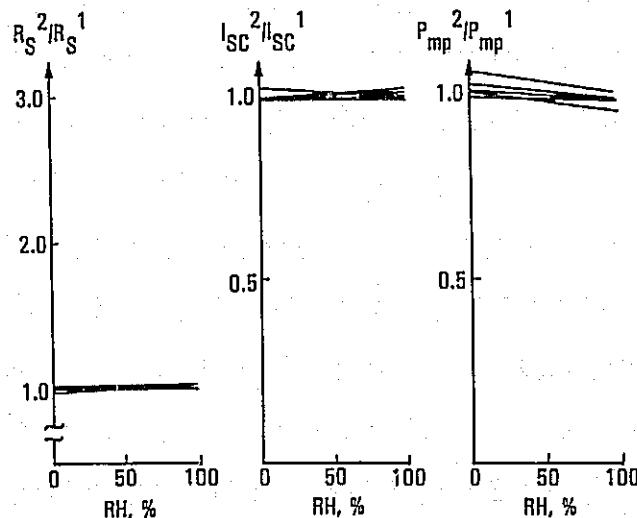


DEPENDENCE ON RELATIVE HUMIDITY OF  
NORMALIZED SERIES RESISTANCE, SHORT  
CIRCUIT CURRENT, AND MAXIMUM POWER  
OUTPUT

→ SILVER PASTE CELLS IN RTV  
AFTER 1944 h EXPOSURE

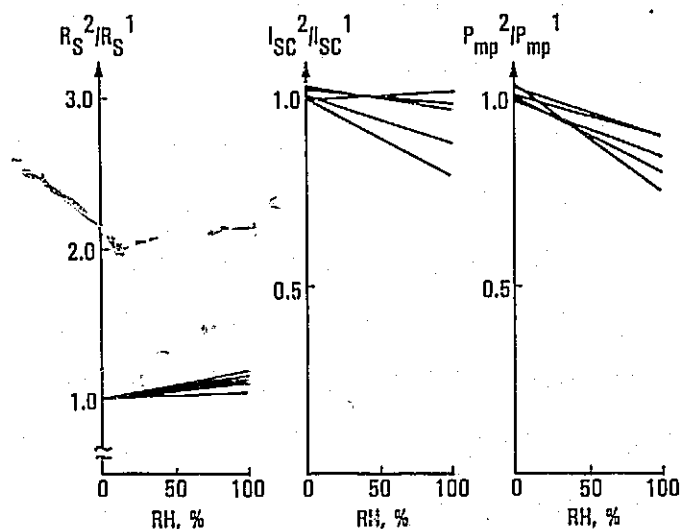


DEPENDENCE ON RELATIVE HUMIDITY OF  
NORMALIZED SERIES RESISTANCE, SHORT  
CIRCUIT CURRENT, AND MAXIMUM POWER  
OUTPUT  
→ SILVER PASTE CELLS IN PVB  
AFTER 1944 h EXPOSURE



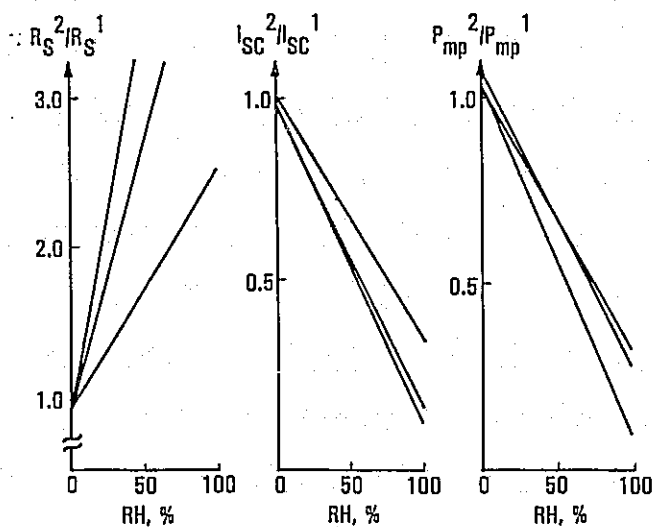
DEPENDENCE ON RELATIVE HUMIDITY OF  
NORMALIZED SERIES RESISTANCE, SHORT  
CIRCUIT CURRENT, AND MAXIMUM POWER  
OUTPUT  
→ Ni-SOLDER CELLS IN EVA  
AFTER 1944 h EXPOSURE

# MODULE TECHNOLOGY



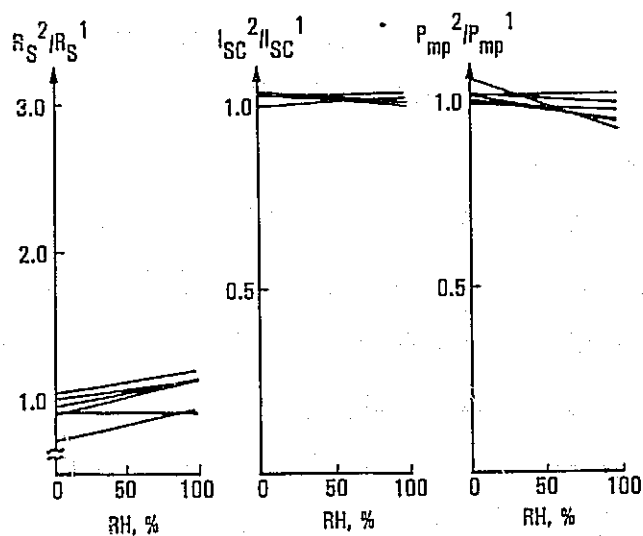
DEPENDENCE ON RELATIVE HUMIDITY OF  
NORMALIZED SERIES RESISTANCE, SHORT  
CIRCUIT CURRENT, AND MAXIMUM POWER  
OUTPUT

→ Ni-SOLDER CELLS IN RTV  
AFTER 1944 h EXPOSURE



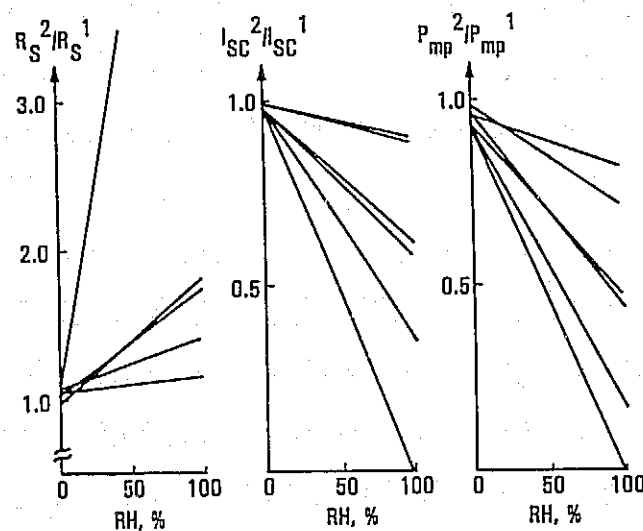
DEPENDENCE ON RELATIVE HUMIDITY OF  
NORMALIZED SERIES RESISTANCE, SHORT  
CIRCUIT CURRENT, AND MAXIMUM POWER  
OUTPUT

→ Ni-SOLDER CELLS IN PVB  
AFTER 1944 h EXPOSURE



DEPENDENCE ON RELATIVE HUMIDITY OF  
NORMALIZED SERIES RESISTANCE, SHORT  
CIRCUIT CURRENT, AND MAXIMUM POWER  
OUTPUT

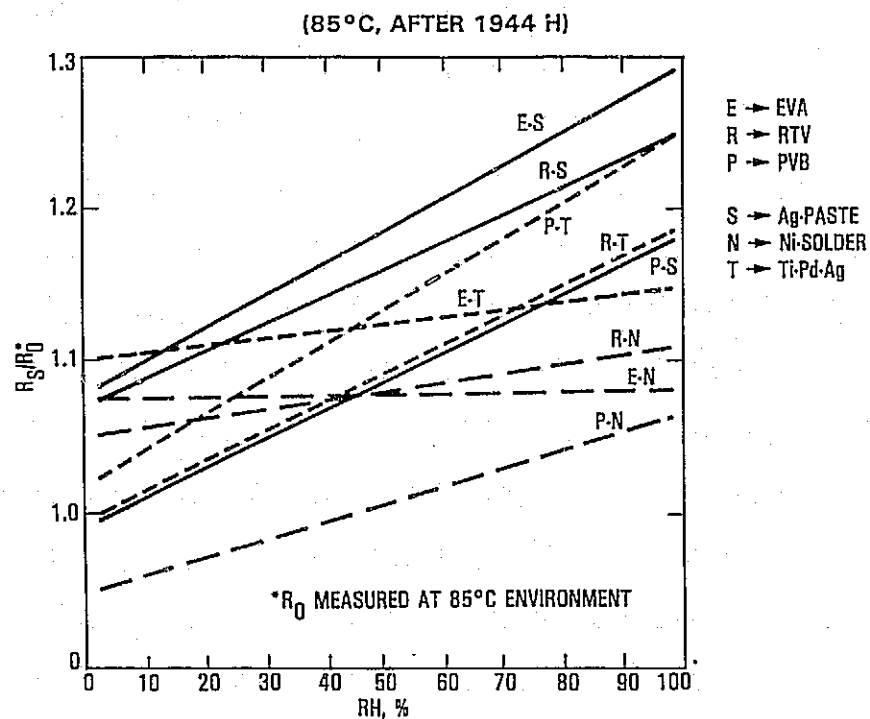
→ TRI-METAL CELLS IN EVA  
AFTER 1944 h EXPOSURE



DEPENDENCE ON RELATIVE HUMIDITY OF  
NORMALIZED SERIES RESISTANCE, SHORT  
CIRCUIT CURRENT, AND MAXIMUM POWER  
OUTPUT

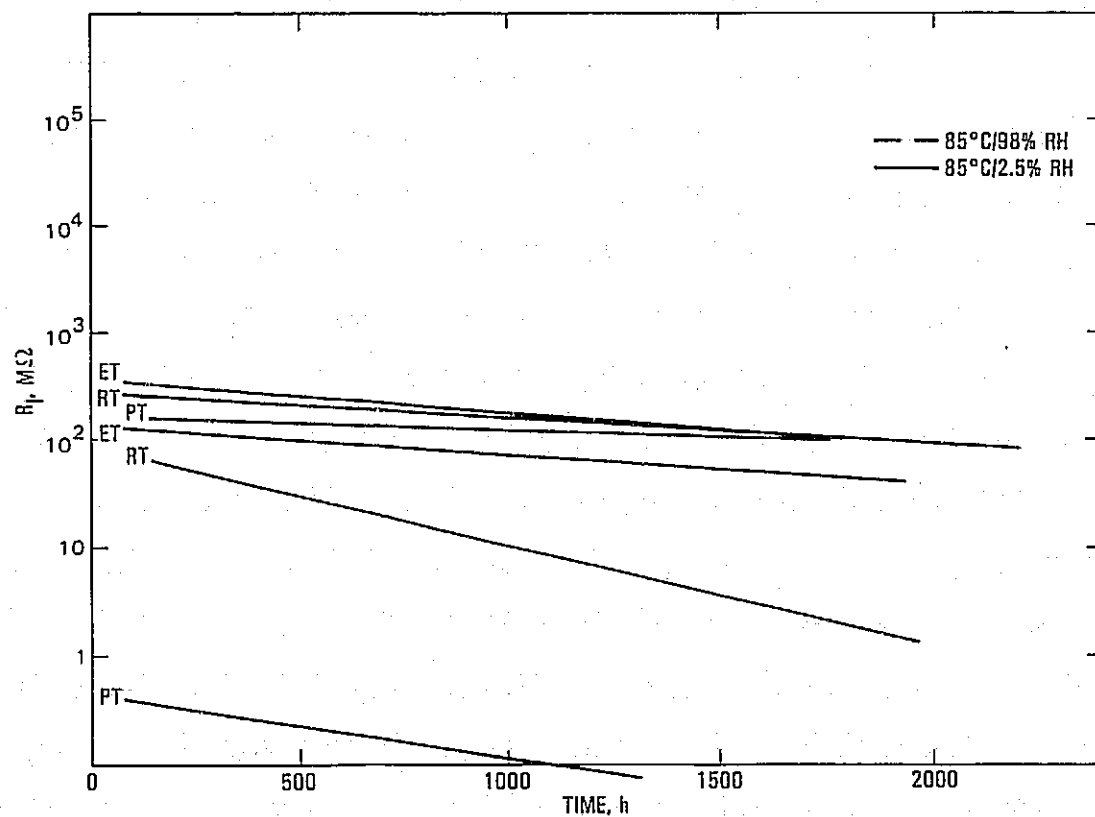
→ TRI-METAL CELLS IN PVB  
AFTER 1944 h EXPOSURE

## Normalized Series Resistance vs Relative Humidity



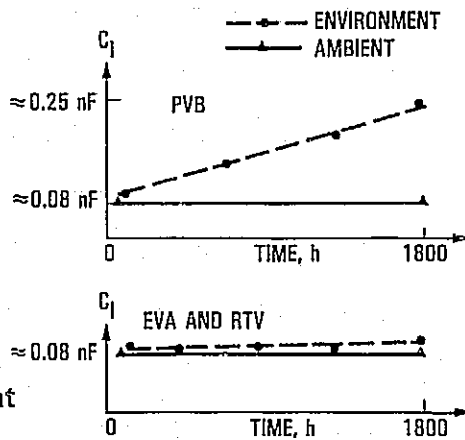
## Insulation Resistance vs Time

Ti-Pd-Ag CONTROL (0 VOLT) SAMPLES



## Insulation Capacitance Data (General)

- Pre-test and post-test insulation capacitance measurements are about the same
- Insulation capacitance increases in value when exposed to environment
- Insulation capacitance increases with time of exposure at a rate dependent on the amount of absorption of water ( $\epsilon \approx 75$ )



## Summary

## Controlling corrosion in photovoltaic modules

- Use polymer encapsulants featuring low moisture absorption and high resistivity at working environments
- PVB, EVA, RTV performance is comparable in dry environments, but if used in moist environments, PVB should be provided adequate protection such as thin metal-film moisture barriers
- Use of silver-paste metallizations should be limited to low-moisture environments
- In high-moisture-level environments, use electrochemically passive metallizations such as Ti-Pd-Ag and Ni-solder



## Controlling Corrosion in Photovoltaic Modules

- **Anodic passivation**

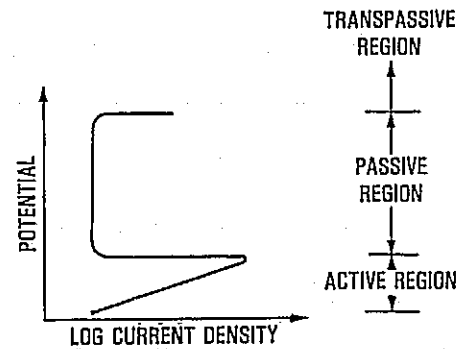
Use electrochemically passive metallizations at working environments; this may require coating the cell or adding inhibitors to the metallization or the encapsulant

- **Cathodic passivation**

Reduce the rate at which oxygen reacts at the cathode ( $\text{H}_2\text{O} + \frac{1}{2}\text{O}_2 + 2\text{e}^- \rightarrow 2\text{OH}^-$ ); this may require cell coatings, encapsulant additives, or the use of foil oxygen barriers

- **Anode-to-cathode conductance**

Use high-resistivity, low-moisture-absorbing encapsulants or foil moisture barriers



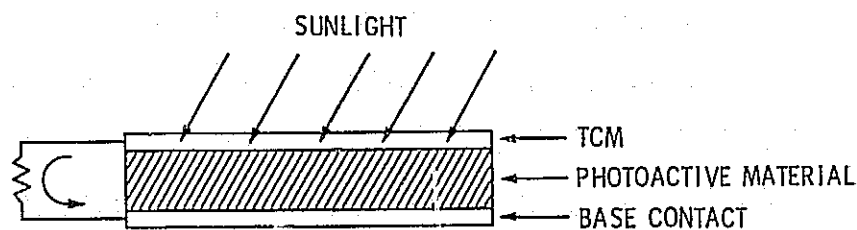
# TRANSPARENT CONDUCTING MATERIALS OVERVIEW

JET PROPULSION LABORATORY

D.R. Coulter

- APPLICATION - UTILIZE ORGANIC/INORGANIC CONDUCTORS TO REPLACE METALS/SEMI-METALS AS CHARGE COLLECTORS AND CONDUCTORS IN PV DEVICES
- GOAL - DEVELOP OPTIMIZED MATERIALS/STRUCTURES TO ACHIEVE A COMBINATION OF TRANSPARENCY AND CONDUCTIVITY CONSISTENT WITH PV PERFORMANCE REQUIREMENTS


## TCM PV Device



- SINGLE CRYSTAL CELLS
- POLYCRYSTALLINE CELLS
- AMORPHOUS CELLS
- THIN FILM DEVICES
- OTHERS

## Organic Conductors

POLYACETYLENE (  $\text{-CH-}$  )

POLYPYRROLE (  )

POLYTHIOPHENE (  )

POLYFURAN (  )

POLY-P-PHENYLENE (  )

### COUNTERIONS (DOPANTS)

$\text{BF}_4^-$

$\text{AsF}_6^-$

$\text{I}_3^-$

Na-POLYSTYRENESULFONATE

POLYSTYRENESULFONIC ACID

POLY-2-ACRYLAMIDO-2-METHYL-1-PROPANESULFONIC ACID

## TCM Program Concerns

- TRADE OFF BETWEEN ELECTRICAL CONDUCTIVITY AND OPTICAL TRANSMISSION
- REFLECTION LOSSES DUE TO INDEX OF REFRACTION MISMATCH WITH PV MODULE MATERIALS
- ELECTRICAL CONTACT (OHMIC, SCHOTTKY)
- EFFECTS OF DOPANTS
- ENVIRONMENTAL STABILITY
- BONDING
- PROCESSABILITY
- COMPATIBILITY WITH PV MODULE MATERIALS/STRUCTURES
- COST

## TCM Task Plan

MATERIALS TASK

PHYSICAL PROPERTY MODELING TASK

ENGINEERING MODELING TASK

PROCESSING TASK

INTERFACIAL SCIENCE TASK

ENVIRONMENTAL DURABILITY TASK

MECHANICAL PROPERTIES TASK

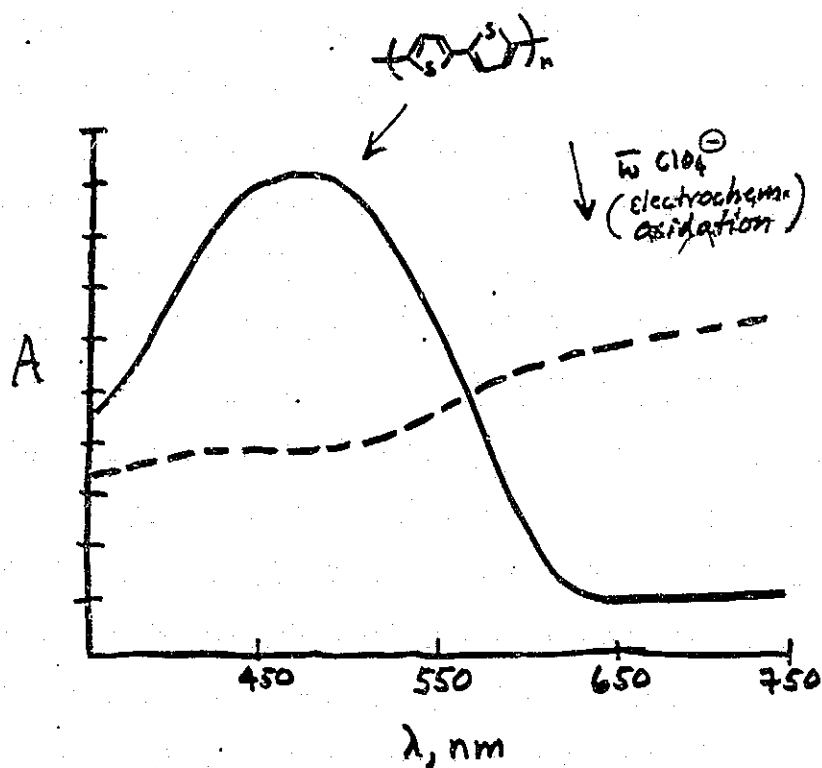
## TCM Summary

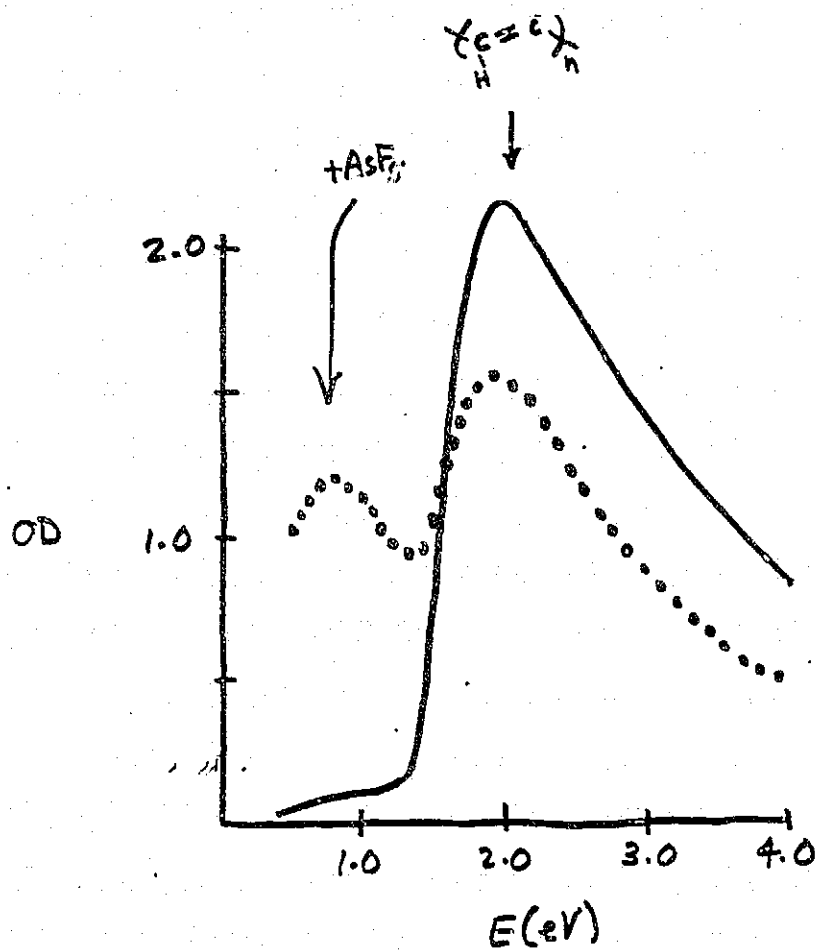
- OBJECTIVE - DEVELOP ORGANIC/INORGANIC CONDUCTORS FOR REPLACEMENT OF METALS/SEMI-METALS AS CHARGE COLLECTORS AND CONDUCTORS IN PV DEVICES
- PARTICIPANTS - JPL, SPRINGBORN, SPECTROLAB, MIT, ROCKWELL
- ACCOMPLISHMENTS
  - IDENTIFICATION OF CANDIDATE ORGANIC CONDUCTORS
  - DEPOSITION OF POLYACETYLENE AND POLYPYRROLE ON SOLAR CELLS
  - PRELIMINARY I-V MEASUREMENTS ON COATED CELLS
  - INITIATION OF MODELING OF OPTICAL/ELECTRICAL PROPERTIES

# TCM TECHNOLOGIES AND PERFORMANCE

MASSACHUSETTS INSTITUTE OF TECHNOLOGY

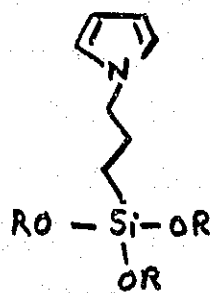
Gary Wnek





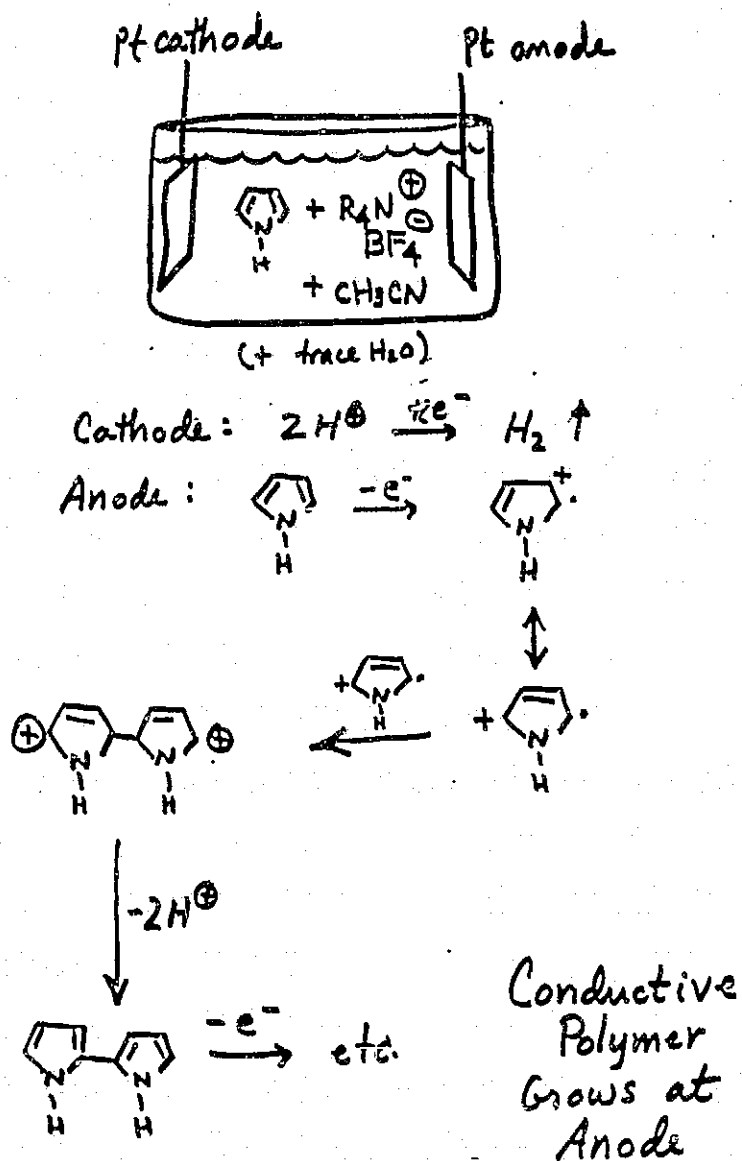
Coupling Agents Can Be Used

e.g.,

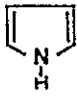


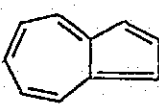
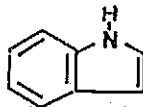


Wrighton et al., MIT

## Electrochemical Deposition



## Electrical Conductivity of Various Materials

ITO		Conductivity	$1000 \Omega^{-1} \text{cm}^{-1}$
Monomer	Structure	Conductivity of doped polymer	
PYRROLE		100-200	(Counter ion $\text{ClO}_4^-$ )
THIOPHENE		10-100	
FURAN		$10^{-2}$ -80	
AZULENE		$10^{-3}$ - $10^{-1}$	
INDOLE		$5 \cdot 10^{-3}$ - $10^{-2}$	

## Polypyrrole Counterions

ANION	CONDUCTIVITY (25 °C), $\Omega^{-1} \text{cm}^{-1}$
$\text{BF}_4^-$	30 - 100
$\text{PF}_6^-$	100
$\text{AsF}_6^-$	100
$\text{ClO}_4^-$	100-200
$\text{HSO}_4^-$	0.3
$\text{CF}_3\text{SO}_3^-$	0.3 - 1
$\text{CH}_3\text{C}_6\text{H}_4\text{SO}_3^-$	20 - 100
$\text{CF}_3\text{COO}^-$	12
$\text{HC}_2\text{O}_4^-$	$10^{-3}$ - $10^{-2}$



## Objective

Assess optical properties (particularly absorption coefficient and refractive index) of candidate conductive polymers

## Requirements

- acceptable transparency (thin films)
- low  $E_{ox}$  (environmental stability)
- $\sigma \geq 100 \Omega^{-1}cm^{-1}$
- acceptable adhesion to substrates

# ORGANIC CONDUCTING POLYMERS: INTERACTIVE MODELING

JPL CONSULTANT

G.F.J. Garlick

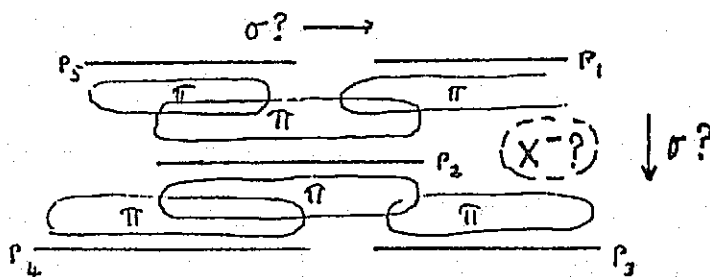
## 1. REVIEW OF BASIC QUANTUM MECHANICAL MODELS

- a) Prominent workers: Heeger, Schrieffer and Su (U.Penn.)  
Bredas and Baughman (Belg. and Allied Corp)
- b) Linear energy band model: gives polymer ionization potential, electron band width and 'semiconductor' band gap. Soliton theory and dopant energy states.
- c) Deficiencies: conflicts with facts e.g. for polypyrroles compared to success with polyacetylene. Does not give inter-polymer transfer process, barrier effects etc. Does not aid in answering the 'big' question: Is high conductivity compatible with low absorption in organic polymer films?

## 2. INTERACTIVE MODELLING

Review existing facts and suggest experiments which discriminate between effects e.g. types of optical absorption, conditions in conduction set by bulk poly chain or barriers between chains. Feed back data to further refine the analysis and finally make conclusions on the 'big' question.

### (Too) Simple Conduction Model



## "Conflict of Interest" Physics

A. ELECTRICAL CONDUCTIVITY

$$\sigma = p e \mu_p \quad \text{--- --- --- 1.}$$

$\sigma$  = CONDUCTIVITY,  $p$  = HOLE CONCENTRATION

$e$  = ELECTRONIC CHARGE,  $\mu_p$  = HOLE MOBILITY

B. OPTICAL ABSORPTION OF FREE CARRIERS

$$\alpha_F = \frac{\lambda^2 g e^3}{4\pi E_0 \epsilon c^3} \left( \frac{p}{m_p^2 \mu_p} \right) \quad \text{--- --- --- 2.}$$

$\alpha_F$  = ABSORPTION COEFFT.  $g \approx 1$ ,  $e$  = ELECTRON CHARGE

$E_0$  = PERMITTIVITY FREE SPACE  $\epsilon$  = DIELECTRIC CONST (= REF. INDEX IN UV-VIS-NEAR I.R.  $c$  = VEL. LIGHT.

$m_p$  = HOLE EFFECTIVE MASS.

C. OPTICAL TRANSITIONS AND ABSORPTION

ABSORPTION DEPENDS ON BAND STRUCTURE, DEEP LEVELS ETC. ASSUME  $\alpha_0 = f(\lambda)$

D. OPTIMUM PERFORMANCE  $\sigma/\alpha_{\text{TOT}}$ 

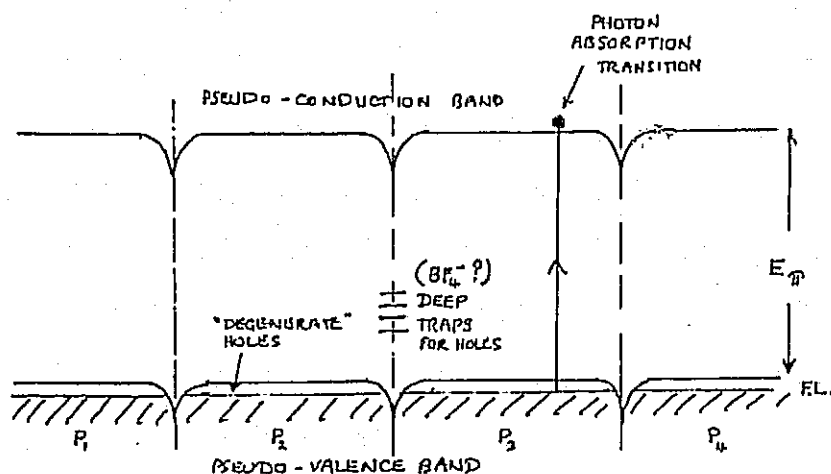
$\sigma$  HIGH -  $\alpha$  LOW :-

$$\frac{\sigma}{\alpha_F} = C \mu^2 \quad \text{IF } \alpha_0 = 0$$

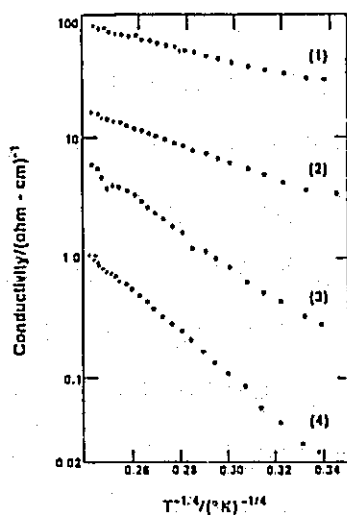
GENERALLY :-

$$\frac{\sigma}{\alpha_{\text{TOT}}} = \frac{p e \mu_p}{\left[ \lambda^2 a p / \mu_p + f(\lambda) \right]}$$

# The Carrier Transport Problem: What Do the Poly-Chain Boundaries Do?

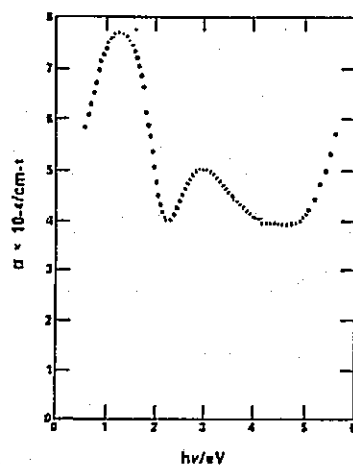


## Variation of Conductivity With Temperature

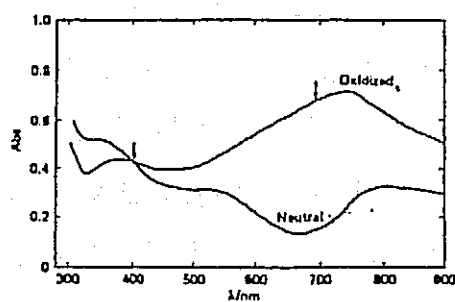


The variation of conductivity with temperature for four samples of poly(p-vinylcarbazole) having different conductivities (Ref. 1).  
 M.A. INDICATES A HOPPING MECHANISM BECAUSE OF  $T^{-1/4}$  DEPENDENCE

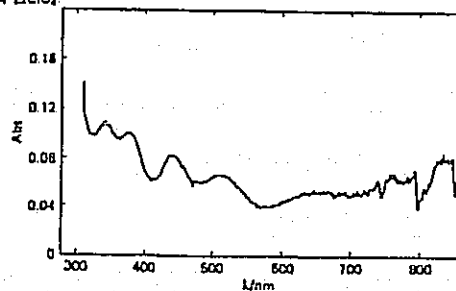
# Absorption Coefficient of Polypyrrole Tetrafluoroborate



The absorption coefficient of polypyrrole tetrafluoroborate (Ref. 3)

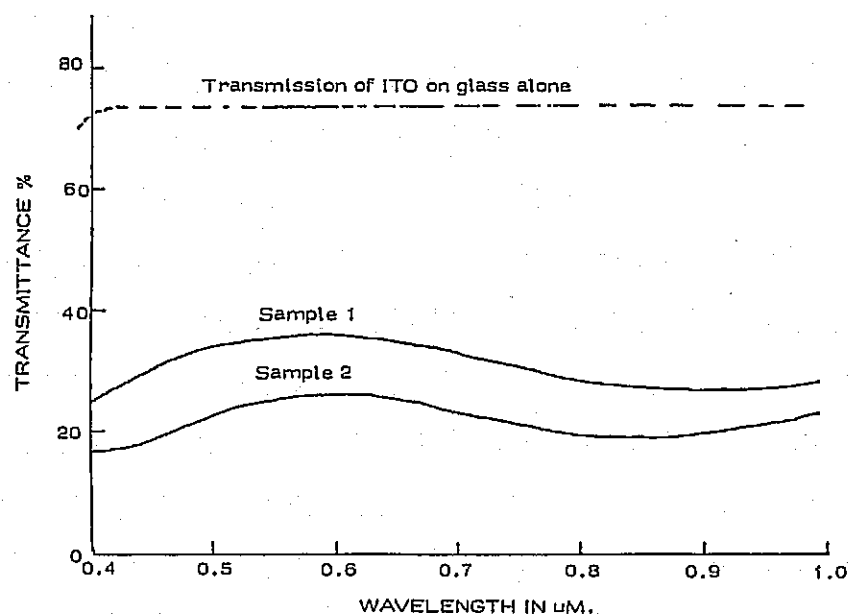


(a) Absorption spectra of polypyrrole film prepared on  $\text{I}_2/\text{O}_2$  by oxidizing (40 mC) pyrrole ( $5.7 \times 10^{-3} \text{ M}$ ) in acetonitrile containing  $0.1 \text{ M LiClO}_4$



(b) Average absorption spectra obtained during 500 combined potential step scans of a acetonitrile solution containing  $1.4 \times 10^{-3} \text{ M}$  pyrrole and  $0.1 \text{ M LiClO}_4$

# Transmission Spectra of Polypyrrole Films on ITO on Glass



# EXPERIMENTAL EVALUATION OF TCMs

SPECTROLAB, INC.

Alexander Garcia III

## Objectives

- MAKE FILMS WITH CONTROLLED CHARACTERISTICS
- ANALYSES UNDER CONTROLLED CONDITIONS
- INTERACTIVE MODELING
- FEASIBILITY PREDICTION

## Overall Plan

SET UP FOR ANODIC DEPOSITION

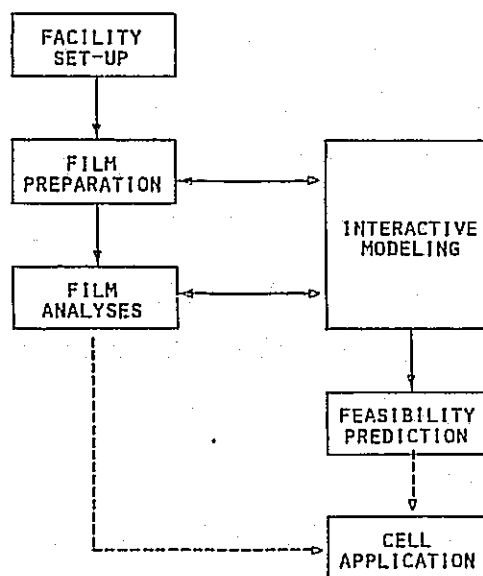
ADAPT EQUIPMENT FOR SPECIAL MEASUREMENTS

DETERMINE BEST OVERALL MODEL

DETERMINE FEASIBILITY FROM MODEL

APPLY MATERIAL TO CELLS

## Work Flow



## Experimental Setup for Film Deposition

- IBM EC/225 POLARGRAPHIC/VOLTAMMETRIC ANALYZER

- VOLTAMMETRY
- CYCLIC VOLTAMMETRY




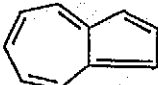
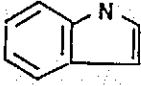
- ESC 680 DIGITAL COULOMETER



## Analytical Measurements

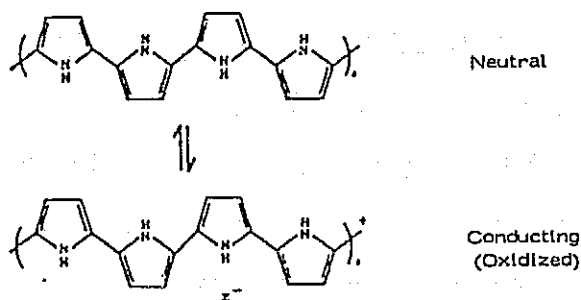
- 1) CYCLIC VOLTAMMETRY
- 2) CRYOGENIC MEASUREMENTS
  - A. ELECTRICAL
  - B. OPTICAL
- 3) SEM
- 4) RESISTANCE MEASUREMENTS 4-POINT/VAN DER PAUW
- 5) AC CONDUCTANCE/CAPACITANCE
- 6) IV DARK AND LIGHT
- 7) PHOTO-INJECTION
- 8) DISPERSION SPECTRUM

## Electrical Conductivity of Various Materials

ITO Monomer	Structure	Conductivity $1000 \Omega^{-1} \text{cm}^{-1}$ Conductivity of doped polymer
PYRROLE		30-100 (Counter ion $\text{ClO}_4^-$ )
THIOPHENE		10-100
FURAN		10-80
AZULENE		$10^{-3} - 10^{-1}$
INDOLE		$5 \cdot 10^{-3} - 10^{-2}$

## Conducting Organic Polymers

## CONDUCTING POLYMER FORMATION (Polypyrrole)



## Polypyrrole Counterions

ANION	CONDUCTIVITY (25 °C), $\Omega^{-1} \text{ cm}^{-1}$
$\text{BF}_4^-$	30 - 100
$\text{PF}_6^-$	100
$\text{AsF}_6^-$	100
$\text{ClO}_4^-$	100-200
$\text{HSO}_4^-$	0.3
$\text{CF}_3\text{SO}_3^-$	0.3 - 1
$\text{CH}_3\text{C}_6\text{H}_4\text{SO}_3^-$	20 - 100
$\text{CF}_3\text{COO}^-$	12
$\text{HC}_2\text{O}_4^-$	$10^{-3} - 10^{-2}$

# ENCAPSULATION DESIGN ANALYSIS

SPECTROLAB, INC.

Alexander Garcia III

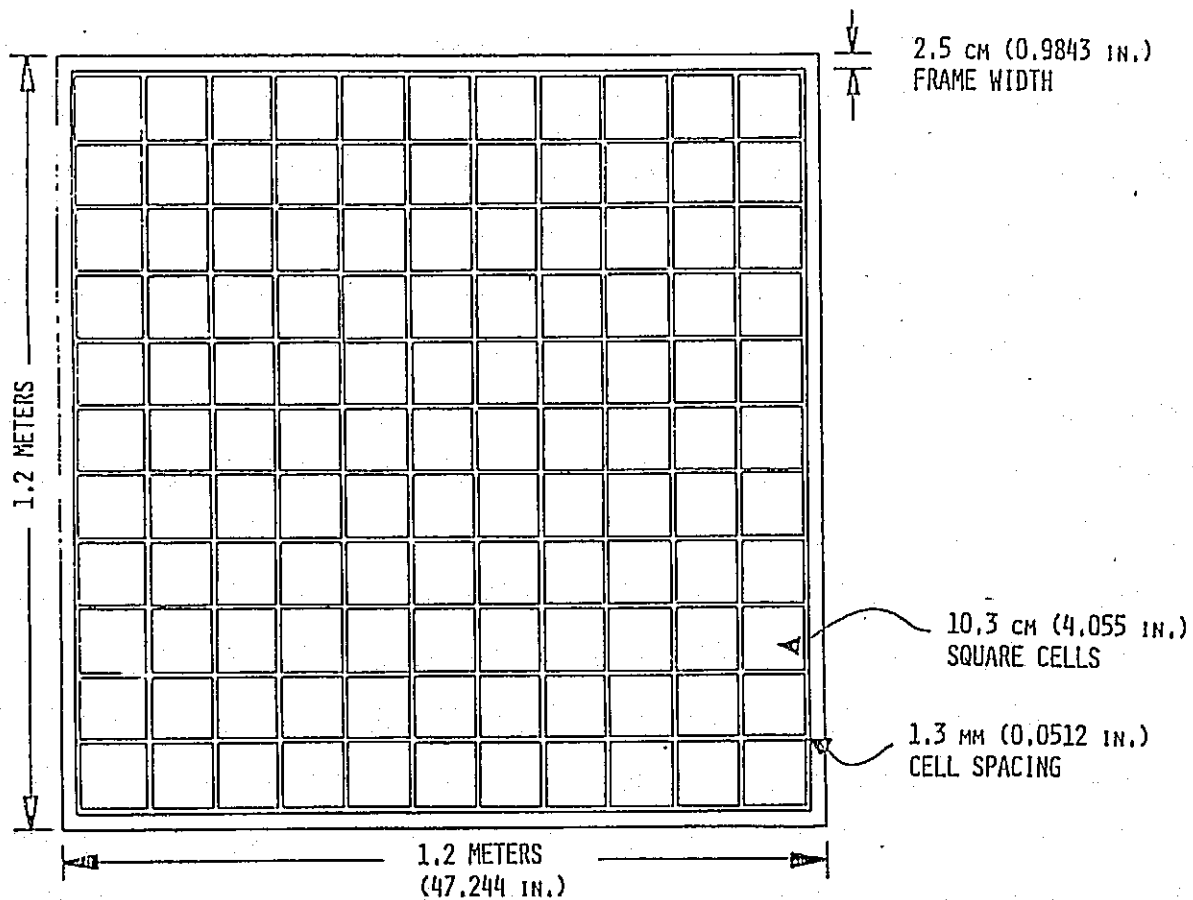
## Objectives

- ANALYTICAL METHODOLOGY
- VERIFICATION
- DESIGN AIDS, MASTER CURVES
- RESEARCH DIRECTION
- TCM

## Today's Topics

- STRUCTURAL ANALYSES
  - DEFLECTION
  - THERMAL
- ELECTRICAL ISOLATION STUDIES

# Module Concept



## Parameter Limits

### STRUCTURAL PANEL

$E_{SP}$ : 0.75-30 MSI  
 $T_{SP}$ : 0.04 - 0.25 IN.  
 $\alpha_{SP}$ : 7-24  $\mu\text{IN}/\text{IN}/^{\circ}\text{C}$

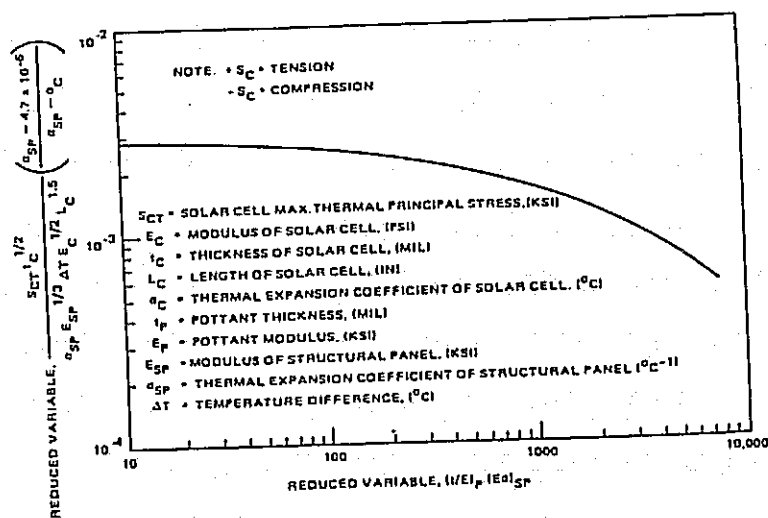
### POTTANT

$E_P$ : 0.5-2.5 KSI  
 $T_P$ : 0.001 - 0.020 IN.

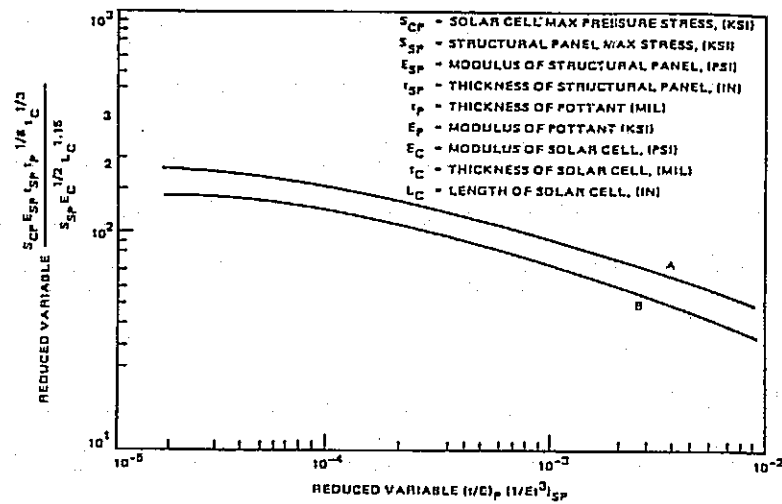
### CELL

$E_C$ : 5 - 30 MSI  
 $T_C$ : 0.005 - 0.015 IN.  
 $\alpha_C$ : 1 - 12  $\mu\text{IN}/\text{IN}/^{\circ}\text{C}$   
 $L_C$ : 1 - 4 IN.

## Thermal Stress Master Curve



## Pressure Stress Master Curve



## Caveats

- GUIDE NOT ABSOLUTE
- VERIFICATION INCOMPLETE

## Electrical Isolation Studies

- FINITE ELEMENT MODEL
- ELECTRICAL/THERMAL ANALOGY
- NASTRAN

## Thermal-Electrical Analogy

## DIFFUSION EQUATIONS

$$\nabla \cdot (\epsilon \nabla V) + \rho = 0$$

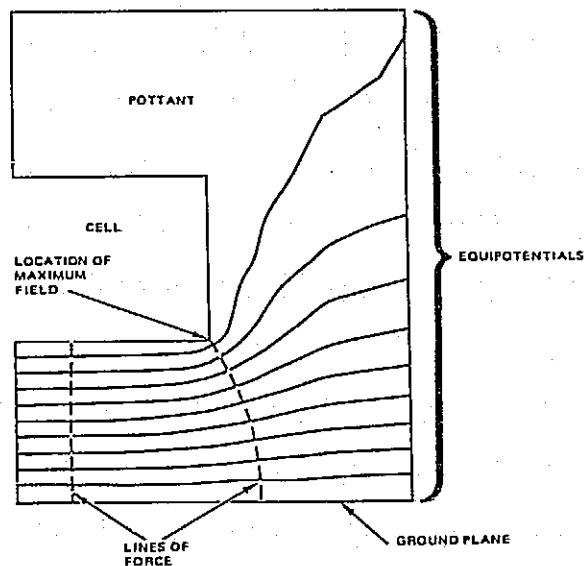
ELECTRICAL

$$\nabla \cdot (k \nabla T) + \dot{q} = \rho c \left( \frac{\partial T}{\partial t} \right)$$

THERMAL

THERMAL PARAMETER		ELECTRICAL PARAMETER	
TEMPERATURE	T	POTENTIAL	V
THERMAL CONDUCTIVITY	k	PERMITTIVITY	$\epsilon$
TEMPERATURE GRADIENT	$\nabla T$	ELECTRIC FIELD	$\vec{E} = -\nabla V$
HEAT FLUX	$-k \nabla T$	ELECTRIC DISPLACEMENT	$\vec{D} = \epsilon \vec{E}$
INTERNAL HEAT GENERATION	$\dot{q}$	CHARGE DENSITY	$\rho = \nabla \cdot \vec{D}$

## Electric Field Distribution in Module

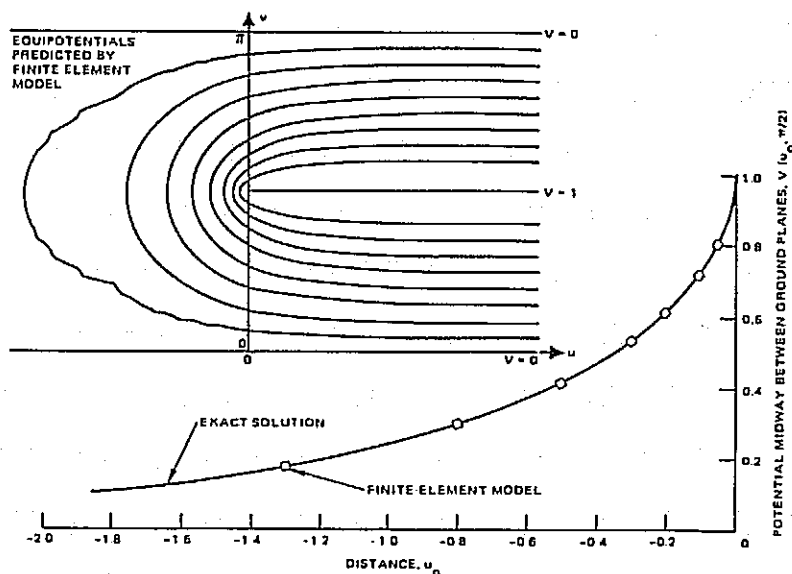


## Maximum Field Calculation

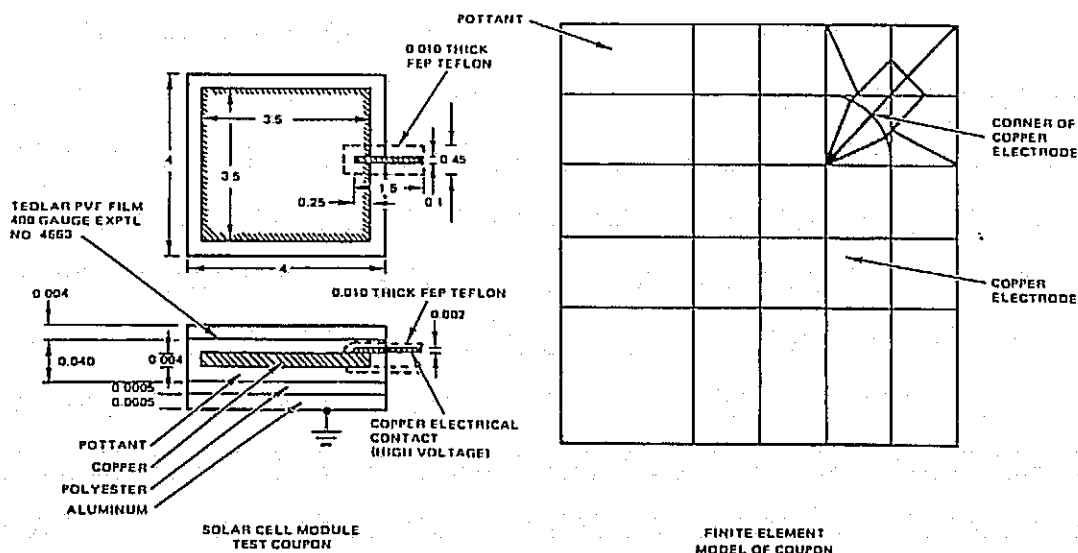
## PROCEDURE:

- 1) CALCULATE POTENTIAL DISTRIBUTION
- 2) CURVE FIT TO FUNCTION V (D)
- 3) CALCULATE SURFACE FIELD

## Potential Distribution for Blunted Knife-Edged Slab

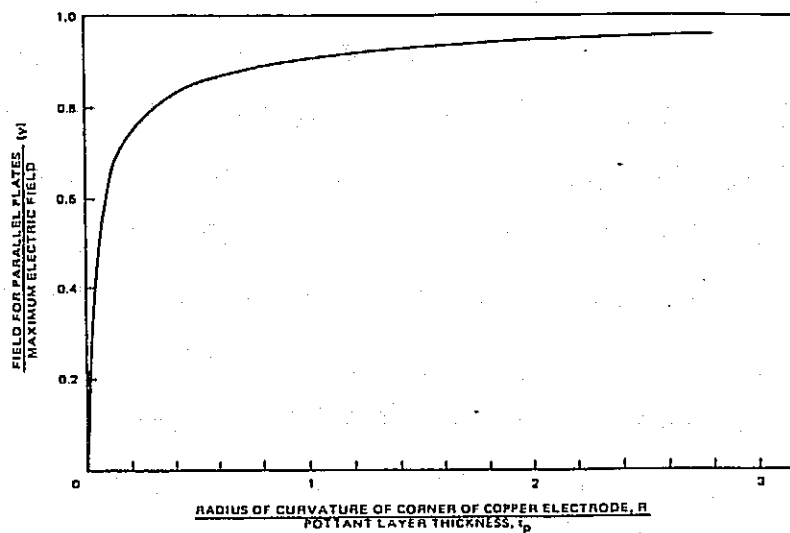


## Electrical Isolation Test Coupon and Finite-Element Model of It

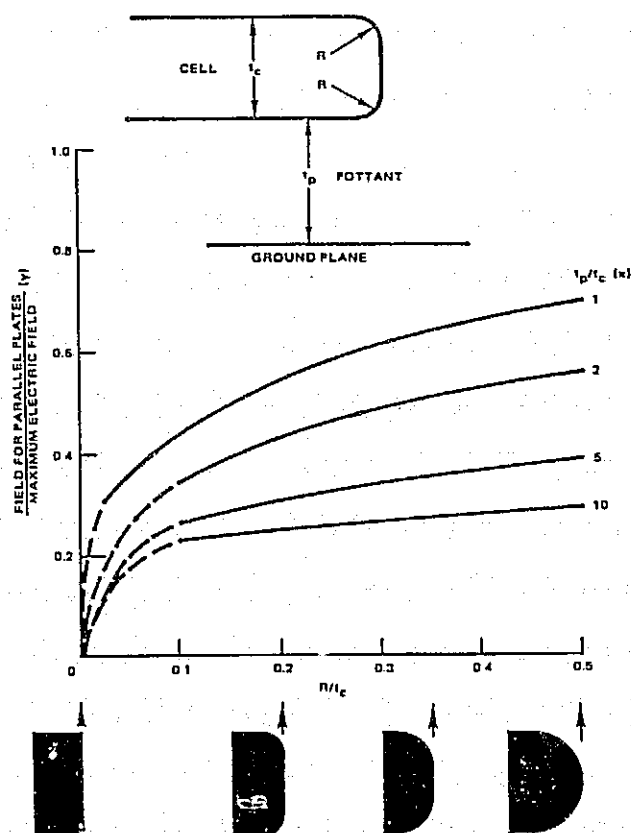




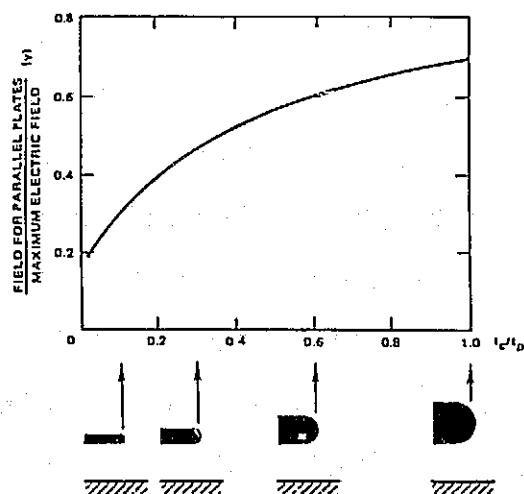
# Square Test Coupon: Effect of Coupon Corner Radius of Curvature on Electrical Stress Intensification Factor



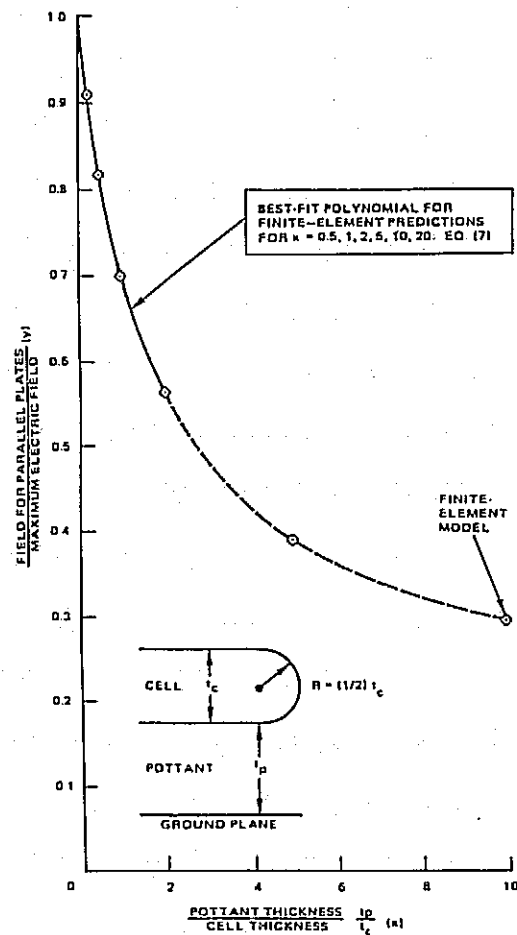
# Disc-Shaped Cell: Effect of Cell Edge Radius of Curvature on Electrical Stress Intensification Factor



# Disc-Shaped Cell: Effect of Cell Thickness on Electrical Stress Intensification Factor



# Disc-Shaped Cell: Limit of Electrical Stress Intensification Factor as Pottant Becomes Very Thin



## Conclusions

- VISIBLE ELECTRICAL MODEL

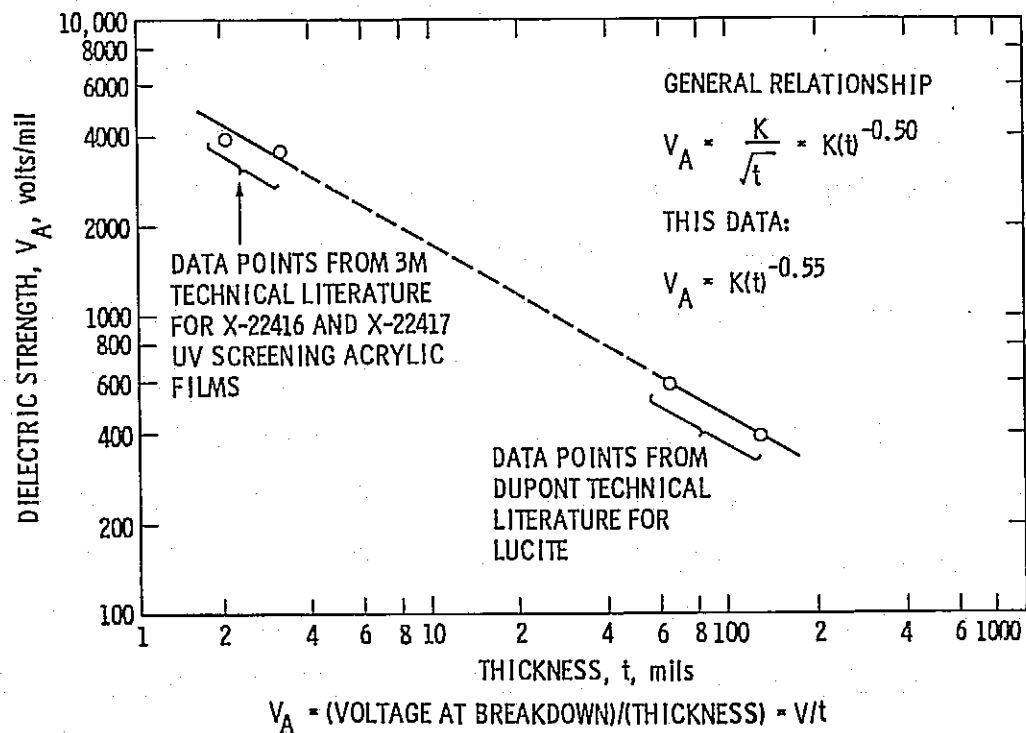
- REAL WORLD VALUE OF R NECESSARY

# ELECTRICAL INSULATION STABILITY

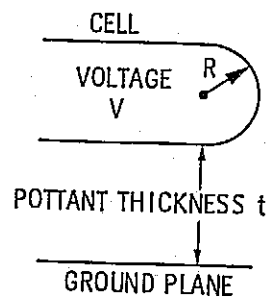
JET PROPULSION LABORATORY

Edward F. Cuddihy

## Dielectric Strength of PMMA Acrylic



## Spectrolab Computer Data



$V_A / (dV/dt)_{\max}$	$(t/2R)$
0.9116	0.25
0.8200	0.50
0.7004	1.00
0.5648	2.00
0.3916	5.00
0.2968	10.00
0.2305	20.00
0.1898	50.00

$$V_A = V/t = (dV/dt)_{\max} (2R)^{0.54} (t + 2R)^{-0.54}$$

## Similarity of Dielectric Strength Equations

EMPIRICAL  $\longrightarrow V_A = K t^{-1/2}$

COMPUTER THEORY  $\longrightarrow V_A = (dV/dt)_{\max} (2R)^{1/2} (t + 2R)^{-1/2}$

GENERAL FORM

$$V_A = K (t + a)^{-n}$$

$$V_A = K a^{-n} = (dV/dt)_{\max} \text{ AT } t = 0$$

## Needle Electrodes: Exact Solution for Tip-to-Tip

$$(dV/dt)_{\max} = \frac{V_A t (1 + 2R/t)^{1/2}}{2R \tanh^{-1} \left\{ t / (t + 2R) \right\}^{1/2}}$$

$$\text{AS } t \longrightarrow 0$$

$$V_A = (dV/dt)_{\max} (2R) (t + 2R)^{-1}$$

## Needle Electrodes: Exact Solution for Tip-to-Ground-Plane

$$(dV/dt)_{\max} = 2 V_A t P / \ln(Q)$$

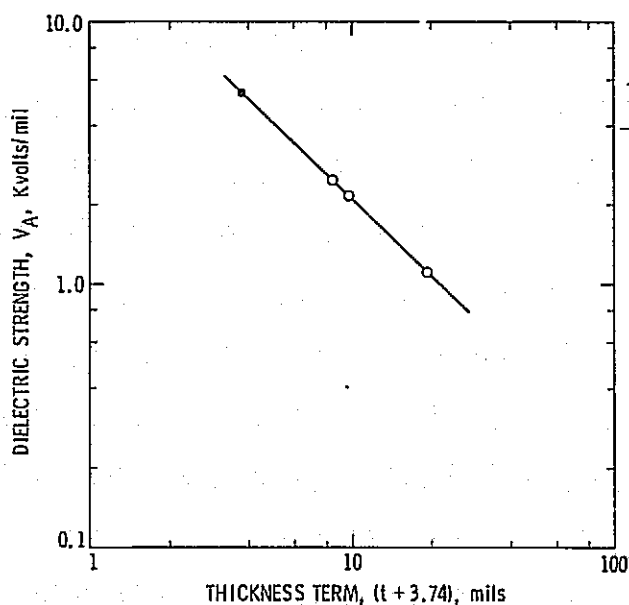
$$P = (1 + R/t)^{1/2} / R$$

$$Q = \{2t + R + 2t^{1/2}(t + R)^{1/2}\} / R$$

AS  $t \rightarrow 0$

$$V_A = (dV/dt)_{\max} (R)^{0.7} (t + R)^{-0.7}$$

## Dielectric Strength of A-9918 EVA



THICKNESS t, mils	AVERAGE DC BREAKDOWN VOLTAGE, KV	AVERAGE DIELECTRIC STRENGTH, V <sub>A</sub> = V/t, KV/mil
4.7	11.7	2.49
6.0	13.0	2.17
15.7	17.6	1.12

$$V_A = 19173 (t + 3.74)^{-0.96}$$

$$(dV/dt)_{\max} @ t = 0 = 5404 \text{ volts/mil}$$

## Comparison of EVA and PMMA Dielectric Strength Data

### EXPERIMENTAL DATA FIT

PMMA

$$V_A = 8009 (t + 0.87)^{-0.63}$$

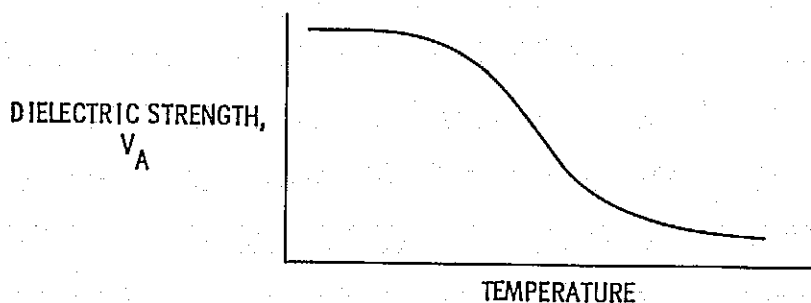
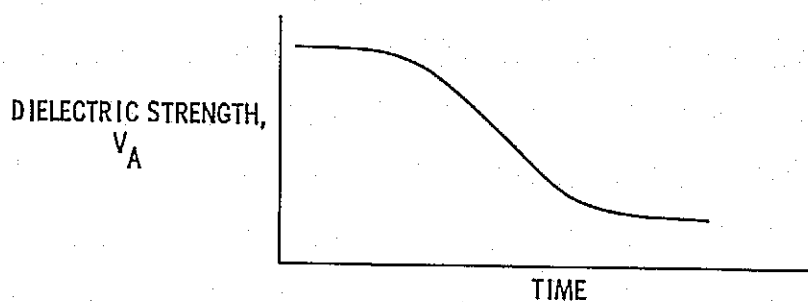
$$(EL)/(GP) \quad (dV/dt)_{\max} = (8009) (0.87)^{-0.63} = 8740 \text{ volts/mil}$$

EVA

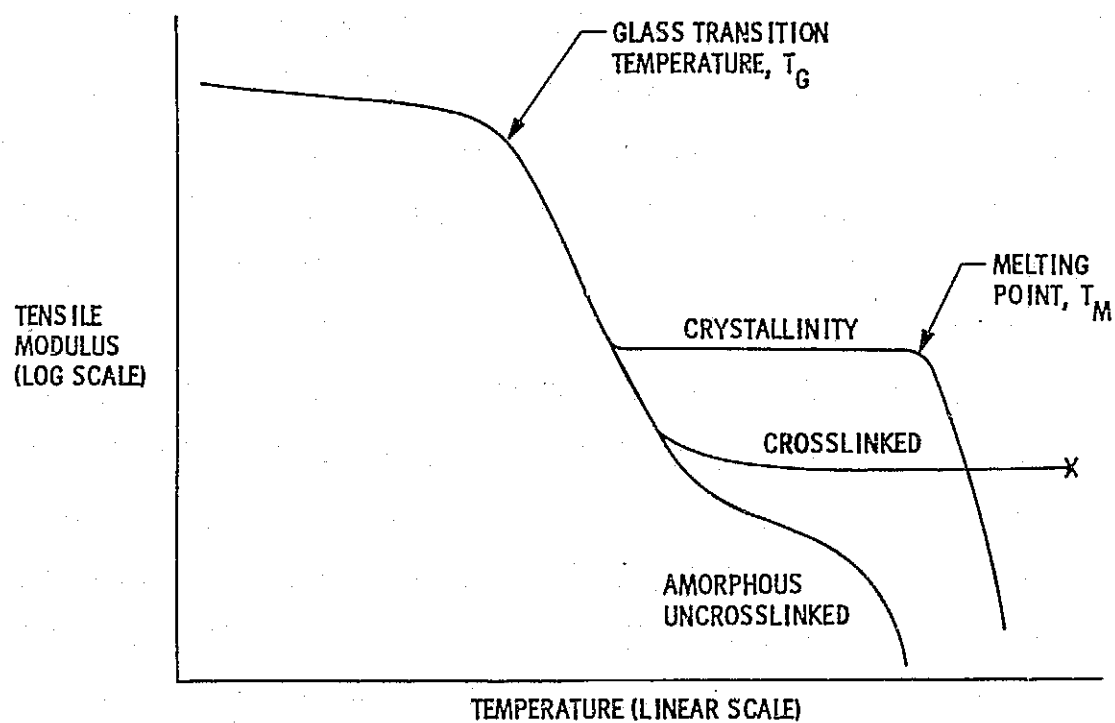
$$V_A = 19173 (t + 3.74)^{-0.96}$$

$$(EL)/(EL) \quad (dV/dt)_{\max} = (19173) (3.74)^{-0.96} = 5404 \text{ volts/mil}$$

### Dc Voltage Dielectric Strength Behavior (Literature)

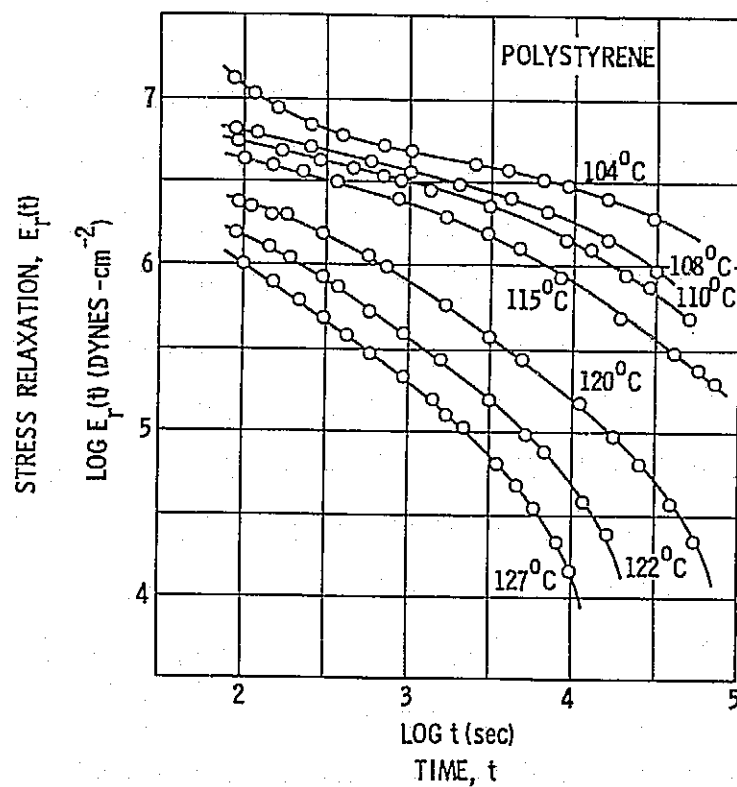


# Generalized Mechanical Property Behavior of Crosslinked and Crystalline Polymers

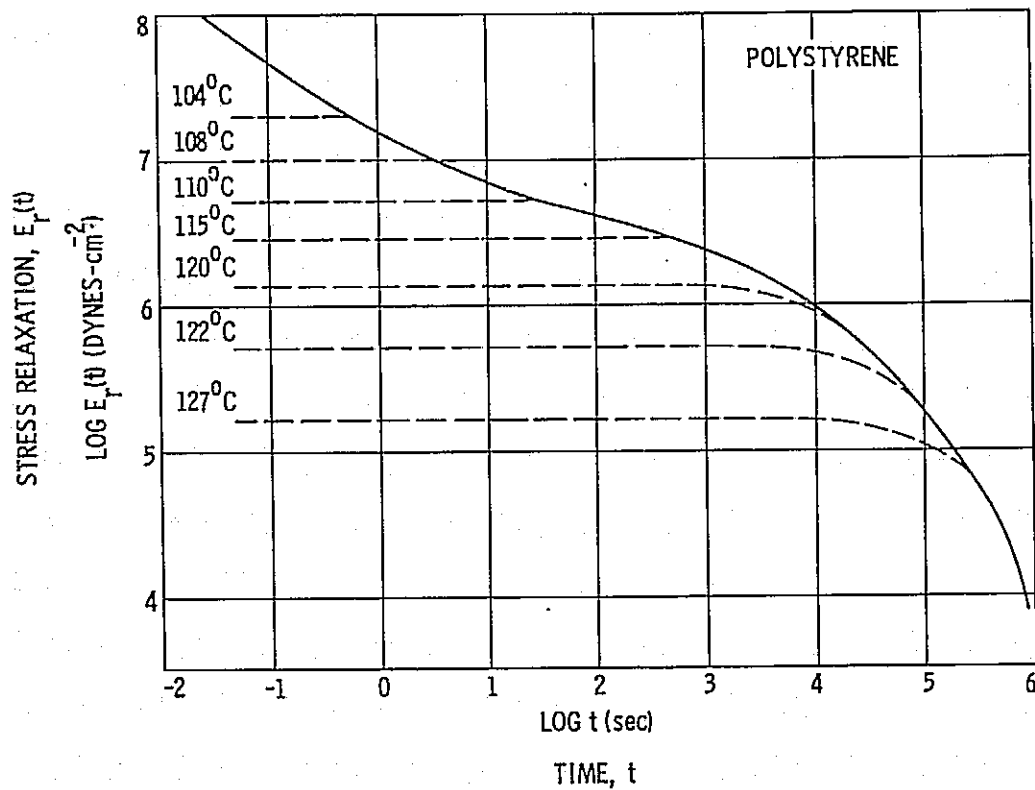




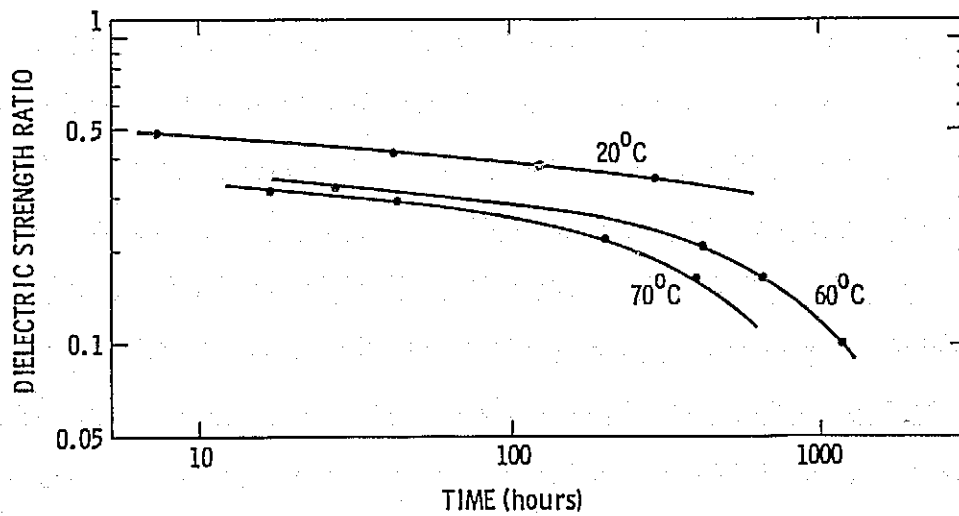
## Time-Temperature Superposition: Parametric Data Curves



# Time-Temperature Superposition: Master Curve for Time Extension



## Dielectric Strength of Polyethylene



DATA SOURCE: PROFESSOR LUCIANO SIMONI  
UNIV. OF BOLOGNA (ITALY)

# THEORETICAL AND EXPERIMENTAL ENCAPSULANT STABILITY

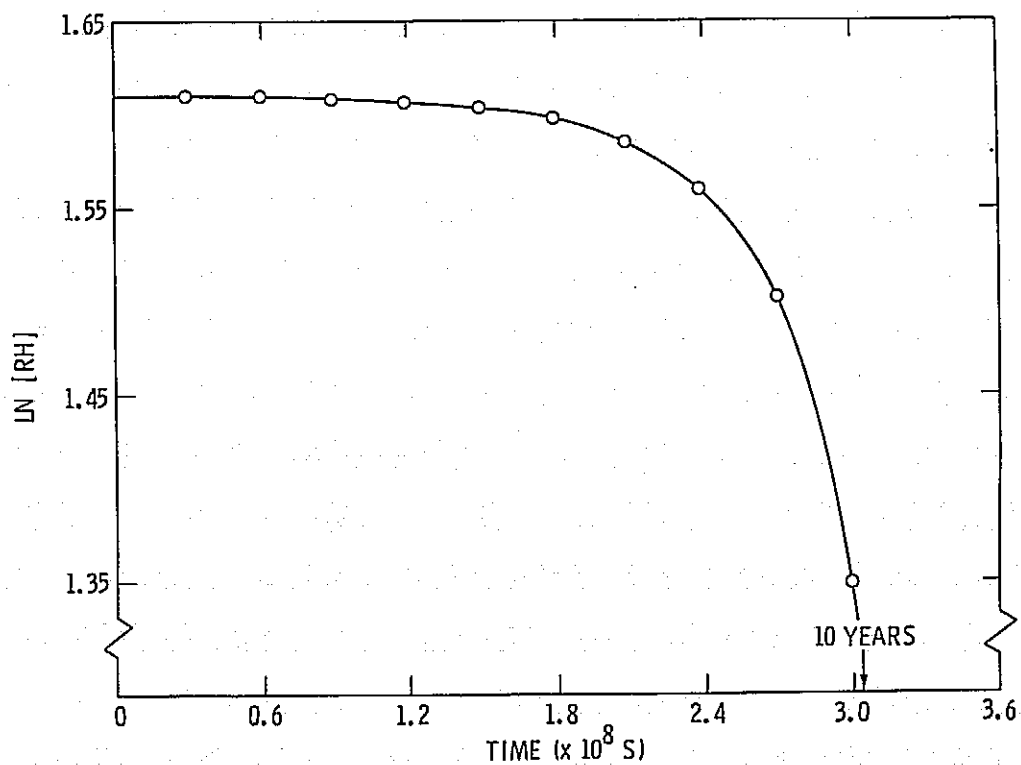
JET PROPULSION LABORATORY

R. Liang

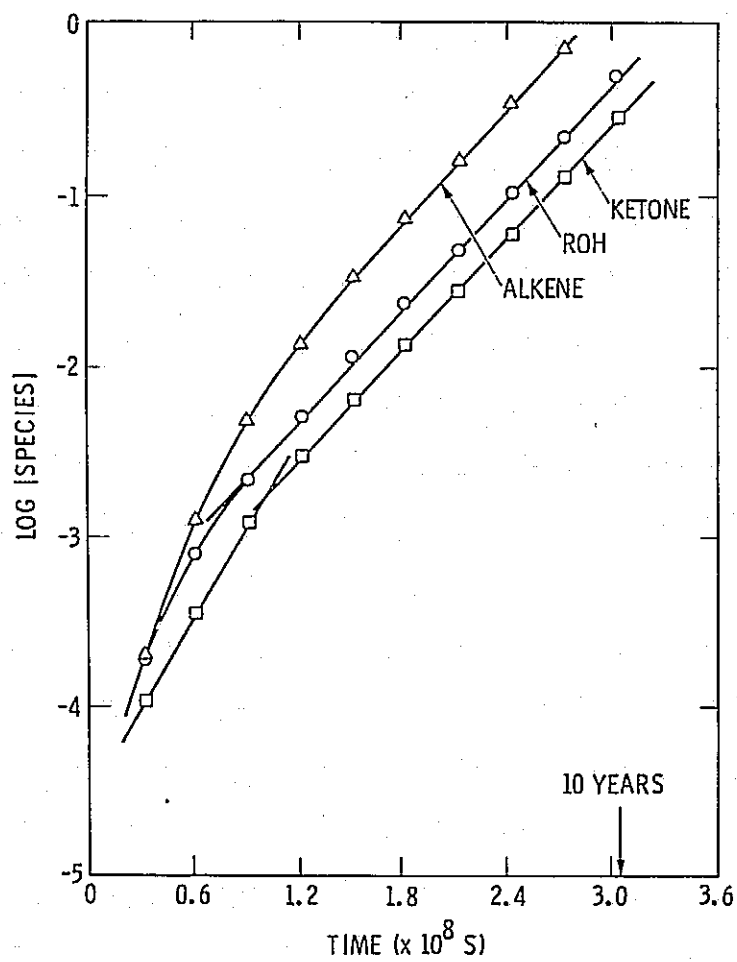
## Agenda

- THEORETICAL MODELLING OF EVA OUTDOOR PHOTODEGRADATION (U. OF TORONTO)
- EXPERIMENTAL INVESTIGATION OF POLYMER DEGRADATION AND DEVELOPMENT OF ACCELERATED TESTING TECHNOLOGY
- PHOTOTHERMAL TESTING OF ENCAPSULANT MATERIALS

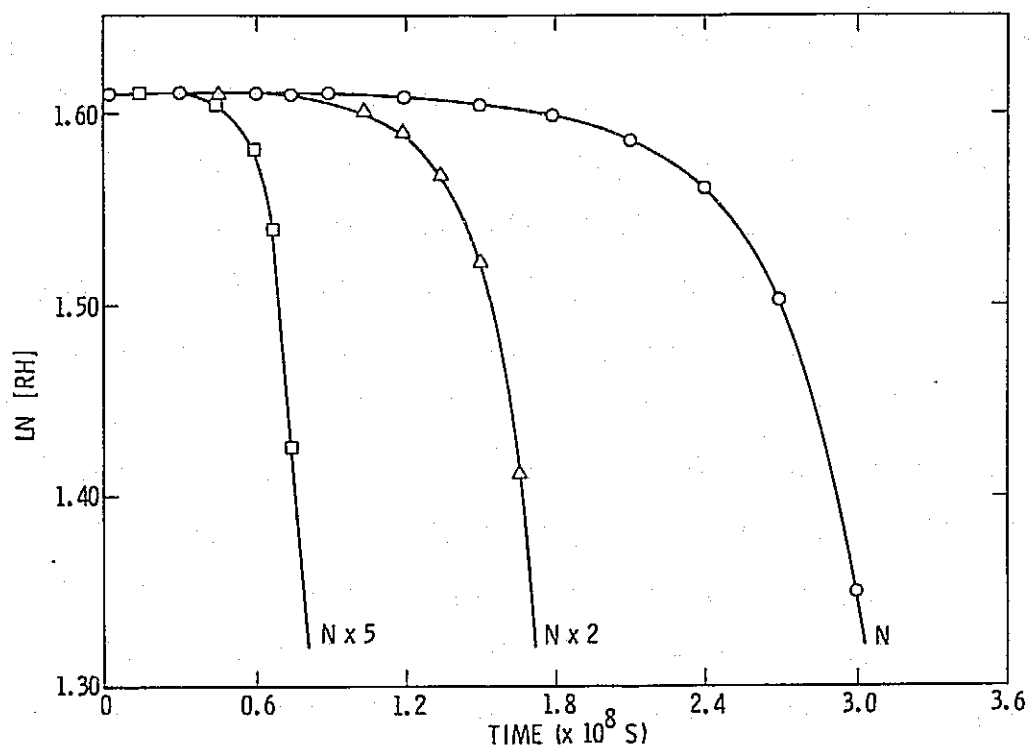
## Photooxidation versus Time



Log (Species) versus Time

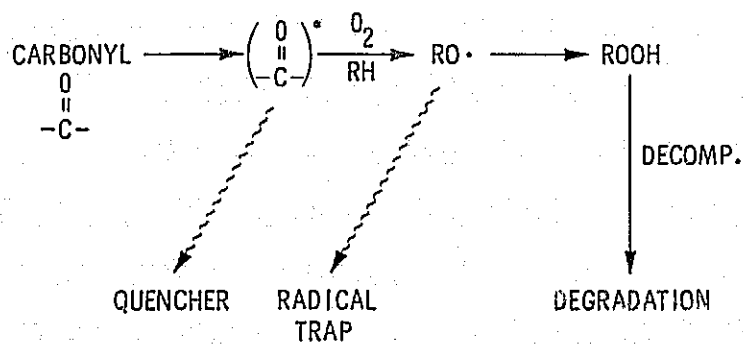
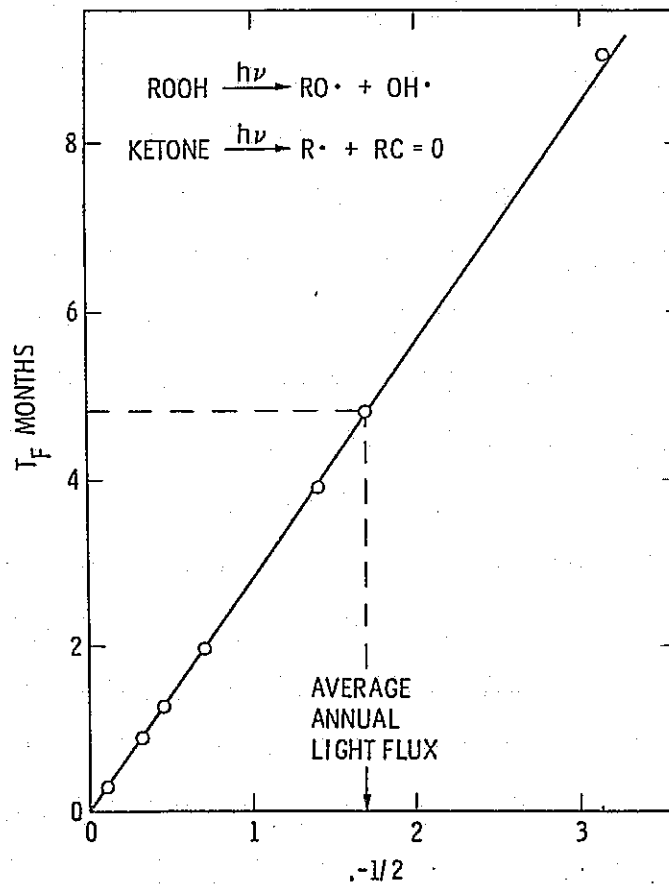


## Photooxidation as a Function of Intensity of Light

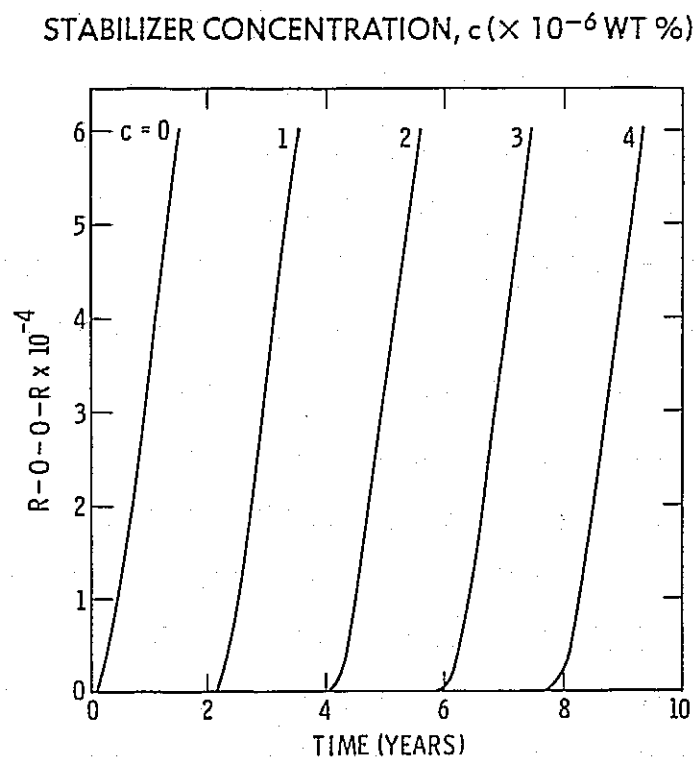


# Photooxidation of Unstabilized PE

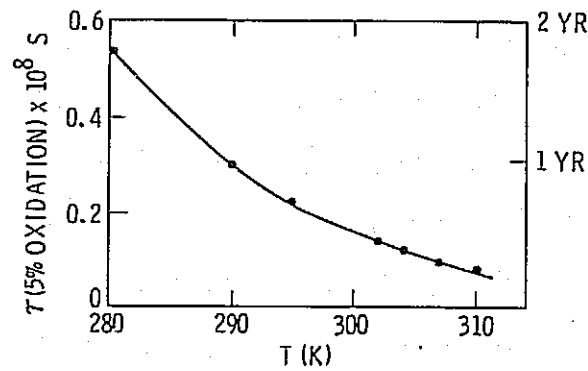
TIME TO FAILURE AS A FUNCTION OF LIGHT INTENSITY



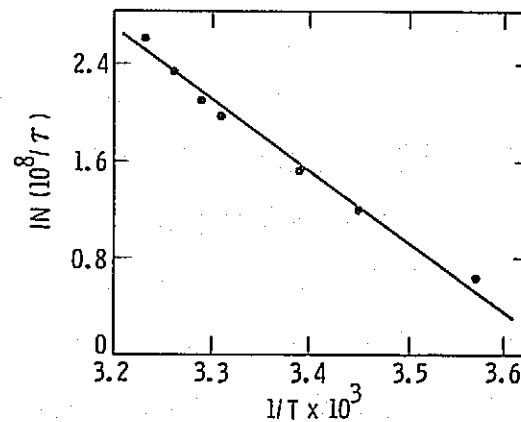
## Effect of Stabilizer on Formation of Crosslinks



## Time to Failure (5% Oxidation) as a Function of Temperature



## Arrhenius Plot of the Rate of Oxidation (k versus 1/T)

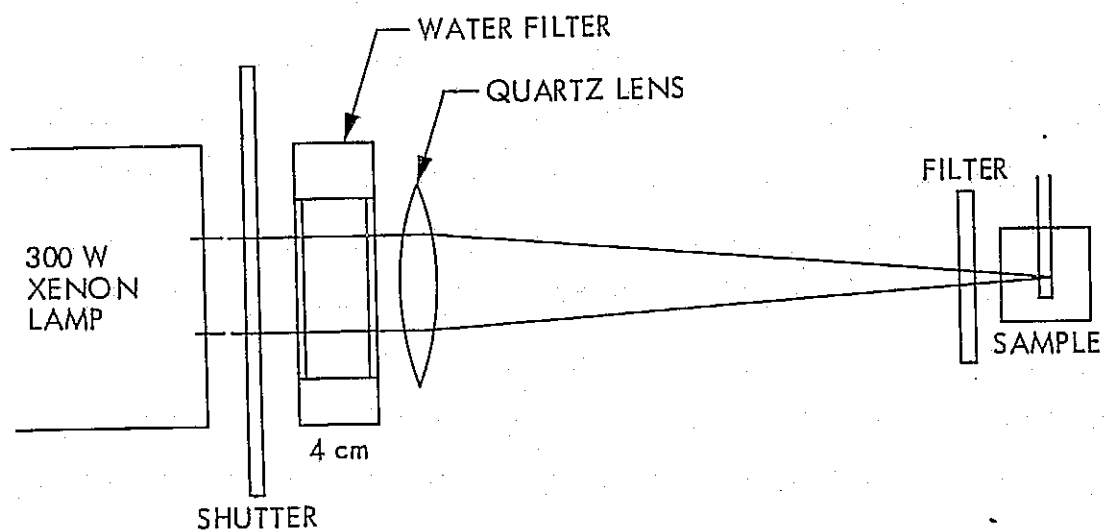


## Conclusion

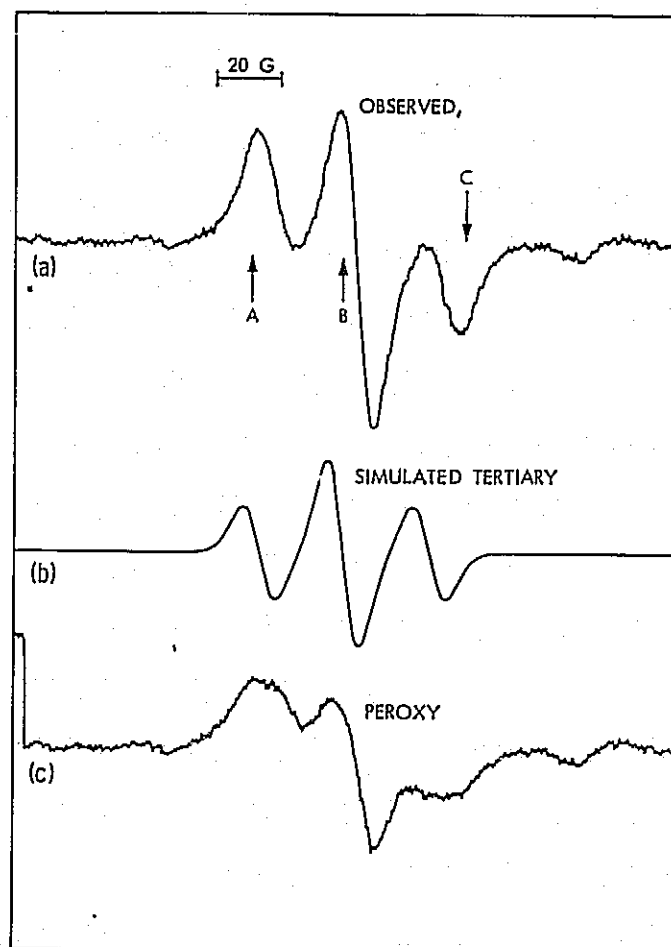
- TIME TO FAILURE  $\propto \sqrt{\text{LIGHT INTENSITY}}$
- PEROXIDE LIFETIME
- "APPARENT ENERGY OF ACTIVATION" OF  
10 Kcal (45°F - 100°F)



# Flash ESR Apparatus

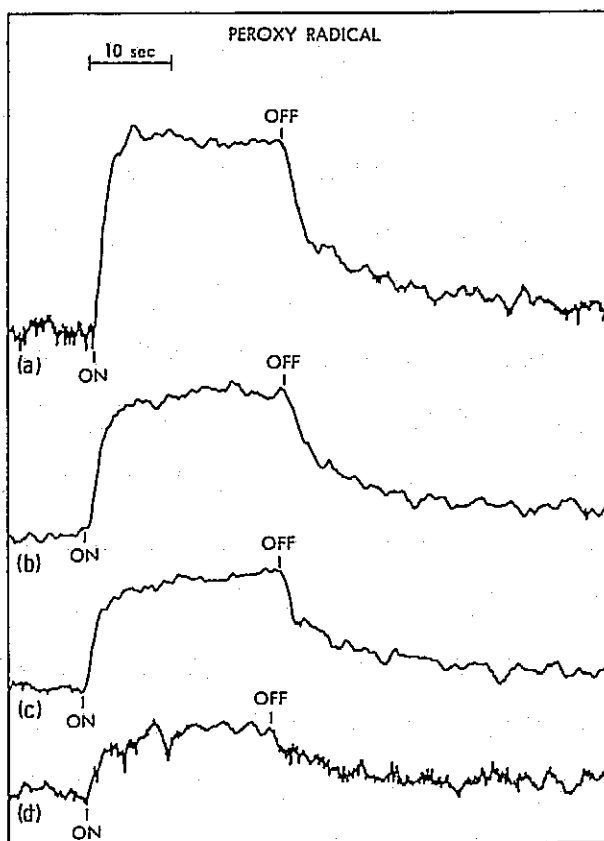


# In-Situ, Steady-State ESR Spectrum of Photo-Irradiated PnBA at Room Temperature in Air



# Time Profile and Intensity of Peroxy Radical as a Function of Light Intensity

a). 100% b). 46% c). 26% d). 12%



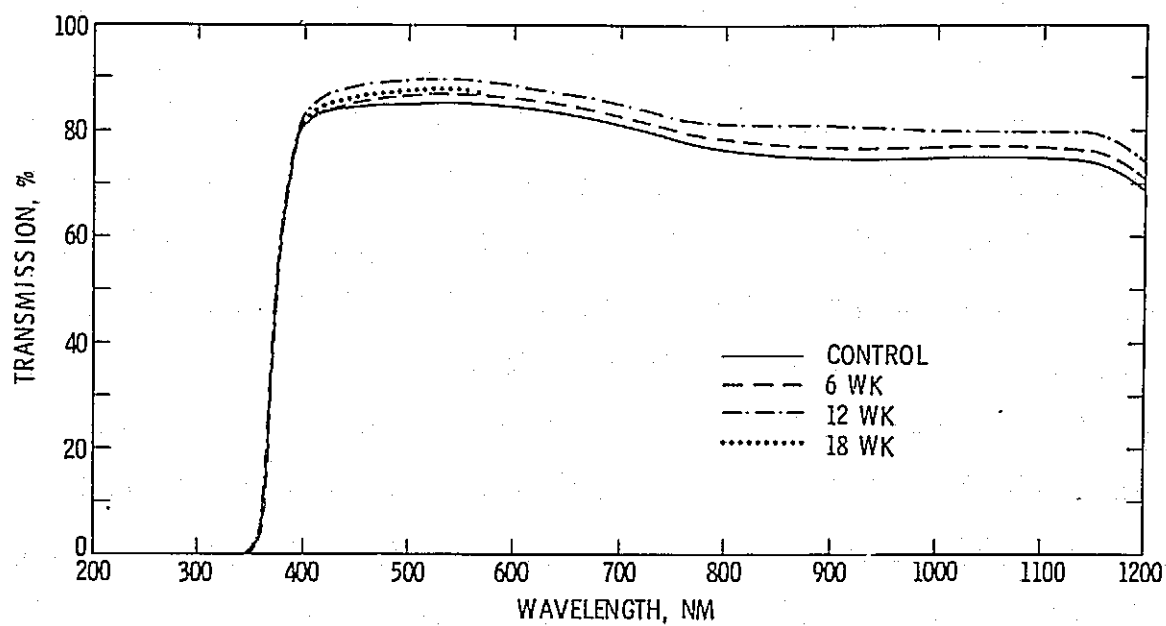
### Concentration of Transient Radicals as a Function of Light Intensity

SAMPLE No.	LIGHT INTENSITY (I)	$\sqrt{I}$	NORMALIZED OBSERVED ESR INTENSITY	
			AT PEAK A	AT PEAK C
1	1.0	1.0	1.0	1.0
2	2.2	1.5	1.8	1.6
3	3.9	2.0	2.5	2.2
4	8.3	2.9	3.2	2.6

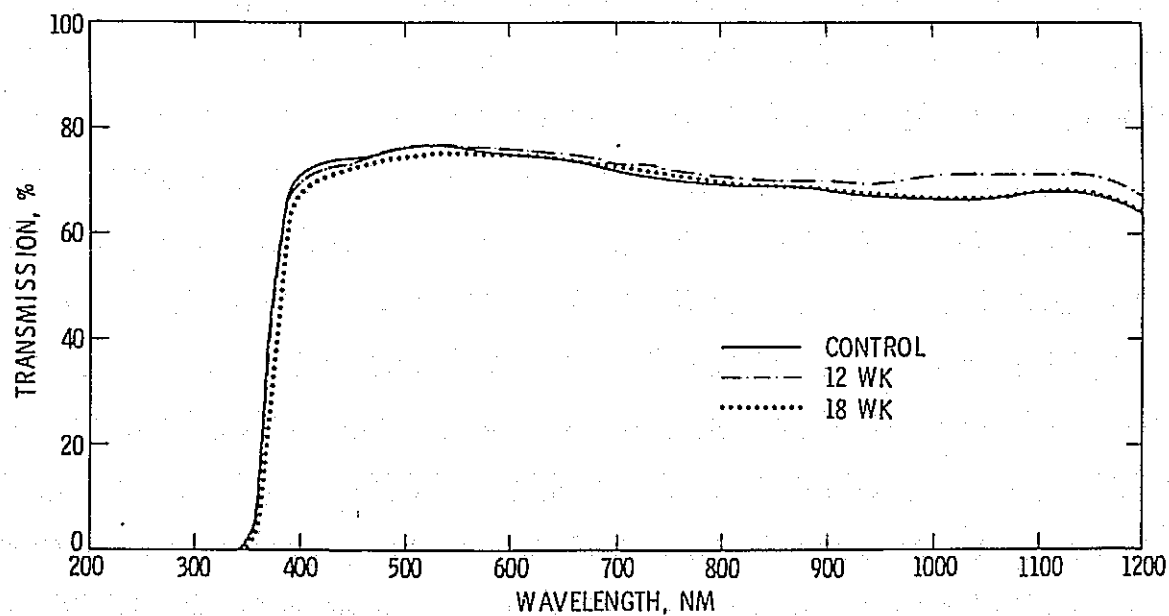
### Conclusions

- HALF LIFE OF  $\text{ROO}^\bullet$  RADICAL MEASURED TO BE 5 SEC
- CONCENTRATION OF CROSSLINKING RADICAL IS PROPORTIONAL TO SQUARE ROOT OF LIGHT INTENSITY
- TEMPERATURE AND PHOTON FLUX CORRELATION WILL BE EVALUATED

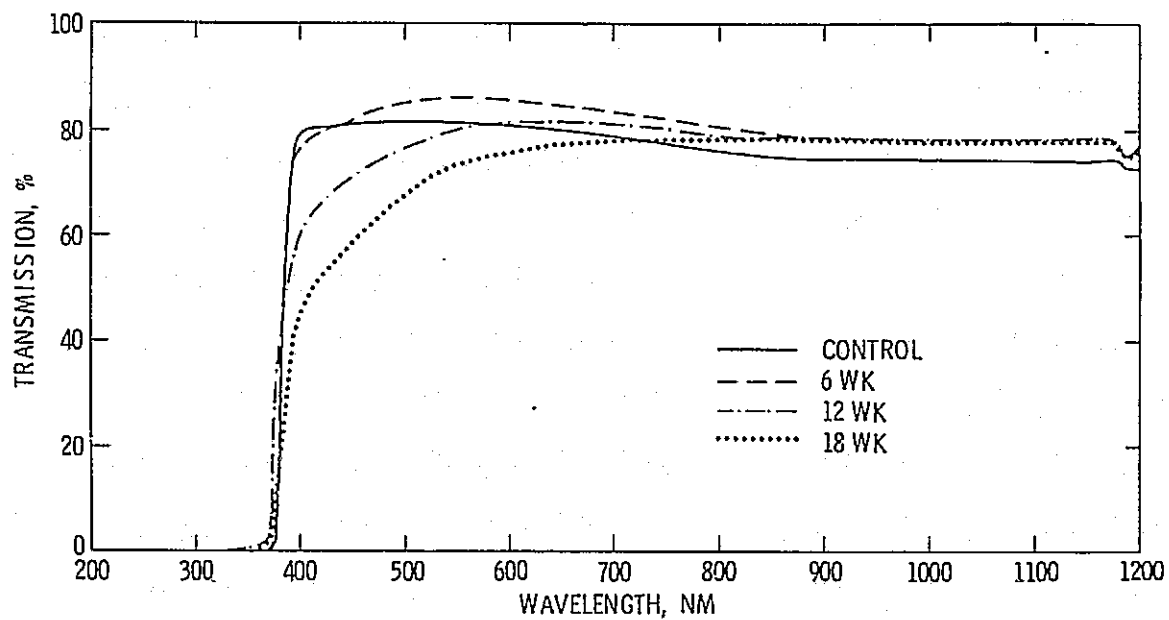
## Photothermal Aging of EVA Under Sunadex at 85°C, 6 Suns



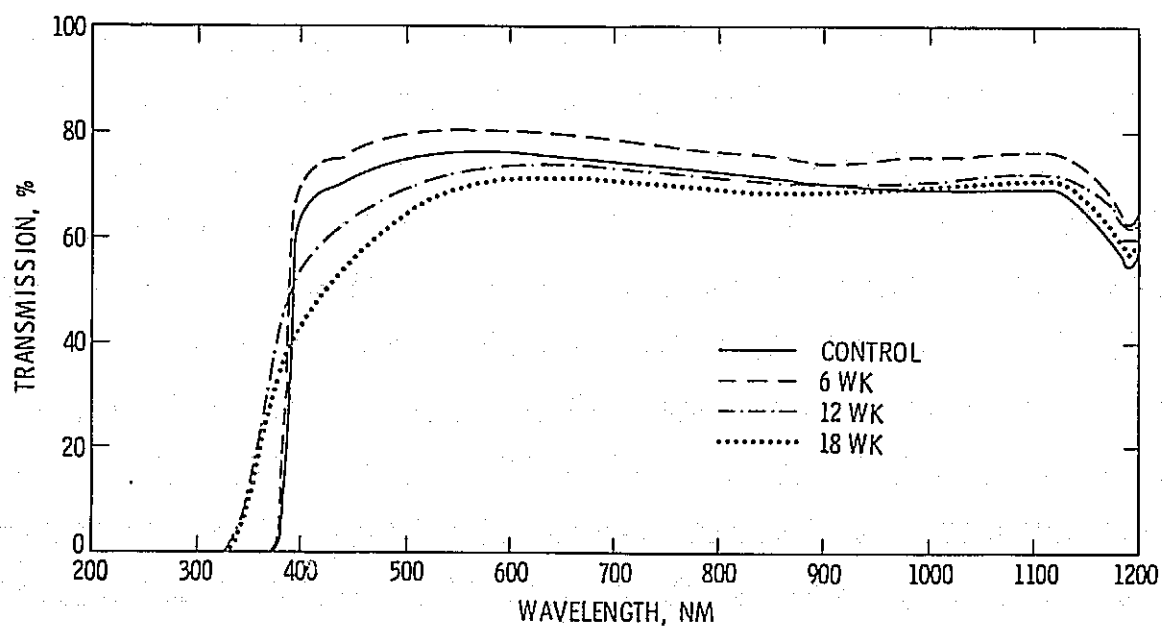
## Photothermal Aging of EMA Under Sunadex at 85°C, 6 Suns



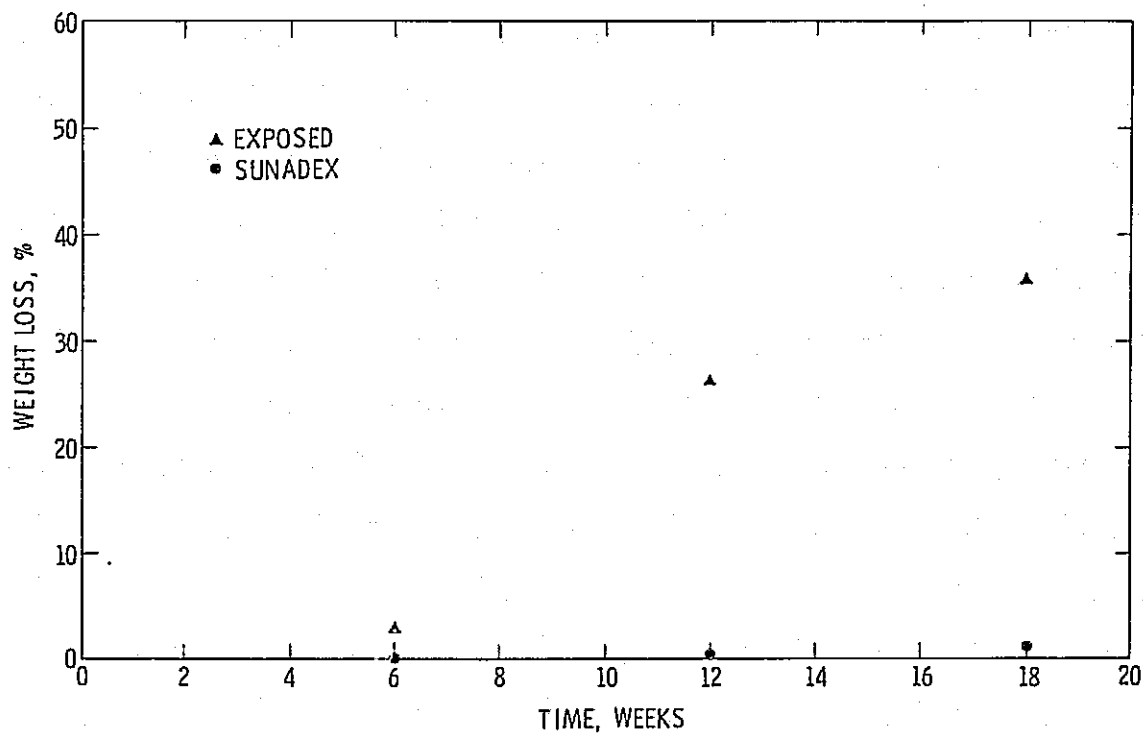
## Photothermal Aging of PVB Under Sunadex at 85°C, 6 Suns



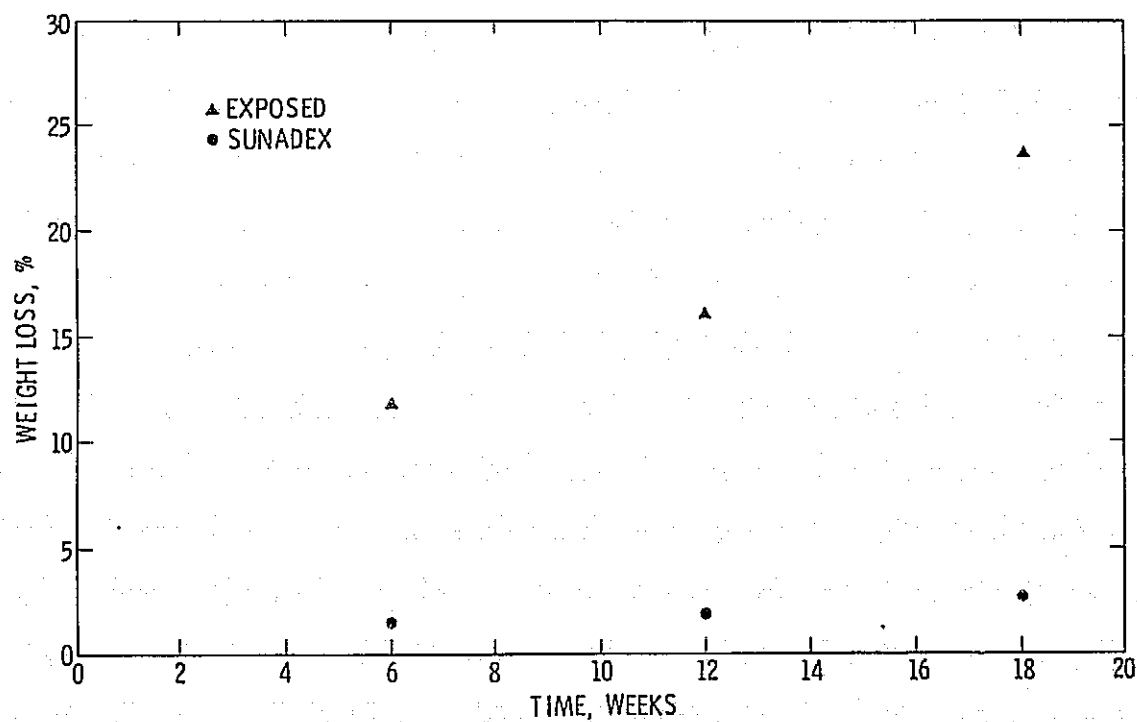
## Photothermal Aging of PnBA Under Sunadex at 85°C, 6 Suns



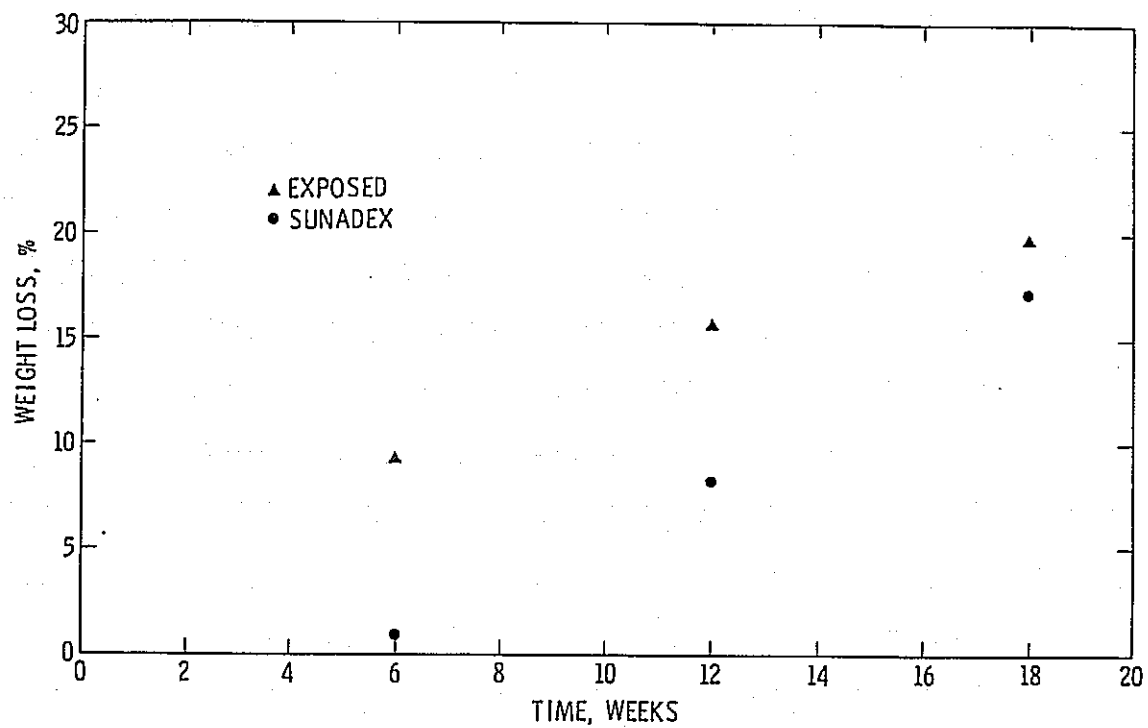
## Photothermal Aging of EVA at 85°C, 6 Suns



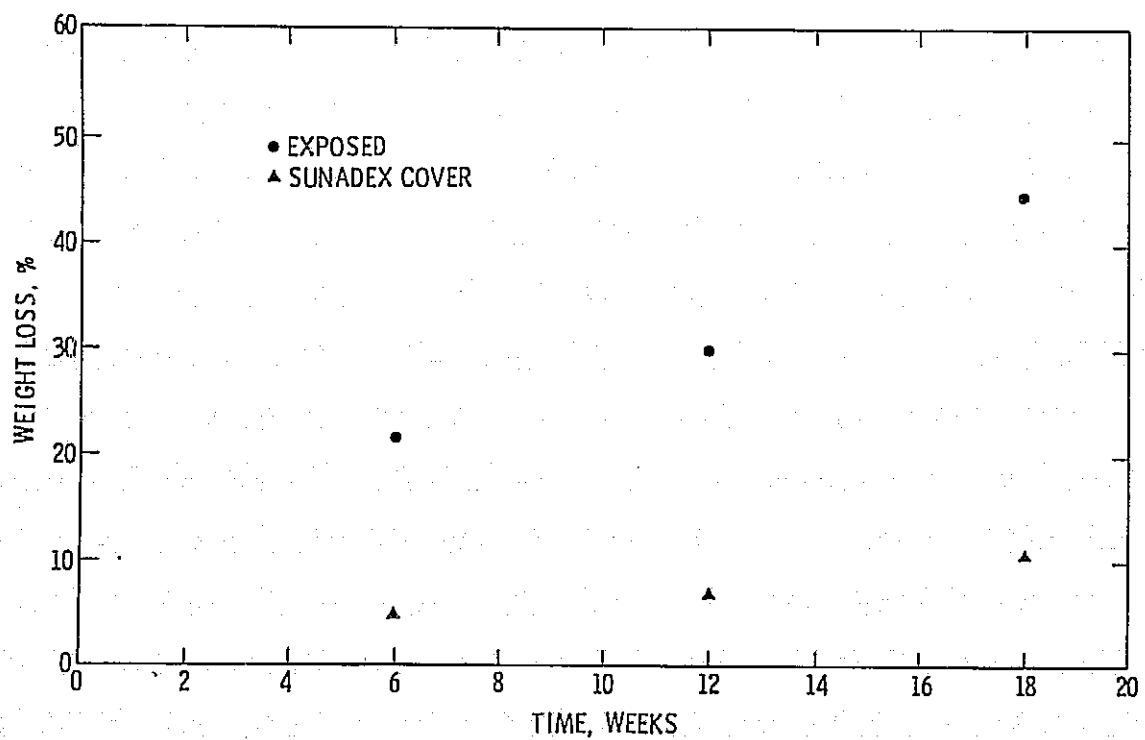
## Photothermal Aging of EMA at 85°C, 6 Suns



## Photothermal Aging of PnBA at 85°C, 6 Suns



## Photothermal Aging of PVB at 85°C, 6 Suns





# POLYMER-METAL INTERFACE BOND STABILITY

UNIVERSITY OF CINCINNATI

F.J. Boerio

## Goal - Enhanced Reliability and Durability of

adhesive bonds between polymers used as  
encapsulation potants and metals used as  
supports or electrical interconnects

## Encapsulation Pottant

ethylene/vinyl acetate (EVA) copolymer

## Metal Supports or Interconnects

steel

aluminum

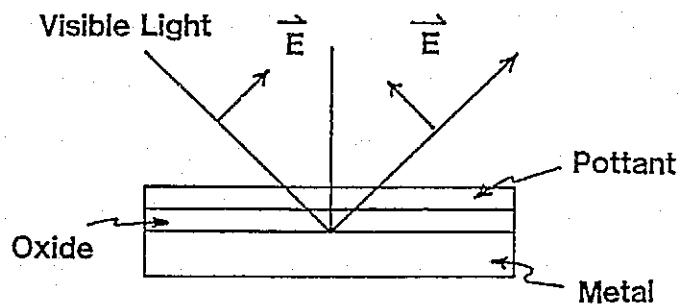
copper

nickel

## Strategies

1. Develop in-situ, non-destructive technique  
for determining stability of polymer/metal  
(oxide) interface.
2. Determine nature of degradation reactions  
occurring at polymer/metal (oxide)  
interface and develop methods for  
inhibiting those reactions.

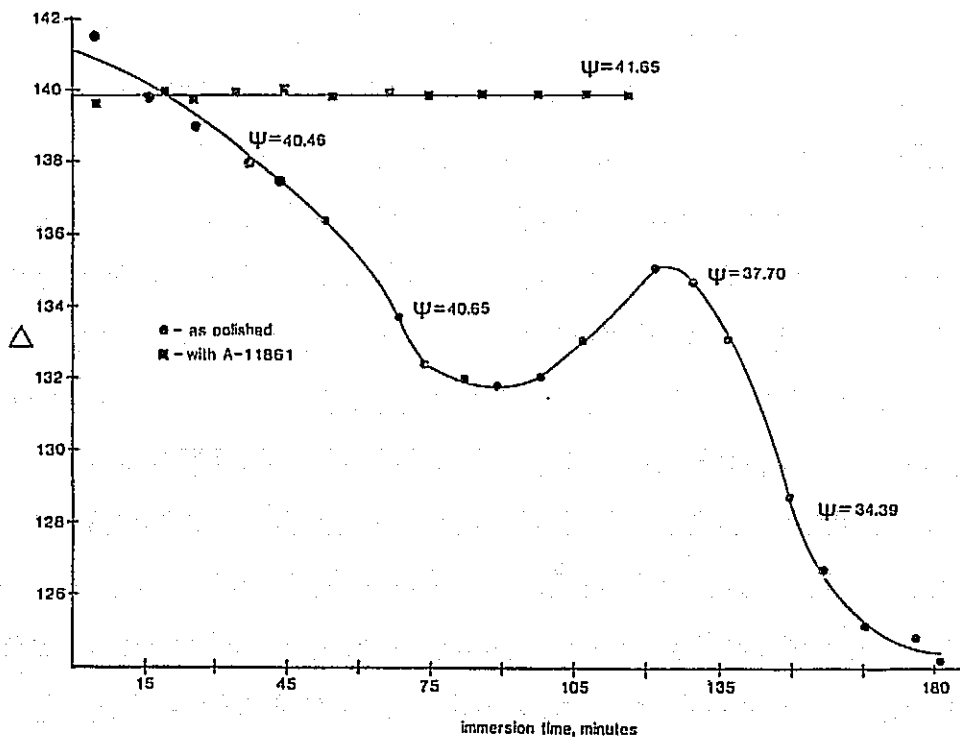
## Ellipsometry for Determining Stability of Polymer-Metal Interfaces



### Advantages

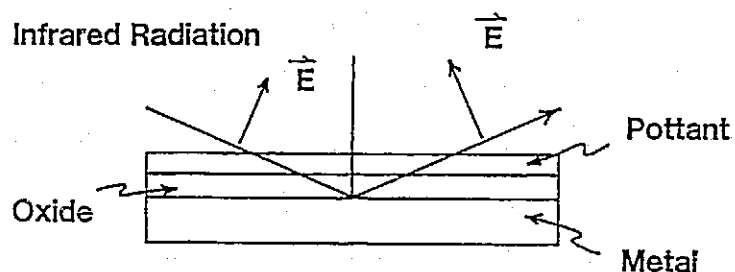
- non-destructive
- extreme sensitivity
- in-situ analysis

## Ellipsometry Parameter $\Delta$ vs Immersion Time



Plot of ellipsometry parameter  $\Delta$  versus immersion time in water at 40°C for polished aluminum mirrors with and without thin films (~20 Å) of A-11861 primer.

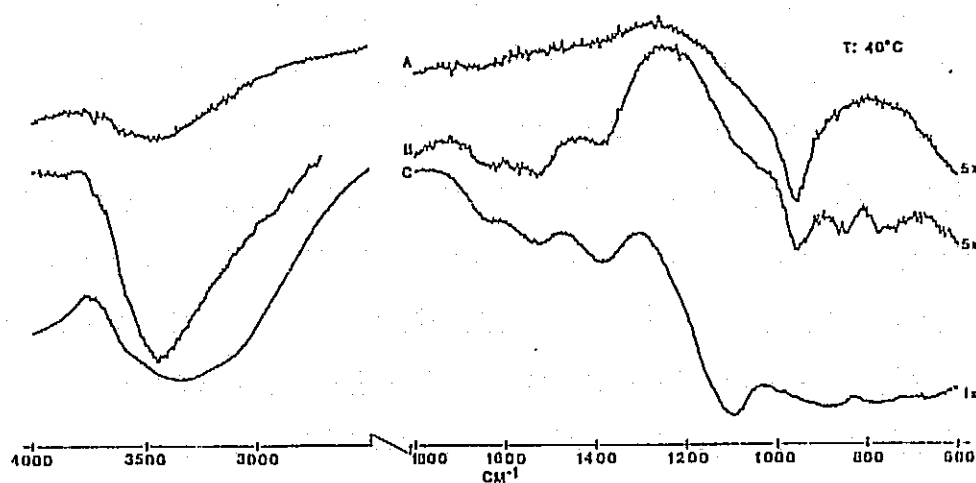
## Infrared Spectroscopy for Determining Chemistry of Polymer-Metal Interfaces



### Advantages

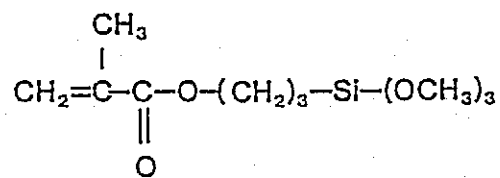
- non-destructive
- high sensitivity
- chemical information
- oxides
- organics

### Infrared Spectra of Oxides

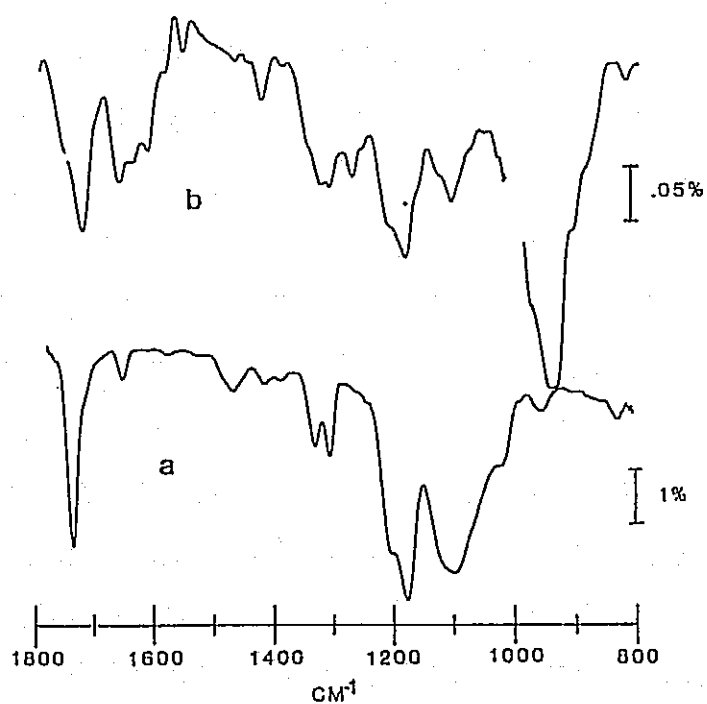


Infrared spectra of oxides formed on mechanically polished 2024 aluminum alloy during immersion in water at 40°C for (A) - one hour, (B) - 16 hours, and (C) - 24 hours.

Active Component in A-11861 Primer Is  
 $\gamma$ -Methacryloxypropyltrimethoxysilane ( $\gamma$ -MPS)



Infrared Spectra



Infrared spectra of (a) multi-molecular layer and  
 (b) mono-molecular layer films formed by A-11861  
 primer on aluminum.

## Conclusions

### CONCLUSIONS

1. ELLIPSONOMETRY IS EFFECTIVE FOR NDE OF POLYMER/METAL INTERFACES.
2. IR IS EFFECTIVE FOR CHEMISTRY OF INTERFACES.

### FUTURE WORK

1. APPLY THESE TECHNIQUES TO INTERFACES BETWEEN EVA AND OTHER METALS SUCH AS Ni AND Cu.
2. MAKE RECOMMENDATIONS FOR PROPER FORMULATION AND APPLICATION OF PRIMERS FOR BONDING EVA TO METALS.

## SILICON MATERIAL

R. Lutwack, Chairman

This session comprised presentations on continuing research efforts to develop processes for producing low-cost semiconductor-grade silicon and to extend the understanding of the effects of impurities and cell design on the performance of solar cells. Two additional efforts are described: one on a chemical vapor transport technique, and one on an electrochemical refining method.

# DICHLOROSILANE RESEARCH PROCESS

HEMLOCK SEMICONDUCTOR CORP.

## Chemical Vapor Deposition of Polysilicon From DCS

### TECHNOLOGY

POLYCRYSTALLINE SILICON

### REPORT DATE

SEPTEMBER, 1983

### APPROACH

CHEMICAL VAPOR DEPOSITION OF POLY-SILICON FROM DICHLOROSILANE (DCS)

### STATUS

PROJECT COMPLETE

PDU OPERATED SUCCESSFULLY

### CONTRACTOR

HEMLOCK SEMICONDUCTOR CORPORATION

\$15.60/KG MANUFACTURING COST  
PROJECTED FOR 1000 TN/YR PLANT

PURITY OF DEPOSITED SILICON  
IS SEMICONDUCTOR GRADE

### GOALS

ESTABLISH PROCESS FEASIBILITY THROUGH  
LABORATORY EXPERIMENTS AND COMPONENT  
TESTING

DEPOSITION GOAL OF 2.0 GM/HR/CM  
DEMONSTRATED

INVESTIGATE CRITICAL ELEMENTS OF PROCESS  
VIA OPERATION OF PROCESS DEVELOPMENT UNIT

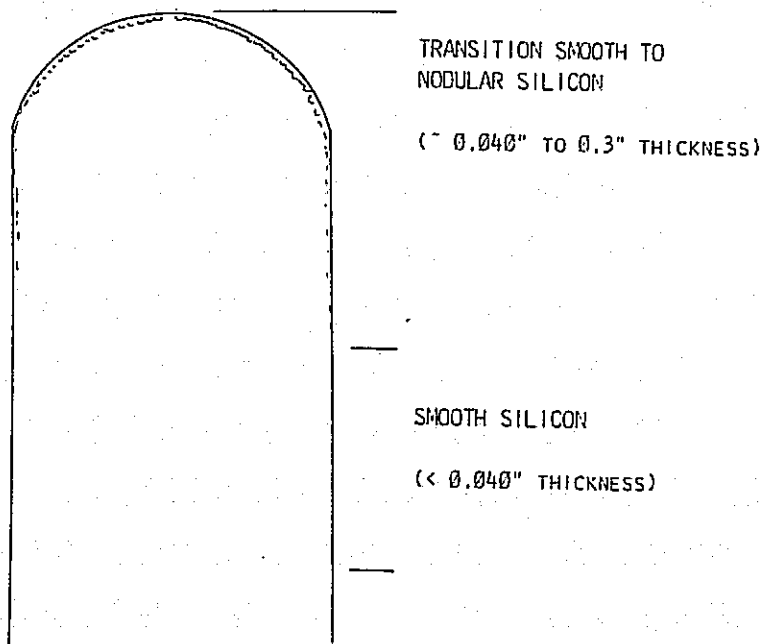
POWER CONSUMPTION GOAL OF  
60 KWH/KG DEMONSTRATED

POLYSILICON PRICE OF LESS THAN \$21/KG  
(1980 \$, 1000 - MT/YR, 20% ROI) AND PURITY  
APPROACHING OR EQUALLING SEMICONDUCTOR-  
GRADE POLYSILICON

## Summary of DCS Performance for Intermediate Reactor

ROD DIAMETER	80 MM ROD DIAMETER		
PARAMETER CONDITION	SILICON DEPOSITION RATE (GH <sup>-1</sup> CM <sup>-1</sup> )	CONVERSION (MOLE %)	POWER CONSUMPTION (KWH/KG)
A	1.59	37.5	89.6
B	1.74	35.0	88.8
C	2.00	35.1	82.0
D	1.61	41.6	93.9
GOAL	2.0	40	60

## Bell-Jar Silicon Deposition (Model 8D Reactor)





## Current Objectives

### DEMONSTRATE

2.0 GM/HR/CM DEPOSITION RATE

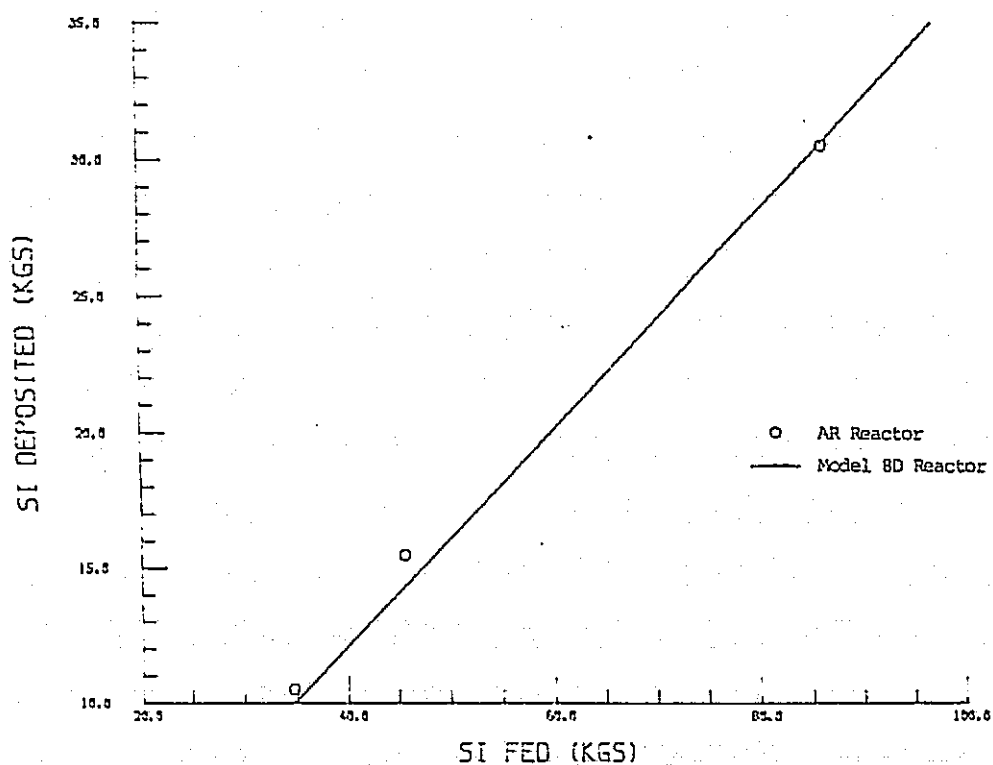
60 KWH/KG POWER CONSUMPTION

40% CONVERSION

IN A COOLED WALL (<500°C INSIDE TEMPERATURE) DEPOSITION REACTOR

INVESTIGATE SUITABILITY OF VARIOUS METALS AS MATERIALS OF CONSTRUCTION FOR DEPOSITION REACTORS AND COMPONENTS.

### Conversion Data Plot (4.46 g/h-cm Feed)



## SILICON MATERIAL

### Results of High-Performance Runs

RUN	FEED RATE GM/HR/CM	DEPOSITION RATE GM/HR/CM	POWER CONSUMPTION KWH/KG	CONVERSION %
547	13.39	2.28	59	17.1
528	7.44	1.83	78	24.7
540	7.44	2.21	85	29.7
GOAL		2.0	60	40

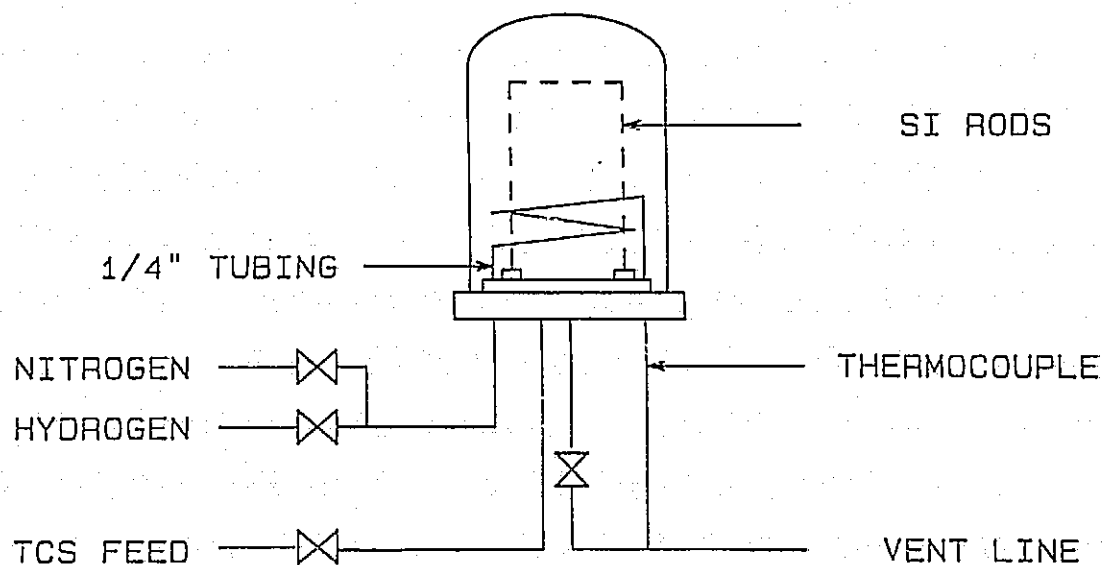
### Materials-of-Construction Test: Objectives

DETERMINE SUITABILITY OF VARIOUS METALS AS LOW COST, HIGH DURABILITY, MATERIALS OF CONSTRUCTION FOR DEPOSITION REACTORS AND COMPONENTS.

IDENTIFY WHICH OF THE MATERIALS WARRANT FURTHER INVESTIGATION BY ESTABLISHING A RANK ORDER ON ADDITION TO SILICON OF:

ELECTRICALLY ACTIVE CONTAMINANTS  
CARBON  
METALLIC IMPURITIES

### Materials of Construction: Reactor Configuration



# Materials-of-Construction Testing Results for Electrically Active Impurities and Carbon

MATERIAL	REACTOR RUN NO.	BORON PPBA	DONOR PPBA	AL (+) AS (-)	CARBON PPMA
BASELINE	394-184	0.11	1.53	0.01	
304 SS	394-185	0.05	1.77	0.03	
304 SS	(1) 394-186	0.07	0.57	0.20	7.36
304 SS	(1) 394-187	0.07	0.84	0.15	
BASELINE	394-188	0.11	0.87	0.12	
MONEL #1	394-189	0.13	1.05	0.17	4.56
MONEL #2 (1)	394-190	0.29	1.08	0.49	3.22
MONEL #3 (1)	394-191	0.04	0.45	0.12	
BASELINE	394-192	0.07	0.51	0.00	
CARBON STEEL #1	394-193	0.07	0.48	0.04	1.49
CARBON STEEL #2	(1) 394-194	0.07	0.98	0.16	8.59
CARBON STEEL #3	(1) 394-195	0.04	1.14	-0.08	
BASELINE	394-196	0.03	0.45	0.10	
HASTALLOY #1	394-198	0.10	1.04	0.10	0.14
HASTALLOY #2	(1) 394-199	0.05	0.43	0.00	9.86
HASTALLOY #3	(1) 394-200	0.08	0.55	0.06	
BASELINE	394-201	0.04	0.49	0.00	
BASELINE	394-202	0.08	0.30	0.03	
316 SS #1	394-203	0.05	1.28	0.41	
316 SS #2	(1) 394-204	0.04	0.33	0.03	5.77
316 SS #3	(1) 394-205	0.03	0.39	0.01	

(1) LOST SINGULARITY.

# SILICON MATERIAL

## Mass Spectrographic Results: ppba in Polycrystalline Silicon

ELEMENT	394-185 304 SS #1	394-186 304 SS #2	394-189 Monel #1	394-190 Monel #2	394-193 Carbon Steel #1	394-194 Carbon Steel #2	394-199 Hastalloy B #2	394-204 316 SS #2
AL	6.0	60	190	57	207	20	18	63
FE	2.9	2.9	81	27	31	31	2.6	93
HI	2.0	1.9	1.8	1.8	2.0	20	1.7	2.0
MG	0.6	5.1	16	4.8	0.6	0.6	1.2	5.4
CR	4.5	1.7	15	15	0.3	0.3	0.3	17
MN	0.1	0.1	0.1	0.1	0.1	0.1	0.3	0.1
CU	19	6.0	54	18	19.5	20	5.1	63
MO	0.5	5.4	5.1	15	0.5	54	5.1	6.1
CO	1.3	1.3	1.2	1.2	1.3	1.3	1.2	1.4
NA	3.9	3.9	3.6	1.4	0.3	0.3	1.0	4.2
TI	0.2	18	17	51	5.4	18	1.5	20
V	0.1	0.1	0.3	0.3	0.1	0.1	0.1	0.1
ZR	0.8	0.8	2.1	0.7	0.8	0.8	0.7	0.8
ZN	0.2	0.2	0.2	0.2	0.3	0.3	0.3	0.3
NB	0.1	0.1	0.1	0.1	0.1	0.1	0.1	0.1
PD	0.5	0.5	0.4	0.4	0.5	0.5	0.4	0.5
AG	0.2	0.2	0.2	0.2	0.2	0.2	0.2	0.3
SN	0.4	0.4	0.4	0.4	0.4	0.4	0.3	0.4
W	0.4	0.4	0.4	0.4	0.4	0.4	0.4	0.5

## Materials-of-Construction Test: Rank Order

ORDER FOR

MATERIAL	ELECTRICALLY ACTIVE	CARBON	METALLIC IMPURITIES
304 SS	3	3	2
MONEL 400	5	1	5
CARBON STEEL	4	4	3
HASTALLOY B	2	5	1
316 SS	1	2	4

## Materials-of-Construction Test: Conclusions

ALL MATERIALS CONTRIBUTED SIGNIFICANT AMOUNTS OF CARBON TO THE DEPOSITED SILICON. USE OF LOW CARBON ALLOYS SHOULD BE CONSIDERED.

NO MATERIAL CONTRIBUTED SIGNIFICANT AMOUNTS OF ELECTRICALLY ACTIVE CONTAMINANTS OR METALLIC IMPURITIES.

FURTHER AND MORE RIGOROUS TESTING WOULD BE REQUIRED TO ACCEPT ANY OF THE MATERIALS FOR CONSTRUCTION OF DEPOSITION REACTORS OR COMPONENTS.

## Overall Project Results

1. DCS WAS EFFICIENTLY PRODUCED AT RATES UP TO 70 LB/HR IN THE PROCESS DEVELOPMENT UNIT, (PDU). EMPIRICAL SCALE-UP METHODS WERE PROVIDED.
2. DOWEX MWA-1 ION EXCHANGE RESIN WAS SHOWN TO BE A GOOD CATALYST WITH VERY LONG LIFE.
3. DCS IS EASILY PURIFIED BY DISTILLATION.
4. DCS DECOMPOSITION WAS SUCCESSFULLY DEMONSTRATED WITH RESULTS.

REACTOR TYPE	HOT WALLED	COOLED WALL	GOAL
DEPOSITION RATE GM/HR/CM	2.0	2.21	2.0
POWER CONSUMPTION KWH/KG	82	59	60
CONVERSION %	35.1	17	40

5. PURITY OF PRODUCT SILICON WAS EXCELLENT.
6. EFFICIENCY OF SOLAR CELLS MADE FROM THIS SILICON WAS APPROXIMATELY 103% OF CONTROL SOLAR CELLS.
7. AN EPSDU DESIGN WAS PREPARED BUT THE EPSDU WAS NOT BUILT.
8. A 1000 MT/YR DESIGN WAS DONE TO FACILITATE ECONOMIC EVALUATION.

## SILICON MATERIAL

### Conclusions

THE HSC LOW COST SILICON PROCESS, BASED ON CHEMICAL VAPOR DEPOSITION OF DICHLOROSILANE, IS A VIABLE PROCESS.

CAPACITY OF SUCH A FACILITY, WHEN OPTIMIZED, WILL HAVE TWICE THE CAPACITY OF A COMPARABLE TRICHLOROSILANE BASED PROCESS.

# REFINEMENT BY SILANE

UNION CARBIDE CORP.

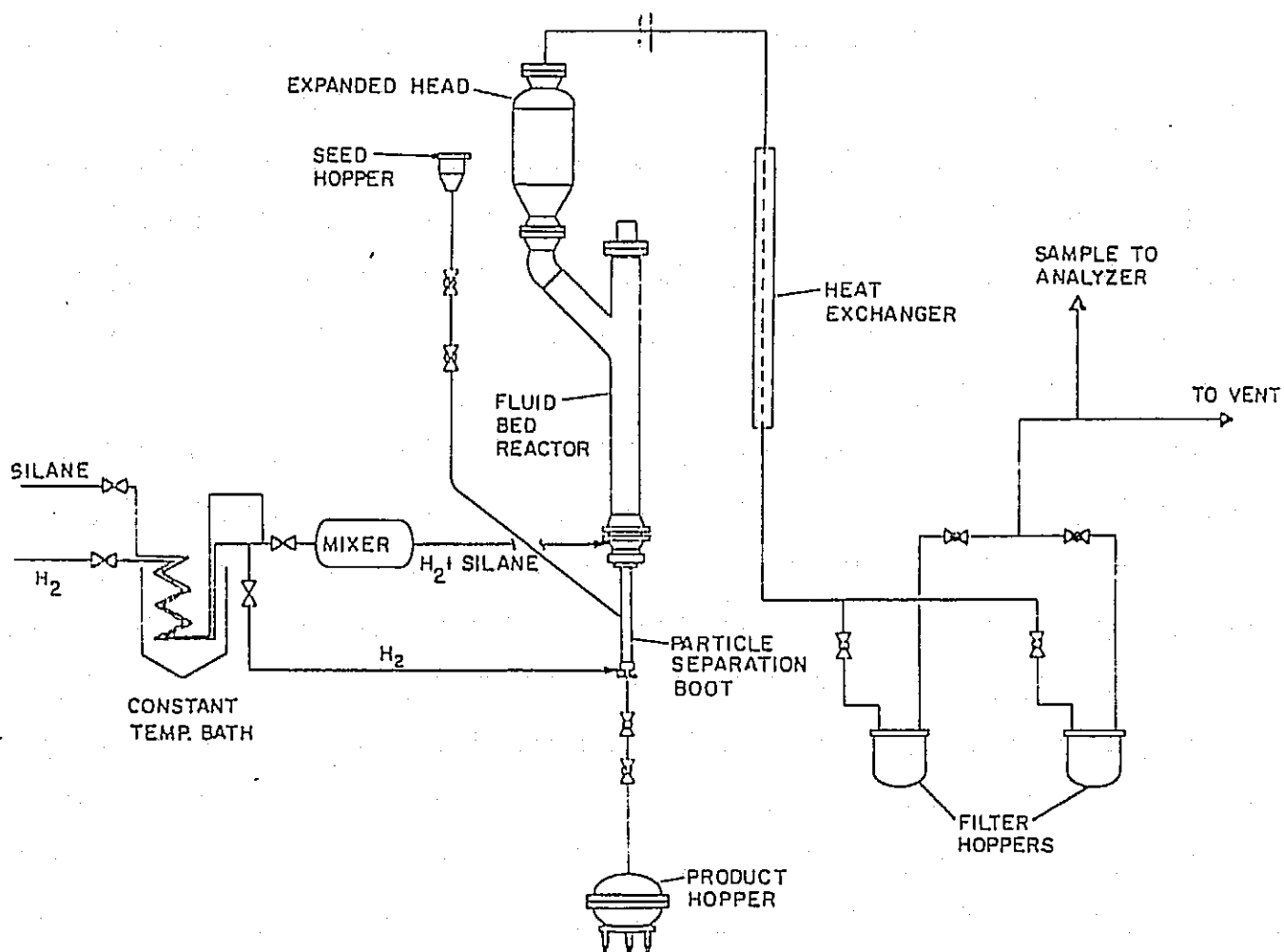
## Silane Decomposition in a Fluidized-Bed Reactor

<b>TECHNOLOGY</b> POLYCRYSTALLINE SILICON R&D	<b>REPORT DATE</b> SEPTEMBER 29, 1983
<b>APPROACH</b> SILANE DECOMPOSITION IN A FLUIDIZED BED REACTOR.  <b>CONTRACTOR</b> UNION CARBIDE CORPORATION	<b>STATUS</b> <ul style="list-style-type: none"><li>• PDU WAS REINSTALLED AT WASHOUGAL, CHECKED OUT AND STARTED UP.</li><li>• PRELIMINARY SHORT DURATION RUNS &amp; COLD FLOW TESTS HELPED TO DETERMINE OPERATING WINDOW.</li><li>• LONG DURATION TESTING IS CURRENTLY IN PROGRESS.</li></ul>
<b>GOALS</b> <ul style="list-style-type: none"><li>• DEMONSTRATE PROCESS FEASIBILITY.</li><li>• DETERMINE OPERATING WINDOW.</li><li>• CONDUCT LONG-DURATION TESTS.</li><li>• DEMONSTRATE SILICON PURITY.</li></ul>	

### Silane Decomposition R&D: Specific Objectives of Current Phase

- COMPLETE THE REINSTALLATION OF FLUID BED PDU AT WASHOUGAL.
- RESTART EXPERIMENTS WITH HIGH PURITY SILANE FROM EPSDU.
- CONDUCT LONG-DURATION TESTS.
- ESTABLISH PRELIMINARY DETERMINATION OF SILICON PURITY.

## Fluid-Bed Reactor PDU





## Run Summary: Short-Duration Tests

RUN NO.	DURATION	MAXI SILANE CONCENTRATION	COMMENTS
C-3	7.5 hrs.	20%	<ul style="list-style-type: none"> <li>• Two-cone distributor</li> <li>• Inadequate U/Umf</li> <li>• Agglomerates</li> </ul>
D-1	2 hrs.	10%	<ul style="list-style-type: none"> <li>• Single cone distributor</li> <li>• Low U/Umf</li> <li>• Improper temp. distribution</li> </ul>
D-2	10 hrs.	21.3%	<ul style="list-style-type: none"> <li>• Low U/Umf</li> <li>• Smooth operation</li> <li>• Voluntary shut-down</li> </ul>
D-3	4.5 hrs	21%	<ul style="list-style-type: none"> <li>• Low U/Umf</li> <li>• Improper fluidization</li> </ul>

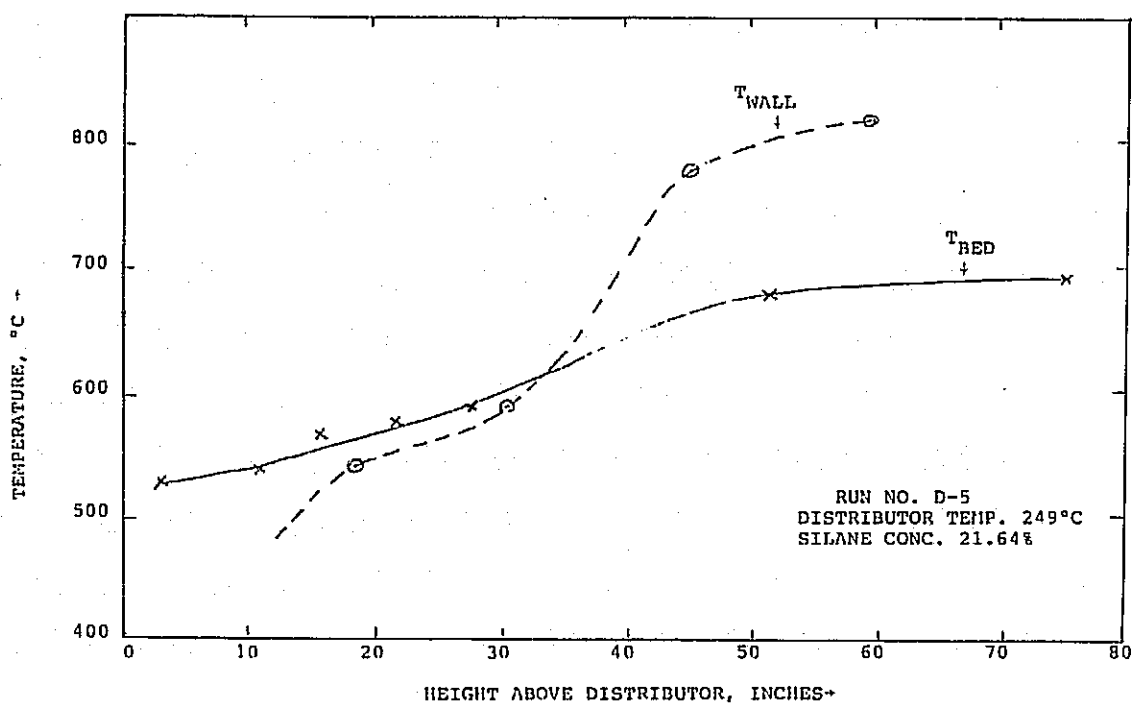
NOTE: Following the above runs, cold model tests were conducted to enable accurate prediction of Umf. Corrected  $\epsilon_{mf}$  &  $\phi$  values were used for subsequent experiments.

## Run Summary: Long-Duration Tests

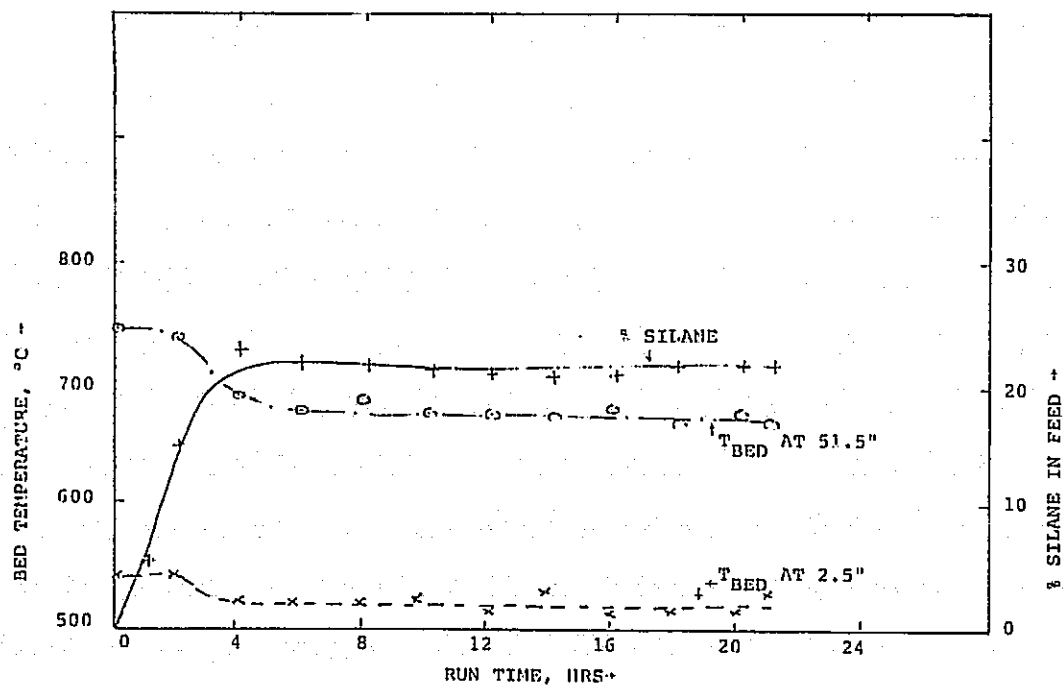
RUN NO.	DURATION	MAX. SILANE CONCENTRATION	COMMENTS
D-4	20 hrs.	23%	<ul style="list-style-type: none"> <li>• Smooth, steady state run</li> <li>• High <math>\Delta p</math> through distributor</li> <li>• Bed volume increased to fill up reactor</li> </ul>
D-5	21 hrs.	21.7%	<ul style="list-style-type: none"> <li>• Smooth, steady state run</li> <li>• Bed volume increased to fill up reactor</li> <li>• Product withdrawal valve rupture</li> </ul>
D-7	14 hrs.	23%	<ul style="list-style-type: none"> <li>• Smooth, steady state run</li> <li>• Shutdown because of silane leak</li> </ul>

# SILICON MATERIAL

## Fluid-Bed Reactor Wall & Bed Temperature Profiles



## Feed Silane & Bed Temperature as a Function of Run Time



## Fluid-Bed Silane Decomposition R&D: Summary

- 6 INCH DIAMETER PDU WAS REINSTALLED AT WASHOUGAL, CHECKED OUT AND STARTED UP WITH HIGH PURITY SILANE.
- SHORT DURATION TESTS (2-10hrs) WERE CONDUCTED TO ESTABLISH OPERATING WINDOW.
- COLD MODEL TESTS WERE CONDUCTED TO DETERMINE PARTICLE PROPERTIES & FLUIDIZATION CHARACTERISTICS.
- LONG DURATION TESTS ARE IN PROGRESS. LONGEST SINGLE RUN TIME TO DATE IS 21 HOURS.
- PRELIMINARY EVALUATION OF SILICON PURITY WILL BE ESTABLISHED BY FY 1983 PROGRAM.

## Areas of Concern and Future Work

- IMPROVED GAS DISTRIBUTOR
  - Closed Loop Oil Cooling
  - Reusable After Cleaning
- CONTAMINATION FROM HOT REACTOR WALL
  - Liner Treatment
- SEED PARTICLE GENERATION
  - Minimize Contamination
- PRODUCT WITHDRAWAL
  - Suitable Valves to Close Against Hot Solid Particles

# JPL IN-HOUSE FLUIDIZED-BED REACTOR RESEARCH

## JET PROPULSION LABORATORY

George Hsu

### Summary of Key 6-in. FBR Experiments (Series II)

RUN No. AND DATE	DISTRIBUTOR	SILICON SEED			EXPERIMENTAL CONDITIONS						PRODUCTION RATE (kg/hr)	OVERALL MASS-BALANCE			
		WEIGHT (kg)	dp (μm)	LEACHING	TEMP (°C)	SILANE CONCENTRATION (%)	DURATION (min)	WU ml		SUPERFI- CIAL VELOCITY cm/sec		% IN BED	% OF DUST IN FILTER	% AS DUST IN LINES	% WALL DEPOSIT
102 3/31/83	ONE LAYER OF 325 MESH SCREEN	11.5	207.4	NO	700	20	74	5	5	13.85	0.78	84.8	14.3	NONE	NONE
							16	3.75	4.0	10.4					
							15	2.5	3.0	6.9					
							OVERALL	-	-	-					
105 4/13/83	MULTILAYER SCREEN DISTRIBUTOR	11.27	214.8	NO	700	20	74	5.0	5.0	14.8	0.96	93.7	3.7	0.87	NONE
109 5/24/83	ONE LAYER OF 325 MESH SCREEN	11.0	226.4	YES	700	20	237	5.0	5.0	16.5	0.99	88	13.2	2.1	NONE
110 6/7/83	MULTILAYER SCREEN	11.0	238.5	NO	700	80	21	5.0	5.0	15.2	3.9	88	4.3	-	NONE
						60	49	5.0	5.0	16.3					
						OVERALL									
111 6/10/83	ONE LAYER OF 325 MESH SCREEN	11.5	238.54	YES	700	30	480	5.0	5.0	18.2	1.93	100	10	0.6	NONE
112 8/17/83	TWO LAYERS OF 325 MESH SCREENS	11.0	196.1	NO	700	80	9	5.0	5.0	10.3	2.6	93.3	9.3	-	-
						60	29	5.0	5.0	11.0					
						OVERALL									

RUN No. AND DATE	DISTRIBUTOR	SILICON SEED			EXPERIMENTAL CONDITIONS						PRODUCTION RATE (kg/hr)	OVERALL MASS-BALANCE			
		WEIGHT (kg)	dp (μm)	LEACHING	TEMP (°C)	SILANE CONCENTRATION (%)	DURATION (min)	WU ml		SUPERFI- CIAL VELOCITY cm/sec		% IN BED	% AS DUST IN FILTER	% AS DUST IN LINES	% WALL DEPOSIT
113 6/23/83	TWO LAYERS OF 325 MESH SCREENS	11.0	220.84	NO	700	80	13	5.0	1.0	13.0	2.9	96.8	6.9	0.5	
						60	53	5.0	1.0						
						OVERALL									
114 7/7/83	TWO LAYERS OF 325 MESH SCREENS	11.0	204.62	NO	650	20	33	5.0	<1	14.4	1.5	89.2	5.3	6.2	0.8
						90	20.3	5.0	<1	12.85					
						60	14.0	5.0	<1	12.41					
						OVERALL									
115 7/13/83	TWO LAYERS OF 325 MESH SCREENS	10.24	231.82	PRODUCT OF RUN No. 111	650	50	300	5.0	<1	16.5	2.8	92.8	7.0	2.3	0.4
116 7/25/83	TWO LAYERS OF 325 MESH SCREENS	9.8	202.48	NO	650	80	27	5.0	<1	11.4	3.0	84.6	10.8	7.3	NONE
117 7/27/83	TWO LAYERS OF 325 MESH SCREENS	10.0	194.26	NO	650	50	59	5.0	<1	11.6	1.8	83.1	7.5	4.2	NONE
119 8/11/83 2nd FBR	TWO LAYERS OF 325 MESH SCREENS	0.8	232.1	YES	650	65	60	5.0	0	15.7	0.31	85	4.6	NONE	2.5
120 8/16/83 20% SILANE INJECT. AT 6 in. ABOVE DISTRIB. 2 in. FBR	TWO LAYERS OF 325 MESH SCREENS	1.0	232.1	YES	650	65	120	5.0	0	15.7	0.33	87	3.0	NONE	6.82

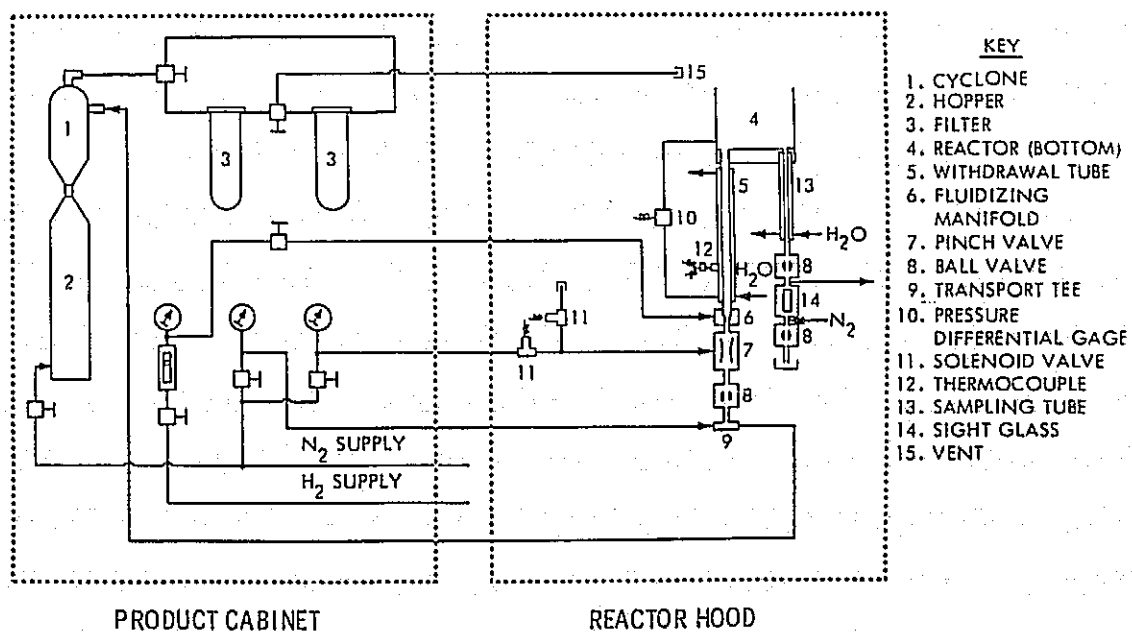
## Significant Progress Since 21st PIM

- NEW FEATURES FOR THE 6-INCH FBR
- IMPROVEMENTS FOR FBR TECHNOLOGY
- PRELIMINARY PREPARATION FOR PURITY INVESTIGATION
- UNDERSTANDING OF FUNDAMENTAL MECHANISM

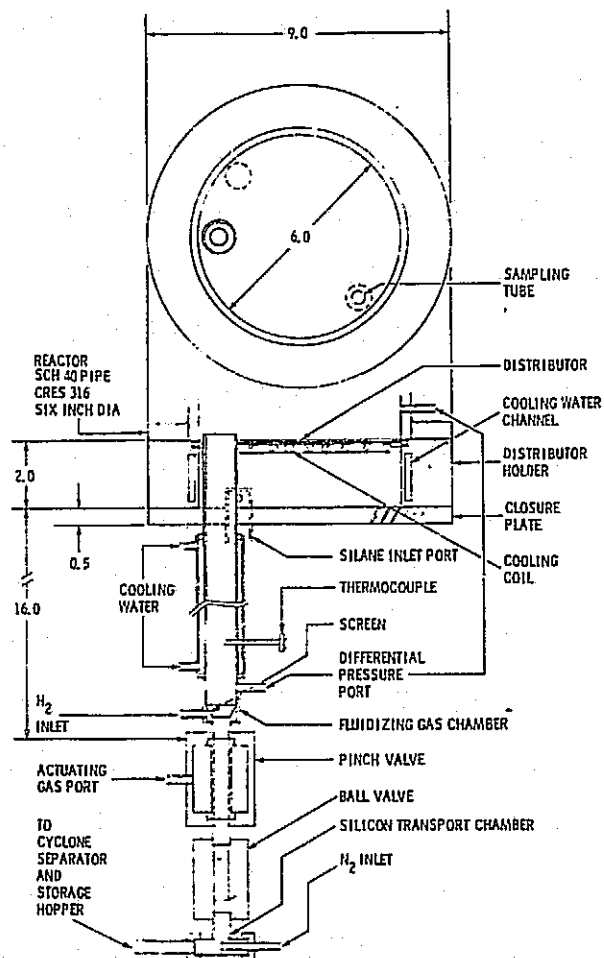
## New Features

- THE 6-INCH FBR IS EQUIPPED WITH A PRODUCT WITHDRAWAL SYSTEM
- IT ENABLES THE CONTINUOUS OPERATION
- A HIGH WITHDRAWAL RATE, 3 KG/HR., HAS BEEN DEMONSTRATED

## Overall Product Withdrawal and Collection System



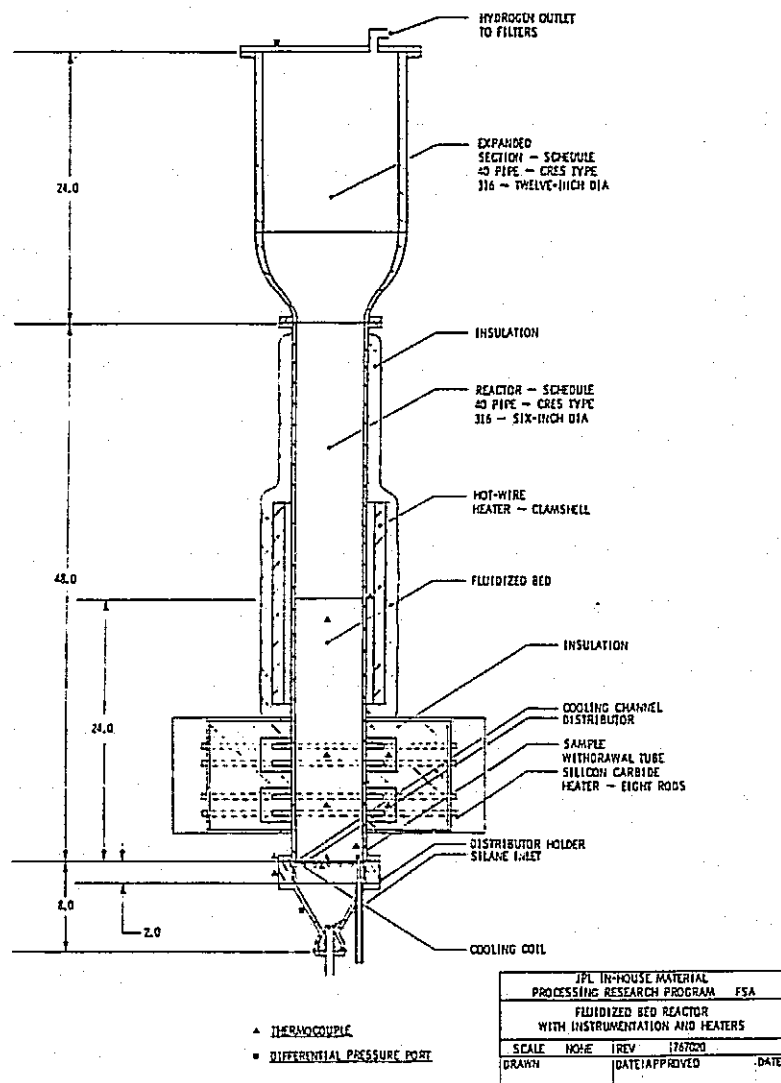
## Silicon Withdrawal System



## Long-Duration Experiment

- A LONG-DURATION EXPERIMENT AT 30%  
SILANE AND 700°C FOR 8 HOURS WAS  
DEMONSTRATED. THE PRODUCT WAS  
CONTINUOUSLY WITHDRAWN AT A RATE  
OF 1.5 KG/HR.

# SILICON MATERIAL



## Improvements in FBR Technology

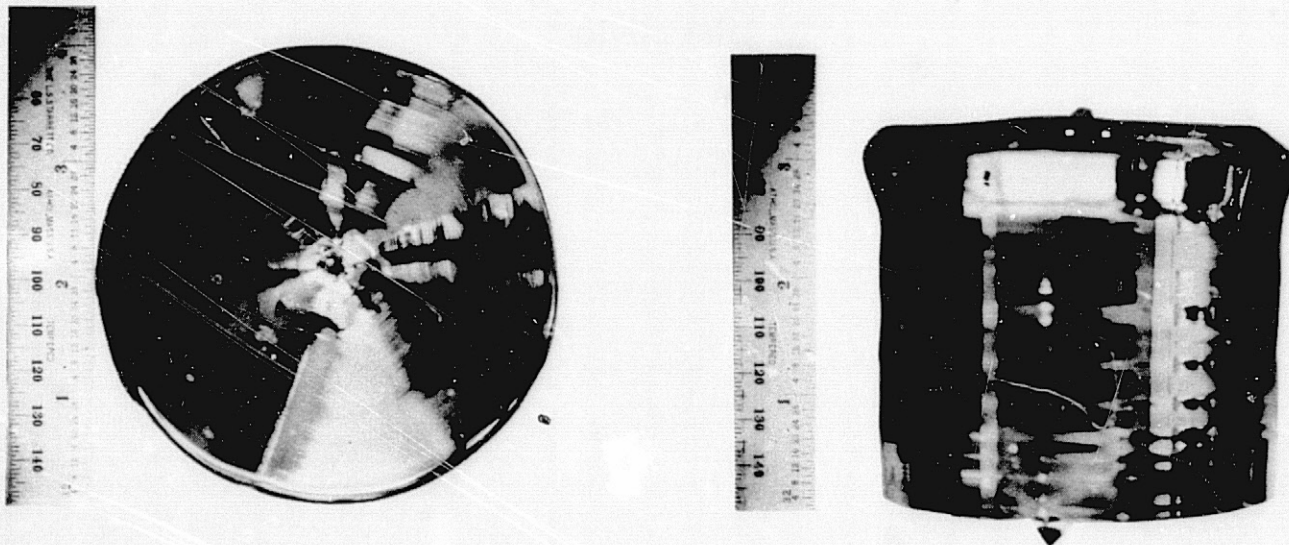
- SMALL OPENING OF DISTRIBUTOR, DOUBLE-LAYER MESH 325 SCREEN
- TEMPERATURE (650°C RATHER THAN 700°C)
- ADDITIONAL INJECTION PORT ABOVE THE DISTRIBUTOR TO ENHANCE THE SCAVENGING EFFECT

## Preliminary Purity Investigation

- AN EXPERIMENT ON HIGH SILANE CONCENTRATION (RUN 115) WAS CONDUCTED AT 630°C AND 50% SILANE CONCENTRATION FOR A DURATION OF 5 HOURS. A TOTAL OF 14 KG OF SILICON WAS PRODUCED AND THE LEVEL OF FINES WAS DETERMINED TO BE 9.3%.
- MELTING OF UNETCHED FBR POLYCRYSTALLINE PARTICLES IN A CRUCIBLE WAS ESTABLISHED:

PARTICLE DENSITY	2.3 GM/CC
BULK DENSITY	1.5 GM/CC
MELTING POINT	1410°C
- A 4-INCH Cz INGOT WAS PULLED.  
AFFECTED BY THE QUALITY OF SEED USED, THE RESULTING INGOT WAS PARTIALLY POLY -  
ALTHOUGH THE MAJORITY WAS SINGLE.

### Cz Ingot From FBR Product (JPL Run #115, 7/13/83)





## Solar-Cell \* Electrical Data

(PRELIMINARY PURITY INVESTIGATION)

	<u>V<sub>OC</sub> (MV)</u>	<u>J<sub>SC</sub> (MA/CM<sup>2</sup>)</u>	<u>CFF (%)</u>	<u><math>\eta</math> (%)</u>
TOP (AVE)	570	28.7	76	12.5
RANGE	564 - 574	27.5 - 29.5	73 - 78	11.7 - 12.9
MID (AVE.)	565	28.9	74	12.1
BOTTOM (AVE.)	567	27.9	77	12.2
C <sub>2</sub> CONTROL	586	30.7	77	13.9

\*2 x 2 (CM) BASELINE CELLS WITH MLAR BY ASEC (9/22/83)

## Resistivity\*

TOP	1.91	OHM-CM
MID	1.83	OHM-CM
BOTTOM	1.83	OHM-CM

\*RESISTIVITY OF WAFERS FROM 4-INCH C<sub>2</sub> INGOT PULLED FROM  
PRELIMINARY FBR PARTICLES.

## Findings on Inductively Coupled Plasma Emission Spectroscopy

- POSSIBLE CONTAMINATION FROM DIGESTION SOLVENTS, HF AND  $\text{HNO}_3$
- DETECTION LIMIT - PPM LEVEL
- REPRODUCIBILITY - POOR

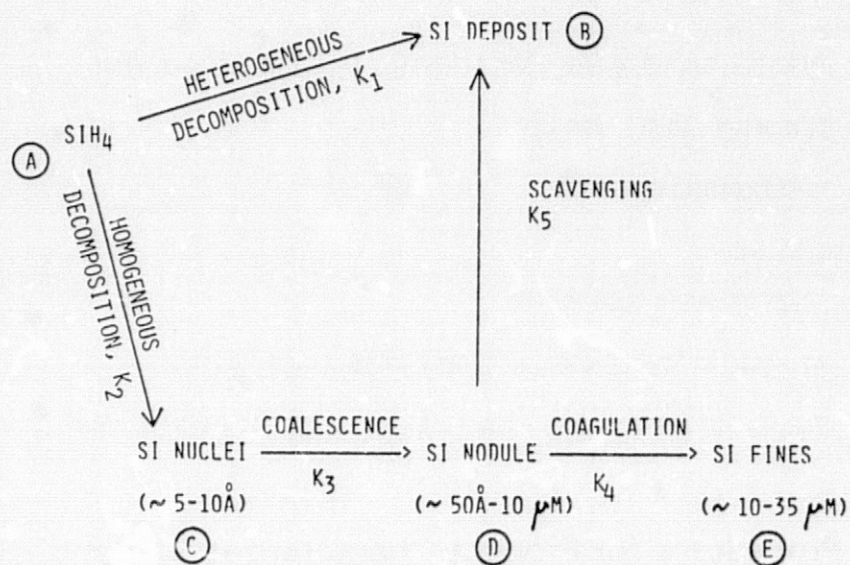
### CONCLUSIONS:

- ICPES IS NOT A GOOD METHOD
- AT MOST, IT CAN BE USED TO SCREEN GROSS CONTAMINATION
- THE WAY TO PREPARE SEED IS A CRITICAL MATTER FROM PURITY POINT OF VIEW

## Procedures for Product Characterization Identified

- IMPURITY CONTENT - NAA  
GROSS CONTAMINATION - ICPES
- RESISTIVITY - CRYSTAL PULL TO WAFER
- CELL EFFICIENCY - WAFER TO CELL
- O, H, C CONTENT (QUALITATIVE) - SECONDARY ION MASS SPECTROSCOPY (SIM)
- CRYSTALLINE STRUCTURE - X-RAY DIFFRACTION
- MORPHOLOGY AND SURFACE GROWTH - SEM (EDAX)
- SIZE DISTRIBUTION - SCREEN ANALYSIS

## Diagram of Fluidized-Bed Silicon Deposition



Nodular Surface Growth of Silicon Seed Particles in FBR (Run #8, 20%  $\text{SiH}_4$  at  $550^\circ\text{C}$ )



## FBR Publications to Come

- "FINES FORMATION IN FLUIDIZED BED SILANE PYROLYSIS" - JOURNAL OF ELECTROCHEMICAL SOCIETY, 1983.
- "FLUIDIZED BED SILICON DEPOSITION" - 1984 IEEE PHOTOVOLTAIC SPECIALIST CONFERENCE AT FLORIDA (FUNDAMENTAL PARTICLE GROWTH MECHANISM)
- "SILICON PRODUCTION IN A FLUIDIZED BED REACTOR" - I & EC PRODUCT R & D (CHEMICAL ENGINEERING REACTOR ASPECTS)

## Future Activities

- PURITY AND PRODUCT CHARACTERIZATION
- SEED PREPARATION

FLUID JET MILLING - INITIAL FEASIBILITY TESTS INDICATED 60% OF THE PARTICLES FRACTURED (FROM 700  $\mu$ M TO MINUS 500  $\mu$ M)

# ELECTROCHEMICAL PRODUCTION OF SILICON

ENERGY MATERIALS CORP.

## Program Objectives

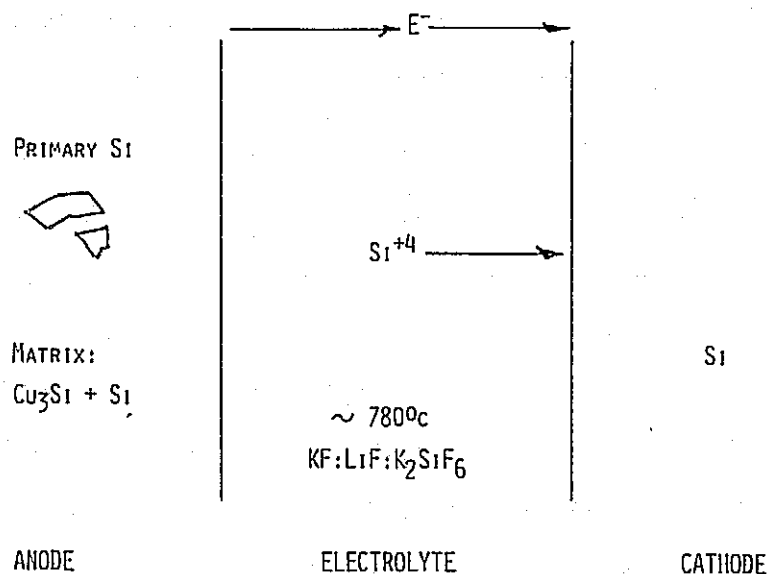
- DESIGN AND BUILD CELL TO PRODUCE 50 GM/HR
- DETERMINE OPERATING CONDITIONS AND RUN CELL CA. 40 HOURS TO PRODUCE 2KG OF SI
- THEORETICAL ANALYSIS AND MODEL OF ANODE IMPURITY AND SI DEPLETION BEHAVIOR, CORRELATE WITH EXPERIMENTAL OBSERVATIONS
- ANALYZE ECONOMIC POTENTIAL OF LARGE SCALE PRODUCTION

## Background

- PROCESS INVENTED AND DEMONSTRATED BY JERRY OLSON OF S.E.R.I.
- KEY ELEMENT IS  $\text{Cu}_3\text{Si}$  - SI ANODE
- LOW TEMPERATURE ( $\sim 1000^\circ\text{C}$ ) FABRICATION OF Mg - SI ANODE
- $D_{\text{SI}} \gg D_{\text{METALS}}$  IN  $\text{Cu}_3\text{Si}$

# SILICON MATERIAL

## Electrorefining Process



## Typical Impurity Concentrations (ppma)

Impurity	MgSi	Electrorefined Si
Al	>3400.0	1.0
B	17.0	0.7
Ba	9.4	<0.02
Ca	290.0	<0.07
Cu	—	0.2
Cr	40.0	<0.2
Fe	>2500.0	0.1
Mg	85.0	0.9
Mn	550.0	0.03
Mo	1.4	<0.03
Ni	39.0	<0.1
P	14.5	3
S	7.0	0.4
Ti	290.0	<0.1
V	250.0	<0.05
Zr	13.0	<0.03

## System Design Considerations

- SI PRODUCTION RATE OF 50 GM/HR
- CAPABILITY OF PRODUCING 2 KG/RUN: ~ 40 HRS
- MINIMAL CONTAMINATION FROM FURNACE ENVIRONMENT

## Experimental Procedure

- DRY SALT MIXTURE:  $350^{\circ}\text{C} + 10^{-3}$  TORR
- MELT SALTS AND PRE-ELECTROLYSIS REMOVAL OF IMPURITIES
- SILICON ELECTROLYSIS:  $100 \text{ MA/CM}^2$
- ANALYZE ANODE (STRUCTURE, IMPURITY DISTRIBUTION),  
ELECTROLYTE PURITY, DEPOSITED SILICON

## Anode Behavior

- IMPURITY DISTRIBUTION
  - MODEL PROFILES ASSUMING DIFFUSIONAL BEHAVIOR
  - SURFACE EFFECTS?
  - SILICIDE FORMATION?
  - DETERMINE IMPURITY DISTRIBUTION AFTER USE
- SILICON DEPLETION
  - MODEL POROSITY CAUSED BY SILICON OUT-DIFFUSION
  - METALLOGRAPHICALLY DETERMINE PORE DISTRIBUTION AFTER USE

## Progress

- MAJOR EQUIPMENT ITEMS IN-HOUSE
- DESIGN PHASE ESSENTIALLY COMPLETE
- MODELLING EFFORT INITIATED

## Plans

- COMPLETE FABRICATION OF SYSTEM
- OPERATE SYSTEM AND ANALYZE ANODE BEHAVIOR, ELECTROLYTE PURITY
- CORRELATE OBSERVATIONS WITH THEORETICAL MODELS

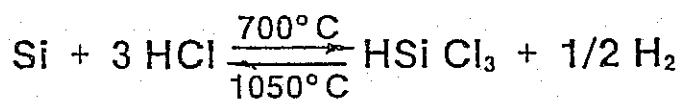
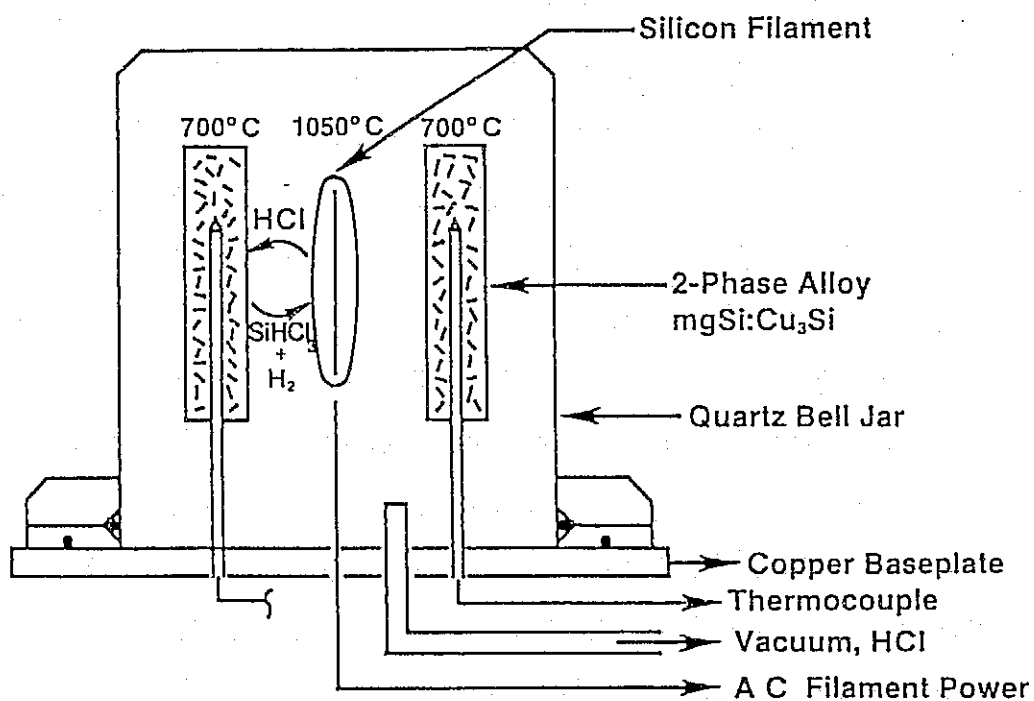


# ENHANCED SILICON PURIFICATION IN A CHEMICAL VAPOR TRANSPORT SYSTEM

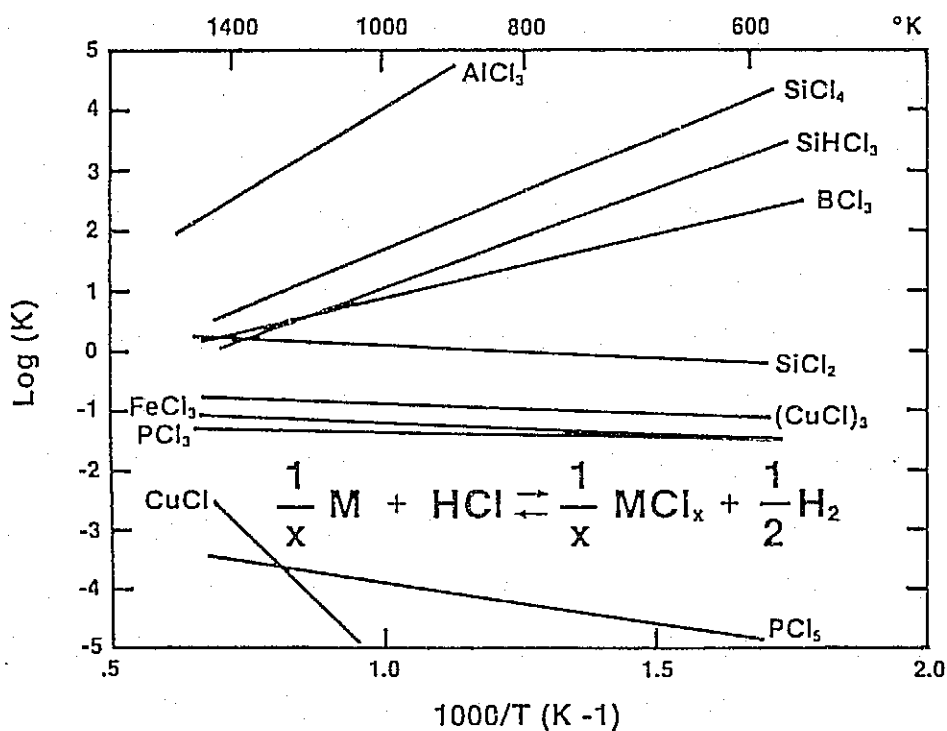
SOLAR ENERGY RESEARCH INSTITUTE

R. Powell  
J.M. Olson

Reactor



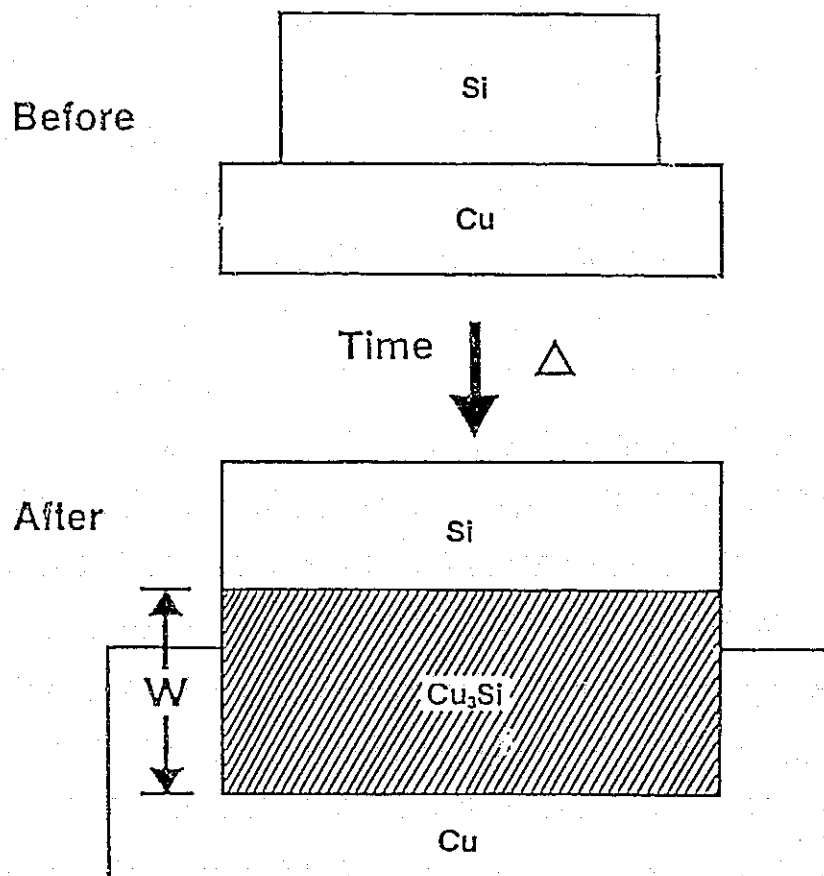
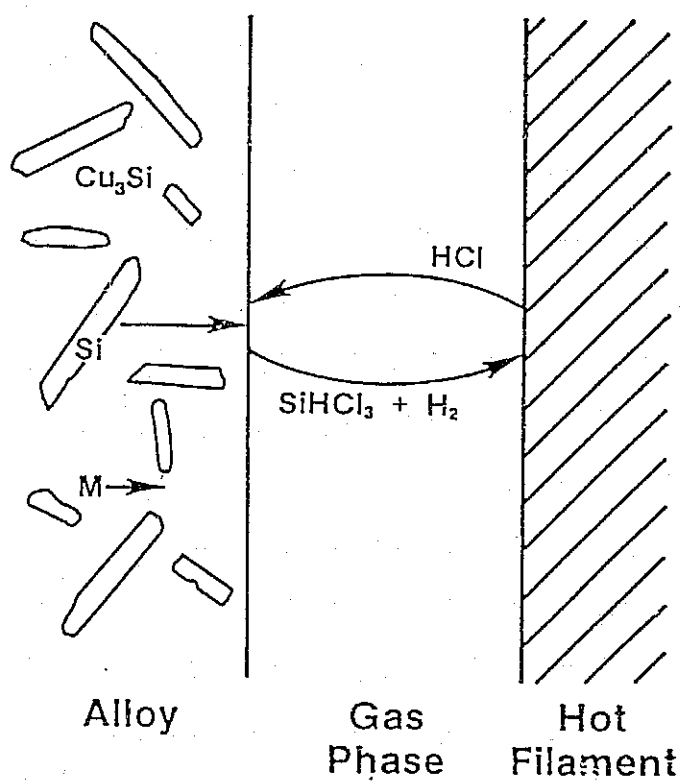
# SILICON MATERIAL



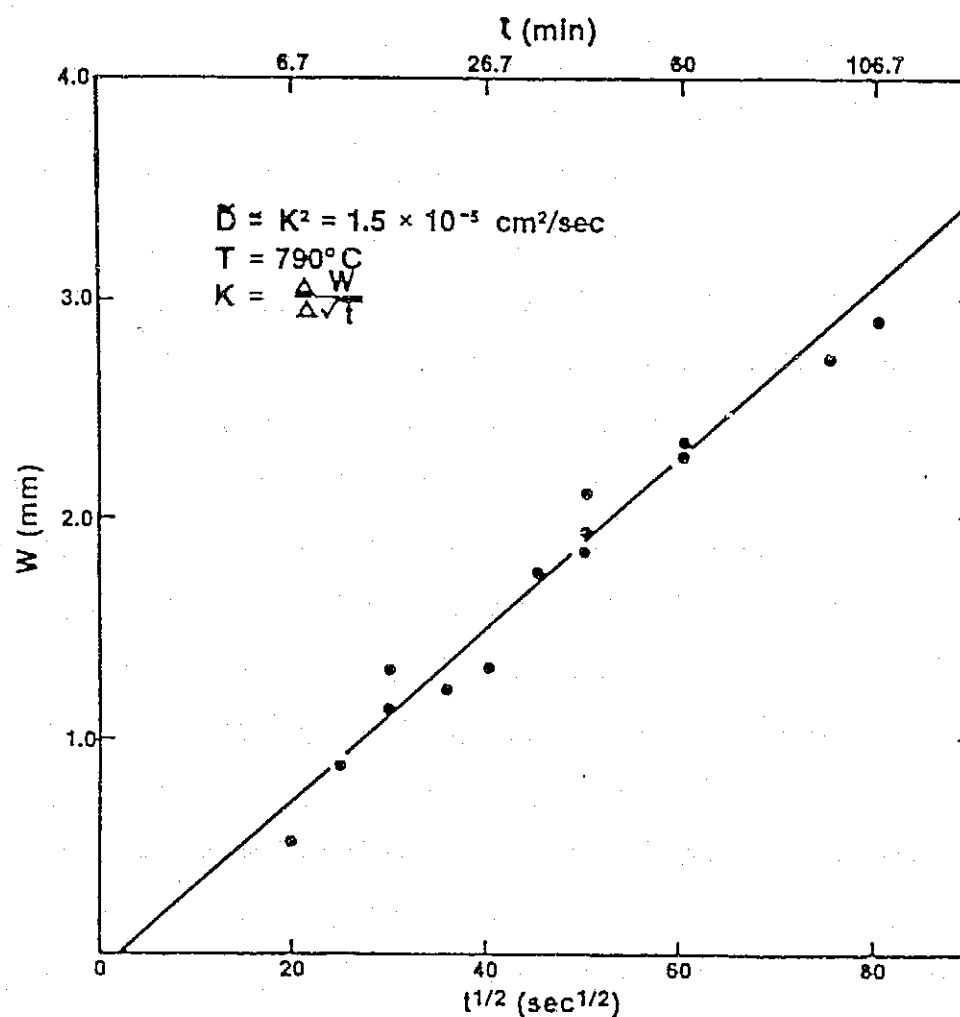
Impurity	mgSi (ppma)	CVT Refined (ppma)	CZ Recrystallized (ppba)	Degradation Threshold† (ppba)
Cu	—	0.12 - 0.15	0.05 - 0.06	200
B	117	< 0.26	< 210	—
P	15	0.16 - 1.8	56 - 630	10 <sup>4*</sup>
Al	> 3400	< 0.1 - 0.98	< 0.2 - 2	20
Fe	> 2500	< 0.13 - 0.50	< 8.3 × 10 <sup>-4</sup> - 3.2 × 10 <sup>-3</sup>	1
Mn	550	< 0.15	2.0 × 10 <sup>-3</sup>	2
Ca	290	< 0.07 - 0.2	—	—
Ti	290	< 0.06	< 1.2 × 10 <sup>-4</sup>	0.02
V	250	< 0.055 - 0.44	2 × 10 <sup>-4</sup> - 2 × 10 <sup>-3</sup>	0.02
Ni	39	< 0.13 - 1.9	< 0.02 - 0.25	< 1
Zr	13	< 0.09	< 1.5 × 10 <sup>-6</sup>	—
Mo	1.4	< 0.09	< 4.0 × 10 <sup>-6</sup>	< 10 <sup>-3</sup>

†R. H. Hopkins, et. al. (n-type base)

\*p-type base



# SILICON MATERIAL



## Electrical Properties

CONDUCTIVITY TYPE

N

RESISTIVITY AS GROWN:

$0.1 - 1 \text{ } \Omega\text{-CM}$

RESISTIVITY AFTER RECRYSTALLIZATION:

$0.08 \text{ } \Omega\text{-CM}$

HALL MOBILITY:

$524 \text{ cm}^2/\text{V-SEC}$

CARRIER CONCENTRATION:

$1.45 \times 10^{17} \text{ cm}^{-3}$

## Deposition Results

$T_{\text{ALLOY}}$  = 700° C  
 $CL/H$  = 0.3  
 $P$  = 650 TORR  
 $DEP \cdot AREA$  = 20  $CM^2$

$MASS \text{ FLUX}$  = 0.5  $G \text{ CM}^{-2} \text{ HR}^{-1}$

$SPACE\text{-}TIME \text{ YIELD}$  =  $10^{-3} \text{ HR}^{-1}$

## Summary

- Simple closed system
- Solid state purification mechanism
- Inherent radiation shields
- Recyclable copper

# PROBABILISTIC ANALYSIS OF SILICON COST

## JET PROPULSION LABORATORY

L. Reiter

The objectives of this analysis are threefold: to approach the question of silicon cost from a probabilistic viewpoint, to determine how the Silicon Materials Task is doing vis-a-vis the DOE program goals, and to provide a broader basis for planning and analysis. The viewgraphs provide a general outline of the study: its approach, assumptions, limitations, and results.

There is some information that makes the presentation easier to understand: in the assumptions section, the 20% property tax rate, 16% debt, etc. These are all standard IPEG economic assumptions (see IPEG Computer Program User's Guide, JPL Internal Document No. 5101-156, Rev. A). The cost-estimating multipliers are based on work done under JPL Contracts Nos. 956045 and 954343 by the Texas Research and Engineering Institute and by Lamar University, respectively. These studies treated total plant investment as a multiple of equipment cost.

In the limitations section: it is important to bear in mind the limitation on the cost results. These costs, which include profit, are not intended to reflect actual market prices but rather to predict technologically achievable costs. No attempt was made to include market conditions (e.g., glut or surplus) or corporate strategies (e.g., one company undercutting another to take a larger market share). These costs are in the proper format for comparison with DOE goals.

Results are presented as cumulative probability curves; any point on the curves represents a cost in 1982 \$/kg for a technology and a probability that the actual technologically achievable cost will be equal to or less than that cost. The three curves were derived independently from the computer model.

The composite curves were produced by allowing the technologies to compete within the computer model, which randomly selects a point on each of the three technology curves and compares them for lowest cost. This was done for 2500 scenarios. As expected, the Union Carbide Corp. fluidized-bed reactor (FBR) dominates. The next curve does not include the FBR process, since it is on a longer time line than the other 10 processes. In both composite curves a \$60/kg default cost was included along with a probability of unsuccessful development for each process: 5% for the FBR, 2% each for the other two. The curve shows that the probability that none of the processes will be successfully developed (from an R&D perspective) is very small. Commercialization strategy considerations are not included.

The final viewgraph that needs explanation is the one on cost sensitivities. For each technology, the base (median or 50%) case is plotted. Each variable is then allowed to vary over its entire range, one at a time. The resulting graphs show the sensitivity of silicon cost to each variable. Note that the EQPT bars on the graph are actually the total plant investment for each process (including the multipliers mentioned above) and that the scale on the Union Carbide Komatsu process is different.

## Silicon Cost Study

- Reduction of silicon price necessary to produce low-cost PV modules
- Previous analyses based on point estimates: no information about uncertainty, risk vs payoff
- Probability of achieving DOE program goals
  - \$20/kg (1982 \$) low-cost
  - \$16/kg target
- Basis for future planning or analyses

## Study Outline

- Focus on PV program processes, semiconductor grade
  - Hemlock semiconductor DCS process
  - Union Carbide silane process with:
    - (1) Komatsu reactor
    - (2) Fluidized-bed reactor
- Approach
  - Develop cost-estimating methodology
  - Obtain data
  - Perform analysis based on the data
- Assumptions and limitations
- Results
  - Silicon cost distributions
  - Cost drivers
- Conclusions

## Approach

- Derive and validate IPEG equation
- Encode data from
  - JPL experts
  - Industry
  - Literature
  - 23 distributions in all
- Analyze results using SIMRAND
  - Monte Carlo simulation
  - Sum inputs
  - Perform IPEG cost-estimating
  - Two cycles through analysis

## Assumptions

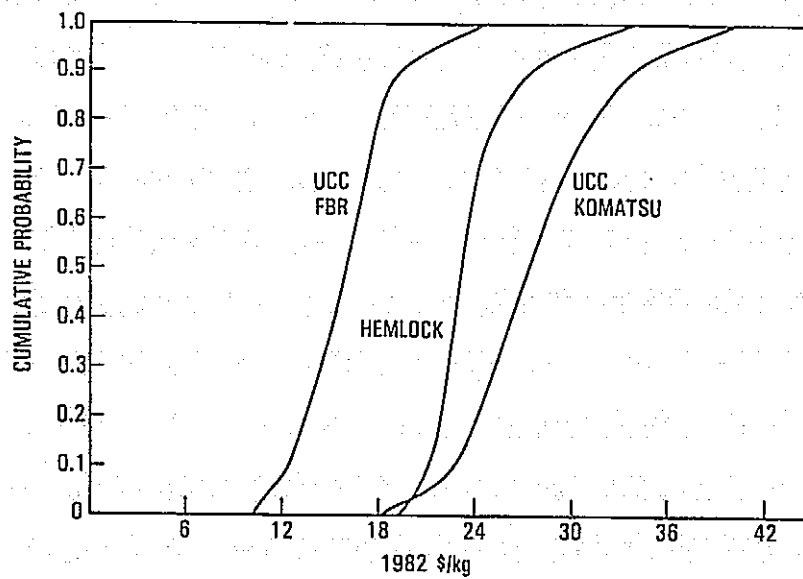
- Process plants
  - Not a prototype
  - Steady-state operation
  - 1000 MT/yr
- DOE funding
- Economics
  - 20% return on equity
- Cost-estimating multipliers
  - From Lamar/TREI
  - Based on equipment cost
  - 15% contingency
  - 10-year equipment lifetime



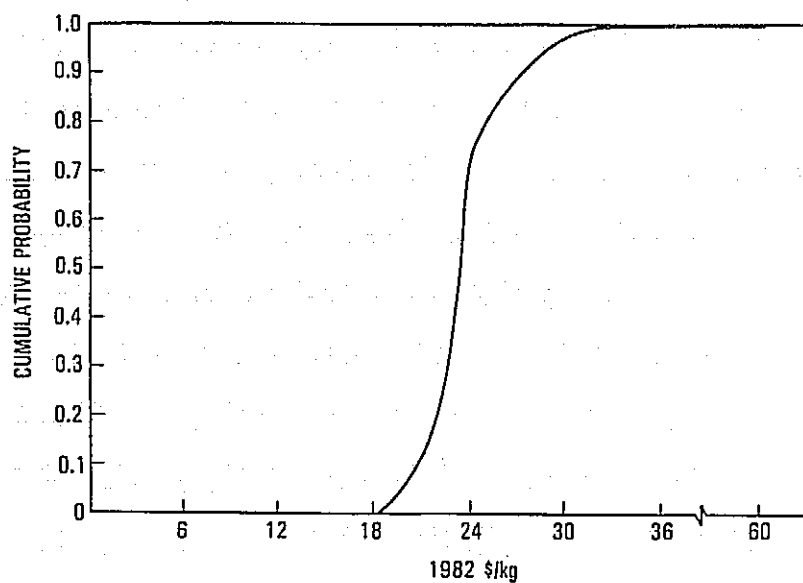
## Limitations

- Data
  - 23 distributions — limited to 3 processes
  - Some issues were proprietary
- Cost results
  - Technically achievable cost (including profit)
  - Does not include market conditions or corporate strategy

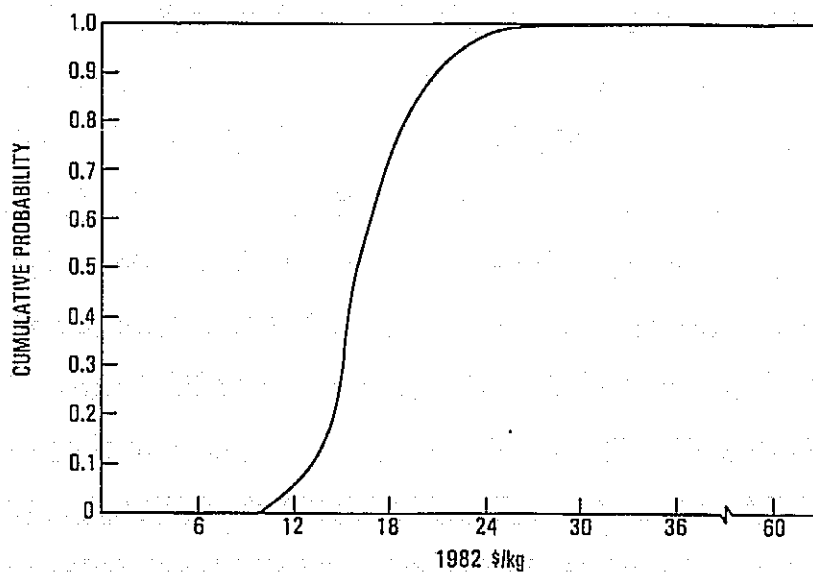
## Results



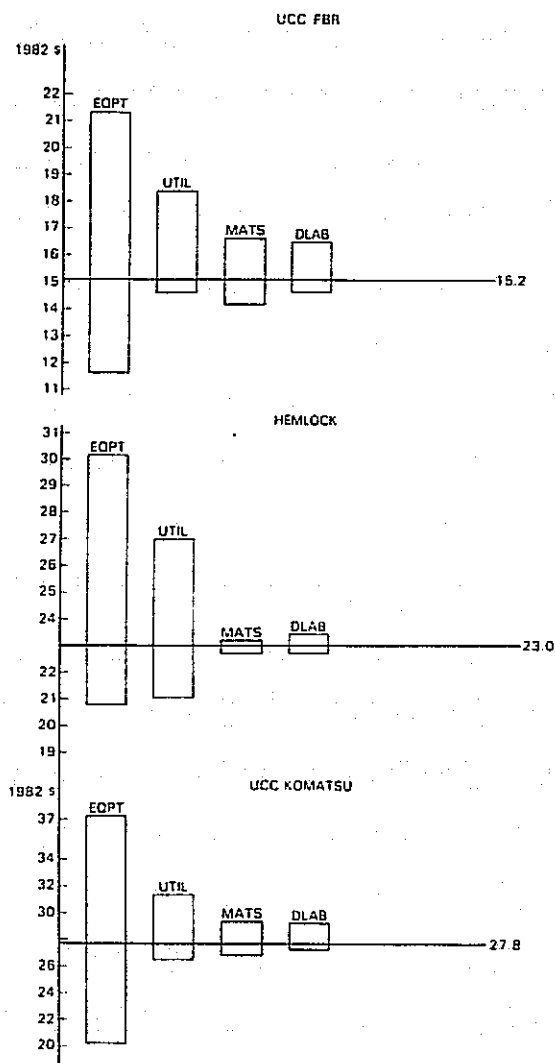
### Composite Silicon Cost: No FBR



### Composite Silicon Cost



## Cost Sensitivities



## Conclusions

- Long-term silicon prices are 90% likely to be \$20 (1982 \$) or less
- Nearer-term silicon prices are 90% likely to be \$27 (1982 \$) or less
- These are technologically feasible prices; market and strategic considerations are not included
- There is a 55% chance of meeting the DOE target for the silicon materials

# DEVICE STRUCTURE AND ANALYSIS

C.T. SAH ASSOCIATES

C.T. Sah

## Objectives

### □ TASK 1

Theoretical and experimental studies of impurity related energy levels, densities of levels and electron-hole thermal capture-emission rates at these levels.

### □ TASK 2

Generation of mathematical models to describe experimental results on, and to specify materials properties and device structures required for very-high-efficiency solar cells.

## Progress Summary

### □ TASK 1

Thermal capture rate measurements on the two Titanium double-donor levels are near completion using a new variation of the Capacitance Transient Spectroscopy method which gives all four majority and minority carrier capture rates on one diode. Will be reported in the future.

### □ TASK 2

Optimum base design analysis on about 100 extended BSF cells are completed. Report was distributed in the mail. Will be summarized in this presentation.

## SILICON MATERIAL

<b>TECHNOLOGY</b> MATERIAL LIMITATIONS ON HIGH EFFICIENCY SOLAR CELL PERFORMANCE	<b>REPORT DATE</b> 09/29/1983 22nd PIM (15 months)
<b>APPROACH</b> ANALYSIS OF EFFECTS OF DRIFT FIELD ON THIN-BASE SILICON CELL PERFORMANCE  <b>CONTRACTOR</b> C. T. SAH ASSOCIATES	<b>STATUS</b> <input type="checkbox"/> COMPUTER-AIDED ANALYSIS (CAA) USING THE EXACT TRANSMISSION LINE METHOD. <ul style="list-style-type: none"> <li>• ABOUT 100 CELLS ANALYZED,</li> <li>• INTERBAND AUGER RECOMBINATION LIMIT IN              THE EMITTER DEMONSTRATED.</li> <li>• RESULTS REPORTED IN FIRST TECHNICAL              REPORT (DOE/JPL-956289-83/1, July 1983).</li> </ul>
<b>GOALS</b> <ul style="list-style-type: none"> <li>• DETERMINE THE IMPROVEMENT OF THE              TOLERANCE TO RESIDUAL RECOMBINATION              IMPURITIES AND PHYSICAL DEFECTS BY              EXTENDING THE BACK SURFACE FIELD              DEEP INTO THE BASE OF THIN-BASE              SILICON SOLAR CELLS.</li> </ul>	<input type="checkbox"/> THERMAL CAPTURE RATE DETERMINATION. <ul style="list-style-type: none"> <li>• NEW CAPACITANCE TRANSIENT METHOD DEVE-              LOPED GIVING BOTH ELECTRON AND HOLE              CAPTURE RATES ON ONE DIODE.</li> <li>• MEASUREMENTS ON DOUBLE-DONOR TITANIUM              CENTER NEAR COMPLETION.</li> </ul>

## Outline

- ☐ REVIEW OF ANALYSIS METHOD
  - Mathematical Technique
  - Computer Model
  - Device and Material Parameters
- ☐ RESULTS OF OPTIMUM CELL DESIGNS
  - P+/N/N+ Low Resistivity Cells
  - Base Resistivity Effects
  - Immunity to Base Recombination
  - Emitter Interband-Auger-  
 Recombination Limited Performance
- ☐ SUMMARY
- ☐ PLAN

## Summary

- 20  $\mu\text{m}$  EXBSF sufficient to reach 20% EFF plateau for 50  $\mu\text{m}$  cells with 20  $\mu\text{s}$  base lifetime.
- EFF improved by extending the BSF from 2  $\mu\text{m}$  (18%) to 20  $\mu\text{m}$  (20%).
- Immunity to recombination density improved by a factor of 2.5 by extending BSF from 5  $\mu\text{m}$  to 40  $\mu\text{m}$  at  $10^{12} \text{ cm}^{-3}$ .
- P+/N/N+ better than N+/P/P+ due to interband Auger recombination in the emitter.
- Emitter recombination limiting JSC and EFF in EXBSF cells.

## Plan

- Analysis for optimum emitter design.

## Computer-Aided Analysis (CAA) Using the Exact Transmission Line Model

• Numerical Solution of the Solar-Cell or Semiconductor Equations using a FORTRAN program, the CIRCUIT TECHNIQUE FOR SEMICONDUCTOR-DEVICE ANALYSIS (CTSA)

- △ 7 General Semiconductor Equations
- △ Expanded to 7 Steady-State Equations plus 7 Small-Signal or Small-Error Equations
- △ Synthesize the two corresponding transmission line circuits with 198 lump sections each for the cell.
- △ Make an initial guess of the d.c. electric potentials at equilibrium (dark and zero bias).
- △ Get the values of the small-error circuit elements.
- △ Solve, by matrix inversion of the  $199 \times 3$  small-error matrix, to get the corrections of the 199 d.c. potentials.
- △ Iterate until the change is less than  $10^{-6}$ .
- △ Increase the photocurrent,
- △ Repeat the iteration as above until convergence is reached for the three potentials (quasi-Fermi potentials for electrons, holes and the electric potential) at the 199 nodes.
- △ Repeat above until photocurrent reaches AM1. JSC is obtained.
- △ Step d.c. voltage by 50 mV.
- △ Repeat above until zero current is reached. VOC is obtained.
- △ Least Squares Fit around maximum power point.
- △ Computer EFF and EE at Pmax.
- △ Computation completed for one cell.

## SILICON MATERIAL

### •COMPUTER MODELS

- Δ Nonuniform size of the 198 lumped sections required.
- Δ Four regions are required: (LUMPS)
  - \*Diffused Emitter Layer 25
  - \*Junction Space-Charge Layer 50
  - \*Quasi Neutral Base Layer 73
  - \*Extended Back Surface Field 50
- Δ Adjacent lump section size must not differ by more than 3.
- Δ Different lump numbers required for different base doping.

### •DEVICE AND MATERIAL PARAMETERS

- ## See Next Three Viewgraphs ##
- Δ Dopant and Recombination Impurity Concentration Profiles.
- Δ Interband Auger and Double Acceptor Zinc Recombination Rate Parameters.
- Δ Examples of Steady-State Local Lifetimes.
- ΔΔ DETAILS GIVEN IN TWO ARTICLES IN IEEE TRANSACTION ON ELECTRON DEVICES.

### ≡ OPTIMUM CELL DESIGNS ILLUSTRATED

#### •P+/N/N+ Low Resistivity ( $10^{17}\text{cm}^{-3}$ )

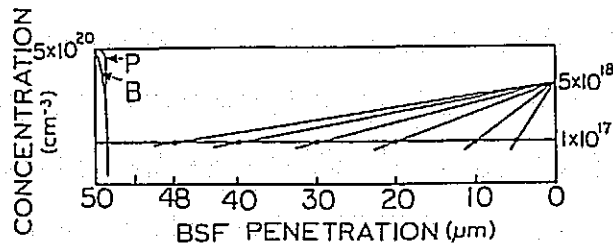
- Δ 20% EFF reached for 20  $\mu\text{m}$  EXBSF.
- Δ 18% EFF or less for 2  $\mu\text{m}$  BSF.
- ΔΔ 20  $\mu\text{s}$  base lifetime.
- ΔΔ 50  $\mu\text{m}$  cell thickness.

#### •Base Resistivity Effects (P+/N/N+)

- ΔΔ 20  $\mu\text{s}$  base lifetime at  $1.0 \times 10^{17}\text{cm}^{-3}$
- ΔΔ 25  $\mu\text{s}$  base lifetime at  $5.0 \times 10^{15}\text{cm}^{-3}$
- Δ High level effect in base. FF
- Δ Base recombination effect. JSC
- Δ Base minority carrier conc. VOC
- Δ Base minority carrier conc. EFF



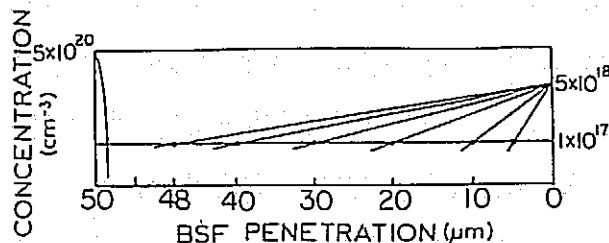
## Device and Material Parameters Used



- $C_0 = 2.5 \times 10^{20} \text{ cm}^{-3}$  Front Surface
- $C_B = 1.0 \times 10^{17} \text{ cm}^{-3}$  Bulk Doping (Constant)  
or  $5.0 \times 10^{15} \text{ cm}^{-3}$
- $C_L = 5.0 \times 10^{18} \text{ cm}^{-3}$  Back Surface
- $N_{TT} = 1.0 \times 10^{12} \text{ cm}^{-3}$  Double Acceptor Zn Recombination Center (Constant)

### • IMPURITY CONCENTRATION PROFILES

- Δ Boron:  $1 - Z^{2/3}$
- Δ Phosphorus:  $\exp(-Z^6)$  NORMAL
- Δ Phosphorus:  $1 - Z^{2/3}$  B-LIKE (emitter only)
- Δ Zinc: Constant



### • INTERBAND AUGER RECOMBINATION

$$C_n^n = C_p^n = 2.80 \times 10^{-31} \text{ cm}^6/\text{s}$$

$$C_p^p = C_n^p = 0.99 \times 10^{-31} \text{ cm}^6/\text{s}$$

### • ZINC (Double Acceptor)

$$\Delta E_V + 664 \text{ meV}$$

$$C_{n1} = 2.0 \times 10^{-12} \text{ cm}^3/\text{s}$$

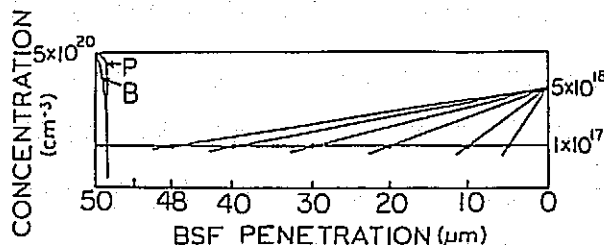
$$C_{p2} = 6.0 \times 10^{-8} \text{ cm}^3/\text{s}$$

$$\Delta E_V + 326 \text{ meV}$$

$$C_{n0} = 2.0 \times 10^{-8} \text{ cm}^3/\text{s}$$

$$C_{p1} = 5.0 \times 10^{-8} \text{ cm}^3/\text{s}$$

## SILICON MATERIAL



STEADY-STATE LOCAL LIFETIMES  $N_{TT}=10^{12}$

④ BASE ( $x=0.7\mu m$ )  $C_B=10^{17}$   $E_V+326$  meV

• p+/n/n+ 20  $\mu s$

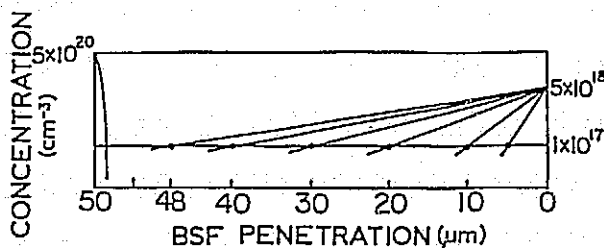
• n+/p/p+ 50  $\mu s$

④ EMITTER ( $x=0.17\mu m$ ) Auger

• p+/n/n+ 3140 ps

• n+/p/p+ 269 ps NORMAL

• n+/p/p+ 1113 ps B-LIKE



### Effect of Zinc Impurity on Silicon Solar-Cell Efficiency

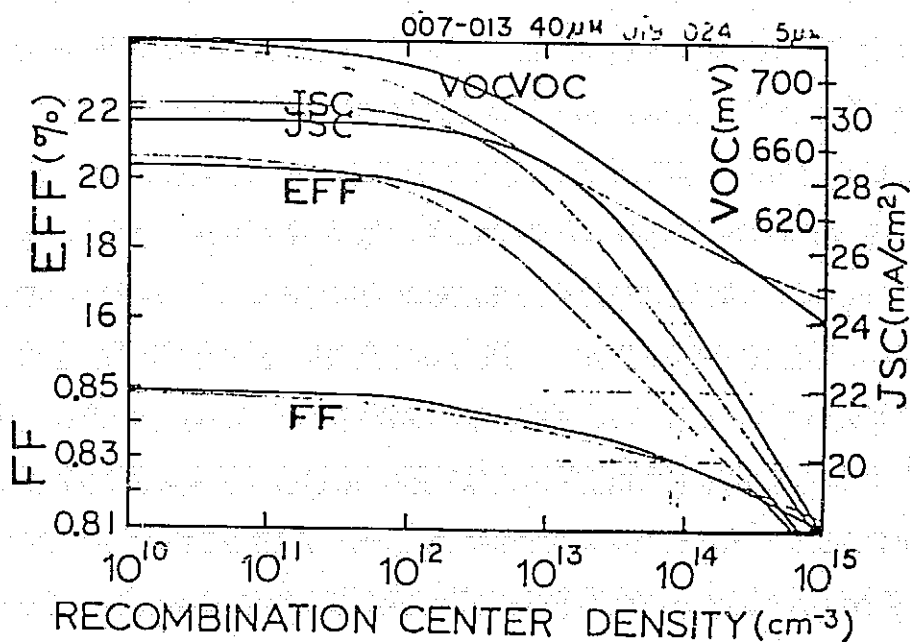
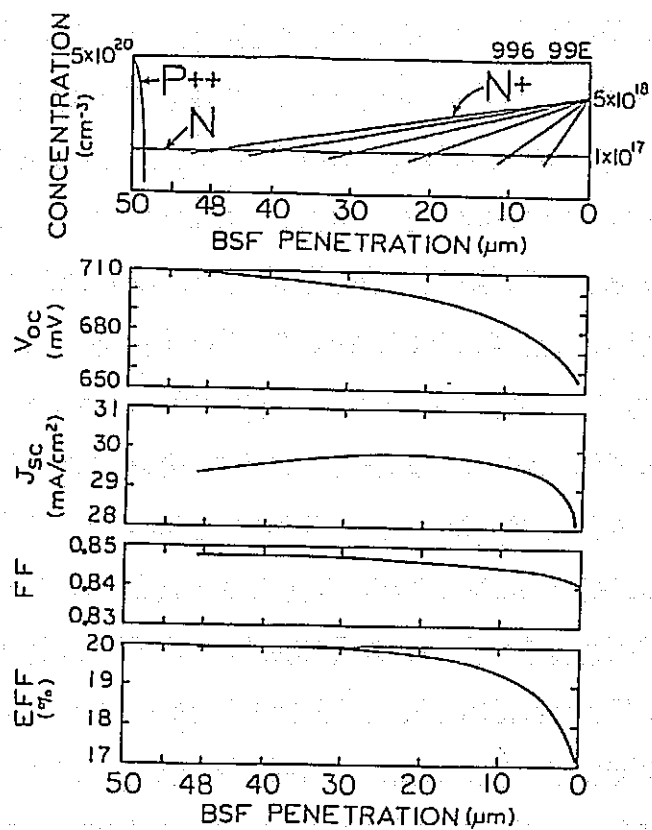
CHIH-TANG SAH, FELLOW, IEEE, PHILIP CHIO'S HO CHAM, CHI-KUO WANG, ROBERT L-Y. SAH, STUDENT MEMBER, IEEE, K. ALAN YAMAKAWA, AND RALPH LUTWACK

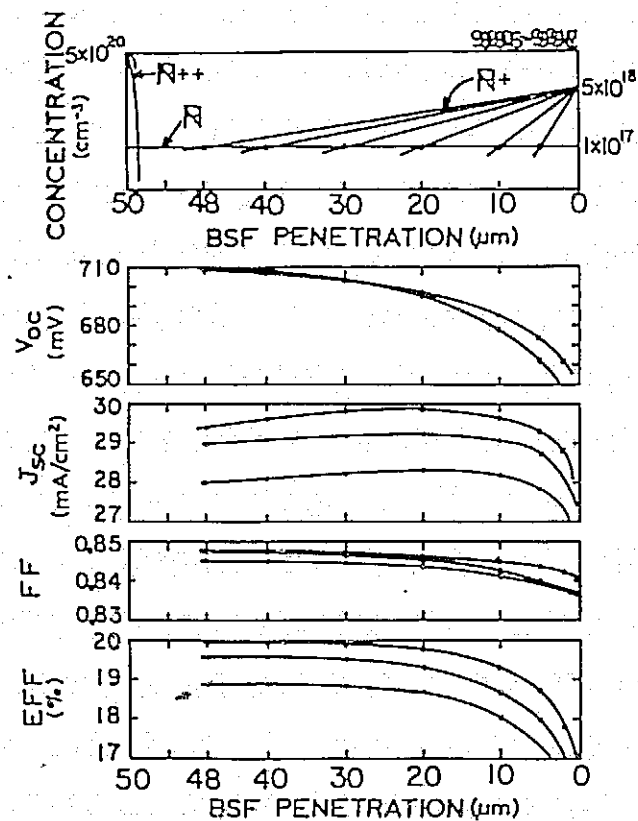
IEEE TRANSACTION ON ELECTRON DEVICES  
VOL. ED-28, 304-313, MARCH 1981

### Effect of Thickness on Silicon Solar Cell Efficiency

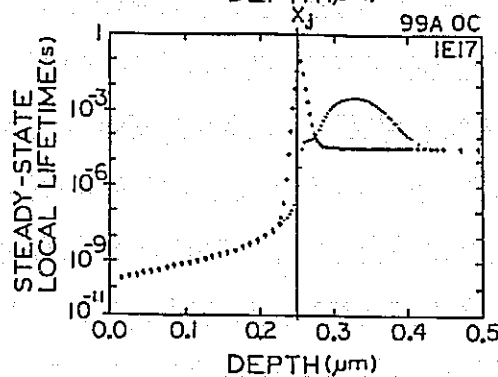
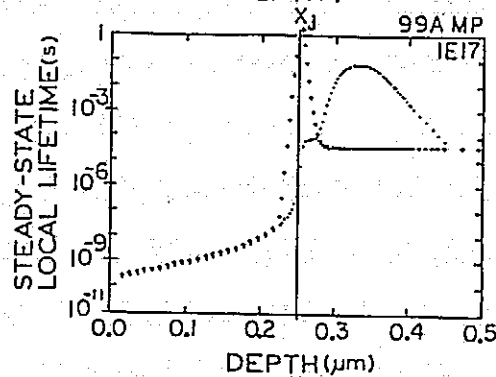
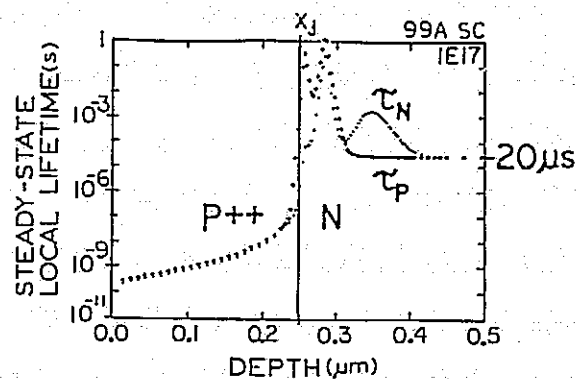
CHIH-TANG SAH, FELLOW, IEEE, K. ALAN YAMAKAWA, AND RALPH LUTWACK

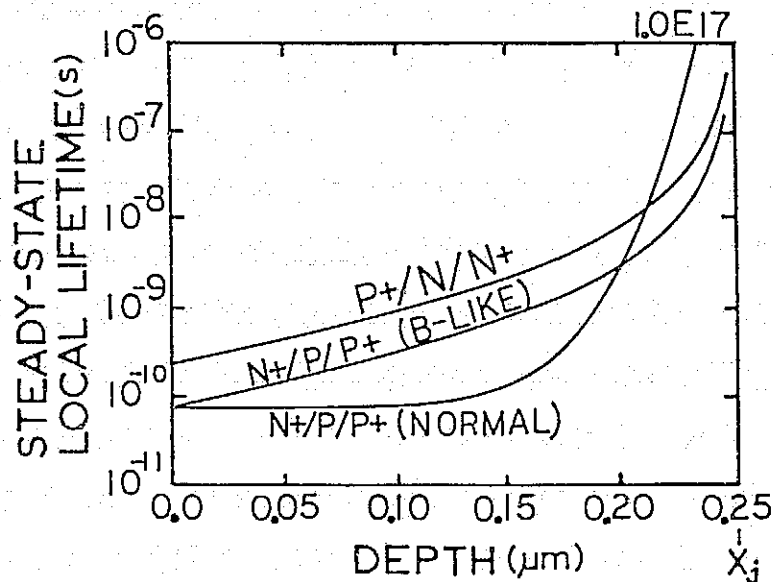
IEEE TRANSACTION ON ELECTRON DEVICES  
VOL. ED-29, 903-908, MAY 1982





# SILICON MATERIAL





### • OPTIMUM EMITTER $\lesssim 20\%$

- $\Delta E_G$  carrier screening
- F-D statistics
- $\mu_{\text{minority}} \lesssim \mu_{\text{majority}}$   
trapping at tails of band edge states
- Surface & interface recombination reduction  
Oxidized surface  
oxide traps - life? 30yr

### • DEFECTIVE EMITTER MODEL

- $\Delta E_{\text{eff}}$
- LATERAL EFFECTS

## Summary

- 20  $\mu\text{m}$  EXBSF sufficient to reach 20% EFF plateau for 50  $\mu\text{m}$  cells with 20  $\mu\text{s}$  base lifetime.
- EFF improved by extending the BSF from 2  $\mu\text{m}$  (18%) to 20  $\mu\text{m}$  (20%).
- Immunity to recombination density improved by a factor of 2.5 by extending BSF from 5  $\mu\text{m}$  to 40  $\mu\text{m}$  at  $10^{12} \text{ cm}^{-3}$ .
- P+/N/N+ better than N+/P/P+ due to interband Auger recombination in the emitter.
- Emitter recombination limiting JSC and EFF in EXBSF cells.

## Plan

- Analysis for optimum emitter design.

# **SOLAR CELL EFFICIENCY ESTIMATION METHODOLOGY AND ANALYSIS**

**JET PROPULSION LABORATORY**

**Anant R. Mokashi**

- **OBJECTIVE**
- **PROBLEM DEFINITION**
- **CELL PERFORMANCE**
- **MATHEMATICAL MODEL**
- **APPROACH**

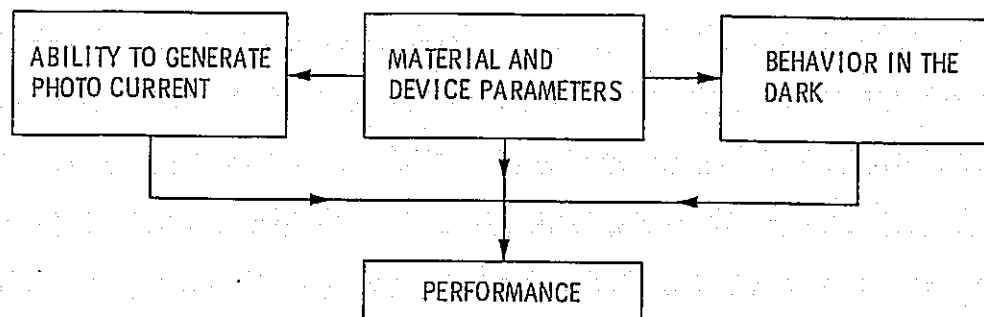
## **Objective**

- **EVALUATE PERFORMANCE OF HIGH EFFICIENCY SOLAR CELLS OF INNOVATIVE AND CONCEPTUAL DESIGNS FOR ACHIEVING NEAR 20% EFFICIENCY**
- **DEVELOP A COMPUTER MODEL FOR SIMULATING SOLAR CELL PERFORMANCE**
- **PERFORM SENSITIVITY ANALYSIS BY VARYING THE MATERIAL AND DEVICE PARAMETERS**
- **CORRELATE THE IMPACT OF CELL PROCESSING STEPS ON PARAMETER VALUES AND CELL PERFORMANCE**



## SILICON MATERIAL

### Problem Definition



### Solar-Cell Performance

CONTROLLED BY:

MATERIAL AND SURFACE PROPERTIES

DEVICE DESIGN

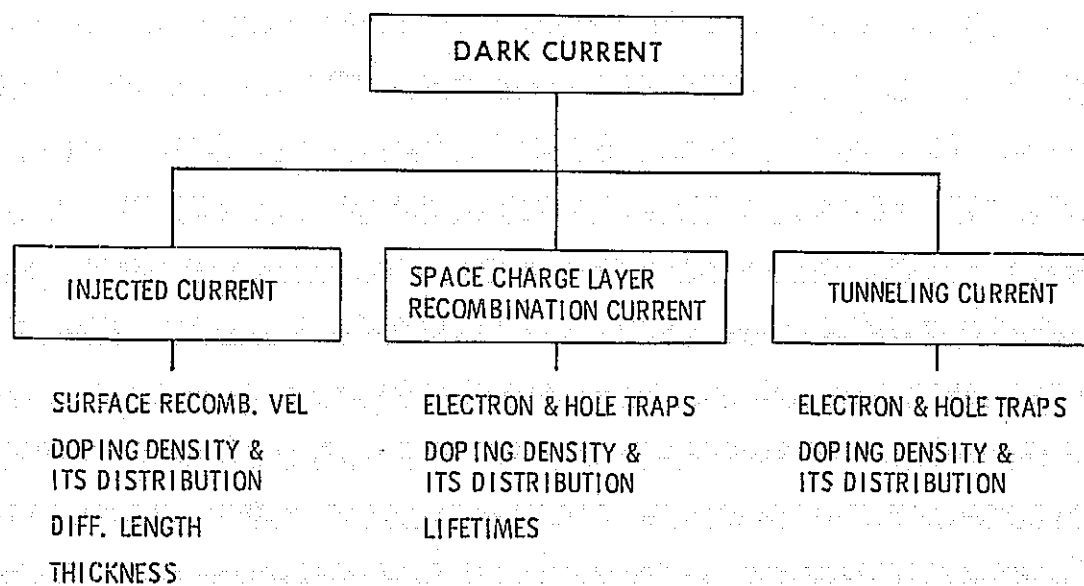
DEVICE PROCESSING STEPS, ETC.

MEASURED BY:

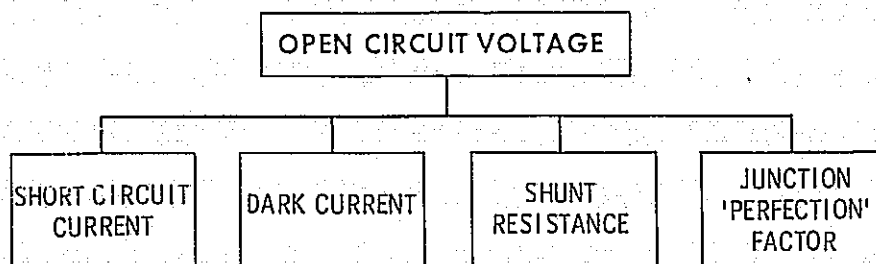
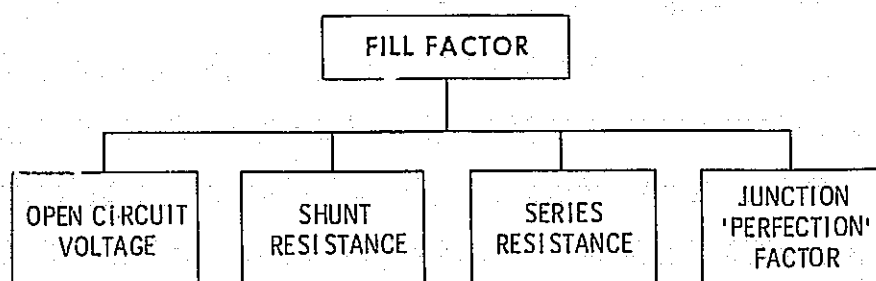
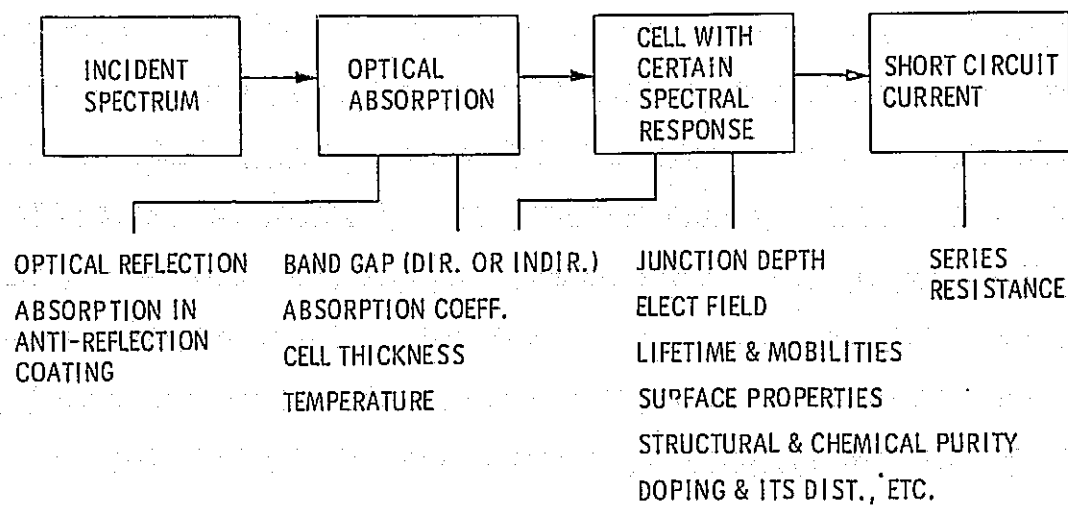
DARK I-V CHARACTERISTICS (SATURATION CURRENT -  $I_0$ )

LIGHT I-V CHARACTERISTICS ( $I_{sc}$ ,  $V_{oc}$ , FF)

SPECTRAL RESPONSE (COLLECTION EFFICIENCY)



## Short-Circuit Current



## Procedure

### 1st ITERATION

- UNIFORMLY DOPED FRONT & BASE REGIONS WITH HIGH LIFETIMES
- IDEALIZED CONDITIONS OF
  - NO SERIES RESISTANCE
  - NO SHUNT RESISTANCE
  - NO REFLECTION FROM FRONT SURFACE
  - NO CONTACT AREA LOSSES

### COMPUTATION

- SHORT CIRCUIT CURRENT
- OPEN CIRCUIT VOLTAGE
- EFFICIENCY

2nd ITERATION     INTRODUCE THE EFFECTS OF LOSS MECHANISMS (RESISTANCES, CONTACT AREA, REFLECTION, (DOPING DISTRIBUTION ETC.)

THUS                TECHNOLOGY DEPENDENT FEATURES CAN THEREBY BE SEPARATED FROM THE INHERENT FEATURES

## Mathematical Model

- INCORPORATION OF DEVICE PHYSICS AS ACCURATELY AS POSSIBLE (RECOMBINATION, GENERATION, HEAVY DOPING EFFECTS, SURFACE EFFECTS & MOBILITY)
- MODELING CELLS OF MANY DIFFERENT DESIGNS
- PREDICTION OF THE EFFECT OF EACH DEVICE PARAMETER ON DEVICE PERFORMANCE & EFFECT OF PROCESSING STEPS ON OTHER PARAMETERS (EX. DIFFUSION PROCESS STEP TO ACHIEVE DEEPER JUNCTION WOULD ALSO AFFECT LIFETIME)
- SPACIAL DISTRIBUTION OF HOLES ELECTRONS
- EVALUATION OF CELL PERFORMANCE ( $I_{sc}$ ,  $V_{oc}$ ,  $PM$ , ETC.)

## Semiconductor Equations

### BASIC EQUATIONS

- POISSON'S EQUATION
- HOLE CONTINUITY EQUATION
- ELECTRON CONTINUITY EQUATION

### SUPPLEMENTARY EQUATIONS

- GENERATION EQUATION
- TRANSPORT EQUATION
- RECOMBINATION EQUATION, ETC.

## Approach

- BOUNDARY VALUE PROBLEM
- NUMERICAL ANALYSIS
- EXISTING MODELS
- MODIFICATIONS & IMPROVEMENTS

# CELL PROCESSING AND HIGH-EFFICIENCY CELLS

D.B. Bickler, Chairman

Reports of research progress in cell processes and high-efficiency cells were presented by 11 contractors, SERI, and JPL.

Westinghouse Electric Corp. Advanced Energy Systems Division reported on its liquid-applied, dried and fired dopant and oxide mask preparations. Cell performance equivalent to gaseous diffusion and Silox masking has been demonstrated repeatedly. Meniscus coating and belt-furnace firing were shown to be feasible processes. Material from the Kayex Corp.-developed shot tower was used to make cells equivalent to cells from Siemens-process polysilicon. A seven-minute videocassette showed a Kulicke and Soffa, Inc.-developed automatic cell interconnection machine. This machine ultrasonically bonds (interconnects) 180 cells in 10.5 minutes with high yield.

Investigation of performance-limiting mechanisms in large-grain polycrystalline (Semix and Wacker) material was reported by Solarex Corp. A series of test wafers, each containing 400 minicells, was fabricated. Illuminated I-V testing showed that the current density is dominated by bulk recombination and not by grain-boundary effects. Inclusions were found in most, but not all, of the minicells with high shunt conductance and poor performance. Damaged-backside gettering was shown to improve cell performance by migration of impurities when impurities and not inclusions are determining performance. Dc plasma hydrogenation equipment has been completed and will be used for additional performance-improvement studies.

Research on nonnoble front-metallization processes was reported by Spectrolab, Inc. Solderability is a major problem in the molybdenum-tin-titanium hydride thick-film system. A two-step firing cycle is a possible solution. No shunting problems have been found with this system. Early work with transparent conductive coatings showed problems with firing in a reducing atmosphere. A number of different analytical tools (I-V, SEM, TGA and DSC) are being used to characterize each thick-film ink formulation.

J. Parker of Electrink, Inc., gave a short summary of the status of nonnoble metal systems. A copper system with lead as a sintering medium has been demonstrated. Oxide scavenging by metallic fluorides and Teflon powder was tried. Dopants of aluminum-silicon and germanium were incorporated in some tests. Successful back contacts were shown. Front contacts with copper were not successful. Silver or copper metal pads on aluminum BSF were demonstrated; nuclear resonance profiling for hydrogen was performed.

Laser-assisted cell metallization processing research was reported by Westinghouse Electric Corp. Research Division. This new contract was still in a study phase, so only theoretical concepts such as pyrolytic (heat-induced) and photolytic (light-induced) deposition techniques could be discussed. Many benefits in cell processing are envisioned from laser technology.

M. A. Nicolet of California Institute of Technology presented experimental results of diffusion-barrier studies. Contact resistivity and barrier height of a titanium nitride passive barrier and iron-tungsten,

## CELL PROCESSING AND HIGH-EFFICIENCY CELLS

nickel-molybdenum and nickel-tungsten amorphous metal films have been measured. Film quality is strongly dependent on the deposition process used. Thermal and metallurgical stability tests have been started.

R. Daniel of JPL described a metallization cost-comparison methodology that permits improved visibility of the tradeoffs involved in use of various metallization systems. This methodology is helpful in assessing the value of new research efforts as well as ranking the already-characterized systems.

Spire Corp. presented details of an 18% high-efficiency cell fabricated by ion implantation. Both the phosphorus front junction and the boron back-surface field were ion-implanted. The boron implant was annealed at 950°C, then at 550°C; the front junction was annealed using the usual Spire three-step process. Front contacts were plated to 10  $\mu\text{m}$  thickness. A study of ion implantation of ribbon and polycrystalline material is being made. Some interesting thermal processing effects have been noted.

D. Fitzgerald of JPL discussed his recent ion-cluster beam efforts. A research deposition system is nearly complete. Advantages of such a system are: low temperatures, medium vacuum requirement, good deposition rates, surface cleanliness, no carrier gas, control of crystallinity, strong adhesion and the capability of depositing compounds.

Some molecular-beam epitaxially grown cells were fabricated at University of California at Los Angeles but poor reverse leakage currents were found, due to the location of the depletion region. Additional computer modeling shows that tandem cells are potentially more efficient than single cells. Additional modeling and cell fabrication are planned to achieve the optimal design for a tandem cell.

Applied Solar Energy Corp. presented results of its investigation into the use of microcrystalline silicon for heterojunction or window layer on single-crystal silicon. Considerable experimental difficulty has resulted in test values well below calculated values. Additional tests are planned.

Professor M. Wolf of the University of Pennsylvania has been analyzing high-efficiency cell designs and measuring minority-carrier lifetime by use of a spectral LBIC method. This work was carried out on epitaxially grown test samples. Lifetimes of 12 microseconds were found along with good saturation current density and excess current density values. The intermediate conclusion is that the CVD-epi process can be compatible with achievement of a 20% solar cell.

An overview of high-efficiency cell activity at SERI was presented by J. Milstein. Five contracts are currently active at SERI as a result of a RFP soliciting fundamental research directed toward increasing polycrystalline cells beyond 14% efficiency and single-crystal cells beyond 17%. All contractors are performing satisfactorily.

# **LASER-ASSISTED SOLAR-CELL METALLIZATION PROCESSING**

**WESTINGHOUSE ELECTRIC CORP.**

**S. Dutta**

## **Potential Advantages of Laser Deposition Techniques for Photovoltaic Systems**

- **High Resolution**
- **No Photolithography**
- **Clean And Contamination - Free**
- **In-Situ Sintering**
- **Low Contact Resistance**

## **Laser-Assisted Deposition Techniques**

### **Pyrolytic Deposition (Thermal)**

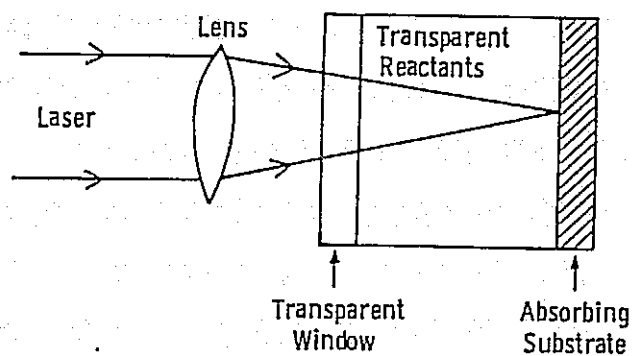
- **Laser Chemical Vapor Deposition (LCVD)**
- **Laser Deposition From Solutions**

### **Photolytic Deposition (Non-Thermal)**

- **Laser Photodissociation Of Vapors**
- **Laser Photodissociation Of Solutions**

## Pyrolytic Deposition

### Laser Chemical Vapor Deposition (LCVD)



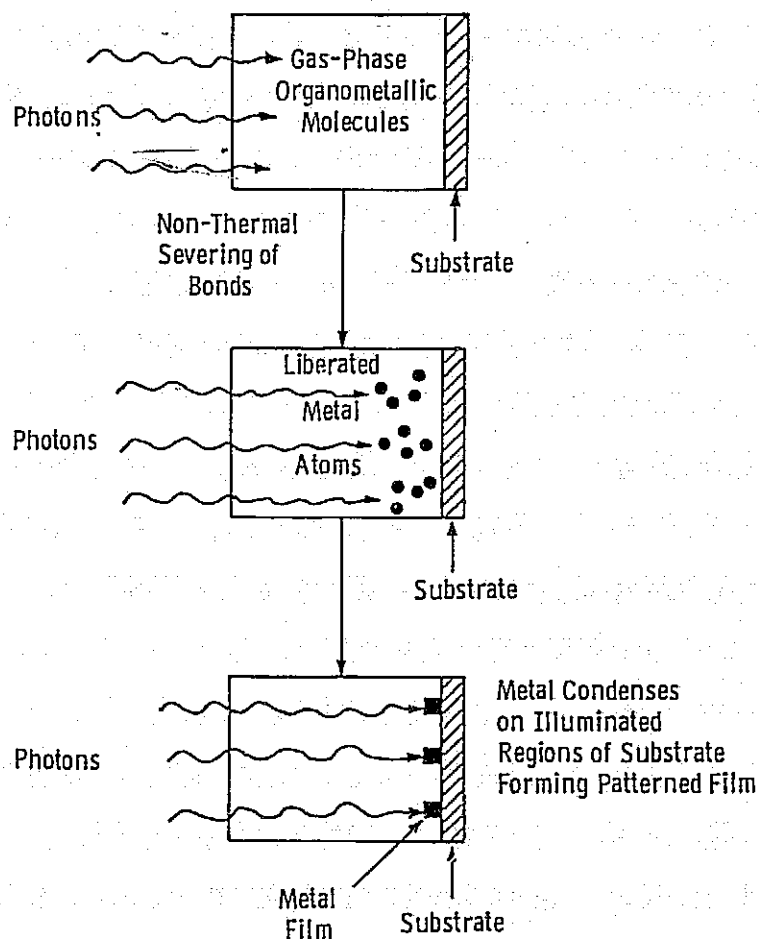
Schematic of LCVD Apparatus



## Photolytic Deposition

### Laser-Induced Photodecomposition of Gas-Phase Organometallic Compounds:

This Technique is Fundamentally Different from Thermally Based Laser Processes



## Applications to Photovoltaic Metallization Systems

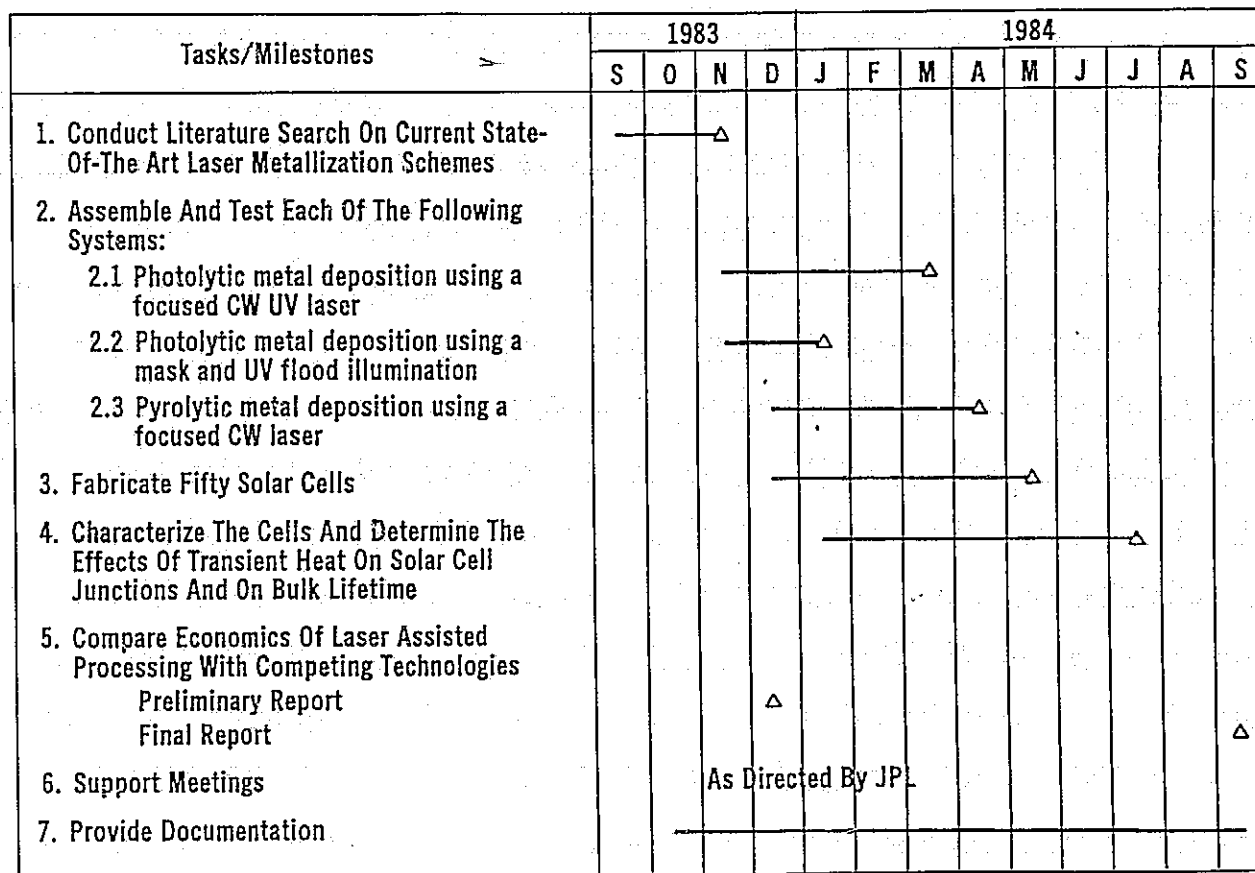
### **Laser Thermal Deposition From Vapors (Or Solutions):**

- **Clean, Maskless Process**
- **Possibility Of Interfacing With Laser Annealing And Diffusion Techniques**
- **Ability To Perform Laser-Assisted Electroplating For Rapid Metal Buildup**

### **Laser Photodeposition From Vapors (Or Solutions):**

- **Possibility Of Two Or Three Layer Metal Deposition (Diffusion Barrier, Galvanic Buffering)**
- **Flood Illumination Using Mask For Rapid Throughput**
- **Possibility Of Using Repeated Laser Pulses For Film Buildup**

## Laser-Assisted Solar-Cell Metallization Processing Milestone Chart



# PROCESS RESEARCH ON POLYCRYSTALLINE SILICON MATERIAL (PROPSM)

SOLAREX CORP.

Jerry Culik

## PROPSM Program

- 0 IDENTIFY MECHANISMS LIMITING CELL PERFORMANCE (SHORT-CIRCUIT CURRENT, OPEN-CIRCUIT VOLTAGE, FILL-FACTOR, PEAK POWER) IN LARGE-GRAIN POLYCRYSTALLINE SILICON SHEET MATERIAL.
- 0 DEVELOP SOLAR CELL FABRICATION PROCESSES, COMPATIBLE WITH LIMITING MECHANISMS, TO IMPROVE PERFORMANCE.

## Summary of Thickness-Resistivity Matrix Evaluation

- 0 MECHANISMS LIMITING LIGHT-GENERATED CURRENT ARE THE SAME AS THOSE IN SINGLE-CRYSTAL.  $I_{sc}$  IS DOMINATED BY MINORITY-CARRIER DIFFUSION LENGTH WITHIN THE BULK OF THE GRAINS.
- 0  $V_{oc}$  TENDS TO DECREASE SLIGHTLY AS THE BASE THICKNESS INCREASES, AND TO INCREASE AS THE BULK RESISTIVITY DECREASES. SIMILAR TO SINGLE-CRYSTAL SILICON.
- 0 FILL-FACTOR OF POLYCRYSTALLINE CELLS IS NOT SIGNIFICANTLY DIFFERENT FROM THAT OF SINGLE-CRYSTAL CONTROLS.
- 0 BOTH  $V_{oc}$  AND FILL-FACTOR OF POLYCRYSTALLINE CELLS HAVE SUBSTANTIAL SCATTER.

## Minicell Evaluation

J. CULIK

K. GRIMES

1. FABRICATE 400 PHOTODIODES (ON 5 MM CENTERS, 0.19 CM<sup>2</sup> AREA) ACROSS 10CM X 10CM POLYCRYSTALLINE SILICON WAFERS USING MESA STRUCTURE FOR ISOLATION.
2. MEASURE ILLUMINATED I-V CHARACTERISTICS ACROSS WAFER.
3. LOCATE AREAS WHICH SUFFER FROM REDUCED V<sub>OC</sub> AND/OR FILL- FACTOR.
4. DETERMINE CAUSE:
  - o SHUNT CONDUCTANCE.
  - o DARK I-V ANALYSIS FOR J<sub>0NO</sub>, J<sub>SC0</sub>, AND N-FACTOR.
  - o DEFECT ETCH OF SERIAL WAFER FOR DISLOCATION CONTENT.
  - o LIGHT-SPOT SCANNING TO LOCATE ELECTRICALLY ACTIVE GRAIN AND SUB-GRAIN BOUNDARIES.

## Minicell Evaluation: Samples

1. SEMIX BRICK 71-01E: TOP, MIDDLE, BOTTOM
2. SEMIX BRICK C4-108, MIDDLE
3. SEMIX BRICK C4-116B, MIDDLE
4. WACKER SILSO
5. CZ SINGLE-CRYSTAL

## Minicell Evaluation: Process

- 0 250  $\pm$   $\mu$ M THICKNESS
- 0 80 OHM/ $\square$  DIFFUSION
- 0 MESA ETCH - REMOVE 10  $\mu$ M BETWEEN CELLS
- 0 ALUMINUM PASTE BSF
- 0 Ti/Pd, ELECTROPLATED Ag FRONT TAB CONTACT; FULL Ti/Pd/Ag REAR CONTACT

## Minicell Evaluation: Illuminated I-V Characteristics

WAFER	N (CELLS)	J <sub>sc</sub> (mA/cm <sup>2</sup> )	V <sub>oc</sub> (mV)	FF (%)
SC11-1 (SINGLE-CRYSTAL)	241	30.3 (0.4)	580 (15)	61.7 (4.2)
71-01E, TOP	294	27.9 (0.6)	562 (16)	66.3 (5.7)
71-01E, MIDDLE	255	27.9 (0.8)	560 (19)	63.9 (7.2)
71-01E, BOTTOM	271	26.1 (0.5)	520 (42)	55.5 (9.6)
C4-108	287	28.2 (1.9)	540 (55)	56.9 (11.0)
C4-116B	329	29.4 (1.6)	559 (14)	64.6 (3.3)
WACKER SILSO	308	27.5 (0.8)	551 (14)	63.6 (5.2)

MEAN (STANDARD DEVIATION ABOUT MEAN)

MEASURED AT 135 mW/cm<sup>2</sup>, AMO, 25°C

### Minicell Evaluation: Illuminated I-V Characteristics Summary

- 0  $I_{SC}$  OF POLYCRYSTALLINE CELLS IS 3 TO 14 PERCENT LOWER THAN SINGLE-CRYSTAL; SCATTER IS SIMILAR TO SINGLE-CRYSTAL.
- 0  $V_{OC}$  OF POLYCRYSTALLINE CELLS IS 20 TO 60 MV LOWER THAN SINGLE-CRYSTAL; SCATTER SIMILAR TO SINGLE-CRYSTAL, BUT SCATTER FROM TWO WAFERS (C4-108 AND 71-01E, BOTTOM) IS SIGNIFICANTLY GREATER.
- 0 FILL-FACTOR ALSO SIMILAR, EXCEPT FOR TWO WAFERS THAT ARE SIGNIFICANTLY LOWER (C4-108 AND 71-01E, BOTTOM).

### Minicell Evaluation: Shunt Conductance

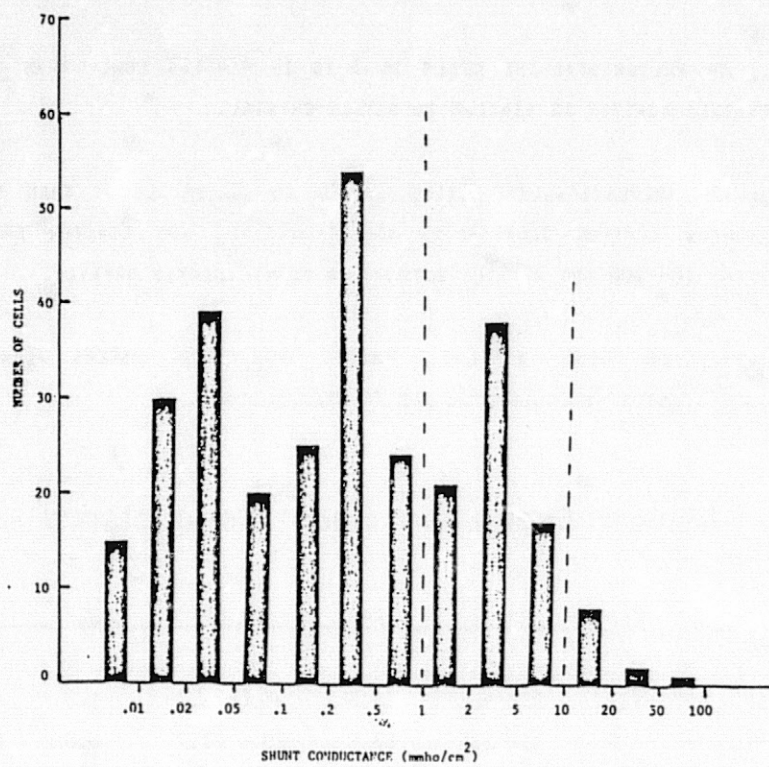
WAFER	$V_{OC}$	RANGE	FF	RANGE	$G_S$	RANGE
71-01E, TOP	562	512-583	66.3	46.0-73.3	1.9	0.0- 55.9
71-01E, MIDDLE	560	414-585	63.9	29.6-73.7	6.8	0.0- 90.8
71-01E, BOTTOM	520	263-554	55.5	28.4-70.4	10.0	0.0-100.8
C4-108	540	169-586	56.9	26.0-71.2	13.8	0.0-154.1
C4-116B	559	522-588	64.6	50.4-70.2	1.5	0.0- 19.2
WACKER SILSO	551	434-582	63.6	36.2-70.9	3.3	0.0- 41.9

- 0 HIGH SHUNT CONDUCTANCE CORRELATES WITH LOW  $V_{OC}$  (AND LOW FILL-FACTOR).
- 0 RANGE OF  $V_{OC}$  (AND FILL-FACTOR) INCREASES AS RANGE OF  $G_S$  INCREASES.
- 0 HIGH SHUNT CONDUCTANCE WITH LARGE RANGE CORRELATES WITH PRESENCE OF MANY INCLUSIONS.

### Minicell Evaluation: Shunt Conductance Histograms

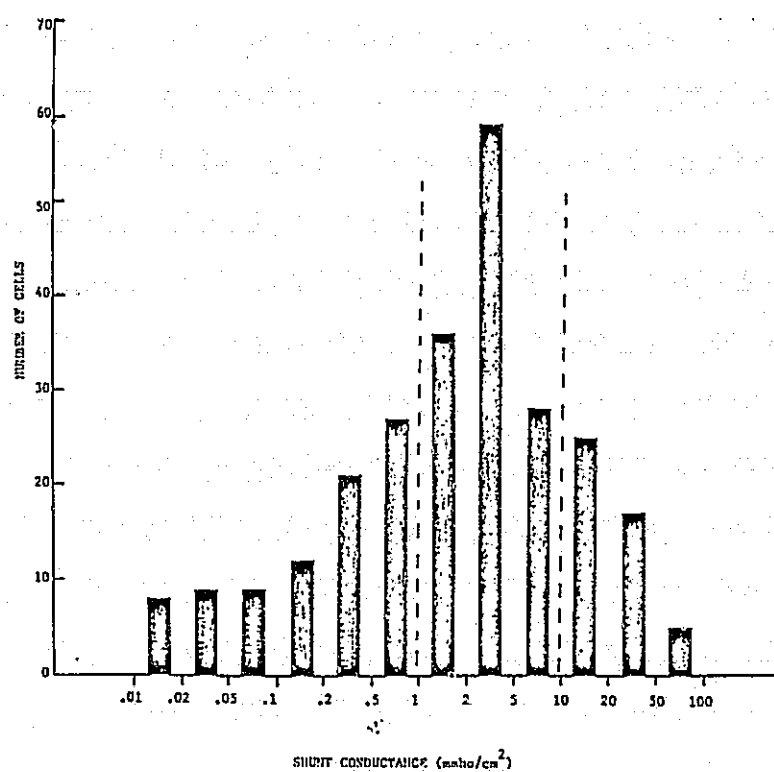
- 0 VERY LITTLE EFFECT ON  $V_{OC}$  AND FILL-FACTOR WHEN  $G_S$  IS LESS THAN 1  $MMHO/CH^2$ .
- 0 >20% DECREASE IN FILL FACTOR AND PEAK-POWER WHEN  $G_S$  IS GREATER THAN 10  $MMHO/CH^2$ .

71-01E, Top

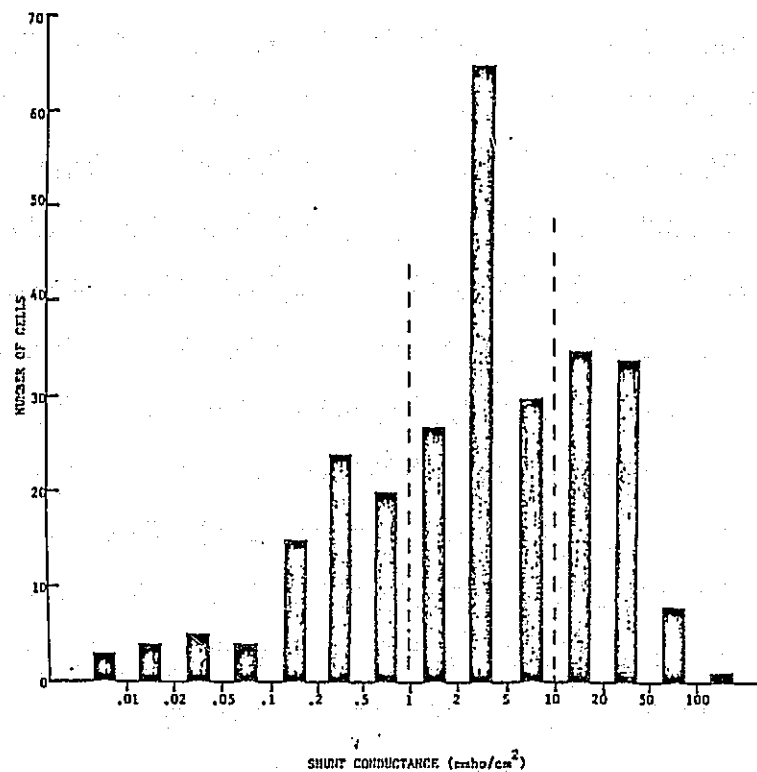




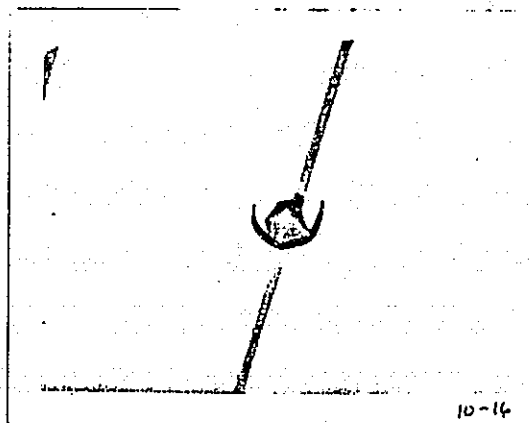
71-01E, Middle



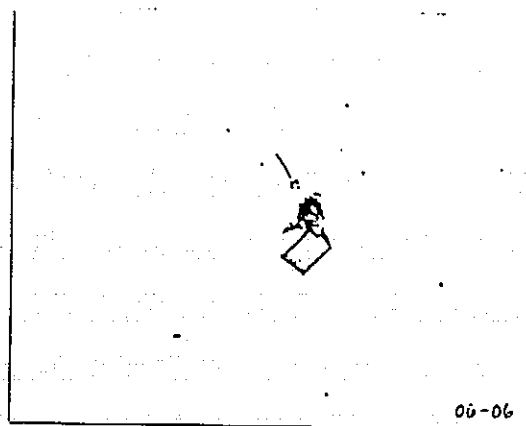
# 71-01E, Bottom



## Minicell Evaluation: Inclusions



C4-108 (50X)



71-01E, BOTTOM (20X)

## Minicell Evaluation: Dark I-V Analysis

- o LOCATE CELLS IN WAFER C4-116B THAT HAVE SIGNIFICANTLY LOWER  $V_{OC}$  NOT DUE TO INCLUSIONS, THAT IS,  $G_S$  LESS THAN  $1 \text{ MH}\Omega/\text{CH}^2$ .
- o MEASURE  $I_{SC}$ - $V_{OC}$ , TO AVOID SERIES RESISTANCE (NO GRID).
- o DETERMINE  $J_{QNO}$ ,  $J_{SCO}$ , N-FACTOR.

Minicell Evaluation: Spatial Dark I-V Analysis,  
Wafer C4-116B

	2	3	4
13	579 66 $4.9 \times 10^{-9}$ $9.2 \times 10^{-5}$ 2.1 4 2	563 65 $3.3 \times 10^{-9}$ $7.0 \times 10^{-5}$ 2.1 3 1	561 62 $4.3 \times 10^{-9}$ $8.4 \times 10^{-4}$ 22 27 10
14	568 66 $7.2 \times 10^{-9}$ $9.3 \times 10^{-5}$ 2.0 5 3	556 60 $8.9 \times 10^{-9}$ $1.2 \times 10^{-1}$ .47 12 15	566 63 $7.1 \times 10^{-9}$ $6.8 \times 10^{-5}$ 1.9 6 3
15	563 68 $9.5 \times 10^{-9}$ $8.5 \times 10^{-4}$ 2.6 3 3	567 68 $9.3 \times 10^{-9}$ $1.5 \times 10^{-2}$ 4.4 7 3	561 63 $9.6 \times 10^{-9}$ $9.9 \times 10^{-3}$ 3.6 4 5

$V_{OC}$	FF
$J_{QNO}$	
$J_{SCO}$	
N-FACTOR	
$\Delta V$	$\Delta FF$

Minicell Evaluation: Dark I-V Analysis Summary,  
Minicell Wafer C4-116B

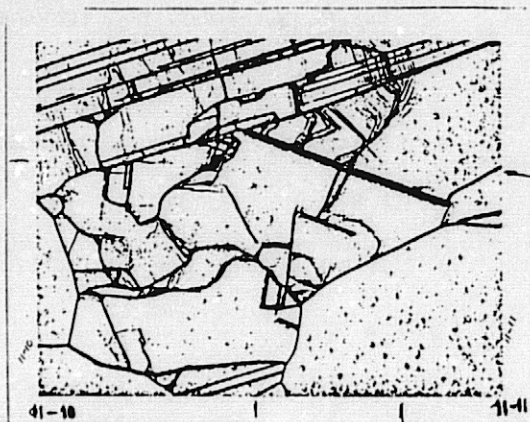
- o  $J_{QNO}$  VARIES FROM  $5 \times 10^{-9} \text{ MA/CH}^2$  TO  $1 \times 10^{-8} \text{ MA/CH}$ , THAT IS, EFFECTIVE MINORITY-CARRIER DIFFUSION LENGTH VARIES BY FACTOR OF TWO.
- o SOME CELLS HAVE  $J_{QNO}$  GREATER THAN  $2 \times 10^{-8} \text{ MA/CH}^2$ .
- o MORE THAN HALF OF CELLS LOSE 5 TO 20 MV DUE TO  $J_{SCO}$ , FEW CELLS LOSE MORE THAN 20 MV.
- o MUCH OF  $V_{OC}$  SCATTER IS ACCOUNTED FOR BY  $J_{QNO}$ .

### Minicell Evaluation: Dislocation Etch, Minicell Wafer C4-116B



CELL 9-4

$$J_{QNO} = 1.3 \times 10^{-3} \text{ mA/cm}^2$$



CELLS 11-10 AND 11-11

$$J_{QNO} (11-10) = 1.1 \times 10^{-8} \text{ mA/cm}^2$$

$$J_{QNO} (11-11) = 5.8 \times 10^{-9} \text{ mA/cm}^2$$

- o MANY CELLS WITH EXCESS  $J_{QNO}$  HAVE AREAS OF HIGH DISLOCATION DENSITY.
- o LIGHT SPOT SCAN TO DETERMINE ELECTRICALLY ACTIVE GRAIN AND SUB-GRAIN BOUNDARIES.

### Minicell Evaluation: Summary

- o DEGRADATION AND SCATTER IN  $V_{OC}$  AND FILL-FACTOR MAY, FOR SOME WAFERS, BE DUE TO INCLUSIONS, WHICH ACT AS RESISTIVE SHUNTS.
- o  $I_{SC}$  IS DOMINATED BY BULK DIFFUSION LENGTH.
- o FOR MINI-CELL WAFER C4-116B,  $V_{OC}$  MAY BE REDUCED 5 TO 20 mV DUE TO  $J_{SCO}$ ; HOWEVER,  $V_{OC}$  IS DOMINATED BY  $J_{QNO}$ , AND SCATTER IS LARGELY DUE TO VARIATIONS IN  $J_{QNO}$ .

## Damage Gettering

J. CULIK

S. RONCIN

1. SELECT, QUARTER AND ETCH LOW DIFFUSION LENGTH POLYCRYSTALLINE WAFERS FROM SEMIX BRICK C4-87E; SINGLE-CRYSTAL CONTROLS.
2. DAMAGE BACKSIDE BY SANDBLASTING WITH 320 MESH ALUMINUM OXIDE POWDER, CLEAN.
3. HEAT-TREAT AT 1000°C IN FLOWING NITROGEN; 1, 5, OR 25 HOURS.
4. ETCH SURFACE DAMAGE (20  $\mu$ m).
5. FABRICATE 2cm X 2cm SOLAR CELLS.

## Damage Gettering: Single-Crystal Controls

ANNEAL TIME (HOURS)	N (CELLS)	I <sub>sc</sub> (mA)	V <sub>oc</sub> (mV)	FF (%)	PP (mW)
0	16	108 (1)	589 (8)	74.1 (4.0)	47.4 (3.1)
1	16	104 (2)	564 (7)	73.9 (4.7)	43.4 (2.6)
5	13	101 (4)	557 (11)	76.0 (4.3)	43.1 (3.0)
25	11	103 (2)	558 (13)	72.8 (4.0)	41.9 (3.6)

MEAN (STANDARD DEVIATION ABOUT MEAN)

MEASURED AT 135 mW/cm<sup>2</sup>, AMO, 25°C. NO AR COATING.0 I<sub>sc</sub>, V<sub>oc</sub>, AND PP DECREASE WITH TIME AT 1000°C

## Damage Gettering: Polycrystalline Wafer C4-87E

ANNEAL TIME (HOURS)	N (CELLS)	I <sub>sc</sub> (mA)	V <sub>oc</sub> (mV)	FF (%)	PP (mW)
0	8	83 (3)	520 (4)	73.1 (1.2)	31.8 (1.1)
1	20	78 (2)	503 (6)	70.8 (2.0)	27.9 (1.4)
5	16	98 (2)	530 (4)	70.2 (2.0)	36.6 (1.1)
25	14	88 (4)	514 (4)	70.4 (0.8)	32.0 (1.3)

MEAN (STANDARD DEVIATION ABOUT MEAN)

MEASURED AT 135 mW/cm<sup>2</sup>, AMO, 25°C. NO AR COATING.

- o ONE HOUR AT 1000°C DEGRADES I<sub>sc</sub>, V<sub>oc</sub>, AND FF.
- o 5 HOURS AT 1000°C RESULTS IN SIGNIFICANT IMPROVEMENT IN I<sub>sc</sub>, V<sub>oc</sub>, AND PP.

## Damage Gettering: Dark I-V Analysis

SEMIX C4-87E, WAFERS 31 AND 36

ANNEAL TIME (HOURS)	CELL	I <sub>sc</sub> (mA)	V <sub>oc</sub> (mV)	J <sub>QNO</sub> (X 10 <sup>-8</sup> mA/cm <sup>2</sup> )	J <sub>SC0</sub> (X 10 <sup>-4</sup> mA/cm <sup>2</sup> )	N FACTOR
0	31A-3	83	517	2.0	5.2	2.0
	36A-3	82	517	2.0	6.6	2.0
1	31B-4	78	510	2.7	2.8	1.9
	36B-4	77	502	3.8	5.5	2.0
5	31C-1	96	535	1.3	11.6	2.3
	36C-1	101	533	1.1	3.2	1.9
25	31D-2	90	515	2.6	17.1	2.2
	36D-2	91	515	2.0	6.0	2.0

## Damage Gettering: Summary

- 0 SECCO ETCH OF SERIAL WAFERS INDICATES LOW  $I_{sc}$  IS NOT DUE TO DISLOCATIONS.
- 0 IF LOW  $I_{sc}$  IS DUE TO IMPURITIES, THEN IMPROVEMENT RESULTS FROM GETTERING OF THOSE IMPURITIES WHICH INCREASES  $L$ , DECREASES  $J_{QNO}$ , AND INCREASES  $J_L$ .
- 0 THEREFORE BOTH  $I_{sc}$  AND  $V_{oc}$  IMPROVE.
- 0 ADDITIONAL TIME AT 1000°C PROBABLY DEGRADES  $L$  BY SAME MECHANISM FOUND IN CZOCHRALSKI SINGLE-CRYSTAL SILICON.

## Conclusions

- 0 PERFORMANCE OF CAST POLYCRYSTALLINE MATERIAL MAY BE LIMITED BY PRESENCE OF INCLUSIONS, WHICH ACT AS RESISTIVE SHUNTS; DENSITY OF INCLUSIONS INCREASES TOWARD BOTTOM OF BRICK.
- 0  $V_{oc}$  IS CONTROLLED BY  $J_{QNO}$ , NOT  $J_{SCO}$ ;  $J_{QNO}$  MAY VARY UP TO AN ORDER OF MAGNITUDE ACROSS WAFER.
- 0  $J_{QNO}$  CAN BE REDUCED IN SHORT DIFFUSION LENGTH MATERIAL BY HEAT TREATMENT AT 1000°C FOR 5 HOURS WITH DAMAGED BACKSIDE.

## CELL PROCESSING AND HIGH-EFFICIENCY CELLS

### Plans

- o EVALUATE MINI-CELL DARK I-V CHARACTERISTICS IN SEMIX 71-01E, TOP AND WACKER SILSO TO DETERMINE SPATIAL VARIATION OF  $J_{QNO}$ .
- o LIGHT SPOT SCANNING TO CORRELATE EXCESS  $J_{QNO}$  WITH STRUCTURE.
- o ADDITIONAL MEASUREMENTS ON GETTERED CELLS.

### Damage Gettering Comparisons

COMPARE NO-DAMAGE TO ALUMINUM OXIDE, SILICON DIOXIDE, AND GLASS BEAD DAMAGE  
SINGLE-CRYSTAL SILICON

	N (CELLS)	$I_{sc}$ (mA)	$V_{oc}$ (mV)	FF (%)	PP (mW)
NO-DAMAGE	12	116 (1)	600 (2)	78.2 (0.9)	54.4 (0.7)
ALUMINUM OXIDE	12	115 (1)	596 (7)	78.4 (1.8)	53.8 (1.2)
SILICON DIOXIDE	12	115 (1)	596 (9)	76.6 (3.6)	52.9 (3.1)
GLASS BEADS	8	116 (1)	596 (6)	75.0 (3.4)	52.2 (3.0)

MEAN (STANDARD DEVIATION ABOUT MEAN)  
MEASURED AT 135 mW/cm<sup>2</sup>, AMO, 25°C. NO AR COATING.



## Damage Gettering Comparisons (Cont'd)

COMPARE NO-DAMAGE TO ALUMINUM OXIDE AND GLASS BEAD DAMAGE  
POLYCRYSTALLINE SILICON

	WAFER	N	I <sub>sc</sub>	V <sub>oc</sub>	FF	PP
		(CELLS)	(mA)	(mV)	(%)	(mW)
NO-DAMAGE	30A	4	74 ± 2	522 ± 4	73.4 ± 0.3	28.6 ± 1.0
	37A	4	72 ± 2	519 ± 6	73.2 ± 1.3	27.7 ± 1.7
ALUMINUM OXIDE	30B	4	68 ± 2	511 ± 5	74.6 ± 0.6	26.2 ± 0.7
	37B	4	67 ± 1	509 ± 2	74.9 ± 0.4	25.6 ± 0.3
GLASS BEADS	30D	4	78 ± 1	529 ± 3	73.8 ± 0.3	30.7 ± 0.6
	37D	4	74 ± 1	526 ± 2	74.7 ± 0.2	29.4 ± 0.4

MEASURED AT 135 mW/cm<sup>2</sup>, AMO, 25°C. NO AR COATING

COMPARE ALUMINUM OXIDE, SILICON DIOXIDE, AND GLASS BEAD DAMAGE  
POLYCRYSTALLINE SILICON

	WAFER	N	I <sub>sc</sub>	V <sub>oc</sub>	FF	PP
		(CELLS)	(mA)	(mV)	(%)	(mW)
ALUMINUM OXIDE	38B	3	83 ± 2	537 ± 6	74.9 ± 0.9	33.4 ± 1.8
	40B	4	79 ± 2	529 ± 3	74.5 ± 0.9	31.3 ± 0.6
SILICON DIOXIDE	38C	4	84 ± 6	537 ± 11	75.7 ± 0.9	34.2 ± 3.0
	40C	1	74	520	74.3	28.6
GLASS BEADS	38D	3	94 ± 1	558 ± 2	75.7 ± 0.0	39.8 ± 0.9
	40D	4	94 ± 2	558 ± 2	75.7 ± 0.3	39.7 ± 0.8

MEASURED AT 135 mW/cm<sup>2</sup>, AMO, 25°C. NO AR COATING.

# A NONNOBLE FRONT METALLIZATION PROCESS

SPECTROLAB, INC.

Alexander Garcia III

JET PROPULSION LABORATORY

Brian Gallagher

## Objectives

- OPTIMIZATION, EVALUATION AND DEMONSTRATION OF A NOVEL METALLIZATION SYSTEM
- Mo/Sn/TiH SYSTEM
- ITO CONDUCTIVE AR SYSTEMS

## Approach

- SCREEN PRINTING
- AIR FIRING
- REDUCING ATMOSPHERE
- CONDUCTIVE AR COATING (ITO)

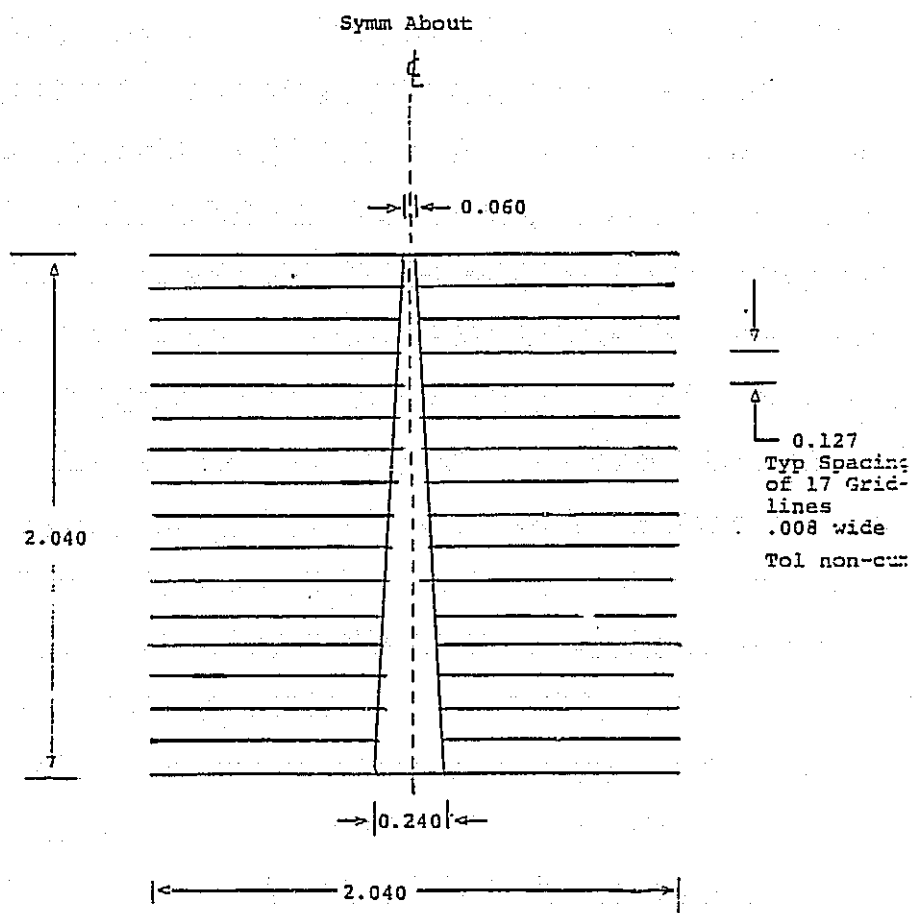
# CELL PROCESSING AND HIGH-EFFICIENCY CELLS

## Metallization Paste Formulations

	A (RH 3659)	B	C	D	E	F	G
MOLYBDENUM (SYLVANIA 280-325)	19.5	50.0	70.0	49.0	48.0	19.5	19.5
TIN (ATLANTIC EQUIPMENT ENGINEERS SN 266)	80.0	49.5	29.5	49.0	48.0	80.0	80.0
TITANIUM HYDRIDE (FERRO PLANT FX-41)	0.5	0.5	0.5	2.0	4.0	0.5	0.5
FRIT						5.0	5.0

ALL PASTES USE THICK FILM SYSTEMS ORGANIC VEHICLE

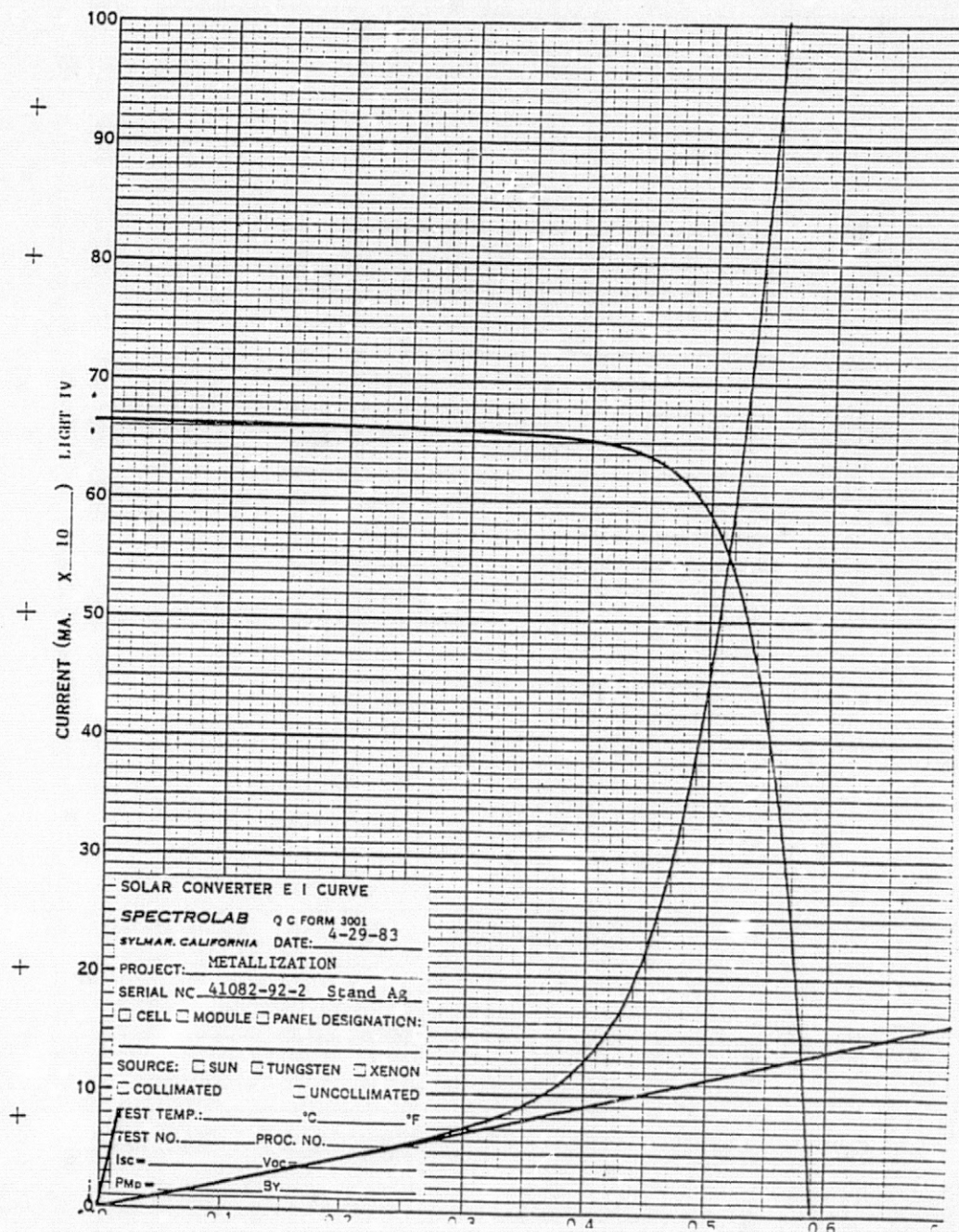
## Front Metallization Pattern



## Mo-Sn versus Ag

CELL	$V_{OC}$	$I_{SC}$	$I_{500}$	$P_{MAX}$	FF	E
1728M-90 (Mo/Sn)	.601	.678	.596	.229	.73	10.5%
1728M-72 (Ag)	.601	.680	.600	.302	.74	10.6%

# Standard Ag Cell





## Typical Mo-Sn Cell

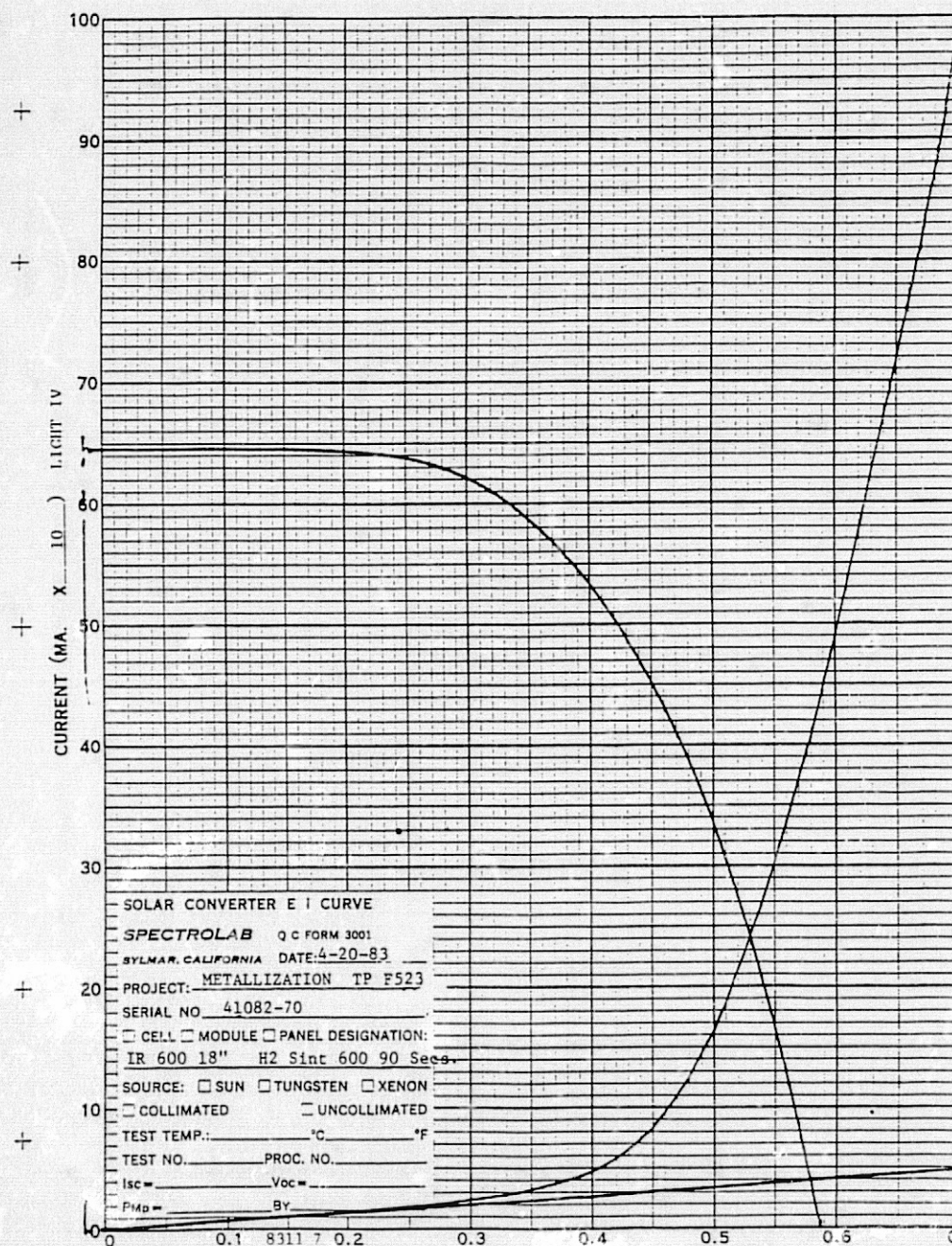


Table 1

Cell	Prefire		Gas	Fire		V <sub>oc</sub>	I <sub>sc</sub>	I <sub>500</sub>
	Temp.	Belt		Temp.	Time			
41082-70	600	18	H <sub>2</sub>	600	1.5	593	643	351
41082-79	600	18	H <sub>2</sub>	600	5.0	595	646	416
41082-81	600	18	H <sub>2</sub>	600	10.0	591	665	360
41082-85	600	18	H <sub>2</sub>	600	15.0	592	667	353
41082-83	600	18	H <sub>2</sub>	550	15.0	580	654	291

### Conclusions

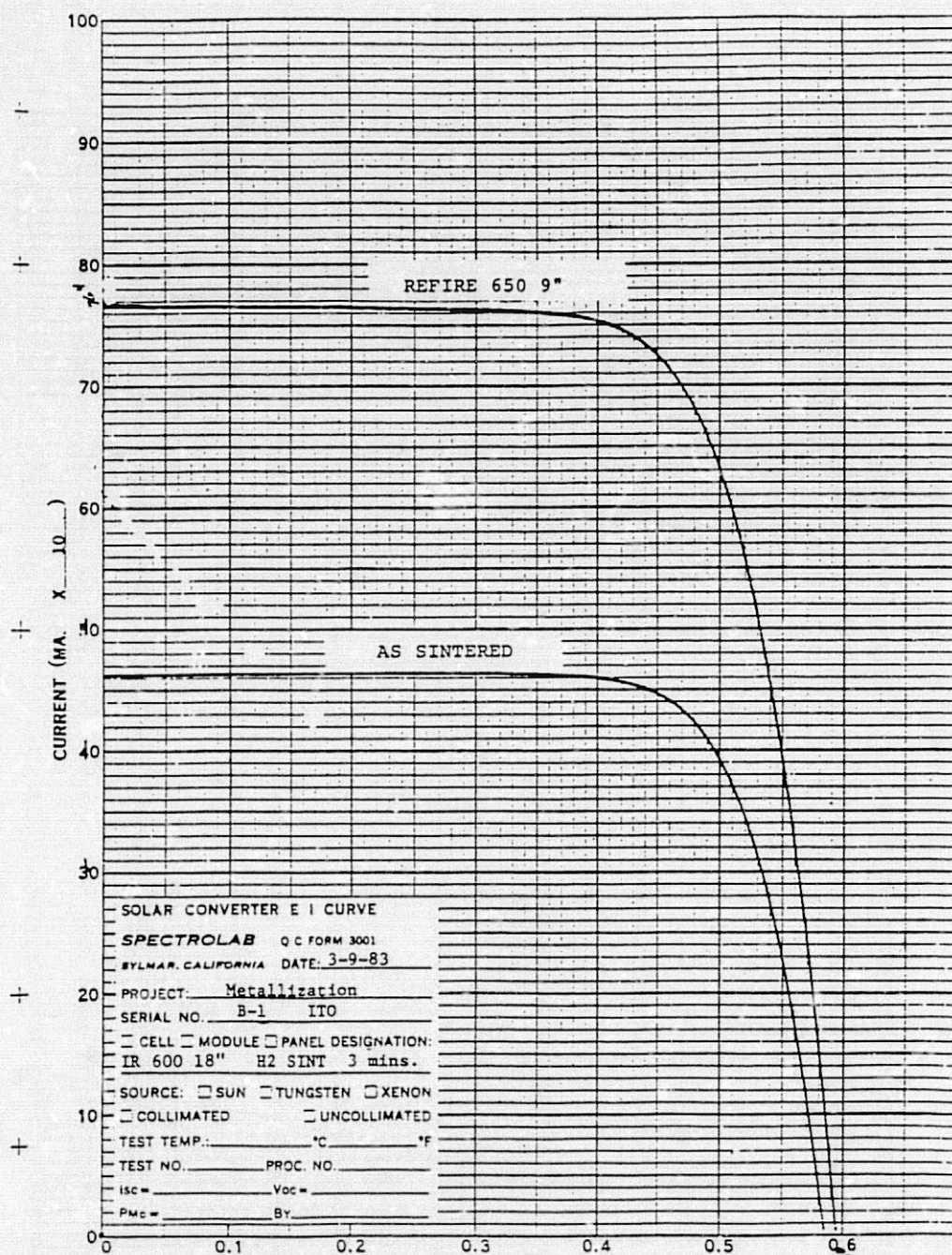
- Mo/Sn HAS ADEQUATE CONDUCTIVITY FOR SCREEN PRINTING
- SHUNTING IS NEVER A PROBLEM
- SOLDERABILITY A MAJOR PROBLEM
- TWO-STEP PROCESSING A POSSIBLE SOLUTION

### ITO Results

- GOOD ADHESION PARTICLES - ITO
- POOR ADHESION PARTICLE-PARTICLE  
(REDUCED IN H<sub>2</sub>)
- ITO AR VALUE IS DESTROYED BY REDUCING ATMOSPHERE
- REOXIDATION NECESSARY
- SHUNTING OCCURS ABOVE 600°C

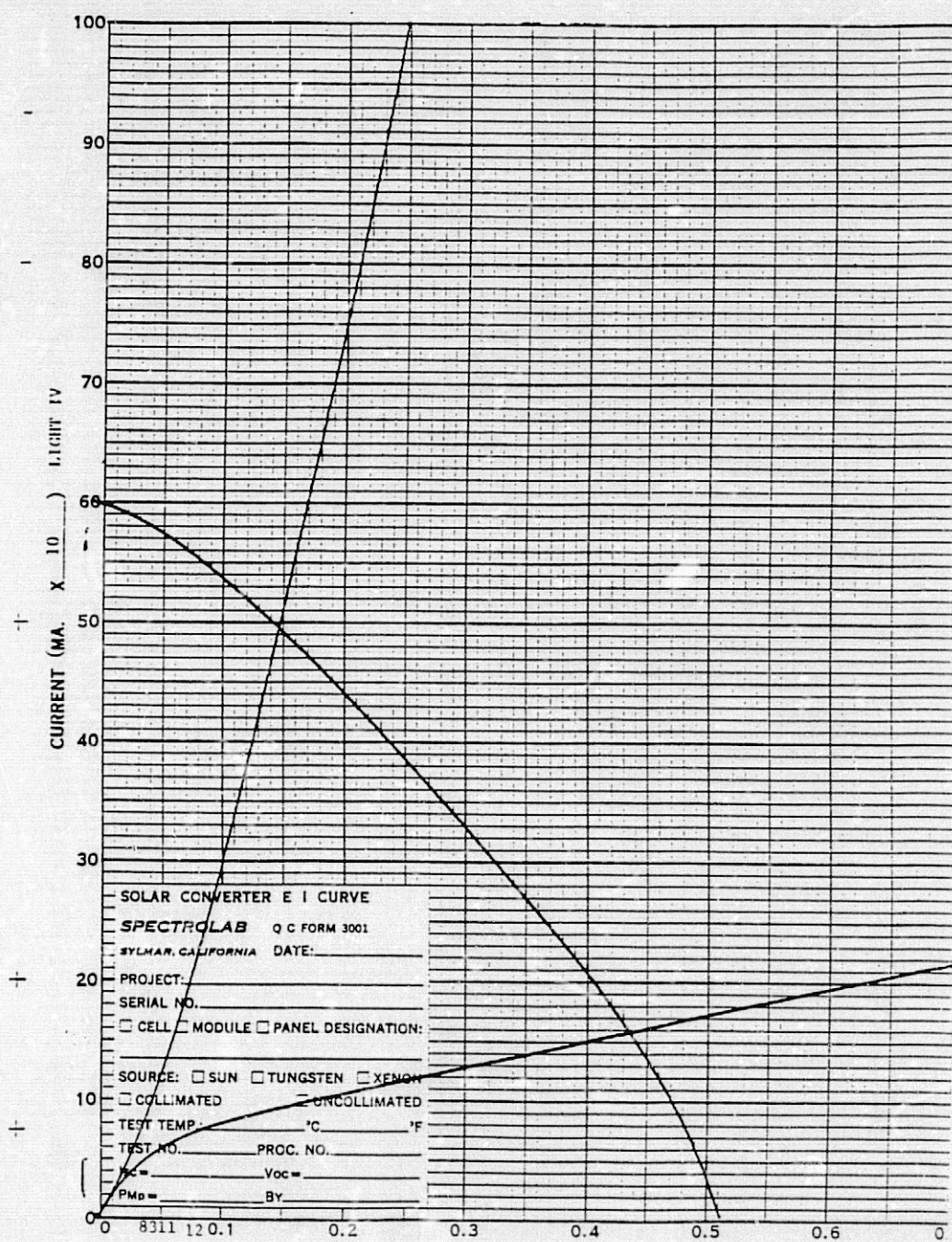


# CELL PROCESSING AND HIGH-EFFICIENCY CELLS





## ITO Shunted Cell

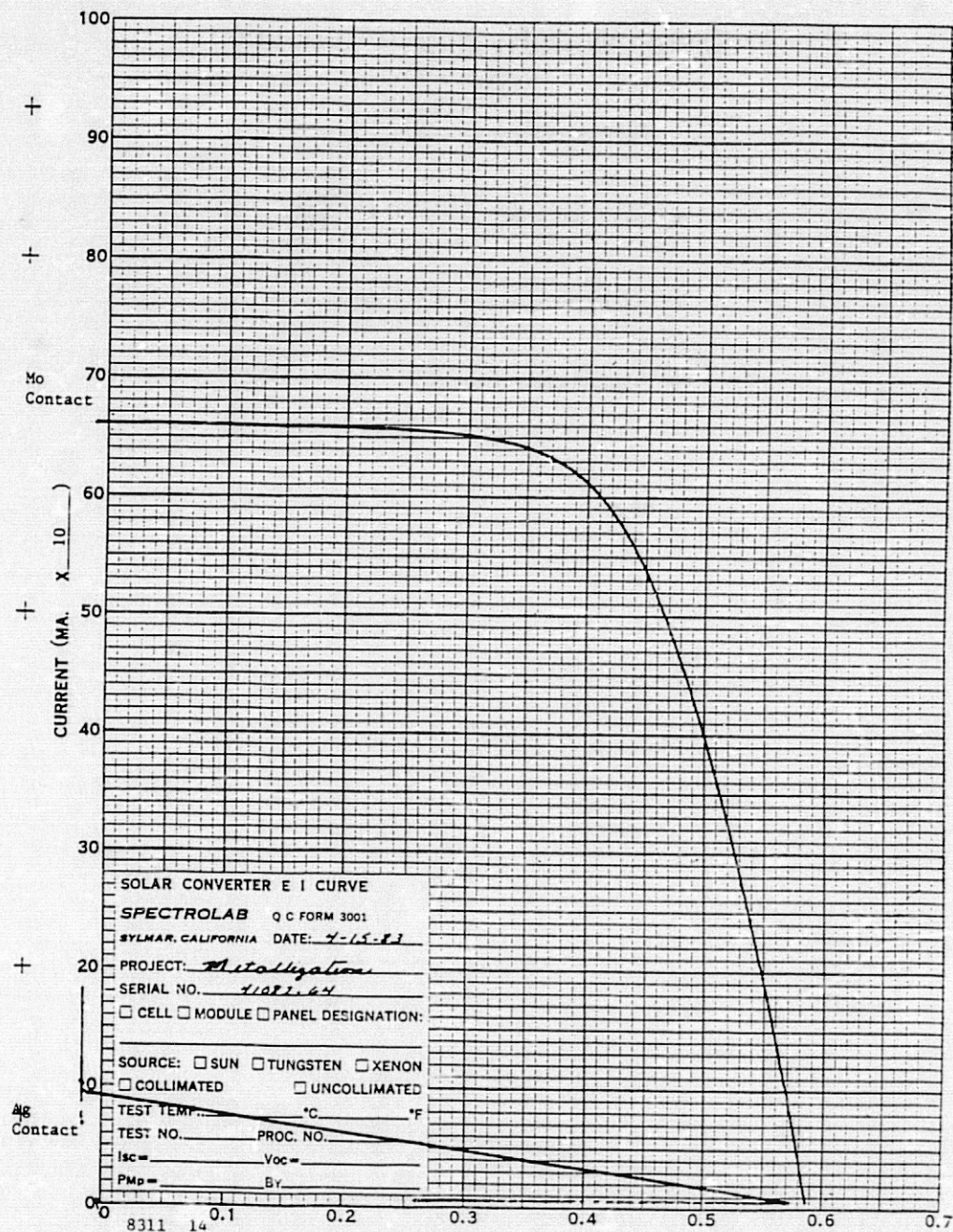


## Problems With Hydrogen Reduction

- POOR ADHESION
- FRIT DOES NOT APPRECIABLY WORK
- SI-POWDER BOND A PROBLEM
- SOLDERING A PROBLEM

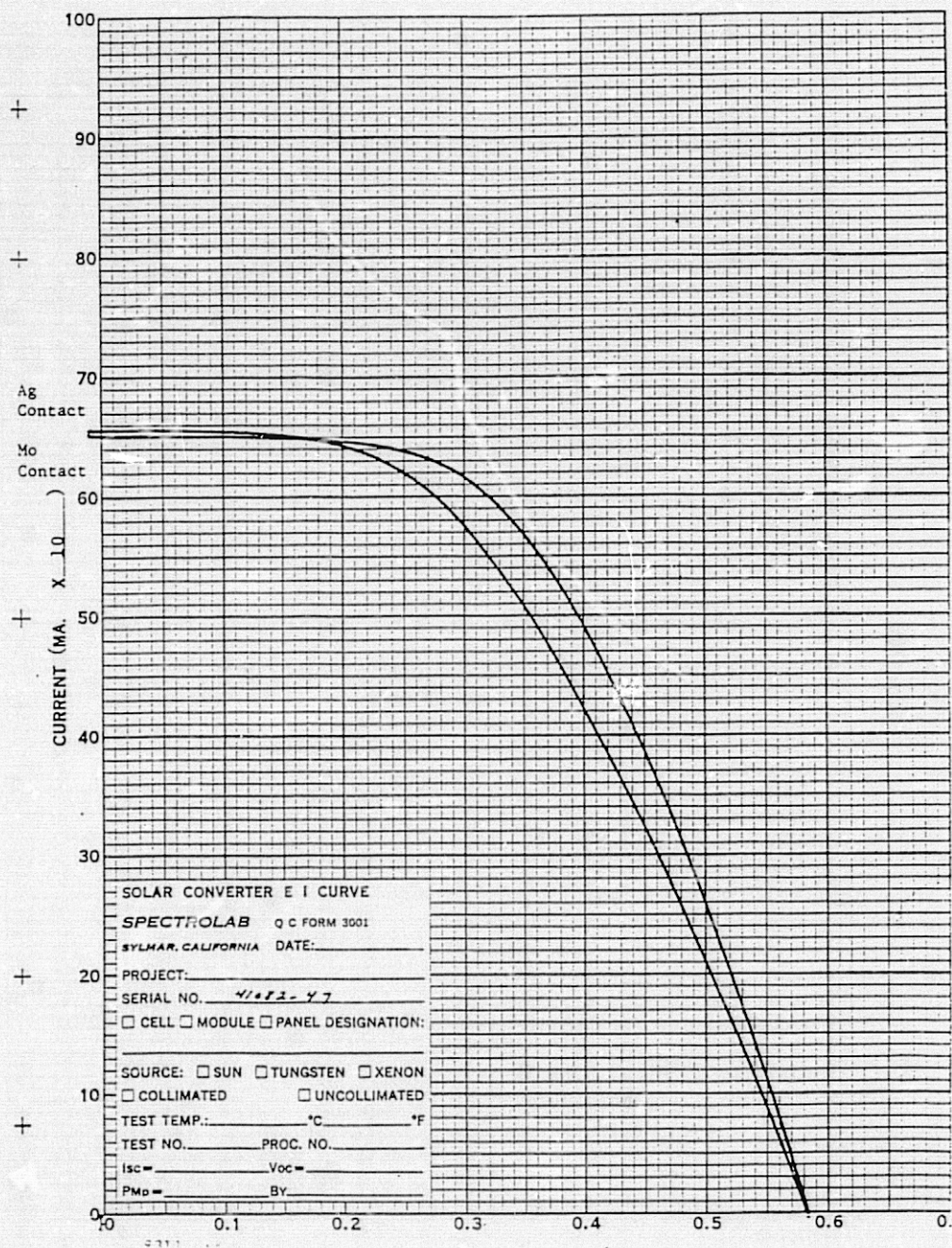


# CELL PROCESSING AND HIGH-EFFICIENCY CELLS



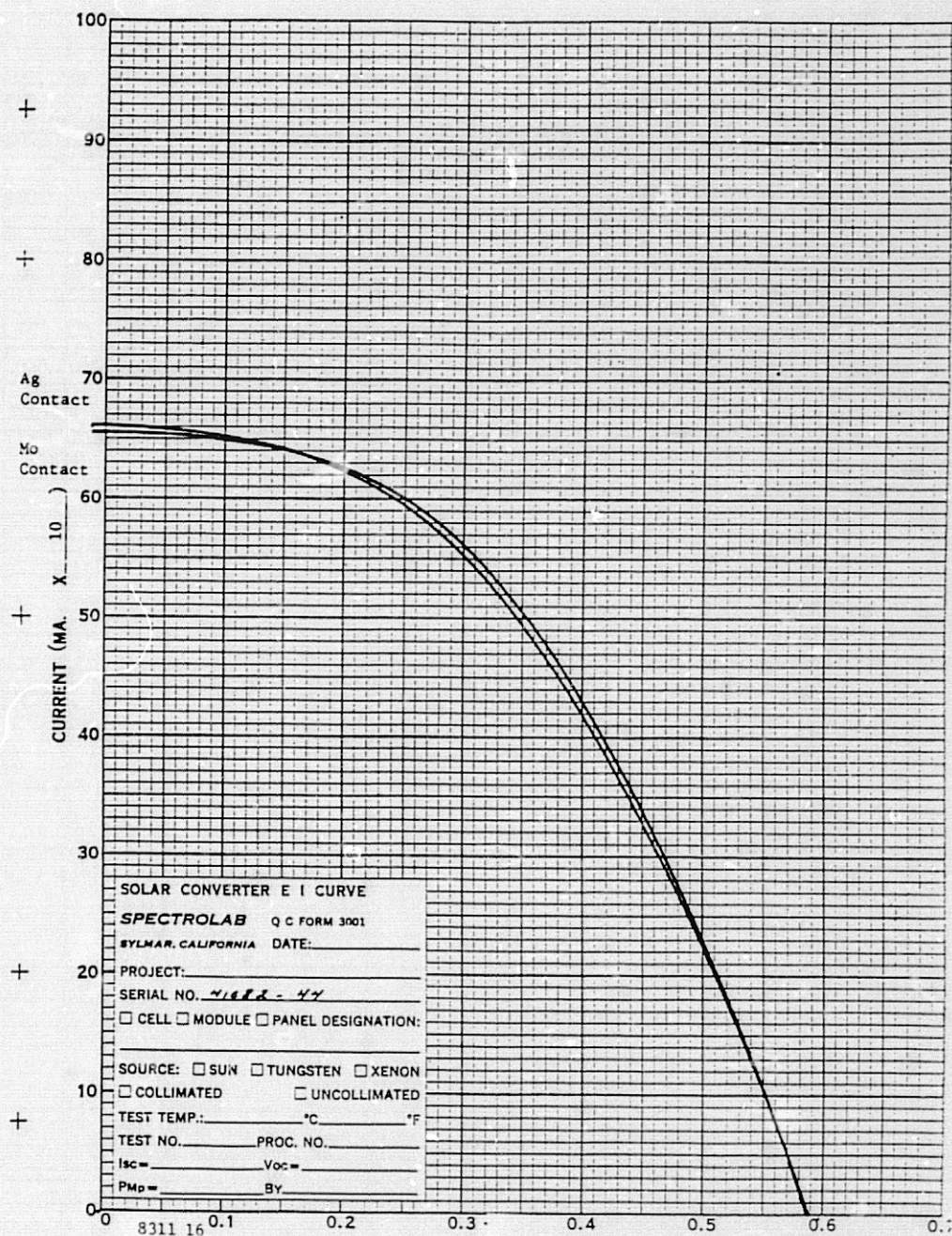


# CELL PROCESSING AND HIGH-EFFICIENCY CELLS





# CELL PROCESSING AND HIGH-EFFICIENCY CELLS



## CELL PROCESSING AND HIGH-EFFICIENCY CELLS

## Paste Formulations

<u>Paste</u>	<u>Frit (Pb)</u>	<u>Frit 90</u>	<u>Frit 494</u>	<u>Teflon</u>	<u>V-26</u>	<u>V-38</u>
A			X		X	
B			X	X	X	
C		X			X	
D		X		X	X	
E			X			X
F			X	X		X
G		X				X
H		X		X		X
I	X				X	
J	X					X
K					X	
L						X

## Vehicle Formulation

	<u>V-38</u>	<u>V-26</u>
$\alpha$ -TERPINCOL	43.62	88.00
BUTYL CARBITAL ACETATE	43.62	
ETHYL CELLULOSE N-14	9.76	
THIXATROL ST	3.00	
ELVACITE 2042		9.00
TROYKYD XYZ		3.00

# CELL PROCESSING AND HIGH-EFFICIENCY CELLS

## Frits Investigated

	<u>\$450</u>	<u>#90</u>	<u>#494</u>
K <sub>2</sub> O	1.80	0.41	2.20
Na <sub>2</sub> O	2.36	6.33	2.03
CaO	5.98	13.97	9.35
MgO	0.32	0.76	0.41
PbO	31.72	-	-
Al <sub>2</sub> O <sub>3</sub>	3.50	9.75	5.09
B <sub>2</sub> O <sub>3</sub>	13.76	13.92	7.99
SiO <sub>2</sub>	40.56	54.86	55.66
SrO	-	-	6.08
BaO	-	-	11.19
MP°C	827	843	

## Analytical Approach

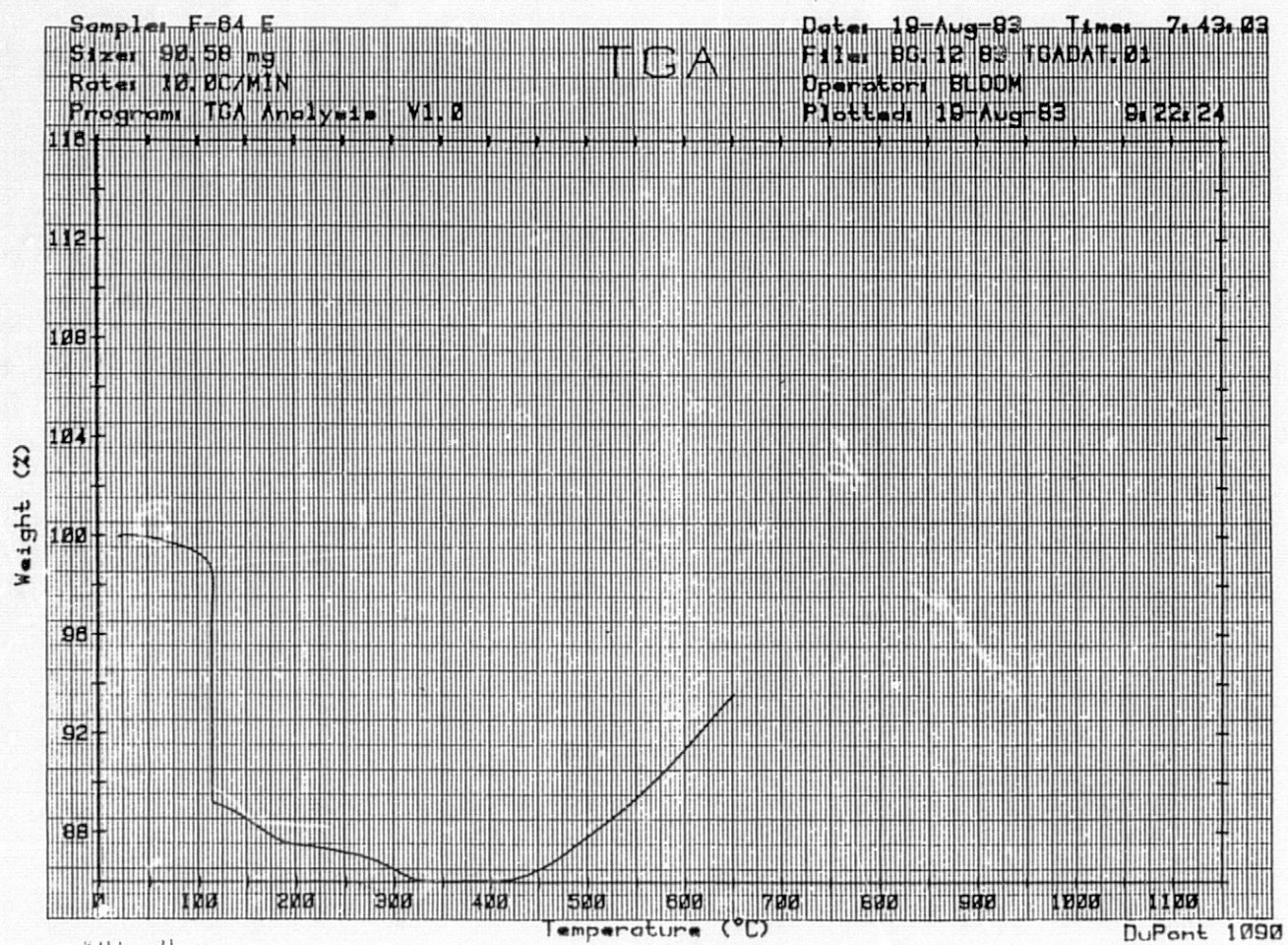
- IV ANALYSIS

- SEM

- TGA

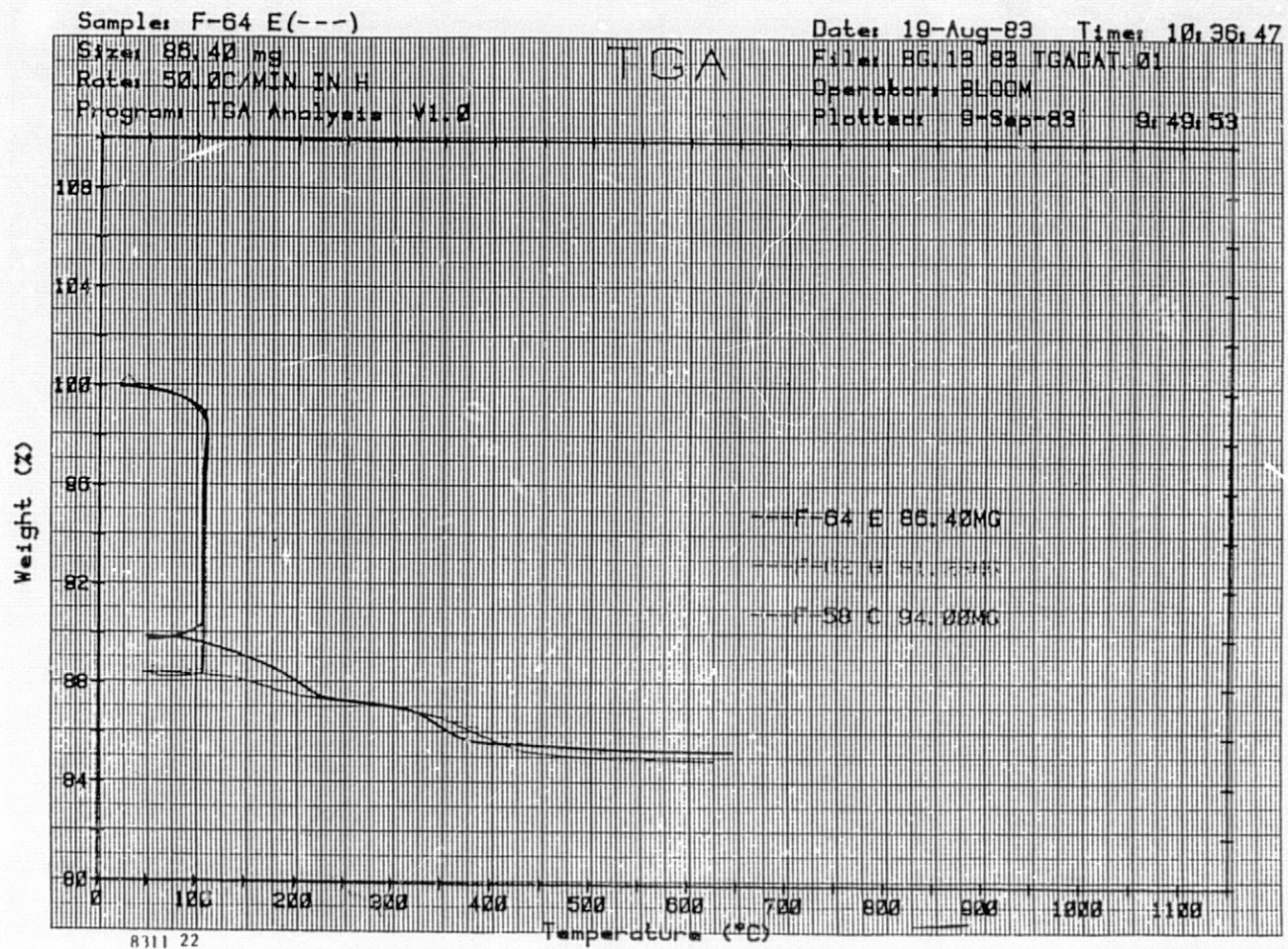
- DSC

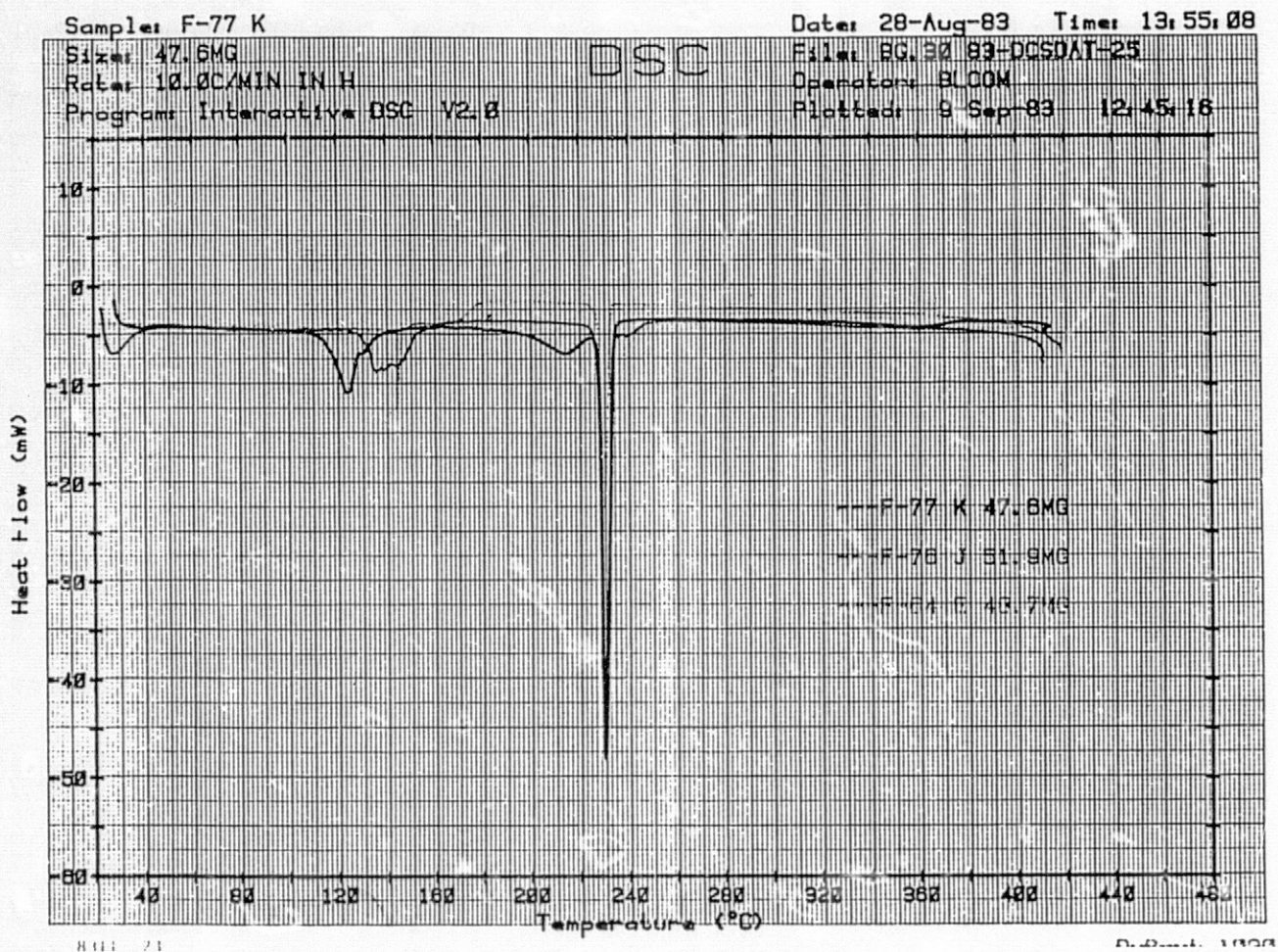




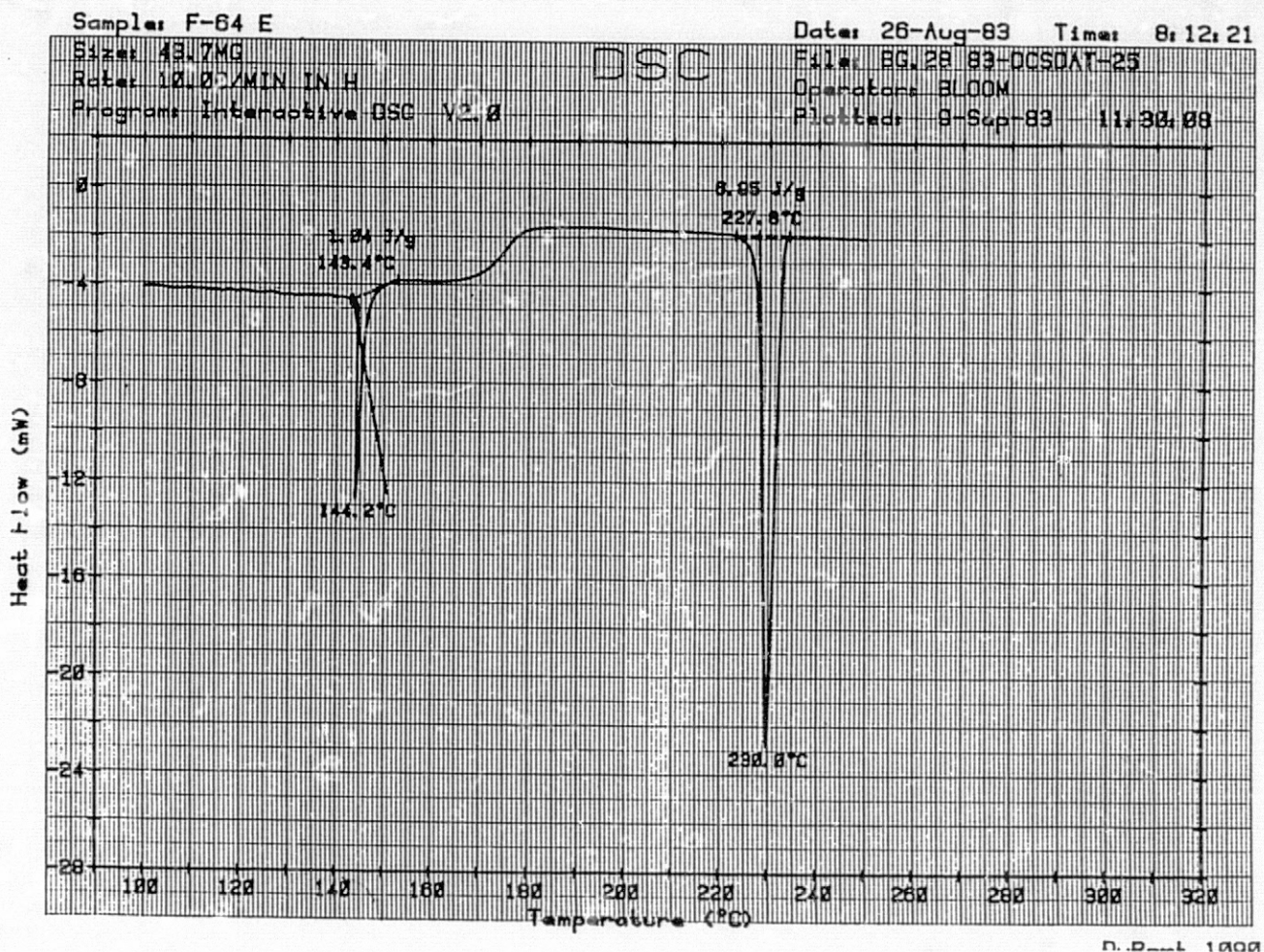


# CELL PROCESSING AND HIGH-EFFICIENCY CELLS









### Future Work

- TITANIUM RESINATE
- BORANE PYRIDINE
- MOLYBDENUM OXIDE
- ORGANO-SILANES
- DRY HYDROGEN

# PROCESS RESEARCH OF NON-Cz SILICON MATERIAL

WESTINGHOUSE ELECTRIC CORP.

C.M. Rose  
R.B. Campbell

## Alternative Liquid-Boron Solutions Investigated

<u>Supplier</u>	<u>Liquid Mask Solution</u>	<u>Liquid Boron Solution</u>
Filmtronics	700A	FB201
Emul-s-one	B100	B201
Allied Chemical	X600*	XB150*
Diffusion Technology	U1A	B60

\*These are experimental products.

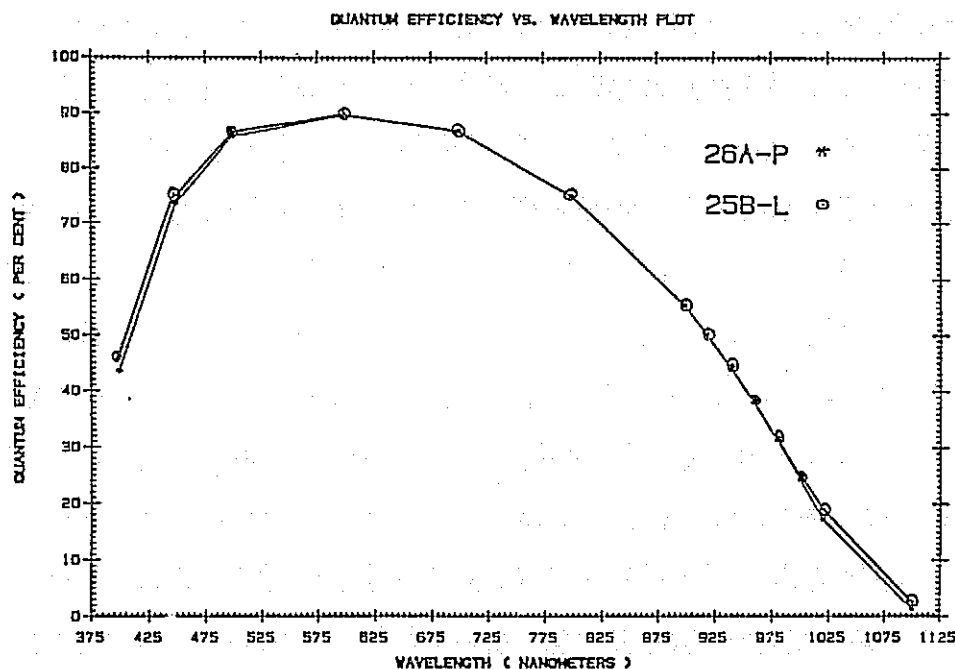
## Liquid Diffusion-Mask Study Summary

- Automated Application Technique Qualified
- Time/Temperature Parameters Determined for Post-Application Bake
- Film Thickness Investigations Completed
- Effects of Furnace Atmospheres Determined
- Post-Diffusion Mask Removal Problems Eliminated
- Mask Quality Equivalent to CVD  $\text{SiO}_2$
- Process Now Incorporated in Baseline Sequence

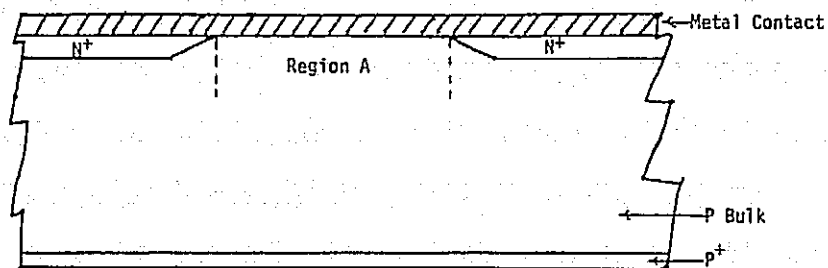
## Liquid Junction Formation Studies

- Automated Application Technique Qualified
- Optimum Time/Temperature Determined for Boron Drive
- Optimum Time/Temperature Determined for Phosphorus Drive
- Vendor Survey Completed
- Belt Furnace Drive Feasibility Established

## Quantum Efficiency Measurements for Liquid and Gaseous-PH Diffused Cells



## Low Shunt-Resistance Mechanism for Liquid PH Doping Experiments



**NOTE:** No  $N^+$  diffusion or very shallow diffusion in Region A.  
Metal contact shorts  $N^+$  and P regions giving a low  $R_{shunt}$ .

## Liquid Phosphorus Study Results

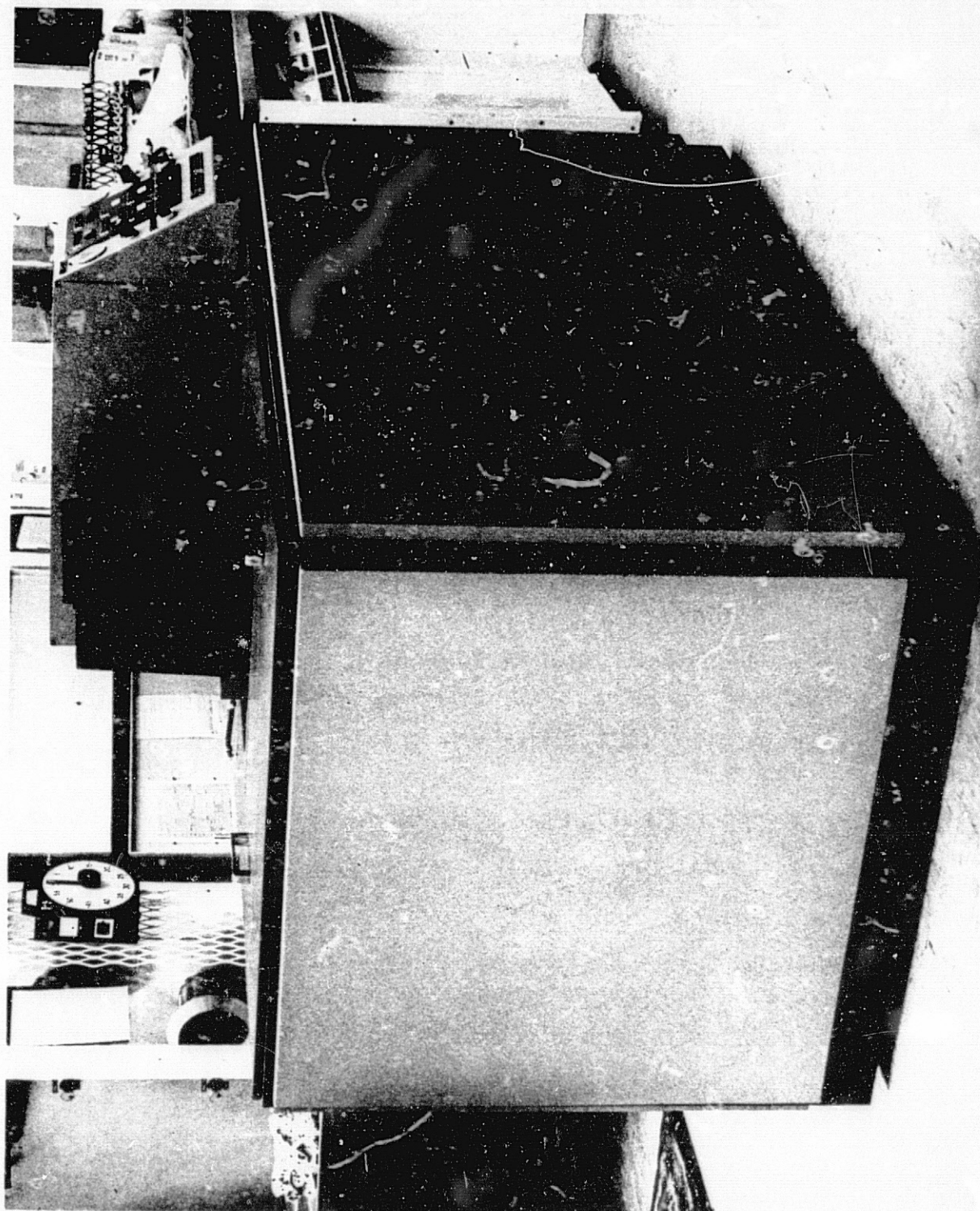
- Experiments Run Using Liquid Boron and Liquid Masks
- Uniformity and Continuity of PM Liquid Critical
- Efficiency Comparison From Recent Experiments

	<u>No. of Cells</u>	<u>Avg. Efficiency</u>
Baseline ( $POCl_3$ ) Process	76	13.3%
Liquid Ph Process	66	13.2%

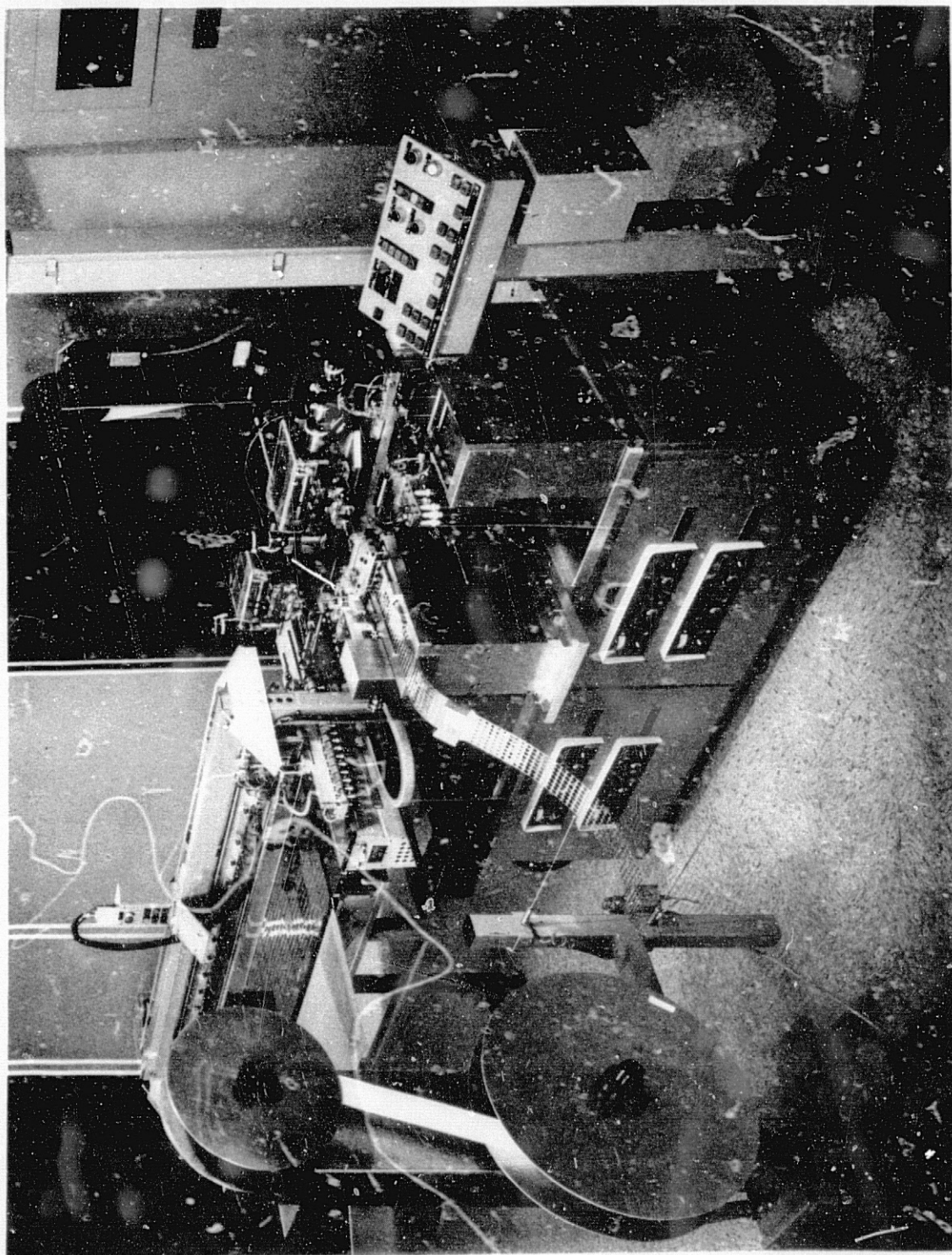
- Properties Controlled By Emitter Region
- Large Scale Verification Runs Planned



Meniscus Coating Equipment



K&S Automatic Cell Interconnect Station





## Conclusions

- All Program Tasks Completed Within Budget
- Liquid Boron/Liquid Diffusion Mask Processes Incorporated into (W) Baseline Sequence
- Meniscus Coater Qualified for Liquid Application
- Feasibility of Belt Furnace Junction Drive Established
- Costing Studies Show Liquid Dopant/Liquid Mask Decrease Overall Production Costs by 3%
- Ion Implantation Material Delivered to JPL
- Silicon Shot Tower Installed/Material Qualified

# THIN-FILM DIFFUSION BARRIERS

CALIFORNIA INSTITUTE OF TECHNOLOGY

M. A. Nicolet

The objective of this program is to improve the stability of metal contacts to semiconductors by means of thin-film diffusion barriers, with emphasis on applications to solar cells. Two types of thin-film barriers have been investigated:

- (1) Passive barriers, as typically represented by reactively sputtered TiN, and
- (2) Amorphous metallic films, as represented by RF-sputtered binary alloys.

## Reactively Sputtered TiN Films

The contact resistivity of reactively sputtered TiN films deposited on Si has been measured. On solar-cell-type  $p^+$ -Si (doped to about  $10^{20}$  B atoms/cm<sup>3</sup>), the contact resistivity is about  $3 \times 10^{-4} \Omega\text{cm}^2$ ; on  $n^+$ -Si (doped to about  $2 \times 10^{20}$  P atoms/cm<sup>3</sup>), it is about  $1.5 \times 10^{-5} \Omega\text{cm}^2$  for as-deposited films. These values are sufficiently low to qualify these barriers for solar concentrations of approximately 50 for  $p^+$ -type cells and significantly beyond 100 for  $n^+$ -type cells. Upon thermal annealing (600°C, 15 min in vacuum), the contact resistivity converges to a common value of 6 or  $7 \times 10^{-5} \Omega\text{cm}^2$ . This effect has been studied in detail. It can be explained in terms of sputtering damage that produces donor-like traps near the Si surface. A model assuming an exponential decrease of the trap concentration with depths with a characteristic decay length of 45 Å accounts well for the observed characteristics [forward and reverse  $I(V)$ , and  $C(V)$ ]. Thermal annealing reduces the trap concentration. The trap-free value of the barrier height,  $\phi_B$ , derived from these data is 0.55 V or  $\phi_{Bn}$  and 0.57 for  $\phi_{Bp}$ , including barrier height lowering by image forces. A further test of the effectiveness of reactively sputtered TiN thin-film diffusion barriers has been performed with Al overlayers on NiSi/Si contacts. Diodes where the Al is in direct contact with NiSi fail rapidly under thermal annealing. Diodes with a reactively sputtered TiN film interposed between the Al and the NiSi successfully pass annealing tests at 500°C for hours. Similar studies are in progress with Al overlayers on other silicides. These contact schemes are of interest to Si integrated circuits.

## Sputtered Amorphous Metallic Binary Alloy Films

We have formed a number of amorphous metallic binary alloy films by sputtering of compound targets whose elemental combination and composition conformed to the structural difference rule. The contact resistivity of Fe-W,

## CELL PROCESSING AND HIGH-EFFICIENCY CELLS

Ni-Mo and Ni-W was determined for the as-deposited and for annealed amorphous films on solar-cell-type  $p^+(10^{20} \text{ B/cm}^3)$  and  $n^+(\approx 2 \times 10^{20} \text{ P/cm}^3)$  Si. In all cases, the contact resistivity is in the  $10^{-6} \Omega\text{cm}^2$  range, or below, and changes little upon annealing up to  $500^\circ\text{C}$  for 30 min. The values are so low as to be of potential interest to VLSI applications. The barrier heights have also been determined. They differ little ( $0.61 \leq B_n/V \leq 0.65$ , and  $0.44 \leq B_p/V \leq 0.45$ ) for as-deposited films, and change little ( $\leq 0.06 \text{ V}$ ) upon annealing ( $500^\circ\text{C}$ , 30 min). We presently investigate the thermal stability of the amorphous films themselves, and their usefulness as diffusion barriers in complete contact schemes.

At this point, the reactively sputtered TiN films still have an edge over the sputtered amorphous metallic films as diffusion barriers, because the successful operation in complete contact schemes of solar cells has been demonstrated only for TiN. Metallurgical stability tests indicate that amorphous metallic films cease to be functional barriers as soon as the films recrystallize.

## Thin-Film Diffusion Barriers

### STRUCTURE

#### SINGLE-CRYSTAL

Minimal Defects	unpractical
Minimal Diffusivities	

#### AMORPHOUS

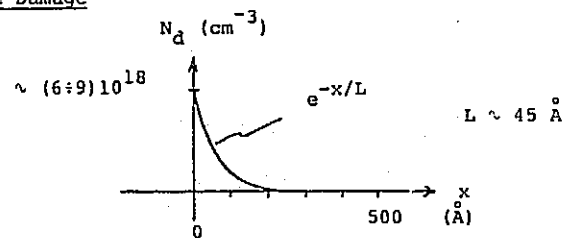
No Extended Defects	attractive
Low Diffusivities	novel

#### POLYCRYSTALLINE

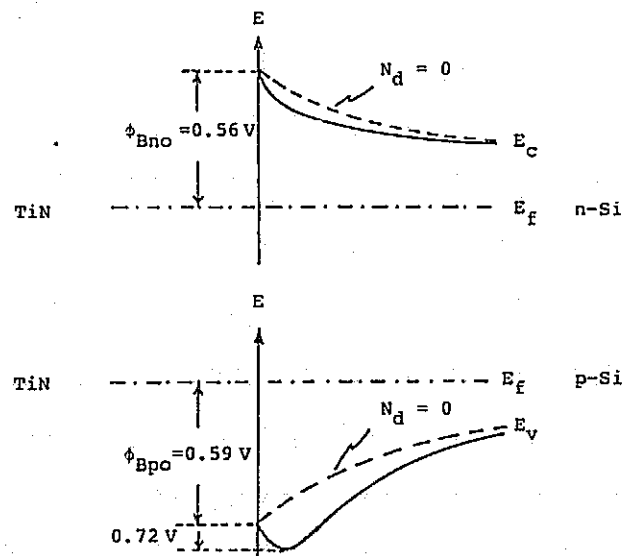
Extended Defects	practical
High Diffusivity Paths	problematic

## Reactively dc-Sputtered TiN on n- and p-Silicon

### Surface Damage



### Potential Distribution



$\phi_B$  After Annealing ( $> 600^\circ\text{C}$ , 15 min)

$$\phi_{Bn} = 0.55 \text{ V}$$

$$\phi_{Bp} = 0.57 \text{ V}$$

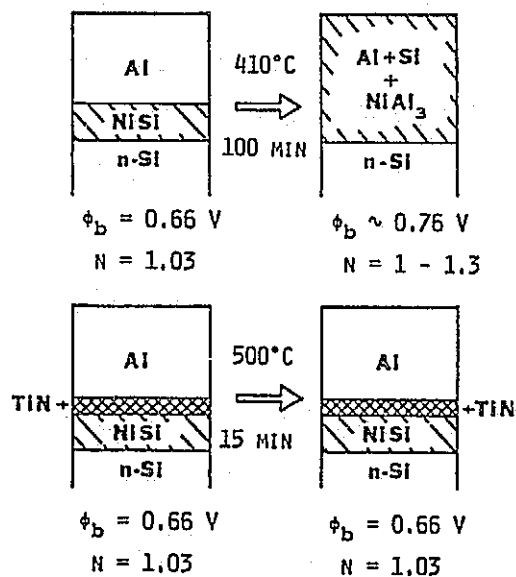
## Theoretical Values

Theoretical Values of Characteristic Length  $L$  and Traps Concentration  $N_{ts}$  for DC Sputtered TiN on n- and p-Type Silicon.

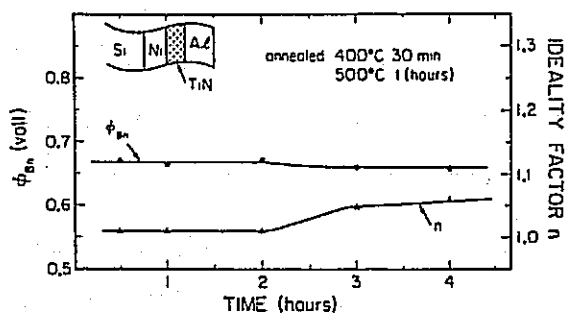
Thermal Treatment	$L$ (Å)	$N_{ts}$ for n-Si (cm <sup>-3</sup> )	$N_{ts}$ for p-Si (cm <sup>-3</sup> )
as-deposited	45	$9.3 \times 10^{18}$	$5.7 \times 10^{18}$
450°C, 15 min	45	$6.1 \times 10^{18}$	$2.7 \times 10^{18}$ *
500°C, 15 min	45	$5.1 \times 10^{18}$	$2.0 \times 10^{18}$
600°C, 15 min	45	$2.2 \times 10^{18}$	$\leq 1.1 \times 10^{18}$

REMARKS: \* The thermal treatment is 400°C, 15 min.

## Al-NiSi-n-Si Schottky Diode



## CELL PROCESSING AND HIGH-EFFICIENCY CELLS



Barrier height,  $\phi_{Bn}$ , and ideality factor,  $n$ , of n-Si/NiSi/TiN/Al Schottky diodes as a function of annealing duration at 500°C.

## Measured Contact Resistivity

Measured Contact Resistivity,  $\rho_c$ , for Amorphous Fe-W, Ni-Mo, and Ni-W Contacts on Silicon.

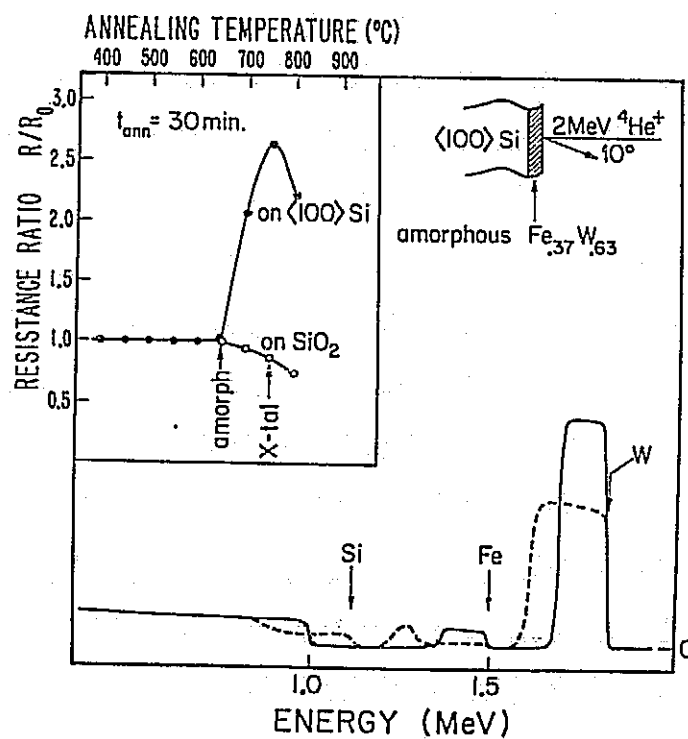
Contact Resistivity ( $\mu\Omega\text{cm}$ ) Heat Treatment	Fe <sub>45</sub> W <sub>55</sub>		Ni <sub>42</sub> Mo <sub>58</sub>		Ni <sub>36</sub> W <sub>64</sub>	
	$n^+(1 \times 10^{20}/\text{cm}^3)$	$p^+(1 \times 10^{20}/\text{cm}^3)$	$n^+(2 \times 10^{20}/\text{cm}^3)$	$p^+(1 \times 10^{20}/\text{cm}^3)$	$n^+(2 \times 10^{20}/\text{cm}^3)$	$p^+(1 \times 10^{20}/\text{cm}^3)$
as-deposited	0.1±0.05	2.8±0.8	1.1±0.3	1.3±0.4	1.4±0.3	0.89±0.02
400°C, 30 min	0.2±0.10	1.1±0.3			1.1±0.3	0.18±0.05
500°C, 30 min	0.1±0.05	1.1±0.3	1.0±0.3	0.8±0.3	2.0±0.3	0.35±0.05

## Measured Barrier Height

Measured Barrier Height  $\phi_{bn}$ ,  $\phi_{bp}$  for Amorphous  
Fe-W, Ni-Mo, and Ni-W Contacts to Silicon.

Heat Treatment	Barrier Height ( $\pm 0.01$ eV)	Fe <sub>45</sub> W <sub>55</sub>		Ni <sub>42</sub> Mo <sub>58</sub>		Ni <sub>36</sub> W <sub>64</sub>	
		$\phi_{bn}$	$\phi_{bp}$	$\phi_{bn}$	$\phi_{bp}$	$\phi_{bn}$	$\phi_{bp}$
as-deposited		.61		.69	.44	.65	.45
400°C, 30 min		.65				.65	.43
500°C, 30 min				.66	.44	.65	.39

## Backscattering Yield (Arbitrary Units)



# METALLIZATION COST COMPARISON

## JET PROPULSION LABORATORY

R.W. Aster

### Introduction

- Original concept first presented at 21st PIM (January 1983)
- Work expanded to 25 candidate processes for the PV metallization systems Research Forum, March 1983

#### Update

- Changes in some metallization parameters as suggested by Martin Wolf
- Use of a higher-efficiency cell baseline for the advanced processing concepts

#### Purpose of Analysis

- Compare costs and effectiveness of SOA metallization and potential advanced metallization concepts
- Estimate the potential impact of R&D in this area
- Develop an analysis approach that can be applied to key process steps where cost and performance tradeoffs are necessary

### Study Limitations

- There are many metallization processes; only 25 have been analyzed so far
- SOA metallization costs are typically based on commercial experience of industry
- Advanced metallization costs are typically based on laboratory-scale experiments and extrapolations
- There are two basic reliability issues:
  - Immediate mechanical and subsequent electrical test yields. (This has been addressed by this study)
  - Lifetime (e.g., 20-year) performance. (This has not yet been addressed)
- Compatibility with other process steps and with unusual sheet specifications will not be addressed
- Back metallization cost and performance data not included in the evaluation



## Methodologies Used

### Electrical Performance

Grid optimization model provides:

- Optimum spacing and dimensions (within process constraints) for the grid design
- Metallization coverage and volume
- Power lost in the cell from which the relative electrical performance is derived

### Cost

Focus on front metallization process steps such as masking, metal deposition, sintering, mask removal, and plate up

- Determine cost of using a copper ribbon to improve the current-carrying capability of the bus bar
- Use IPEG2 to calculate total cost of front metallization

## Cost and Relative Performance Results

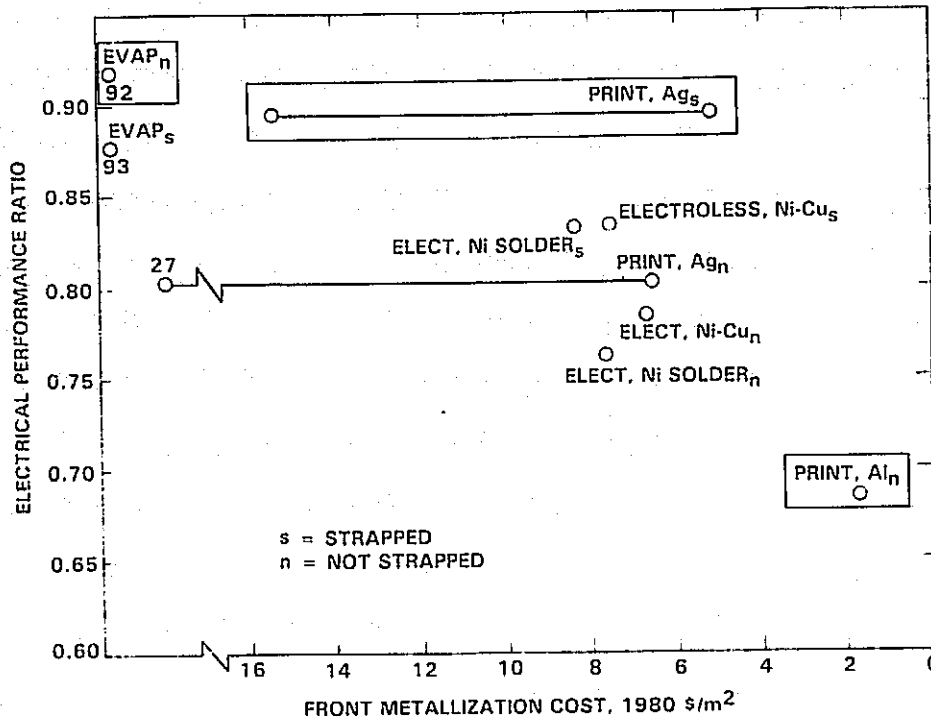
### SOA

Process or System	Strapped		Not Strapped	
	Performance Ratio	Cost, \$/m <sup>2</sup>	Performance Ratio	Cost, \$/m <sup>2</sup>
Evaporation	0.919	91.8	0.875	92.7
Print Ag	0.892	5.2 - 15.4	0.803	6.6 - 26.6
Print AL	—	—	0.679	1.7
Electroless Ni-Solder	0.833	8.4	0.760	7.7
Electroless Ni-Cu	0.835	7.6	0.788	6.7

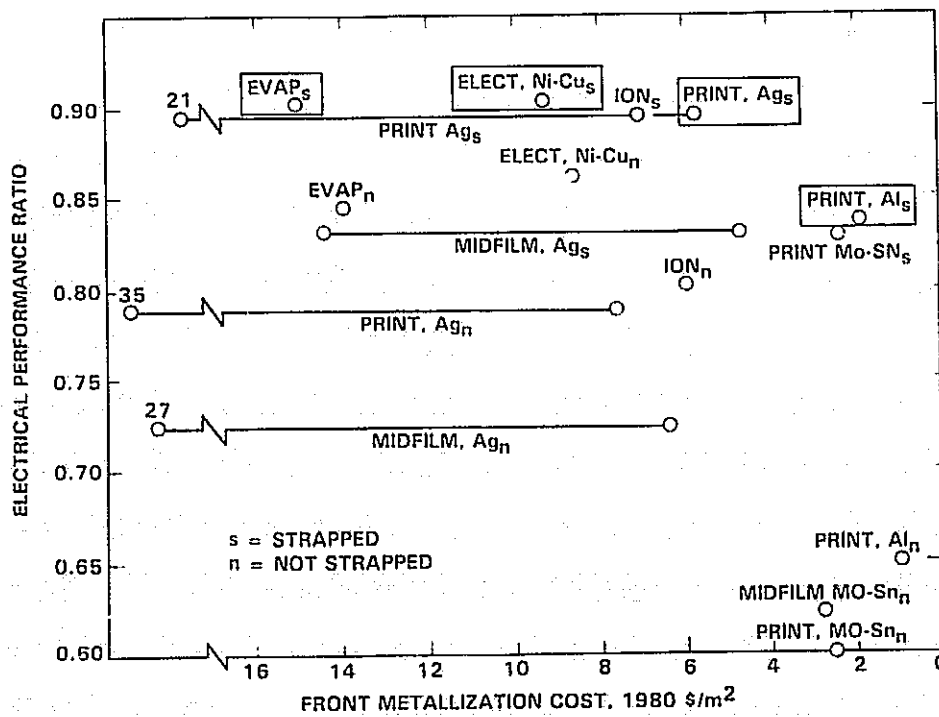
### Advanced

Process or System	Strapped		Not Strapped	
	Performance Ratio	Cost, \$/m <sup>2</sup>	Performance Ratio	Cost, \$/m <sup>2</sup>
Evaporation	0.904	15.1	0.848	14.1
Print Ag	0.880	5.7 - 21.3	0.785	7.6 - 34.7
Print A	0.839	1.9	0.650	1.0
Print Mo-Sn	0.835	2.2 - 2.6	0.600	2.0 - 3.0
Midfilm Ag	0.835	4.7 - 14.2	0.722	6.4 - 26.7
Midfilm Mo-Sn	0.817	2.7 - 3.1	0.617	2.4 - 3.4
Ion Plating Ti-Ni-Cu	0.880	7.0	0.816	6.0
Electroless Ni-Cu	0.906	9.6	0.864	8.6

# Efficient Frontier: State of The Art (SOA)



# Efficient Frontier: Advanced Systems



## Optimization

An ideal solution would have zero cost and 100% relative efficiency (upper right hand corner). Below this point, tradeoff lines can be drawn that give equally preferred points. These lines tradeoff cost versus efficiency and rely on total area-related system cost to determine their slope.

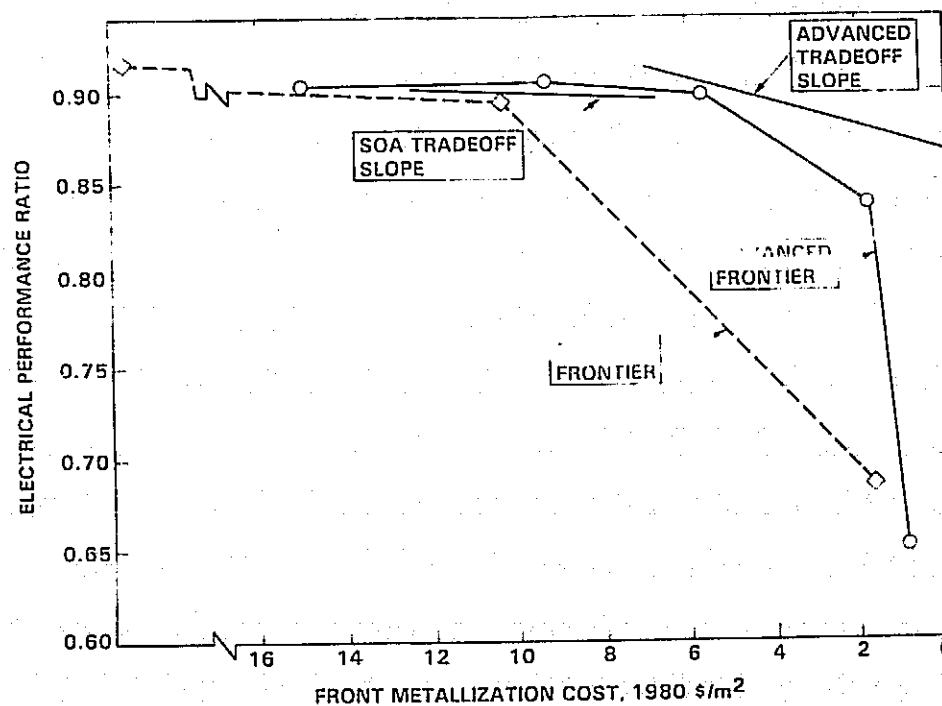
The optimal realistic solution lies on the tradeoff line that is closest to the ideal solution. The slope of the tradeoff line is approximated by the expression:

$$1 / (1000 \text{ W/m}^2 \cdot \text{module efficiency} \cdot \text{area-related system costs})$$

For example:

	Baseline Efficiency	Area-related System Costs	Slope
SMUD SOA	0.11	\$11/W	$8.26 \times 10^{-4}$
Advanced	0.14	\$1.2/W	$5.95 \times 10^{-3}$

## Combined Efficient Frontiers



## Summary

- Cost and effectiveness of metallization systems have been compared
- Twenty-five processes have been examined so far
- This study shows that metallization R&D could lead to significant advances in low-cost, high-performance processing
- R&D emphasis should be placed on those processes that are either on or close to the efficient frontier and the tradeoff slope. Careful consideration should be given to the other processes before additional R&D attention is given them

# EVALUATION OF THE ION IMPLANTATION PROCESS FOR PRODUCTION OF SOLAR CELLS FROM SILICON SHEET MATERIALS

SPIRE CORP.

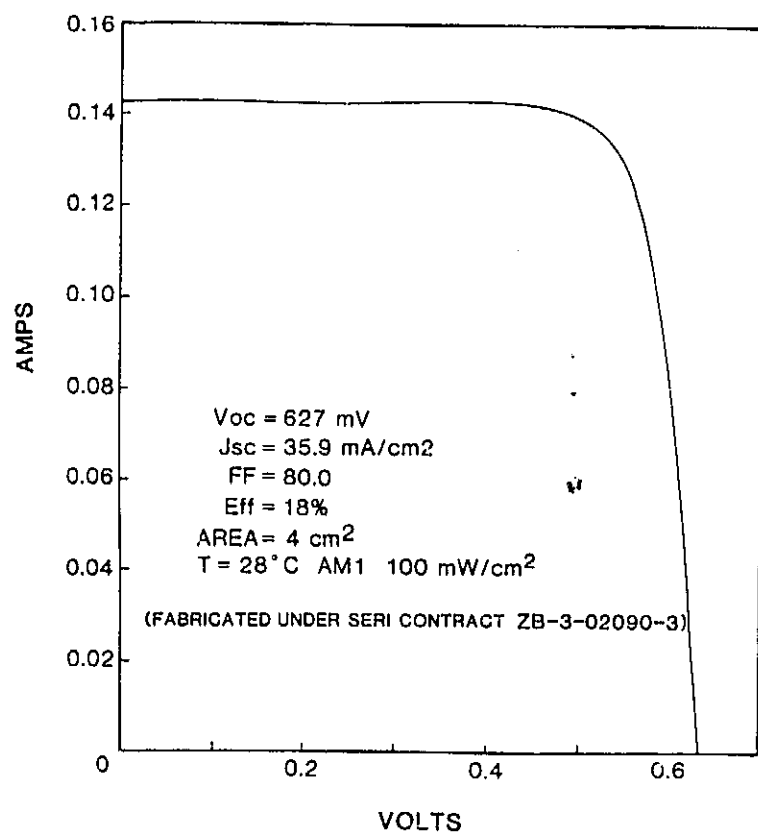
M.B. Spitzer

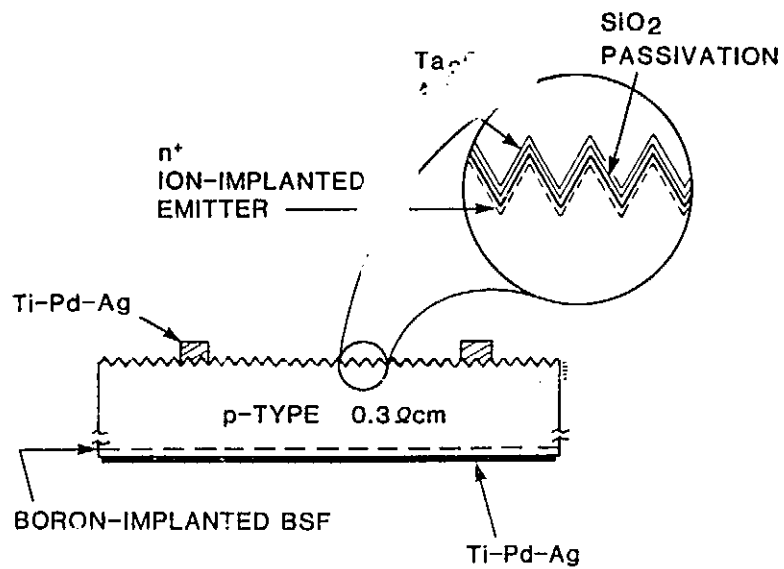
**Materials Studied: Dendritic Web,  
EFG, Cz, HEM, Semix and Silso**

## Advantages of Ion Implantation

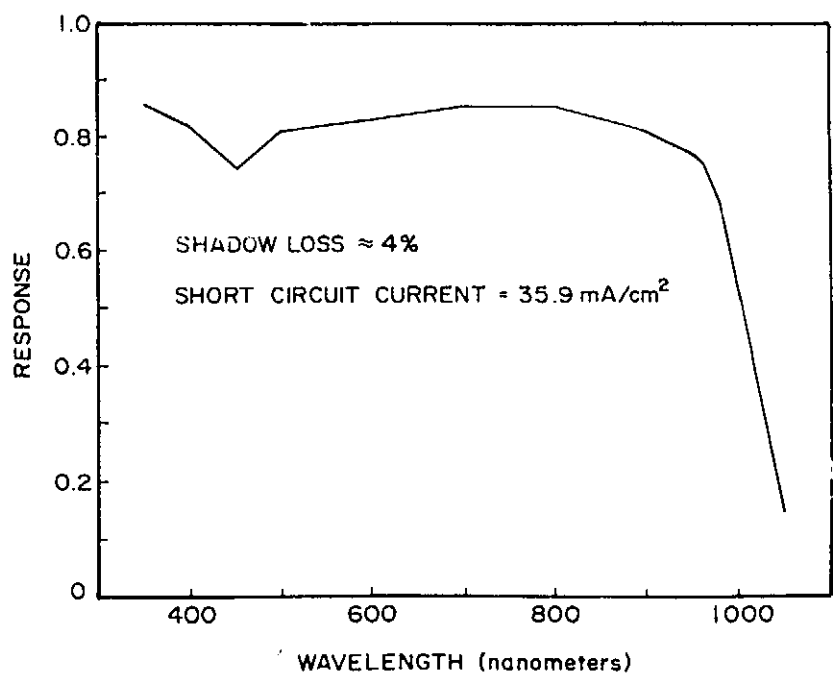
- HIGH PROCESS UNIFORMITY
- DRY, EFFLUENTLESS PROCESS
- HIGH CELL CONVERSION EFFICIENCY

### Illuminated I-V Characteristics of a High-Efficiency Si Cell





### External Quantum Efficiency



## Important Cell Features

- LOW SHEET RESISTIVITY  
( $R < 100 \Omega/\square$ )
- NO DEAD LAYER
- SURFACE PASSIVATION  
FOR IMPROVED  $J_{sc}$  AND  $V_{oc}$

---

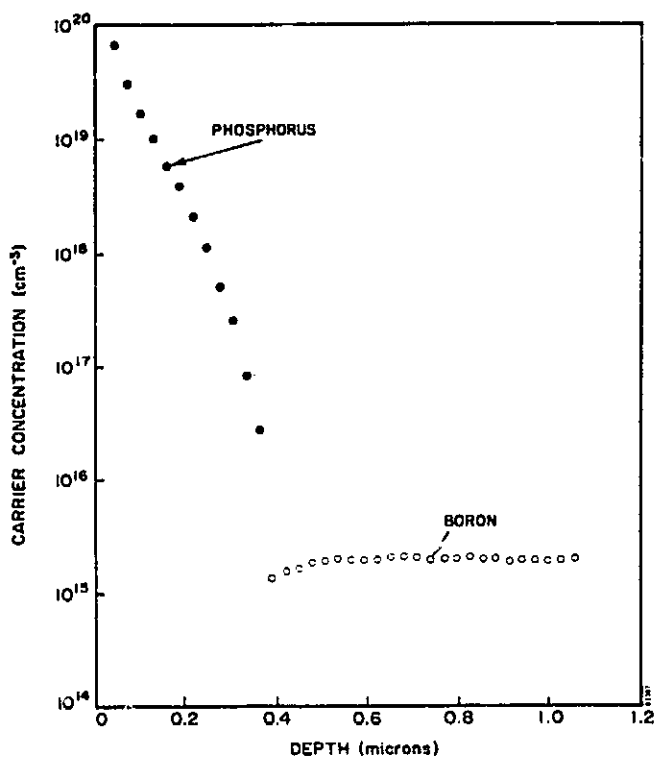
CONCLUSION: ION IMPLANTATION IS IDEAL FOR  
HIGH EFFICIENCY CELL  
FABRICATION.

## Baseline Fabrication Sequence for Dendritic-Web Solar Cells

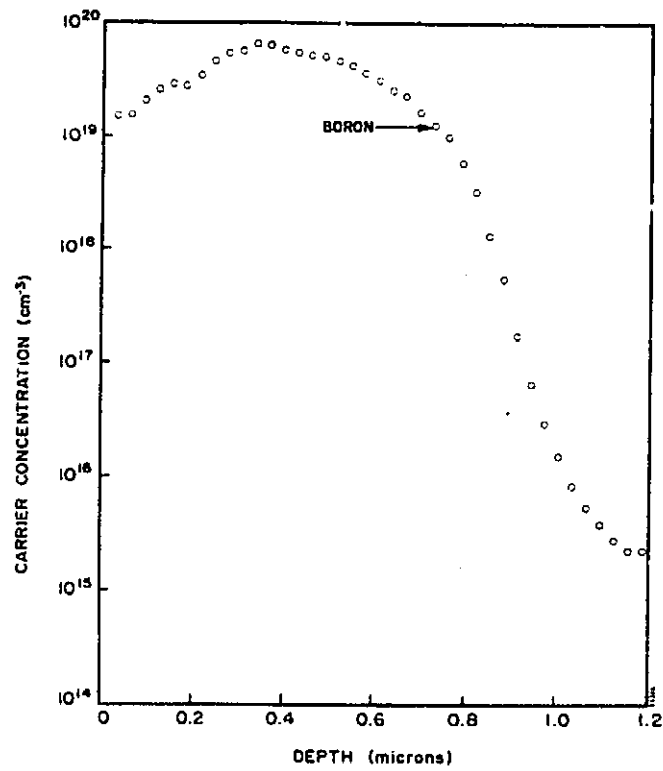
1. REMOVE DENDRITES
2. CLEAN
3. IMPLANT BACK  
 $11B^+$   
50 KEV  
 $5 \times 10^{15} \text{ ION}/\text{CM}^2$
4. ANNEAL  
 $950^\circ\text{C} - 2 \text{ HRS.}$   
 $550^\circ\text{C} - 2 \text{ HRS.}$
5. IMPLANT FRONT  
 $31P^+$   
10 KEV  
 $2.5 \times 10^{15} \text{ IONS}/\text{CM}^2$
6. ANNEAL  
 $550^\circ\text{C} - 2 \text{ HRS.}$   
 $850^\circ\text{C} - 15 \text{ MIN.}$   
 $550^\circ\text{C} - 2 \text{ HRS.}$
7. APPLY PHOTOLITHOGRAPHY
8. EVAPORATE CONTACTS ON FRONT AND BACK  $Ti-Pd-Ag$
9. LIFT OFF AND SINTER
10. PLATE FRONT METAL  $10 \mu\text{M}$
11. SAW TO SIZE  $2 \text{ CM} \times 2 \text{ CM}$
12. TEST



## Ion-Implanted Junction in Dendritic Web



## Ion-Implanted BSF in Dendritic Web



### Emitter Anneal Matrix for Phosphorus Implantation at 10 keV

THREE-STEP ANNEAL TEMP (°C) (2 HRS, 15 MIN, 2 HRS)	DENDRITIC WEB				FLOAT ZONE CONTROLS			
	Voc (mV)	Jsc (mA/cm <sup>2</sup> )	FF (%)	EFF (%)	Voc (mV)	Jsc (mA/cm <sup>2</sup> )	FF (%)	EFF (%)
550/850/550°C	524	18.9	75.6	7.48	584	23.2	78.6	10.6
550/900/550°C	531	18.7	76.1	7.59	602	22.4	76.3	10.3
550/950/550°C	554	19.9	73.9	8.28	602	22.4	76.3	10.3

NO AR COATINGS WERE EMPLOYED.

### Emitter Anneal Matrix for Phosphorus Implantation at 5 keV

THREE-STEP ANNEAL TEMP (°C) (2 HRS, 15 MIN, 2 HRS)	WEB				FLOAT ZONE CONTROLS			
	Voc (mV)	Jsc (mA/cm <sup>2</sup> )	FF (%)	EFF (%)	Voc (mV)	Jsc (mA/cm <sup>2</sup> )	FF (%)	EFF (%)
550/850/550°C	521	18.6	71.6	6.94	594	23.3	77.5	10.7
550/900/550°C	537	19.5	75.8	7.96	593	22.2	73.6	9.71
550/950/550°C	515	17.4	75.5	6.77	582	21.0	73.8	9.0

NO AR COATINGS WERE EMPLOYED.

### Experiments in Progress

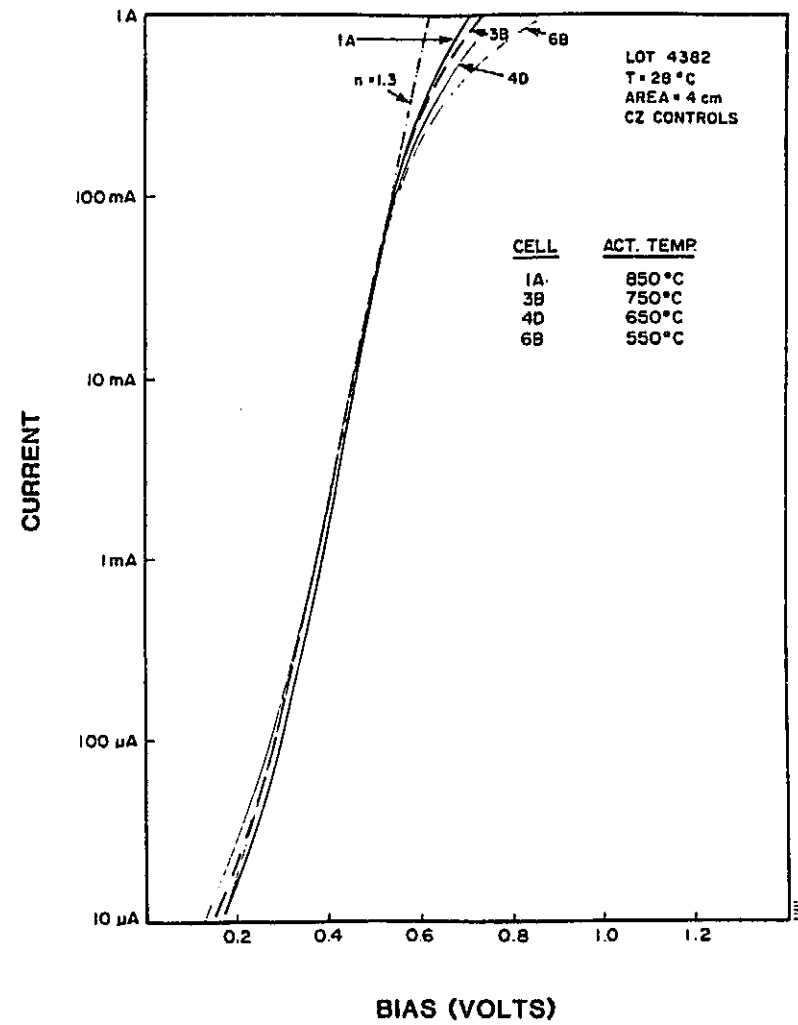
- FABRICATION OF HIGH EFFICIENCY CELLS  
FROM DENDRITIC WEB USING  
METICULOUS PROCESSING
- PREPARATION OF ION IMPLANTED WEB  
SOLAR CELLS FOR FABRICATION OF  
CELLS AT WESTINGHOUSE

**Average AM1 Performance of the Cz Control Group**

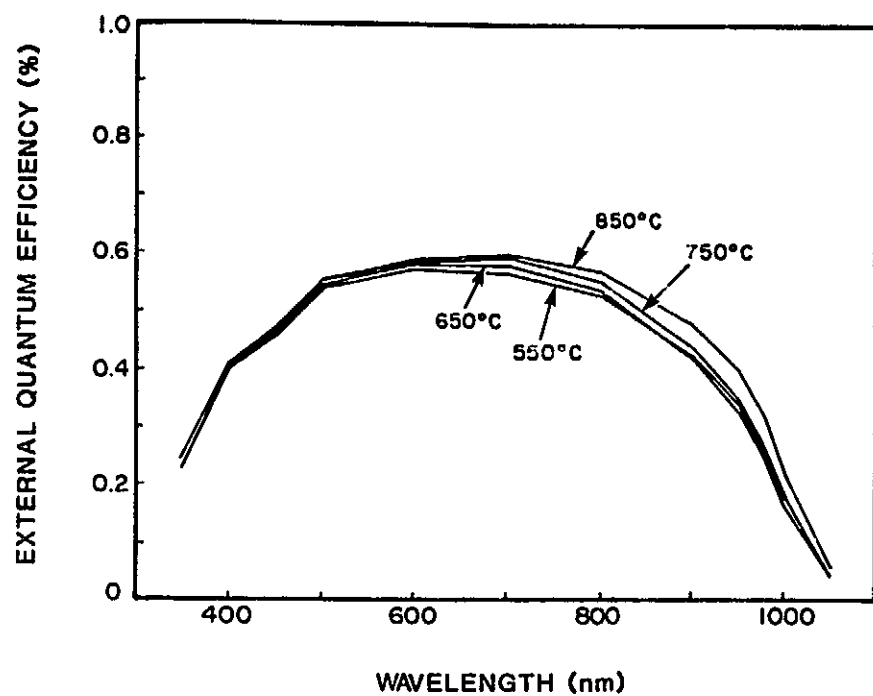
ACTIVATION TEMPERATURE	Voc (mV)	Jsc (mA/cm <sup>2</sup> )	FF (%)	EFF (%)	EFF x 1.4 (%)
5500C	526	24.3	71.1	9.09	12.7
6500C	529	24.3	71.9	9.24	12.9
7500C	533	23.9	75.2	9.60	13.4
8500C	543	23.9	77.1	10.0	14.0
3-STEP	533	22.3	73.5	9.07	12.7

NOTES: INSOLATION LEVEL IS 100 mW/cm<sup>2</sup>, T = 280C, AREA = 4 cm<sup>2</sup>.

Dark I-V Characteristics of the Cz Control Cells



## EFG Group

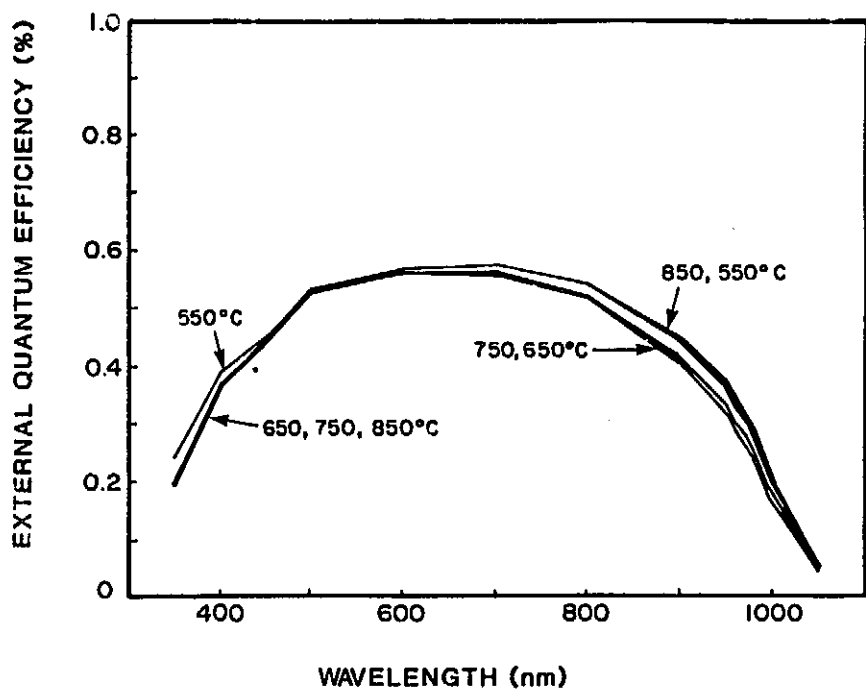


## Average AM1 Performance of the EFG Group

ACTIVATION TEMPERATURE	Voc (mV)	Jsc (mA/cm <sup>2</sup> )	FF (%)	EFF (%)	EFF x 1.4 (%)
550°C	502	20.2	70.8	7.18	10.1
650°C	512	21.1	68.1	7.33	10.3
750°C	517	21.4	70.5	7.81	10.9
850°C	505	22.1	68.9	7.68	10.8
BEST CELL	526	22.3	72.9	8.39	11.7

NOTES: INSOLATION LEVEL IS 100 mW/cm<sup>2</sup>, T = 28°C, AREA = 4 cm<sup>2</sup>.

### Silso Group

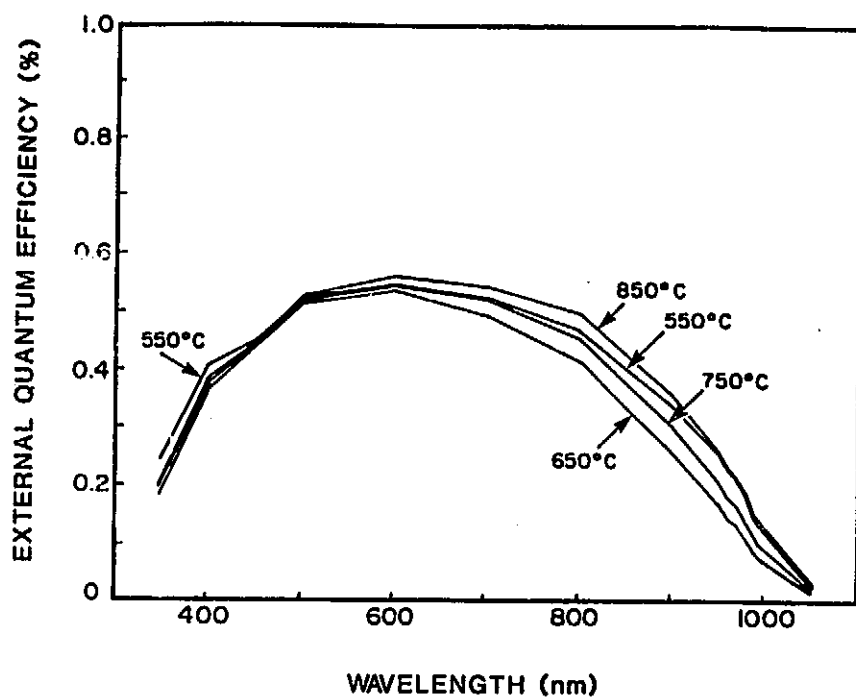


### Average AM1 Performance of the Silso Group

ACTIVATION TEMPERATURE	V <sub>oc</sub> (mV)	J <sub>sc</sub> (mA/cm <sup>2</sup> )	FF (%)	EFF (%)	EFF x 1.4 (%)
550°C	519	21.5	73.6	8.20	11.5
650°C	514	21.0	73.3	7.91	11.1
750°C	519	21.1	73.8	8.07	11.3
850°C	528	21.4	75.8	8.56	12.0
3-STEP	523	20.8	75.0	8.15	11.4
BEST CELL	533	21.9	75.6	8.82	12.4

NOTES: INSOLATION LEVEL IS 100 mW/cm<sup>2</sup>. T = 28°C. AREA = 4 cm<sup>2</sup>.

## HEM Group



## Average AM1 Performance of the HEM Group

ACTIVATION TEMPERATURE	V <sub>oc</sub> (mV)	J <sub>sc</sub> (mA/cm <sup>2</sup> )	FF (%)	EFF (%)	EFF x 1.4 (%)
550°C	529	20.5	74.3	8.07	11.3
650°C	520	18.9	73.9	7.25	10.2
750°C	526	19.2	73.5	7.42	10.4
850°C	549	21.2	76.2	8.86	12.4
3-STEP	553	20.3	74.0	8.33	11.7
BEST CELL	567	21.9	74.6	9.25	13.0

NOTES: INSOLATION LEVEL IS 100 mW/cm<sup>2</sup>, T = 28°C, AREA = 4 cm<sup>2</sup>.



**Pulsed Electron-Beam Annealing of Sheet Silicon Materials**

MATERIAL (NO. OF CELLS)	Voc (mV)	Jsc (mA/cm <sup>2</sup> )	FF (%)	EFF (%)	EFF x 1.4 (%)
CZ (15)	521	23.3	68.9	8.93	11.7
BEST CZ	534	23.4	75.9	9.48	13.3
HEM (15)	525	22.3	70.9	8.29	11.6
BEST HEM	531	22.8	73.1	8.87	12.4
SILSO (15)	519	21.0	69.5	7.60	10.6
BEST SILSO	542	21.5	73.3	8.53	11.9

**Task 2 Status**

- COMPARISON OF THERMAL ANNEAL TO PEBA IN PROGRESS
- THERMAL ANNEAL STUDIES COMPLETE FOR EFG, HEM, AND SILSO
- THERMAL ANNEAL STUDIES OF SEMIX IN PROGRESS

## Summary

- ION IMPLANTATION OF DENDRITIC WEB HAS BEEN STUDIED
- THERMAL ANNEAL STUDIES INDICATE INTERESTING TEMPERATURE EFFECTS
- ION IMPLANTATION HAS BEEN USED FOR FABRICATION OF SILICON CELLS WITH 18% EFFICIENCY\*

---

\*UNDER SERI CONTRACT ZB-3-02090-3

# CLUSTER ION BEAM DEPOSITION

## JET PROPULSION LABORATORY

D.J. Fitzgerald

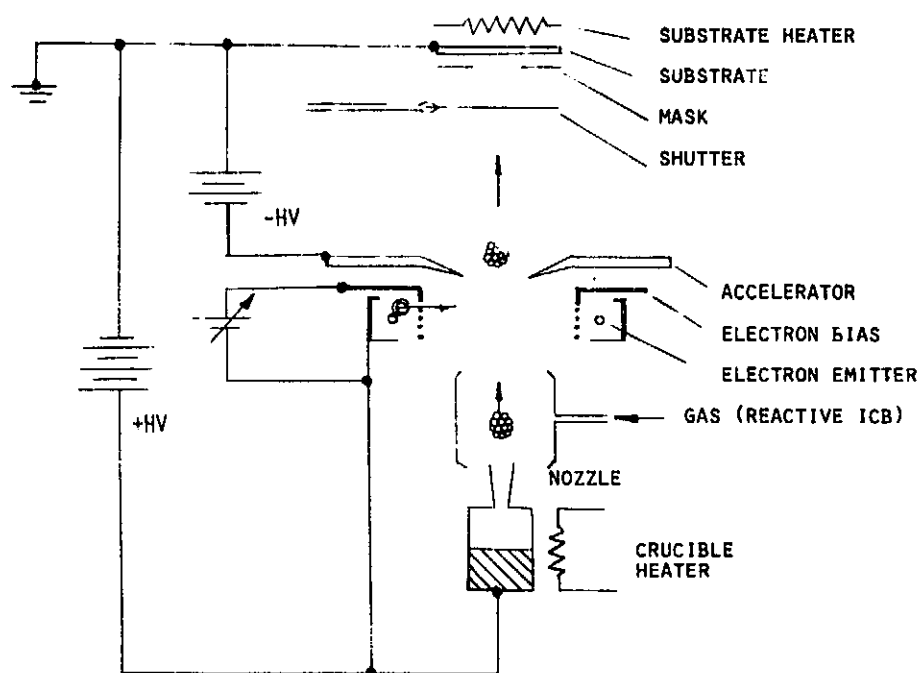
### Objectives

- ° CHARACTERIZE ION CLUSTER BEAM (MASS, ENERGY CHARGE).
- ° DEPOSIT Ag ON Si WITHOUT Pd, Ti OR SINTER.
- ° EVALUATE DEPOSITION QUALITY AS FUNCTION OF ICB SOURCE PARAMETERS AND SUBSTRATE TEMPERATURE.
- ° COMPARE WITH CONVENTIONAL TiPdAg SYSTEM.

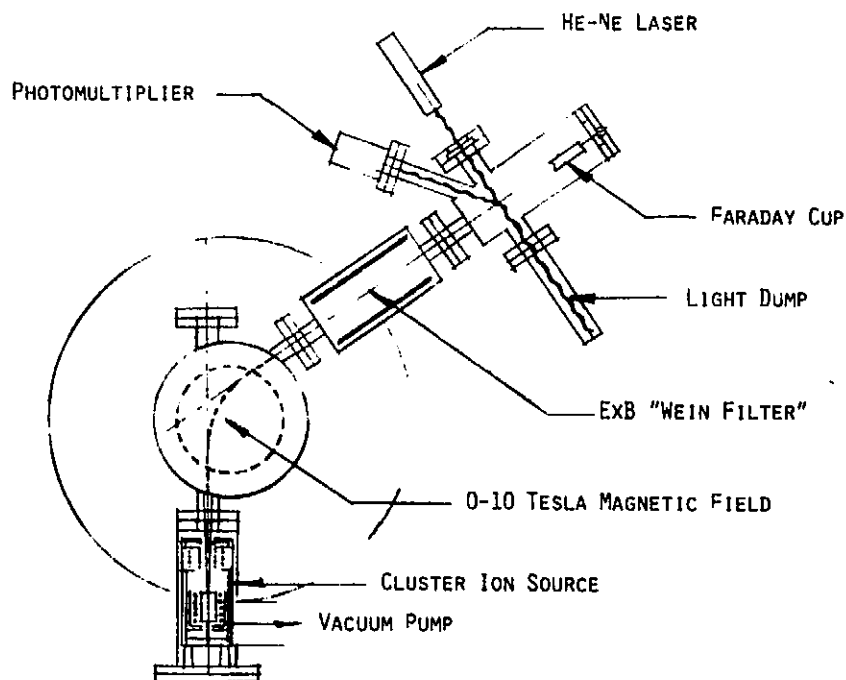
### (Claimed) Advantages of ICB

- ° MEDIUM VACUUM CONDITIONS REQUIRED ( $10^{-6}$  TORR)
- ° SUBSTRATES AT LOW TEMPERATURE ( $<500^{\circ}\text{C}$ )
- ° REASONABLE DEPOSITION RATES ( $0.05 - 0.5 \mu\text{m}/\text{min}$ )
- ° MAINTAINS SURFACE CLEANLINESS (SPUTTER ACTION)
- ° MAY USE PURE MATERIALS (NO CARRIER GAS)
- ° CONTROL OF CRYSTALLINITY (AMORPHOUS/SINGLE CRYSTAL)
- ° STRONG ADHESION (HIGH PACKING DENSITY)
- ° COMPOUND DEPOSITS (DIRECT OR REACTIVE ICB)

## Ion Cluster Beam (ICB) Deposition



## ICB Characterization Apparatus



## Status

- ° DEPOSITION VACUUM CHAMBER OPERATIONAL.
- ° SILVER ICB SOURCE DESIGN COMPLETE.
- ° SAMPLE HOLDER DESIGN IN PROGRESS.
- ° ICB SOURCE POWER SUPPLIES UNDER CONSTRUCTION.
- ° ICB CHARACTERIZATION APPARATUS 50% COMPLETE.

# MOLECULAR-BEAM EPITAXIAL GROWTH OF SILICON SOLAR CELLS

UNIVERSITY OF CALIFORNIA, LOS ANGELES

F.G. Allen

- ADVANTAGES:
- DOPING LEVEL CONTROLLABLE FROM  $10^{14}$  TO  $10^{19} \text{ cm}^{-3}$
  - DEPTH CONTROL TO  $< 100\text{\AA}$
  - ARBITRARY ARRANGEMENT OF PROFILE
  - REPRODUCIBLE FOR TEST OF OPTIMUM DESIGN
  - CAN GROW MULTIJUNCTION CASCADE CELLS
  - CAN GROW FRONT SURFACE FIELDS  
EVEN FOR THIN ( $0.5\mu$ ) FRONT LAYERS

- DISADVANTAGES:
- EXPENSIVE PROCESS (U.H.V.)
  - MATERIAL QUALITY STILL POOR AT JUNCTIONS
  - HARD TO GROW LAYERS  $> 10\mu$  DEEP
  - STILL UNPROVEN

## Solid-Phase Epitaxial Growth During MBE

### NEW METHOD:

- EVAPORATE SILICON ONTO CLEAN SUBSTRATE AT ROOM TEMPERATURE
- CO-EVAPORATE n OR p DOPANTS (Sb OR Ga) AS DESIRED FOR PROFILE
- RE-GROW CRYSTAL LAYER BY SOLID PHASE EPITAXY BY HEATING SUBSTRATE TO 560 C, FOR 30 MINUTES/MICRON

### ADVANTAGES:

- ABSOLUTELY SHARP DOPING PROFILES (NO DIFFUSION AT 560 C)
- NO CARRY-OVER OR TRANSIENT SMEARING
- ALL DOPANTS HAVE UNITY STICKING COEFFICIENTS - EASY CONTROL
- HIGHER MAXIMUM DOPING LEVELS ATTAINED - TO  $>10^{19} \text{ cm}^{-3}$

### DISADVANTAGES:

- HARD TO GET PERFECT CRYSTAL AT INTERFACE

## UCLA Silicon MBE Problems

POOR CRYSTAL QUALITY, p-n JUNCTIONS

### SYMPTOMS:

- HIGH REVERSE CURRENT
- SOFT BREAKDOWN
- RAPID ETCHING OF LAYER
- DIFFUSION OF Al THROUGH LAYER

### TESTS:

- MOBILITY VS DOPING
- TEM EXAMINATION
- RBS OF SPE SAMPLE
- SIMS ANALYSIS
- SURFACE AUGER
- X-RAY FLUORESCENCE
- DLTS

### RESULTS:

- GOOD AS BULK
- SOME AREAS  $< 10^4 \text{ cm}^{-2}$
- EXCELLENT EXCEPT AT INTERFACE
- $\left\{ \begin{array}{l} \text{SOME C} \\ \text{SOME O} \end{array} \right\}$  AT INTERFACE
- USUALLY O.K.
- SOME NICKEL IMPURITY ?
- NO RESULTS

## Parameters for Efficiency Calculations

Depth of top junction =  $0.5 \mu$

Thickness of second  $n^+$  layer and  $p^+$  layers =  $0.2 \mu$

Total width is varied

All surface recombination velocities set equal to zero

$$N_{A^+} = 10^{19} \text{ cm}^{-3}$$

$$N_D = 5 \times 10^{19} \text{ cm}^{-3} \implies L_p = 7.2 \mu$$

$$D_p = 1.295 \text{ cm}^2/\text{s}$$

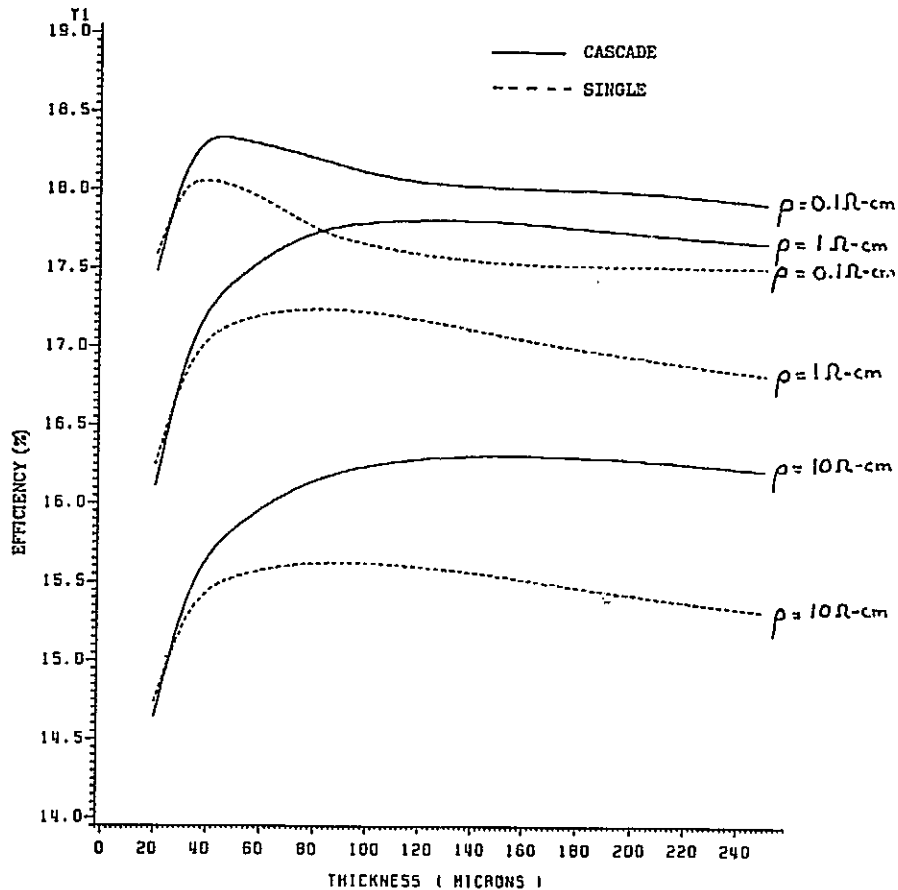
$$\tau_p = 0.4 \mu\text{s}$$

$\rho$ ( $\Omega\text{-cm}$ )	$N_D$ ( $\text{cm}^{-3}$ )	$D_n$ ( $\text{cm}^2/\text{s}$ )	$\tau_n$ ( $\mu\text{s}$ )	$W$ ( $\mu$ )	$L_n$ ( $\mu$ )
0.1	$5 \times 10^{17}$	10.9	2.5	0.05	52.2
1	$1.5 \times 10^{16}$	27	10	0.28	164
10	$1.25 \times 10^{15}$	36	15	0.93	232

Data taken from Hovel Semiconductors and Semimetals



## Efficiency vs Thickness for Cascade and Single Cells



## Status of UCLA-JPL Program

### 1. MBE EXPERIMENTAL PROGRAM:

- DEVELOPMENT OF SILICON SOLID PHASE EPITAXY EXTENDS AVAILABLE DOPING LEVELS TO  $10^{19} \text{ cm}^{-3}$
- POOR QUALITY MATERIAL AT p-n JUNCTIONS HAS THUS FAR PRECLUDED GOOD SOLAR CELLS

### 2. COMPUTER MODELING OF SILICON CASCADE CELLS:

- PROGRAM IS WORKING AND ALLOWS RAPID COMPARISON AS ALL PARAMETERS ARE VARIED
- INITIAL RESULTS SHOW, FOR CASCADE vs SINGLE CELL:
  - INCREASE IN  $\eta$  BY  $\sim 1\%$  OUT OF 15%
  - $\sim 3\%$  IMPROVEMENT IN  $\eta$  BY ADDING FRONT SURFACE FIELD

# MICROCRYSTALLINE SILICON CELLS

APPLIED SOLAR ENERGY CORP.

<b>TECHNOLOGY</b> MICROCRYSTALLINE SILICON GROWTH FOR HETEROJUNCTION SOLAR CELLS	<b>REPORT DATE</b> 9-29-83
<b>APPROACH</b> 1) DEPOSIT P-TYPE MICROCRYSTALLINE SI (m-Si) ON N-TYPE SINGLE CRYSTALLINE SI (c-Si) TO FORM HETEROJUNCTION 2) DEPOSIT P-TYPE M-SI ON P-n JUNCTION FORM- ED IN c-Si TO FORM A WINDOW LAYER <b>CONTRACTOR</b> APPLIED SOLAR ENERGY CORPORATION BOSTON COLLEGE	<b>STATUS</b>
<b>GOALS</b> 1) TO STUDY THE POTENTIAL OF M-SI AS A Voc ENHANCER IN BOTH HETEROJUNCTION AND HETEROFACE SYSTEMS. 2) INVESTIGATE THE POSSIBILITY OF LOW COST SOLAR CELL MANUFACTURE BY USING M-SI.	

## Properties of Microcrystalline Si

- |                                    |                               |
|------------------------------------|-------------------------------|
| 1) CRYSTALLINE DIMENSION:          | HUNDREDS OF ANGSTROMS         |
| 2) ENERGY BANDGAP:                 | 1.7eV                         |
| 3) GROWTH METHOD:                  | E-GUN EVAPORATION             |
| 4) HYDROGENATED IN HYDROGEN PLASMA |                               |
| 5) CONDUCTIVITY:                   | MUCH HIGHER THAN $\alpha$ -Si |

## Various Structures to Be Studied

### 1) HETEROJUNCTION

P-TYPE M-Si  
N-TYPE C-Si

### 2) HETEROFACE

P-TYPE M-Si  
P-TYPE C-Si  
N-TYPE C-Si

### 3) P m-Si/p c-Si TESTING STRUCTURE

P-TYPE M-Si  
P-TYPE C-Si

## Results

HETEROJUNCTION:

MAX  $V_{oc}$  ~480mV

HETEROFACE:

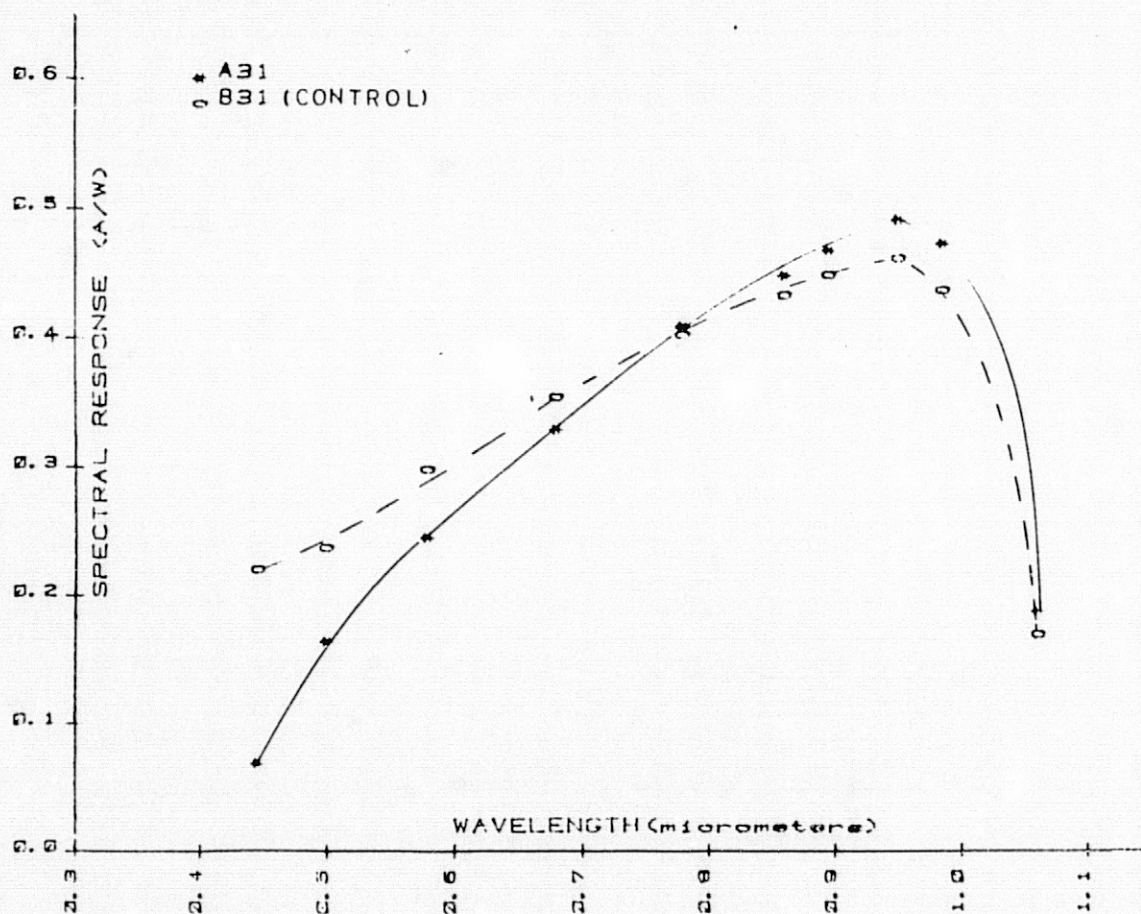
SLIGHT PROMISE SEEN

P-P TESTING STRUCTURE:

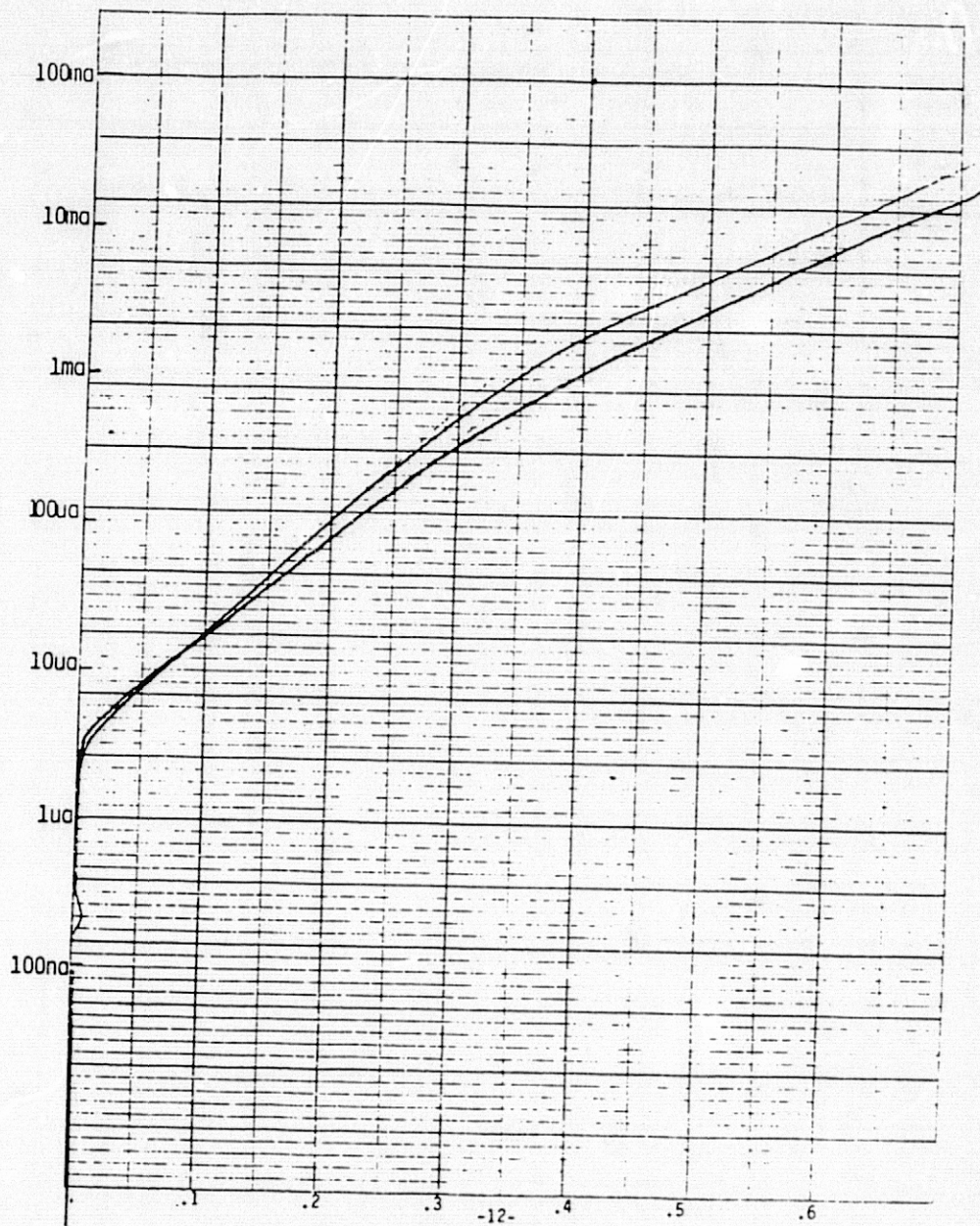
IN MANY CASES INDICATION OF  
MINORITY CARRIER COLLECTION  
INSTEAD OF REPULSION AND UP TO  
NEGATIVE  $V_{oc}$  OF 146mV WAS SEEN.

### Comparison of Heteroface m-Si Cells With Controls Made From the Same Wafers

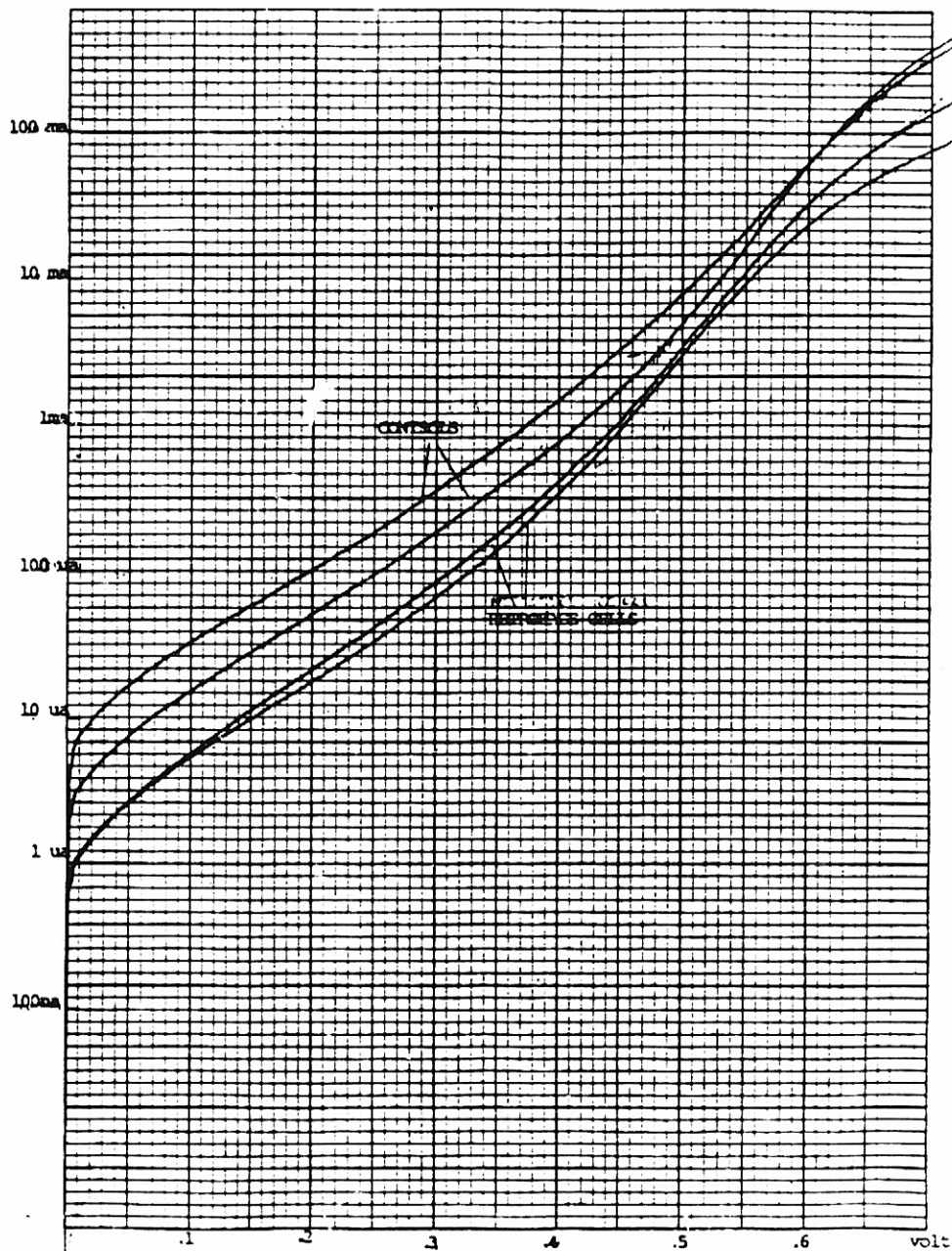
Wafer		Cells With m-Si Window Layer		Control Cells	
		Voc (mV)	Jsc (mA/cm <sup>2</sup> )	Voc (mV)	Jsc (mA/cm <sup>2</sup> )
T2	Ave. Range	563 556-568	19.2 19.1-19.4	561 560-562	21.5 21.1-21.7
T3	Ave. Range	569 566-570	19.3 19.0-19.6	555 550-558	20.9 20.4-21.3
T4	Ave. Range	559 554-562	19.2 19.2	562 560-564	21.5 21.3-21.5



### Dark Currents of Selected Heterojunction Cells







### Preliminary Results in Reciprocal Structure (n-m-Si)

HETEROJUNCTION: UP TO 230mV.

N-N TESTING STRUCTURE: ONLY SLIGHT CARRIER COLLECTION  
IF ANY.

HETEROFACE: YET TO BE TESTED.

# HIGH-EFFICIENCY CELL CONCEPT

UNIVERSITY OF PENNSYLVANIA

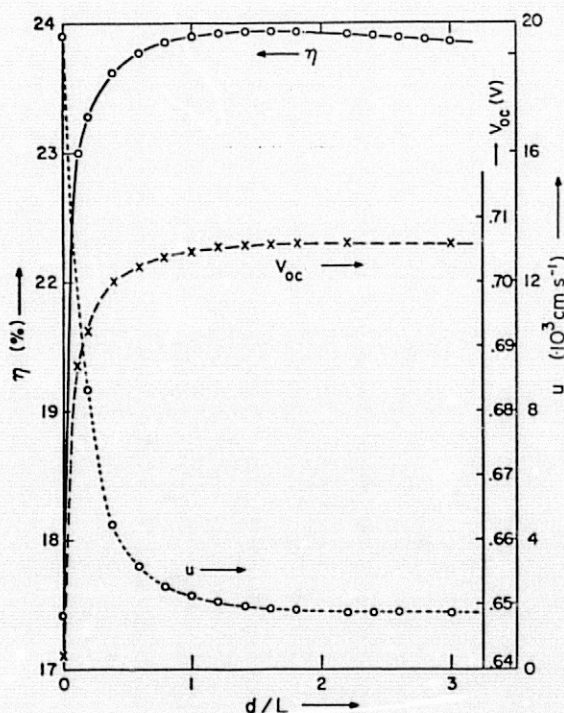
M. Wolf

## Near-Optimum Si Solar Cell Structure (AM1)

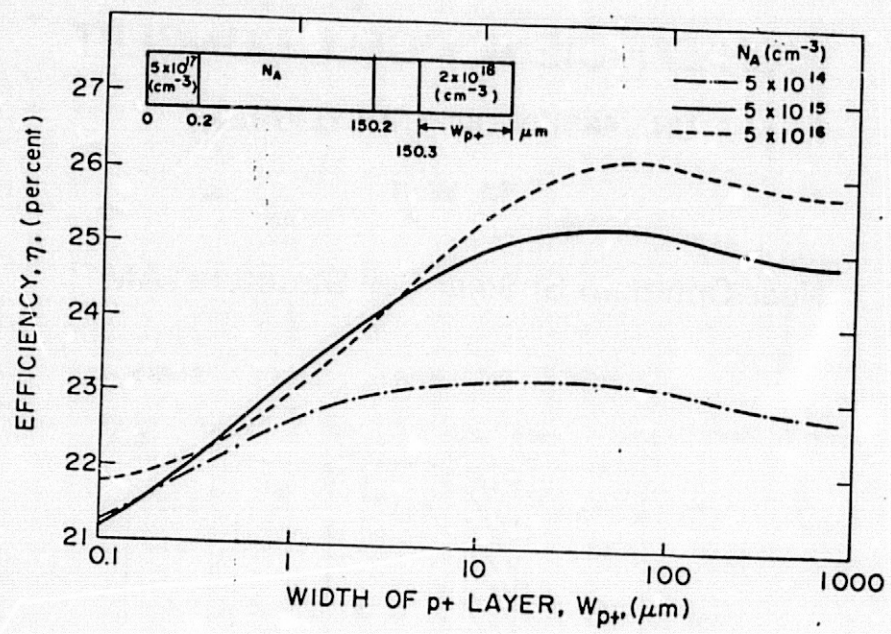
	FRONT	PN	BASE 1	BASE 2	BASE 3	
$u_d (\leftarrow)$ [cm s <sup>-1</sup> ]	200 (p)	52.6 (n)	225 (n)	52.8 (n)	2.1 · 10 <sup>3</sup> (n)	1 · 10 <sup>6</sup> (n)
$N_{DORA}$ [cm <sup>-3</sup> ]	5 · 10 <sup>17</sup> - 2 · 10 <sup>18</sup>		5 · 10 <sup>16</sup>	—	2 · 10 <sup>18</sup>	
$L_{p,orn}$ [μm]	36.3		226	88.4	34.5	
$E$ [V cm <sup>-1</sup> ]	1.93 · 10 <sup>3</sup>		0	9.55 · 10 <sup>3</sup>	0	
$u_L (\rightarrow)$ [cm s <sup>-1</sup> ]	—	1 · 10 <sup>9</sup> (p)	1 · 10 <sup>9</sup> (n)	2.6 · 10 <sup>3</sup> (n)	1.03 · 10 <sup>5</sup> (n)	—
$x$ [μm]	0	0.186	0.340	60	60.1	100

$j_L = 39.79 [\text{mA cm}^{-2}]$	(C.F.) = 0.847	FRONT: $j_L = 6.2 [\text{mA cm}^{-2}]$ ; $j_0 = 1.3 \cdot 10^{-15} [\text{A cm}^{-2}]$
$V_{oc} = 0.705 [\text{V}]$	= 23.92 [%]	BASE: $j_L = 31.0 [\text{mA cm}^{-2}]$ ; $j_0 = 5.7 \cdot 10^{-14} [\text{A cm}^{-2}]$

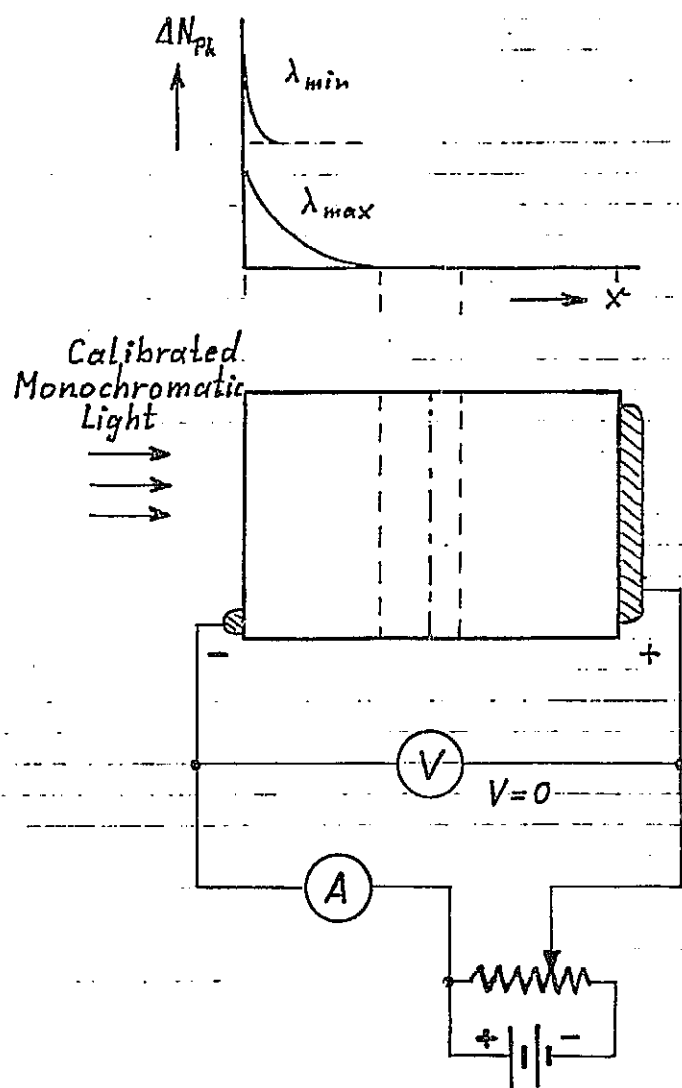




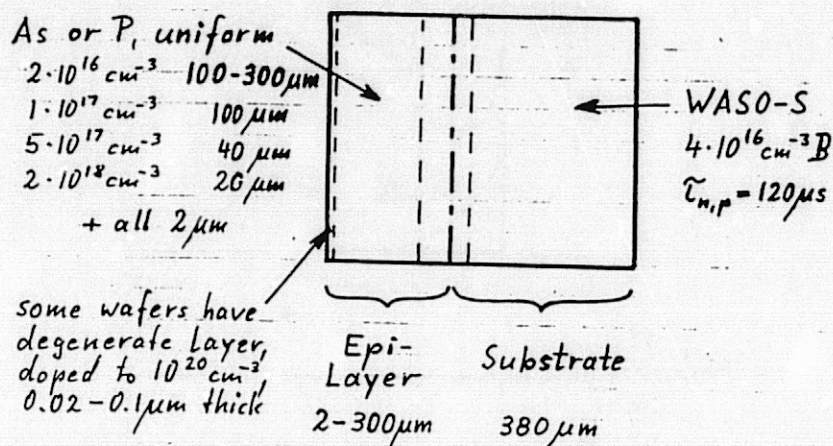




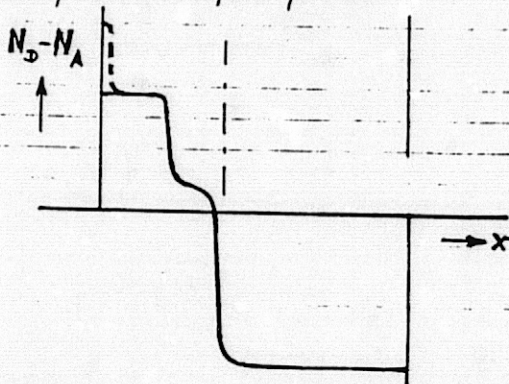
# Calibrated Spectral LBIC



# The Test Devices



Test-Devices are electroless Ni-plated, strip contact front, whole surface p-side.



### Minority Carrier Lifetimes of Wacker Boron-Doped Float-Zone Ingots

Wacker Lot No.:	5.04	5.06	5.05	5.07	bought by Spectrolab
Type	WASO-S	WASO-S	WASO	WASO	WASO-S
nominal $\rho$ ( $\Omega$ cm)	0.2-0.4	14	0.2-0.4	100	0.75
measured by Spectro-Lab: $\rho$ ( $\Omega$ cm)	0.39	14.7	0.32	108	0.77
$L$ ( $\mu$ m)	448	1970	335	1390	959
calculated, using mobilities from H. Wolf:					
$\rho_p$ ( $\text{cm}^{-3}$ )	$4 \cdot 10^{16}$	$8.5 \cdot 10^{14}$	$5 \cdot 10^{16}$	$1.25 \cdot 10^{14}$	$1.9 \cdot 10^{16}$
$\mu_p$ ( $\text{cm}^2/(\text{Vs})$ )	400	500	390	500	430
$\rho_{\text{calc}}$ ( $\Omega$ cm)	0.39	14.7	0.32	108	0.765
$\mu_n$ ( $\text{cm}^2/(\text{Vs})$ )	690	1200	670	1230	800
$D_n$ ( $\text{cm}^2/\text{s}$ )	17.6	30.8	17.2	31.6	20.5
$\tau_n$ ( $\mu$ s)	120	1260	65	610	450
Measured at Wacker. $\tau_n$ ( $\mu$ s)	-	1000 - 1200	-	400 - 700	-

Absorption Coefficients for Si at 300K (in  $\text{cm}^{-1}$ )

Wavelength (nm)	Dash- Newman	ORNL (1)	Runyan (2)	Mobil Solar	ASTM Approx'n to Runyan (3)
200	$1.65 \cdot 10^6$				
250	$1.72 \cdot 10^6$				
300	$1.65 \cdot 10^6$	$1.65 \cdot 10^6$			
350	$9.2 \cdot 10^5$	$1.08 \cdot 10^6$			
400	$8.2 \cdot 10^4$	$1.07 \cdot 10^5$	$7.16 \cdot 10^4$		
450	$2.7 \cdot 10^4$	$3.06 \cdot 10^4$	$2.44 \cdot 10^4$		
500	$1.23 \cdot 10^4$	$1.38 \cdot 10^4$	$1.23 \cdot 10^4$		$8.99 \cdot 10^3$
550	$7.5 \cdot 10^3$	$7.15 \cdot 10^3$	$7.25 \cdot 10^3$		$6.21 \cdot 10^3$
600	$5.0 \cdot 10^3$	$4.54 \cdot 10^3$	$4.26 \cdot 10^3$		$4.3 \cdot 10^3$
650	$3.6 \cdot 10^3$	$3.18 \cdot 10^3$	$2.78 \cdot 10^3$		$2.97 \cdot 10^3$
700	$2.6 \cdot 10^3$	$2.23 \cdot 10^3$	$1.98 \cdot 10^3$		$2.03 \cdot 10^3$
750	$1.8 \cdot 10^3$	$1.31 \cdot 10^3$	$1.355 \cdot 10^3$		$1.36 \cdot 10^3$
800	$1.2 \cdot 10^3$		$8.8 \cdot 10^2$		$8.87 \cdot 10^2$
850	$8 \cdot 10^2$		$5.5 \cdot 10^2$		$5.55 \cdot 10^2$
900	$4.9 \cdot 10^2$		$3.3 \cdot 10^2$		$3.25 \cdot 10^2$
950	$2.3 \cdot 10^2$		$1.7 \cdot 10^2$	$1.82 \cdot 10^2$	$1.71 \cdot 10^2$
1000	$9 \cdot 10^1$		$7.2 \cdot 10^1$	$8.31 \cdot 10^1$	$7.45 \cdot 10^1$
1050	$3.3 \cdot 10^1$		$4.1 \cdot 10^1$	$3.42 \cdot 10^1$	$2.08 \cdot 10^1$
1100	$1 \cdot 10^1$				
1150	$1 \cdot 10^0$				

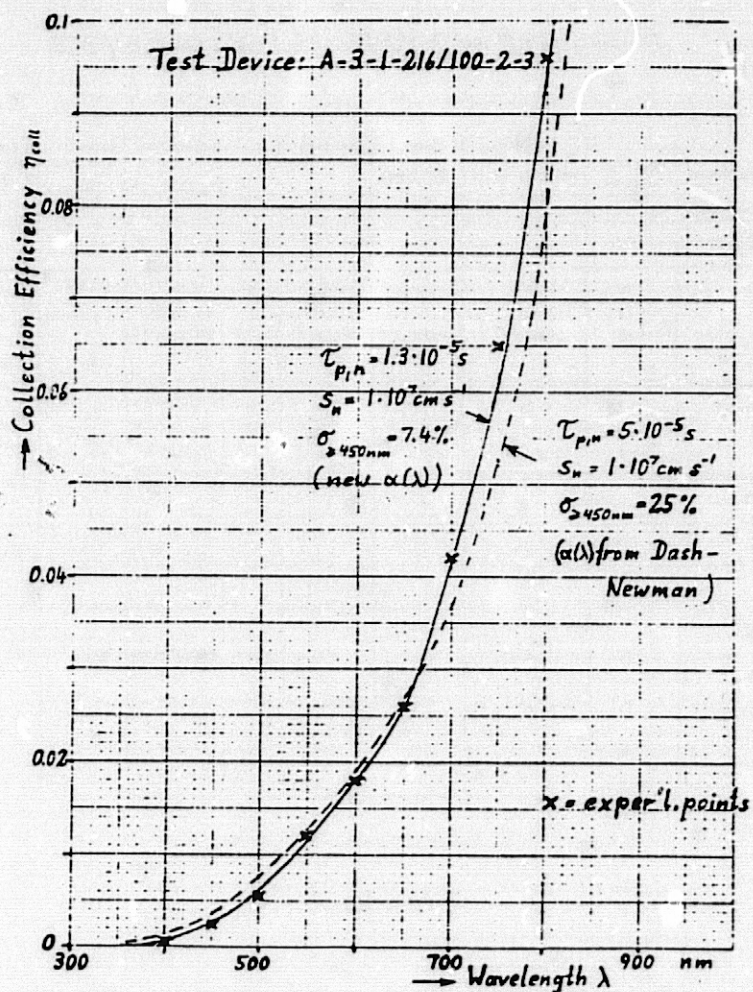
Like Runyan to 900 nm

- (1) G.E. Jellison, Jr., and S.A. Modine, "Optical Constants for Silicon at 300K and 10K, Determined from 1.64 to 4.73 eV by Ellipsometry", Oak Ridge National Lab. Report ORNL/TM-8002. Contract # W-7405-eng-26; Feb. 1982.
- (2) SMU Report SMU-83-13 (1967).
- (3) ASTM Standard Method F391 (Part 43 of the ASTM Standards.):  

$$\alpha = \{0.526376 - 1.14425 \lambda^{-1} + 0.585368 \lambda^{-2} + 0.039958 \lambda^{-3}\} \cdot 10^4 \text{ cm}^{-1}$$

$$(\lambda \text{ in } \mu\text{m})$$





## Measurement Results on Epi Layers

Test Device Number	Measured Lifetime $\mu s$	Surface Recombination Velocity $cm\ s^{-1}$	"Dead-Layer" Thickness $\mu m$	Standard Deviation %	Area $cm^2$	Saturation Calculated $J_{01}\ Acm^{-2}$	Current Measured $J_{01}\ Acm^{-2}$	Excess Saturation $J_{02}\ Acm^{-2}$	Current Slope $A_2$
A-3-1-216/100-1-10	-12								
A-3-1-216/100-2-1	10	$5 \cdot 10^6$	-	10.6	3.9	$2 \cdot 10^{-12}$	$5 \cdot 10^{-12}$	$3 \cdot 10^{-8}$	1.68
-3	$\begin{Bmatrix} 13 \\ 16 \end{Bmatrix}$	$\begin{Bmatrix} 1 \cdot 10^7 \\ 3 \cdot 3 \cdot 10^5 \end{Bmatrix}$	$\begin{Bmatrix} - \\ 0.3 \end{Bmatrix}$	$\begin{Bmatrix} 7.4 \\ 3.3 \end{Bmatrix}$	4.25	$\begin{Bmatrix} 2 \cdot 10^{-12} \\ 1.9 \cdot 10^{-12} \end{Bmatrix}$	$\begin{Bmatrix} 1.9 \cdot 10^{-12} \\ 1.3 \cdot 10^{-12} \end{Bmatrix}$	$\begin{Bmatrix} 1 \cdot 10^{-8} \\ 1 \cdot 3 \cdot 10^{-8} \end{Bmatrix}$	$\begin{Bmatrix} 1.9 \\ 1.77 \end{Bmatrix}$
-4					3.85				
A-3-1-216/100-3-1	0.50	$5 \cdot 10^5$	-	10.4	4.0	$6 \cdot 10^{-12}$	$1 \cdot 10^{-11}$	$8 \cdot 10^{-9}$	2.0
-2	$\begin{Bmatrix} 0.875 \\ 0.875 \end{Bmatrix}$	$\begin{Bmatrix} 1 \cdot 10^7 \\ 2.3 \cdot 10^5 \end{Bmatrix}$	$\begin{Bmatrix} - \\ 0.2 \end{Bmatrix}$	$\begin{Bmatrix} 7.0 \\ 6.8 \end{Bmatrix}$	4.25	$\begin{Bmatrix} 5 \cdot 10^{-12} \\ 5 \cdot 10^{-12} \end{Bmatrix}$	$\begin{Bmatrix} 9 \cdot 10^{-12} \\ 9 \cdot 10^{-12} \end{Bmatrix}$	$\begin{Bmatrix} 2 \cdot 10^{-8} \\ 2 \cdot 10^{-8} \end{Bmatrix}$	$\begin{Bmatrix} 2.18 \\ 2.18 \end{Bmatrix}$
A-3-1-216/100-4-1									
P-3-2-517/40-1-3	20 (100)	$\begin{Bmatrix} 1 \cdot 10^5 \\ 1 \cdot 10^5 \end{Bmatrix}$	$\begin{Bmatrix} 0.3 \\ 0.3 \end{Bmatrix}$	$\begin{Bmatrix} 7.8 \\ 7.4 \end{Bmatrix}$	3.5	$6 \cdot 10^{-13}(B)$	$8 \cdot 10^{-11}$	$3 \cdot 10^{-8}$	1.54
P-3-2-517/40-2-2									
-3	20	$3 \cdot 10^4$	1.07	7.2	5.5	$6 \cdot 10^{-13}(B)$	$1 \cdot 10^{-11}$	$1 \cdot 10^{-6}$	2.37
Same, but 3.9um etched off (Thickness assumed as 32um)	14	$8 \cdot 10^4$	0.6	8.2					

## Conclusions

1. CALIBRATED SPECTRAL LBIC CAN YIELD BELIEVABLE MINORITY CARRIER LIFETIME VALUES WHEN CORROBORATED WITH SATURATION CURRENT DETERMINATION, OR OTHER INDEPENDENT MEASUREMENTS.
2. SI CVD EPI CAN YIELD LAYERS WITH MINORITY CARRIER LIFETIME ADEQUATE FOR HIGH EFFICIENCY SOLAR CELLS (~20% AM1).
3. CVD EPI WITH  $SiHCl_3$  AT 1150°C CAN BE CARRIED OUT ON FLOAT ZONE SI WITHOUT GREATLY REDUCING THE SUBSTRATE MINORITY CARRIER LIFETIME.
4. THE DEFECT DENSITY AT THE SUBSTRATE-EPI LAYER INTERFACE CAN BE HELD LOW ENOUGH TO GENERATE ACCEPTABLE EXCESS CURRENT, IF LOCATED IN THE JUNCTION SPACE CHARGE REGION.
5. NOT ALL EPI-LAYERS ARE THE EXPECTED SIMPLE STRUCTURES WHICH FACILITATE INTERPRETATION OF THE MEASURED DATA. EXTENSIVE DEVICE ANALYSIS IS NEEDED IN SOME CASES TO UNDERSTAND THEIR PERFORMANCE.



Table 1: List of Symbols

$j_L$	light-generated current density [ $A\ cm^{-2}$ ]	$T$	absolute temperature [K]	$\zeta = \frac{x}{L}$	normalized length coordinate
$j_d$	diode current density resulting from $V_d$ , regardless of illumination [ $A\ cm^{-2}$ ]	$D$	diffusion constant [ $cm^2\ s^{-1}$ ]	$\zeta^* = \frac{x_N}{L}$	normalized optical pathlength to layer boundary nearer pn junction for light incident on front surface ( $x=0$ )
$j_{0,k}$	saturation current density flowing into an infinitely thick layer $k$ [ $A\ cm^{-2}$ ]	$L$	diffusion length [cm]	$\zeta^* = \frac{d-x_N}{L}$	dto. for light incident on back surface ( $x=d$ )
(GP)	geometry factor for saturation current into a layer of finite thickness	$E$	electric field strength [ $V\ cm^{-1}$ ]	$\zeta^* = \frac{2d-x_N}{L}$	dto. for light internally reflected at back surface after one pass from the front surface
$V_d$	bias voltage applied across built-in potential barrier of diode [V]	$G$	generation rate [ $cm^{-3}\ s^{-1}$ ]	$F_n = \frac{qEL_n}{2kT}$	normalized drift potential difference for electrons as minority carriers
$s$	surface recombination velocity [ $cm\ s^{-1}$ ]	$U$	recombination rate [ $cm^{-3}\ s^{-1}$ ]	$F_p = -\frac{qEL_p}{2kt}$	dto. for holes
$u$	charge carrier transport velocity [ $cm\ s^{-1}$ ]	$N_{ph}$	photon flux penetrating illuminated surface of solar cell [ $cm^{-2}\ s^{-1}$ ]	$r = (1+F^2)^{1/2}$	factor expressing effect of drift relative to diffusion
Subscripts refer quantities to:					
$q$	electron charge [ $1.6 \cdot 10^{-19} A\ s$ ]	$n$	"electrons as charge carriers"; alternately, if used as subscript on a carrier concentration: "in n-type region"	$a' = \alpha L$	normalized absorption coefficient
$k$	Boltzmann constant [ $1.38 \cdot 10^{-23} J\ s\ K^{-1}$ ]	$p$	"holes as charge carriers"; alternately, if used as subscript on a carrier concentration: "in p-type region"	$\sigma = \frac{uL}{Dr} + \frac{F}{r}$	normalized transport velocity
$n$	electron density [ $cm^{-3}$ ]	$O$	"thermal equilibrium"	$b = \frac{1}{r}(\alpha' - F)$	normalized "effective absorption coefficient" for photons penetrating from front surface
$p$	hole density [ $cm^{-3}$ ]	$J$	"pn junction"	$b = -\frac{1}{r}(\alpha' + F)$	dto. for photons penetrating from back surface
$x$	length coordinate normal to illuminated surface of cell; $x=0$ at illuminated surface, $x>0$ in direction towards back of cell. [cm]	$N$	"near" boundary, defined for determination of current generation in active layers, as the boundary nearer to the transition region; or, for transformations of $u$ or $n$ ( $p$ ) across passive layers, as the boundary towards which transformation is made		
$d$	total thickness of solar cell [cm]	$F$	"far" boundary, defined as the layer boundary which is not "near" boundary		
$t$	time [s]				
$\alpha$	absorption coefficient [ $cm^{-1}$ ]				
$\lambda$	wavelength [cm]				
$\tau$	minority carrier lifetime [s]				

# CRYSTALLINE SILICON SOLAR CELL TASK: STATUS OF HIGH-EFFICIENCY PROGRAMS

SOLAR ENERGY RESEARCH INSTITUTE

Joseph B. Milstein

## Objective of the High-Efficiency RFP

THE INTENT OF THIS RFP IS TO SOLICIT FUNDAMENTAL RESEARCH PROJECTS DIRECTED TO INCREASING SILICON SOLAR CELL EFFICIENCY TO LEVELS SUPERIOR TO PRESENT SILICON SOLAR CELLS (I.E., GREATER THAN 14% FOR POLYCRYSTALLINE CELLS, AND GREATER THAN 17% FOR SINGLE CRYSTAL CELLS), AND VALIDATING IDEAS BY FABRICATION EXPERIMENTS. THE INTENT OF THE RFP IS TO CONSIDER PROPOSALS WHICH PRESENT NEW CONCEPTS AND APPROACHES IN CELL DESIGN AND/OR NEW TECHNIQUES IN CELL FABRICATION, INCLUDING THEORETICAL ANALYSIS, CONCEPT VALIDATION, AND A PLAN FOR BRINGING THE NEW CONCEPT TO FRUITION IN AN EXPERIMENTAL VERIFICATION. RESPONSES TO THIS RFP WHICH MERELY PROPOSE EVOLUTIONARY CHANGES OF CURRENT TECHNOLOGY WILL NOT BE CONSIDERED. AN EXAMPLE OF SUCH AN EVOLUTIONARY CHANGE IS THE PROPOSAL TO CONTROL THE THERMAL DIFFUSION OF A DOPANT WHICH CREATES A P/N JUNCTION WITH GREATER PRECISION THAN CURRENTLY AVAILABLE, AND WHICH IS EXPECTED TO IMPROVE CELL EFFICIENCY ONLY marginally OVER THAT PRESENTLY AVAILABLE, WITH NO CHANGE IN UNDERLYING PHYSICAL METHODS OR CONCEPTS.

RFP ISSUED MARCH 18, 1982



## High-Efficiency Programs

ORGANIZATION/P.I./CONTRACT NO.	PERIOD	FUNDING	APPROACH
UNIVERSITY OF PENNSYLVANIA (SUBTIER CONTRACT TO SPECTROLAB) PROF. MARTIN WOLF XB-2-02090-1	11/15/82 TO 11/14/83	\$147,319	FABRICATION AND EVALUATION OF WOLF'S CONCEPTUAL CELL
UNIVERSITY OF FLORIDA PROF. FREDERIK A. LINDHOLM XB-3-02090-2	01/01/83 TO 12/31/83	\$94,585	FABRICATION AND EVALUATION OF QBGF DRIFT FIELD CELL
SPIRE CORPORATION DR. MARK B. SPITZER 7B-3-02090-3	12/23/82 TO 12/31/83	\$117,976	FABRICATION AND EVALUATION OF HI-LOW EMITTER AND HYBRID CELL STRUCTURES BASED ON BSF CELL DESIGN
WESTINGHOUSE ELECTRIC CORP. R & D CENTER DR. AJEET ROHATGI XB-3-02090-4	12/01/82 TO 11/30/83	\$98,547	FABRICATION AND EVALUATION OF ADVANCED DESIGN, INCLUDING ABRUPT STEPPED EMITTER, MIS CONTACTS, MULTI-LAYER AR COATING, OPTICALLY REFLECTING BACK, AND GA BSF.
UNIVERSITY OF WASHINGTON JOINT CENTER FOR GRADUATE RESEARCH PROF. LARRY C. OLSEN	10/01/82 TO 09/20/83	\$114,010	FABRICATION AND EVALUATION OF MINP CELL
		TOTAL FUNDING: \$572,537	

## Results

### SPIRE CORPORATION

18.0%, 4.005 cm<sup>2</sup> CELL VERIFIED AT SERI

$V_{OC} = 522$  mV,  $J_{SC} = 35.1$  mA/cm<sup>2</sup>, FF = .801

(IMPROVED FROM CA. 15.5% AT CONTRACT INITIATION)

### WESTINGHOUSE ELECTRIC CORPORATION

17.1%, 1.01 cm<sup>2</sup> CELLS (3) VERIFIED AT SERI

TYPICAL PARAMETERS:

$V_{OC} = 504$  mV,  $J_{SC} = 35.5$  mA/cm<sup>2</sup>, FF = .796

(IMPROVED FROM CA. 15.4% AT CONTRACT INITIATION)

### JCGS

15.4%, 3.98 cm<sup>2</sup> CELL VERIFIED AT SERI

$V_{OC} = 525$  mV,  $J_{SC} = 31.5$  mA/cm<sup>2</sup>, FF = .780

(IMPROVED FROM CA. 11.7% AT CONTRACT INITIATION)

## Details of Spire Cell

CELL FABRICATED IN 0.3 OHM-CM P-TYPE (100) FZ SILICON WAFER THICKNESS 380 MICRONS

B ION IMPLANTED, THERMALLY ANNEALED BSF (MINORITY CARRIER DIFFUSION LENGTH APPROX. 150 MICRONS, IMPLYING INEFFECTIVENESS OF BSF)

FRONT SURFACE TEXTURE-ETCHED

P ION IMPLANTED, THERMALLY ANNEALED EMITTER PASSIVATING OXIDE ON FRONT

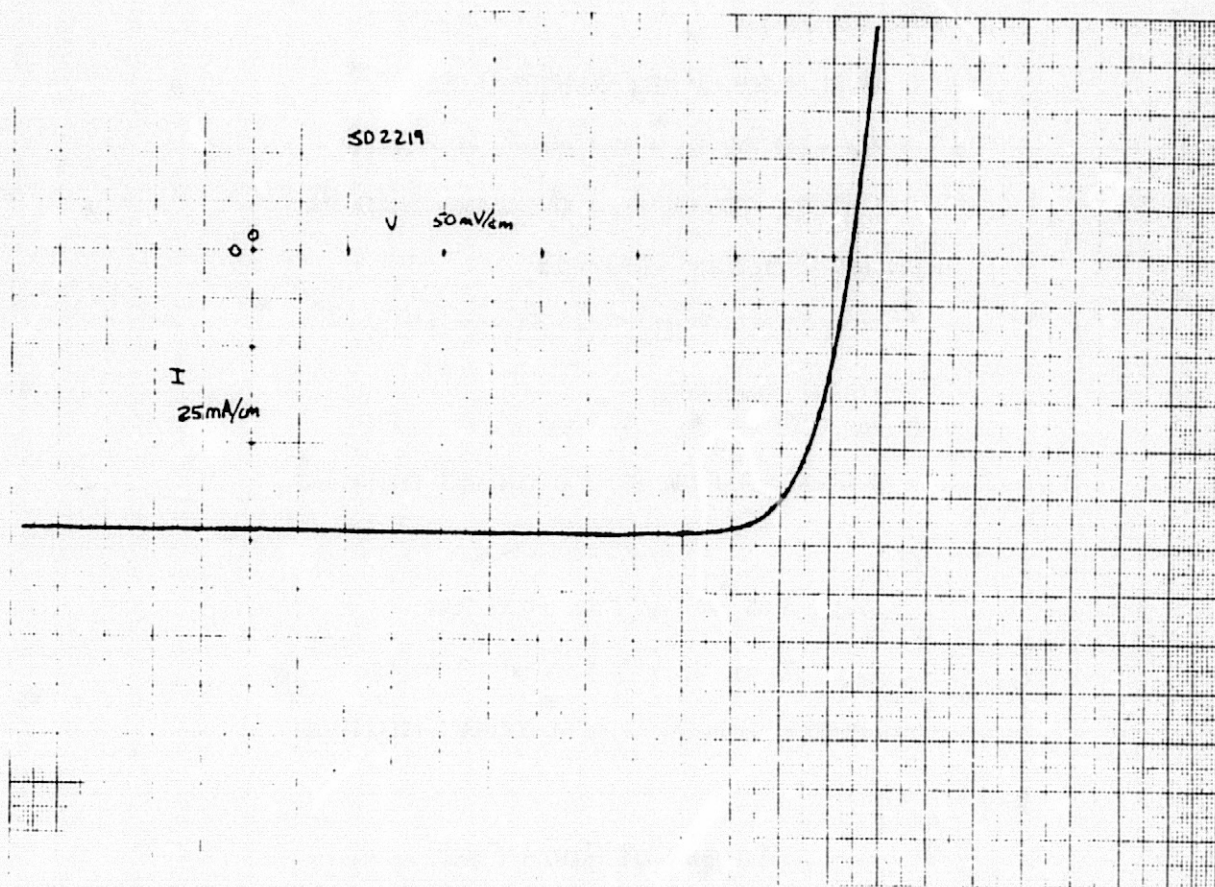
APPROX. 4% METALLIZATION (Ti-PD-AG) FRONT CONTACT FULL Ti-PD-AG BACK CONTACT

Ta<sub>2</sub>O<sub>5</sub> AR COATING

TEST CELL



### Spire 18.0% Cell



### Details of Westinghouse Cell

CELL FABRICATED IN 4 OHM-CM P-TYPE (111) FZ SILICON WAFER 250 MICRON THICKNESS

B  $\text{Br}_3$  DIFFUSION FOR BSF

$\text{POCl}_3$  DIFFUSED EMITTER

OXIDATION FOR SURFACE PASSIVATION

AR COATING WITH  $\text{TiO}_2$

OPEN OXIDE FOR METALLIZATION (FRONT AND BACK)

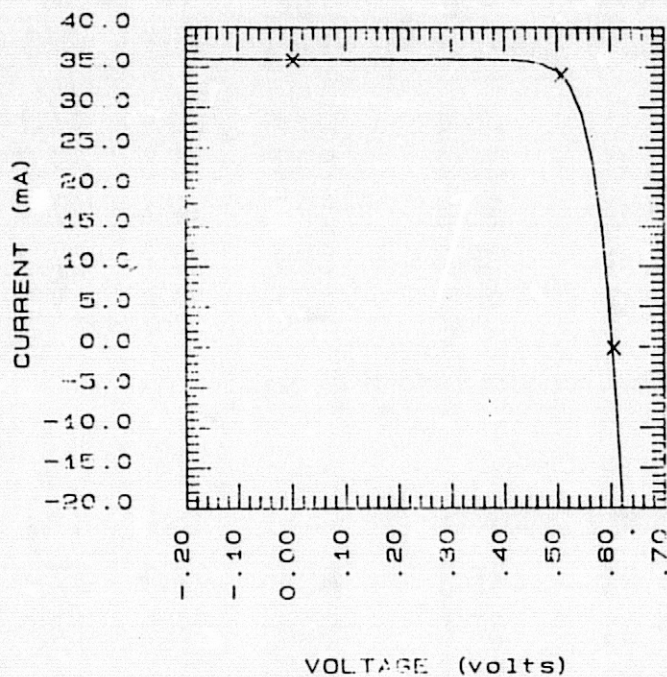
METALLIZATION (APPROX. 3% FRONT, APPROX. 3% BACK CONTACT, FULL REAR COVERAGE)

ETCH MESA

TEST.

# B-Doped Si n<sup>+</sup>pp<sup>+</sup> HIEFY-4-5

SAMPLE: SD2183 Voc = 0.6042 volts  
 DATE: AUG 5 1993 15:38 Jsc = 35.60 mA/cm<sup>2</sup>  
 TEMP = 28.0 C Fill factor = 79.54 %  
 AREA = 1.010 cm<sup>2</sup> Efficiency = 17.11 %



Vmax = 0.5064 V  
 Imax = 34.12 mA  
 Isc = 35.96 mA

Oxide-Passivated Solar Cells on  
Boron-Doped 4  $\Omega$ -cm Float-Zone Silicon

Cells Tested At Westinghouse

Cell ID	Area (cm <sup>2</sup> )	J <sub>sc</sub> (mA/cm <sup>2</sup> )	V <sub>oc</sub> (mV)	FF (%)	$\eta$ (%)
HIEFY 4-4	1.0	36.1	599	79.4	17.1
-5	1.0	36.2	600	79.3	17.2
-6	1.0	36.4	598	78.5	17.1
-7	1.0	36.2	599	79.1	17.2
-8	1.0	36.3	597	79.5	17.2

Above Cells Tested At SERI

Cell ID	Area (cm <sup>2</sup> )	J <sub>sc</sub> (mA/cm <sup>2</sup> )	V <sub>oc</sub> (mV)	FF (%)	$\eta$ (%)
HIEFY 4-4	1.01	35.5	604	79.6	17.1
-5	1.01	35.6	604	79.5	17.1
-6	1.01	35.9	605	78.6	17.1
-7	1.01	35.4	604	79.7	17.0
-8	1.01	35.3	603	79.8	17.0

\*AM1, 100 MW/cm<sup>2</sup> Illumination

\*Run # HIEFY 4, Base 2



## Comparison of Cell Parameters

A COMPARISON OF CELL PARAMETERS OF  
A BASELINE  $n^+ - p - p^+$  CELL AND 17.2 %  
OXIDE PASSIVATED CELL ON  $4 \Omega\text{-cm}$  FZ SILICON

PARAMETER	BASELINE $n^+ - p - p^+$ CELL	17.2 % OXIDE PASSIVATED CELL
$J_{sc}$	$33.4 \text{ mA/cm}^2$	$36.1 \text{ mA/cm}^2$
$V_{oc}$	583 mV	600 mV
FF	0.78	0.794
$\eta$	15.2 %	17.2 %
$R_s$	$0.5 \Omega/\text{cm}^2$	$0.21 \Omega/\text{cm}^2$
$R_{sh}$	$104 \text{ K}\Omega/\text{cm}^2$	$190 \text{ K}\Omega/\text{cm}^2$
$J_{o1}$	$3.7 \times 10^{-12} \text{ A/cm}^2$	$2 \times 10^{-12} \text{ A/cm}^2$
$J_{o2}$	$1.7 \times 10^{-7} \text{ A/cm}^2$	$7.7 \times 10^{-7} \text{ A/cm}^2$

### Quantum Efficiency vs Wavelength

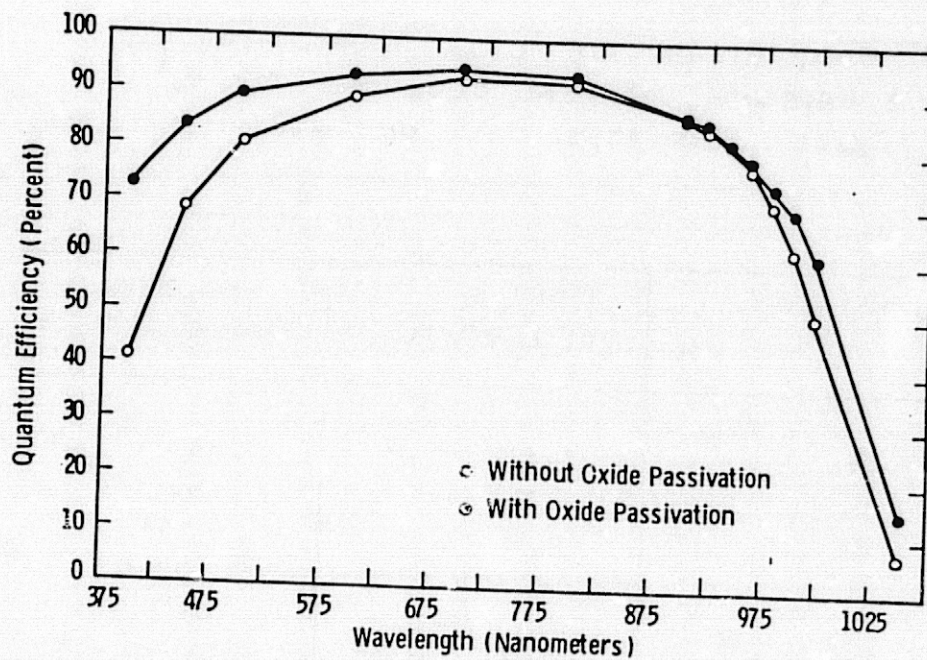
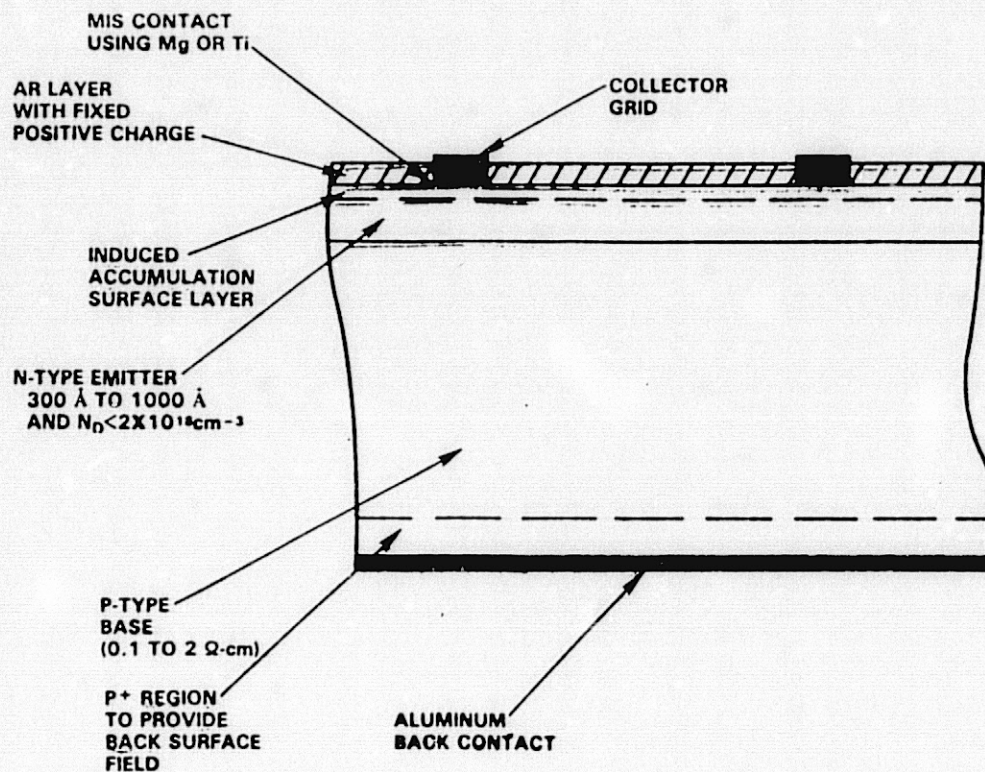


Fig. 1 - Quantum efficiency vs. wavelength plot for an unpassivated cell and 17.2% efficient oxide passivated cell on 4  $\Omega$ -cm float zone silicon

### Details of JCGS Cell

CELL FABRICATED IN 0.2 OHM-CM P-TYPE (100) FZ SILICON WAFER THICKNESS 375 MICRONS  
P DIFFUSED EMITTER 0.2 MICRON DEEP  
AL BACK CONTACT (500°C HEAT TREATMENT)  
FRONT OXIDE  
MG GRID DEPOSITED ON FRONT (12 LINES/CM), APPROX. 5% SHADOWING  
AL FRONT GRID OVERCOATED  
SiO<sub>2</sub> AR COATING  
TEST CELL





### Other Features of the Crystalline-Silicon Solar-Cell Task

ELECTRICALLY ACTIVE DEFECTS STUDIES INCLUDING EFFECTS OF HYDROGEN PASSIVATION

GROWTH OF SILICON RIBBONS BY LASS AND ESP TECHNIQUES



# STATUS: NONNOBLE METAL SYSTEMS

ELECTRINK, INC.

J. Parker

## Concept

- COST EFFECTIVE ALL METAL PRINTABLE SYSTEM
  - CONDUCTIVE METAL
  - SINTERING MEDIUM
  - OXIDE SCAVENGER
  - DOPANTS

## Status

- Cu-BASED BACK CONTACT
- Cu-BASED FRONT CONTACT
- Ag OR Cu METAL ON BSF Al INK
- RESONANCE NUCLEAR PROFILING FOR HYDROGEN
- CONTRACT TERMINATED

## Future Recommendations

- ESTABLISH REPRODUCIBILITY
- CONTINUE METAL TO METAL INTERFACE STUDIES
- STUDY FUNDAMENTAL ROLE OF HYDROGEN

# MODULE TECHNOLOGY

L.D. Runkle, Chairman

John Griffith reviewed recent experiences at JPL in testing modules to the requirements of the Block V specification. Although correlation of the effects of increasing the high-potential voltage test, extending the thermal cycling, and imposing the humidity-freeze requirement awaits experience in the field, module manufacturers are responding to the challenge to meet these tests. Module designs now appearing are generally able to survive the 200 thermal cycles without interconnect fatigue or electrical degradation. In the recent past, about 25% of the modules tested in the humidity-freeze cycles have suffered significant electrical degradation.

Dan Runkle of JPL described the physical and electrical characteristics of a number of modules produced by foreign manufacturers. Those samples subjected to the Block V environmental requirements appear to be nearly equivalent to domestic modules procured under the Block V requirements.

Bob Weaver reviewed module endurance testing at the JPL sites. Modules from Blocks I and II continue to fail at a rate that shows no trend for either acceleration or deceleration. Block III modules are beginning to show failures, and Block IV modules have been in the field too short a time to show anything but a slight deterioration of fill factor.

Paul Willis described activities at Springborn Laboratories, Inc., whose objective is to identify and develop low-cost module construction materials. This includes pottants, outer-cover films, substrates, antisoiling treatments, ultraviolet stabilizers and the like. Also described were materials lifetime and aging studies and results of field exposures.

M.J. Nowlan of Spire Corp. reported on progress being made in developing a hermetic seal for the perimeters of encapsulated modules. The technique under investigation involves an electrostatic bond of a strip of aluminum foil to the glass superstrate, and an ultrasonic weld of the back-cover foil to the strip.

C.C. Gonzalez of JPL reviewed a recent investigation of hot-spot heating on the Sacramento Municipal Utility District (SMUD) 10 kW verification array. The study focused on the current imbalances that result from the typical multiple paralleling of module strings in central-station arrays. The SMUD test results indicate the existence of current imbalances and aggravated hot-spot heating when the number of cells per substring is decreased to three or less. The SMUD modules have three cells per substring.

An overview of the bypass diode design tradeoffs contract was presented by N.F. Shepard of General Electric Co. Tentative findings include: a possible cost advantage exists in using encapsulated bypass diodes if externally-mounted diodes require more than one minute of installation time or cost more than \$2.10 to install; current-sharing among parallel-connected diodes can be achieved by adding series resistance to each diode; and diode reliability can be enhanced by derating the reverse voltage and limiting the junction temperature to no more than 125°C. Features of an advanced-design enclosure for externally mounted diodes was also presented.



## MODULE TECHNOLOGY

D.H. Otth of JPL reviewed the development of a qualification test procedure for assessing the reliability of both integral and externally mounted module bypass diodes. Design criteria that would ensure acceptable field reliability and a step-by-step procedure using the diode forward voltage drop to measure the junction temperature were included in the presentation. Manufacturers were invited to participate in the development of a final qual-test procedure that would be included in a future JPL design specification document.

L.C. Wen of JPL discussed residential array thermal considerations. The prototype buildings at the Southwest Residential Experiment Station were investigated and the results provide a qualitative understanding of different mounting features. Air ventilation of array back surfaces was identified as a key factor in array thermal performance.

C.C. Gonzalez of JPL summarized improvements in the methodology for selecting the preferred irradiance level and ambient temperature for measuring module (array) power output and showed that the NOCT-based power rating can predict annual PV energy production to within 1% accuracy for moderate climates. Also discussed were approaches to fine-tuning the NOCT-based rating system for site-specific ambient temperature and I-V fill factor.

# BLOCK V TEST RESULTS

JET PROPULSION LABORATORY

John S. Griffith

## Contents

- RESULTS OF THE NEW TESTS
- SOME UNEXPECTED RESULTS WITH ALUMINIUM
- SUMMARY

## Review of Block V Tests

TEST	BLOCK V	BLOCK IV
HIPOT	3000 V	2000 V
TEMPERATURE CYCLES	50	50
ADDED TEMPERATURE CYCLES	150	--
HUMIDITY	20 HRS 85°C, 85% RH 1/2 HR @ -40°C, 10 CYCLES	5 DAYS AT 20°C AND 40°C, 95% RH
MECHANICAL CYCLING	SAME	
TWIST	SAME	
HAIL	25 mm ICEBALLS	19 mm
HOTSPOT	3 CELLS, 100 HOURS	--



### Results of Block V Tests on 10 Commercial, 6 Georgetown U., 4 Block V Module Types

PROBLEM	FAILURE	DEFECT	PERCENT OF 20 TYPES AFFECTED	PERCENT OF MODULES IN AFFECTED TYPES
	X	ELECTRICAL FAILURE	35	56
	X	DELAMINATION, BUBBLES	20	90
	X	HOTSPOT	5	100
	X	HIPOT	10	65
	X	TORN, FRACTURED INTERCONNECTS	10	100
	X	CONTINUITY	10	100
	X	LOOSE FRAME OR LOOSE GASKETS	5	100
	X	ENCAPSULANT CURE	5	100
	X	LOOSE TERMINALS	5	75
X		BACKSKIN DELAM, WRINKLED OR CRACKED	35	94
X		DELAMINATION, BUBBLES, DISCOLORATION	30	88
X		J-BOX CRACKING OR LOOSE	15	36
X		CRACKED CELLS	25	25

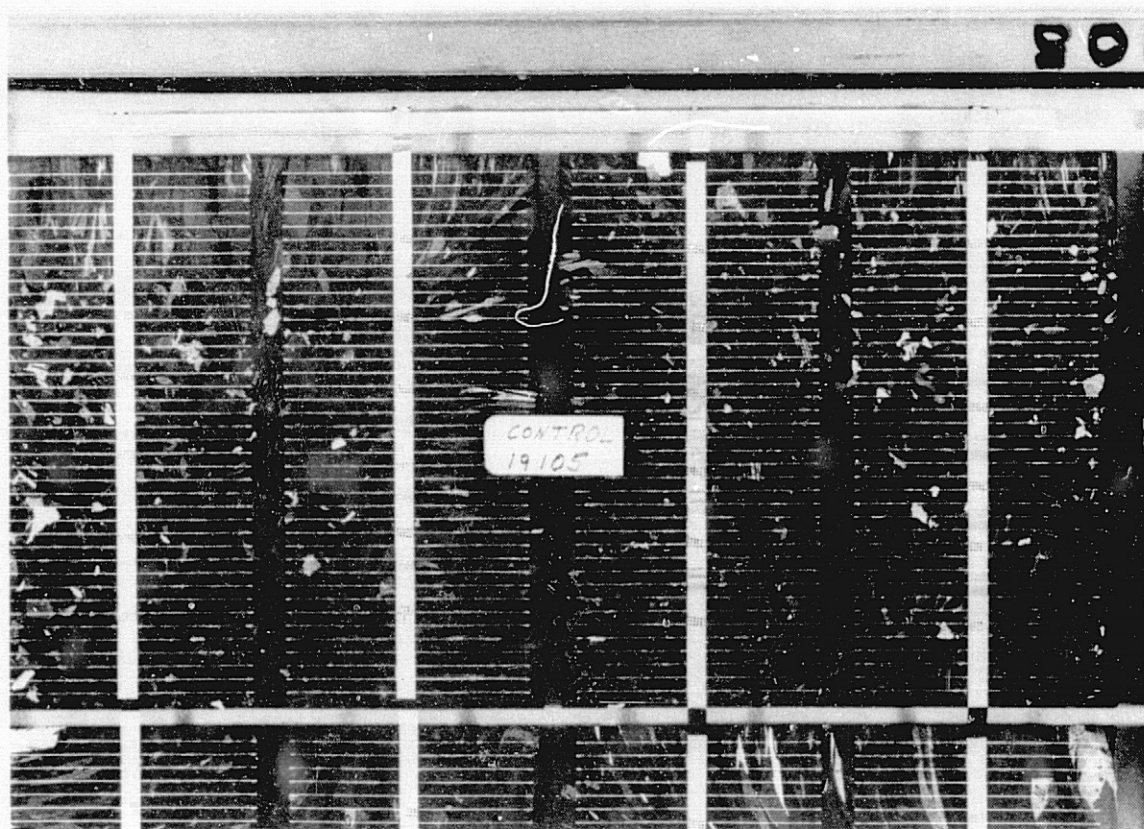
### How Effective Are the New Tests?

- A RELATIVELY HIGH PERCENTAGE OF THE MODULES FAIL
- ARE THE TESTS TOO SEVERE?
  - THE NEW HUMIDITY AND TEMPERATURE TESTS  
PROVIDE THE EQUIVALENT OF LONGER FIELD LIFE
- PROOF OF EFFECTIVENESS MUST WAIT YEARS FOR  
FIELD RESULTS
- TESTS APPEAR TO BE EFFECTIVE AND THE BEST  
AVAILABLE NOW

### Unexpected Test Results

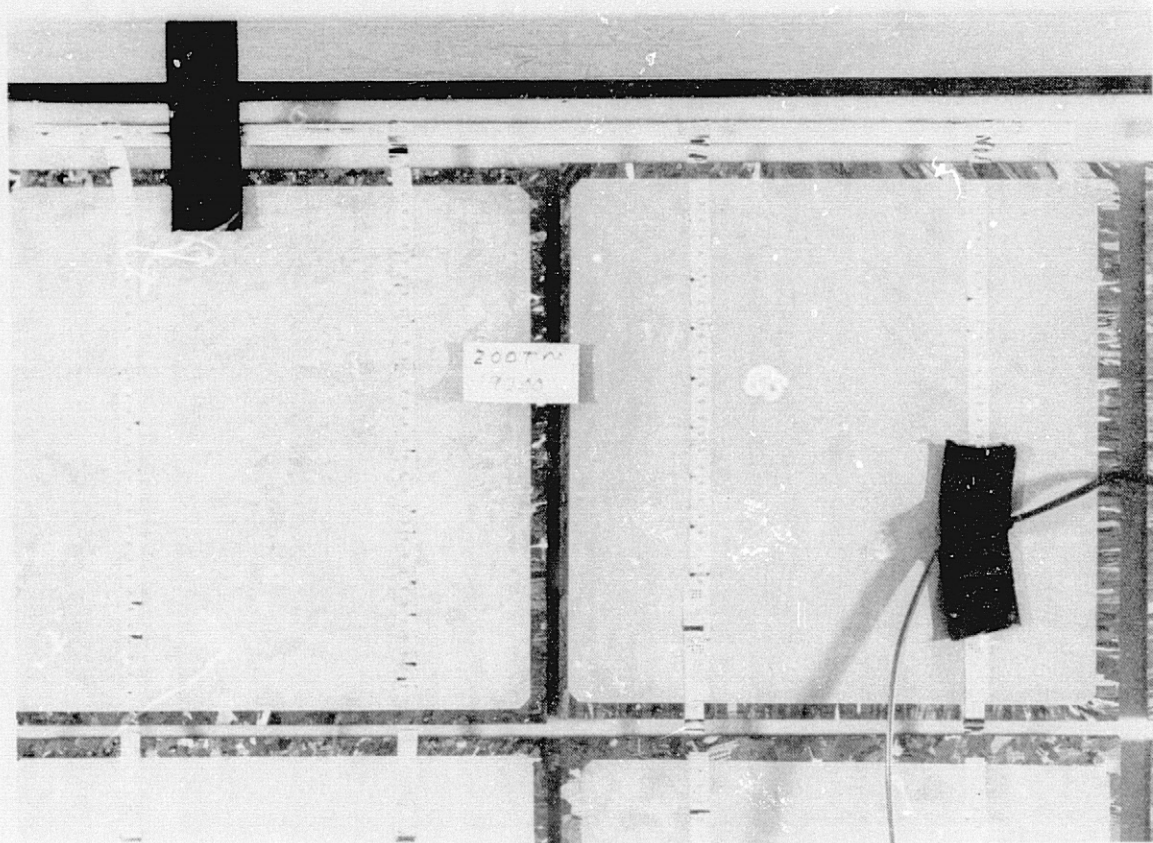
- FAILURE OF BUSBARS AND INTERCONNECTS MADE OF PURE ALUMINUM
- THE 200 TEMPERATURE CYCLE TEST DESIGNED TO SHOW INTERCONNECT  
WEAKNESSES REVEALS OTHER PROBLEMS

# Control Module With Interconnects at Right Angles to Bus Bar

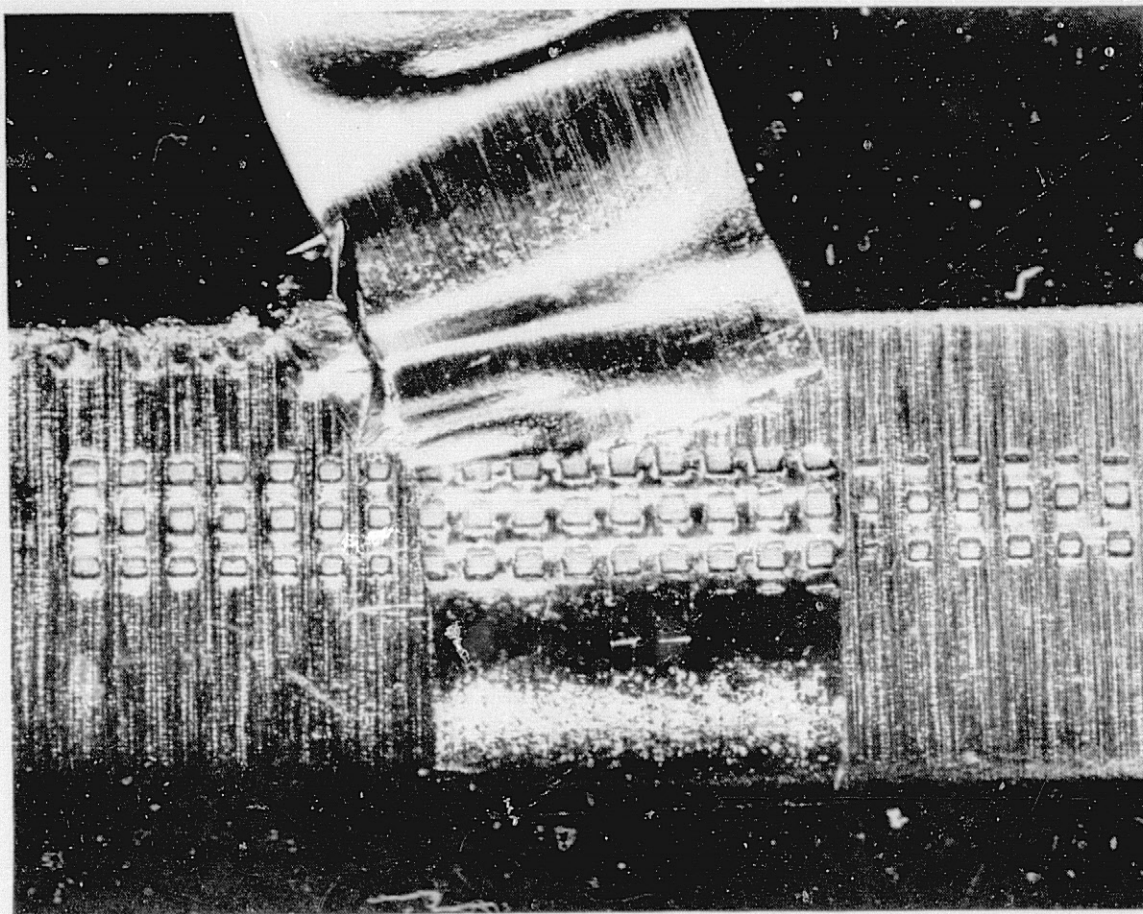




## Interconnects Displaced After 200 Temperature Cycles

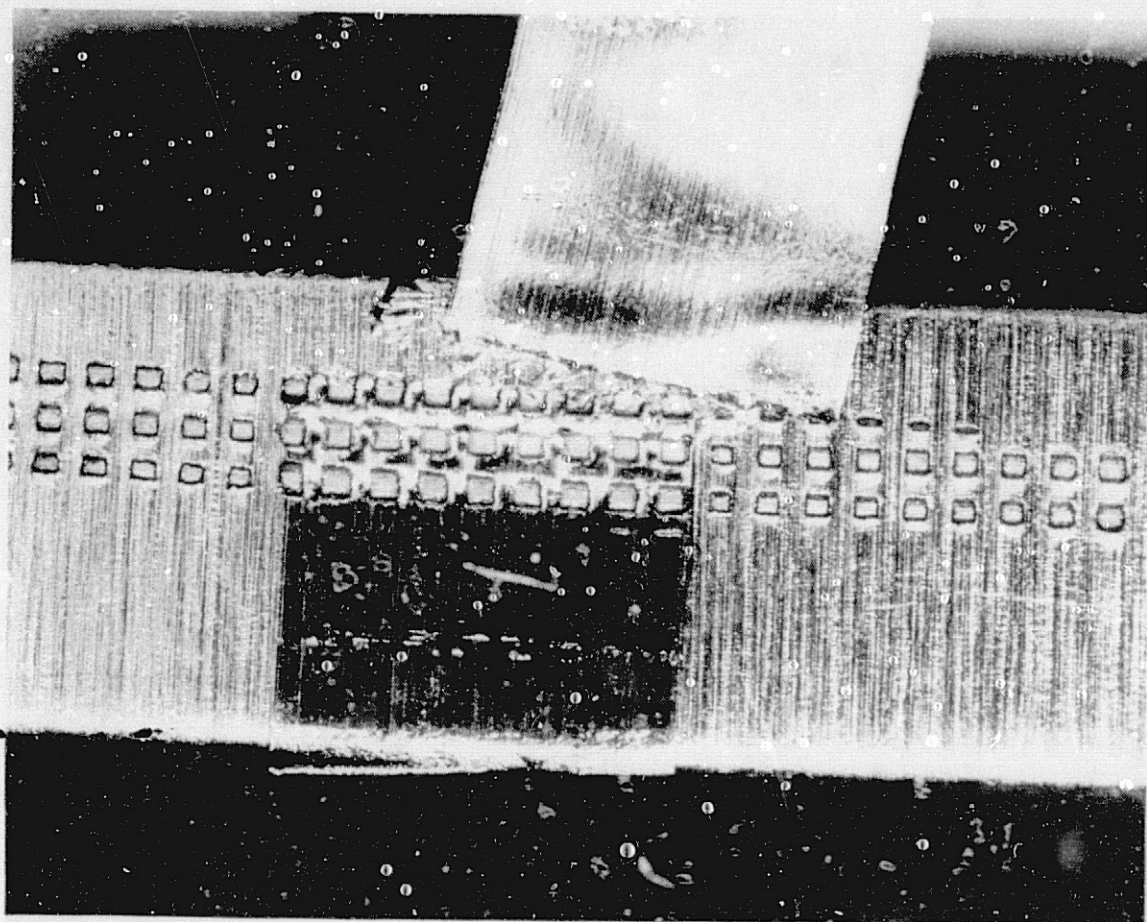


Closeup of Torn Interconnect





# Interconnect Separated From Bus Bar

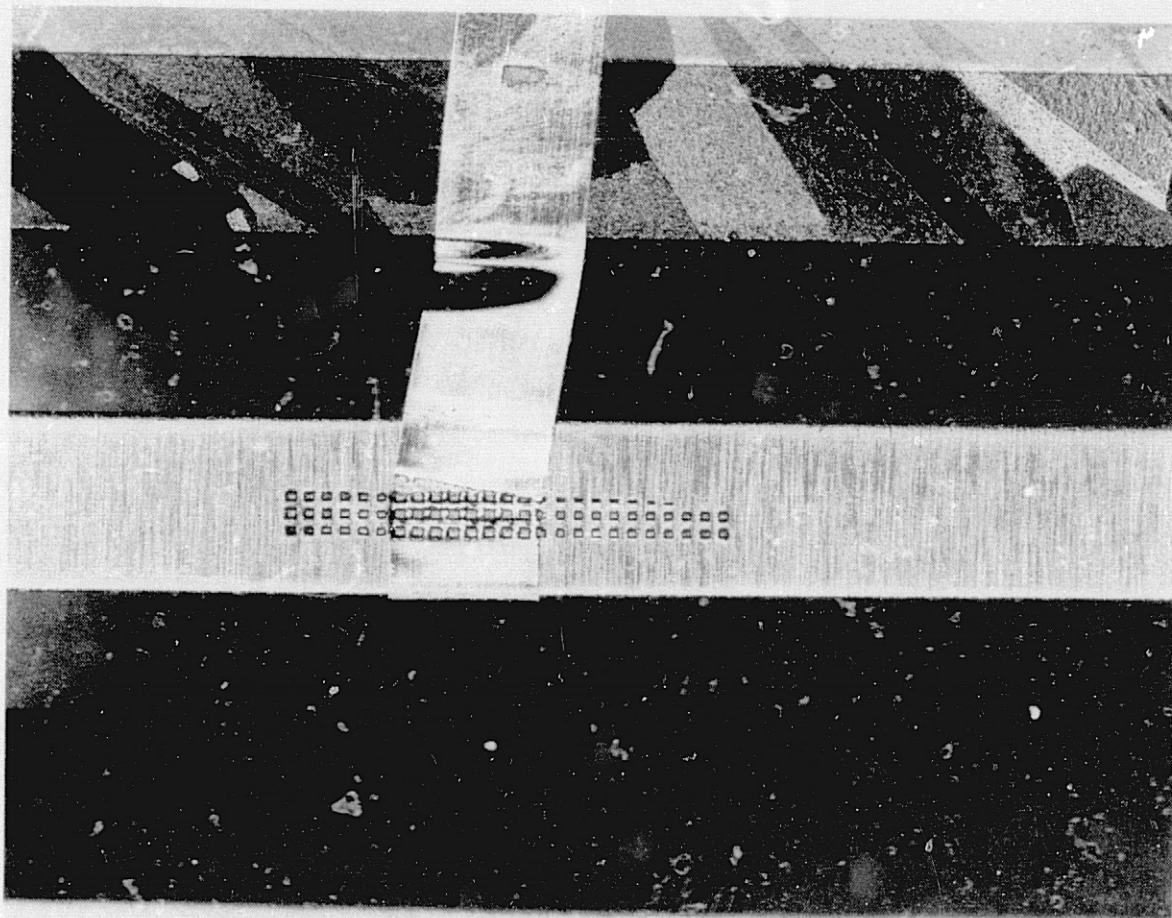


After 100 Cycles on Another Module:  
Used to Measure Bus Bar Elongation





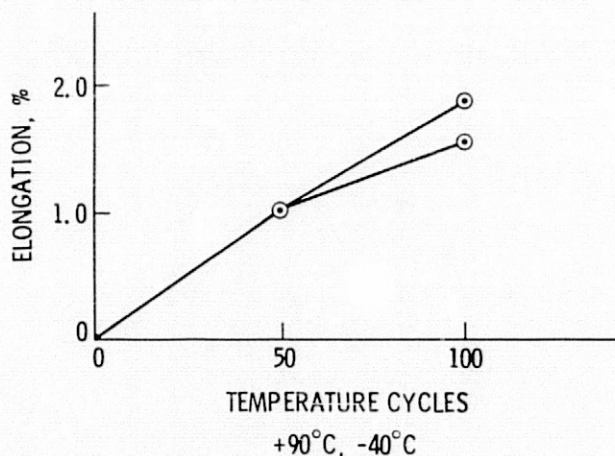
## Torn Interconnects on Latter Module



## Elongation of Aluminum Bus Bars

- METAL: ALUMINUM -- PROBABLY PURE
- DIMENSIONS: 0.04 x 0.41 x 18.1 cm (0.015 x 0.161 x 7.13 inches)
- ENCAPSULANT: PVB
- TEMP. CYCLING TEST
  - ELONGATION INCREASES WITH EACH CYCLE
  - INTERCONNECTS PARTIALLY OR COMPLETELY SEPARATED FROM BUSBAR
- TENSILE TEST
  - DISSECTED BUSBAR HAD ULTIMATE STRENGTH OF 11,300 psi
  - ELONGATION WAS 45%
- THREE CYCLE TEMPERATURE TEST OF FREE STRIP OF 1100 (PURE) ALUMINUM AND A MODULE
  - ELONGATION WAS 0.13% IN THE FREE STRIP vs 0.15 AND 0.20% IN THE BUSBAR
- RATCHETING OR CREEP CONFIRMED BY KAISER ALUMINUM CO.

### Bus Bar Elongation: Temperature Cycling Test of a New Module

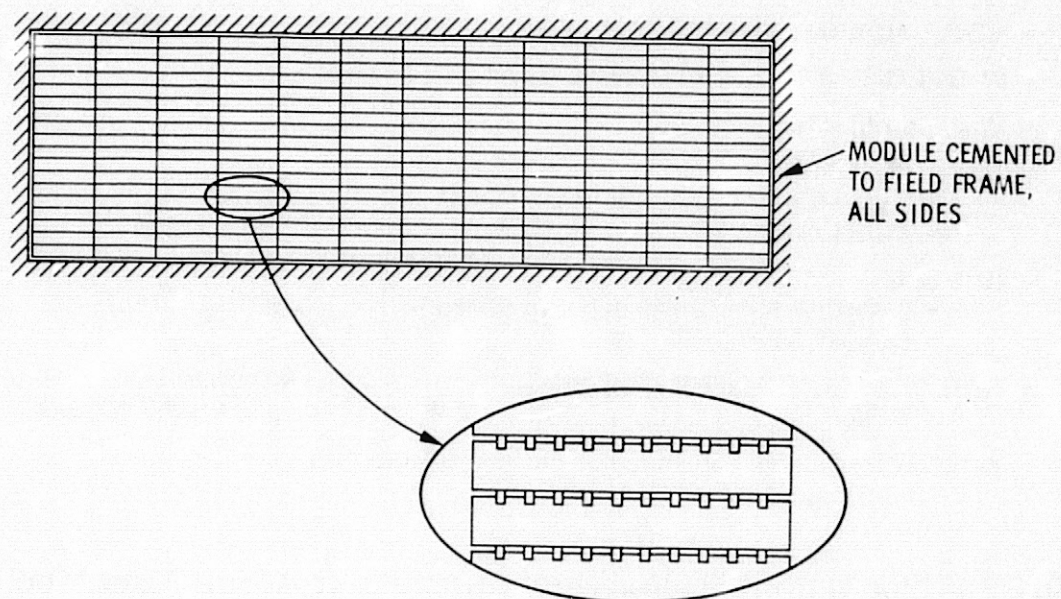


### Interconnect Failure: Test History

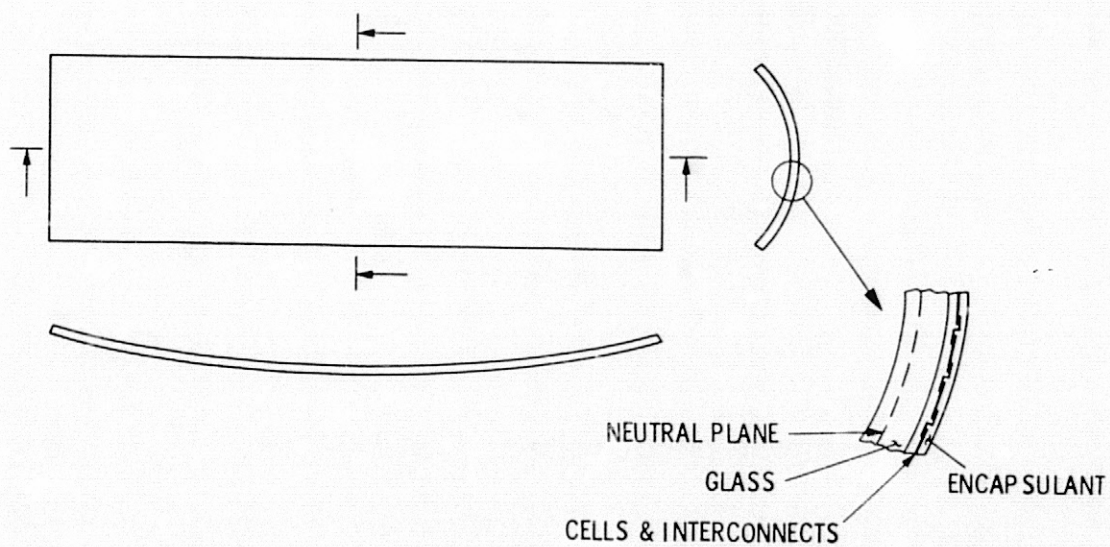
- |   |   |
|---|---|
| • 50 AND 200 TEMPERATURE CYCLES   | NO INTERCONNECT FATIGUE OR ELECTRICAL DEGRADATION |
| • 10 HUMIDITY-FREEZE CYCLES   | 8% ELECTRICAL DEGRADATION OF 1 OF 4 MODULES       |
| • MECHANICAL CYCLING  | -6, -8, -15, -17 % ELECTRICAL DEGRADATION, RESP.  |
| • FAILURE ANALYSIS SHOWED MULTIPLE INTERCONNECT BREAKAGE OCCURRED DURING MECHANICAL CYCLING |   |



### Cell Layout



### Module Under Pressure Loading



## Remedies for Interconnect Fractures

- CHANGE ORIENTATION OF CELLS  $90^0$
- COPPER OR CLAD METAL INTERCONNECTS ARE SUPERIOR TO ALUMINUM
  - REF: GORDON MON, RON ROSS PAPER, 16th PV SPECIALISTS CONFERENCE
- USE THICKER CLASS

## Polymer-Aluminum Back-Surface Films

- A TEDLAR/ALUMINUM/TEDLAR MATERIAL STRETCHED DUE TO ENCAPSULANT GAS BUBBLES
- TEDLAR SHRANK BACK TO ORIGINAL SHAPE
- ALUMINUM WRINKLED
- CONTINUED CYCLING MADE THE PROBLEM WORSE

## Results (Sometimes Unexpected) From the Added 150-Temperature-Cycle Test

- COMMERCIAL MODULE - ENCAPSULANT SOFTENED AND FLOWED OUT OF MODULE. PROBLEM NOT OBSERVED DURING 50 TEMPERATURE CYCLE OR HUMIDITY-FREEZE TEST.
- BLOCK IV MODULE (TESTED PER BL. VI) - ELECTRICAL FAILURE OF ONE MODULE. DEGRADATION AFTER 50 CYCLES WAS NEGLIGIBLE.
- VARIOUS MODULES - ELECTRICAL ISOLATION PROBLEMS, CRACKED CELLS, DELAMINATION, AND INTERCONNECT FATIGUE AND BREAKAGE.



## Conclusion

THE ADDED 150 TEMPERATURE CYCLES ARE A VALUABLE EXTENSION TO THE 50 CYCLE TEST.

## Summary

- AFTER BLOCK V TESTS OF MANY MODULES, THE TESTS APPEAR TO BE EFFECTIVE. THEY ARE DESIGNED TO BE EQUIVALENT TO LONGER FIELD LIFE.
- PURE ALUMINUM IS A POOR BUSBAR, INTERCONNECT MATERIAL FOR MANY APPLICATIONS
  - ALUMINUM BUSBARS ARE DIMENSIONALLY UNSTABLE IN TEMPERATURE CYCLING
  - ALUMINUM INTERCONNECTS CAN RAPIDLY FATIGUE DURING PRESSURE CYCLING
- THE 200 TEMPERATURE CYCLING TEST HAS GREAT VALUE BEYOND DETECTING INTERCONNECT FATIGUE.

# FOREIGN MODULE PERFORMANCE

JET PROPULSION LABORATORY

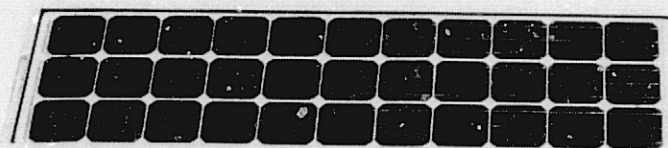
L. D. Runkle

## Physical Characteristics

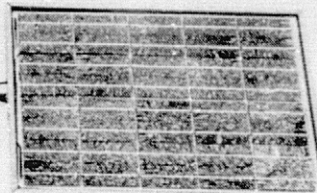
Mfr	Size, m		Superstrate	Encapsulant	Rear Cover	Electrical Connection	Packing Factor
	Length	Width					
AEG	0.563	0.459	Glass	PVB	Glass	Pigtail	0.77
China K	0.467	0.237	Glass	Silicone	Metal	Connector	0.49
China L	0.448	0.341	Glass	Silicone	Glass	Pigtail	0.76
China M	0.611	0.267	Glass	Silicone	Glass	Pigtail	0.54
Kyocera	0.950	0.445	Glass	EVA	Tedlar	J-Box	0.84
Tideland	1.023	0.414	Glass	AP	Glass	J-Box	0.67
Toyomenka	0.951	0.399	Glass	PVB	Polymer	Pigtail	0.73



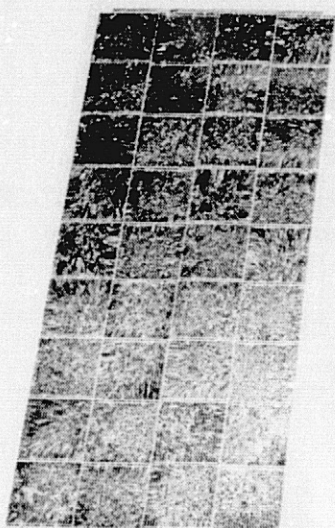
## Typical 1983 Modules



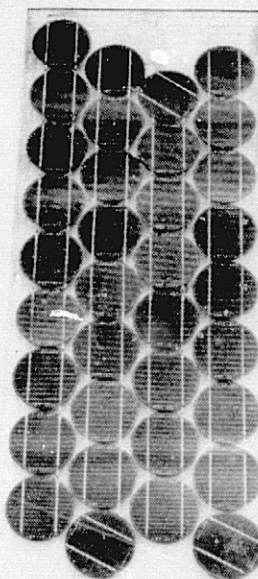
SOLAVOLT  
USA



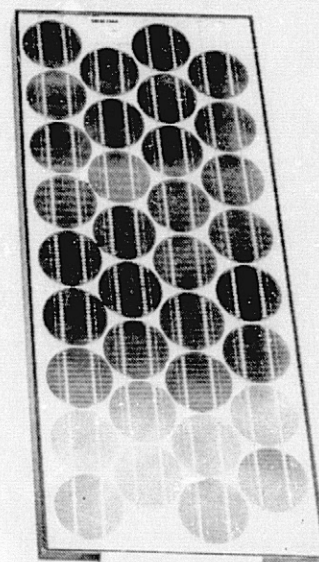
AEG-TELEFUNKEN  
GERMANY



KYOCERA  
JAPAN

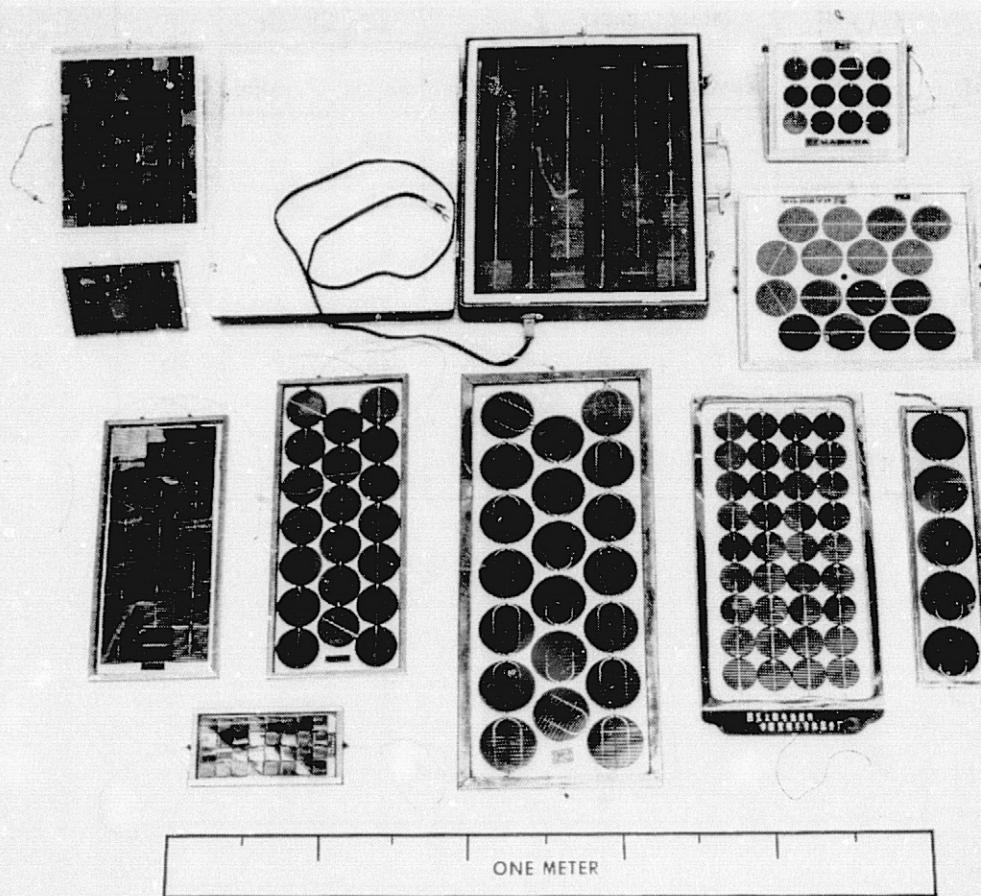


TIDELAND SIGNAL  
AUSTRALIA/USA



TOYOMENKO  
JAPAN

Chinese Modules

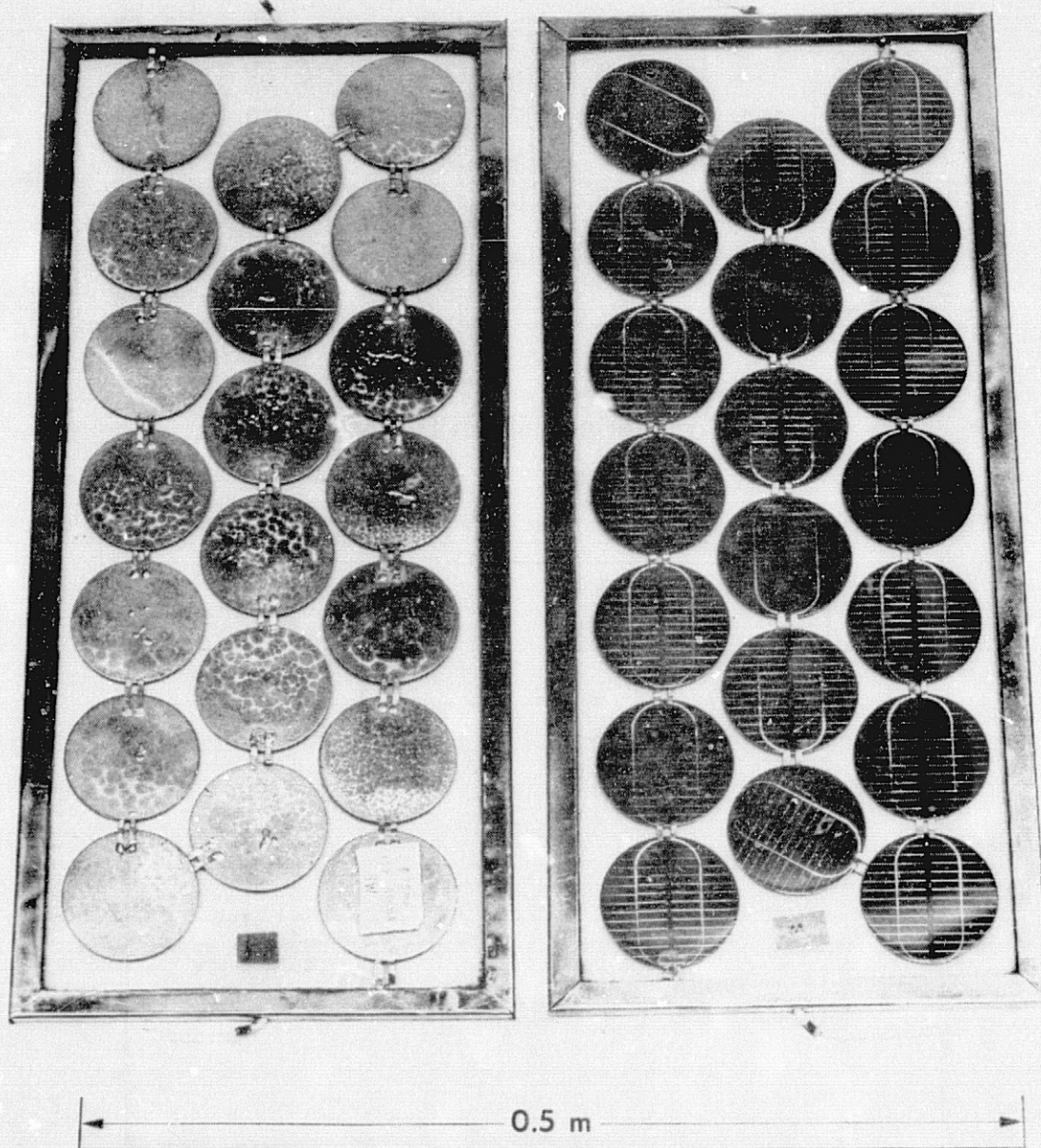




## Cell and Circuit Characteristics

Mfr	Cell Size, cm	Interconnects		Cell Material	Cell Circuit		Diodes
		Number	Contacts		Series	Parallel	
AEG	10x10	2	Mult	Poly	20	1	No
China K	4.4 dia	1	1	Cz	36	1	No
China L	4.9x4.9	1	1	Cz	48	1	No
China M	7.45 dia	2	2	Cz	20	1	No
Kyocera	10x10	2	2	Poly	36	1	No
Tideland	10 dia	2	Mult	Cz	36	1	No
Toyomenka	10.2 dia	2	Mult	Cz	34	1	No

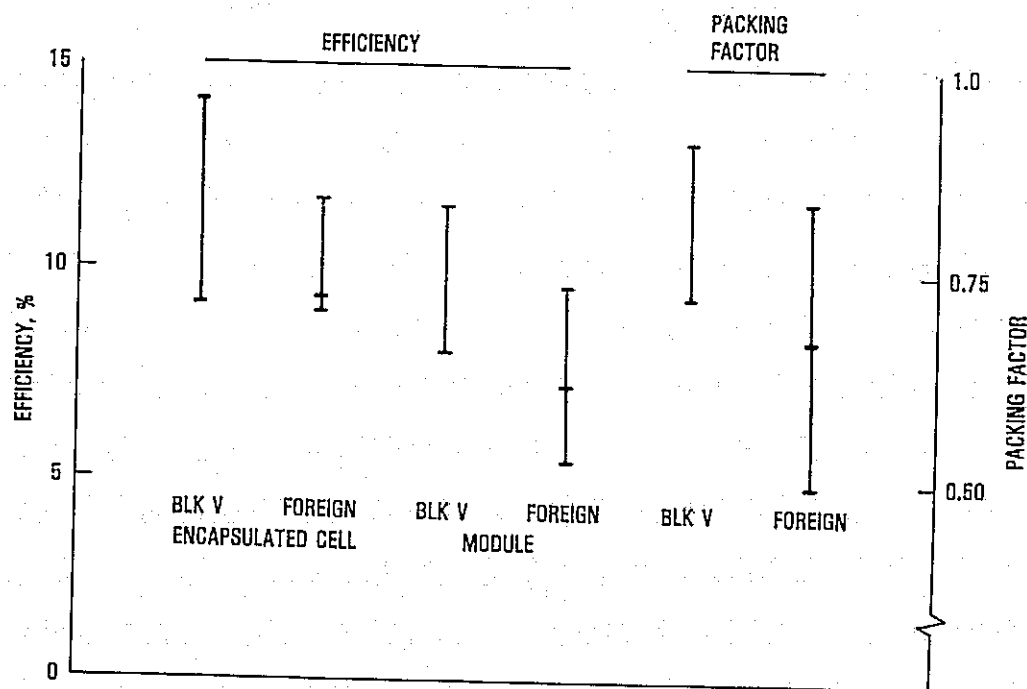
Back and Front Views of Chinese Module



## Electrical Performance

Mfr	P <sub>MAX</sub> , W	V <sub>P</sub> MAX, V	I <sub>P</sub> MAX, A	Fill Factor	Encaps'd Cell Eff'y, %	Module Eff'y, %
AEG	18.8	8.9	2.11	0.71	9.4	7.2
China K	5.8	16.0	0.36	0.70	10.6	5.2
China L	10.5	20.6	0.51	0.68	9.0	6.8
China M	8.5	8.5	1.00	0.70	9.7	5.2
Kyocera	40.5	15.8	2.56	0.70	11.3	9.6
Tideland	33.2	16.7	1.99	0.74	11.7	7.8
Toyomenka	32.0	15.2	2.11	0.73	11.6	8.4

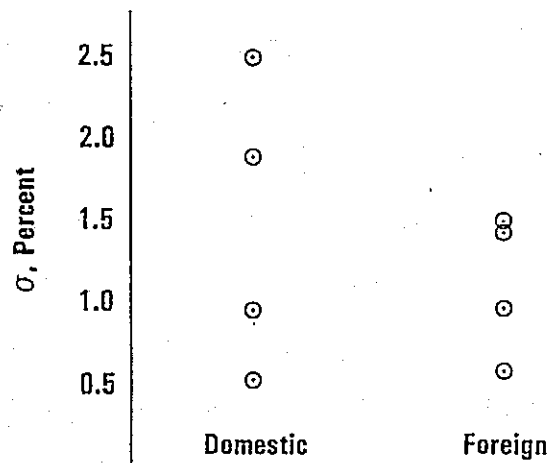
## Comparison With Block V



## Product Consistency

1 $\sigma$  variation in module power output

Sample size = 10 modules



## Qualification Testing

Tests: Block V specification

Hi-pot

Continuity

T-50, T-150

HF-10

MI-10K

Hot spot

Hail

## Conclusions

- Chinese samples on par with Block II
- Other foreign samples somewhat less than Block V
- Foreign modules appear to be intended for remote applications



# MODULE DURABILITY: FIVE YEARS' FIELD EXPERIENCE

JET PROPULSION LABORATORY

R.W. Weaver

## Objectives of Field-Test Activity

- To obtain in-field performance data for life-cycle endurance evaluation
- To determine degradation characteristics and failure modes as they relate to module design characteristics
- To provide verification data to qualification testing
- To perform field tests to identify module performance problems in an operational (array configuration) environment
- To obtain array performance data at operational array installations

## Field-Testing History

- 1977
  - Established four sites in Southern California
  - Automatic data acquisition system installed at the JPL site (Blocks I and II modules)
- 1978
  - Acquired 12 more test sites from Lewis Research Center (Blocks I and II modules)
  - Developed a portable module I-V data acquisition system
  - Initiated semiannual inspections of remote sites
  - Block III modules deployed to sites
- 1979
  - Data analysis techniques developed and applied to all data available
- 1981
  - Remote sites decommissioned
- 1982
  - Started Block IV deployment
- 1983
  - Initiated Testing of Block IV Modules and Arrays



## Testing Process

- Baseline I-V data acquired during installation
- Modules and arrays stressed using fixed resistors
- Periodic I-V data acquired
- All data adjusted to standard conditions
- Performance evaluated

## JPL Test Sites

Category	Locale	Latitude (degrees)	Altitude (feet)	Key Features
Extreme Weather	Fort Clayton, CZ	9	0	Typical tropic; Hot and humid; 100 inch-per-year rainfall
	Fort Greely, AK	64	1,270	Semi-arctic; dry, cold and windy; -30°F winters
Marine	Point Vicente, CA	34	0	Cool, damp mornings and clear afternoons; corrosive salt spray
	Key West, FL	25	0	Hot and humid; corrosive salt spray
	San Nicholas Island, CA	34	0	Somewhat milder than Key West
Mountain	Table Mountain, CA	34	7,500	Typical alpine environment; heavy winter snows and mild summers; high-velocity winds
	Mines Peak, CO	40	13,000	Clear and cold; high-velocity winds, max. UV
High Desert	*Goldstone, CA	35	3,400	Very hot and dry summers; clear skies
	Albuquerque, NM	35	5,200	Dry with clear skies; an abundance of UV
	Dugway, UT	40	4,300	Cold winters, hot summers; alkaline soil
Midwest	Crane, IN	39	0	Typical midwest; hot humid summers, cold snowy winters
Northwest	Seattle, WA (Fort Lewis)	47	0	Typical northwest; mild temperatures and an abundance of rain
Upper Great Lakes	Houghton, MI	47	750	Mild summers, severe winters
Urban Southern California	*JPL, Pasadena, CA	34	1,250	Primary test site - hot summers and mild winters; very high pollution environment
Urban Coastal	New London, CT	41	0	Typical New England Coastal
	New Orleans, LA	30	0	Hot and very humid; high-pollution environment

\*Retained as test sites

## Goldstone Site

Block No.	Retained at Site	Relocated		Totals
		JPL	TM	
I	19	40	20	79
II	8	24	10	42
III	13	9	8	30
Totals	40	73	38	151

All modules within 1% of baseline as of August 1981

## JPL Site

## Modules:

- Six from each manufacturer, not stressed (ARCO, ASEC, Motorola, Photowatt, Solarex, Spire)
- Periodic data taken

## Arrays:

- Nine months in field
- Design characteristics

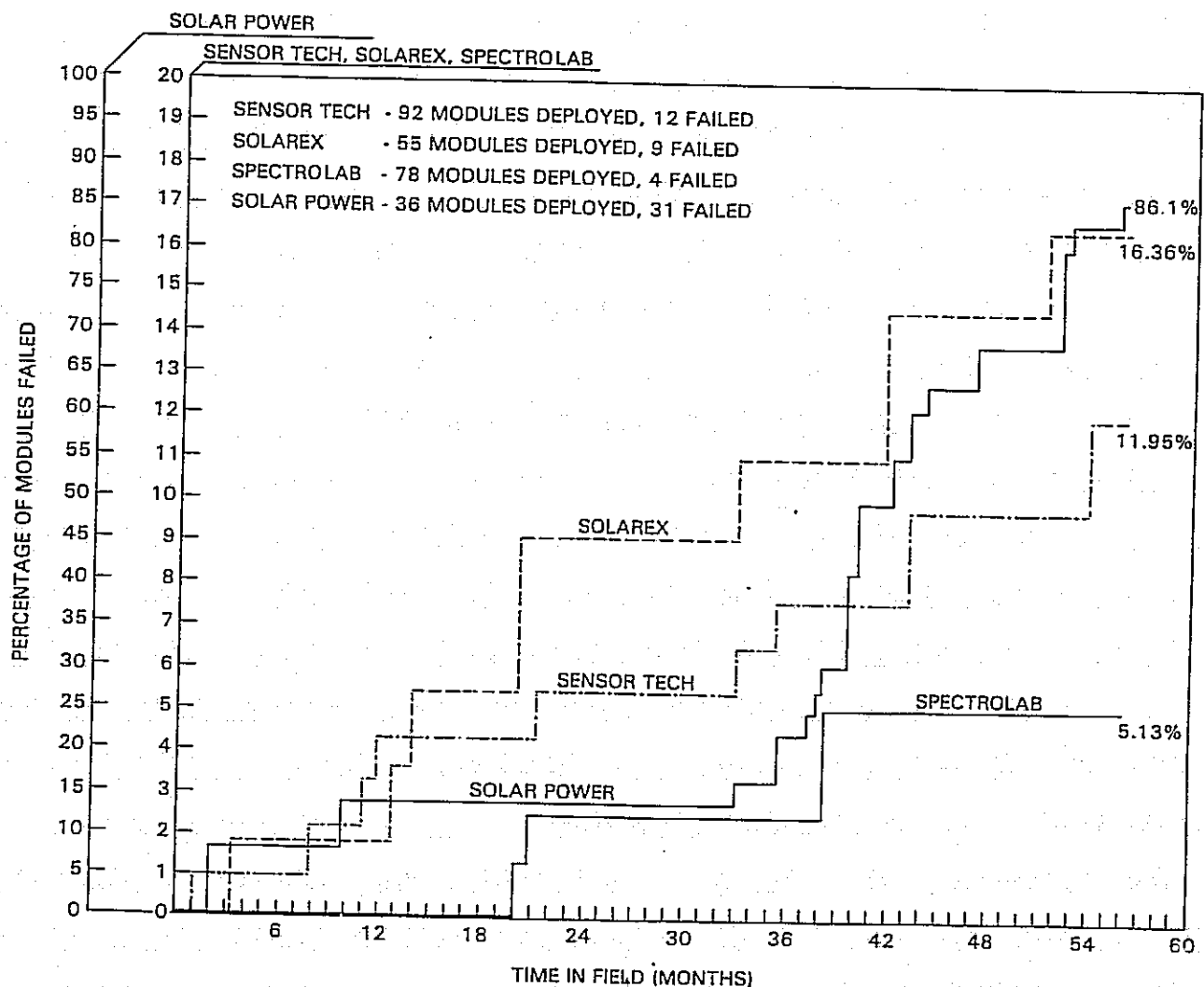
Manufacturer	Configuration	$I_{sc}$ , A	$V_{oc}$ , W	$W_p$	Fill Factor
ARCO	18, Series	2.4	350	580	0.69
ASEC	12, Series	5.1	220	800	0.71
Motorola	20, Series	2.5	360	660	0.73
Photowatt	11, Series	7.0	75	370	0.69
Solarex	22, Series	4.5	385	1200	0.69
GE*	4, P; 20, S	9.4	200	1200	0.64

\*GE hex shingles

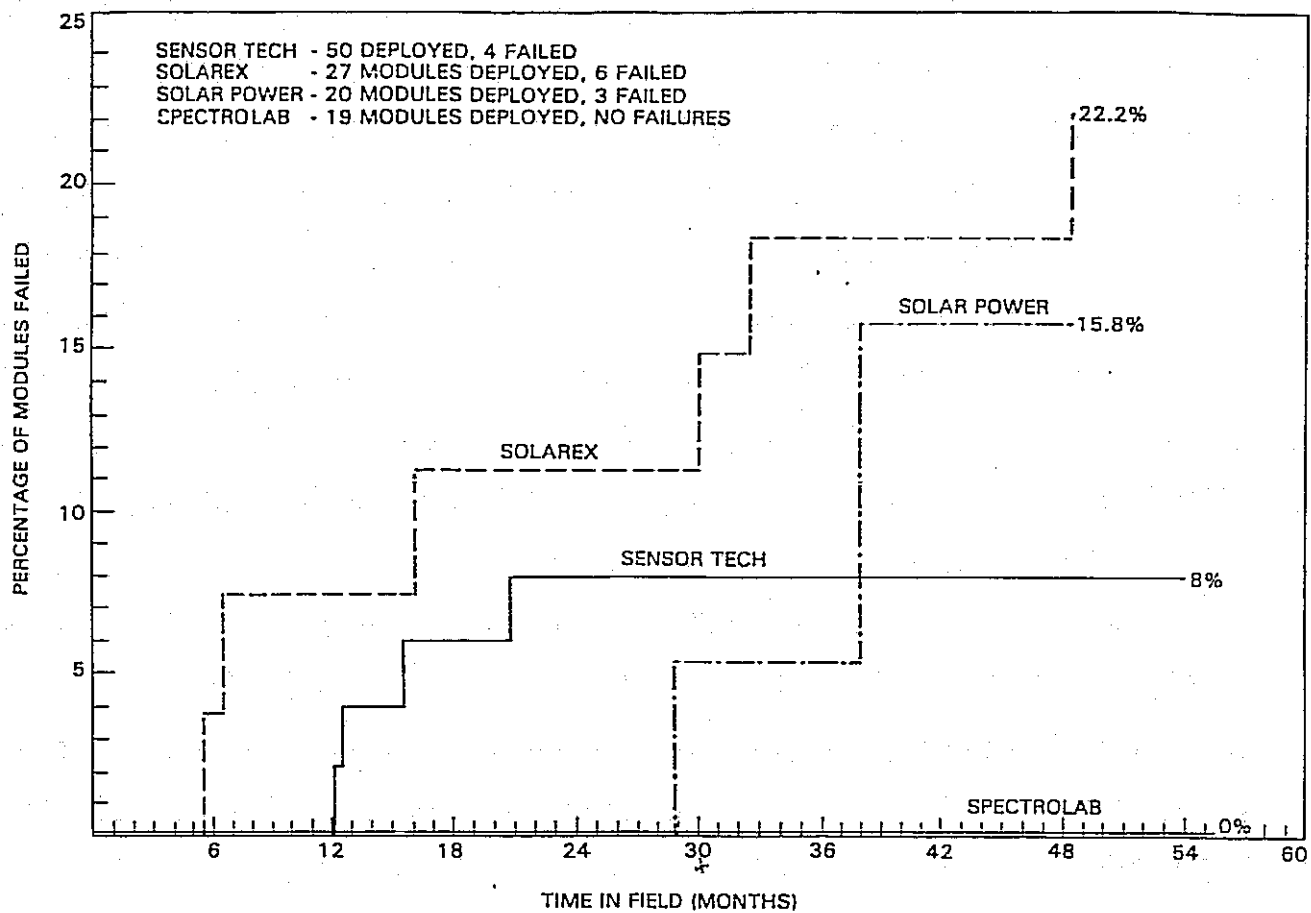
## Florida Solar Energy Center

- Marine environment, hot and humid
- Block IV modules, six each of:  
ARCO, ASEC, Motorola, Photowatt, Solarex, Spire
- Installed and initial tests, October 1982
- Resistor stressed
- Weekly visual inspections by FSEC
- Due for I-V tests October 1983

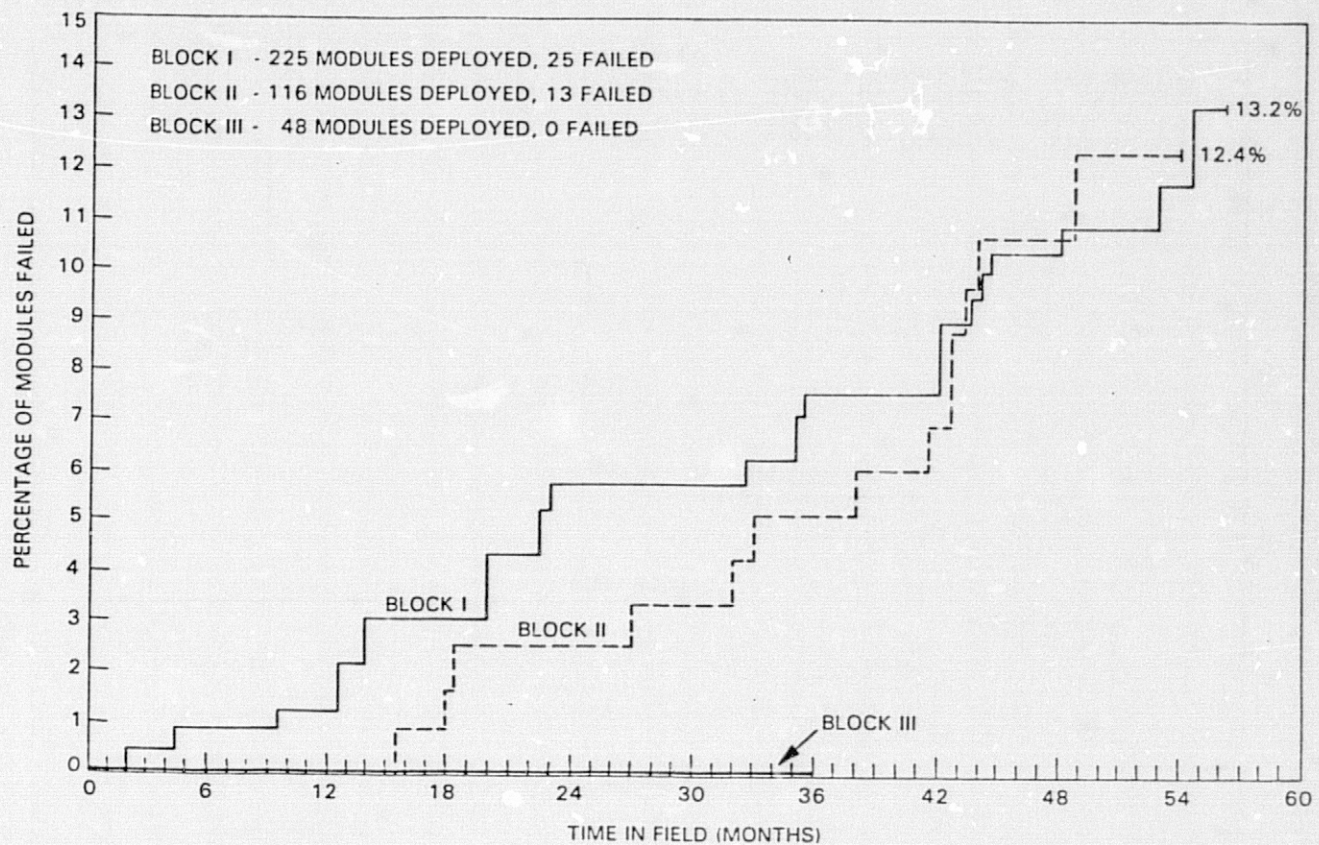
### Failure Rates of Block I Modules



## Failure Rates of Block II Modules

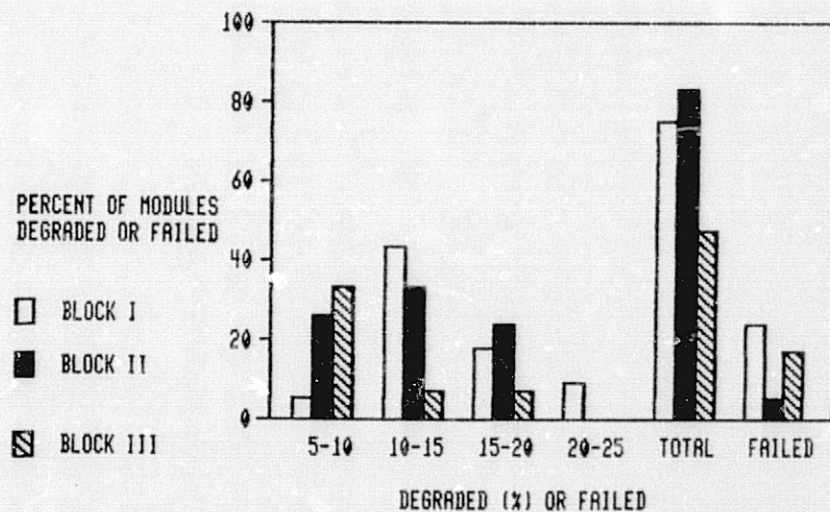


### Failure Rates for Blocks I, II and III Modules

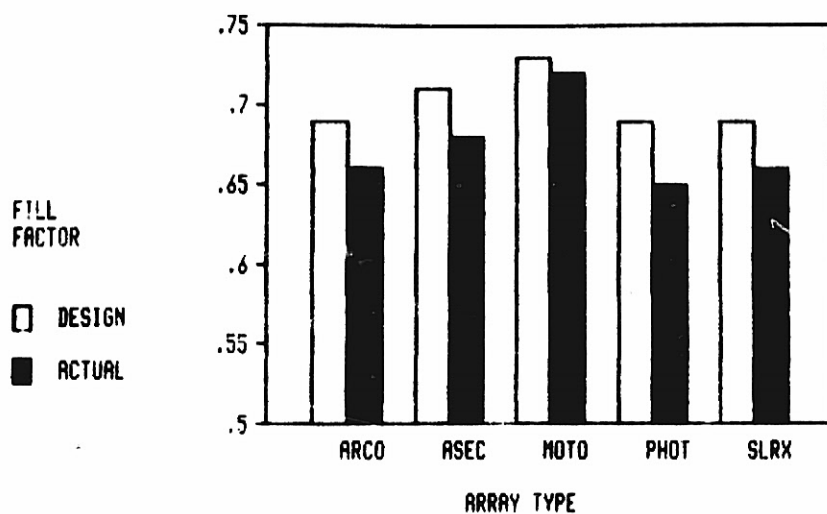


SOLAR POWER BLOCK I NOT INCLUDED

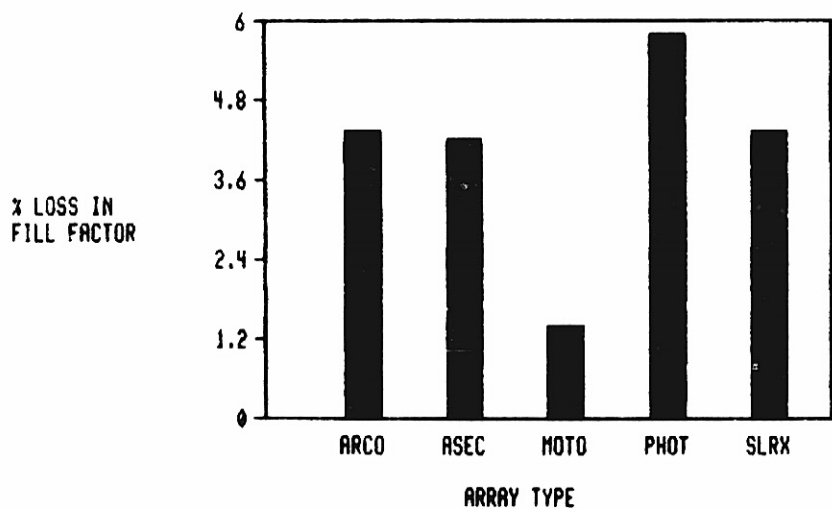
### Goldstone Results, 1981 to 1983



### Array Performance: Fill Factors



### Array Performance: Loss in FF, %



## Primary Causes of Failures

- Cracked cells
  - Impact
  - Burst
  - Defect
  - Hot Spotting
- Broken interconnects
  - Fatigue
  - Design
  - Assembly
- Terminals and connectors
  - Design
  - Corrosion
  - Grounding

## Other Reasons for Loss of Module Output

### Dirt

- 2% to 12% loss
- Partially correctable by cleaning
- Glass is best self-cleaner

### Discoloring of encapsulant

### Thermal-related

- Cycling effects
- Expansion stress
- Match materials or compensate

### NSMD

- San Nicolas Island, Mines Peak, Point Vicente

## Conclusions

- Electrical degradation or failure is not necessarily a function of physical appearance
- Three primary known causes of failures were cracked cells, broken interconnects, and electrical shorts
- Most severe environment is hot and humid
- No apparent failures due to array environment

## Plans

- Acquire data at Goldstone and FSEC annually
- Reduce amount of module data acquired at JPL site
- Acquire array data at JPL site under varying load conditions
- Continue off-Lab support function on request



# ENCAPSULATION MATERIALS AND PROCESSING

SPRINGBORN LABORATORIES, INC.

Identify and Develop Low-Cost Module  
Construction Materials:

## PHASE I

- POTTANTS
- OUTER COVER FILM
- SUBSTRATES
- ANTI-SOILING TREATMENTS
- ULTRAVIOLET STABILIZERS
- FABRICATION CONCEPTS
- ADHESIVES/PRIMERS

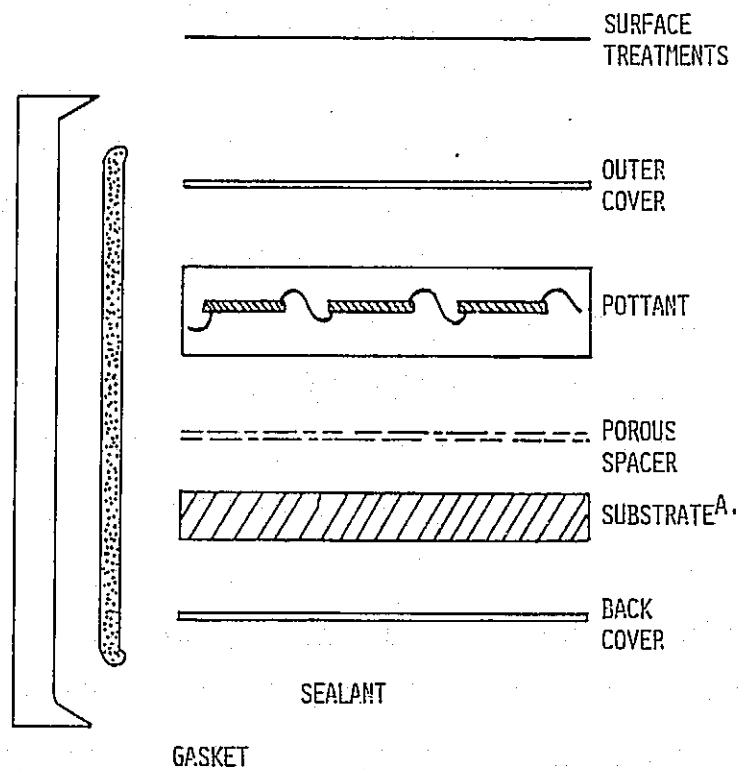
## PHASE II

(TECHNOLOGY READINESS)

- OPTIMIZED MATERIALS FORMULATION
- MATERIALS LIFETIME AND AGING STUDIES
- FIELD EXPOSURES

## Module Components (Essential)

- PLUS ADHESIVES WHERE NEEDED



A. ELIMINATED IN SUPERSTRATE DESIGN

## Candidate Polymer Encapsulation Materials (Overview)

SUPERSTRATE: LOAD BEARING TOP COVER  
SODA - LIME GLASS (LOW IRON)

POTTANTS: MECHANICAL STRESS RELIEF, ELECTRICAL ISOLATION,  
CELL POSITIONING, ENVIRONMENTAL ISOLATION,  
CORROSION BARRIER

ETHYLENE/VINYL ACETATE (EVA) }  
ETHYLENE/METHYL ACRYLATE (EMA) } LAMINATION TYPES

ALIPHATIC POLYURETHANE (PU) }  
POLY(BUTYL ACRYLATE) (BA) } CASTING TYPES

OUTER COVERS: PROVIDES HARD SOIL RESISTANT SURFACE, UV  
SCREENING, MECHANICAL BARRIER

TEDLAR 100BG30UT, TEDLAR 4462

ACRYLAR 22417

NON-SCREENING TYPES? KYNAR, FEP

POROUS SPACER: PROVIDES FIXED SPACING FOR MECHANICAL,  
DIELECTRIC ISOLATION: EVACUATION PATH  
DURING LAMINATION

CRANEGLASS (NON-WOVEN GLASS CLOTH)

BACK COVER: MECHANICAL BARRIER, ELECTRICAL ISOLATION  
EMISSIVITY FOR COOLING MODULE

KORAD 63000, TEDLAR 150BS30WH

SCOTCHPAR 20CP - WHITE (POLYESTER)

OTHER WHITE FILMS?

GASKETS: EPDM RUBBER

(PAWLING RUBBER CO.)

## Sealants

### FUNCTION AND PROPERTIES:

- PREVENTS INTRUSION OF RAINWATER
- SELF HEALING
- INEXPENSIVE
- WEATHERABLE
- NON-STAINING (NO SOLVENTS)
- APPLICABLE!

### SELECTIONS:    POLYSULFIDES, BUTYLS, URETHANES, OLEFIN/ACRYLIC COPOLYMERS

- BUTYLS MEET ALL CRITERIA EXCEPT APPLICATION
- AUTOMOTIVE TWO-PART URETHANES MAY BE BEST CHOICE
- MORE WORK NEEDED

## Substrates

MILD STEEL - \$0.25/FT<sup>2</sup> - CORROSION SENSITIVE

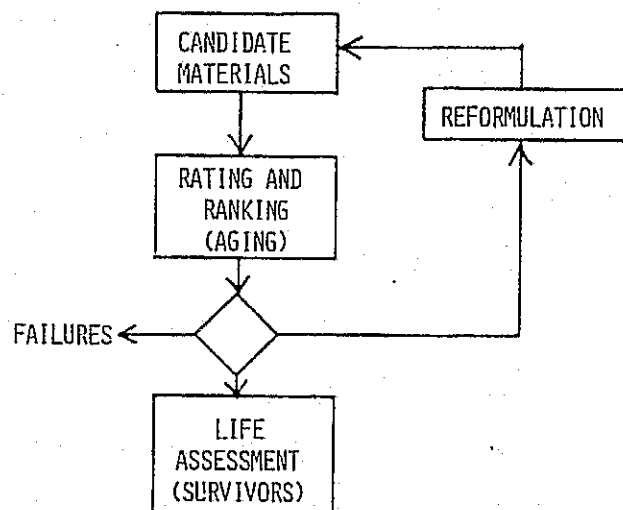
- COMBINATION OF PRIMERS AND COATINGS UNDER EVALUATION BY EXPOSURE AND SALT SPRAY
- BAKED INORGANIC CORROSION BARRIER, "ALSEAL 518"<sup>A</sup>, 1.5 MILS, APPROX. 10¢/FT<sup>2</sup>, 3,500 HOURS SALT SPRAY - MINOR CORROSION
- COMBINE WITH TOPCOAT WILL PROBABLY BE COST EFFECTIVE

HARDBOARD - \$0.15/FT<sup>2</sup> - HYGROSCOPIC SENSITIVITY

- INVESTIGATE FILMS/COATINGS TO DAMP OUT HYGROSCOPIC RESPONSE
  - NEED LOW COST, LOW VISCOSITY, LOW TEMPERATURE ADHESIVES TO BOND:
    - DAMPING FILMS
    - "SPLIT PROCESS" MODULES TO HARDBOARD
- ( ECONOMICS IN PROGRESS )

A. COATINGS FOR INDUSTRY, INC. SOUDERTON, PA.

## Accelerated Aging Program



### CONDITIONS:

- THERMAL STRESS (HEAT AGING)
- ULTRAVIOLET STRESS (UV EXPOSURE)
- CATALYTIC STRESS (METAL CORROSION)
- HYDROLYTIC STRESS (WATER)
- COMBINATIONS

## Data Correlation

OVERALL DEGRADATION REACTION IS COMPOSITE OF MANY COMPETING CHEMICAL REACTIONS IN COMPLEX RELATIONSHIP<sup>(A)</sup>

### DATA TREATMENT

#### 1. FIRST ORDER BEHAVIOR

- SUMMATION OF REACTIONS APPROXIMATES FIRST ORDER BEHAVIOR (ARRHENIUS)

#### 2. INDUCTION PERIOD BEHAVIOR

- REACTION KINETICS SUDDENLY CHANGE
- PLOT OF LOG PROPERTY VS TIME SHOWS SHARP ONSET OF DEGRADATION AT END OF INDUCTION PERIOD

### EMPIRICAL

- STRESS CONDITIONS SIMILAR TO MODULE APPLICATION
- INFORMATION USEFUL WITHOUT CORRELATION

(A) CHEMICAL MECHANISM CONSISTANT WITH DEGRADATION IN MODULE APPLICATION

## Encapsulant Properties (Major Emphasis on Pottants)

### RELEVANT MATERIAL PROPERTIES FOR MODULE SERVICE LIFE:

<u>MECHANICAL:</u>	CREEP RESISTANCE (GEL) TENSILE STRENGTH YOUNG'S MODULUS ELONGATION
<u>OPTICAL:</u>	INTEGRATED TRANSMISSION OVER 0.4 TO 1.1 MICRONS
<u>CHEMICAL:</u>	INERTNESS OF ENCAPSULANT TO CELL HARDWARE  DEGRADATION (WEATHERING)  INVENTORY OF ADDITIVES (STABILIZERS) IN POLYMER WITH TIME (HPLC)
<u>DIELECTRIC:</u>	ELECTRICAL ISOLATION OF CONDUCTIVE COMPONENTS (HI POT AND LEAK CURRENT)



## Thermal Degradation

- FREE RADICAL CHAIN REACTIONS WITH OXYGEN:
- DEGRADATION IS COMPOSITE OF MANY REACTIONS
- 60° , 80° , 105° , 130° C

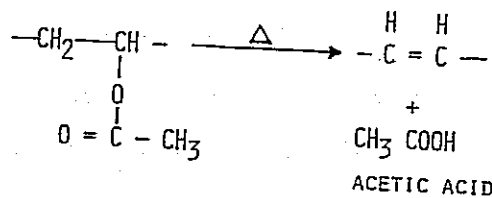
### ANTIOXIDANTS

PRIMARY: FUNCTION AS FREE RADICAL TRAPS

SECONDARY: CATALYZE DECOMPOSITION OF HYDROPEROXIDES  
VIA IONIC MECHANISMS: NO FREE RADICALS

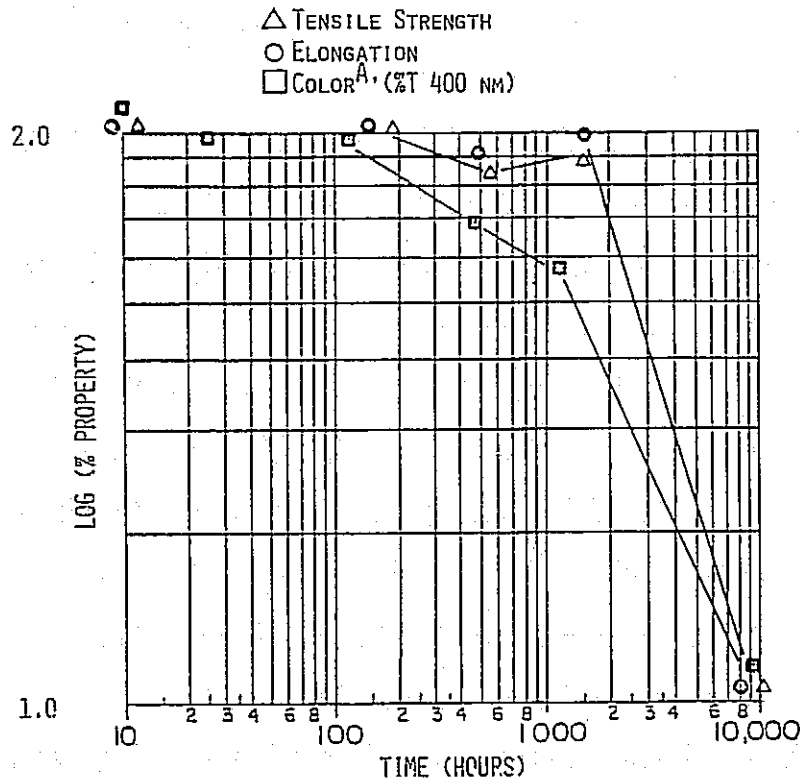
### ETHYLENE VINYL ACETATE (EVA)

"THERMOLYSIS" REACTION



- DOES NOT APPEAR TO BE A PROBLEM

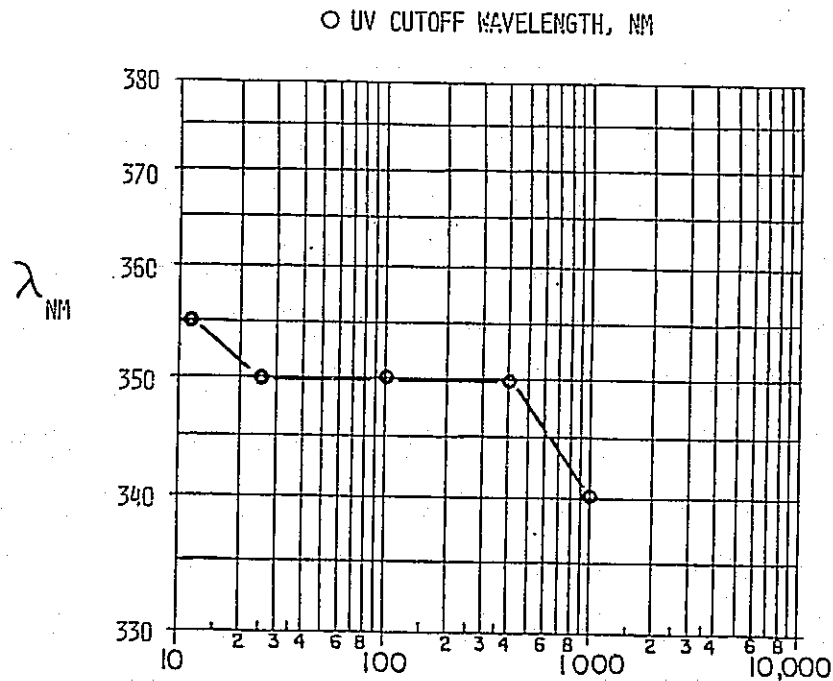
# Thermal Aging: EVA A-9918, 130°C



- MECHANICAL PROPERTIES ALMOST GONE AFTER 7200 HOURS (STILL HAS 74% T OPTICAL)
- NO CHANGE IN OPTICAL, MECHANICAL OR ELECTRICAL PROPERTIES AFTER:  
 7200 HRS - 90°C  
 1000 HRS - 105°C

A. AIR AND NITROGEN VALUES APPROXIMATELY THE SAME.

# Thermal Aging: EVA A-9918, 105°C



- DATA THE SAME IN BOTH AIR AND NITROGEN
- ALMOST NO CHANGE IN OTHER PROPERTIES AFTER 1000 HOURS
- RESULTS SUGGEST VOLATILE LOSS OF STABILIZER (UV ABSORBER)

## Thermal Aging

EMA 13439

80°C	1,000 HRS	NO CHANGE
105°C	1,000 HRS	NO CHANGE
130°C	1,000 HRS	COLOR ONLY (20% AT 400 NM)

POLYURETHANE  
Z-2591

80°C	1,000 HRS	NO CHANGE
105°C	1,000 HRS	COLOR ONLY ( 10% AT 400 NM )
130°C	250 HRS	COMPLETE LOSS OF ALL PROPERTIES

PVB  
SAFLEX PT-10

80°C	1,000 HRS	NO CHANGE
105°C	250 HRS	STRONG COLOR
130°C	CANNOT BE RUN DUE TO FLOW	

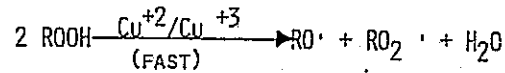
- ETHYLENE COPOLYMER POTTANTS HAVE GOOD  
THERMAL ENDURANCE

## Metal-Catalyzed Degradation

COPPER AND OTHER MULTIVALENT METALS<sup>A</sup>  
ACCELERATE OXIDATION REACTIONS IN POLYMERS

### METAL CATALYSIS:

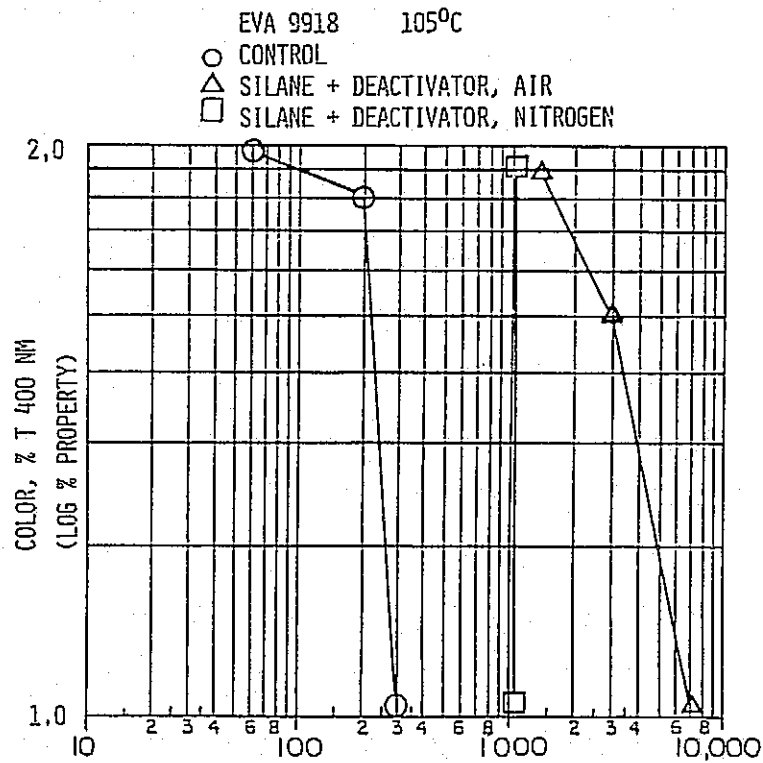
- SOLUBLE IONS ARE VERY CATALYTIC



- EFFECT WELL KNOWN IN WIRE AND CABLE INDUSTRY
- METAL DEACTIVATORS:  
COMPLEXING AGENTS FUNCTION TO INSOLUBILIZE  
THE METAL ION (0.2 PHR)
- COPPER TREATMENT: Z6030 SILANE (COPPER SCREEN)
- THERMAL AGE, AIR AND NITROGEN, 105°C
- MONITOR % T 400 NM (YELLOWING)

A. NO REACTION WITH ALUMINUM OR 60/40 SOLDER  
SILVER, TITANIUM OR NICKEL

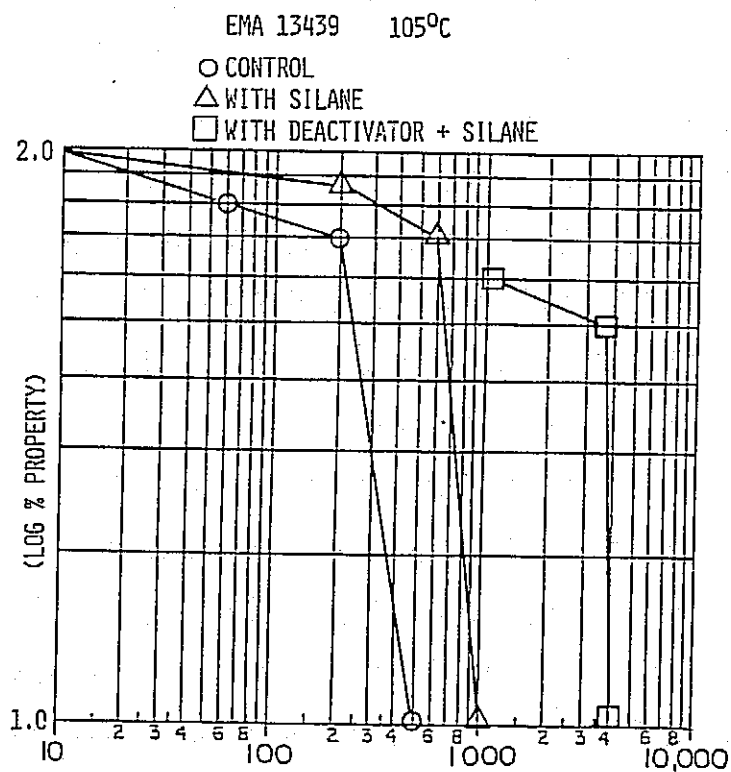
# Metal Deactivation (Copper Screen)



IN AIR, LIFE IMPROVEMENT FACTOR ~ 4

IN NITROGEN, LIFE IMPROVEMENT FACTOR ~ 24

# MODULE TECHNOLOGY



- LASTS 4000 HOURS AT 105°C WITH BOTH DEACTIVATOR AND SILANE
- LIFE IMPROVEMENT FACTOR ~8

## Photodegradation Experiments

- CARBON - CARBON BOND DEGRADES AT 80 KCAL/MOLE  
SUNLIGHT (UV) CONTAINS THIS AMOUNT OF ENERGY

### RS/4 SUNLAMP EXPOSURE

- MEDIUM PRESSURE MERCURY ARC LAMP IN GLASS ENVELOPE
- FILTERED TO REMOVE WAVELENGTHS BELOW 295 NM
- 1300 HOURS OF RS/4 EQUIVALENT TO ONE YEAR OUTDOOR  
SOLAR ULTRAVIOLET (50°C)

### THREE CONDITIONS

1. RS/4 EXPOSURE, 50°C
  - CLOSE TO ARRAY OPERATING TEMPERATURE
2. RS/4 EXPOSURE, 50°C, WATER SPRAY CYCLE
  - INTRODUCES HYDROLYTIC STRESS
  - SIMULATES RAINWATER EXTRACTION
3. RS/4 EXPOSURE, 85°C
  - ROOFTOP MODULE TEMPERATURE
  - FASTER ACCELERATION RATE

(RESULTS IN SHORTER TIME)



## RS/4 Fluorescent Sunlamp Exposure

EVA POTTANT A 9918  
(No COVER FILM)

CLEAR STABILIZED EVA EXPOSED 40,000 HOURS,  
SOLAR UV EQUIVALENT, 30 YEARS

	<u>TOTAL INTEGRATED TRANSMISSION</u>	<u>ULTIMATE ELONGATION</u>	<u>TENSILE STRENGTH</u>	<u>COLOR</u>
	(%)	(%)	(PSI)	(%T 400)
CONTROL	91	510	1890	75
EXPOSED 40,000 HRS.	<u>90</u>	<u>480</u>	<u>1480</u>	<u>14</u>
% CONTROL	99%	94%	78%	20%

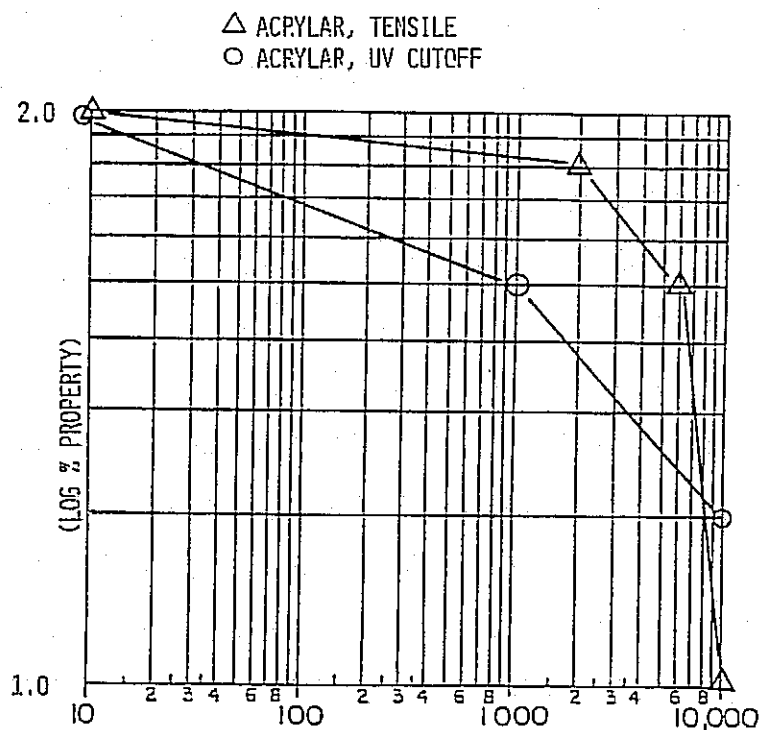
- SPECIMEN NOW SHOWING SMALL SURFACE CRACKS, TERMINATED
- UNSTABILIZED ELVAX 150 (EVA) BECOMES SOFT, TACKY, -  
LOSES PHYSICAL PROPERTIES IN LESS THAN 1000 HOURS

## RS/4 Data (50°C)

• EVA AND EMA WITH TBEC	8,000 HRS	NO CHANGE
• EVA FORMULATION WITH UV-2098 SCREENER	12,000 HRS	NO CHANGE
• ELVAX 150 - L101 BEHIND SUNADEX	3,000 HRS	DEGRADATION ONSET (TENSILE)
• EMA 13439	10,000 HRS	NO CHANGE (SLIGHT COLORATION)
• POLYURETHANE	14,000 HRS	NO CHANGE (SOME COLORATION)
• PVB (PT-10X WITHOUT GLASS)	500 HRS	LOSS OF ALL PROPERTIES DARK COLOR
• TEDLAR 100BG30UT	25,000 HRS	NO CHANGE
• ACRYLAR 22417 ACRYLIC FILM	12,000 HRS	OK, BRITTLE (LOW ELONGATION)
• SCOTCHPAR 20 CP - WHITE POLYESTER	10,000 HRS	DEGRADATION ONSET (ELONGATION)
• TEDLAR 150BS30WH	10,000 HRS	ONSET OF DEGRADATION (8% OF TENSILE AT 25,000 HRS.)

- RESULTS TAKE A LONG TIME

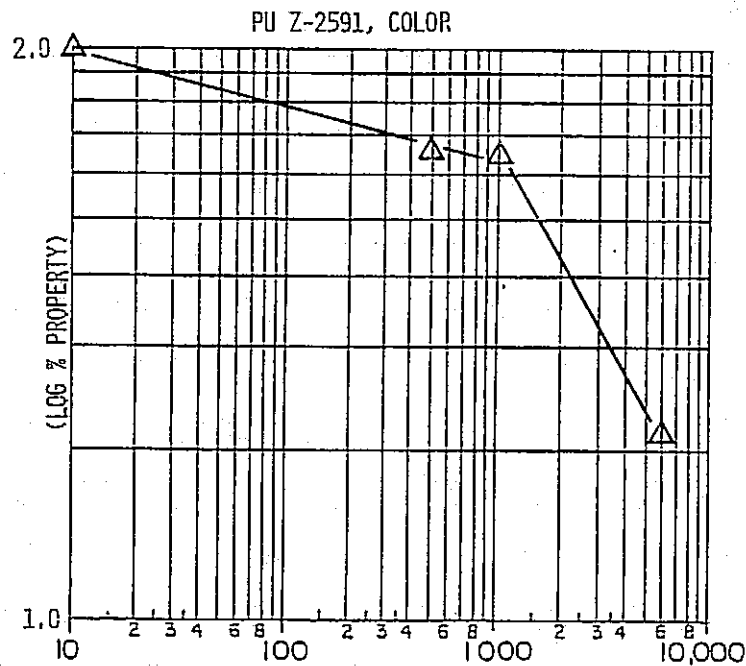
RS/4, Wet (50°C)



NO CHANGE AT 10,000 HOURS:

- EVA 9918
- EMA 13439
- PU Z 2591

## RS/4 (85°C)



AT 5,000 HOURS NO CHANGE:

- EVA 9918
- EMA 15257
- TEDLAR 100B30UT

A. GOOD STABILITY !

## RS/4 Data (85°C)

- CROSSLINKED ELVAX 150 BEHIND GLASS

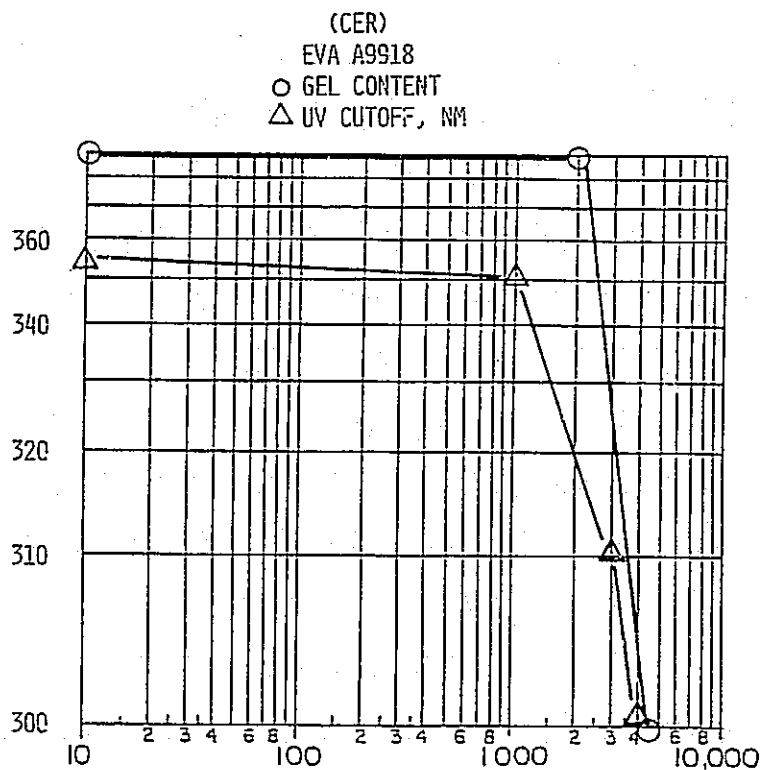
DEGRADES IN LESS THAN 1,000 HRS  
PALE YELLOW COLOR  
NO MEASUREABLE PROPERTIES

- EVA/UV SCREENER (UV-2098)

BUT NO TINUVIN 770  
DEGRADES IN APPX. 1,000 HRS.

- SEVERE CONDITION
- DEMONSTRATES IMPORTANCE OF HALS TYPE STABILIZER

# Controlled Environment Reactors<sup>A</sup>



COMPLETELY DEGRADED AT 4000 HOURS

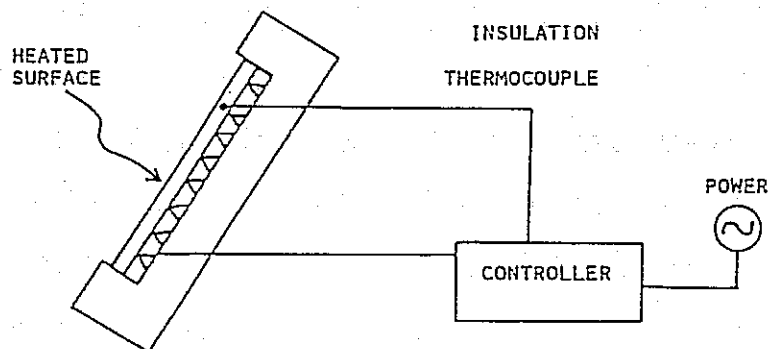
300 NM CUTOFF SUGGESTS NO STABILIZER LEFT - PRECEDES DEGRADATION

A. MEDIUM PRESSURE MERCURY LAMP, 50°C DAILY WATER SPRAY

## Accelerated Aging Test Program

### OUTDOOR PHOTOTHERMAL AGING

- USE NATURAL SUNLIGHT, AVOIDS SPECTRAL DISTRIBUTION PROBLEMS WITH ARTIFICIAL LIGHT SOURCES
- USES TEMPERATURE TO ACCELERATE THE PHOTOTHERMAL REACTION
- INCLUDES DARK CYCLE REACTIONS
- INCLUDES DRY/RAIN EXTRACTION
- SILICONE RUBBER HEATERS - IN OPERATION ONLY DURING SUNLIT HOURS



## Outdoor Photothermal Reactors (Opt)

70°C

NO CHANGE 2000 HOURS

90°C AND 105°CTERMINATED<sup>A</sup> AT:

EVA A 9918

2000 HOURS

EMA 15257

2000 HOURS

PU Z-2591

2000 HOURS

EVA 16718 A

1000 HOURS

(UV2098, TBEC)

EVA 16718 B

~500 HOURS

(NO TINUVIN 770)

- NO DECREASE IN UV CUTOFF WAVELENGTH  
(UV SCREENER LOSS)
- LOSS OF HINDERED AMINE STABILIZER?  
HEAT PLUS RAIN? 16718-A
- RAINFALL DURING EXPOSURE, 9.7 INCHES

A. LOSS OF MECHANICAL PROPERTIES, SEVERE COLORATION AT 105°C

## Co-Reacted Stabilizers

### UV SCREENER TYPE:

- AMERICAN CYANAMIDE CYASORB UV-2098  
BENZOPHENONE ESTER TYPE  
97% NON-EXTRACTABLE IN CURED EVA COMPOSITIONS

### HALS (HINDERED AMINE) TYPE:

- KNOWN TO BE SYNERGISTIC WITH BENZOPHENONE AND BENZOTRIAZOLE UV ABSORBERS
- POLYMERIC COMPOUNDS AVAILABLE:  
CYASORB UV-3346 (AMERICAN CYANAMIDE)  
CHIMASORB 944 (CIBA-GEIGY)
- REACTIVE (MONOMERIC) TYPES?  
U.S. PATENTS FOUND FOR:  
CIBA-GEIGY  
AMERICAN CYANAMIDE  
SANKYO KK



## Adhesion Experiments

EVA TO GLASS, SUBSTRATE, COVER FILMS:

POTTANT TO:	PRIMER	CONTROL	ADHESION , LBS/IN WIDTH	
			2 HOURS BOILING WATER	2 WEEKS WATER IMMERSION
EVA A9918 :				
SUNADEX	11861	32	28	30
MILD STEEL	11861	> 30	> 30	> 30
TEDLAR 200BS30WH	68040	> 30	> 30	> 30
TEDLAR 100BG30UT	107D	> 30	> 13	> 30
SCOTCHPAR 20CPW (POLYESTER)	14719	35.7	31.3	21.3
COPPER	16180	32.5	43.4	37.6
KYNAR 450	68040	5.7	6.1	4.1
SOLDER	16160	9.8	9.0	7.7
ALUMINUM	16180	6.5	3.7	3.2
PLEXIGLASS	68040	40.2	42.4	44.1

EVA TO GLASS, SUBSTRATE, COVER FILMS:

		ADHESION, LBS/IN WIDTH		
<u>POTTANT TO:</u>	<u>PRIMER</u>	<u>CONTROL</u>	<u>2 HOURS BOILING WATER</u>	<u>2 WEEKS WATER IMMERSION</u>
EVA 15295 (TBEC CURE):				
SUNADEX	11861	51.3	32.9	33.3
MILD STEEL	11861	8.0	5.2	2.3
ALUM!NUM	16180	5.6	3.0	3.0

• LOWER VALUES WITH MILD STEEL INDICATE  
DIFFERENCE IN CHEMISTRY FROM A9918

# MODULE TECHNOLOGY

## EVA TO GLASS, SUBSTRATE, COVER FILMS:

		ADHESION, LBS/IN WIDTH		
POTTANT TO:	PRIMER	CONTROL	2 HOURS BOILING WATER	2 WEEKS WATER IMMERSION
EMA 15257:				
SUNADEX	11861	BROKE	64	45
TEDLAR 100BG30UT	68040	- - -	FILM TORE - - -	- - -
SCOTCHPAR	14719	5.0	6.8	1.5
PU Z-2591:				
SUNADEX	Z6020	31	37	45
KOPAD 63000 (BACK COVER)	Z6020	4.1	2.5	2.7

- MORE WORK NEEDED ON PRIMERS FOR  
TEDLAR COVER FILMS, SOLDER

## SELF - PRIMING FORMULATIONS ( TO SUNADEX GLASS)

POTTANT/ PRIMER	LEVEL (PHR)	BOND STRENGTH, LBS/IN	
		CONTROL *	TWO MONTHS* STORAGE
EVA A9918	0.25	42	44
Z-6030	0.05	29	24
EVA 15295/ Z-6030	0.25	31	32
	0.05	10.9	9.5
EMA 15257/ Z-6030	0.25	57.4	58
	0.05	49.0	39.3

\* BONDS ALSO STABLE TO WATER IMMERSTION AND BOILING WATER

- STABLE TO STORAGE CONDITIONS
- EFFECTIVE OPTION IN EVA AND EMA (AT LOW LEVELS)  
TO GLASS
- EFFECTIVE AT LOW LEVELS

## Antisoiling Experiments

### SURFACE CHEMISTRY

- . HARD
- . SMOOTH
- . HYDROPHOBIC
- . OLEOPHOBIC
- . ION FREE
- . LOW SURFACE ENERGY

### SURFACE INVESTIGATED

- . SUNADEX GLASS
- . TEDLAR (100 BG 30 UT)
- . ACRYLAR (ACRYLIC FILM )

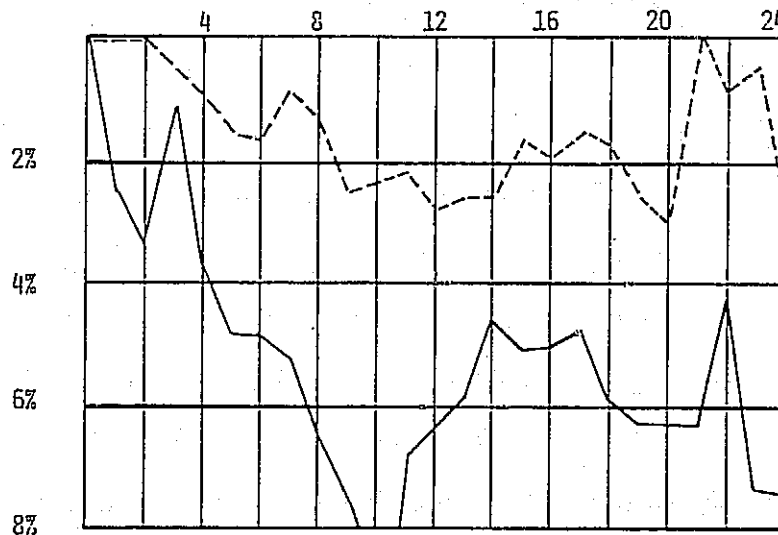
### TREATMENTS REMAINING

- . 1-2668 FLUOROSILANE (3M)
- . E-3820 PERFLUORODECANOIC ACID/  
SILANE (DOW CORNING)

## Soiling Experiments

TWENTY FOUR MONTHS EXPOSURE  
ENFIELD, CONNECTICUT

% LOSS IN  $I_{SC}$  WITH STANDARD CELL TREATED  
TEDLAR 10C08G300UT  
(SUPPORT ON GLASS )  
MONTHS EXPOSURE



———— CONTROL, NO COATING

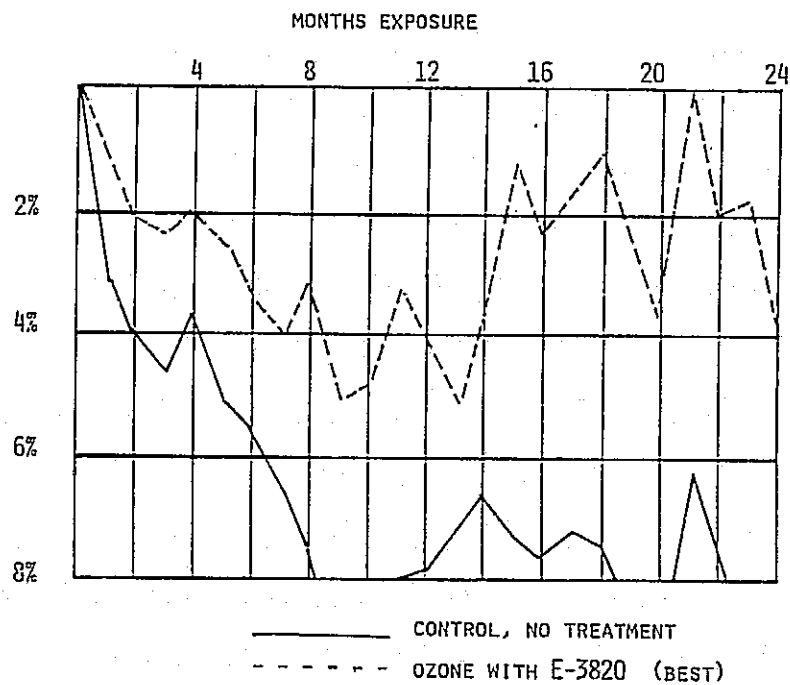
----- E-3820 COATING (BEST)

ESTIMATED AVERAGE POWER IMPROVEMENT, 3.8%

# MODULE TECHNOLOGY

TWENTY FOUR MONTHS EXPOSURE  
ENFIELD, CONNECTICUT

% LOSS IN  $I_{SC}$  WITH STANDARD CELL TREATED ACRYLAR  
(SUPPORTED ON GLASS)

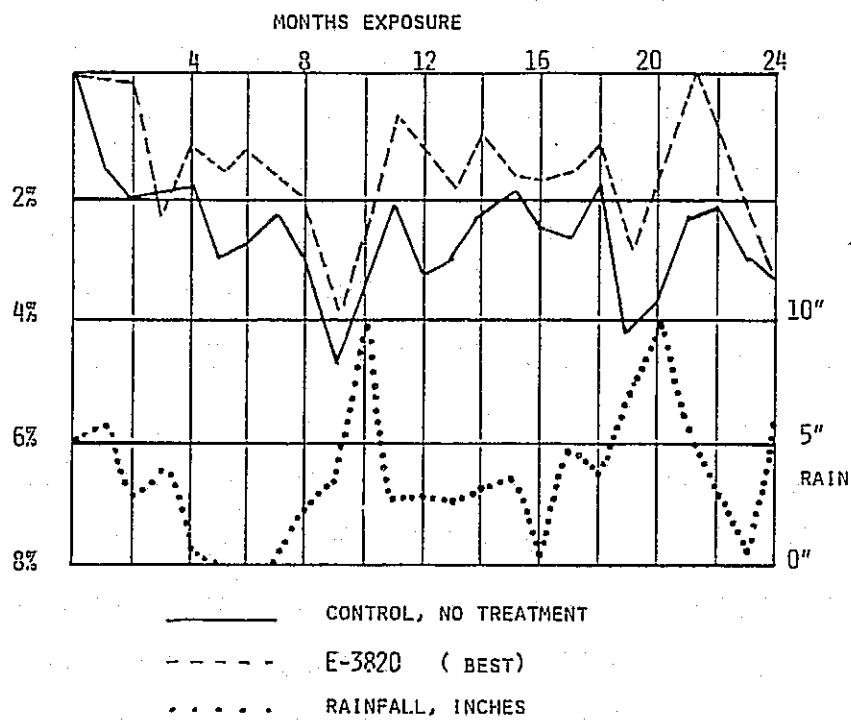


ESTIMATED AVERAGE POWER IMPROVEMENT, 3.9%

# MODULE TECHNOLOGY

TWENTY FOUR MONTHS EXPOSURE  
 ENFIELD, CONNECTICUT

% LOSS IN  $I_{SC}$  WITH STANDARD CELL TREATED  
 SUNADEX GLASS



ESTIMATED AVERAGE POWER IMPROVEMENT, 1%

## Additional Activities

### SUPPORT SERVICES

#### DOW CORNING:

ED PLUEDDEMANN

- ADVANCED PRIMER FORMULATIONS
- ADHESIVES

#### CASE WESTERN RESERVE UNIVERSITY : DR. JACK KOENIG

- "DRIFT" ANALYSIS OF PRIMER AT INTERFACE FOR DIAGNOSTICS

#### UNIVERSITY OF CINCINNATI: DR. BOERIO

- POLYMER - METAL INTERFACES

### TRANSPARENT CONDUCTIVE MATERIALS

- SURVEY OF POLYMER DEPOSITION METHODS
- ENVIRONMENTAL STABILITY CONSIDERATIONS
- SOLAR CELL ADHESION
- ENCAPSULATION PROCESS MATERIAL COMPATABILITY

## Conclusions

### ACCELERATED AGING

- SEVERITY OF CONDITIONS  
RS/4 TYPES THERMAL 130°C CER  
OPT 105°C COPPER 105°C
- PROPERTIES LEAST AFFECTED: DIELECTRIC, OPTICAL  
AND MECHANICAL
- FIRST PROPERTY TO CHANGE: COLOR (YELLOW)
- DEGRADATION: PREDOMINANTLY INDUCTION PERIOD TYPE,  
FEM FIRST ORDER

### THERMAL

- EVA AND EMA VERY THERMALLY STABLE
- EVIDENCE FOR VOLATILE LOSS OF UV STABILIZERS

### METAL

- AVOID EXPOSED COPPER :  
DEACTIVATORS + SILANE BUY TIME
- NO REACTIONS OBSERVED WITH ALUMINUM,  
60/40 SOLDER, NICKEL, SILVER

### PHOTO-THERMAL

- RS/4 CONDITIONS REQUIRE LONG EXPOSURES TO EVALUATE  
STABLE MATERIALS
- CER AND OPT CONDITIONS GIVE RESULTS IN MONTHS, NOT  
YEARS (REALISTIC)
- STABILIZER EXTRACTION PRECEDES DEGRADATION HALS  
MATERIALS?



## MODULE TECHNOLOGY

### ADHESION:

- MANY GOOD PRIMERS FOR EVA 9918
- MORE WORK REQUIRED FOR EVA/TBEC, EMA, PU
- SELF PRIMING POTTANTS (EVA, EMA)  
WORK WELL !

### ANTI-SOILING:

- FLUROSILANE CHEMISTRY BEST.
- STILL ACTIVE AFTER 2 YEARS
- ESTIMATED POWER IMPROVEMENTS.  
SUNDEX GLASS 1%  
ORGANIC FILMS 3-4 %

## Future Work

- NON-SCREENING OUTER COVER FILMS
- BACK COVER (WHITE FILM ) ALTERNATIVES
- SEALANTS (APPLICATION METHODS )
- GLUES FOR HARDBOARD PROTECTIVE FILMS AND SPLIT  
PROCESS OPERATION
- AGING STUDIES:
  - STABILIZER INVENTORY  
(QUANTITATE LOSSES)
  - EVALUATE NON-FUGITIVE HALS
  - EVA, EMA ADVANCED FORMULATIONS  
(WITH TBEC, UV-2098 STABILIZER)
  - OPT, CER - MORE EMPHASIS
- PRIMERS:
  - MORE WORK - EMA , PU
  - INTERNAL PRIMERS FOR CELLS AND METALIZATION
  - BOND DURABILITY (AGING)

## Advanced Formulations

"ADVANCED INDUSTRIAL VERSION "

EVA 16718A

- EVALUATION SAMPLES AVAILABLE
- FAST TBEC CURE SYSTEM
- BETTER SHELF STABILITY
- CO-REACTIVE UV STABILIZER  
(CYASORB UV-2098)
- WITH OR WITHOUT INTERNAL  
PRIMER

# HERMETIC EDGE SEALING OF PHOTOVOLTAIC MODULES

SPIRE CORP.

M.J. Nowlan

## OBJECTIVE

INVESTIGATE THE USE OF AN ELECTROSTATIC BONDING (ESB) AND ULTRASONIC WELDING PROCESS TO PRODUCE HERMETIC EDGE SEALS ON SOLAR CELL MODULES.

## PROGRAM TASKS

- 1- DEVELOP ESB TECHNIQUES  
FOR BONDING AI FOIL TO GLASS
- 2- DEVELOP ULTRASONIC WELDING TECHNIQUES  
FOR BONDING AI FOIL TO AI FOIL
- 3- DEMONSTRATE EFFECTIVENESS OF  
DEVELOPED TECHNIQUES BY FABRICATING  
SAMPLE MODULES AND QUANTIFYING  
SEAL HERMETICITY

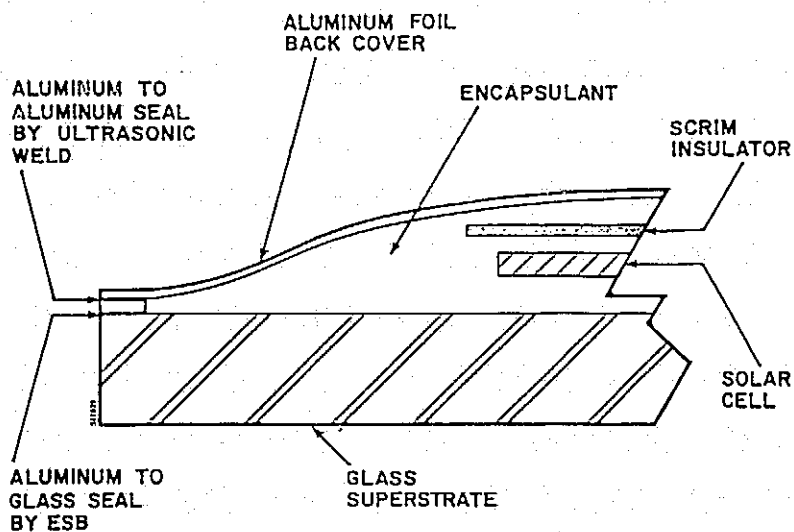
## ANTICIPATED BENEFITS

- REDUCED  $H_2O$  VAPOR TRANSMISSION
- REDUCED  $O_2$  TRANSMISSION
- UV AND TEMPERATURE STABLE SEAL

## APPLICATIONS

- MODULES IN SEVERE ENVIRONMENTS
  - COASTAL AND MARINE SITES
  - HOT AND HUMID REGIONS
- REMOTE LOCATIONS
  - REDUCED MAINTENANCE AND REPLACEMENT COSTS
- MODULES WITH SENSITIVE COMPONENTS
  - THIN FILM CELLS
- EXTENDED LIFETIME FOR STANDARD MODULES

### Module With Hermetic Seal



## ESB Development

### SELECT MATERIALS

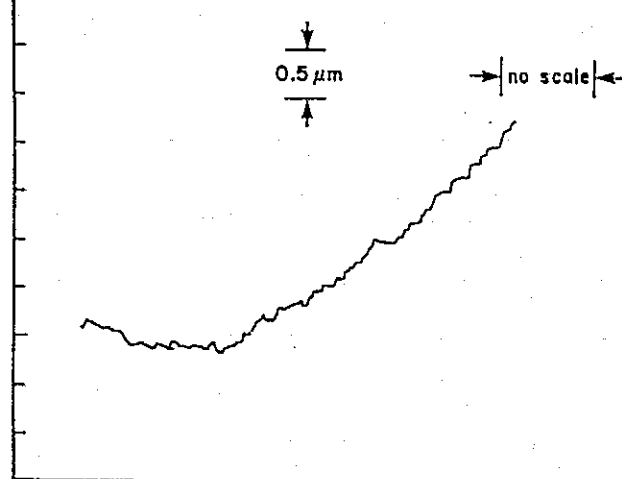
- FLOAT SODA LIME SILICATE (WINDOW) GLASS
  - 1/8" THICK - TYPICAL FOR MODULES
  - INTRINSICALLY SMOOTH ( $\leq 100\text{\AA}$ )
  - HIGH MOBILE ION CONTENT
    - 13%  $\text{Na}_2\text{O}$
    - 9.3%  $\text{CaO}$
- ALUMINUM FOIL
  - 1100-0 ALLOY -SOFT TEMPER
  - LOW YIELD STRENGTH
  - 2 MILS ( $51\text{ }\mu\text{m}$ ) THICK
  - THICK ENOUGH TO WELD
  - THIN ENOUGH FOR PLASTIC DEFORMATION

### PROCESS RESEARCH

- INVESTIGATE ESB IN AIR
  - TRAPPED AIR ( $.13\text{ }\mu\text{m Al}$ ) POCKETS
  - NO POCKETS ( $1.3\text{ }\mu\text{m Al}$ ) BUT
  - REDUCED ADHESION - LESS BONDED AREA
  - ROTATING DISK ELECTRODE SHOULD
  - BE TRIED ON  $.13\text{ }\mu\text{m Al}$
- OPTIMAL CONDITIONS
  - PRESSURE  $\geq 60\text{ PSI}$
  - TEMP =  $250^\circ\text{C}$  TO  $350^\circ\text{C}$
  - VOLTAGE  $\geq 500\text{ V}$  FOR ONE MINUTE
- ROTATING DISK ELECTRODE ESB SHOWN FEASIBLE
  - EXPERIMENTAL SET-UP
  - BETTER PROCESS CONTROL  $\rightarrow$  REPRODUCIBILITY

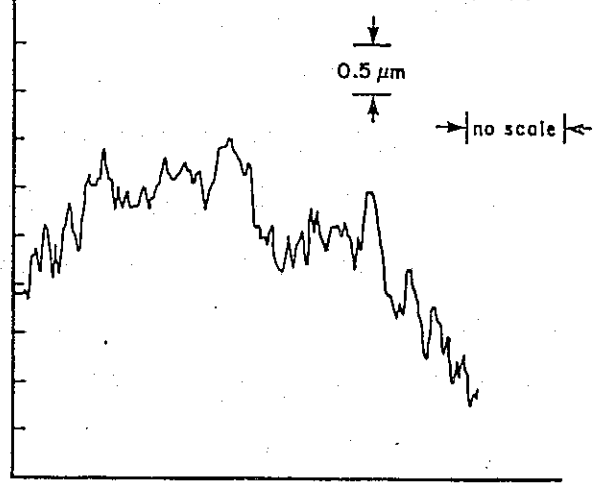
# MODULE TECHNOLOGY

SMOOTH SIDE OF 2 MIL ALUMINUM FOIL



$\leq 0.13 \mu\text{m}$  PEAK TO PEAK

ROUGH SIDE OF 2 MIL ALUMINUM FOIL



$\leq 1.35 \mu\text{m}$  PEAK TO PEAK

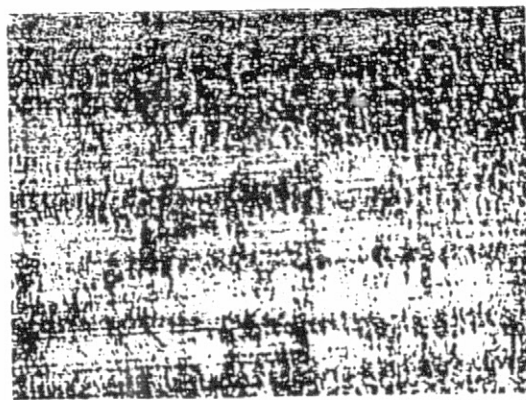
ESB of Al Foil to Glass

(52x)



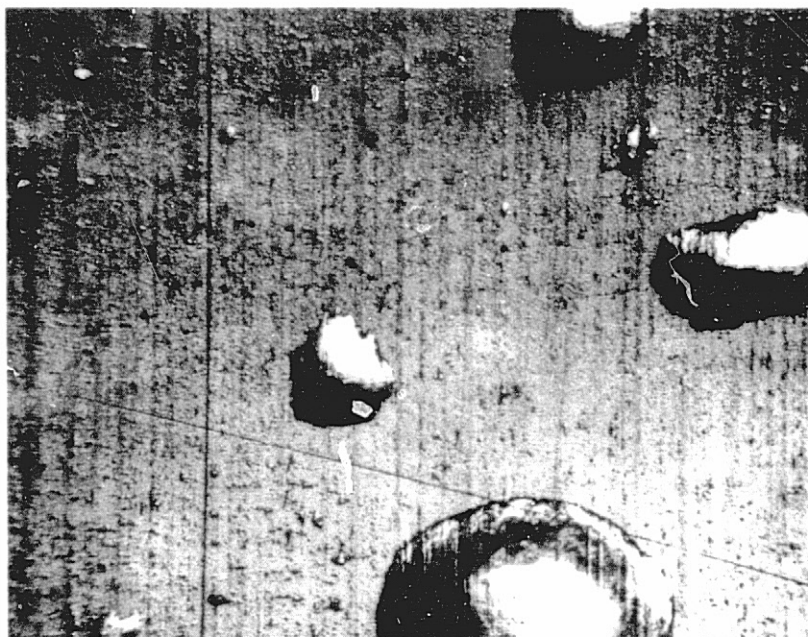
SMOOTH SIDE

— 1 mm —



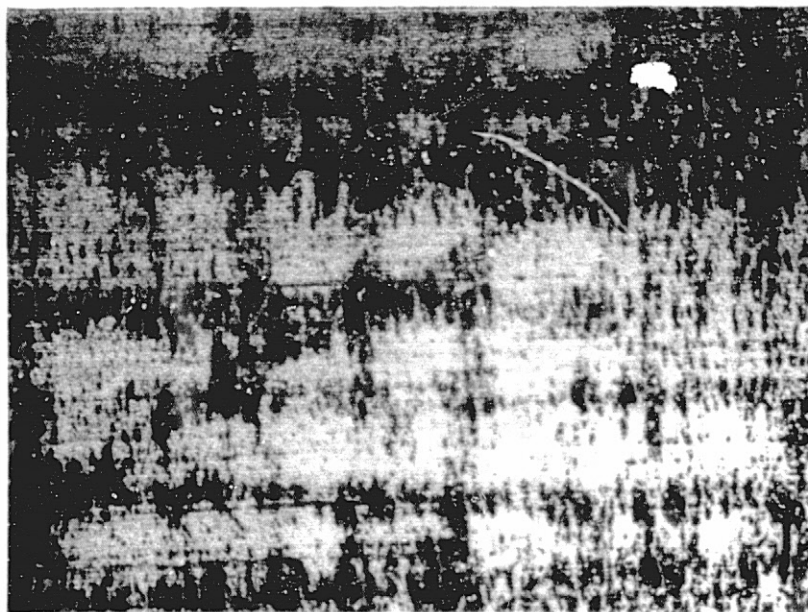
ROUGH SIDE

# ESB OF Al FOIL TO GLASS (52x)



SMOOTH SIDE

— 1 mm —

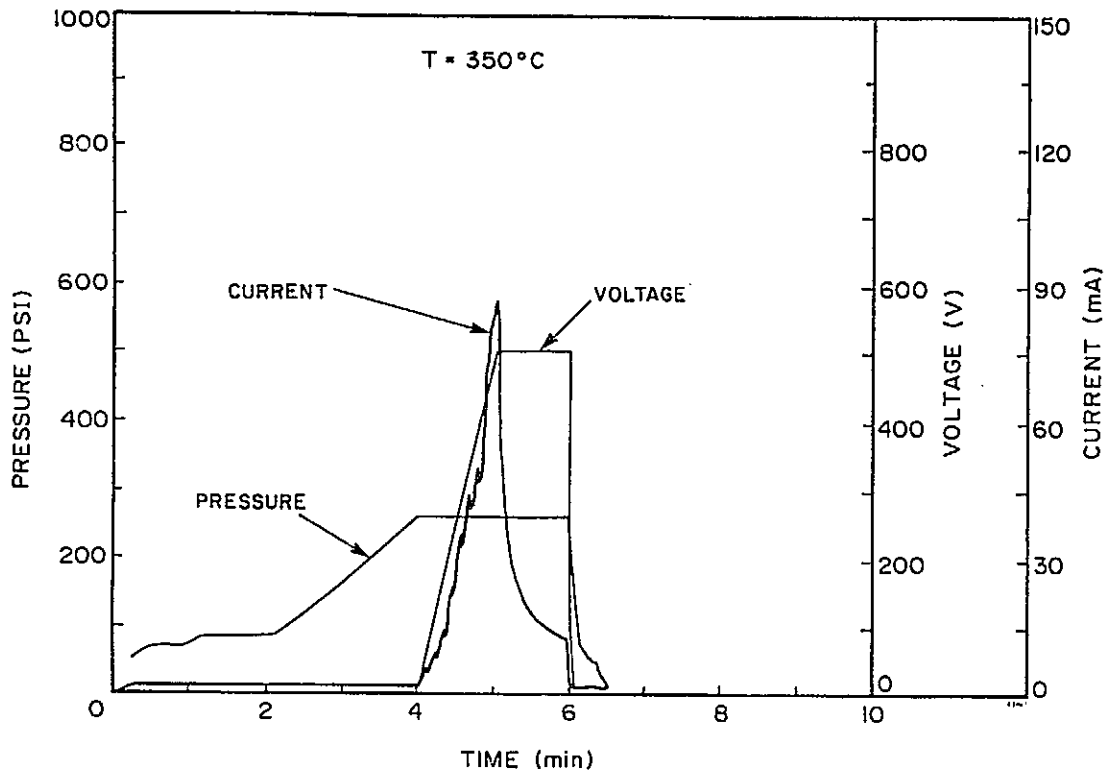


ROUGH SIDE

83011P



## ESB Cycle



## Ultrasonic Welding Development

### POWER SUPPLY

- FREQUENCY: 50 kHz
- POWER: 100 W INTO  $8\Omega$  LOAD

### WELD TIP

- ROTATING DISK FOR SEAM WELDING
- VERTICAL FORCE BY AIR CYLINDER
- TRAVERSE BY RACK AND PINION DRIVE

### OPTIMAL CONDITIONS

- ULTRASONIC POWER = 50%
- TRAVERSE SPEED = 208 cm/minute
- VERTICAL FORCE = 3.6 kg

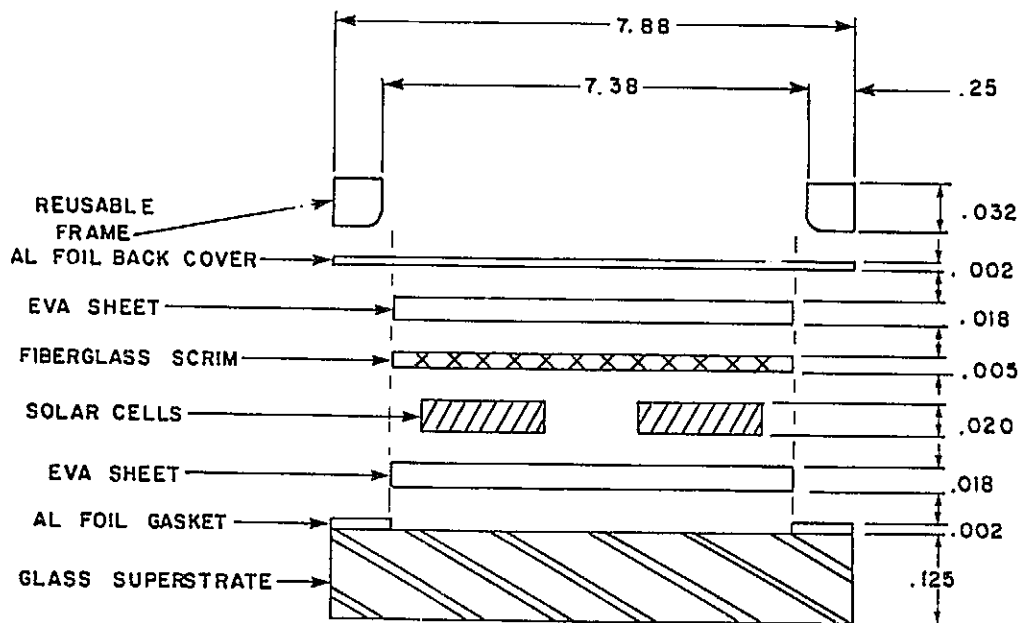
### RESULTS

- NO DAMAGE TO ESB GLASS-AI SEAL
- GOOD QUALITY WELDS
  - BOND STRENGTH > AI FOIL

## Hermetic Edge Seal Process Sequence

- ATTACH AL FOIL GASKET TO GLASS PERIMETER BY ESB
  - GLASS MUST BE SMOOTH ( $\sim 1 \mu\text{m}$ ) AT PERIMETER
- ENCAPSULATE MODULE USING STANDARD TECHNIQUES
  - LAMINATION OR CASTING
  - INSIDE OF MODULE BACK COVER IS AL FOIL AT PERIMETER
- ATTACH AL BACK COVER TO AL GASKET BY ULTRASONIC SEAM WELDING

## Module Encapsulation Assembly



## Leak Testing

MIL-STD-883B, METHOD 1014.4, SEAL

## NONDESTRUCTIVE TEST FOR HERMETICALLY SEALED PACKAGES

## ● FINE LEAK - HELIUM

- 60 PSIG He FOR 2 HOURS
- MASS SPECTROMETER LEAK DETECTOR

S/N	LEAK RATE, R <sub>1</sub> (10 <sup>-7</sup> atm cc/sec He)	
01	21	} GROSS LEAKS LATER DETECTED
02	27	
04	55	
05	49	
07	22	
08	32	
09	51	
10	23	
11	27	} NO GROSS LEAKS DETECTED
26	2.8	

## ● GROSS LEAK - FLUOROCARBON

- 60 PSIG DETECTOR FLUID FC-72 (3M)  
FOR 2 HOURS
- 0 PSIG, 125°C INDICATOR FLUID FC-40 (3M)

OBSERVE BUBBLES OF GASEOUS FC-72

- IDENTIFY SOURCE OF LEAKS
- MODIFY SEALING PROCESS

## Conclusions

ESB TECHNIQUE DEVELOPED IN AIR FOR  
SEALING AI FOIL TO GLASS

- BOND STRONGER THAN AI FOIL

ULTRASONIC WELDING TECHNIQUE DEVELOPED FOR  
SEALING BACK COVER FOIL TO GASKET FOIL

- NO DEGRADATION OF ESB SEAL

SAMPLE MODULES

- FABRICATED
- LEAK TESTED

HERMETIC SEALING PROVEN FEASIBLE

FUTURE RESEARCH RECOMMENDATIONS

- ROTATING DISK ELECTRODE ESB
  - NECESSARY FOR LARGE ( $M^2$ ) AREAS
  - INSENSITIVE TO GLASS THICKNESS VARIATIONS AND WAVES
  - INDEPENDENT OF GLASS SIZE
  - ELIMINATE TRAPPED AIR (SMOOTH FOILS)
    - BOND FRONT
    - HIGH PRESSURE
  - SHALLOW ZONE HEATING
    - REDUCE ENERGY CONSUMPTION
    - ELIMINATE GASKET

# SMUD HOT-SPOT TEST RESULTS

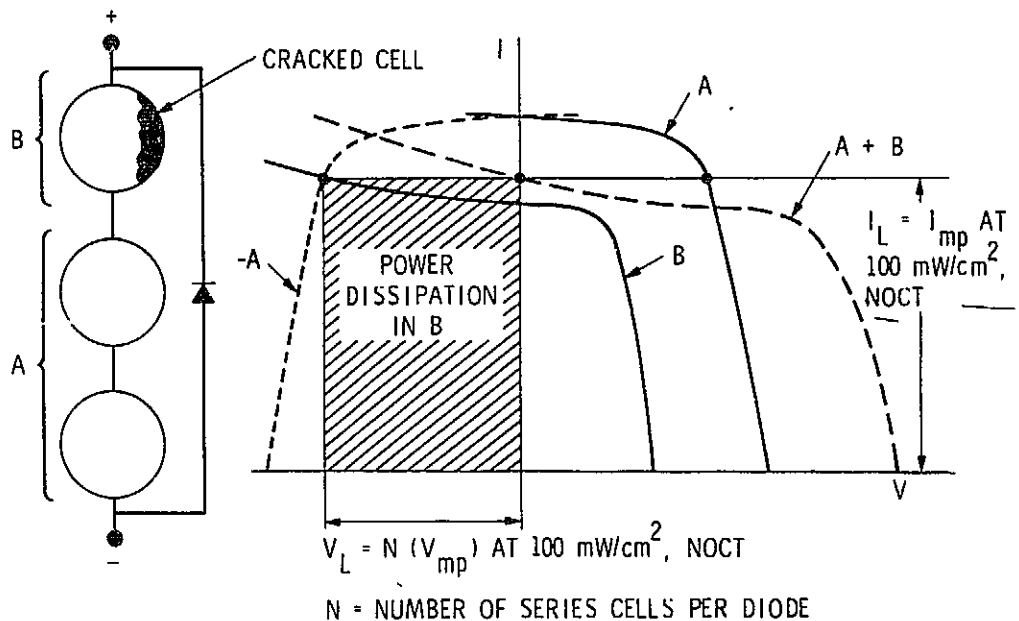
JET PROPULSION LABORATORY

C.C. Gonzalez

## Background

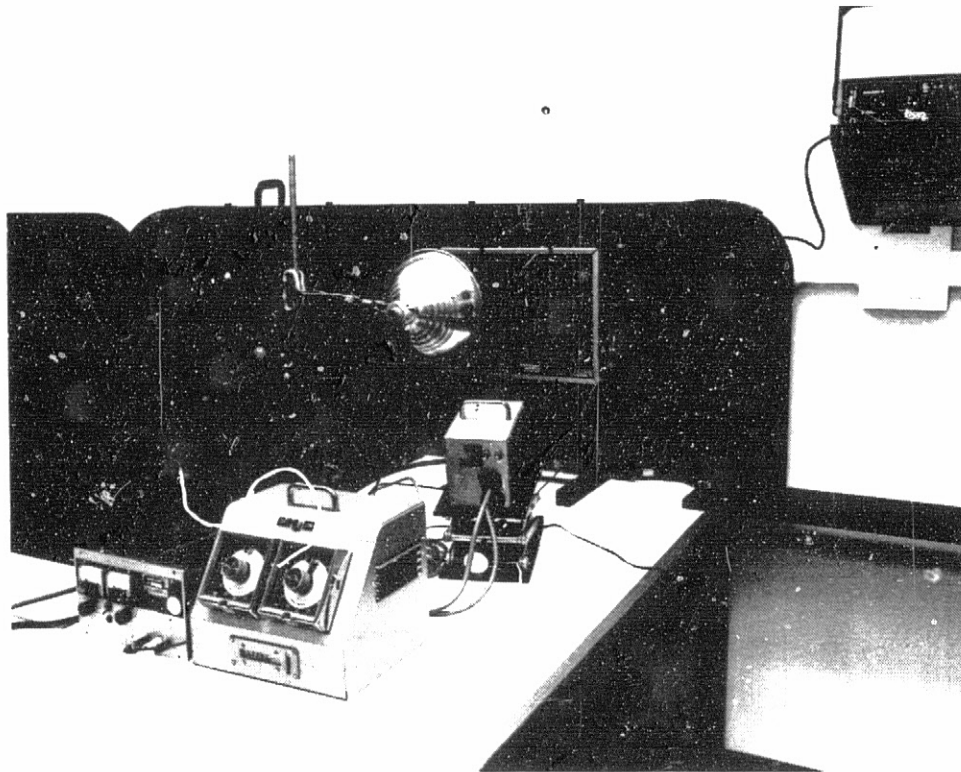
- Cells whose short-circuit current is below applied source-circuit current go into reverse voltage (back bias)
- Causes of low short-circuit current are:
  - Cracked cells
  - Shadowed cells
  - Open interconnects
- Back-biased cells absorb power equivalent to product of cell current and back-bias voltage
- Modules can suffer permanent damage such as cell cracking, cell shorting and encapsulation delamination

## Selection of Test Voltage and Current for Type A Cell

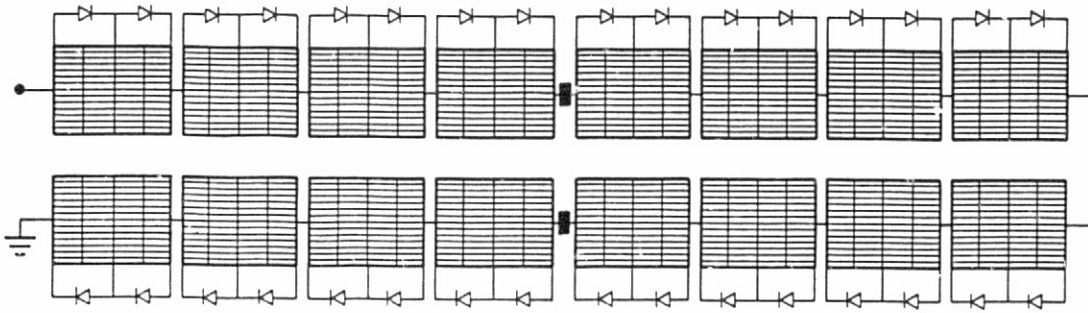


## Hot-Spot Test

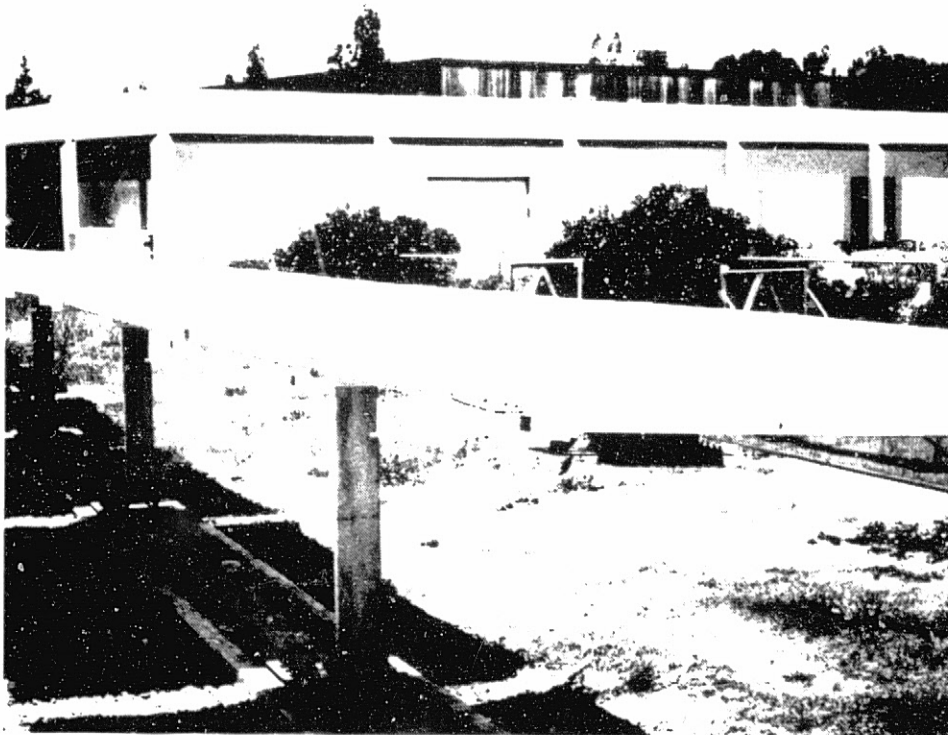
- Laboratory test developed to determine hot-spot susceptibility of modules
  - Key features:
    - Applied test current equivalent to cell short circuit current
    - Applied back-bias voltage determined by bypass diode frequency
    - Thermal boundary conditions for 100 mW/cm<sup>2</sup>, 40°C ambient
    - 100 hours test duration



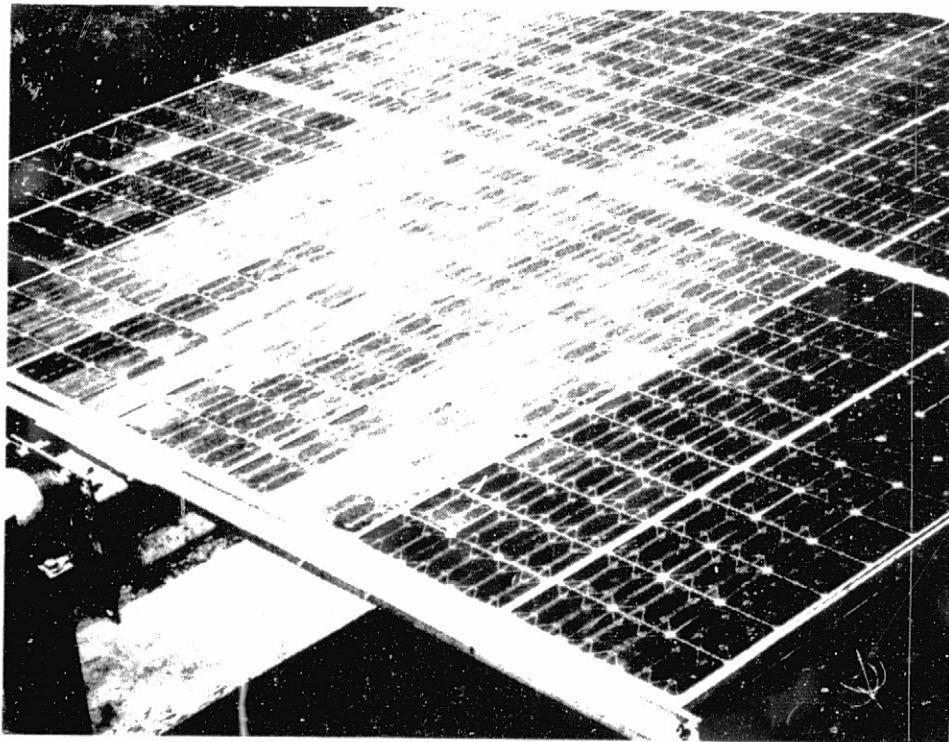
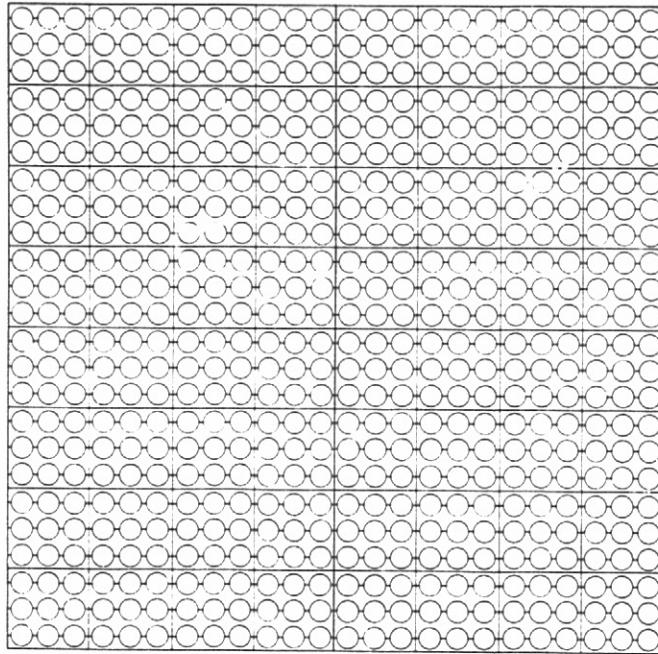
## SMUD Source-Circuit Electrical Configuration



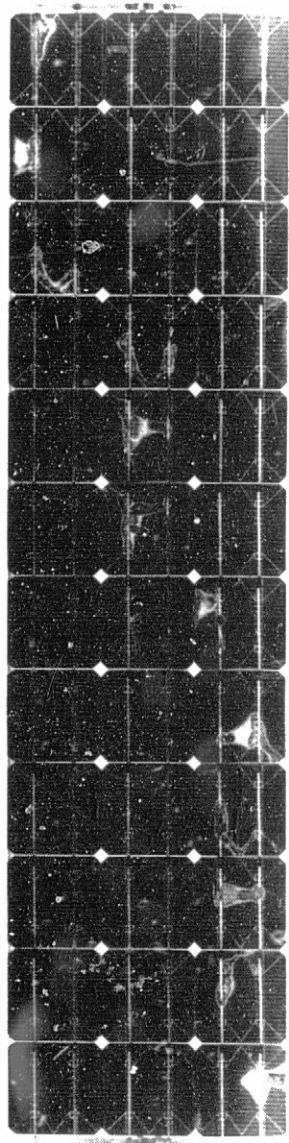
Source Circuit: 2 arrays  
16 panels  
64 series blocks (modules)  
24 cells in parallel  
12 cells per substring  
Approx. 21 kW at STC  
Approx. 56 A

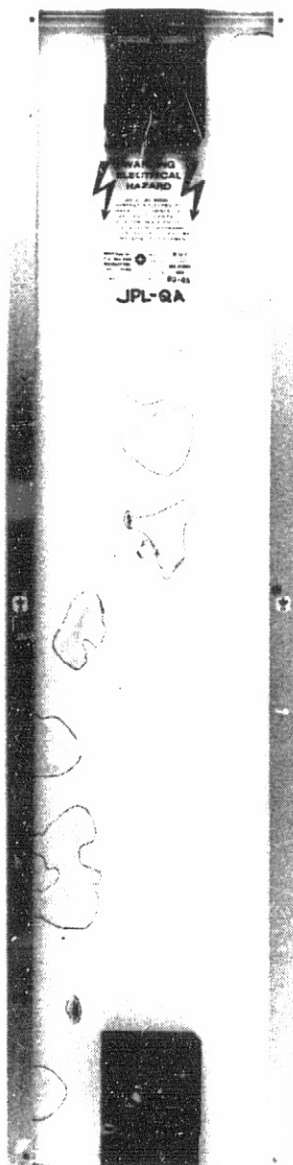


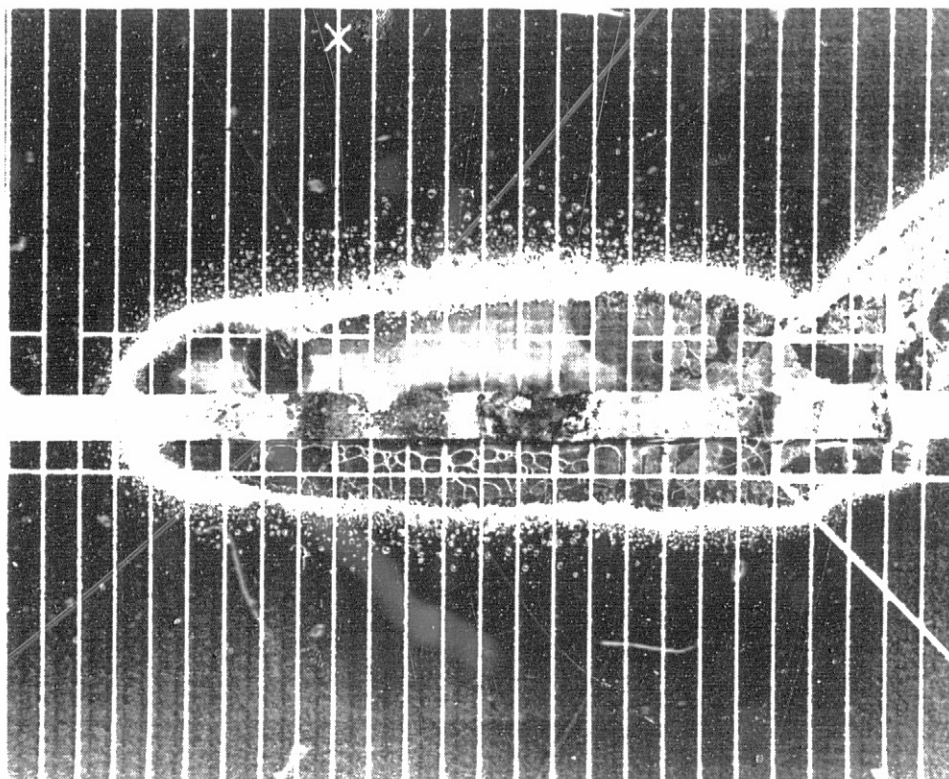
## SMUD Module and Panel Configuration

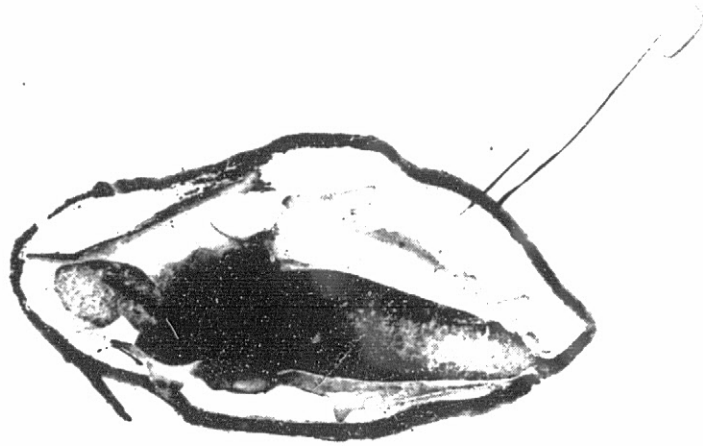




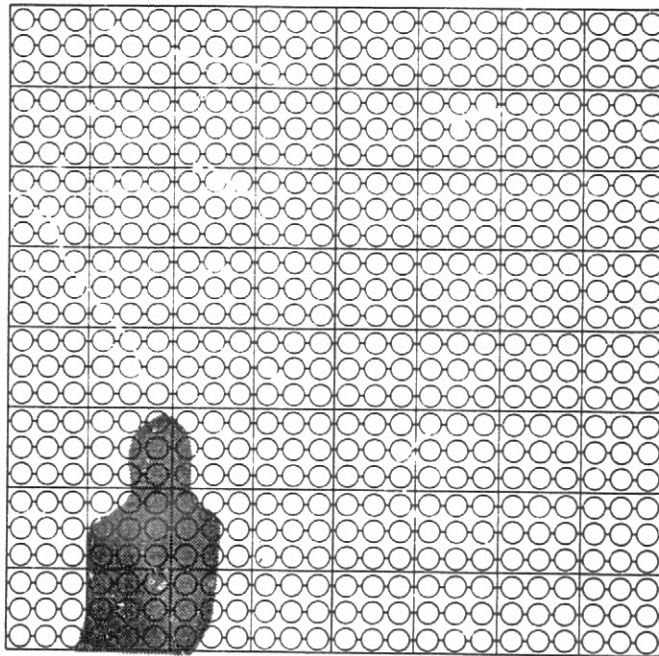




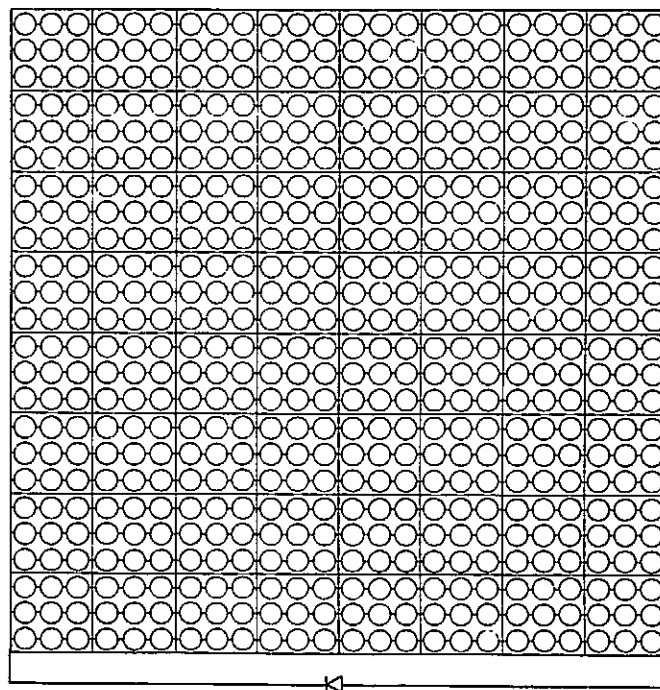




**SMUD Module and Panel Configuration:  
With Diffuse Shadow**



## SMUD Module and Panel Configuration: With Bypass Diode

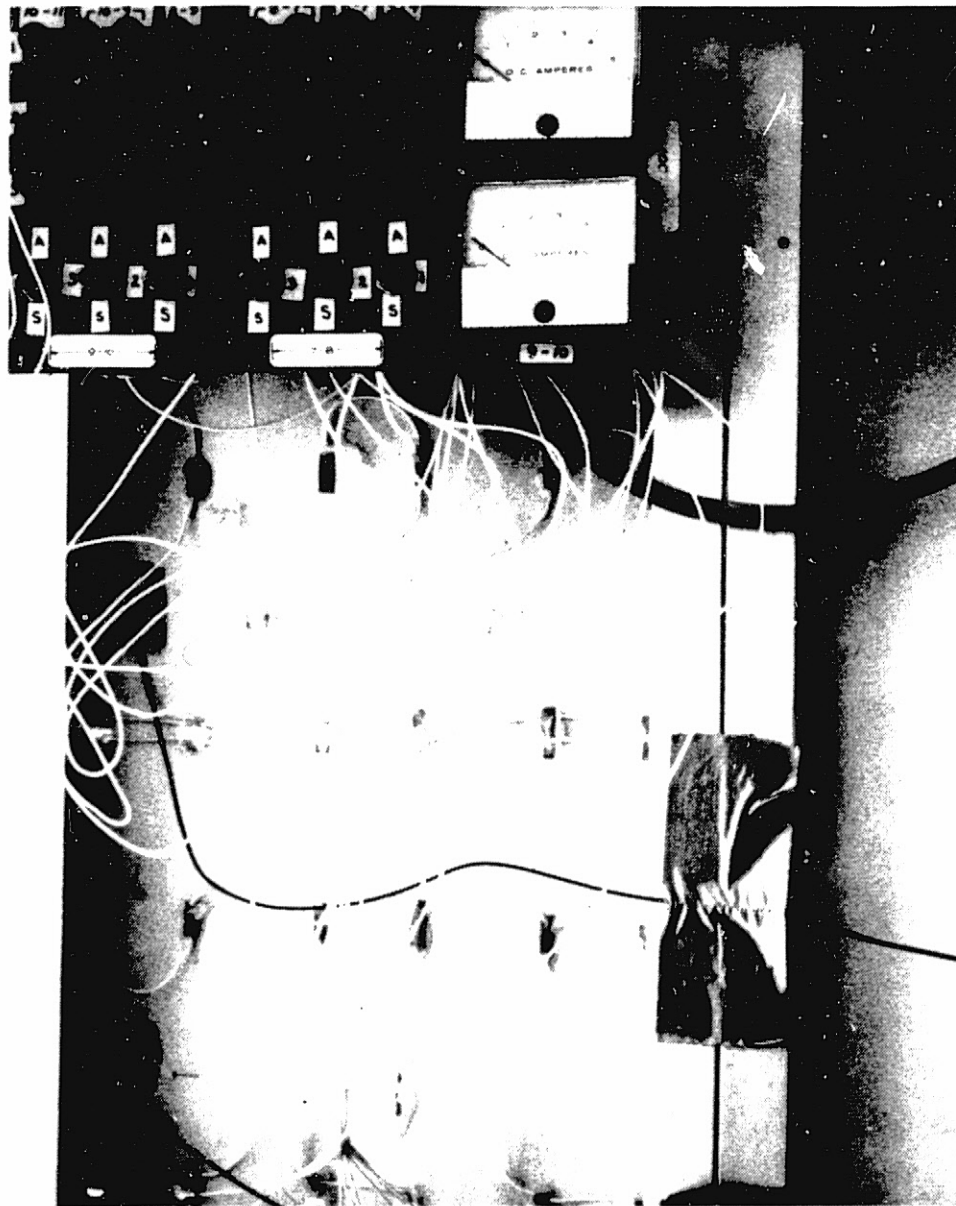


### Test Objectives

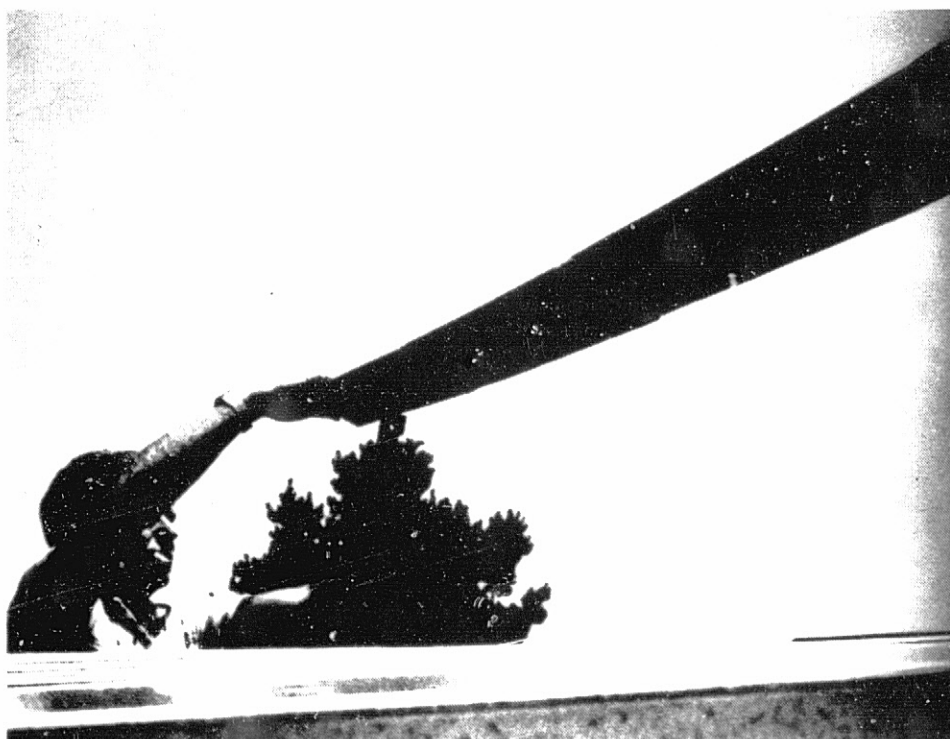
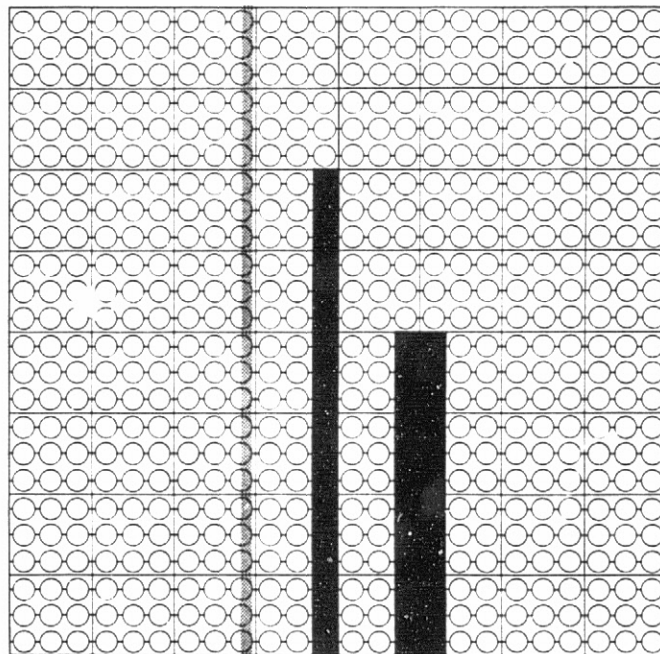
- Compare hot-spot temperatures achieved under field conditions with those obtained from present laboratory hot-spot tests
- Assess extent of current imbalance versus cross-tie frequency
- Assess effects of different shadow patterns and shadow densities

### Test Procedure

- Tests performed on verification array with bypass diodes around every two modules
  - Use of instrumented modules — number of cross ties varied
  - Measurement of cell currents and back-bias voltages
  - Use of IR camera to indicate existence of hot-spots and estimate temperature increases in conjunction with thermocouples
  - Use of shadow patterns of varying size and density



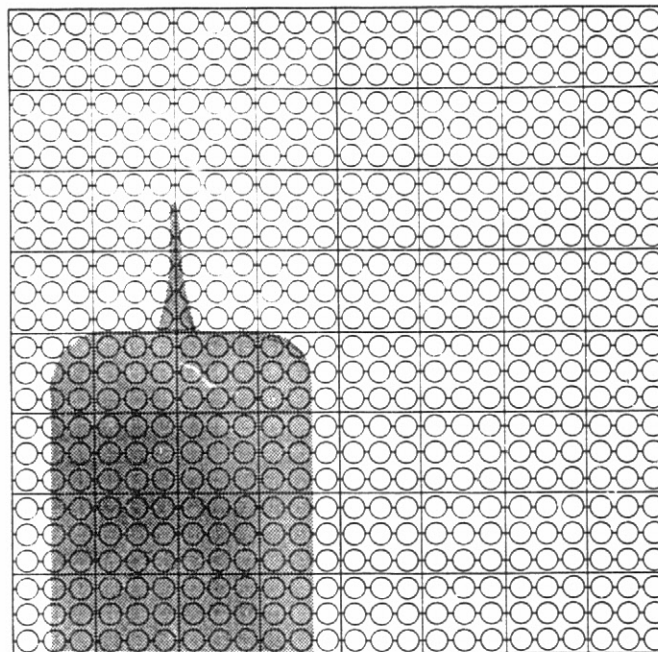
# SMUD Module and Panel Configuration: Shadow Patterns Used in Test



## Test Observations

- Sensitivity to shadow size (amount of cell coverage) and density
  - Partial cell coverage and diffuse shadows produce greatest heating for high-shunt-resistance cells; changes to full cell coverage for low shunt resistance ( $\approx 5\Omega$ )
  - Hot spots occur in shadowed area
- Occurrence of current imbalance and severe hot-spot heating noted with three or fewer cells per substring
- Hot-spot temperature in field is in general greater than in laboratory ( $150^{\circ}$ - $200^{\circ}\text{C}$ )

## SMUD Module and Panel Configuration: Actual Field Shadow





## Future Work

- Continue full-scale module tests under more controlled conditions (only two series x n parallel modules required for test because of bypass diode)
- In-depth study of types of shadows that lead to hot-spot problems
- Determine relationship for difference in increase in hot-spot temperature between parallel cell strings and single cell strings
- Determine the effect of adjacent hot cells on hot-spot temperature rise

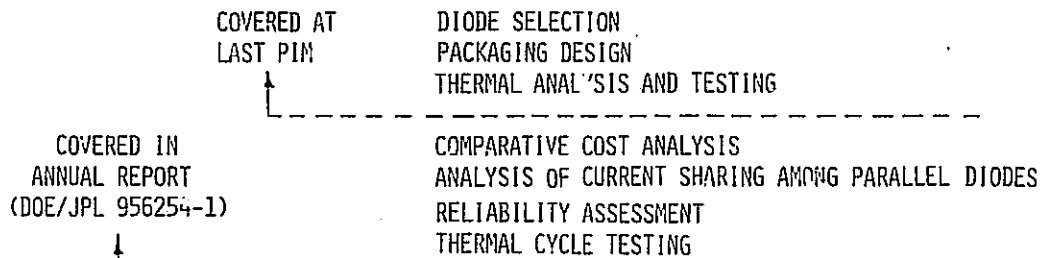
# BYPASS DIODE DESIGN TRADEOFFS

GENERAL ELECTRIC CO.

N.F. Shepard, Jr.

## Study Areas

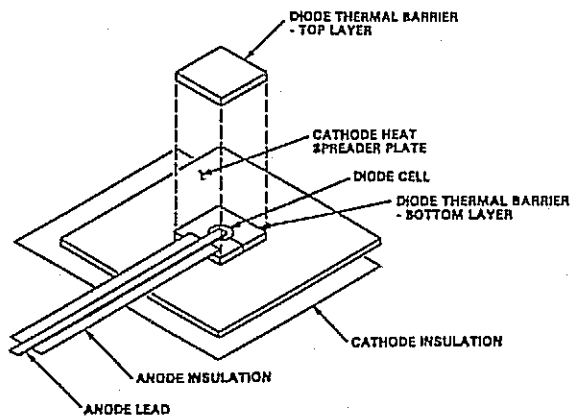
### ENCAPSULATED BYPASS DIODES (INTEGRAL WITH MODULE LAMINATE)



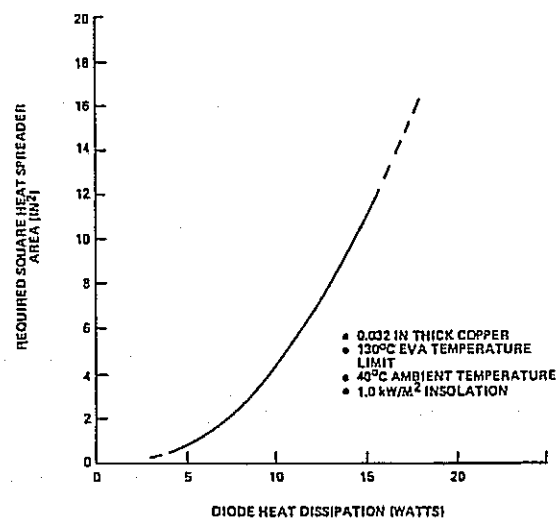
### EXTERNALLY-MOUNTED BYPASS (AND BLOCKING) DIODES

DIODE SELECTION  
PACKAGING DESIGN  
COST ANALYSIS

## Encapsulated Bypass Diodes: Packaging Concept



CONFIGURATION

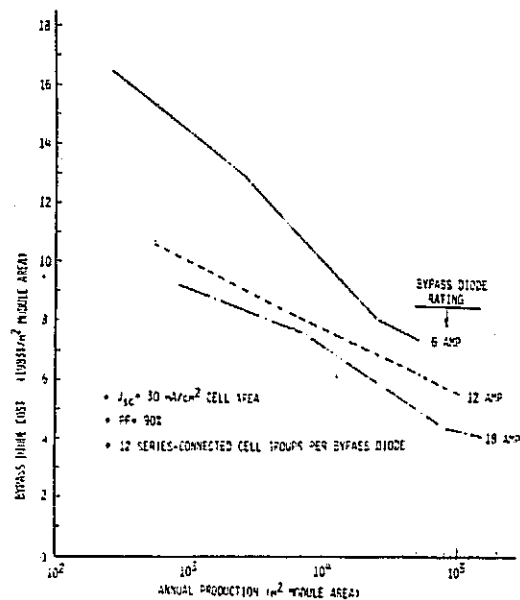


THERMAL PERFORMANCE

## Comparative Cost Analysis

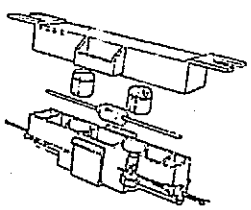
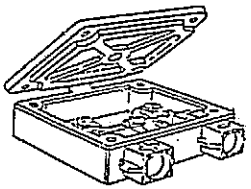
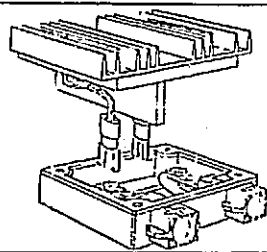
DESIGN PARAMETERS

RATED BYPASS CURRENT (AMPERES)	DIODE CELL MANUFACTURER/RATING	0.032" THICK SQUARE COPPER HEAT SPREADER PLATE SIZE (INCHES)	COPPER ANODE LEAD	
			THICKNESS (INCHES)	WIDTH (INCHES)
6	SEMICON/20 AMP	0.90	0.005	0.120
12	SEMICON/40 AMP	2.10	0.007	0.170
18	SEMICON/50 AMP	3.30	0.010	0.180

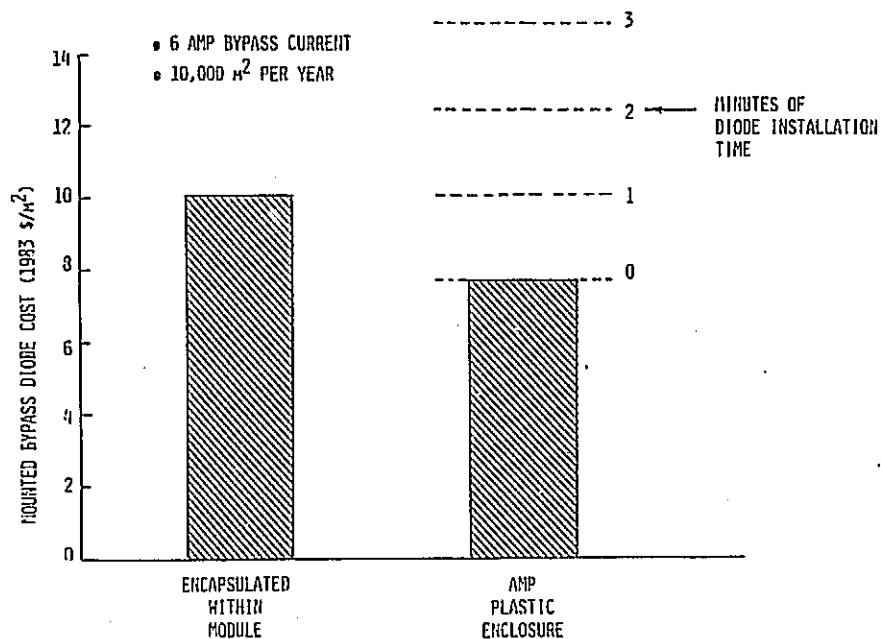


ESTIMATED FOB FACTORY PRICE

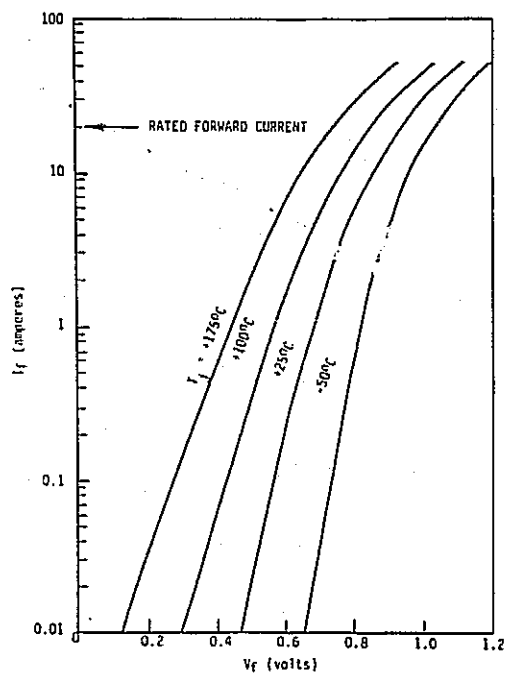
SELLING PRICE (1983\$) OF PACKAGED DIODES IN AMP INC. PLASTIC ENCLOSURES

QUANTITY	6 AMP	8 AMP	30 AMP
			
1000	2.50	3.90	7.80
5000	2.35	2.95	5.70
20000	2.15	--	--

## MODULE TECHNOLOGY

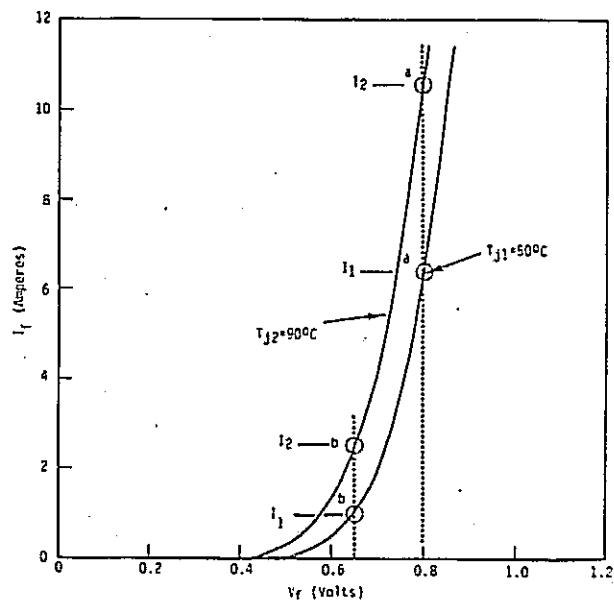
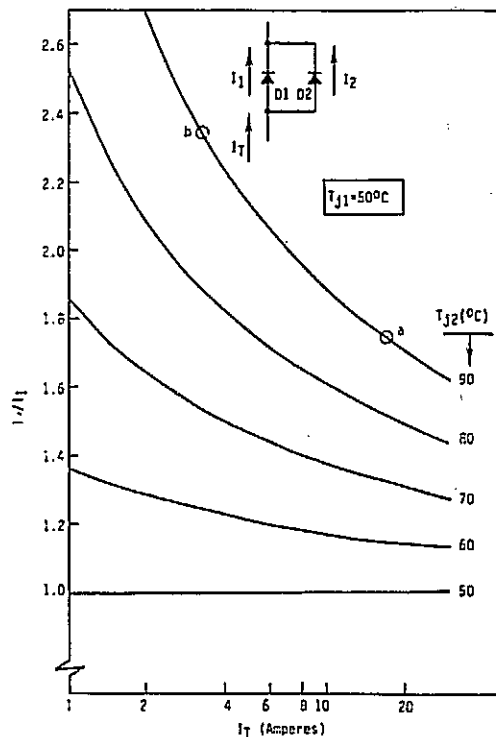


## Bypass Diode Current Sharing: Forward I-V Characteristics

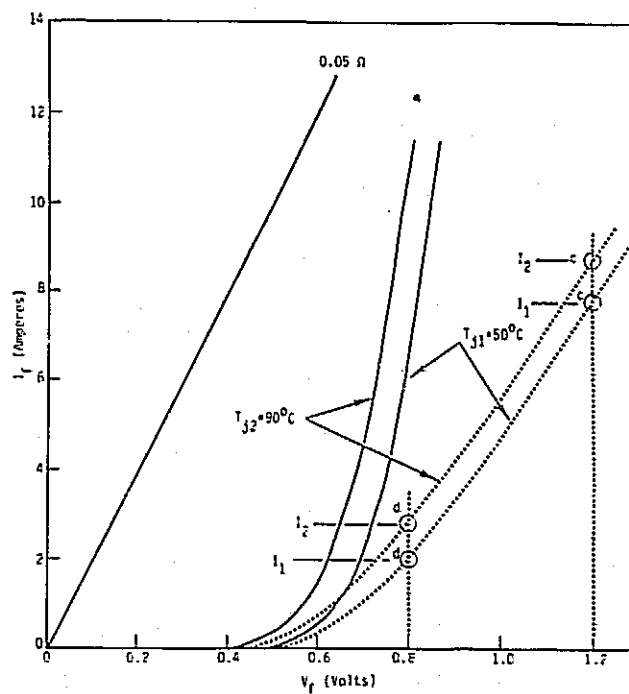
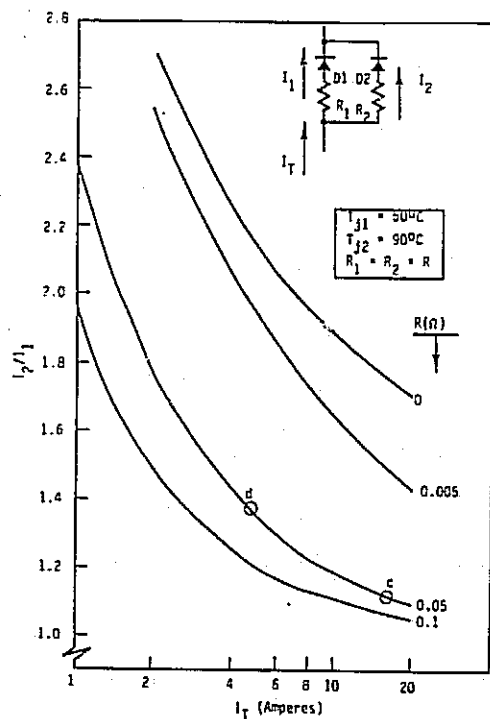


PN JUNCTION DIODE

# Bypass Diode Current Sharing: Parallel pn Diodes (Without Series Resistance)



# Bypass Diode Current Sharing: Parallel pn Diodes (With Series Resistance)



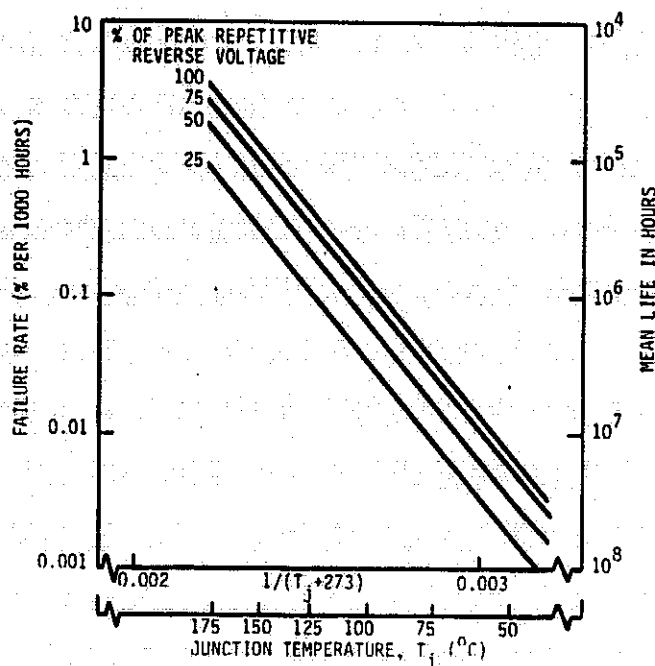
## Bypass Diode Reliability Considerations

OPERATING CONDITIONS:

- PROLONGED OPERATION WITH THE PERIODIC APPLICATION OF A LOW REVERSE VOLTAGE
- OCCASIONAL OPERATION IN A FORWARD CONDUCTION MODE

DESIGNING FOR HIGH RELIABILITY

- DERATE REVERSE VOLTAGE
- LIMIT JUNCTION TEMPERATURE TO 125°C UNDER WORST CASE FORWARD CONDUCTION CONDITIONS
  - MAXIMUM AMBIENT TEMPERATURE
  - MAXIMUM INSULATION



FAILURE RATE FOR A TYPICAL  
RECTIFYING DIODE

## Externally Mounted Diode: Requirements

### APPLICATIONS:

APPLICATION	SYSTEM VOLTAGE	SOURCE CIRCUIT CURRENT	SOURCE CIRCUIT POWER	SYSTEM POWER
RESIDENTIAL	200V	5A	1 kW	4 TO 6 kW
INDUSTRIAL	400V	25A	10 kW	100 kW
CENTRAL STATION	400V	60A	24 kW	1 TO 5 MW
CENTRAL STATION	1000V	60A	60 kW	1 TO 5 MW

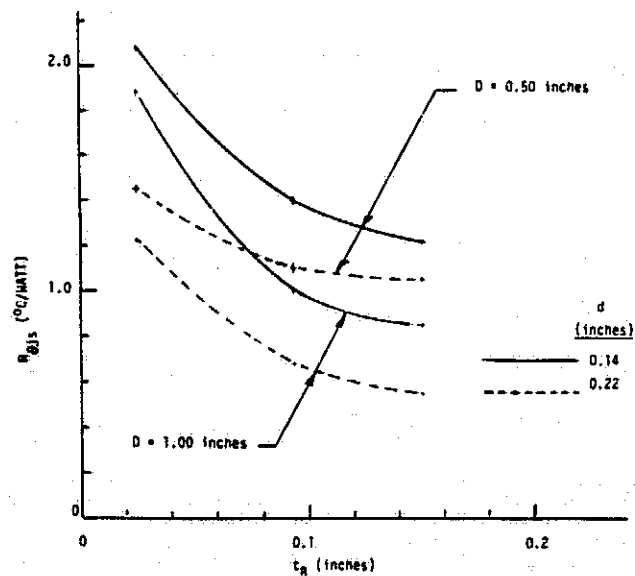
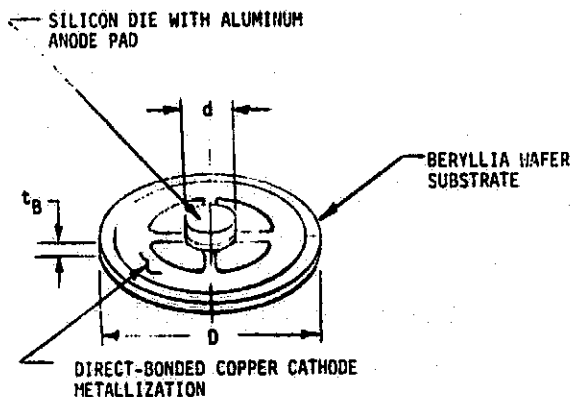
### DRIVING DESIGN REQUIREMENTS:

WITHSTANDING VOLTAGE =  $2 \times \text{SYSTEM VOLTAGE} + 1000$

LEAKAGE  $\leq 50 \mu\text{A}$

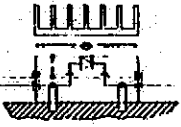
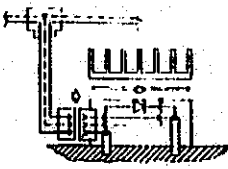
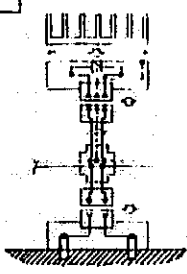
(AFTER WATER SPRAY, HUMIDITY, AND CORROSIVE  
ATMOSPHERE TESTS)

## Externally Mounted Diode: Diode Cell Mounting Approach

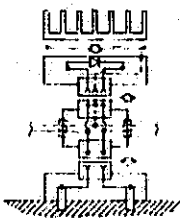
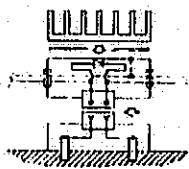
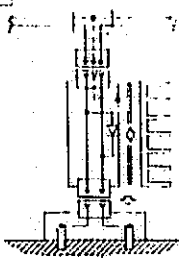


- REDUCES JUNCTION-TO-SINK THERMAL RESISTANCE
- ELIMINATES STUD PACKAGE AND ASSOCIATED MOUNTING HARDWARE
- REDUCES THERMAL STRESSES IN SOLDER JOINT BETWEEN SILICON DIE AND HEAT SPREADER
- ASSURES ADEQUATE DIELECTRIC STRENGTH

## Externally Mounted Diode: Configuration Evaluation

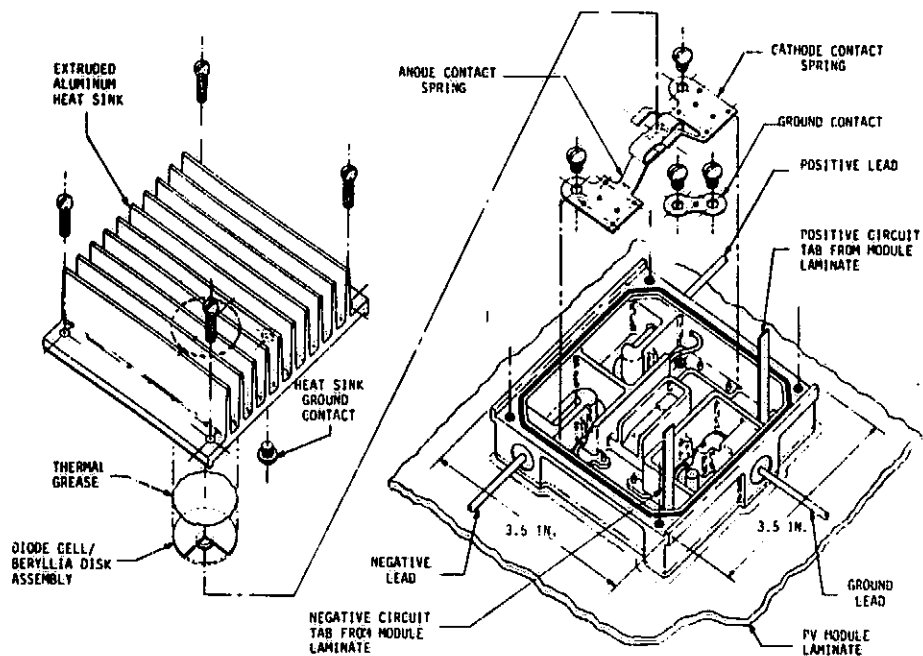
CONFIGURATION →	A	B	C
PARAMETER/CHARACTERISTIC			
NUMBER OF CONNECTION PAIRS	0	1	2
NUMBER OF SEPARABLE PARTS	1	2	4
NUMBER OF SCREW TERMINALS	4	3	3
ARCING UPON MODULE DISCONNECT	YES	YES	POSSIBLE
FIELD ASSEMBLY REQUIRED FOR INSTALLATION	3 CRIMP JOINTS	1 PLUG	2 PLUGS + DIODE MODULE MOUNTING
DIODE FIELD REPLACEMENT REQUIREMENTS	REMOVE HEAT SINK COVER AND REPLACE DIODE	REMOVE HEAT SINK COVER AND REPLACE DIODE	UNPLUG AND REPLACE DIODE/HEAT SINK MODULE
RELATIVE FACTORY COST ( $R_{FC}$ )	1*	2	4
RELATIVE INSTALLATION COST ( $R_{IC}$ )	3	1	4
RELATIVE DIODE REPLACEMENT COST ( $R_{RC}$ )	5	3	1
TOTAL RELATIVE COST $10 R_{FC} + 50 R_{IC} + \frac{1}{10} R_{RC}$	109	50	163

\* 1 = LOWEST, 4 = HIGHEST

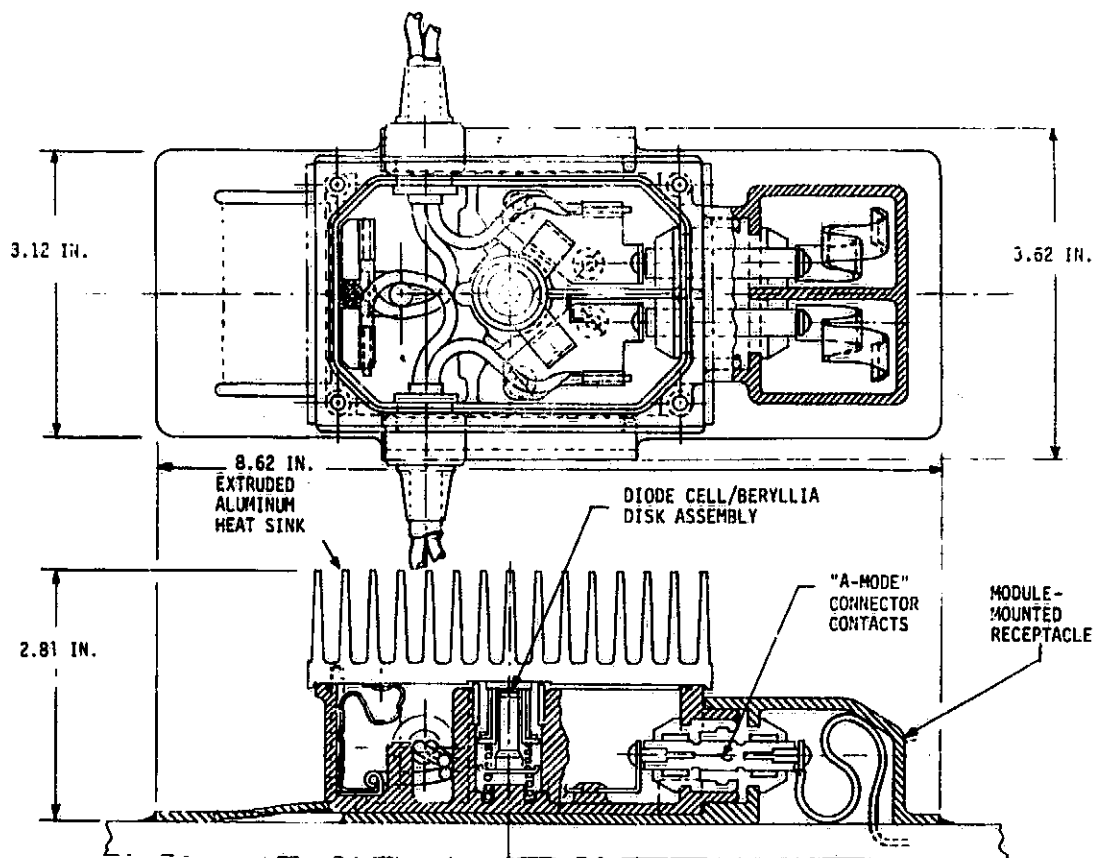
CONFIGURATION →	D	E	F
PARAMETER/CHARACTERISTIC			
NUMBER OF CONNECTION PAIRS	2	1	2
NUMBER OF SEPARABLE PARTS	1	2	4
NUMBER OF SCREW TERMINALS	4	4	4
ARCING UPON MODULE DISCONNECT	POSSIBLE	NO	POSSIBLE
FIELD ASSEMBLY REQUIRED FOR INSTALLATION	2 PLUGS	1 PLUG	2 PLUGS
DIODE FIELD REPLACEMENT REQUIREMENTS	UNPLUG AND REPLACE DIODE/HEAT SINK MODULE	REMOVE HEAT SINK COVER AND REPLACE DIODE	UNPLUG AND REPLACE DIODE/HEAT SINK MODULE
RELATIVE FACTORY COST ( $R_{FC}$ )	3	2	3
RELATIVE INSTALLATION COST ( $R_{IC}$ )	2	1	2
RELATIVE DIODE REPLACEMENT COST ( $R_{RC}$ )	1	3	2
TOTAL RELATIVE COST $10 R_{FC} + 50 R_{IC} + \frac{1}{10} R_{RC}$	45	50	96



## Externally Mounted Diode: Junction-Box Packaging



## Externally Mounted Diode: Harness Connector Packaging



## Conclusions

- IF THE MODULE DESIGN DICTATES MULTIPLE BYPASS DIODES, THE MODULE DESIGNER SHOULD
  - USE AN INTERNALLY ENCAPSULATED PACKAGING APPROACH WITH PN JUNCTION DIODE CELLS
  
- FOR ALL OTHER CASES WHERE BYPASS DIODES ARE INDICATED, THE ARRAY DESIGNER SHOULD
  - PACKAGE THE BYPASS DIODE INTEGRAL WITH THE MODULE CONNECT MEANS ON THE HARNESS SIDE OF THE MODULE CONNECTOR INTERFACE
    - AVOID PARALLEL MODULE CONNECTIONS WITHIN A SOURCE CIRCUIT
  - USE UNPACKAGED PN JUNCTION DIODE CELLS MOUNTED TO BeO HEAT SPREADERS
  - LIMIT BYPASS CIRCUIT CURRENT TO 25 AMPERES

# **BYPASS DIODE QUALIFICATION TEST DEVELOPMENT**

## **JET PROPULSION LABORATORY**

**D.H. Otth**

### **Objective**

- **Define design criteria for bypass diodes to ensure acceptable field reliability**
- **Develop a qualification test for assessing conformance to design criteria**
  - **Diodes integral with modules**
  - **Externally mounted diodes**

### **Approach**

- **Define design criteria in terms of maximum diode junction temperature under worst-case field conditions of 100 mW/cm<sup>2</sup>, 40°C air temperature and 1.0 I<sub>SC</sub> under these conditions**
  - **Addresses diode maximum current adequacy**
  - **Addresses heat-sink adequacy**
- **Develop test to determine diode junction temperature in situ using readily available laboratory test instruments**
  - **Use diode forward-voltage drop versus temperature to sense junction temperature**
  - **Extrapolate temperature to 100 mW/cm<sup>2</sup>, 40°C field thermal conditions from laboratory temperature using NOCT relationships**

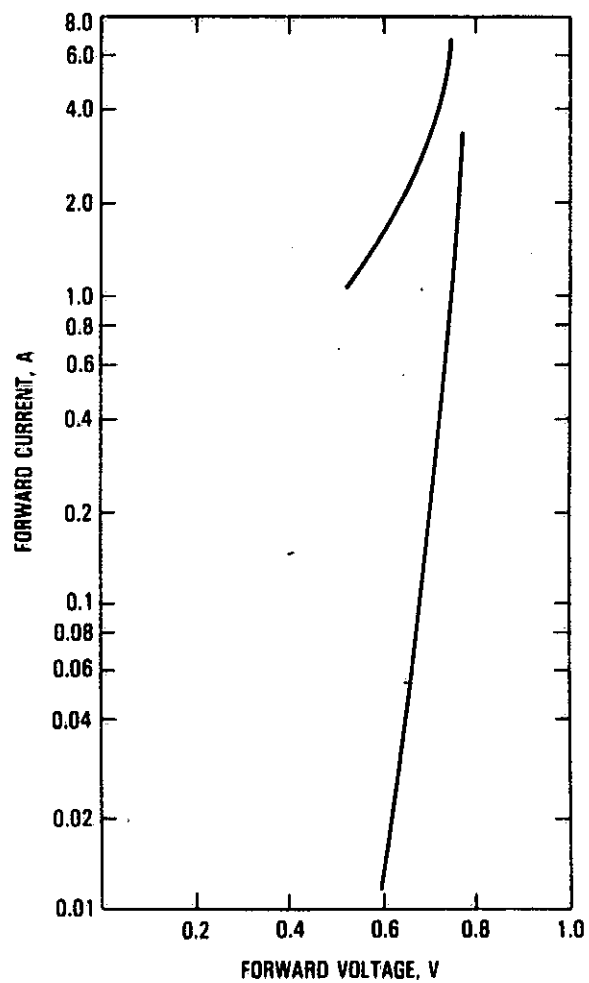
## Design Criteria

- **Published diode junction allowables**

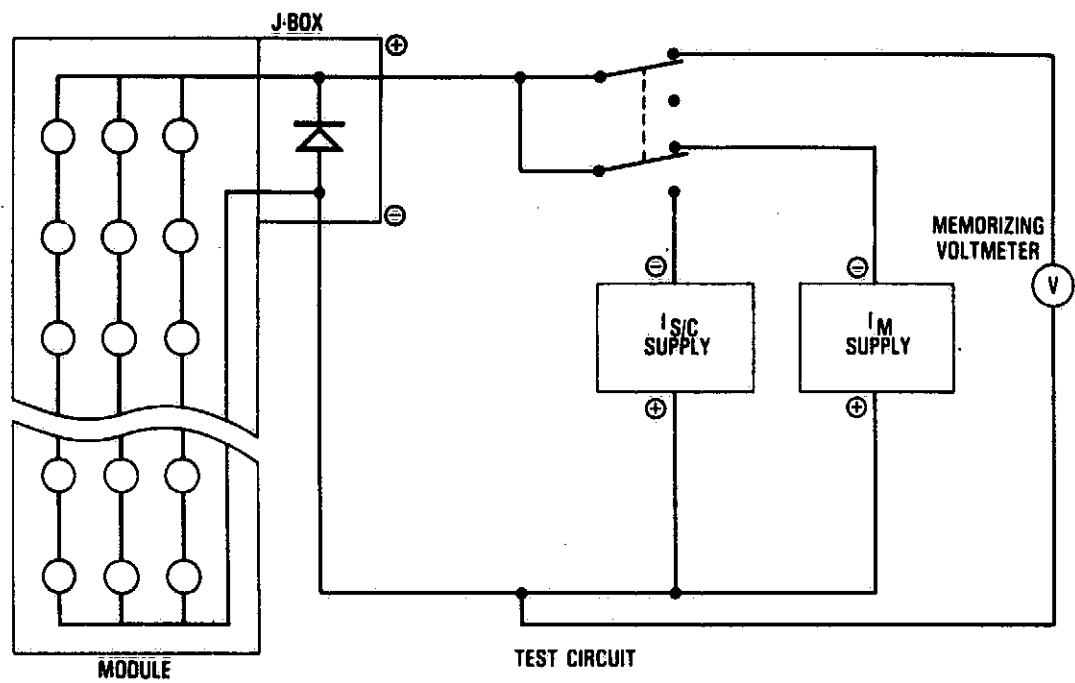
Diode Type	Maximum Allowable Junction Temperature	Derated Temperature for Long-Term Reliability
p-n	175°C	125°C
Schottky	125°C	75°C

- **Maximum allowable junction temperature not to be exceeded under conditions of 100 mW/cm<sup>2</sup>, 40°C ambient, 1.5 I<sub>SC</sub>**
- **Derated junction temperature not to be exceeded under conditions of 100 mW/cm<sup>2</sup>, 40°C ambient, 1.0 I<sub>SC</sub>**

### Typical p-n Diode Curve



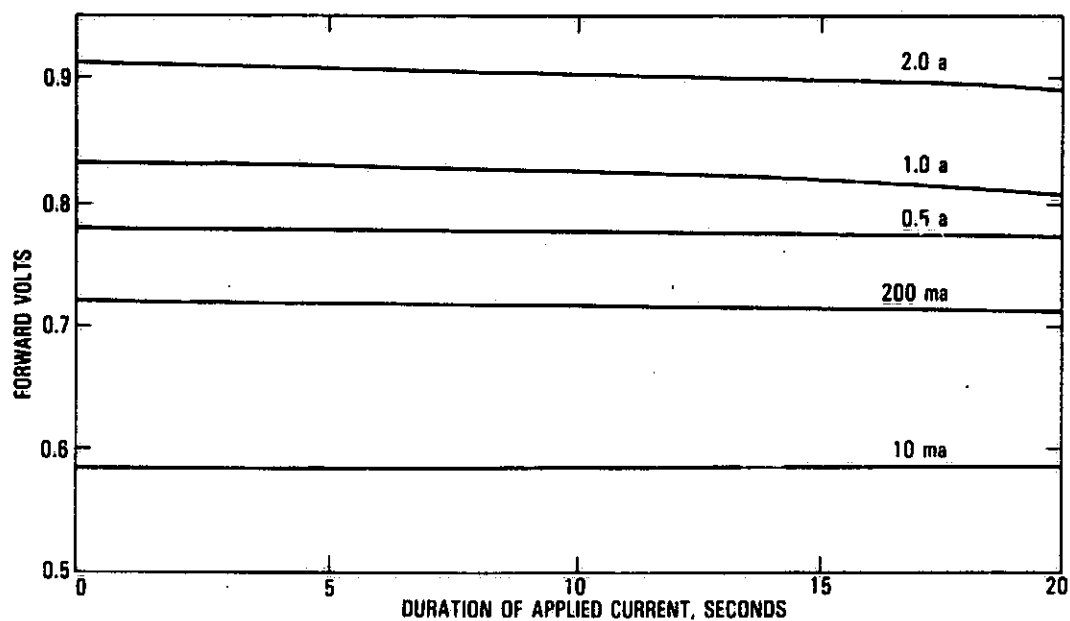
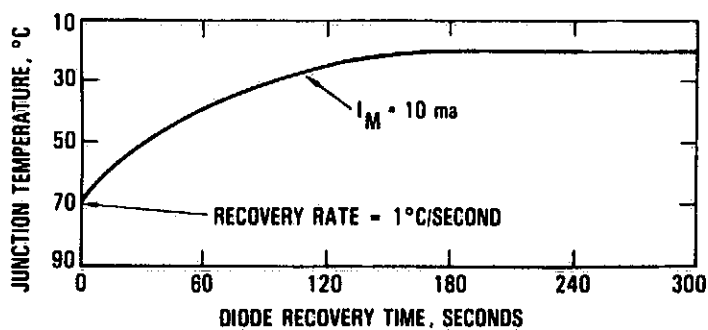
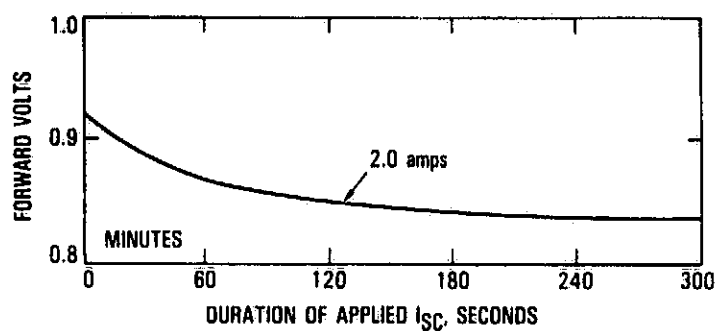
Test Circuit for Measuring Bypass Diode  
Junction Temperature

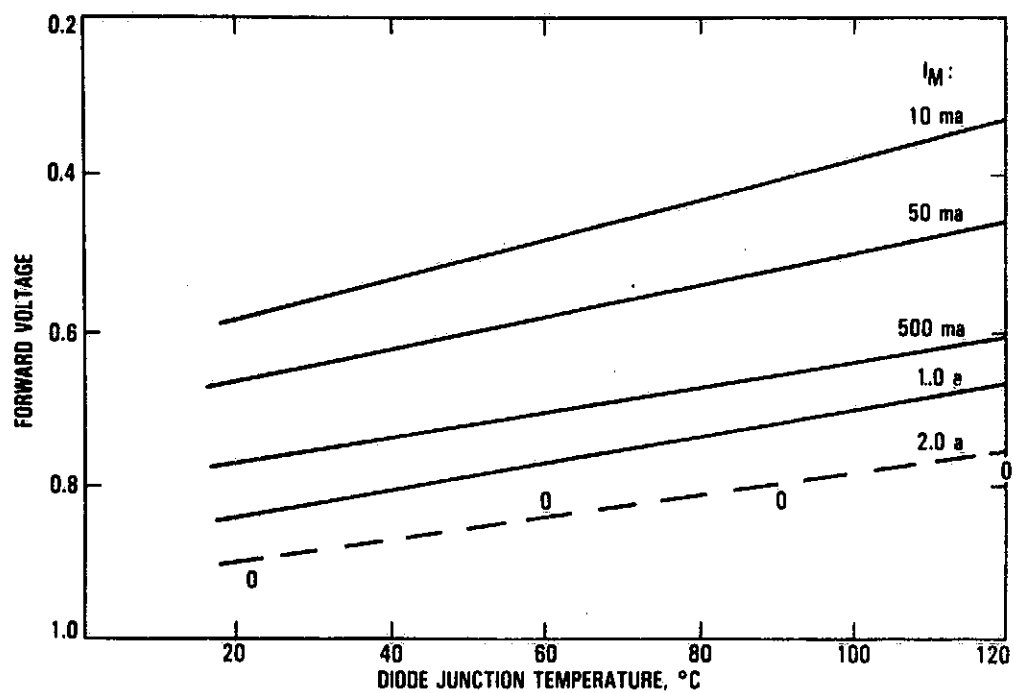


Leakage Current Test

Results

Reverse Volts	Module Type					
	1			2		
	I (μa)			I (ma)		
	Cover	W/O Cover	¼ in. Tilt	Cover	W/O Cover	¼ in. Tilt
0.5	81.7	81.7	82.2	0.57	0.57	0.59
0.6	—	—	—	0.68	0.68	0.72
0.7	113.4	113.4	113.7	0.79	0.79	0.83
0.8	129.3	129.3	129.6	0.91	0.91	0.94
0.9	144.5	144.5	145.6	1.02	1.02	1.05
1.0	160.6	160.6	163.5	1.13	1.13	1.18

**p-n Diode Response to  $I_M$  Currents****Diode Response to Applied  $I_{SC}$  and  $I_M$  Currents**

**p-n Diode Junction Temperature versus Voltage**



## Test Procedure

- Determine diode forward voltage drop versus junction temperature at a chosen measurement current ( $I_M$ )
  - Use three oven temperatures  
25°C, 60°C, 90°C
  - $I_M$  value is selected to provide good linear response with temperature (e.g., without heating junction significantly) and two orders of magnitude above module leakage current (without diode) in dark
- Apply test current ( $I_{S/C}$  at 100 mW/cm<sup>2</sup>) to module in dark at room temperature environment until diode reaches thermal equilibrium (1/2 hour)
- Instantaneously (<1/2 sec) apply  $I_M$  and measure diode forward voltage drop
- Determine diode junction temperature ( $T_j$ ) by extrapolating 25°C – 60°C – 90°C data
- Calculate qualification junction temperature ( $T_{jq}$ ) from:

$$T_{jq} = T_j + 1.25(\text{NOCT}) + T_{\text{room}} - 15^\circ\text{C}$$

## Sample Test

Module $I_{S/C}$ @ 100 mW/cm <sup>2</sup>	$I_M$	V	$T_j$ 1	$T_{jq}$ 2
2.0 amps	10.0 ma	0.46V	69°C	126.5°C

1  $T_j$  – Diode Junction Temperature in room environment

2  $T_{jq}$  – Diode Junction Temperature for module in 40°C ambient and 100 mW/cm<sup>2</sup> illumination

## Plans

- Develop details for extrapolating measured temperature to 100 mW/cm<sup>2</sup>, 40°C field conditions
- Address test procedure for modules containing multiple diodes
- Work with manufacturers in arriving at final criteria and tests
  - Invite comments
  - Invite modules for trial testing

# THERMAL INVESTIGATION OF RESIDENTIAL PHOTOVOLTAIC ARRAYS

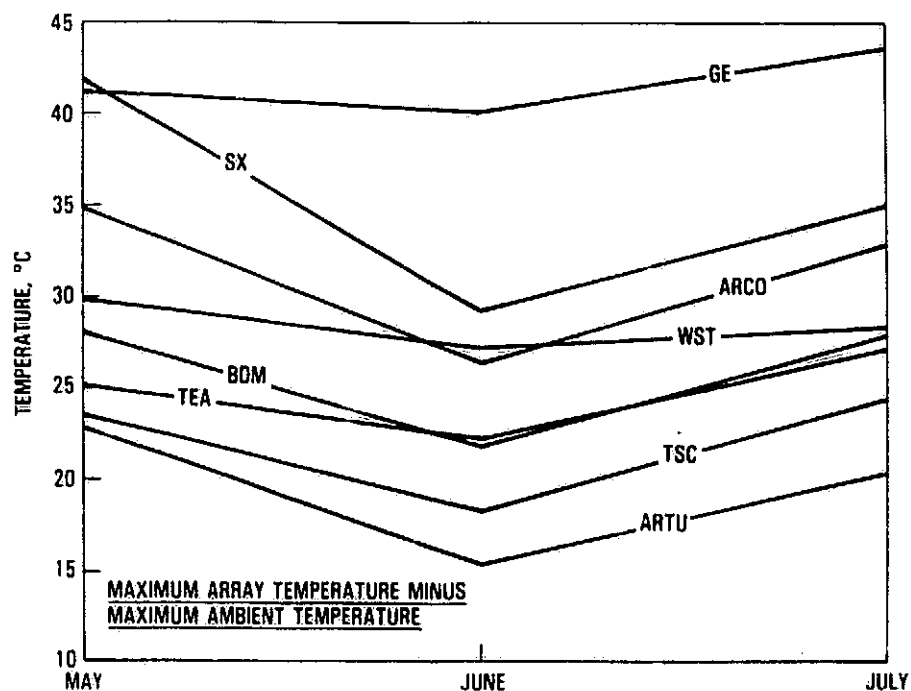
JET PROPULSION LABORATORY

L. Wen

## Concerns

- Observation of unexpected large temperature differences among southwest residential experiment station (SW RES) arrays
- Effects of cell temperature on array lifetime and performance

## SW RES



## Study Objectives

- Generic understanding of relative merits of alternative array concepts
  - RES arrays
  - Other candidate concepts
- To generate generic recommendations relative to array thermal features (sensitivities)
- To provide algorithms for predicting temperatures of various RES array design options
  - Detailed (transient simulation)
  - Simplified (for system trade-off)
  - ASHRAE-type design guide (annual performance)

## Factors Affecting Array Thermal Performance

- Module thermal characteristics
- Boundary conditions
  - Solar irradiance
  - Ambient temperature
  - Ground reflection and radiation
  - Sky radiation
  - Wind convection
- Design parameters
  - Insulation
  - Air ventilation

## SW RES Prototype Systems

Mounting Technique  Module Type				
	Direct	Rack	Integral	Stand-Off
Motorola		TEA		BDM
ARCO Res	ARCO			
GE Shingle	GE			
ARCO ASI			WST	ARTU
ASEC			TriSolar	
Solarex				Solarex

## Study Approach

- Use SW RES prototypes as test beds
- Develop detailed thermal network models
- Calibrate model and boundary parameters
- Validate/correct design variables by comparing transient simulation with test data
- Exercise resultant models to normalize comparisons and perform sensitivity studies
  - Generic understanding of underlying parameters
  - Sensitivity of thermal features

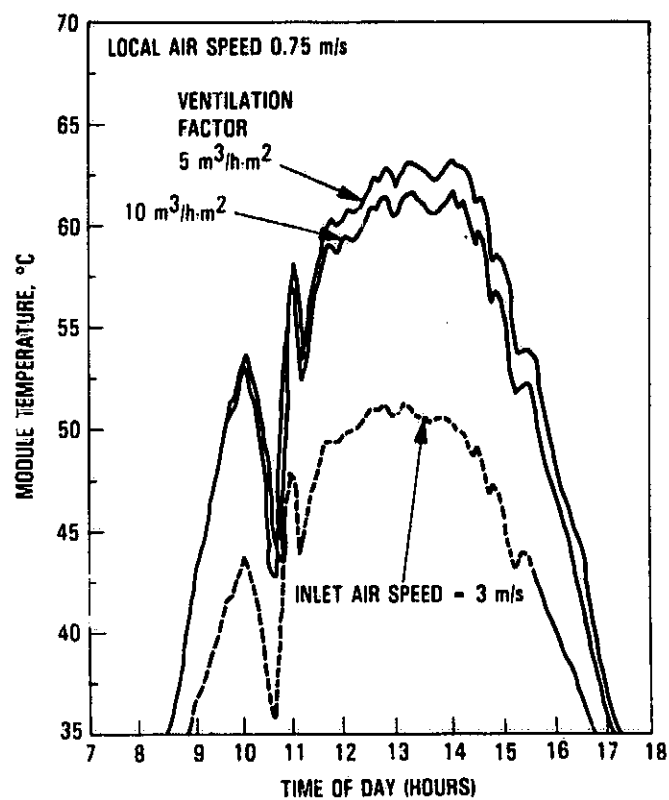
## Simulation Methodology

- Thermal analyzer – SINDA
- Nodal network models
  - Materials and dimensions
  - Thermal-optical measurements (TRW)
  - Heat transfer correlations (earlier studies)
- Boundary conditions: 2 representative days
  - Pyranometers on tilted roofs
  - Wind condition at 30-ft post
  - Ambient temperature
  - Power conversion
- Test data
  - Measured cell and substrate temperature

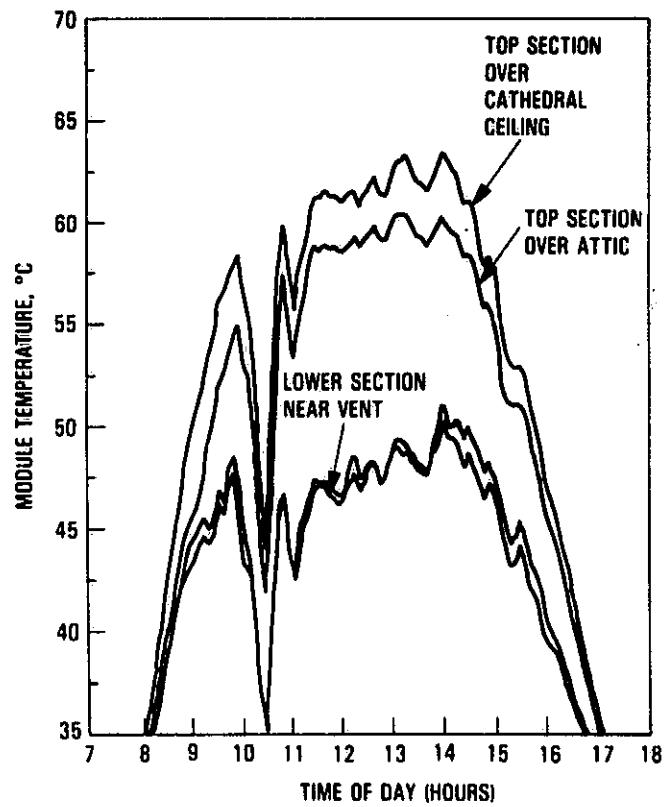
## Calibration and Validation

- Calibration
  - Using GE prototype as baseline to verify the assumed models for wind profile and convection
- Model parameter adjustments
  - All prototypes
  - Iterate simulation variables to match test data
  - Local air speed
  - Ventilation factor

## Simulated Temperature Profiles for Westinghouse Prototype on Day 268

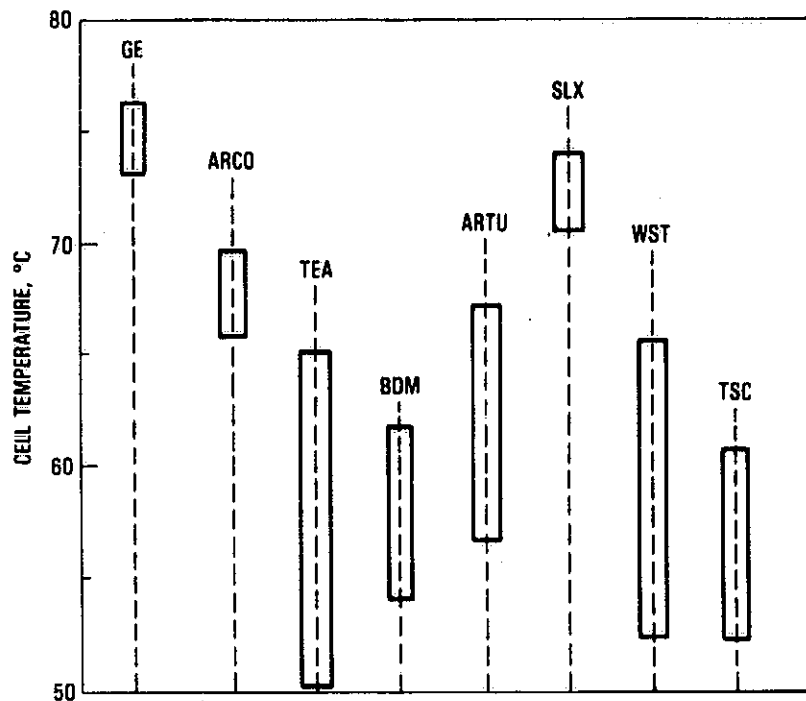


### Measured Temperature Profiles for Westinghouse Prototype on Day 268

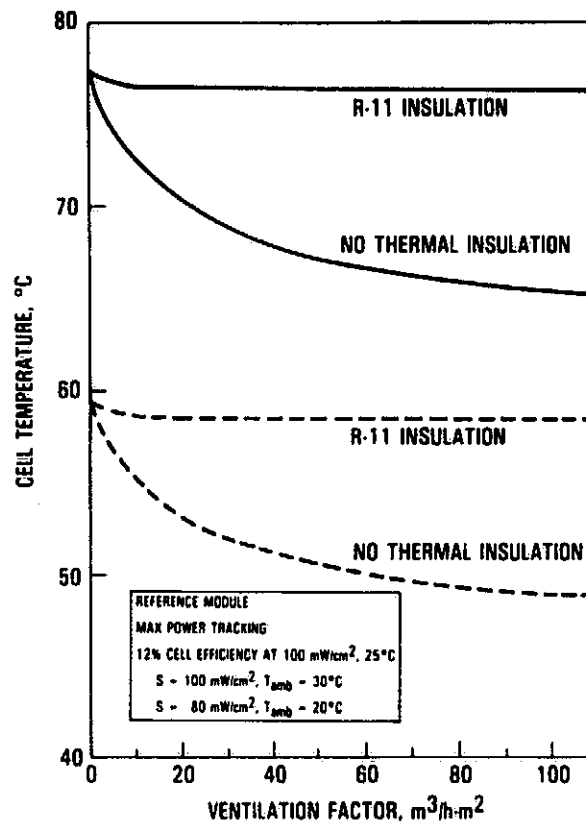




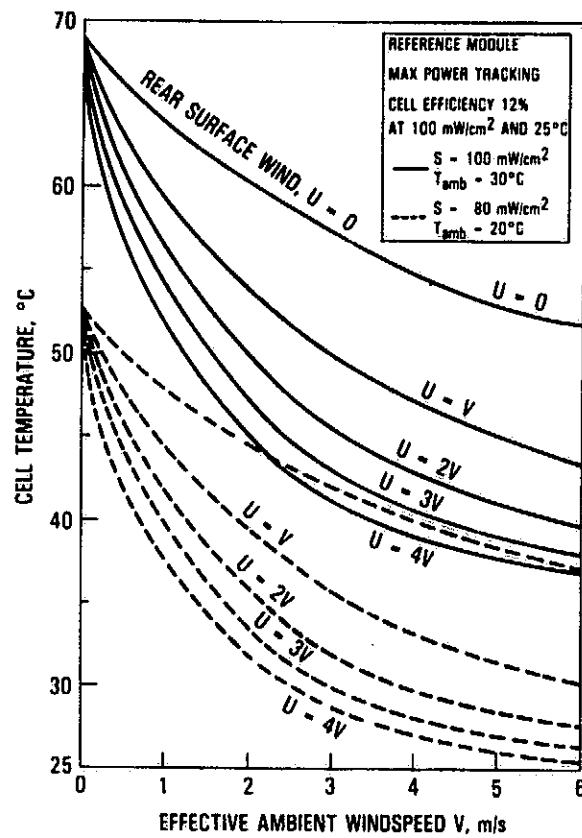
## Cell Temperature Levels Under Normalized Environmental Conditions



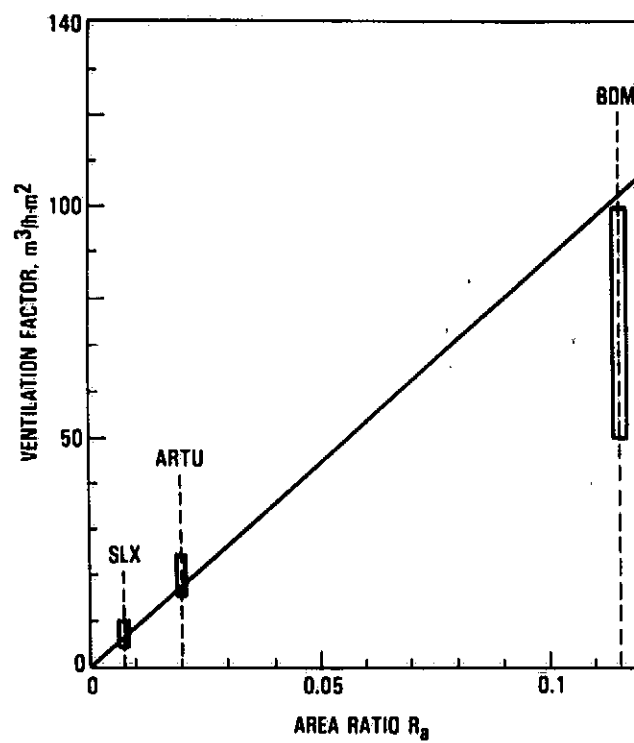
## Direct-Mounted Arrays



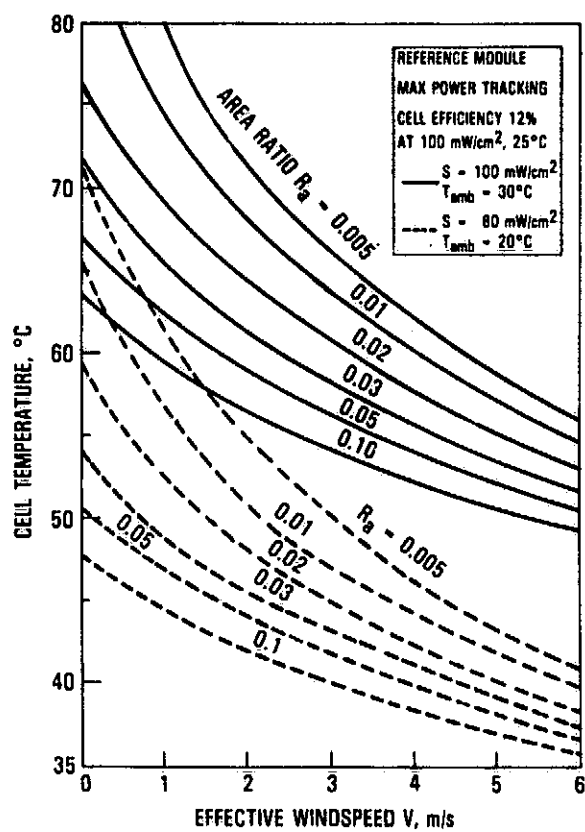
## Effect of Wind Distribution on Cell Temperature Levels



# Ventilation Factor and Area Ratio



## Cell Temperature Levels for Stand-Off Mounted Arrays



## Array Temperature Level in Nominal Test Environment

Array Temperature	Degrees Above NOCT	Mounting Arrangement
Hot	10 to 15	<ul style="list-style-type: none"> <li>• Direct mounted with back insulated</li> <li>• Stand-off mount with low channel height</li> <li>• Integral mount with small vent</li> </ul>
Medium	5 to 10	<ul style="list-style-type: none"> <li>• Direct mounted, exposed to ventilated attic</li> <li>• Stand-off mount, high channel</li> <li>• Integral mount, medium-sized vent</li> </ul>
Cold	-5 to +5	<ul style="list-style-type: none"> <li>• Rack mounted</li> <li>• Integral mounted with large vent</li> <li>• Stand-off mounted high channel and large separation between subarrays</li> </ul>

### Conclusions

- Air ventilation of the array back surface is a key factor in array thermal performance
- Preliminary results provide qualitative understanding of different mounting features

### Future Work

Additional studies are under way to:

- Provide quantitative correlation between design parameters (vent size, stand-off height) and simulation variables (ventilation factor)
- Determine relationship between effective wind speed and measuring altitude
- Simplify algorithms in predicting array temperatures

# ANNUAL ENERGY PREDICTION BASED ON NOCT

## JET PROPULSION LABORATORY

C.C. Gonzalez

### Background

- Consideration of NOCT array energy prediction method

$$E = \int S(t) \eta(T, S) dt \approx \eta(T_r, S_r) \int S(t) dt$$

NOCT determined for  $T_r = 20^\circ\text{C}$ ,  $S_r = 80\text{mW}/\text{cm}^2$

- Concern involving adequacy of energy prediction relative to:
  - Site-specific energy determination
  - Fill-factor dependency

### Objectives

- To provide an approach for fine-tuning the NOCT method in order to address shortcomings
  - Site-specific ambient-temperature dependencies
  - Fill-factor dependencies
- To provide a detailed assessment of the energy-prediction accuracy of the NOCT method

## Approach

- Obtain modified NOCT algorithms with site-specific parameters and fill-factor differentiation

$$\begin{aligned}
 E &= \int_{yr} S(t) \eta(T, S) dt \\
 &\approx \eta(T_r, S_r) \int_{yr} S(t) dt \\
 &\approx \phi(T) [1 - \psi(K_T) (0.7 - FF)] \cdot \eta(20, 80) \int_{yr} S(t) dt
 \end{aligned}$$

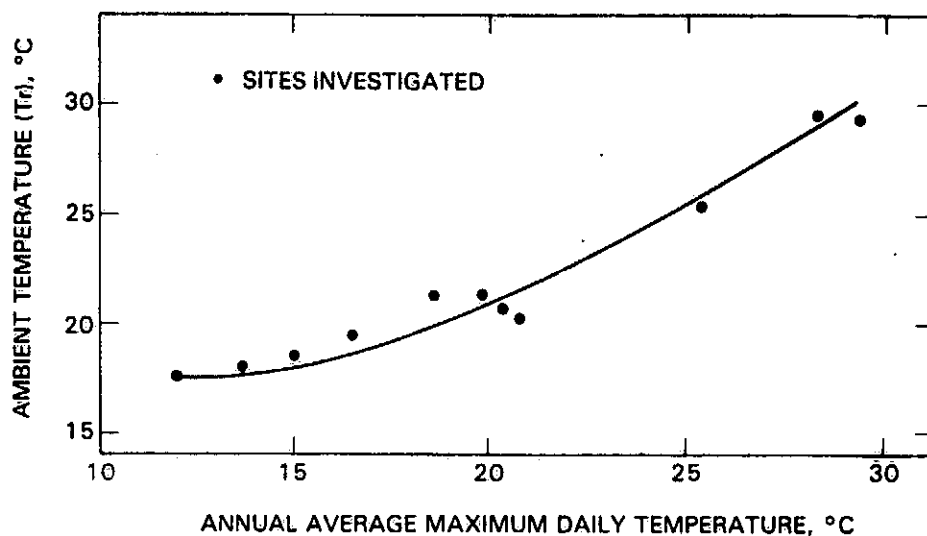
## Parameter Determination

- Determine parameters by minimizing the least-square energy prediction error based on:
  - Various module thermal-response characteristics ( $k = 0.30-0.45$ )
  - Various fill factors ( $0.60-0.75$ )
  - Hour-by-hour integration using SOLMET data for each site
- Correlate computer-determined parameters with generic weather atlas data
  - Annual average maximum daily temperature
  - Annual average  $K_T$  index



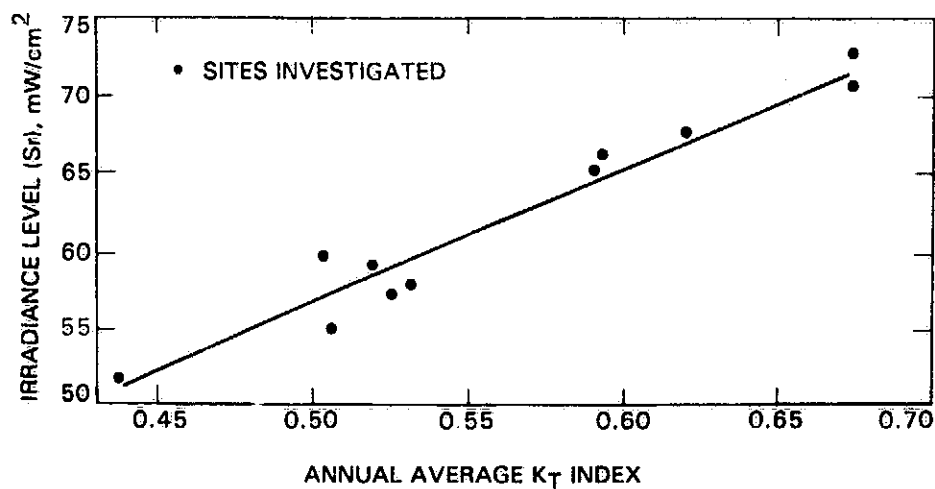
# Optimum Reference Ambient Temperature vs Site Annual Maximum Daily Temperature

$$E = \eta (T_r, S_r) \int_{yr} S(t) dt$$



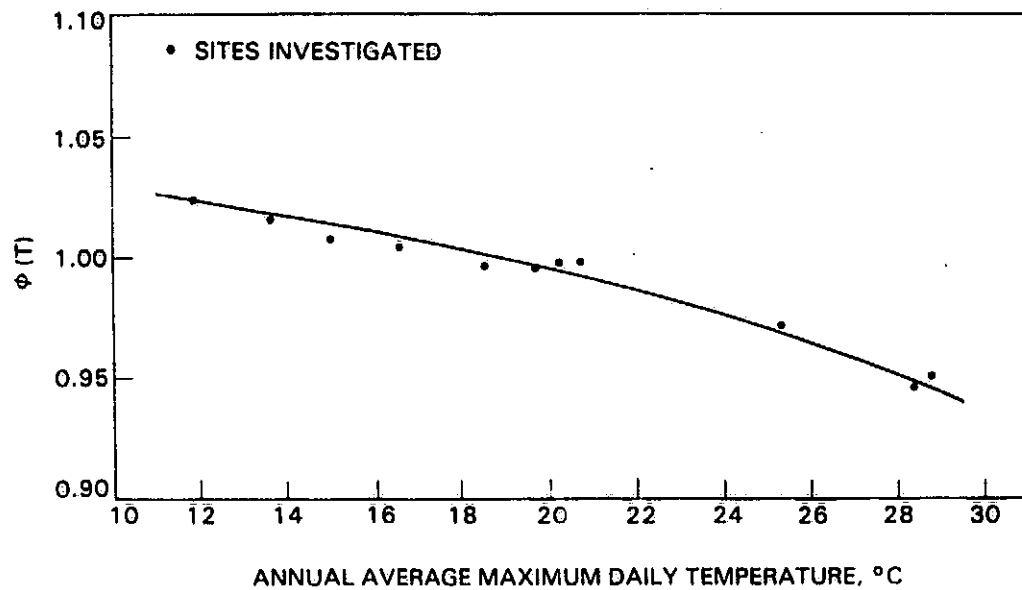
# Optimum Reference Irradiance Level vs Site Annual Average KT Index

$$E = \eta (T_r, S_r) \int_{yr} S(t) dt$$

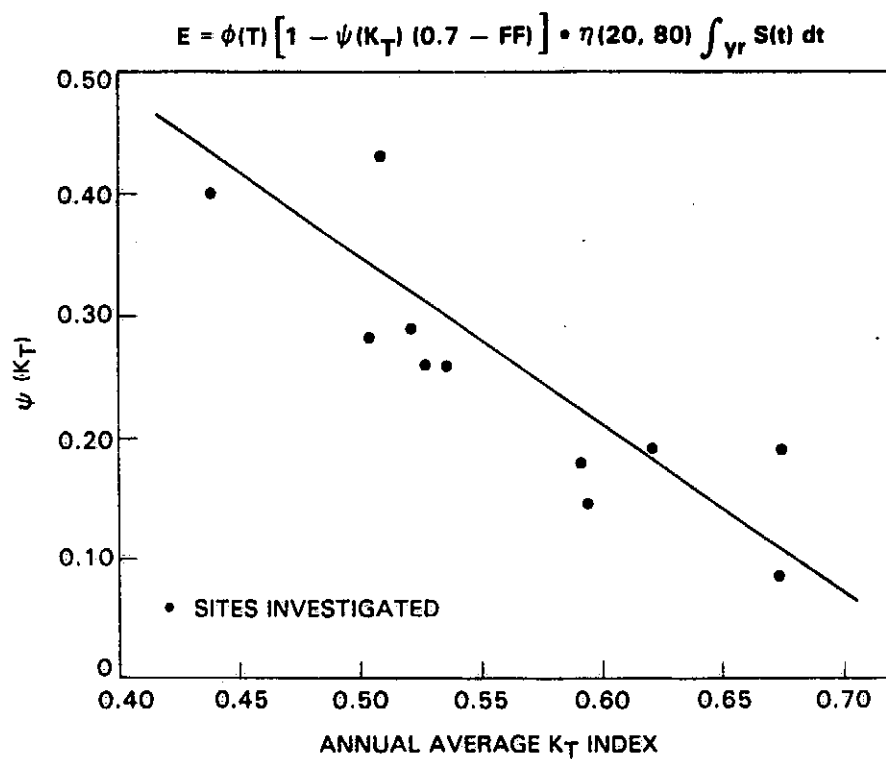


# **Ambient Temperature Correction Factor $\phi(T)$ vs Site Annual Average Maximum Daily Temperature**

$$E = \phi(T) \left[ 1 - \psi(K_T) (0.7 - FF) \right] \cdot \eta(20, 80) \int_{yr} S(t) dt$$



### Irradiance Level Correction Factor $\psi(K_T)$ vs Site Annual Average $K_T$ Index



## Sample Results for NOCT = 46°C

Site	Fill Factor	$\left( \text{Energy Prediction Algorithm} \right) / \int_{\text{yr}} S(t) \eta(T,S) dt$		
Site Ref. Cond. T, °C; S, mW/cm <sup>2</sup>		T = 20°C S = 80 mW/cm <sup>2</sup>	Site Spec. Ref. Cond.	T = 20°C S = 80 mW/cm <sup>2</sup> Plus Correction Factor
Albuquerque T = 21.4, S = 71.4	0.70	1.002	0.993	0.994
	0.60	1.011	0.991	0.992
Boston T = 18.2, S = 51.0	0.70	1.003	0.997	1.016
	0.60	1.044	0.998	1.012
Miami T = 29.0, S = 57.0	0.70	1.060	0.999	1.009
	0.60	1.106	0.995	1.017
Phoenix T = 30.0, S = 71.4	0.70	1.050	0.993	0.995
	0.60	1.070	0.995	1.003

## Conclusions

- NOCT-based energy-prediction algorithm adequate in most cases but significantly over-predicts for sites with hot climates
- Other single-temperature and irradiance reference conditions have similar problems
- Attainment of improved accuracy beyond NOCT-based algorithm requires a site-specific approach
  - Use of site-specific reference conditions
  - Use of site and fill-factor adjustment of the NOCT-baseline condition
- Site-specific approaches lead to energy-prediction errors of less than 1%